This publication is available free of charge from: https://doi.org/10.6028/NIST.IR.8271

NISTIR 8271 DRAFT SUPPLEMENT

Face Recognition Vendor Test (FRVT)

Part 2: Identification

Patrick Grother
Mei Ngan
Kayee Hanaoka
Information Access Division
Information Technology Laboratory

This document is a draft supplement of NIST Interagency Report 8271

2022/06/13

National Institute of Standards and Technology
U.S. Department of Commerce

This publication is available free of charge from: https://doi.org/10.6028/NIST.IR.8271

NISTIR 8271 DRAFT SUPPLEMENT

Face Recognition Vendor Test (FRVT)

Part 2: Identification

Patrick Grother
Mei Ngan
Kayee Hanaoka
Information Access Division
Information Technology Laboratory

This document is a draft supplement of NIST Interagency Report 8271

February 2022

U.S. Department of Commerce
Gina M. Raimondo, Secretary

National Institute of Standards and Technology
Laurie E. Locascio, NIST Director and Undersecretary of Commerce for Standards and Technology

This publication is available free of charge from: https://doi.org/10.6028/NIST.IR.8271

RELEASE NOTES

2022-06-08: The 1:N track of the FRVT remains open.

- This document is the seventeenth draft update to NIST Interagency Report 8271. It includes results for algorithms submitted by three first-time participants: Digidata, DiluSense Technology, and Vietnam Posts and Telecommunications Group.
- The document also includes results for algorithms from five returning developers: Canon Inc, Imagus Technology, Neurotechnology, Thales, and Samsung S1.

2022-04-28: The 1:N track of the FRVT remains open.

- This document is the sixteenth draft update to NIST Interagency Report 8271. It includes results for algorithms submitted by one first-time participants: Hangzhuo AIlu Network Information Technology.
- The document also includes results for algorithms from three returning developers: HyperVerge Inc, Qnap Security, and Realnetworks Inc.
- The 1:N results page has been updated.

2022-03-30: The 1:N track of the FRVT remains open.

- This document is the sixteenth draft update to NIST Interagency Report 8271. It includes results for algorithms submitted by two first-time participants: Intellivision, and Pangiam.
- The document also includes results for algorithms from three returning developers: Fujitsu Research and Development Center, Idemia, and Gorilla Technology.
- The 1:N results page has been updated.

2022-02-23: The 1:N track of the FRVT remains open.

- This document is the fifteenth draft update to NIST Interagency Report 8271. It includes results for algorithms submitted by four first-time participants: Cloudwalk - Moontime Smart Technology, Decatur Industries Inc, NotionTag Technologies Private Limited, and Reveal Media Ltd.
- The document also includes results for algorithms from three returning developers: Cognitec Systems GmbH, Sensetime Group, and Viettel Group
- The 1:N results page has been updated.

2022-01-20: The 1:N track of the FRVT remains open.

- This document is the fourteenth draft update to NIST Interagency Report 8271. It includes results for algorithms recently submitted by two first-time participants: Daon and SQIsoft.
- The document also includes results for algorithms from five returning developers: Cyberlink Corp, NEC, Neurotechnology, Paravision, and Rank One Computing.
- The 1:N results page has been updated.

2021-12-16: The 1:N track of the FRVT remains open.

- This document is the thirteenth draft update to NIST Interagency Report 8271. It includes results for algorithms from six returning developers: Dahua Technology, Imagus Technology, Line Corporation, N-Tech Lab, Qnap Security, and Realnetworks Inc.
- The 1:N results page has been updated.

2021-11-22: The 1:N track of the FRVT remains open.

- ▷ This document is the twelfth draft update to NIST Interagency Report 8271. It includes results for algorithms recently submitted by three first-time participants Clearview AI, Griaule, and Mantra Softech India.
- ▷ This document and the 1:N results page also include results for algorithms from six returning developers: Acer Incorporated, Canon, Dermalog, Samsung S1, VisionLabs, and Veridas Digital Authentication.

2021-10-28: The 1:N track of the FRVT remains open.

- ▷ This document is the eleventh draft update to NIST Interagency Report 8271. It includes results for algorithms recently submitted by three first-time participants (20Face, Fujitsu Research and Development Center, and Vision-Box), and five returning participants (Alchera, Gorilla Technology, Tevian, Thales-Cogent, and Visidon). Visidon
- ▷ Both the main 1:N results page and the small-gallery paperless travel page have been updated.

2021-09-21: The 1:N track of the FRVT remains open. Three news items:

- ▷ This document is the tenth draft update to NIST Interagency Report 8271. It includes results for algorithms recently submitted by six first-time developers: Cubox, Fincore, HyperVerge, Qnap Security, Staqu Technologies, and Tripleize (Aize, 3-ize).
- ▷ It includes results also for four returning developers: Cognitec Systems, Incode Technologies, Innovatrics, Neurotechnology, and Rank One Computing.

2021-08-02: The 1:N track of the FRVT remains open. Three news items:

- ▷ This document is the nineth draft update to NIST Interagency Report 8271. It includes results for algorithms recently submitted by eight participants: Cyberlink Corp, NEC Corp, N-Tech Lab, Realnetworks Inc., Sensetime Group, Veridas Digital, Viettel Group, and Vigilant Solutions.
- ▷ Algorithms submitted since July 24 will be included in the next update scheduled for September 9, 2021.
- ▷ A new report, NIST Interagency Report 8381 - FRVT Part 7: Identification for Paperless Travel and Immigration, has been released [PDF, webpage]. It documents the use of FRVT 1:N algorithms in positive access control and immigration status update travel applications where the enrolled population size is as low as 420 people for aircraft boarding, and 42 000 for an airport security line. These population sizes are much smaller than those used in the main 1:N evaluation. Going forward, we will update the report and webpage with results for new algorithms.

2021-07-07: The 1:N track of the FRVT remains open. One update:

- ▷ This document is the eighth draft update to NIST Interagency Report 8271. It include results for an algorithm from one participant: Kakao Enterprises.

2021-06-22: The 1:N track of the FRVT remains open. Three updates:

- ▷ This is the seventh draft of the update to NIST Interagency Report 8271. It includes results for algorithms from three new participants: Line Corporation, Rendip, and Samsung S1 Corp.
- ▷ We have also added results for algorithms from five returning developers: Imagus Technology, Kneron, Tevian, Visidon, and Xforward AI Technology.
- ▷ The algorithm-specific report cards (examples: 1, 2, and 3) now include figures showing how low threshold values can be used to reduce candidate list lengths for human review, while (usually) elevating miss rates (FNIR) only modestly. The reports also feature some minor additions and clarifications.

2021-03-26: The 1:N track of the FRVT remains open. Three updates:

This publication is available free of charge from: https://doi.org/10.6028/NIST.IR.8271

This publication is available free of charge from: https://doi.org/10.6028/NIST.IR.8271

- ▷ This is the sixth draft of the update to NIST Interagency Report 8271. It includes results for algorithms from three returning developers: Neurotechnology, Guangzhou Pixel Solutions, and Tech5 SA.
- ▷ We have added results on the webpage and in the report for a new ageing dataset in which border crossing photos are searched against a gallery of border crossing photos collected between 10 and 15 years prior to the mated search photos. See section 2 for a description of the images. Table 1 has a new entry describing the experiment.
- ▷ We will mostly discontinue running the mugshot ageing test, reserving it for algorithms that show high accuracy on the new border-crossing set.

2021-03-26: Regarding the fifth draft of the update to NIST Interagency Report 8271:

- ▷ In addition have added results for first algorithms from two new participants: Viettel Group and Veridas Digital Authentication Solutions.
- ▷ We have added results for algorithms from two returning developers: Idemia and Cognitec Systems.
- ▷ In addition to the report, the results page and its hyperlinked report cards have been updated.

2021-02-08: Regarding the fourth draft of the update to NIST Interagency Report 8271:

- ▷ We have added results for eight algorithms submitted by eight developers: Cyberlink, Dermalog, Imagus, Paravision, Sensetime, Trueface, Vigilant Solutions, and X-Forward AI. With the exception of Trueface, all of these developers have participated previously.
- ▷ We anticipate updating this report again in the first week of March 2021.
- ▷ The main results page has been revised with tabs for the investigative and lights-out identification tables, and a new tab dedicated to speed and resource consumption.
- ▷ The report cards (example here) hyperlinked from the results page have been revised to improve content and format.

2020-12-14: Regarding third draft of the update to NIST Interagency Report 8271:

- ▷ We have added results for fifteen algorithms submitted by thirteen developers. The four first-time participants are: Acer, Akurat Satu Indonesia, Canon, and Xforward AI Technology. The ten returning developers are: AllGoVision, Cyberlink Corp, Dahua Technology, Deepglint, Guangzhou Pixel Solutions, IIT Vision, Innovatrics, Rank One Computing, Scanovate, Sensetime Group, Synesis, and VisionLabs.
- ▷ We have added two new datasets to the evaluation: First a set of "visa-border" photos, representing search of an airport immigration lane photo against a database of closely ISO standard portraits; second a "visa-kiosk" set representing search of a photo collected in a registered traveller kiosk against the same ISO portrait gallery. The images are described in section 2.1.
- ▷ As in previous reports, we include results for searching mugshots against a mugshot gallery containing a single image of each of 12 million people. However we have suspending running searches against a gallery in which multiple lifetime photos per person are present, because this is computationally expensive. We retain a N = 3 million search test dedicated to ageing in which mugshots taken up to 18 years after the first photograph are searched - see Table 7.
- ▷ Tables containing computational resource information, Table 2. . ., now include duration of the finalization step, in which search algorithms can, at their option, build fast-search data structures.
- ▷ We have linked revised per-algorithm PDF report cards from the main results page.
- ▷ We have regenerated all figures and tables to drop algorithms submitted before June 2018. Results for prior algorithms appear in archived editions of this report.
- ▷ Going forward, we anticipate producing more frequent updates to this report. Developers may submit one algorithm to this evaluation every four calendar months.

2020-03-24: Regarding the second draft of the update to NIST Interagency Report 8271:

- ▷ Adds results for three algorithms from three developers, Dermalog, Innovatrics, and Synesis.
- ▷ Adds Table 7 on ageing showing the increase in false negative rates with time elapsed between two photos. Some of the results were contained in graphs in prior editions of this report, but the table adds results for some newly submitted algorithms.
- ▷ Adjusts frontal mugshot results (for recent and lifetime consolidated galleries) to include the effect of removing some images that should not have been included in image test sets. These images were mostly profile views, images of tattoos containing faces, images of faces on tee shirts, and images of photographs on walls behind the intended subject. This affects many tables and reduces false negative identification rates for all algorithms. The reduction is larger for "recent" enrollments than for "lifetime consolidated" ones with the consequence that accuracy on recent images is now superior.

2020-02-26: Regarding the first draft of the update to NIST Interagency Report 8271:

- ▷ Adds results for 38 algorithms from 31 different developers, eleven of whom are entirely new to the 1:N track of FRVT. These are Allgovision, Cyberlink, Deepsea Tencent, Farbar F8, Imperial College London, Intsys MSU, Kedacom, Kneron, Pixelall, and Scanovate.

This publication is available free of charge from: https://doi.org/10.6028/NIST.IR.8271

This publication is available free of charge from: https://doi.org/10.6028/NIST.IR.8271

DISCLAIMER

Specific hardware and software products identified in this report were used in order to perform the evaluations described in this document. In no case does identification of any commercial product, trade name, or vendor, imply recommendation or endorsement by the National Institute of Standards and Technology, nor does it imply that the products and equipment identified are necessarily the best available for the purpose.

INSTITUTIONAL REVIEW BOARD

The National Institute of Standards and Technology's Research Protections Office reviewed the protocol for this project and determined it is not human subjects research as defined in Department of Commerce Regulations, 15 CFR 27, also known as the Common Rule for the Protection of Human Subjects (45 CFR 46, Subpart A).

ACKNOWLEDGMENTS

The authors are grateful for the support and collaboration of the the Department of Homeland Security's Science & Technology Directorate (S&T), Office of Biometric Identity Management (OBIM), and Customs and Border Protection (CBP).

Additionally, the authors are grateful to staff in the NIST Biometrics Research Laboratory for infrastructure supporting rapid evaluation of algorithms.

This publication is available free of charge from: https://doi.org/10.6028/NIST.IR.8271

Executive Summary

This document is a draft revision of the September 2019 report NIST Interagency Report 8271. That report gave extensive documentation of face recognition applied to mugshots. This report extends that by adding more two more challenging datasets containing images with serious departures from canonical frontal image standards. The report also adds results for algorithms submitted to NIST since in 2019 and 2020. The algorithms, which implement one-to-many identification of faces appearing in two-dimensional images, are prototypes from the research and development laboratories of mostly commercial suppliers, and are submitted to NIST as compiled black-box libraries implementing a NIST-specified C++ test interface. The report therefore does not describe how algorithms operate. The report lists accuracy results alongside developer names and will therefore be useful for comparison of face recognition algorithms and assessment of absolute capability. The report is accompanied by a webpage with sortable results.

The evaluation uses six datasets: frontal mugshots, profile view mugshots, desktop webcam photos, visa-like immigration application photos, immigration lane photos, and registered traveler kiosk photos. These datasets are sequestered at NIST, meaning that developers do not have access to them for training or testing. This aspect is important because face recognition algorithms are very often deployed without the developer having access to the customers image data. A possible exception to this would be in a cloud-based application where the operational image data is uploaded to a cloud operated by a face recognition developer.

The major result in NIST IR 8271 was that massive gains in accuracy have been achieved in the years 2013 to 2018 and these far exceed improvements made in the prior period, 2010 to 2013. While the industry gains were broad - at least 30 developers' algorithms outperformed the most accurate algorithm from late 2013, there remains a wide range of capability. While this report shows accuracy gains only over the period 2018-2020, the most accurate algorithm reported here is substantially more accurate than anything reported in NIST IR 8271. This is evidence that face recognition development continues apace, and that FRVT reports are but a snapshot of contemporary capability.

From discussion with developers, the accuracy gains stem from the adoption of deep convolutional neural networks. As such, face recognition has undergone an industrial revolution, with algorithms increasingly tolerant of poorly illuminated and other low quality images, and poorly posed subjects. One related result is that a few algorithms correctly match side-view photographs to galleries of frontal photos, with search accuracy approaching that of the best c. 2010 algorithms operating on purely frontal images. The capability to recognize under a 90-degree change in viewpoint - pose invariance - has been a long-sought milestone in face recognition research.

With good quality portrait photos, the most accurate algorithms will find matching entries, when present, in galleries containing 12 million individuals, with rank one miss rates of approaching 0.1%. The remaining errors are in large part attributable to long-run ageing, facial injury and poor image quality. Given this impressive achievement - close to perfect recognition - an advocate might claim that cooperative face recognition is a solved problem, a statement that can be refuted with the following context and caveats:

- ▷ **Mugshots vs. less constrained captures:** The low error rates reported here are attained using mostly excellent cooperative live-capture mugshot images collected with an attendant present. Recognition in other circumstances, particularly those without a dedicated photographic environment and human or automated quality control checks, will lead to declines in accuracy. This is documented here for side-view images, poorer quality webcam images, and, particularly, for newly introduced ATM-style kiosk photos that were not originally intended for automated face recognition. In this case, recognition error rates are much higher, often in excess of 20% even with the more accurate algorithms which variously remain intolerant of face cropping (at image edge) and of large downward head pitch.

- ▷ **Algorithm accuracy spectrum:** Recognition accuracy is very strongly dependent on the algorithm and, more

This publication is available free of charge from: https://doi.org/10.6028/NIST.IR.8271

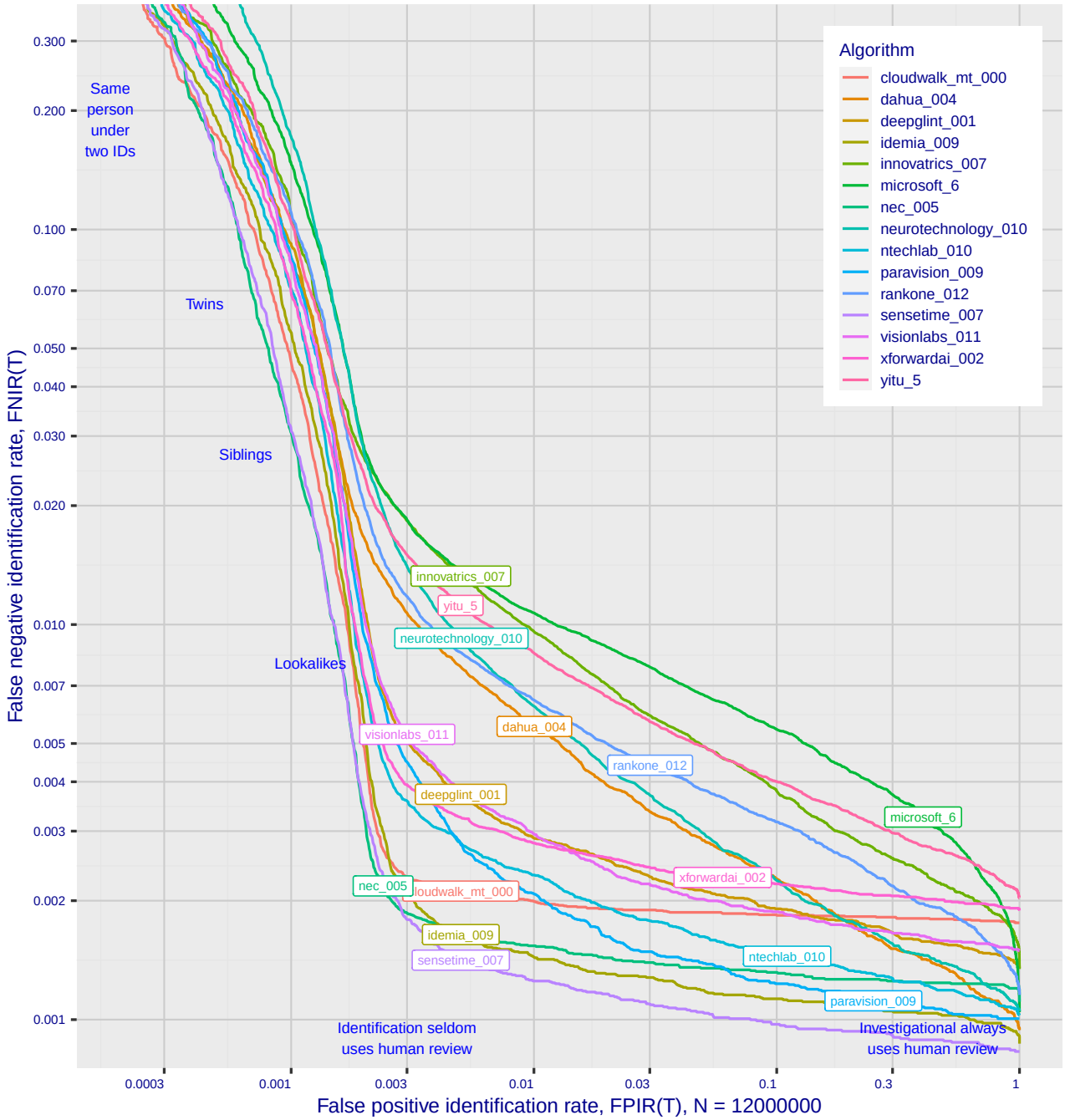

Figure 1: Identification miss rates across the false positive range. N = 12 million individuals are enrolled with one recent image.

generally, on the developer of the algorithm. False negative error rates in a particular scenario range from a few tenths of one percent to beyond fifty percent. This is tabulated exhaustively later: For example Table 11 shows accuracy across datasets. Figure 1 here compares algorithms on mugshot searches in a consolidated gallery of 12 million subjects and 12 million photos. Many algorithms do not achieve the low error rates noted above, and while many of those may still be useful and valuable to end-users, only the most accurate excel on poor quality images and those collected long after the initial enrollment sample.

▹ **Versioning:** While results for up to ten algorithms from each developer are reported here, the intra-provider

accuracy variations are usually smaller than the inter-provider variations. That said different versions give an order of magnitude fewer misses. Some developers demonstrate speed-accuracy tradeoffs[1]. See Figs. 18, 19.

▷ **Low similarity scores:** In thousands of mugshot cases the correct gallery image is returned at rank 1 but its similarity score is nevertheless low, below some operationally required score threshold. This is not so important when face recognition is used for "lead generation" in investigational applications because human reviewers are specifically required to review potentially long candidate lists and the threshold is effectively 0. In applications where search volumes are higher and labor is not available to review the results from searches, a higher threshold must be applied. This reduces the length of candidate lists and false positive identification rates at the expense of increased false negative miss rates. The tradeoff between the two error rates is reported extensively later.

▷ **Population size:** As the number of enrolled subjects grows, some mates are displaced from rank one, decreasing accuracy. As tabulated later for N up to 12 million, false negative rates generally rise slowly with population size. This enables use of face recognition in very large populations. However in most positive and negative identification applications[2], a score threshold is set to limit the rate at which non-mate searches produce false positives. This has the consequence that some mated searches will report the mate below threshold, i.e. a miss, even if it is at rank 1. The utility of this is that many non-mated searches will return no candidate identities at all. As the error-tradeoff characteristic shows, investigational miss rates on the right side are very low but then rise steadily (in the center region) as threshold is increased to support "lights-out" applications, and ultimately rise quickly (left side) as discussed below. Thus, if we demand that just one in one thousand non-mate searches produce any false positives, the most accurate algorithms there (Sensetime-004 and NEC-3) would fail on between 3 and 5% of mated searches. Even though the graph shows results for the most accurate algorithms, all but two would fail to find the mate in more than 8% of mated searches. While the two most accurate algorithms produce a relatively flat error tradeoff until the threshold is raised to limit false positives to about 1 in 400 non-mated searches[3]

Thereafter, as the threshold is raised to further reduce false positives, miss rates rise rapidly. This means that low false positive identification rates are inaccesible with these algorithms, a result that does not apply for ten-finger identification algorithms. The rapid rise occurs because the lower mate scores are mixed with very high non-mate scores, the low scores from poor image quality and ageing, the high non-mates from the presence of lookalikes persons (doppelgangers), twins (discussed next) and, ultimately, the presence of a few unconsolidated subjects i.e. persons present under multiple IDs.

▷ **False negatives from ageing:** A large source of error in long-run applications where subjects are not re-enrolled on a set schedule is ageing. Changes in facial appearance increase with the time elapsed between photographs. These will depress similarity scores and eventually cause false negatives. All faces age and while this usually proceeds in a graceful and progressive manner, drug use can accelerate this [28]. Elective surgery may be effective in delaying it although this has not been formally quantified with face recognition. As ageing is essentially unavoidable, it can only be mitigated by scheduled re-capture, as in passport re-issuance. To quantify ageing effects, we used the more accurate algorithms to enroll the earliest image of 3.1 million adults and then search

[1] For example, NEC-0 prepares templates much faster than NEC-2 but gives twenty times more misses. Dermalog-5 executes a template search much more quickly than Dermalog-6 but is also much less accurate.

[2] In a positive identification application such as a registered traveler system, a user is making an implicit claim to be enrolled in the system - most users will be. In a negative application, such as with deportees, the implicit claim is that the subejct is not enrolled - most will not be.

[3] The gallery size here is 12 million people, one image per person. Given 331 201 non-mated searches, an exhaustive implementation of one-too-many search would execute almost 4 trillion comparisons. At a false positive identification rate of 0.0025 the number of false positives is, to first order, 828 corresponding to single-comparison false match rate of 828 / 4 trillion = 2.1 10^{-10} i.e. about 1 in 5 billion. Strictly this FMR computation is meaningful only for algorithms that implement 1:N search using N 1:1 comparisons, which is not always the case.

This publication is available free of charge from: https://doi.org/10.6028/NIST.IR.8271

with 10.3 million newer photos taken up to 18 years after the the initial enrollment photo. Figure 2 puts ageing into context by contrasting it with the increase in false negatives that occurs when the number of individuals in an enrollment database becomes larger and the chance of a false positive increases such that higher thresholds may become necessary[4].

The Figure shows, from to bottom, increases in false negative identification rates (FNIR) with the algorithm being tested. This applies to increases due to N on the left side, and increases due to ageing on the right side. The relative spacing of the dots shows that for all algorithms the dependency of FNIR on N (up to 12 million) is considerably less than on ΔT (up to 18 years).

In the inset table, accuracy is seen to degrade progressively with time, as mate scores decline and non-mates displace mates from rank 1 position. More accurate algorithms tend to be less sensitive to ageing. The more accurate algorithms give fewer errors after 18 years of ageing than middle tier algorithms give after four. Note also we do not quantify an ageing rate - more formal methods [2] borrowed from the longitudinal analysis literature have been published for doing so (given suitable repeated measures data). See Figures 60, 84 and 96.

This publication is available free of charge from: https://doi.org/10.6028/NIST.IR.8271

[4]Some algorithms implement stragegies to automatically adjust scores to account for increased population size. This relieves the system owner of having to increase thresholds as N increases.

This publication is available free of charge from: https://doi.org/10.6028/NIST.IR.8271

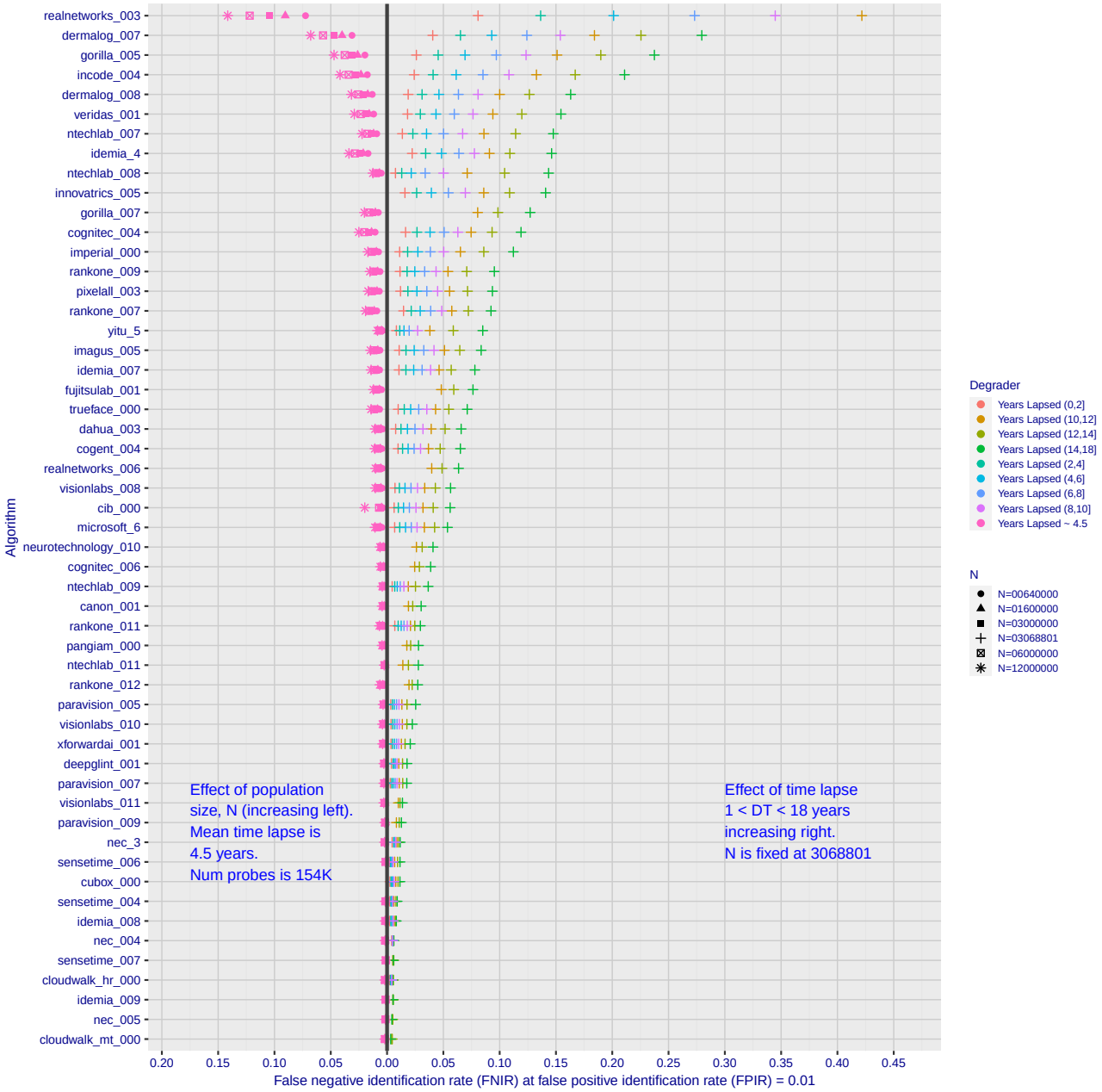

Figure 2: Identification miss rates as a function of enrolled population size, N, and time-lapse, ΔT.

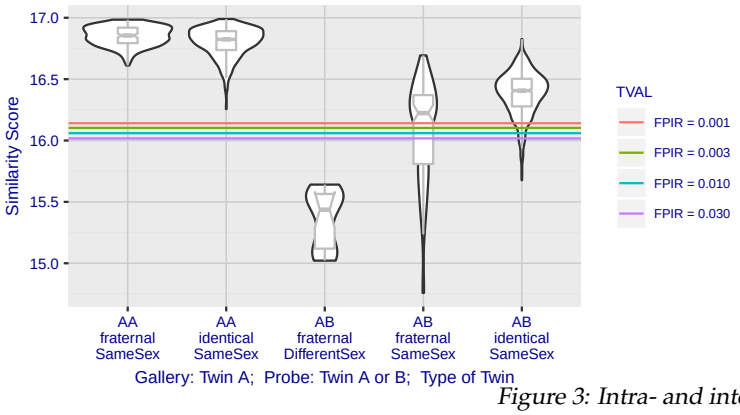

Figure 3: Intra- and inter-twin scores

- **False positives from twins:** By enrolling 640 000 mugshots, adding photos of one twin, and then searching photos of those subjects and their twin the inset figure shows, for one typical algorithm, the similarity is generally greater when searching twins against themselves (A) than when searching twins against their sibling (B) but very often still above even stringent thresholds i.e. those corresponding to one in one thousand searches producing a false positive. Thus twins will very often produce a high-scoring non-match on a candidate list and a false alarm in an online identification system. The plot of Fig. 3 shows that fraternal twins are sometimes correctly rejected at those thresholds - including most different sex twins (at center). Figure **??** shows substantially similar behavior for all algorithms tested. In an investigative search, a twin would typically appear at rank 1, or rank 2 if their sibling happened to also be the gallery. Twins (and triplets etc.) constituted 3.3% of all live births [17] in recent years[5], and because that number is higher today than when the individuals in current adult databases were born, the false positives that arise from twins are now, and will increasingly be, an operational problem. Relative to the United States, twins are born with considerable regional variation. For example they are much less common in East Asia, and much more common in Sub-Saharan Africa [21].

  The presence of twins in the mugshot database is inevitable given its size, around 12.3 million people. As this is not an insignificant sample of the domestic United States population, people with other familial ties will be present also. The data was collected over an extended period and because location information is not available, we are unable to estimate the proportion of the domestic population that is present in the dataset. However, if we assume twins are neither more or less disposed to arrest than the general population, we can estimate that hundreds of thousands of individuals in the dataset are twins. This will affect false positive rates because we randomly set aside 331 201 individuals for nonmate searches, and some proportion of those will be twins with siblings in the gallery.

- **Database integrity:** An operational error rate should be added to all false negative rates in this report reflecting the proportion of images in a real database that are un-matchable. Such anomalies arise from images that: do not contain a face; include multiple persons; cannot be decoded; are rotated by 90° or 180°; depict a face on clothing; and others introduced by a long tail of various clerical errors. While the mugshot trials in this report have been constructed to minimize such effects, they are a real problem in actual operations.

This report is being updated continuously as new algorithms are submitted to FRVT, and run on new datasets. Participation in the one-to-many identification track is independent of participation in the one-to-one verification track of FRVT.

[5]See the CDC's National Vital Statistics Report for 2017: https://www.cdc.gov/nchs/data/nvsr/nvsr67/nvsr67_08-508.pdf

This publication is available free of charge from: https://doi.org/10.6028/NIST.IR.8271

Scope and Context

Audience: This report is intended for developers, integrators, end users, policy makers and others who have some familiarity with biometrics applications. The methods and metrics documented here will be of interest to organizations engaged in tests of face recognition algorithms. Some of these have been incorporated in the ISO/IEC 19795 Part 1 Biometric Testing and Reporting Framework standard, now nearing publication.

Prior benchmarks: Automated face recognition accuracy has improved massively in the two decades since initial commercialization of the various technologies. NIST has tracked that improvement through its conduct of regular independent, free, open, and public evaluations. These have fostered improvements in the state of the art. This report serves as an update to the NIST Interagency Report 8271 on performance of face identification algorithms, published in September 2019.

Demographics: In December 2019, NIST published a first report on demographic dependencies in face recognition, NIST Interagency Report 8280 that documented age, sex and race differentials in one-to-one and one-to-many false positive and false negative rates.

Scope: NIST IR 8271 documented recognition results for four databases containing in excess of 30.2 million still photographs of 14.4 million individuals. That constituted the largest public and independent evaluation of face recognition ever conducted. It includes results for accuracy, speed, investigative vs. identification applications, scalability to large populations, use of multiple images per person, images of cooperative and non-cooperative subjects.

The report also includes results for ageing, recognition of twins, and recognition of profile-view images against frontal galleries. It otherwise does not address causes of recognition failure, neither image-specific problems nor subject-specific factors including demographics. Separate reports on demographic dependencies in face recognition will be published in the future. Additionally out of scope are: performance of live human-in-the-loop transactional systems like automated border control gates; human recognition accuracy as used in forensic applications; and recognition of persons in video sequences (which NIST evaluated separately [9]). Some of those applications share core matching technologies that *are* tested in this report.

Images: Five kinds of images are employed; these are either compared with images of the same kind, or against others from different capture environments as follows. The primary dataset is a set of law enforcement mugshot images (Fig. 5) which are enrolled and then searched with three kinds of images: other mugshots (i.e. within-domain); profile-view photographs (90 degree cross-view); and lower quality webcam images (Fig. 6) collected in similar detention operations (cross-domain). Additionally we compare high quality visa-like photos collected in immigration offices, with: medium quality border crossing images collected in primary immigration lanes; poor quality images collected in ATM-like registered traveller kiosks.

Participation and industry coverage: The report includes performance figures for prototype algorithms from the research laboratories of commercial developers and a few universities. This represents a substantial majority of the face recognition industry, but only a tiny minority of the academic community. Participation was open worldwide. While there is no charge for participation, developers incur some software engineering expense in implementing their algorithms behind the NIST application programming interface (API). The test is a black-box test where the function of the algorithm, and the intellectual property associated with it, is hidden inside pre-compiled libraries.

Recent technology development: Most face recognition research with deep convolutional neural networks (CNNs) has been aimed at achieving invariance to pose, illumination and expression variations that characterize photojournalism and social media images. The initial research [18, 22] employed large numbers of images of relatively few ($\sim 10^4$) individuals to learn invariance. Inevitably much larger populations ($\sim 10^7$) were employed for training [11, 20] but the benchmark, Labeled Faces in the Wild with (essentially) an equal error rate metric [12], represents an easy task,

This publication is available free of charge from: https://doi.org/10.6028/NIST.IR.8271

one-to-one verification at very high false match rates. While a larger scale identification benchmark duly followed, Megaface [15], its primary metric, rank one hit rate, contrasts with the high threshold discrimination task required in most large-population applications of face recognition, namely credential de-duplication, and background checks. There, identification in galleries containing up to 10^8 individuals must be performed using a) very few images per individual and b) stringent thresholds to afford very low false positive identification rates. This track of FRVT was launched to measure the capability of the new technologies, including in these two cases. FRVT has included open-set identification tests since 2002, reporting both false negative and positive identification rates [7].

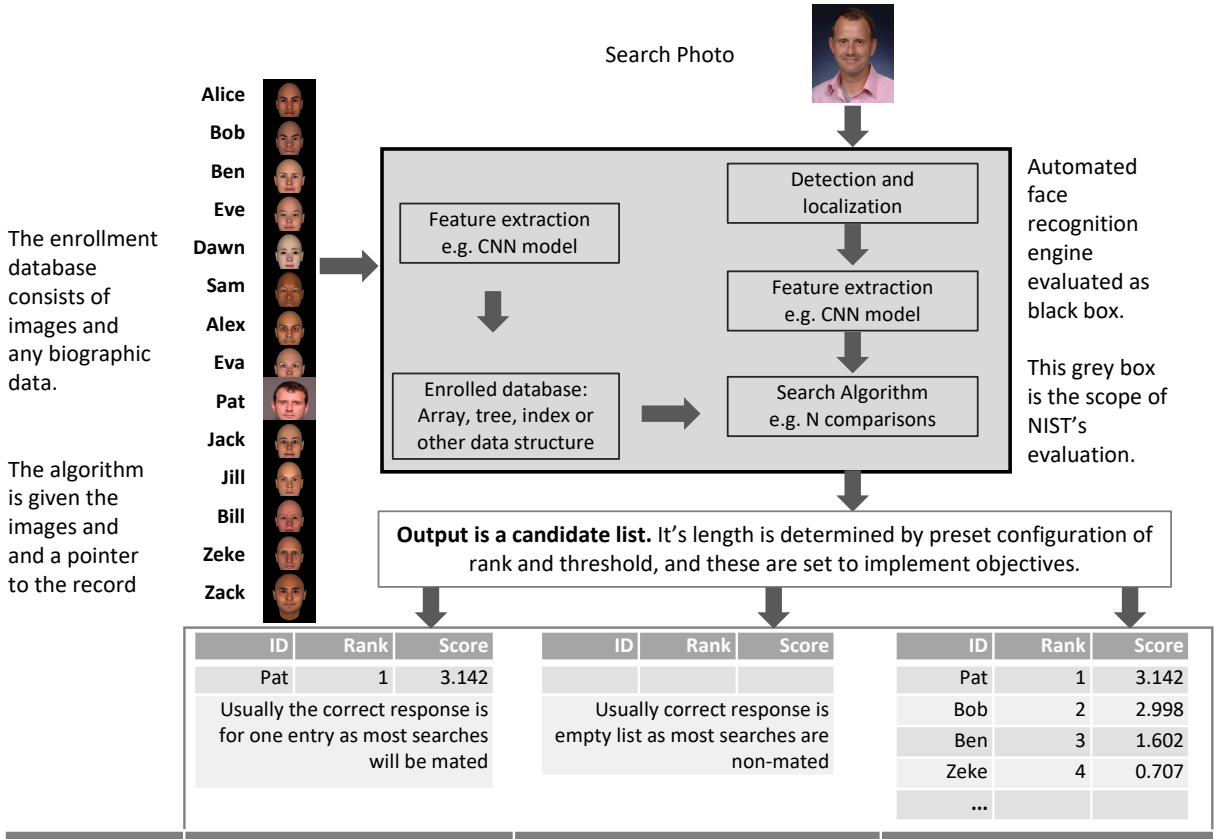

	Positive identification	Negative identification	Post-event investigation
Example	Access to a gym or cruise ship	Watchlist e.g. Detection of deportee or duplicate drivers license applications	Crime scene photos, or of detainee without ID documents.
Claim of identity	Implicit claim to be enrolled	Implicit claim to not be enrolled	No claim: Inquiry
Threshold	High, to implement security objective	High, to limit false positives	Zero
Num. candidates	1	0	L, set by request to algorithm
Human role	Review candidate to assist user in resolution of false negatives, or to detect impostor	Review candidate to determine false positive or correct hit	Review multiple candidates, refer possible hits to examiners see [26]
Intended human involvement frequency	Rare – approx. the false negative identification rate plus prior probability of impostor	Rare – approx. the false positive identification rate plus prior probability of an actual mate	Always
Performance metric of interest	**FNIR at low FPIR. See sec. 3.1, 3.2 and Tables 10, 19**	**FNIR at low FPIR. See sec. 3.1, 3.2 and Tables 10, 19**	**FNIR at ranks 1... 50, say. FPIR = 1. See sec. 3.2 and Table 12, 14, 16**

Performance metrics for applications: This report documents the performance of one-to-many face recognition algorithms. The word "performance" here refers to recognition accuracy and computational resource usage, as measured

This publication is available free of charge from: https://doi.org/10.6028/NIST.IR.8271

by executing those algorithms on massive sequestered datasets.

This report includes extensive tabulation of recognition error rates germane to the main use-cases for face search technology. The Figure below, inspired by the Figure 1 in [23] differentiates different applications of the technolgy. The last row directs readers to the main tables relevant to those applications, respectively threshold-based and rank-based metrics that are special cases of the metrics given in section 3. The terms negative identification and positive identification are taken from the ISO/IEC 2382-37:2017 standardized biometrics vocabulary.

The algorithms are specifically configured for these applications by setting thresholds and candidate list lengths. Both rank-based metrics and threshold-based metrics include tradeoffs. In investigation, overall accuracy will be reduced if labor is only available to review a few candidates from the automated system. Note that when a fixed number of candidates are returned, the false positive identification rate of the automated face recognition engine will be 100%, because a probe image of anyone not enrolled will still return candidates. In identification applications where false positives must be limited to satisfy reviewer labor availability or a security objective, higher false negative rates are implied. This report includes extensive quantification of this threshold-based tradeoff. See Sec. 3

Template diversity: The FRVT is designed to evaluate black-box technologies with the consequence that the templates that hold features extracted from face images are entirely proprietary opaque binary data that embed considerable intellectual property of the developer. Despite migration to CNN-based technologies there is no consensus on the optimal feature vector dimension. This is evidenced by template sizes ranging from below 100 bytes to more than four kilobytes. This diversity of approaches, suggests there is no prospect of a standard template something that would require a common feature set to be extracted from faces. Interoperability in automated face recognition remains solidly based on images and documentary standards for those, in particular the ICAO portrait [27] specification deriving from the ISO/IEC 19794-5 Token frontal [24] standard, which are similar to certain ANSI/NIST Type 10 [26] formats.

Training: The algorithms submitted to NIST have been developed using image datasets that developers do not disclose. The development will often include application of machine learning techniques and will additionally involve iterative training and testing cycles. NIST itself does not perform any training and does not refine or alter the algorithm in any way. Thus the model, data files, and libraries that define an algorithm are fixed for the duration of the tests. This reflects typical operational reality where recognition software, once installed, is fixed and constant until upgraded. This situation persists because on-site training of algorithms on customer data is atypical essentially because training is not a turnkey process.

Automated search and human review: Virtually all applications using automated face search require human review of the outputs at some frequency: Always for investigational applications; rarely in positive identification applications, after rejection (false or otherwise); and rarely in negative identification applications, after an alarm (false or otherwise). The human role is usually to compare a reference image with the query image or the live-subject if present, to render either a definitive decision on "exclusion" (different subjects), or "identification" (same subject), or a declaration that one or both images have "no value" and that no decision can be made. Note that automated face recognition algorithms are not built to do exclusion - low scores from a face comparison arise from different faces *and* poor quality images of the same face.

Human reviewers make recognition errors [5, 19, 25] and are sensitive to image acquisition and quality. Accurate human review is supported by high resolution - as specified in the Type 50, 51 acquisition profiles of the ANSI/NIST Type 10 record [26], and by multiple non-frontal views as specified in the same standard. These often afford views of the ear. Organizations involved in image collection should consider supporting human adjudication by collecting high-resolution frontal and non-frontal views, preparing low resolution versions for automated face recognition [24], and retaining both for any subsequent resolution of candidate matches. Along these lines, the ISO/IEC Joint Technical

This publication is available free of charge from: https://doi.org/10.6028/NIST.IR.8271

Committee 1 subcommittee 37 on biometrics has just initiated projects on image quality assessment and face-aware capture.

This publication is available free of charge from: https://doi.org/10.6028/NIST.IR.8271

Release Notes

FRVT Activities: Since February 2017, NIST has been evaluating one-to-one verification algorithms on an ongoing basis. NIST then restarted FRVT's one-to-many track in February 2018, inviting participants to send up to prototype algorithms. Both tracks allows developers to submit updated algorithms to NIST at any time but no more frequently than four calendar months. This more closely aligns development and evaluation schedules. Results are posted to the web within a few weeks of submission. Details and full report are linked from the Ongoing FRVT site.

FRVT Reports: The results of the FRVT appear in the series NIST Interagency Reports tabulated below. The reports were developed separately and released on different schedules. In prior years NIST has mostly reported FRVT results as a single report; this had the disadvantage that results from completed sub-studies were not published until all other studies were complete.

Date	Link	Title	No.
2014-03-20	PDF	FRVT Performance of Automated Age Estimation Algorithms	7995
2015-04-20	PDF	Face Recognition Vendor Test (FRVT) Performance of Automated Gender Classification Algorithms	8052
2014-05-21	PDF	FRVT Performance of face identification algorithms	8009
2017-03-07	PDF	Face In Video Evaluation (FIVE) Face Recognition of Non-Cooperative Subjects	8173
2017-11-23	PDF	The 2017 IARPA Face Recognition Prize Challenge (FRPC)	8197
2018-11-27	PDF	Face Recognition Vendor Test - Part 2: Identification	8271
2019-09-11	PDF	Face Recognition Vendor Test - Part 2: Identification	8271
2019-12-11	PDF	Face Recognition Vendor Test - Part 3: Demographic Effects	8280
2020-01-03	WWW	Face Recognition Vendor Test (FRVT) - Part 1 Verification	Draft

Details appear on pages linked from `https://www.nist.gov/programs-projects/face-projects`.

Appendices: This report is accompanied by appendices which present exhaustive results on a per-algorithm basis. These are machine-generated and are included because the authors believe that visualization of such data is broadly informative and vital to understanding the context of the report.

Typesetting: Virtually all of the tabulated content in this report was produced automatically. This involved the use of scripting tools to generate directly type-settable LaTeX content. This improves timeliness, flexibility, maintainability, and reduces transcription errors.

Graphics: Many of the Figures in this report were produced using the ggplot2 package running under R, the capabilities of which extend beyond those evident in this document.

This publication is available free of charge from: https://doi.org/10.6028/NIST.IR.8271

Contents

Release Notes 1

Disclaimer 5

Institutional Review Board 5

Acknowledgments 5

Executive Summary 6

Scope and Context 12

Release Notes 16

1 Introduction 18

2 Evaluation datasets 19

3 Performance metrics 25

4 Results 41

Appendices 80

A Accuracy on large-population FRVT 2018 mugshots 80

B Effect of time-lapse: Accuracy after face ageing 125

C Effect of enrolling multiple images 188

D Accuracy with poor quality webcam images 195

E Accuracy for profile-view to frontal recognition 205

F Search duration 209

G Gallery Insertion Timing 219

This publication is available free of charge from: https://doi.org/10.6028/NIST.IR.8271

1 Introduction

One-to-many identification represents the largest market for face recognition technology. Algorithms are used across the world in a diverse range of biometric applications: detection of duplicates in databases, detection of fraudulent applications for credentials such as passports and driving licenses, token-less access control, surveillance, social media tagging, lookalike discovery, criminal investigation, and forensic clustering.

This report contains a breadth of performance measurements relevant to many applications. Performance here refers to accuracy and resource consumption. In most applications, the core accuracy of a facial recognition algorithm is the most important performance variable. Resource consumption will be important also as it drives the amount of hardware, power, and cooling necessary to accommodate high volume workflows. Algorithms consume processing time, they require computer memory, and their static template data requires storage space. This report documents these variables.

1.1 Open-set searches

FRVT tested open-set identification algorithms. Real-world applications are almost always "open-set", meaning that some searches have an enrolled mate, but some do not. For example, some subjects have truly not been issued a visa or drivers license before; some law enforcement searches are from first-time arrestees[6]. In an "open-set" application, algorithms make no prior assumption about whether or not to return a high-scoring result, and for a mated search, the ideal behaviour is that the search produces the correct mate at high score and first rank. For a non-mate search, the ideal behavior is that the search produces zero high-scoring candidates.

Many academic benchmarks execute only closed-set searches. The proportion of mates found in the rank one position is the default accuracy metric. This hit rate metric ignores the score with which a mate is found; weak hits count as much as strong hits. This ignores the real-world imperative that in many applications it is necessary to elevate a threshold to reduce the number of false positives.

[6]Operationally closed-set applications are rare because it is usually not the case that all searches have an enrolled mate. One counter-example, however, is a cruise ship in which all passengers are enrolled and all searches should produce exactly one identity. Another example is forensic identification of dental records from an aircraft crash.

This publication is available free of charge from: https://doi.org/10.6028/NIST.IR.8271

2 Evaluation datasets

This report documents accuracy for four kinds of images - mugshots, webcam, profiles and wild - as described in the following sections.

2.1 Immigration-related images

This report includes benchmark tests sharing a common enrollment of high quality frontal portrait images collected while subject make applications for various immigration benefits. We then search that with two kinds of images, webcam images collected during in-bound immigration and also images collected from registered travelers using a ATM-style kiosk. These are described below and depicted in Figure 4.

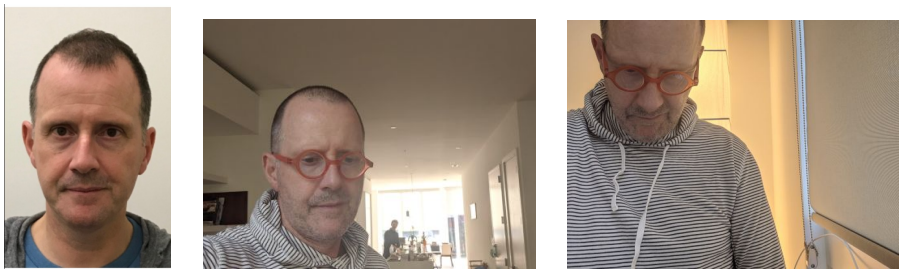

a) Application b) Immigration Lane c) Kiosk

Figure 4: Example photos.

- **Application reference photos**: The images are collected in an attended interview setting using dedicated capture equipment and lighting. The images, at size 300x300 pixels, are smaller than normally indicated by ISO. The images are all high-quality frontal portraits collected in immigration offices and with a white background. As such, potential quality related drivers of high false match rates (such as blur) can be expected to be absent. The images are encoded as ISO/IEC 10918-1 i.e. JPEG. Older images had a compression ration of about 16:1, while newer images, since 2010, are more lightly compressed at 4:1. When these images are provided as input into the algorithm, they are labeled with the type "iso". This report enrols 1 600 000 application images, one per person.

- **Border crossing photos**: Most images are have width 320 and height 240 pixels. They are JPEG compressed at 16:1 i.e. filesize just below 15KB. The images present challenges for face recognition in that subjects often exhibit non-zero yaw and pitch (associated with the rotational degrees of freedom of the camera mount), low contrast (due to varying and intense background lights), and poor spatial resolution (due to inexpensive cameras). There are often subjects standing in the background, usually at very low resolution (see Figure 4b). In such cases, algorithms should detect all faces and determine which is the largest and most centered. When these images are provided as input into the algorithm, they are labeled with the type "wild".

- **Kiosk photos**: These photos were collected from subjects whose attention was focused on interaction with an immigration kiosk. They images were not intended for use with automated face recognition. The camera is situated above a display which the user touches, and is triggered either without directing the subject to look at it, or without waiting for the subject to comply. The images are therefore characterized by pitch-down pose, sometimes exceeding 45 degrees, as in Figure 4c. Yaw-angle variation is mild, with most images close to frontal. The images

This publication is available free of charge from: https://doi.org/10.6028/NIST.IR.8271

have width 320 pixels and height 240 pixels and therefore tall individuals are sometimes cropped. This is often just above the eyes and can occur at the nose or mouth. Conversely, short individuals are sometimes cropped such that only the top part of the face is visible. In a quite small number of cases, there other subjects standing just behind the primary subject such that algoriths should detect all faces and determine which is the largest and most centered. Background ceiling lighting is often visible and this sometimes leads to under-exposure of the face When these images are provided as input into the algorithm, they are labeled with the type "wild".

2.2 Law enforcement images

The main mugshot dataset used is referred to as the FRVT 2018 set. This set was collected over the period 2002 to 2017 in routine United States law enforcement operations. This set yields three subsets

- **Mugshots**: Mugshots comprise about 86% of the database. They have reasonable compliance with the ANSI/NIST ITL1-2011 Type 10 standard's subject acquisition profiles levels 10-20 for frontal images [26]. The most common departure from the standard's requirements is the presence of mild pose variations around frontal - the images of Figure 5 are typical. The images vary in size, with many being 480x600 pixels with JPEG compression applied to produce filesizes of between 18 and 36KB with many images outside this range, implying that about 0.5 bits are being encoded per pixel. When these images are provided as input into the algorithm, they are labeled with the type "mugshot". Example images appear in Fig. 5

  NIST Interagency Report 8238 includes a comparison of this set of mugshots with the smaller and easier sets of mugshots used in tests run in 2010 and 2014.

- **Profile images**: Profile-view images have been collected in law enforcement for more than 100 years, as human capability is improved with orthogonal information. The profile images used in this report were collected during the same session as the frontal mugshot photograph, in the same standardized photographic setup. These would not therefore be used with automated face recognition. A small subset, 200 000 images, were set aside for testing. When these images are provided as input into the algorithm, they are labeled with the type "wild". Example images appear in Fig. 7

- **Webcam images**: The remaining 14% of the images were collected using an inexpensive webcam attached to a flexible operator-directed mount. These images are all of size 240x240 pixels, that are in considerable violation of most quality-related clauses of all face recognition standards. As evident in the figure, the most common defects are non-frontal pose (associated with the rotational degrees of freedom of the camera mount), low contrast (due to varying and intense background lights), and poor spatial resolution (due to inexpensive camera optics) - see examples in Fig 6. The images are overly JPEG compressed, to between 4 and 7KB, implying that only 0.5 to 1 bits are being encoded per color pixel. When these images are provided as input into the algorithm, they are labeled with the type "wild". Example images appear in Fig. 6

These are drawn from NIST Special Database 32 which may be downloaded here.

These images were partitioned in galleries and probesets for the various experiment listed in Table 1.

This publication is available free of charge from: https://doi.org/10.6028/NIST.IR.8271

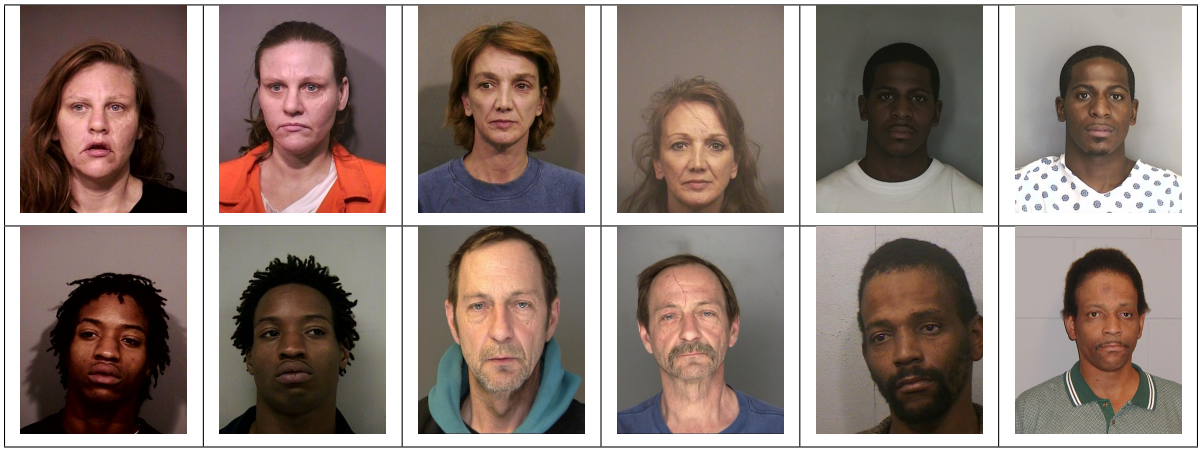

Figure 5: Six mated mugshot pairs representative of the FRVT-2014 (LEO) and FRVT-2018 datasets. The images are collected live, i.e. not scanned from paper. Image source: NIST Special Database 32 the Multiple Encounter Deceased Subjects dataset.

Figure 6: Twelve webcam images representative of probes against the FRVT-2018 mugshot gallery. The first eight images are four mated pairs. Such images present challenges to recognition including pose, non-uniform illumination, low contrast, compression, cropping, and low spatial sampling rate. Image source: NIST Special Database 32 the Multiple Encounter Deceased Subjects dataset.

Figure 7: **[Profile views]** *The three images are a frontal enrollment, subsequent frontal probe, and same-session ninety degree profile view. While collection of both frontal and profile views has been typical in law enforcement for more than a century, the recognition of profile to frontal views has essentially been impossible. However, reasonbly high accuracy results is now possible - see section E.*

This publication is available free of charge from: https://doi.org/10.6028/NIST.IR.8271

Image		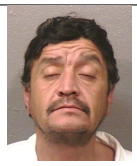		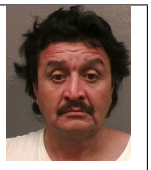
Encounter	1	...	$K_i - 1$	K_i
Capture Time	T_1	...	T_{K_i-1}	T_{K_i}
Role RECENT	Not used	Not used	Enrolled	Search
Role LIFETIME	Enrolled	Enrolled	Enrolled	Search

Figure 8: Depiction of the "recent" and "lifetime" enrollment types. Image source: NIST Special Database 32

2.3 Enrollment strategies

Many operational applications include collection and enrollment of biometric data from subjects on more than one occasion. This might be done on a regular basis, as might occur in credential (re-)issuance, or irregularly, as might happen in a criminal recidivist situation [4]. The number of images per person will depend on the application area. In civil identity credentialing (e.g. passports, driver's licenses), the images will be acquired approximately uniformly over time (e.g. ten years for a passport). While the distribution of dates for such images of a person might be assumed uniform, a number of factors might undermine this assumption[7]. In criminal applications, the number of images would depend on the number of arrests. The distribution of dates for arrest records for a person (i.e. the recidivism distribution) has been modeled using the exponential distribution but is recognized to be more complicated[8].

In any case, the 2010 NIST evaluation of face recognition showed that considerable accuracy benefits accrue with retention and use of *all* historical images [6].

To this end, the FRVT API document provides $K \geq 1$ images of an individual to the enrollment software. The software is tasked with producing a single proprietary undocumented "black-box" template[9] from the K images. This affords the algorithm an ability to generate a *model* of the individual, rather than to simply extract features from each image on a sequential basis.

As depicted in Figure 8, the i-th individual in the FRVT 2018 dataset has K_i images. These are labelled as x_k for $k = 1 \ldots K_i$ in chronological order of capture date. To measure the utility of having multiple enrollment images, this report evaluates three kinds of enrollment:

- ▷ **Recent**: Only the second most recent image, x_{K_i-1} is enrolled. This strategy of enrollment mimics the operational policy of retaining the imagery from the most recent encounter. This might be done operationally to ameliorate the effects of face ageing. Obviously retaining only the most recent image should only be done if the identity of the person is trusted to be correct. For example, in an access control situation retention of the most recent successful *authentication* image would be hazardous if it could be a false positive.

- ▷ **Lifetime-consolidated**: All but the most recent image are enrolled, $x_1 \ldots x_{K_i-1}$. This subject-centric strategy might be adopted if quality variations exist where an older image might be more suitable for matching, despite the ageing effect.

[7] For example, a person might skip applying for a passport for one cycle, letting it expire. In addition, a person might submit identical images (from the same photography session) to consecutive passport applications at five year intervals.
[8] A number of distributions have been considered to model recidivism, see for example [3].
[9] There are no formal face template standards. Template standards only exist for fingerprint minutiae - see ISO/IEC 19794-2:2011.

This publication is available free of charge from: https://doi.org/10.6028/NIST.IR.8271

This publication is available free of charge from: https://doi.org/10.6028/NIST.IR.8271

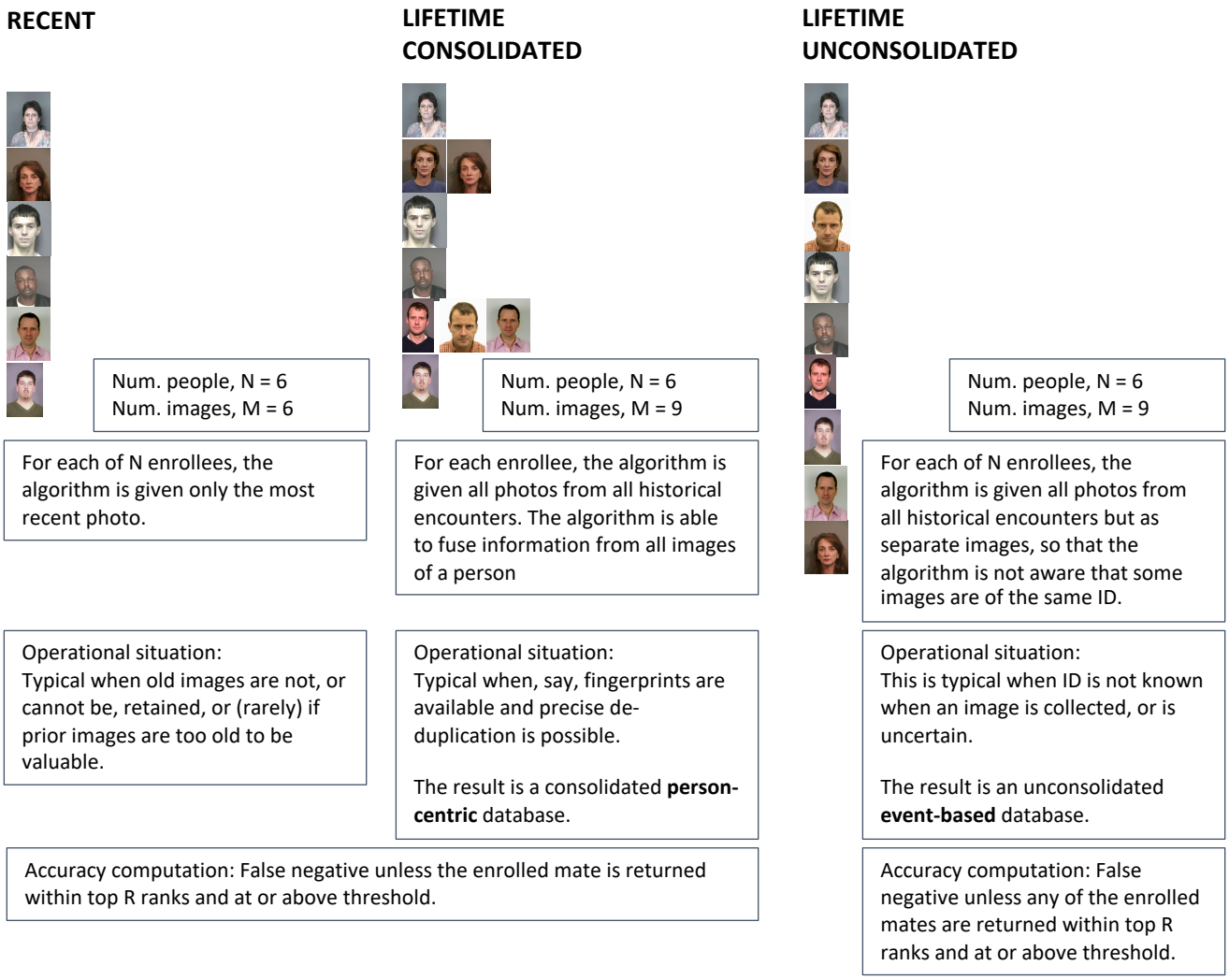

Figure 9: **Enrollment strategies**. *The figure shows the three kinds of enrollment databases examined in this report. Image source: NIST Special Database 32*

	ENROLLMENT				SEARCH			
	TYPE SEE	POPULATION			MATE		NON-MATE	
	SECTION 2.3	FILTER	N-SUBJECTS	N-IMAGES	N-SUBJECTS	N-IMAGES	N-SUBJECTS	N-IMAGES
Mugshot trials from enrollment of single images								
1	RECENT	NATURAL	640 000	640 000	154 549	154 549	331 254	331 254
2	RECENT	NATURAL	1 600 000	1 600 000				
3	RECENT	NATURAL	3 000 000	3 000 000				
4	RECENT	NATURAL	6 000 000	6 000 000				
5	RECENT	NATURAL	12 000 000	12 000 000				
Cross-domain								
13	MUGSHOTS AS ON ROW 2				82 106 WEBCAM	82 106 WEBCAM	331 254 WEBCAM	331 254 WEBCAM
Cross-view								
14	MUGSHOTS AS ON ROW 2				100 000 PROFILE	100 000 PROFILE	100 000 PROFILE	100 000 PROFILE
Mugshot ageing								
17	OLDEST	NATURAL	3 068 801	3 068 801	2 853 221	10 951 064	0	0
Border crossing ageing								
17	OLDEST	NATURAL	1 600 000	1 600 000	903 655	1 922 393	1 393 076	1 680 000
Visa-border								
19	PRIOR	NATURAL	1 600 000 VISA	1 600 000 VISA	80 000 BORDER	80 000 BORDER	80 000 BORDER	80 000 BORDER
20	VISA AS ON ROW 18				21 016 BORDER	21 016 BORDER	21 016 BORDER	21 016 BORDER

Table 1: **Enrollment and search sets**. *Each row summarizes one identification trial. Unless stated otherwise, all entries refer to mugshot images. The term "natural" means that subjects were selected without heed to demographics, i.e. in the distribution native to this dataset. The probe images were collected in a different calendar year to the enrollment image. Missing values in rows 2-12 are the same as in row 1.*

▷ **Lifetime-unconsolidated**: Again all but the most recent image are enrolled $x_1 \ldots x_{K_i-1}$ but now separately, with different identifiers, such that the algorithm is not aware that the images are from the same face. This kind of event- or encounter-centric enrollment is very common when operational constraints preclude reliable consolidation of the historical encounters into a single identity. This aspect also prevents the recognition algorithm from a) building a holistic model of identity (as is common in speaker recognition systems) and b) implementing fusion, for example template-level fusion of feature vectors, or post-search score-level fusion. The result is that searches will typically yield more than one image of a person in the top ranks. This has consequences for appropriate metrics, as detailed in section 3.2.1

NIST first evaluated this kind of enrollment in mid 2018, and the results tables include some comparison of accuracy available from all three enrollment styles.

In all cases, the most recent image, x_{K_i}, is reserved as the search image. For the 1.6 million subject enrollment partition of the FRVT 2018 data, $1 \leq K_i \leq 33$ with $K_i = 1$ in 80.1% of the individuals, $K_i = 2$ in 13.4%, $K_i = 3$ in 3.7%, $K_i = 4$ in 1.4%, $K_i = 5$ in 0.6%, $K_i = 6$ in 0.3%, and $K_i > 6$ is 0.2% for everyone else. This distribution is substantially dependent on United States recidivism rates.

We did not evaluate the case of retaining only the highest quality image, since automated quality assessment is out of scope for this report. We do not anticipate that such strategies will prove beneficial when the quality assessment apparatus is imperfect and unvalidated.

This publication is available free of charge from: https://doi.org/10.6028/NIST.IR.8271

3 Performance metrics

This section gives specific definitions for accuracy and timing metrics. Tests of open-set biometric algorithms must quantify frequency of two error conditions:

- ▷ **False positives**: Type I errors occur when search data from a person who has never been seen before is incorrectly associated with one or more enrollees' data.
- ▷ **Misses**: Type II errors arise when a search of an enrolled person's biometric does not return the correct identity.

Many practitioners prefer to talk about "hit rates" instead of "miss rates" - the first is simply one minus the other as detailed below. Sections 3.1 and 3.2 define metrics for the Type I and Type II performance variables.

Additionally, because recognition algorithms sometimes fail to produce a template from an image, or fail to execute a one-to-many search, the occurrence of such events must be recorded. Further because algorithms might elect to not produce a template from, for example, a poor quality image, these failure rates must be combined with the recognition error rates to support algorithm comparison. This is addressed in section 3.5.

Finally, section 3.7 discusses measurement of computation duration, and section 3.8 addresses the uncertainty associated with various measurements. Template size measurement is included with the results.

3.1 Quantifying false positives

It is typical for a search to be conducted into an enrolled population of N identities, and for the algorithm to be configured to return the closest L candidate identities. These candidates are ranked by their score, in descending order, with all scores required to be greater than or equal to zero. A human analyst might examine either all L candidates, or just the top $R \leq L$ identities, or only those with score greater than threshold, T. The workload associated with such examination is discussed later, in 3.6.

False alarm performance is quantified in two related ways. These express how many searches produces false positives, and then, how many false positives are produced in a search.

False positive identification rate: The first quantity, FPIR, is the proportion of non-mate searches that produce an adverse outcome:

$$\text{FPIR}(N,T) = \frac{\text{Num. non-mate searches where one or more enrolled candidates are returned with score at or above threshold}}{\text{Num. non-mate searches attempted.}} \tag{1}$$

Under this definition, FPIR can be computed from the highest non-mate candidate produced in a search - it is not necessary to consider candidates at rank 2 and above. FPIR is the primary measure of Type I errors in this report.

Selectivity: However, note that in any given search, several non-mate may be returned above threshold. In order to quantify such events, a second quantity, selectivity (SEL), is defined as the *number* of non-mates returned on a candidate list, averaged over all searches.

$$\text{SEL}(N,T) = \frac{\text{Num. non-mate enrolled candidates returned with score at or above threshold}}{\text{Num. non-mate searches attempted.}} \tag{2}$$

where $0 \leq$ SEL(N, T) $\leq$L. Both of these metrics are useful operationally. FPIR is useful for targeting how often an

This publication is available free of charge from: https://doi.org/10.6028/NIST.IR.8271

adverse false positive outcome can occur, while SEL as a number is related to workload associated with adjudicating candidate lists. The relationship between the two quantities is complicated - it depends on whether an algorithm concentrates the false alarms in the results of a few searches or whether it disburses them across many. This was detailed in FRVT 2014, NISTIR 8009. It has not yet been detailed in FRVT 2018.

3.2 Quantifying hits and misses

If L candidates are returned in a search, a shorter candidate list can be prepared by taking the top $R \leq L$ candidates for which the score is above some threshold, $T \geq 0$. This reduction of the candidate list is done because thresholds may be applied, and only short lists might be reviewed (according to policy or labor availability, for example). It is useful then to state accuracy in terms of R and T, so we define a "miss rate" with the general name **false negative identification rate** (FNIR), as follows:

$$\text{FNIR}(N, R, T) = \frac{\text{Num. mate searches with enrolled mate found outside top R ranks or score below threshold}}{\text{Num. mate searches attempted.}} \quad (3)$$

This formulation is simple for evaluation in that it does not distinguish between causes of misses. Thus a mate that is not reported on a candidate list is treated the same as a miss arising from face finding failure, algorithm intolerance of poor quality, or software crashes. Thus if the algorithm fails to produce a candidate list, either because the search failed, or because a search template was not made, the result is regarded as a miss, adding to FNIR.

Hit rates, and true positive identification rates: While FNIR states the "miss rate" as how often the correct candidate is either not above threshold or not at good rank, many communities prefer to talk of "hit rates". This is simply the **true positive identification rate**(TPIR) which is the complement of FNIR giving a positive statement of how often mated searches are successful:

$$\text{TPIR}(N, R, T) = 1 - \text{FNIR}(N, R, T) \quad (4)$$

This report does not report true positive "hit" rates, preferring false negative miss rates for two reasons. First, costs rise linearly with error rates. For example, if we double FNIR in an access control system, then we double user inconvenience and delay. If we express that as decrease of TPIR from, say 98.5% to 97%, then we mentally have to invert the scale to see a doubling in costs. More subtly, readers don't perceive differences in numbers near 100% well, becoming inured to the "high nineties" effect where numbers close to 100 are perceived indifferently.

Reliability is a corresponding term, typically being identical to TPIR, and often cited in automated (fingerprint) identification system (AFIS) evaluations.

An important special case is the **cumulative match characteristic**(CMC) which summarizes accuracy of mated-searches only. It ignores similarity scores by relaxing the threshold requirement, and just reports the fraction of mated searches returning the mate at rank R or better.

$$\text{CMC}(N, R) = 1 - \text{FNIR}(N, R, 0) \quad (5)$$

We primarily cite the complement of this quantity, $\text{FNIR}(N, R, 0)$, the fraction of mates *not* in the top R ranks.

The **rank one hit rate** is the fraction of mated searches yielding the correct candidate at best rank, i.e. CMC(N, 1). While this quantity is the most common summary indicator of an algorithm's efficacy, it is not dependent on similarity scores, so it does not distinguish between strong (high scoring) and weak hits. It also ignores that an adjudicating reviewer is often willing to look at many candidates.

This publication is available free of charge from: https://doi.org/10.6028/NIST.IR.8271

This publication is available free of charge from: https://doi.org/10.6028/NIST.IR.8271

3.2.1 False negative rates for unconsolidated galleries

As detailed in section 2.3 a common type of gallery, here referred to as the lifetime unconsolidate type, is populated with all images of an individual without any association between them. That is, the gallery construction algorithm is not provided with any ID labels that would support processing of a person's images jointly. This constrasts with the lifetime consolidate type where an algorithm may explicitly fuse features from multiple images of a person, or select a best image. In such cases, where the number of enrolled images is a random variable, we define two false negative rates as follows.

The first demands that the algorithm place any of the K_i mates in the top $R \geq 1$ ranks. The proportion of searches for which this does not occur forms a false negative identification rate:

$$\text{FNIR}_{\text{any}}(N, R, T) = 1 - \frac{\text{Num. mate searches where any enrolled mate is found in the top R ranks and at-or-above threshold}}{\text{Num. mate searches attempted.}} \tag{6}$$

The second demands that the algorithm place all K_i mates in the top $R \geq K_i$ ranks. The proportion of searches for which this does not occur forms a false negative identification rate:

$$\text{FNIR}_{\text{all}}(N, R, T) = 1 - \frac{\text{Num. mate searches where all enrolled mates are found in the top R ranks and at-or-above threshold}}{\text{Num. mate searches attempted.}} \tag{7}$$

Placing all mates in the top ranks is a more difficult task than correctly retrieving any image, so it holds that: $\text{FNIR}_{\text{all}} \geq \text{FNIR}_{\text{any}}$. This is evident in the results presented for November 2018 algorithms in Tables starting at **??**.

The information retrieval community might prefer to compute and plot *precision* and *recall*; this is a valid approach, but we advance the two metrics above because they relate to our normal definition of consolidated FNIR, and they cover the two extreme use-cases of wanting any hit vs. all hits.

3.3 DET interpretation

In biometrics, a false negative occurs when an algorithm fails to match two samples of one person – a Type II error. Correspondingly, a false positive occurs when samples from two persons are improperly associated – a Type I error.

Matches are declared by a biometric system when the native comparison score from the recognition algorithm meets some threshold. Comparison scores can be either similarity scores, in which case higher values indicate that the samples are more likely to come from the same person, or dissimilarity scores, in which case higher values indicate different people. Similarity scores are traditionally computed by fingerprint and face recognition algorithms, while dissimilarities are used in iris recognition. In some cases, the dissimilarity score is a distance possessing metric properties. In any case, scores can be either mate scores, coming from a comparison of one person's samples, or nonmate scores, coming from comparison of different persons' samples.

The words "genuine" or "authentic" are synonyms for mate, and the word "impostor" is used as a synonym for nonmate. The words "mate" and "nonmate" are traditionally used in identification applications (such as law enforcement search, or background checks) while genuine and impostor are used in verification applications (such as access control).

An error tradeoff characteristic represents the tradeoff between Type II and Type I classification errors. For identification this plots false negative vs. false positive identification rates i.e. FNIR vs. FPIR parametrically with T. Such plots

are often called detection error tradeoff (DET) characteristics or receiver operating characteristic (ROC). These serve the same function − to show error tradeoff − but differ, for example, in plotting the complement of an error rate (e.g. TPIR = 1 − FNIR) and in transforming the axes, most commonly using logarithms, to show multiple decades of FPIR. More rarely, the function might be the inverse of the Gaussian cumulative distribution function.

The slides of Figures 10 through 15 discuss presentation and interpretation of DETs used in this document for reporting face identification accuracy. Further detail is provided in formal biometrics testing standards, see the various parts of ISO/IEC 19795 Biometrics Testing and Reporting. More terms, including and beyond those to do with accuracy, appear in ISO/IEC 2382-37 Information technology – Vocabulary – Part 37: Harmonized biometric vocabulary.

This publication is available free of charge from: https://doi.org/10.6028/NIST.IR.8271

This publication is available free of charge from: https://doi.org/10.6028/NIST.IR.8271

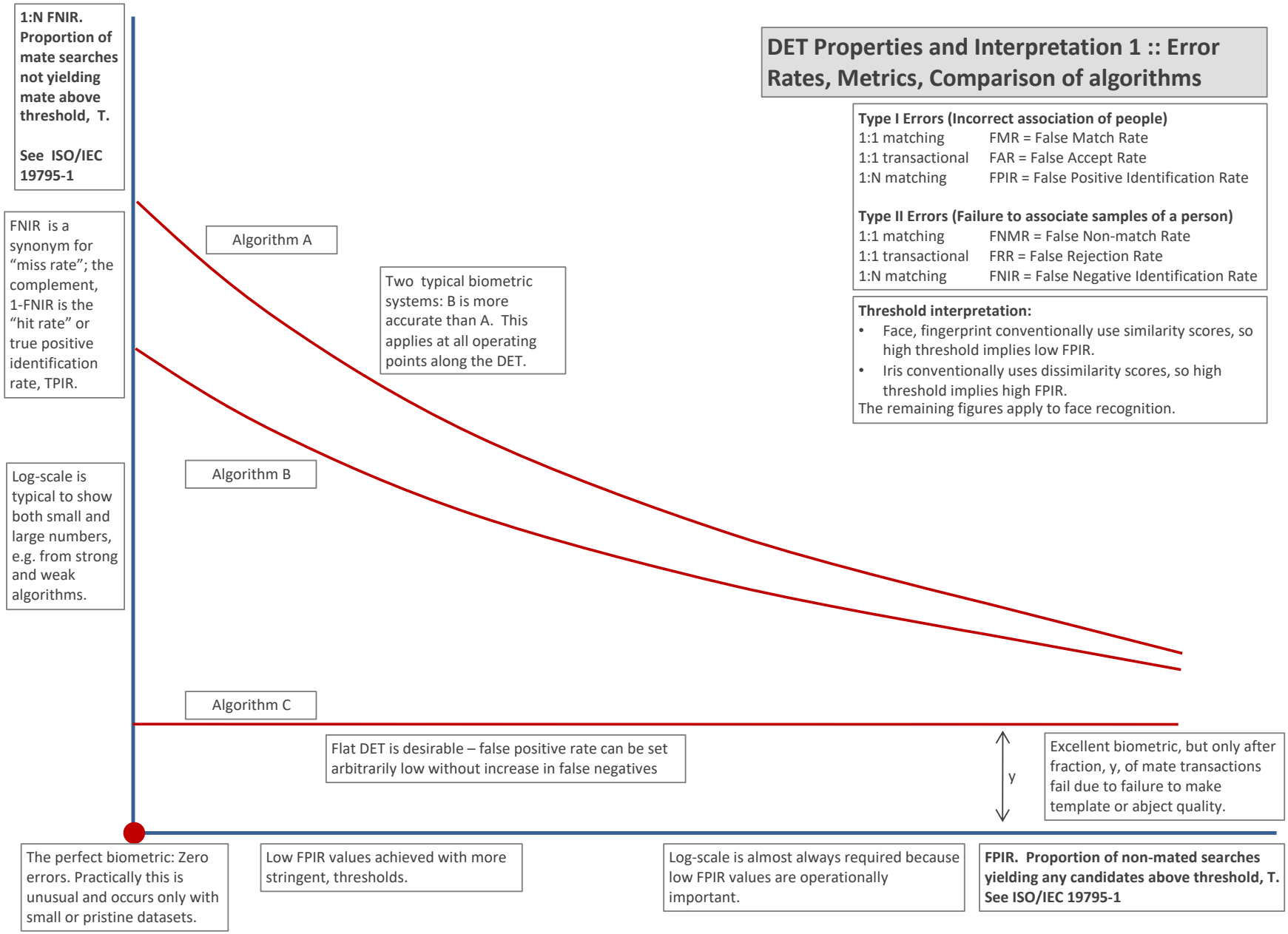

Figure 10: **DET as the primary performance reporting mechanism**.

This publication is available free of charge from: https://doi.org/10.6028/NIST.IR.8271

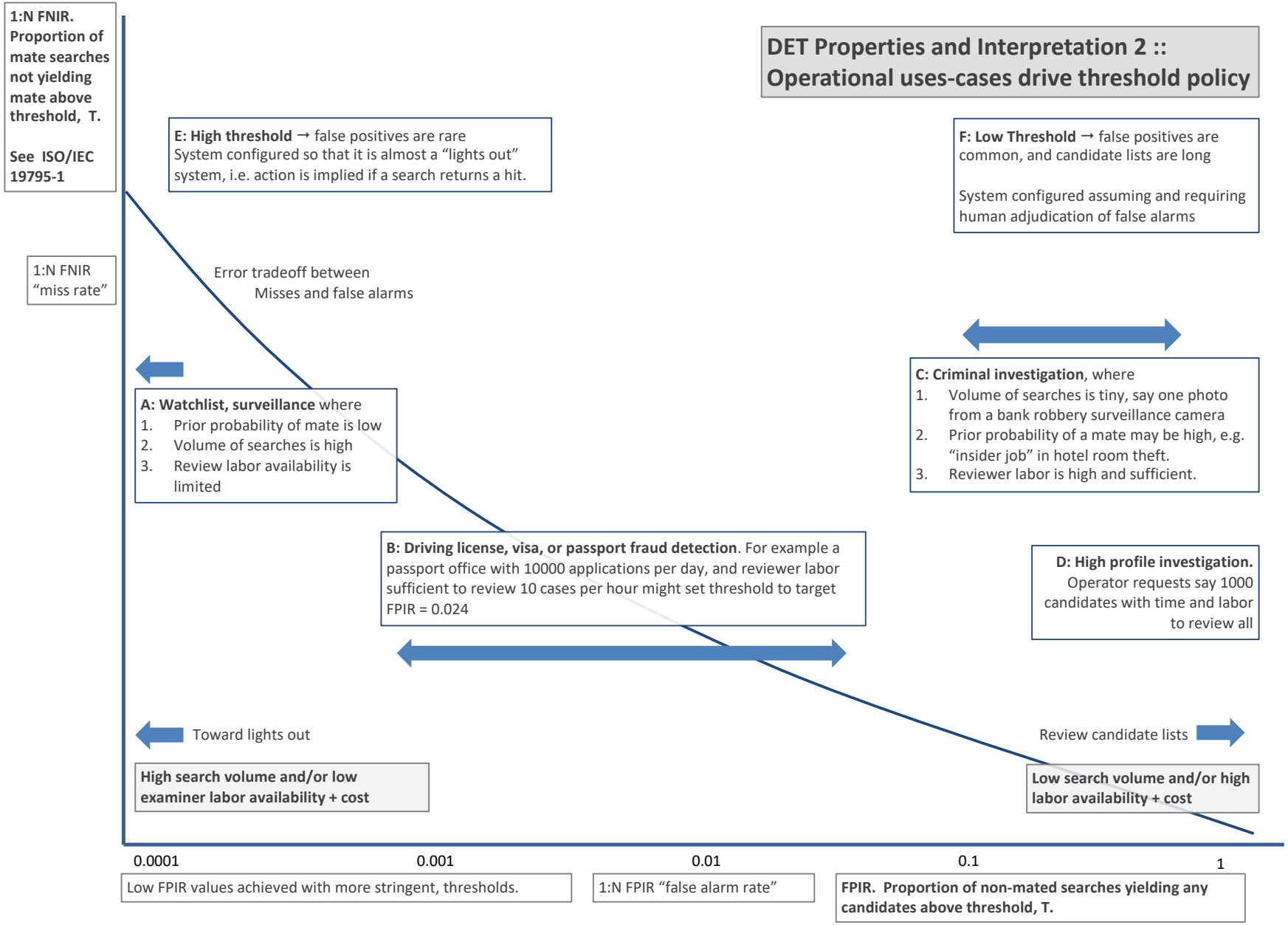

Figure 11: **DET as the primary performance reporting mechanism**.

This publication is available free of charge from: https://doi.org/10.6028/NIST.IR.8271

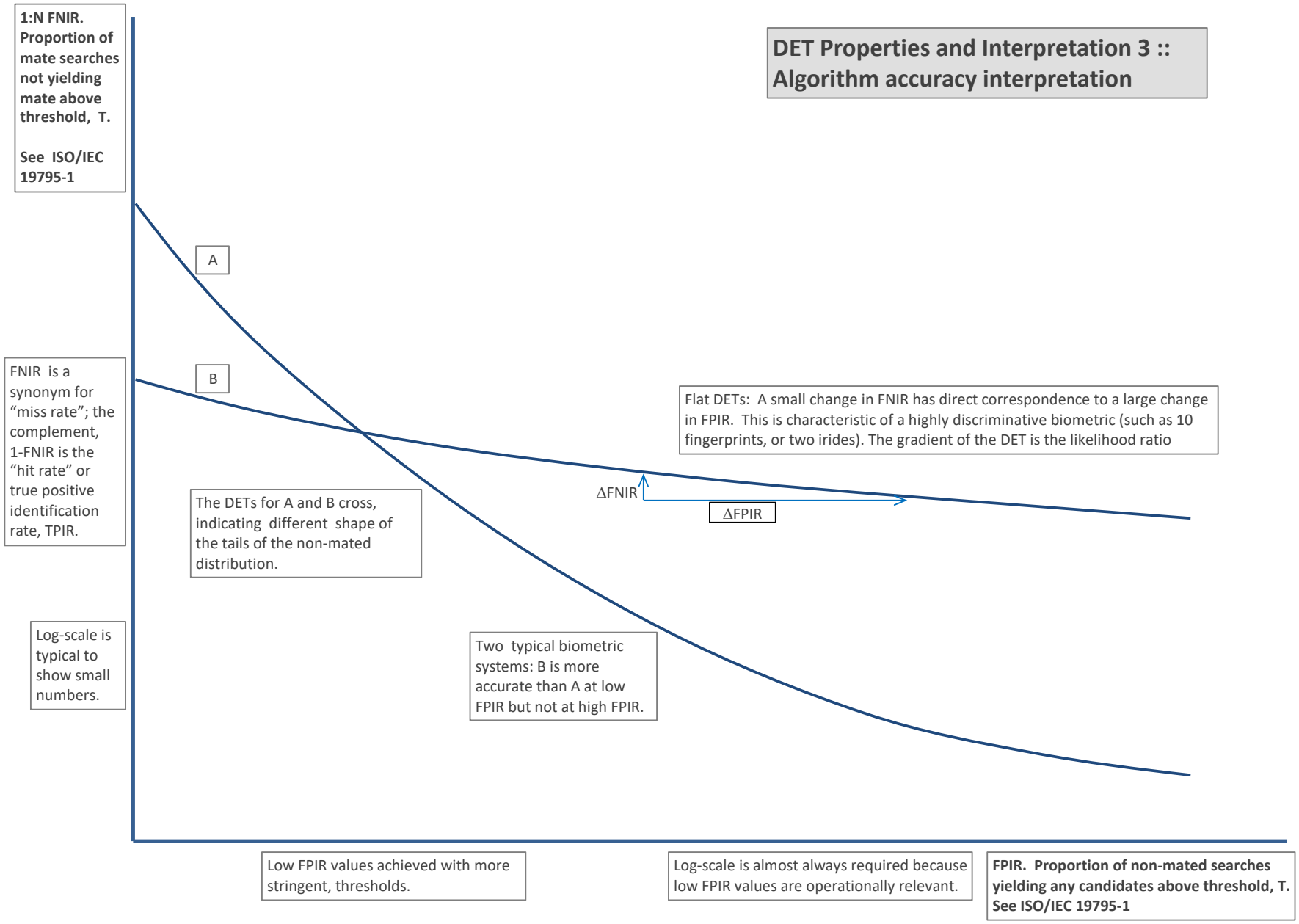

Figure 12: **DET as the primary performance reporting mechanism**.

This publication is available free of charge from: https://doi.org/10.6028/NIST.IR.8271

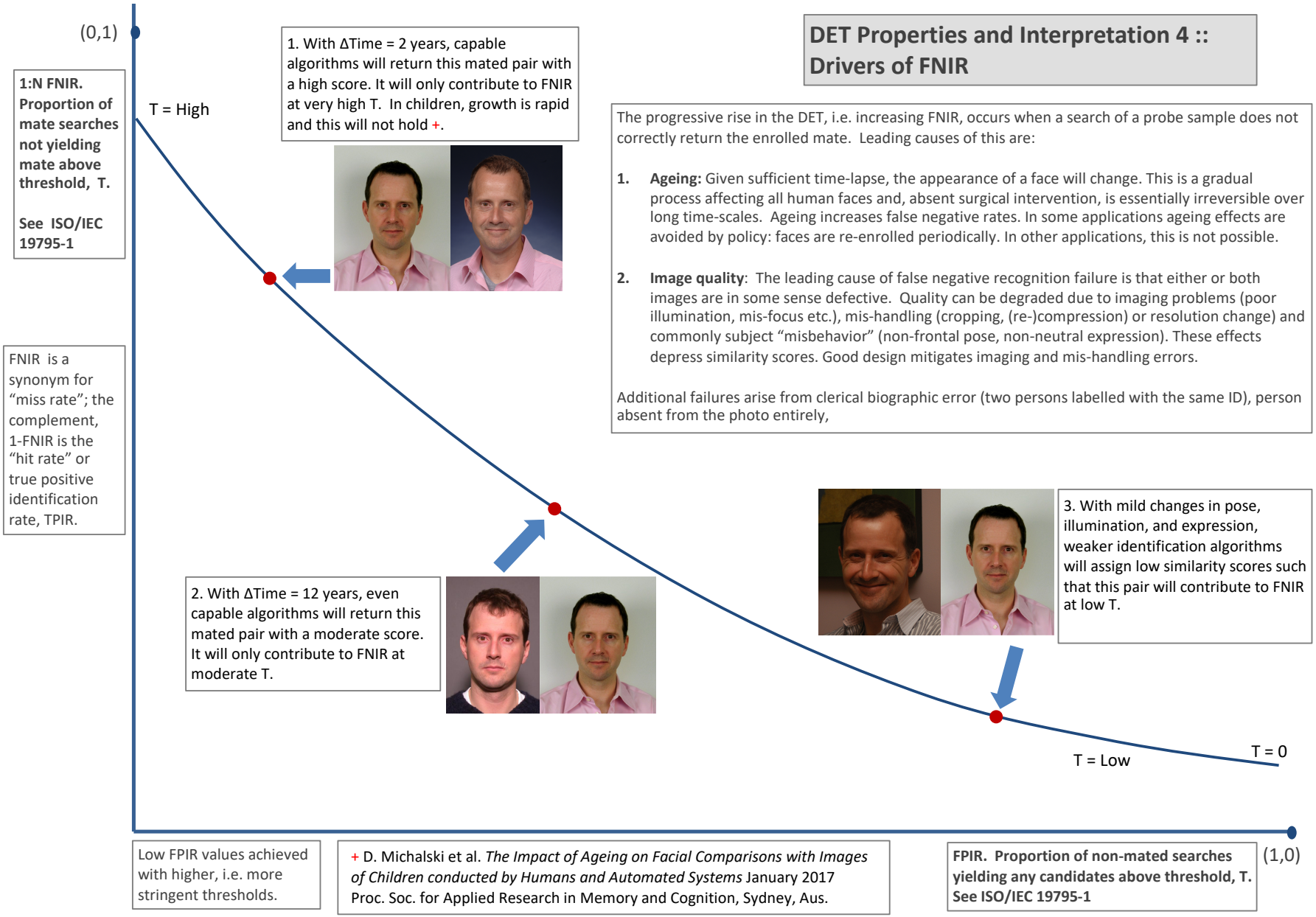

Figure 13: **DET as the primary performance reporting mechanism**.

This publication is available free of charge from: https://doi.org/10.6028/NIST.IR.8271

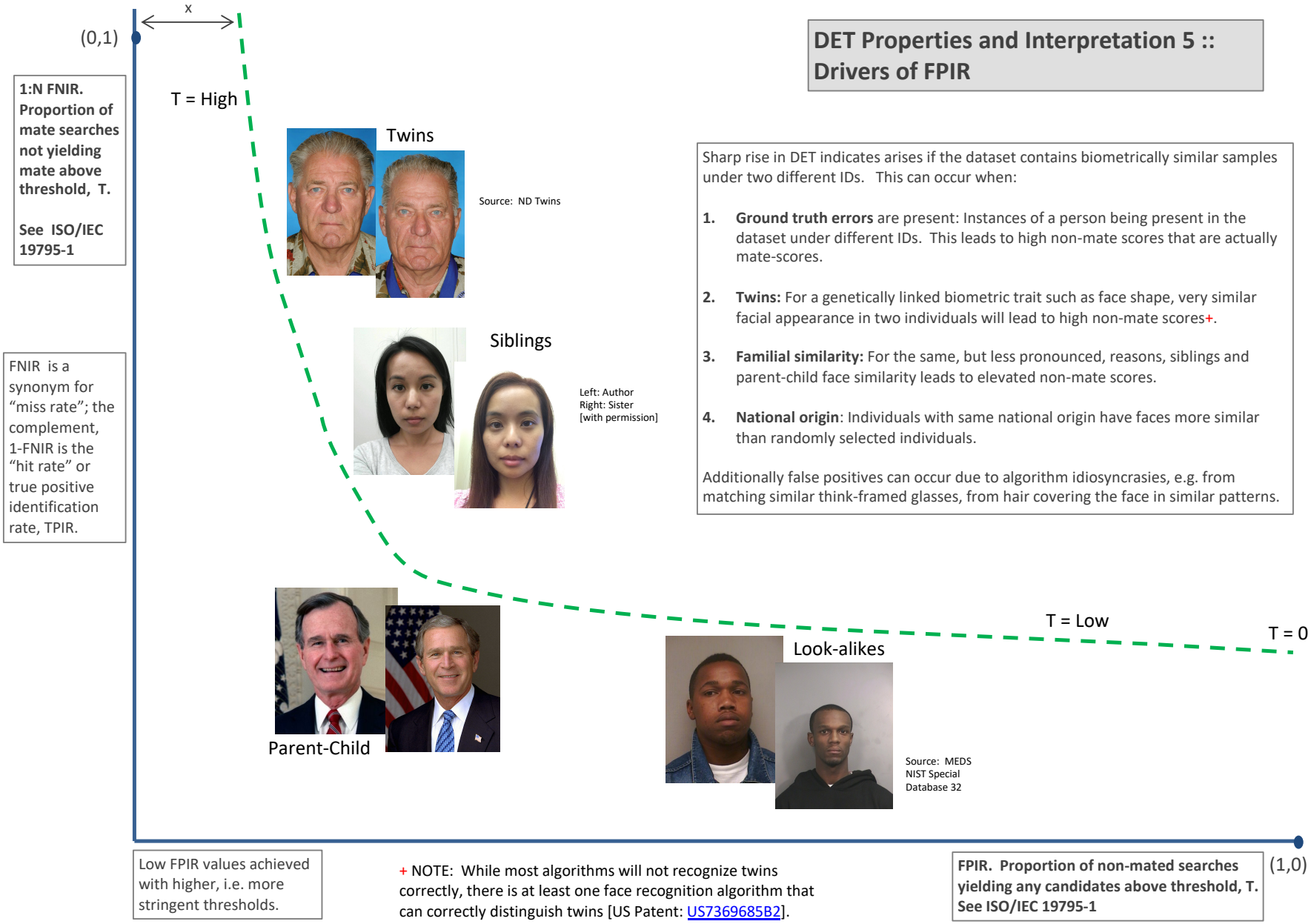

Figure 14: **DET as the primary performance reporting mechanism**.

This publication is available free of charge from: https://doi.org/10.6028/NIST.IR.8271

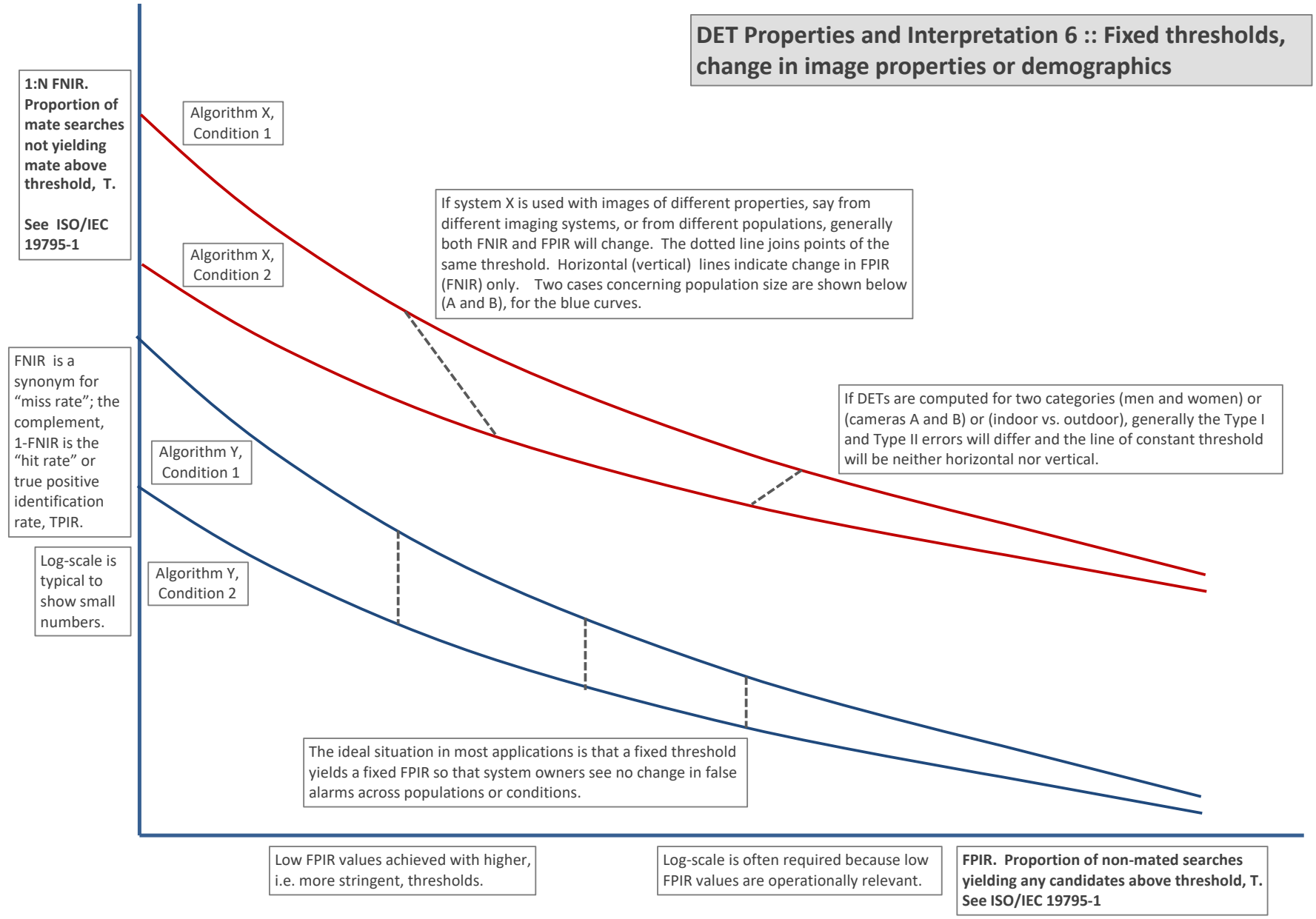

Figure 15: **DET as the primary performance reporting mechanism**.

This publication is available free of charge from: https://doi.org/10.6028/NIST.IR.8271

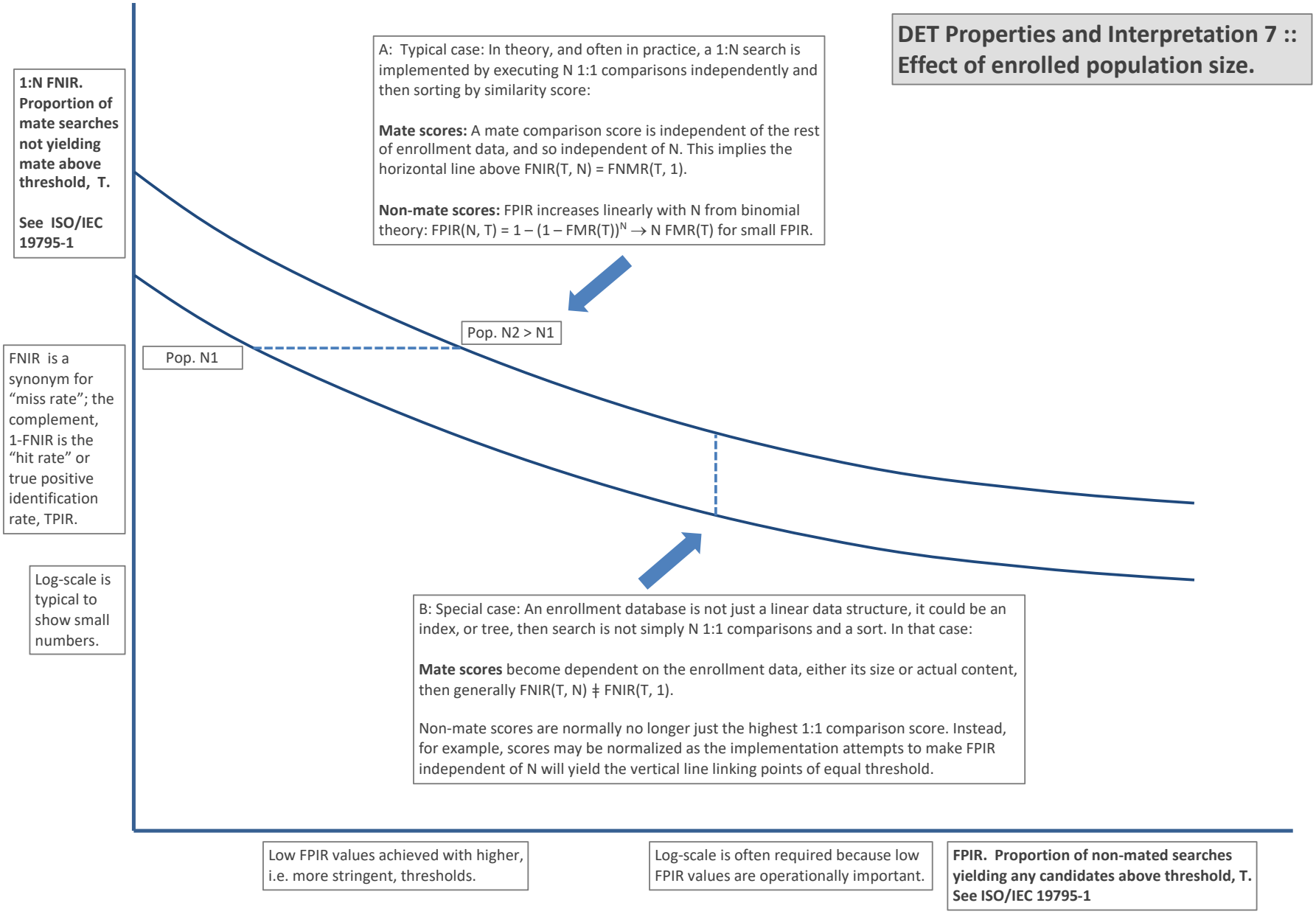

Figure 16: **DET as the primary performance reporting mechanism**.

This publication is available free of charge from: https://doi.org/10.6028/NIST.IR.8271

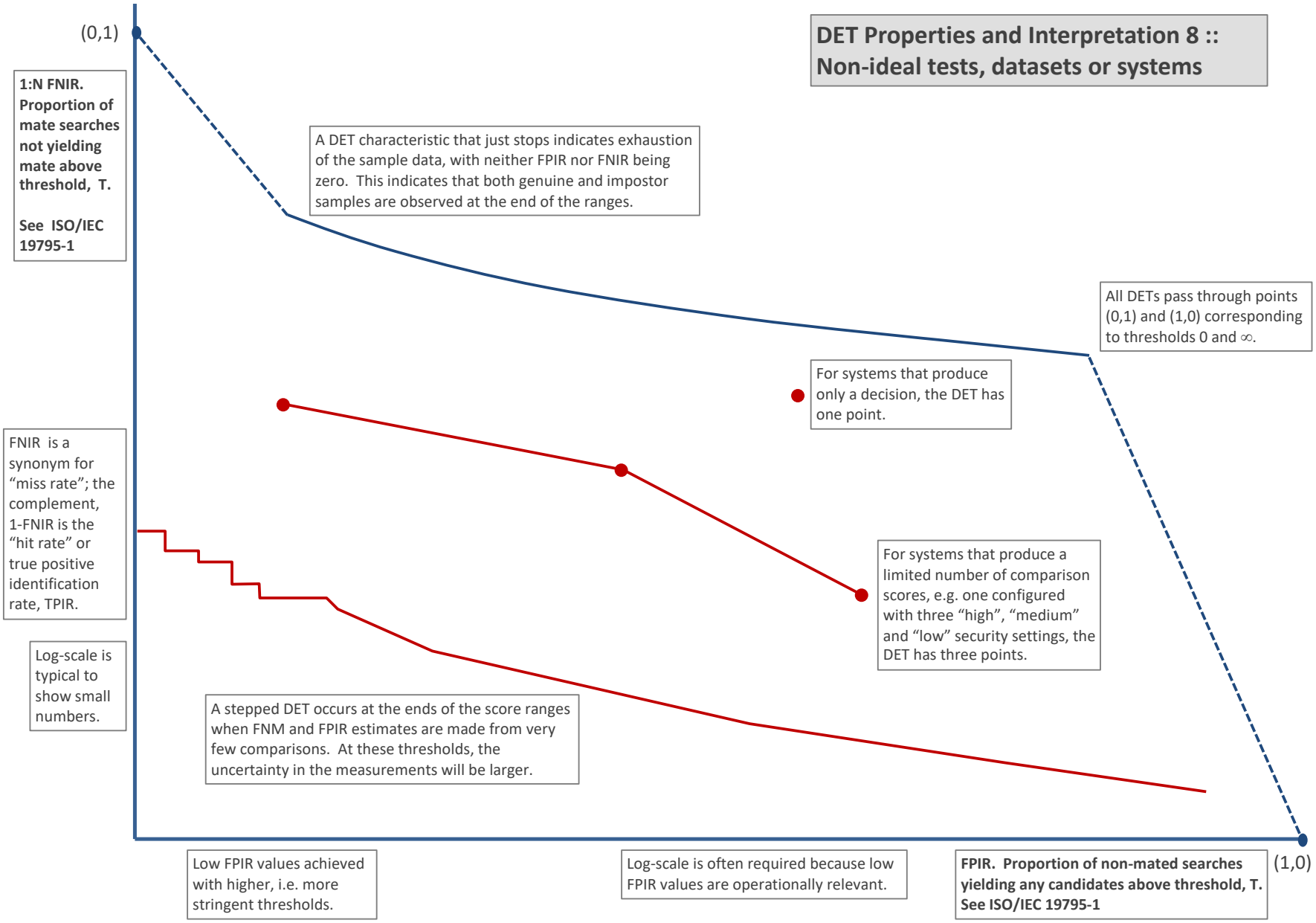

Figure 17: **DET as the primary performance reporting mechanism**.

3.4 Best practice testing requires execution of searches with and without mates

FRVT embeds 1:N searches of two kinds: Those for which there is an enrolled mate, and those for which there is not. The respective numbers for these types of searches appear in Table 1. However, it is common to conduct only mated searches[10]. The cumulative match characteristic is computed from candidate lists produced in mated searches. Even if the CMC is the only metric of interest, the actual trials executed in a test should nevertheless include searches for which no mate exists. As detailed in Table 1 the FRVT reserved disjoint populations of subjects for executing true non-mate searches.

3.5 Failure to extract features

During enrollment some algorithms fail to convert a face image to a template. The proportion of failures is the failure-to-enroll rate, denoted by FTE. Similarly, some search images are not converted to templates. The corresponding proportion is termed failure-to-extract, denoted by FTX.

We do not report FTX because we assume that the same underlying algorithm is used for template generation for enrollment and search.

Failure to extract rates are incorporated into FNIR and FPIR measurements as follows.

- ▷ **Enrollment templates**: Any failed enrollment is regarded as producing a zero length template. Algorithms are required by the API [10] to transparently process zero length templates. The effect of template generation failure on search accuracy depends on whether subsequent searches are mated, or non-mated: Mated searches will fail giving elevated FNIR; non-mated searches will not produce false positives so, to first order, FPIR will be reduced by a factor of $1-\text{FTE}$.

- ▷ **Search templates and 1:N search**: In cases where the algorithm fails to produce a search template from input imagery, the result is taken to be a candidate list whose entries have no hypothesized identities and zero score. The effect of template generation failure on search accuracy depends on whether searches are mated, or non-mated: Mated searches will fail giving elevated FNIR; Non-mated searches will not produce false positives, so FPIR will be reduced. Thus given a measurement of false negative and positive rates made over only those where failures-to-extract did not occur, those rates - call them $\text{FNIR}^\dagger$ and $\text{FPIR}^\dagger$ - could be adjusted by an explicit measurement of FTX as follows

$$\text{FNIR} = \text{FTX} + (1 - \text{FTX})\text{FNIR}^\dagger \tag{8}$$

$$\text{FPIR} = (1 - \text{FTX})\text{FPIR}^\dagger \tag{9}$$

This approach is the correct treatment for positive-identification applications such as access control where cooperative users are enrolled and make attempts at recognition. This approach is not appropriate to negative identification applications, such as visa fraud detection, in which hostile individuals may attempt to evade detection by submitting poor quality samples. In those cases, template generation failures should be investigated as though a false alarm had occurred.

[10] For example, the Megaface benchmark. This is bad practice for several reasons: First, if a developer knows, or can reasonably assume, that a mate always exists, then unrealistic gaming of the test is possible. A second reason is that it does not put FPIR on equal footing with FNIR and that matters because in most applications, not all searches have mates - not everyone has been previously enrolled in a driving license issuance or a criminal justice system - so addressing between-class separation becomes necessary.

This publication is available free of charge from: https://doi.org/10.6028/NIST.IR.8271

This publication is available free of charge from: https://doi.org/10.6028/NIST.IR.8271

3.6 Fixed length candidate lists, threshold independent workload

Suppose an automated face identification algorithm returns L candidates, and a human reviewer is retained to examine up to R candidates, where $R \leq L$ might be set by policy, preference or labor availability. For now, assume also that the reviewer is not provided with, or ignores, similarity scores, and thresholds are not applied. Given the algorithm typically places mates at low (good) ranks, the number of candidates a reviewer can be expected to review can be derived as follows. Note that the reviewer will:

- ▷ Always inspect the first ranked image — Frac. reviewed = 1
- ▷ Then inspect those candidates where mate not confirmed at rank 1 — Frac. reviewed = 1-CMC(1)
- ▷ Then inspect those candidates where mate not confirmed at rank 1 or 2 — Frac. reviewed = 1-CMC(2)

etc. Thus if the reviewer will stop after a maximum of R candidates, the expected number of candidate reviews is

$$M(R) = 1 + (1 - CMC(1)) + (1 - CMC(2)) + \ldots + (1 - CMC(R-1)) \tag{10}$$

$$= R - \sum_{r=1}^{R-1} CMC(r) \tag{11}$$

A recognition algorithm that front-loads the cumulative match characteristic will offer reduced workload for the reviewer. This workload is defined only over the searches for which a mate exists. In the cases where there truly is no mate, the reviewer would review all R candidates. Thus, if the proportion of searches for which a mate does exist is β, which in the law enforcement context would be the recidivism rate [3], the full expression for workload becomes:

$$M(R) = \beta \left(R - \sum_{r=1}^{R-1} CMC(r) \right) \quad + \quad (1-\beta)R \tag{12}$$

$$= R - \beta \sum_{r=1}^{R-1} CMC(r) \tag{13}$$

3.7 Timing measurement

Algorithms were submitted to NIST as implementations of the application programming interface(API) specified by NIST in the Evaluation Plan [10]. The API includes functions for initialization, template generation, finalization, search, gallery insert, and gallery delete. Two template generation functions are required, one for the preparation of an enrollment template, and one for a search template.

In NIST's test harness, all functions were wrapped by calls to the C++ std::chrono::high resolution clock which on the dedicated timing machine counts 1ns clock ticks. Precision is somewhat worse than that however.

3.8 Uncertainty estimation

3.8.1 Random error

This study leverages operational datasets for measurement of recognition error rates. This affords several advantages. First, large numbers of searches are conducted (see Table 1) giving precision to the measurements. Moreover, for the two mugshot datasets, these do not involve reuse of individuals so binomial statistics can be expected to apply to recognition error counts. In that case, an observed count of a particular recognition outcome (i.e. a false negative or false positive) in M trials will sustain 95% confidence that the actual error rate is no larger than some value.

As an example, the minimum number of mugshot searches conducted in this report is M =154 549, and for an observed FNIR around 0.002, the measurement supports a conclusion that the actual FNIR is no higher than 0.00228 at 99% confidence level. On the false positive side, we tabulate FNIR at FPIR values as low as 0.001. Given estimates based on 331 254 non-mate trials, the actual FPIR values will be below 0.00115 at 99% confidence. In conclusion, large scale evaluation, without reuse of subjects, supports tight uncertainty bounds on the measured error rates.

3.8.2 Systematic error

The FRVT 2018 dataset includes anomalies discovered as a result of inspecting images involved in recognition failures from the most accurate algorithms. Two kinds of failure occur: False negatives (which, for the purpose here, include failures to make templates) and false positives.

False negative errors: We reviewed 600 false negative pairs for which either or both of the leading two algorithms did not put the correct mate in the top 50 candidates. Given 154 549 searches, this number represents 0.39% of the total, resulting in FNIR ~ 0.0039. Of the 600 pairs:

- ▷ **A: Poor quality**: About 20% of the pairs included images of very low quality, often greyscale, low resolution, blurred, low contrast, partially cropped, interlaced, or noisy scans of paper images. Additionally, in a few cases, the face is injured or occluded by bandages or heavy cosmetics.
- ▷ **B: Ground truth identity label bugs**: About 15% of the pairs are not actually mated. We only assigned this outcome when a pair is clearly not mated.
- ▷ **C: Profile views**: About 35% included an image of a profile (side) view of the face, or, more rarely, an image that was rotated 90 degrees in-plane (roll).
- ▷ **D: Tattoos**: About 30% included an image of a tattoo that contained a face image. These arise from mis-labelling in the parent dataset metadata.
- ▷ **E: Ageing**: There is considerable time-lapse between the two captures.

All these estimates are approximate. Of these, the tattoo and mislabled images can never be matched. These constitute an accuracy floor in the sample implying that FNIR cannot be below 0.0018[11]. The profile-views, low-quality images, and images with considerable ageing can, in principle, be successfully matched - indeed some algorithms do so - so are not part of the accuracy floor.

[11] This value is the sum of two partial false negative rates: FNIR_B = 0.15 * 0.0039 plus FNIR_D = 0.3 * 0.0039

This publication is available free of charge from: https://doi.org/10.6028/NIST.IR.8271

For the microsoft-4 algorithm the lowest miss rate from (recent entry in Table 24) is FNIR(640 000, 50, 0) = 0.0018. This is close to the value estimated from the inspection of misses. It is below the 0.0039 figure because the algorithm does match some profile and poor quality images, that the yitu-2 algorithm does not.

For many tables (e.g. Table 24), the FNIR values obtained for the FRVT-2018 mugshots could be corrected by reducing them by 0.0018. The best values would then be indistinct from zero. The results in this report *were not* adjusted to account for this systematic error.

False positive errors: As shown in Figure 1 and discussed in Figure 14 many of the DET characteristics in this report exhibit a pronounced turn upward at low false positive rates. The shape can be caused by identity labelling errors in the ground truth of a dataset, specifically persons present in the database under two IDs such that some proportion of non-mate pairs are actually mated. To look for such possibilities, we merged the highest 1000 non-mate pairs produced by three different algorithms which resulted in 1839 unique pairs. This constitutes 0.56% of all non-mate searches. We assert that it is *very* difficult for human reviewers to assign the pairs into the following three categories: twins; doppelgangers; or ground-truth errors (instances of the same person under two IDs). Given this difficulty we made no attempt to correct any possible ground truth errors except by removing 57 pairs in the following categories:

- **A: Profile views**: Thirteen pairs included one or two profile-view images. As described in Figure 135, these can cause false positives.
- **B: Same-session photographs**: For twelve pairs, the images were identical or trivially altered (e.g. cropped) versions of the same photo. These were present under a different ID likely due to some clerical or procedural mistake.
- **C: Tattoos of faces**: There were fourteen instances of tattoo photographs that contained faces causing false matches.
- **D: T-shirt faces**: There were six instances of T-shirt photographs (of Bob Marley and Che Guevara) being detected instead of the face and causing false positives.
- **E: Background faces**: There were twelve instances of one subject appearing in the background of two otherwise correct portrait photos.

Note we did not remove any images where there was a chance that the pair was actually a different person.

In any case, the results in this report have not been adjusted for this systematic error.

This publication is available free of charge from: https://doi.org/10.6028/NIST.IR.8271

4 Results

This section gives extensive results for algorithms submitted to FRVT 2018. Three page "report cards" for each algorithm are contained in a separate supplement. Performance metrics were described in section 3. The main results are summarized in tabular form with more exhaustive data included as DET, CMC and related graphs in appendices as follows:

▷ The three tables 2-4 list algorithms alongside full developer names, acceptance date, size of the provided configuration data, template size and generation time, and search duration data.

- The **template generation duration** is most important to applications that require fast response. For example, an eGate taking more than two seconds to produce a template might be unacceptable. Note that GPUs may be of utility in expediting this operation for some algorithms, though at additional expense. Two additional factors should be considered[12][13].
- The **search duration** is the time taken for a search of a search template into a gallery of N enrollment templates. This performance variable, together with the volume of searches, is influential on the amount of hardware needed to sustain an operational deployment. This is measured here with the algorithm running on a single core of a contemporary CPU. Search is most simply implemented as N computations of a distance metric followed by a sort operation to find the closest enrollments. However, considerable optimization of this process is possible, up to and including fast-search algorithms that, by various means, avoid computation of all N distances.
- The **template size** is the size of the extracted feature vector (or vectors) and any needed header information. Large template sizes may be influential on bus or network bandwidth, storage requirements, and on search duration. While the template itself is an opaque data blob, the feature dimensionality might be estimated by assuming a four-bytes-per-float encoding. There is a wide range of encodings. For the more accurate algorithm, sizes range from 256 bytes to about 2KB bytes, indicating essentially no consensus on face modeling and template design.
- The **template size multiplier** column shows how, given k input images, the size of the template grows. Most implementations internally extract features from each image and concatenate them, and implement some score-level fusion logic during search. Other implementations, including many of the most accurate algorithms, produce templates whose size does not grow with k. This could be achieved via selection of the best quality image - but this is not optimal in handling ageing where the oldest image could be the best quality. Another mechanism would be feature-level fusion where information is fused from all k inputs. In any case, as a black-box test, the fusion scheme is proprietary and unknown.
- The size of the **configuration data** is the total size of all files resident in a vendor-provided directory that contains arbitrary read-only files such as parameters, recognition models (e.g caffe). Generally a large value for this quantity may prohibit the use of the algorithm on a resource-constrained device.

[12] The FRVT 2018 API prohibited threading, so some gains from parallelism may be available on multiple-cores or multiple processors, if the feature extraction code could be distributed across them.

[13] Note also that factors of two or more may be realizable by exploiting modern vector processing instructions on CPUs. It is not clear in our measurements whether all developers exploited Intel's AVX2 instructions, for example. Our machine was so equipped, but we insisted that the same compiled library should also run on older machines lacking that instruction. The more sophisticated implementations may have detected AVX2 presence and branched accordingly. The less sophisticated may be defaulted to the reduced instruction set. Readers should see the FRVT 2018 API document for the specific chip details.

This publication is available free of charge from: https://doi.org/10.6028/NIST.IR.8271

This publication is available free of charge from: https://doi.org/10.6028/NIST.IR.8271

▷ Tables 24-25 report core rank-based accuracy for mugshot images. The population size is limited to N = 1.6 million identities because this is the largest gallery size on which all algorithms were executed. Notable observations from these tables are as follows:

- **Accuracy gains since 2018**: NIST Interagency Report 8238 documented massive gains over those reported in the FRVT 2014 report, NIST Interagency Report 8009. Further gains are documented in this report. Comparing the most accurate algorithm in November 2018, NEC-3, the value of FNIR(N, L, T) reduced from 0.0031 to 0.0024 for the Sensetime-004 algorithm with N = 12 million recent images. The tables show broader gains: many developers have made advances since 2018 with between two and five-fold reduction in errors.
- **Wide range in accuracy**: The rank-1 miss rates vary from FNIR(N, 1, 0) = 0.0012 for sensetime-004 up to about 0.5 for the very fast but inaccurate microfocus-x algorithms. Among the developers who are superior to NEC in 2013, the range is from 0.002 to 0.035 for camvi-3. This large accuracy range is consistent with the buyer-beware maxim, and indicates that face recognition software is far from being commoditized.

▷ Tables 29-30 report threshold-based error rates, FNIR(N, L, T), for N = 1.6 million for mugshot-mugshot accuracy on FRVT 2014, FRVT 2018, and also (in pink) mugshot-webcam accuracy using FRVT 2018 enrollments. Notable observations from these tables are as follows:

- **Order of magnitude accuracy gains since 2014**: As with rank-based results, the gains in accuracy are substantial, though somewhat reduced. At FPIR = 0.01, the best improvement over NEC in 2014 is a 27 fold reduction in FNIR using the NEC_2 algorithm. At FPIR = 0.001, the largest gain is a six-fold reduction in FNIR via the NEC_3 algorithm.
- **Broad gains across the industry**: About 19 companies realize accuracy better than the NEC benchmark from 2014. This is somewhat lower than the 28 developers who succeeded on the rank-1 metric. This may be due to the ubiquity of, and emphasis on, the rank-1 metric in many published algorithm development papers.
- **Webcam images**: Searches of webcam images give FNIR(N, T) values around 2 to 3 times higher than mugshot searches. Notably the leading developers with mugshots are approximately the same with poorer quality webcams. But some developers e.g. Camvi, Megvii, TongYi, and Neurotechnology do improve their relative rankings on webcams, perhaps indicating their algorithms were tailored to less constrained images.

▷ Tables 18, 21, 22 and show, respectively, high-threshold, rank 1, and rank 50 FNIR values for all algorithms performing searches into five different gallery sizes, N = 640 000, N = 1 600 000, N = 3 000 000, N = 6 000 000 and 12 000 000. The FPIR = 0.001 table is included to inform high-volume duplicate detection applications. The Rank-1 table is included as a primary accuracy indicator. The Rank-50 table is included to inform agencies who routinely produce 50 candidates for human-review. The notable results are:

- **Slow growth in rank-based miss rates:** FNIR(N, R) generally grows as a power law, aN^b. From the straight lines of many graphs of Figure 20 this is clearly a reasonable model for most, but not all, algorithms. The coefficient a can be interpreted as FNIR in a gallery of size 1. The more important coefficient b indicates scalability, and often, $b \ll 1$, implies very benign growth in FNIR. The coefficients of the models appear in the Tables 21 and 22.
- **Slow growth in threshold-based miss rates:** FNIR(N, T) also generally grows as a power law, aN^b except at the high threshold values corresponding to low FPIR values. This is visible in the plots of Figure 36 which

show straight lines except for FPIR = 0.001, which increase more rapidly with N above 3 000 000. Each trace in those figures shows FNIR(N, T) at fixed FPIR with both N and T varying. Thus at large N, it is usually necessary to elevate T to maintain fixed FPIR. This causes increased FNIR. Why that would no-longer obey a power-law is not known. However, if we expect large galleries to contain individuals with familial relations to the non-mate search images - in the most extreme case, twins - then suppression of false positives becomes more difficult. This is discussed in the Figures starting at Fig. 10

▷ Figure **??** shows false positives from twins against their enrolled siblings, broken out by type of twin: fraternal or identical. The Figure is based on the enrollment of 104 single images on one of a pair of twins, and then the search of 2354 second images. Note that the dataset is heavily skewed towards identical twins which is not representative of the true population. There is also a skew towards same sex fraternal twin pairs compared to different sex fraternal twin pairs again not representative of the true population.

The notable results are:

- For all algorithms tested, the 1087 mated searches (Twin A vs. Twin A) produce scores almost always above typical operational thresholds, with (not shown) matches at rank 1. The images are of good quality, so this is the result expected from the rest of this report.
- For the 1066 identical twin searches (AB), almost all produce the twin at rank 1, with a few producing the mate at further down the candidate lists rank and low score.
- For the 169 fraternal searches (AB) from same sex pairs, most algorithms give a large number of very high scores, implying false positives at all thresholds. However, there there are long tails containing lower scores that are correctly below threshold. In general, scores that are higher in this distribution are all rank 1 whereas the lower scores have much higher ranks.
- (Not shown) Of the 169, there are 24 fraternal searches (AB) involving different sex twins. Here most algorithms correctly report scores well below the lowest threshold, and usually not on the candidate list at all.

This publication is available free of charge from: https://doi.org/10.6028/NIST.IR.8271

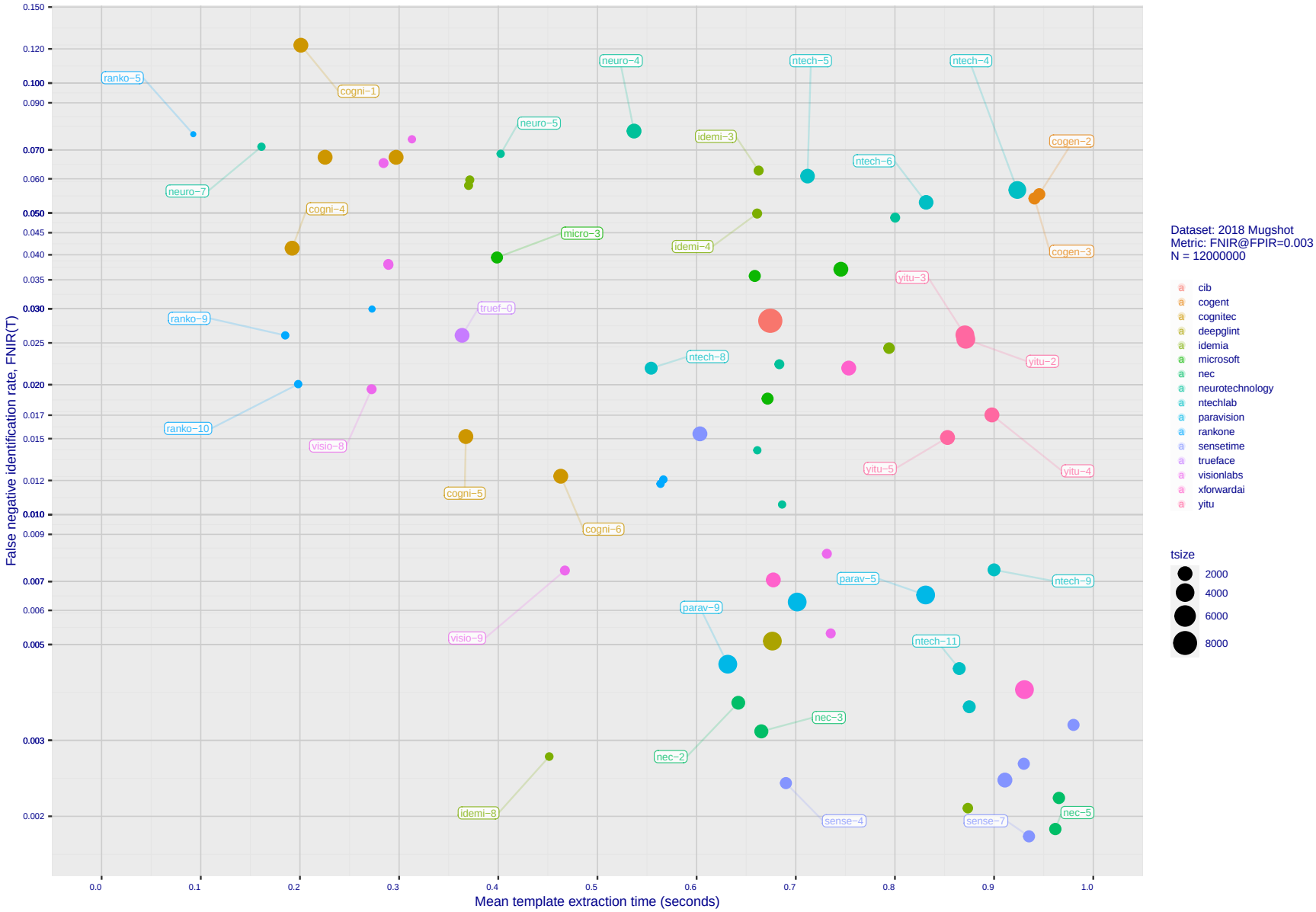

Figure 18: **[Mugshot Dataset] Speed-accuracy tradeoff**. *For developers of the more accurate algorithms the plot shows the tradeoff of high-threshold recognition miss-rates, FNIR(N, N, T) for FPIR(N, T) = 0.003, and template generation time. Developers are coded by color. Template size is encoded by the size of the circle. Some labels are quite distant from the respective point, to avoid superposing text. Without any other influences, the assumption would be that taking time to localize the face, and extract features, would lead to better accuracy. The most notable result, for NEC, is that their slower algorithms are much more accurate than the version that extract features in fewer than 90 milliseconds.*

This publication is available free of charge from: https://doi.org/10.6028/NIST.IR.8271

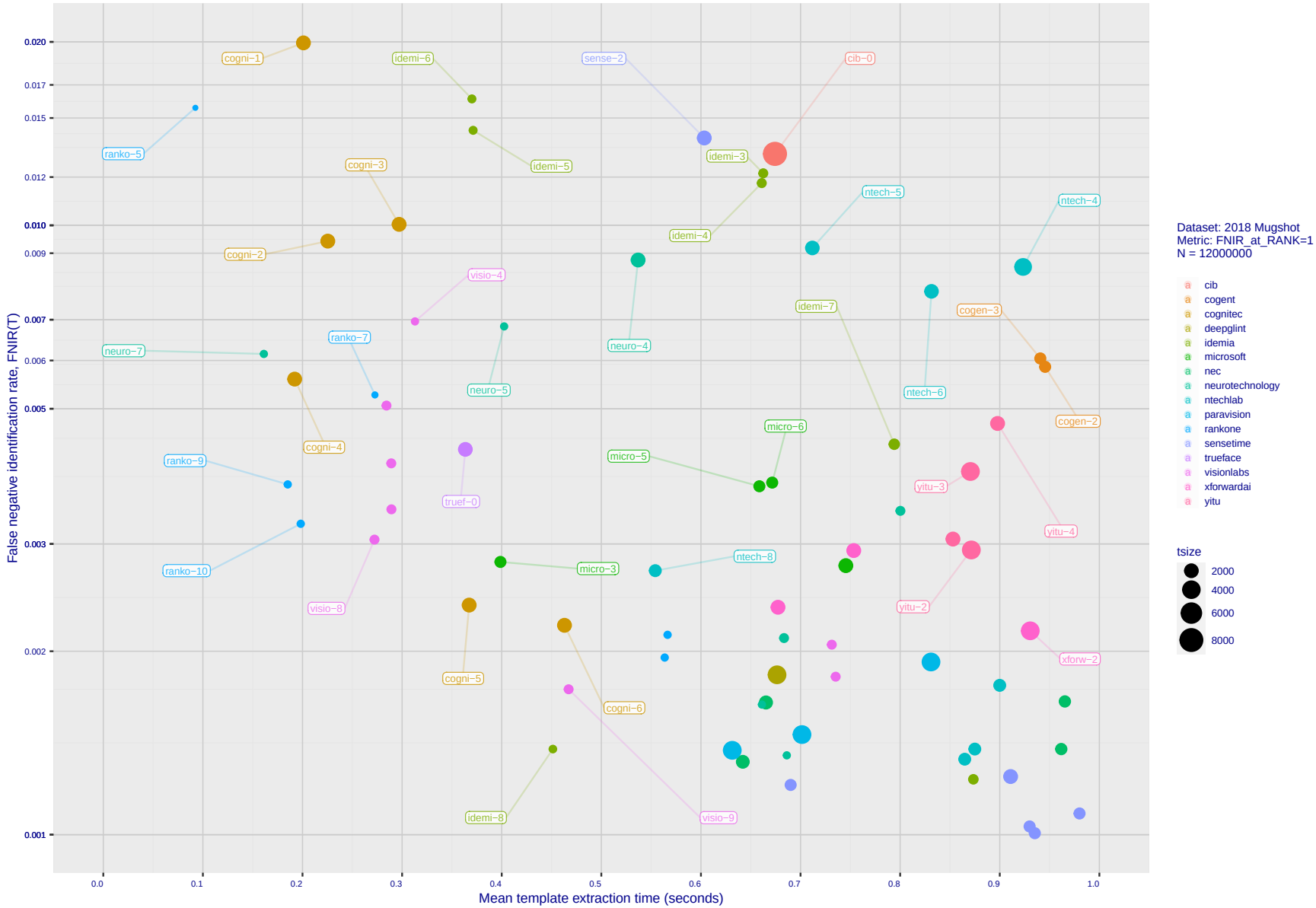

Figure 19: **[Mugshot Dataset] Speed-accuracy tradeoff**. *For developers of the more accurate algorithms the plot shows the tradeoff of rank-one recognition miss-rates, FNIR(N, 1, 0), and template generation time. Developers are coded by color. Template size is encoded by the size of the circle. Some labels are quite distant from the respective point, to avoid superposing text. Without any other influences, the assumption would be that taking time to localize the face, and extract features, would lead to better accuracy. This occurs for NEC with their slower algorithm being much accurate than the version that extract features in fewer than 90 milliseconds.*

This publication is available free of charge from: https://doi.org/10.6028/NIST.IR.8271

	DEVELOPER	SHORT	SEQ.	VALIDATION	CONFIG[1]	LIB[1]	TEMPLATE GENERATION			FINALIZE[2]	SEARCH DURATION[5] MILLISEC					
	FULL NAME	NAME	NUM.	DATE	DATA (MB)	DATA (MB)	SIZE (B)	MULT[3]	TIME (MS)[4]	TIME (S)	L=1	L=50	L=50	L=50	L=50	POWER LAW
										N=1.6M	N=1.6M	N=1.6M	N=3M	N=6M	N=12M	(μs)
1	20Face	20face	000	2021-10-01	112	319	^{120}2048	-	^{20}236	^{67}9	$^{(212)}$6355	$^{(214)}$6341	-	-	-	
2	3Divi	3divi	5	2018-10-26	186	51	^{208}4096	k	^{113}638	^{175}28	$^{(93)}$538	$^{(92)}$537	$^{(87)}$1377	$^{(83)}$2614	$^{(79)}$5530	$^{151}0.07N^{1.1}$
3	3Divi	3divi	6	2018-10-26	187	51	^{38}528	k	^{114}640	^{27}5	$^{(13)}$33	$^{(13)}$33	-	-	-	
4	Acer Incorporated	acer	000	2020-08-12	35	67	^{32}512	-	^{16}198	^{17}4	$^{(59)}$295	$^{(59)}$295	$^{(51)}$623	$^{(77)}$2302	$^{(71)}$4915	$^{182}0.00N^{1.3}$
5	Acer Incorporated	acer	001	2021-11-08	42	610	^{151}2048	-	^{11}184	^{64}9	$^{(106)}$619	$^{(101)}$575	-	-	-	
6	Akurat Satu Indonesia	ptakuratsatu	000	2020-10-23	0	572	^{41}538	-	^{212}905	^{226}28633	$^{(7)}$15	$^{(6)}$16	$^{(6)}$17	$^{(5)}$17	$^{(4)}$17	$^{3}6827.74N^{0.1}$
7	Alchera Inc	alchera	2	2018-10-30	7	14	^{118}2048	k	^{6}114	^{205}63	$^{(190)}$2923	$^{(193)}$2929	-	-	-	
8	Alchera Inc	alchera	3	2018-10-30	251	14	^{114}2048	k	^{89}531	^{206}63	$^{(191)}$2955	$^{(194)}$2956	$^{(167)}$6546	$^{(168)}$15013	$^{(168)}$35262	$^{177}0.10N^{1.2}$
9	Alchera Inc	alchera	004	2021-09-17	476	24	^{102}2048	-	^{187}853	^{189}35	$^{(213)}$6657	$^{(220)}$6851	-	-	-	
10	Alivia / Innovation Sys	isystems	3	2018-10-30	350	784	^{95}2048	1	^{177}825	^{140}16	$^{(71)}$385	$^{(75)}$389	$^{(68)}$979	$^{(66)}$1822	$^{(108)}$9348	$^{183}0.00N^{1.3}$
11	AllGoVision	allgovision	000	2019-07-30	168	150	^{139}2048	k	^{53}404	^{95}12	$^{(194)}$3226	$^{(197)}$3193	$^{(165)}$6129	$^{(165)}$12449	$^{(164)}$25835	$^{86}1.40N^{1.0}$
12	AllGoVision	allgovision	001	2020-07-14	283	126	^{142}2048	-	^{164}777	^{101}13	$^{(193)}$3174	$^{(196)}$3183	$^{(164)}$6073	$^{(163)}$12284	$^{(163)}$25701	$^{84}1.42N^{1.0}$
13	Anke Investments	anke	0	2018-10-30	779	27	^{189}2072	k	^{61}429	^{138}16	$^{(109)}$675	$^{(115)}$748	$^{(94)}$1483	$^{(92)}$2968	$^{(87)}$6148	$^{117}0.21N^{1.1}$
14	Anke Investments	anke	1	2018-10-30	779	27	^{190}2072	k	^{62}430	^{131}15	$^{(114)}$707	$^{(118)}$769	-	-	-	
15	Anke Investments	anke	002	2019-06-27	341	401	^{182}2056	k	^{106}623	^{110}13	$^{(107)}$624	$^{(109)}$682	$^{(84)}$1306	$^{(79)}$2403	$^{(76)}$5082	$^{76}0.30N^{1.0}$
16	Aware	aware	5	2018-10-30	368	27	^{199}3100	k	^{169}792	^{187}34	$^{(17)}$95	$^{(22)}$98	$^{(20)}$203	$^{(18)}$371	$^{(13)}$252	$^{14}4.13N^{0.7}$
17	Aware	aware	6	2018-10-30	368	27	^{2}124	k	^{168}789	^{3}2	$^{(33)}$158	$^{(33)}$162	-	-	-	
18	Ayonix	ayonix	1	2018-10-29	74	2	^{63}1036	k	^{2}12	^{90}11	$^{(55)}$279	$^{(55)}$279	-	-	-	
19	Ayonix	ayonix	2	2018-10-30	74	2	^{64}1036	1	^{1}11	^{116}14	$^{(54)}$279	$^{(54)}$276	$^{(40)}$535	$^{(40)}$1087	$^{(40)}$2284	$^{96}0.11N^{1.0}$
20	Camvi Technologies	camvitech	4	2018-10-30	233	220	^{49}1024	1	^{131}686	^{185}31	$^{(14)}$33	$^{(12)}$32	$^{(11)}$38	$^{(10)}$40	$^{(7)}$48	$^{4}8492.66N^{0.1}$
21	Camvi Technologies	camvitech	5	2018-10-30	257	220	^{52}1024	1	^{154}751	^{183}31	$^{(12)}$31	$^{(10)}$30	-	-	-	
22	Canon Inc	cib	000	2020-10-19	426	127	^{227}8196	-	^{125}674	^{212}113	$^{(195)}$3589	$^{(199)}$3604	$^{(168)}$6738	$^{(166)}$13495	$^{(165)}$27114	$^{31}2.33N^{1.0}$
23	Canon Inc	canon	001	2021-10-27	1139	91	^{207}4096	-	^{202}885	^{161}21	$^{(215)}$6804	$^{(218)}$6789	$^{(183)}$12741	$^{(179)}$25650	$^{(176)}$51922	$^{57}3.82N^{1.0}$
24	Canon Inc	canon	002	2022-04-26	1231	111	^{221}6200	-	^{207}897	^{203}58	$^{(217)}$7673	$^{(221)}$7559	$^{(185)}$14216	$^{(181)}$28503	$^{(179)}$57633	$^{55}4.35N^{1.0}$
25	Clearview AI Inc	clearviewai	000	2021-11-12	358	316	^{210}4096	-	^{159}765	^{180}30	$^{(120)}$802	$^{(106)}$657	$^{(75)}$1134	$^{(69)}$1939	$^{(63)}$3889	$^{20}1.59N^{0.9}$
26	Cloudwalk - Hengrui AI Technology	hr	000	2021-02-10	501	392	^{146}2048	-	^{213}905	^{124}15	$^{(56)}$282	$^{(53)}$276	$^{(42)}$539	$^{(49)}$1268	$^{(57)}$3177	$^{155}0.03N^{1.1}$
27	Cloudwalk - Moontime Smart Technology	cloudwalk	000	2022-01-31	716	573	^{135}2048	-	^{194}869	^{82}10	$^{(82)}$440	$^{(71)}$371	$^{(44)}$547	$^{(39)}$1065	$^{(51)}$2902	$^{23}0.53N^{0.9}$
28	Cognitec Systems GmbH	cognitec	2	2018-10-30	463	26	^{167}2052	k	^{19}225	^{170}27	$^{(167)}$1733	$^{(169)}$1763	$^{(149)}$3660	$^{(144)}$7279	$^{(140)}$13895	$^{81}0.83N^{1.0}$
29	Cognitec Systems GmbH	cognitec	3	2018-10-30	465	26	^{164}2052	k	^{31}297	^{136}16	$^{(166)}$1719	$^{(170)}$1791	$^{(147)}$3638	$^{(143)}$7277	$^{(147)}$14904	$^{106}0.66N^{1.0}$
30	Cognitec Systems GmbH	cognitec	004	2021-03-08	384	60	^{169}2052	-	^{14}192	^{108}13	$^{(165)}$1673	$^{(167)}$1727	$^{(134)}$2904	$^{(132)}$5801	$^{(130)}$11707	$^{26}1.15N^{1.0}$
31	Cognitec Systems GmbH	cognitec	005	2021-07-30	460	61	^{174}2052	-	^{40}367	^{69}9	$^{(157)}$1556	$^{(159)}$1551	$^{(136)}$2916	$^{(140)}$6561	$^{(141)}$13958	$^{123}0.38N^{1.1}$
32	Cognitec Systems GmbH	cognitec	006	2022-02-10	689	61	^{162}2052	-	^{72}463	^{79}10	$^{(134)}$1006	$^{(133)}$1002	$^{(111)}$2097	$^{(107)}$4312	$^{(97)}$7624	$^{115}0.30N^{1.1}$
33	Cubox	cubox	000	2021-08-24	529	298	^{150}2048	-	^{216}917	^{78}10	$^{(196)}$3646	$^{(201)}$4076	$^{(170)}$7605	$^{(169)}$15871	-	$^{116}1.16N^{1.1}$
34	Cyberlink Corp	cyberlink	000	2019-06-12	217	93	^{166}2052	1	^{118}654	^{179}30	$^{(111)}$696	$^{(111)}$701	$^{(88)}$1379	$^{(84)}$2639	$^{(89)}$6214	$^{99}0.28N^{1.0}$
35	Cyberlink Corp	cyberlink	001	2019-10-07	459	102	^{163}2052	1	^{59}423	^{176}28	$^{(112)}$698	$^{(110)}$700	$^{(86)}$1350	$^{(130)}$5524	$^{(133)}$12031	$^{181}0.00N^{1.3}$
36	Cyberlink Corp	cyberlink	002	2020-07-31	333	109	^{219}4140	-	^{147}724	^{217}6875	$^{(154)}$1353	$^{(198)}$3198	$^{(166)}$6138	$^{(162)}$12205	$^{(138)}$13106	$^{18}16.71N^{0.8}$
37	Cyberlink Corp	cyberlink	003	2021-01-05	333	100	^{222}6212	-	^{135}691	^{191}35	$^{(85)}$488	$^{(112)}$723	$^{(91)}$1415	$^{(90)}$2886	$^{(80)}$5643	$^{135}0.12N^{1.1}$
38	Cyberlink Corp	cyberlink	004	2021-07-16	371	100	^{224}6212	-	^{149}728	^{165}23	$^{(87)}$492	$^{(90)}$504	$^{(67)}$923	$^{(55)}$1448	$^{(59)}$3350	$^{22}0.73N^{0.9}$
39	Cyberlink Corp	cyberlink	005	2022-01-07	371	100	^{223}6212	-	^{151}733	^{182}30	$^{(89)}$501	$^{(86)}$498	$^{(80)}$1193	$^{(85)}$2672	$^{(82)}$5693	$^{172}0.03N^{1.2}$
40	DAON	daon	000	2021-12-23	274	2	^{186}2069	-	^{96}583	^{49}8	$^{(92)}$524	$^{(105)}$625	$^{(92)}$1454	$^{(95)}$3097	$^{(91)}$6316	$^{173}0.03N^{1.2}$
41	Dahua Technology Co Ltd	dahua	0	2018-10-29	276	167	^{154}2048	k	^{45}374	^{163}22	-	$^{(51)}$258	-	-	-	
42	Dahua Technology Co Ltd	dahua	1	2018-10-29	276	167	^{157}2048	k	^{41}369	^{172}28	-	$^{(50)}$257	$^{(49)}$602	$^{(46)}$1202	$^{(54)}$3007	$^{162}0.02N^{1.2}$
43	Dahua Technology Co Ltd	dahua	002	2019-12-02	607	137	^{143}2048	k	^{130}685	^{155}19	$^{(45)}$243	$^{(52)}$269	$^{(78)}$1189	$^{(91)}$2950	$^{(94)}$6732	$^{187}0.00N^{1.5}$
44	Dahua Technology Co Ltd	dahua	003	2020-11-18	889	154	^{147}2048	-	^{146}723	^{148}18	$^{(57)}$283	$^{(49)}$249	$^{(37)}$468	$^{(37)}$935	$^{(35)}$1871	$^{33}0.16N^{1.0}$
45	Dahua Technology Co Ltd	dahua	004	2021-11-18	812	116	^{129}2048	-	^{157}758	^{84}11	$^{(79)}$423	$^{(79)}$411	$^{(64)}$871	$^{(58)}$1568	$^{(56)}$3174	$^{88}0.17N^{1.0}$
46	Decatur Industries Inc	decatur	000	2022-02-09	411	383	^{161}2052	-	^{190}863	^{71}9	$^{(168)}$1761	$^{(177)}$2023	$^{(142)}$3361	$^{(145)}$7283	$^{(144)}$14592	$^{60}1.06N^{1.0}$
47	Deepglint	deepglint	001	2019-11-15	448	265	^{209}4096	-	^{127}676	^{188}35	$^{(110)}$677	$^{(157)}$1495	$^{(102)}$1724	$^{(87)}$2747	$^{(90)}$6246	$^{15}25.27N^{0.8}$
48	Dermalog	dermalog	5	2018-10-26	0	440	^{3}128	1	^{88}528	^{216}3155	$^{(1)}$0	$^{(1)}$0	$^{(1)}$0	$^{(1)}$0	$^{(1)}$0	$^{5}66.21N^{0.2}$
49	Dermalog	dermalog	6	2018-10-26	0	453	^{9}256	1	^{84}507	^{4}2	$^{(30)}$142	$^{(30)}$144	$^{(25)}$269	$^{(24)}$531	$^{(23)}$1294	$^{107}0.05N^{1.0}$
50	Dermalog	dermalog	007	2020-02-12	0	424	^{4}128	1	^{56}410	^{1}1	$^{(23)}$98	$^{(20)}$96	$^{(22)}$218	$^{(20)}$429	$^{(20)}$1013	$^{143}0.01N^{1.1}$
51	Dermalog	dermalog	008	2021-01-25	0	531	^{33}512	-	^{43}370	^{19}4	$^{(65)}$335	$^{(45)}$246	$^{(36)}$462	$^{(36)}$924	$^{(34)}$1849	$^{39}0.15N^{1.0}$
52	Dermalog	dermalog	009	2021-11-09	0	318	^{25}512	-	^{36}347	^{14}3	$^{(49)}$253	$^{(46)}$246	$^{(35)}$461	$^{(35)}$923	$^{(33)}$1846	$^{35}0.16N^{1.0}$

Notes	
1	Configuration size does not capture static data present in libraries. Libraries are included but the size also includes any ancillary libraries for image processing (e.g. openCV) or numerical computation (e.g. blas).
2	Finalization is the processing of converting N = 1600000 templates into a searchable data structure an operation which can be a simple copy, or the building of an index or tree, for example. The duration of the operation may be data dependent, and may not be linear in the number of input templates.
3	This multiplier expresses the increase in template size when k images are passed to the template generation function.
4	All durations are measured on Intel®Xeon®CPU E5-2630 v4 @ 2.20GHz processors. Estimates are made by wrapping the API function call in calls to std::chrono::high_resolution_clock which on the machine in (3) counts 1ns clock ticks. Precision is somewhat worse than that however.
5	Search durations are measured as in the prior note. The power-law model in the final column mostly fits the empirical results in Figure 136. However in certain cases the model is not correct and should not be used numerically.

Table 2: Summary of algorithms and properties included in this report. The blue superscripts give ranking for the quantity in that column. Missing search durations, denoted by "-", are absent because those runs were not executed, usually because we did not run on the larger galleries. Caution: The power-law model is sometimes an incorrect model. It is included here only to show broad sublinear behavior, which is flagged in green. The models should not be used for prediction.

This publication is available free of charge from: https://doi.org/10.6028/NIST.IR.8271

	DEVELOPER FULL NAME	SHORT NAME	SEQ. NUM.	VALIDATION DATE	CONFIG[1] DATA (MB)	LIB[1] DATA (MB)	TEMPLATE GENERATION SIZE (B)	MULT[3]	TIME (MS)[4]	FINALIZE[2] TIME (S) N=1.6M	SEARCH DURATION[5] MILLISEC L=1 N=1.6M	L=50 N=1.6M	L=50 N=3M	L=50 N=6M	L=50 N=12M	POWER LAW (μs)
53	Digidata	digidata	000	2022-06-03	248	33	^{148}2048	-	^{92}560	^{215}2444	$^{(2)}$0	$^{(17)}$95	-	-	-	
54	DiluSense Technology	dilusense	000	2022-05-26	311	56	^{112}2048	-	^{23}247	^{169}26	$^{(172)}$1904	$^{(172)}$1898	$^{(146)}$3597	$^{(142)}$7256	$^{(145)}$14689	$^{75}0.88N^{1.0}$
55	FarBar Inc	f8	001	2019-10-03	266	19	^{152}2048	k	^{173}810	^{113}14	-	-	-	-	-	
56	Fincore Ltd	fincore	000	2021-08-18	250	224	^{137}2048	-	^{75}475	^{59}9	$^{(100)}$562	$^{(97)}$560	-	-	-	
57	Fujitsu Research and Development Center	fujitsulab	000	2021-10-12	497	337	^{57}1032	-	^{223}945	^{29}5	$^{(164)}$1668	$^{(163)}$1657	$^{(140)}$3140	$^{(137)}$6320	$^{(136)}$12723	$^{74}0.78N^{1.0}$
58	Fujitsu Research and Development Center	fujitsulab	001	2022-03-15	675	386	^{55}1032	-	^{201}882	^{60}9	$^{(170)}$1854	$^{(171)}$1817	$^{(143)}$3451	$^{(141)}$6986	$^{(142)}$14166	$^{92}0.72N^{1.0}$
59	Gorilla Technology	gorilla	2	2018-10-29	91	1252	^{71}1132	k	^{35}338	^{167}24	$^{(31)}$145	$^{(31)}$146	$^{(26)}$293	$^{(25)}$612	$^{(27)}$1509	$^{141}0.02N^{1.1}$
60	Gorilla Technology	gorilla	3	2018-10-26	94	1252	^{192}2156	k	^{91}559	^{221}12020	-	$^{(178)}$2047	-	-	-	
61	Gorilla Technology	gorilla	004	2020-01-06	182	1244	^{193}2192	k	^{48}388	^{193}41	$^{(58)}$286	$^{(58)}$285	$^{(79)}$1191	$^{(80)}$2416	$^{(75)}$5036	$^{180}0.00N^{1.3}$
62	Gorilla Technology	gorilla	005	2021-02-22	306	1420	^{225}6288	-	^{79}483	^{208}78	$^{(119)}$802	$^{(119)}$799	$^{(96)}$1514	$^{(110)}$4454	$^{(104)}$8820	$^{165}0.05N^{1.2}$
63	Gorilla Technology	gorilla	006	2021-09-30	377	691	^{228}8336	-	^{160}767	^{211}99	$^{(160)}$1626	$^{(160)}$1612	$^{(120)}$2422	$^{(109)}$4422	$^{(109)}$9363	$^{73}0.59N^{1.0}$
64	Gorilla Technology	gorilla	007	2022-02-16	392	322	^{226}6290	-	^{87}526	^{210}89	$^{(117)}$765	$^{(114)}$745	$^{(90)}$1408	$^{(89)}$2823	$^{(83)}$5764	$^{58}0.42N^{1.0}$
65	Griaule	griaule	000	2021-11-01	0	584	^{163}2052	-	^{58}417	^{43}8	$^{(208)}$5827	$^{(212)}$6150	$^{(176)}$11473	$^{(174)}$22952	$^{(171)}$46070	$^{32}3.89N^{1.0}$
66	Guangzhou Pixel Solutions Co Ltd	pixelall	002	2019-07-01	0	165	^{196}2560	k	^{13}190	^{128}15	$^{(151)}$1296	$^{(153)}$1334	$^{(127)}$2526	$^{(122)}$5136	$^{(126)}$11045	$^{97}0.52N^{1.0}$
67	Guangzhou Pixel Solutions Co Ltd	pixelall	003	2019-11-05	0	690	^{195}2560	k	^{140}703	^{164}22	$^{(148)}$1273	$^{(149)}$1307	$^{(124)}$2474	$^{(123)}$5198	$^{(127)}$11141	$^{108}0.46N^{1.0}$
68	Guangzhou Pixel Solutions Co Ltd	pixelall	004	2020-07-02	0	538	^{194}2560	k	^{64}449	^{147}17	$^{(147)}$1259	$^{(148)}$1300	$^{(123)}$2465	$^{(128)}$5492	$^{(128)}$11443	$^{122}0.34N^{1.1}$
69	Guangzhou Pixel Solutions Co Ltd	pixelall	005	2021-03-23	0	717	^{197}2560	-	^{183}840	^{88}11	$^{(159)}$1606	$^{(158)}$1528	$^{(129)}$2609	$^{(119)}$4926	$^{(131)}$11770	$^{66}0.73N^{1.0}$
70	Hangzhuo Allu Network Information Technology	hzailu	000	2022-03-18	855	97	^{48}1024	-	^{116}649	^{89}11	$^{(187)}$2609	$^{(191)}$2551	$^{(162)}$4813	$^{(160)}$9702	$^{(159)}$19338	$^{51}1.50N^{1.0}$
71	Hikvision Research Institute	hikvision	5	2018-10-29	593	9	^{76}1408	1	^{101}607	^{134}16	$^{(127)}$883	$^{(128)}$895	$^{(106)}$1908	$^{(100)}$3792	$^{(110)}$9387	$^{152}0.10N^{1.1}$
72	Hikvision Research Institute	hikvision	6	2018-10-29	593	9	^{77}1408	1	^{99}598	^{137}16	$^{(125)}$871	$^{(127)}$877	-	-	-	
73	HyperVerge Inc	hyperverge	001	2021-08-11	1791	212	^{50}1024	-	^{186}845	^{25}5	$^{(113)}$705	$^{(108)}$681	$^{(85)}$1346	$^{(86)}$2681	$^{(81)}$5680	$^{83}0.32N^{1.0}$
74	HyperVerge Inc	hyperverge	002	2022-04-13	1140	1118	^{51}1024	-	^{219}934	^{63}9	$^{(108)}$661	$^{(107)}$659	$^{(83)}$1292	$^{(73)}$2188	$^{(38)}$2181	$^{16}11.29N^{0.8}$
75	Idemia	idemia	5	2018-10-29	417	48	^{23}352	1	^{44}371	^{26}5	$^{(27)}$137	$^{(28)}$138	$^{(32)}$437	$^{(30)}$724	$^{(29)}$1630	$^{174}0.01N^{1.2}$
76	Idemia	idemia	6	2018-10-29	417	48	^{24}352	1	^{42}370	^{23}4	$^{(28)}$137	$^{(27)}$138	$^{(33)}$442	$^{(33)}$827	$^{(30)}$1646	$^{176}0.01N^{1.2}$
77	Idemia	idemia	007	2020-01-17	738	113	^{47}860	1	^{170}794	^{114}14	$^{(32)}$151	$^{(32)}$152	$^{(54)}$683	$^{(57)}$1481	$^{(55)}$3022	$^{185}0.00N^{1.4}$
78	Idemia	idemia	008	2021-03-15	378	65	^{22}300	-	^{66}451	^{15}3	$^{(26)}$132	$^{(26)}$131	$^{(23)}$247	$^{(22)}$501	$^{(21)}$1013	$^{61}0.07N^{1.0}$
79	Idemia	idemia	009	2022-03-01	735	68	^{45}636	-	^{196}873	^{37}7	$^{(41)}$211	$^{(40)}$205	$^{(31)}$389	$^{(32)}$787	$^{(28)}$1615	$^{78}0.10N^{1.0}$
80	Imagus Technology Pty Ltd	imagus	005	2021-01-15	222	311	^{97}2048	-	^{167}786	^{112}14	$^{(44)}$236	$^{(62)}$313	$^{(52)}$651	$^{(52)}$1361	$^{(43)}$2461	$^{150}0.03N^{1.1}$
81	Imagus Technology Pty Ltd	imagus	006	2021-05-27	248	369	^{117}2048	-	^{211}904	^{72}9	$^{(63)}$317	$^{(43)}$234	$^{(38)}$499	$^{(50)}$1273	$^{(46)}$2727	$^{171}0.01N^{1.2}$
82	Imagus Technology Pty Ltd	imagus	007	2021-11-16	248	366	^{125}2048	-	^{102}609	^{55}9	$^{(43)}$234	$^{(44)}$238	$^{(34)}$442	$^{(34)}$881	$^{(32)}$1765	$^{27}0.16N^{1.0}$
83	Imagus Technology Pty Ltd	imagus	008	2022-05-26	204	335	^{130}2048	-	^{63}445	^{145}17	$^{(98)}$560	$^{(100)}$565	-	-	-	
84	Imperial College London	imperial	000	2019-08-28	461	15	^{141}2048	1	^{95}577	^{100}13	$^{(68)}$360	$^{(74)}$379	$^{(99)}$1626	$^{(104)}$4057	$^{(124)}$10291	$^{188}0.00N^{1.5}$
85	Incode Technologies Inc	incode	2	2018-10-29	71	31	^{122}2048	1	^{29}289	^{133}15	$^{(77)}$411	$^{(76)}$404	-	-	-	
86	Incode Technologies Inc	incode	3	2018-10-29	133	31	^{136}2048	1	^{138}697	^{123}15	$^{(76)}$408	$^{(80)}$412	$^{(60)}$847	$^{(59)}$1608	$^{(69)}$4486	$^{145}0.05N^{1.1}$
87	Incode Technologies Inc	incode	004	2019-06-24	254	50	^{144}2048	1	^{76}475	^{93}12	$^{(69)}$365	$^{(73)}$378	$^{(93)}$1482	$^{(61)}$1660	$^{(53)}$2954	$^{120}0.12N^{1.1}$
88	Incode Technologies Inc	incode	005	2021-07-29	259	21	^{121}2048	-	^{81}500	^{77}10	$^{(62)}$316	$^{(84)}$454	$^{(65)}$890	$^{(67)}$1843	$^{(62)}$3640	$^{134}0.07N^{1.1}$
89	Innovatrics	innovatrics	4	2018-10-30	0	400	^{68}1076	k	^{49}399	^{218}10902	$^{(6)}$8	$^{(4)}$8	$^{(4)}$11	$^{(2)}$9	$^{(3)}$13	$^{9}668.38N^{0.2}$
90	Innovatrics	innovatrics	005	2019-09-30	0	455	^{39}538	1	^{179}827	^{220}11897	$^{(5)}$8	$^{(5)}$8	$^{(3)}$9	$^{(3)}$9	$^{(2)}$9	$^{1}4055.65N^{0.1}$
91	Innovatrics	innovatrics	007	2021-08-16	175	58	^{40}538	-	^{162}777	^{115}14	$^{(22)}$97	$^{(23)}$100	$^{(18)}$188	$^{(19)}$378	$^{(18)}$788	$^{24}0.09N^{1.0}$
92	Intellivision	intellivision	001	2022-03-08	62	130	^{178}2056	-	^{55}406	^{158}20	$^{(72)}$388	$^{(72)}$377	-	-	-	
93	IrexAI	irex	000	2021-02-09	724	46	^{198}3080	-	^{185}844	^{154}19	$^{(105)}$616	$^{(102)}$600	$^{(74)}$1120	$^{(82)}$2477	$^{(84)}$5863	$^{126}0.13N^{1.1}$
94	Kakao Enterprise	kakao	000	2021-06-23	404	124	^{160}2052	-	^{182}835	^{45}8	$^{(42)}$213	$^{(41)}$215	$^{(39)}$510	$^{(38)}$971	$^{(36)}$1955	$^{130}0.05N^{1.1}$
95	Kedacom International Pte	kedacom	001	2019-09-16	239	36	^{21}292	1	^{83}507	^{5}2	$^{(116)}$764	$^{(116)}$760	$^{(107)}$1940	$^{(93)}$2983	$^{(93)}$6623	$^{102}0.31N^{1.0}$
96	Kneron	kneron	000	2020-03-03	366	13	^{111}2048	k	^{86}523	^{105}13	$^{(186)}$2535	$^{(189)}$2506	$^{(161)}$4752	$^{(159)}$9696	$^{(161)}$20926	$^{103}0.95N^{1.0}$
97	Kneron	kneron	001	2021-06-10	270	69	^{138}2048	-	^{74}472	^{61}9	$^{(188)}$2690	$^{(192)}$2642	-	-	-	
98	Line Corporation	line	000	2021-06-02	138	397	^{94}2048	-	^{77}481	^{50}8	$^{(203)}$5433	$^{(207)}$5418	$^{(174)}$10144	-	-	$^{30}3.65N^{1.0}$
99	Line Corporation	line	001	2021-11-21	471	396	^{155}2048	-	^{214}907	^{51}8	$^{(171)}$1872	$^{(175)}$1934	$^{(148)}$3647	$^{(149)}$7675	-	$^{110}0.64N^{1.0}$
100	Lomonosov Moscow State University	intsysmsu	000	2019-08-19	375	168	^{110}2048	1	^{104}614	^{106}13	$^{(80)}$430	$^{(82)}$431	$^{(63)}$860	$^{(62)}$1730	$^{(78)}$5353	$^{160}0.03N^{1.1}$
101	Lookman Electroplast Industries	lookman	3	2018-10-28	203	24	^{20}292	1	^{34}336	^{13}3	$^{(115)}$739	$^{(113)}$745	$^{(89)}$1394	$^{(88)}$2817	$^{(99)}$8286	$^{138}0.13N^{1.1}$
102	Lookman Electroplast Industries	lookman	4	2018-10-28	184	24	^{42}548	1	^{32}320	^{22}4	$^{(131)}$981	$^{(132)}$998	-	-	-	
103	Lookman Electroplast Industries	lookman	005	2019-09-16	239	36	^{43}548	1	^{82}506	^{18}4	$^{(133)}$1005	$^{(134)}$1008	$^{(128)}$2597	$^{(127)}$5446	$^{(105)}$8939	$^{136}0.19N^{1.1}$
104	Mantra Softech India	mantra	000	2021-10-28	460	61	^{173}2052	-	^{57}412	^{76}10	$^{(129)}$916	$^{(129)}$910	$^{(101)}$1714	$^{(99)}$3411	$^{(95)}$6841	$^{36}0.57N^{1.0}$

Notes	
1	Configuration size does not capture static data present in libraries. Libraries are included but the size also includes any ancillary libraries for image processing (e.g. openCV) or numerical computation (e.g. blas).
2	Finalization is the processing of converting N = 1600000 templates into a searchable data structure an operation which can be a simple copy, or the building of an index or tree, for example. The duration of the operation may be data dependent, and may not be linear in the number of input templates.
3	This multiplier expresses the increase in template size when k images are passed to the template generation function.
4	All durations are measured on Intel®Xeon®CPU E5-2630 v4 @ 2.20GHz processors. Estimates are made by wrapping the API function call in calls to std::chrono::high_resolution_clock which on the machine in (3) counts 1ns clock ticks. Precision is somewhat worse than that however.
5	Search durations are measured as in the prior note. The power-law model in the final column mostly fits the empirical results in Figure 136. However in certain cases the model is not correct and should not be used numerically.

Table 3: Summary of algorithms and properties included in this report. The blue superscripts give ranking for the quantity in that column. Missing search durations, denoted by "-", are absent because those runs were not executed, usually because we did not run on the larger galleries. Caution: The power-law model is sometimes an incorrect model. It is included here only to show broad sublinear behavior, which is flagged in green. The models should not be used for prediction.

	DEVELOPER	SHORT	SEQ.	VALIDATION	CONFIG[1]	LIB[1]	TEMPLATE GENERATION			FINALIZE[2]	SEARCH DURATION[5] MILLISEC					
	FULL NAME	NAME	NUM.	DATE	DATA (MB)	DATA (MB)	SIZE (B)	MULT[3]	TIME (MS)[4]	TIME (S)	L=1	L=50	L=50	L=50	L=50	POWER LAW
										N=1.6M	N=1.6M	N=1.6M	N=3M	N=6M	N=12M	(μs)
105	Megvii/Face++	megvii	1	2018-10-28	1703	41	^{201}4096	1	^{108}631	^{186}32	$^{(95)}$552	$^{(98)}$561	$^{(82)}$1222	$^{(78)}$2321	$^{(85)}$5968	$^{144}0.08N^{1.1}$
106	Megvii/Face++	megvii	2	2018-10-28	1735	42	^{212}4096	1	^{111}635	^{184}31	$^{(96)}$553	$^{(95)}$558	-	-	-	
107	MicroFocus	microfocus	5	2018-10-29	94	26	^{15}256	k	^{25}262	^{8}2	$^{(38)}$182	$^{(37)}$186	$^{(29)}$354	$^{(29)}$708	$^{(25)}$1425	$^{53}0.11N^{1.0}$
108	MicroFocus	microfocus	6	2018-10-29	94	26	^{13}256	k	^{24}262	^{10}2	$^{(39)}$183	$^{(36)}$186	-	-	-	
109	Microsoft	microsoft	5	2018-10-29	381	155	^{54}1024	1	^{119}658	^{91}11	$^{(158)}$1606	$^{(164)}$1673	$^{(139)}$3076	$^{(136)}$6302	$^{(139)}$13160	$^{72}0.79N^{1.0}$
110	Microsoft	microsoft	6	2018-10-29	478	155	^{53}1024	1	^{123}671	^{127}15	$^{(161)}$1642	$^{(162)}$1618	$^{(150)}$3710	$^{(138)}$6401	$^{(137)}$12892	$^{91}0.68N^{1.0}$
111	N-Tech Lab	ntech	5	2018-10-30	1685	113	^{89}1940	k	^{144}711	^{202}55	$^{(47)}$243	$^{(48)}$246	$^{(41)}$538	$^{(41)}$1100	$^{(49)}$2867	$^{156}0.02N^{1.1}$
112	N-Tech Lab	ntech	6	2018-10-30	1686	117	^{88}1940	k	^{181}831	^{204}63	$^{(46)}$243	$^{(47)}$246	$^{(43)}$546	$^{(42)}$1104	$^{(50)}$2873	$^{158}0.02N^{1.1}$
113	N-Tech Lab	ntechlab	007	2019-06-25	2450	51	^{200}3348	k	^{171}795	^{207}73	$^{(73)}$393	$^{(81)}$427	$^{(58)}$780	$^{(65)}$1768	$^{(61)}$3499	$^{100}0.16N^{1.0}$
114	N-Tech Lab	ntechlab	008	2020-01-06	1111	51	^{74}1300	k	^{90}554	^{192}36	$^{(37)}$179	$^{(34)}$184	$^{(28)}$341	$^{(28)}$683	$^{(24)}$1395	$^{48}0.11N^{1.0}$
115	N-Tech Lab	ntechlab	009	2021-03-01	1208	42	^{75}1300	-	^{209}899	^{190}35	$^{(36)}$178	$^{(35)}$184	$^{(27)}$336	$^{(27)}$676	$^{(31)}$1704	$^{121}0.05N^{1.1}$
116	N-Tech Lab	ntechlab	010	2021-06-24	351	213	^{72}1280	-	^{197}874	^{30}6	$^{(81)}$440	$^{(83)}$435	$^{(59)}$821	$^{(60)}$1645	$^{(58)}$3337	$^{67}0.22N^{1.0}$
117	N-Tech Lab	ntechlab	011	2021-12-07	679	208	^{73}1280	-	^{191}864	^{32}6	$^{(86)}$488	$^{(85)}$483	$^{(66)}$912	$^{(68)}$1869	$^{(73)}$5003	$^{140}0.07N^{1.1}$
118	NEC	nec	2	2018-10-30	705	35	^{84}1616	k	^{115}642	^{151}18	$^{(74)}$405	$^{(78)}$409	$^{(72)}$1072	$^{(63)}$1755	$^{(68)}$4255	$^{147}0.06N^{1.1}$
119	NEC	nec	3	2018-10-30	774	110	^{85}1712	k	^{121}665	^{159}21	$^{(4)}$7	$^{(3)}$7	$^{(5)}$14	$^{(9)}$40	$^{(10)}$82	$^{166}0.00N^{1.2}$
120	NEC	nec	004	2021-07-19	971	63	^{70}1104	-	^{228}965	^{33}7	$^{(66)}$349	$^{(67)}$351	$^{(53)}$662	$^{(51)}$1330	$^{(45)}$2685	$^{56}0.20N^{1.0}$
121	NEC	nec	005	2021-12-13	922	88	^{69}1104	-	^{227}961	^{34}7	$^{(84)}$473	$^{(93)}$551	$^{(70)}$1017	$^{(71)}$2091	$^{(66)}$4242	$^{64}0.28N^{1.0}$
122	Neurotechnology	neurotech	5	2018-10-30	266	53	^{14}256	k	^{51}402	^{9}2	$^{(123)}$835	$^{(124)}$839	$^{(100)}$1690	$^{(98)}$3219	$^{(106)}$8955	$^{127}0.19N^{1.1}$
123	Neurotechnology	neurotech	6	2018-10-30	564	53	^{12}256	k	^{148}726	^{7}2	$^{(124)}$839	$^{(125)}$842	-	-	-	
124	Neurotechnology	neurotech	007	2019-10-03	57	51	^{8}256	k	^{7}161	^{6}2	$^{(139)}$1118	$^{(139)}$1110	$^{(113)}$2143	$^{(108)}$4397	$^{(107)}$9045	$^{71}0.55N^{1.0}$
125	Neurotechnology	neurotechnology	008	2021-03-22	355	49	^{37}514	-	^{172}800	^{21}4	$^{(142)}$1167	$^{(142)}$1149	$^{(115)}$2266	$^{(113)}$4573	$^{(114)}$9586	$^{79}0.55N^{1.0}$
126	Neurotechnology	neurotechnology	009	2021-09-01	246	82	^{36}513	-	^{129}683	^{11}3	$^{(136)}$1035	$^{(136)}$1049	$^{(109)}$1977	$^{(106)}$4270	$^{(102)}$8756	$^{114}0.32N^{1.1}$
127	Neurotechnology	neurotechnology	010	2022-01-07	247	83	^{10}256	-	^{120}661	^{2}2	$^{(132)}$988	$^{(130)}$984	$^{(104)}$1897	$^{(103)}$3977	$^{(98)}$8048	$^{105}0.36N^{1.0}$
128	Neurotechnology	neurotechnology	012	2022-06-07	247	84	^{11}256	-	^{132}686	^{12}3	$^{(137)}$1036	$^{(138)}$1063	$^{(110)}$2046	$^{(105)}$4179	$^{(101)}$8624	$^{101}0.41N^{1.0}$
129	Newland Computer Co Ltd	newland	2	2018-10-30	96	27	^{103}2048	-	^{189}855	^{129}15	$^{(219)}$8741	$^{(224)}$8854	$^{(189)}$17892	$^{(186)}$39356	-	$^{142}1.32N^{1.1}$
130	Noblis	noblis	1	2018-10-30	114	176	^{145}2048	1	^{17}206	^{125}15	$^{(149)}$1273	$^{(146)}$1272	-	-	-	
131	Noblis	noblis	2	2018-10-30	153	176	^{220}6144	1	^{85}517	^{195}43	$^{(185)}$2513	$^{(190)}$2522	$^{(163)}$5649	$^{(164)}$12432	$^{(170)}$44262	$^{178}0.04N^{1.3}$
132	NotionTag Technologies Private Limited	notiontag	000	2022-01-14	265	945	^{191}2120	-	^{67}453	^{80}10	$^{(218)}$8619	$^{(223)}$8705	$^{(188)}$16652	$^{(185)}$38794	$^{(182)}$90607	$^{146}1.15N^{1.1}$
133	Pangiam	pangiam	000	2022-02-22	453	23	^{153}2048	-	^{112}636	^{146}17	$^{(51)}$276	$^{(63)}$319	$^{(48)}$601	$^{(47)}$1210	$^{(42)}$2443	$^{54}0.18N^{1.0}$
134	Paravision (EverAI)	everai	2	2018-10-30	224	304	^{104}2048	1	^{39}366	^{181}30	$^{(53)}$278	$^{(57)}$283	-	-	-	
135	Paravision (EverAI)	everai	3	2018-10-30	438	304	^{119}2048	1	^{145}717	^{174}28	$^{(52)}$278	$^{(56)}$281	$^{(45)}$572	$^{(43)}$1146	$^{(39)}$2278	$^{93}0.12N^{1.0}$
136	Paravision (EverAI)	everai-paravision	004	2019-06-19	527	128	^{204}4096	1	^{124}672	^{198}45	$^{(97)}$559	$^{(96)}$559	$^{(130)}$2611	$^{(139)}$6445	$^{(143)}$14519	$^{186}0.00N^{1.5}$
137	Paravision (EverAI)	paravision	005	2019-12-11	543	154	^{206}4096	1	^{180}830	^{200}48	$^{(99)}$561	$^{(99)}$564	$^{(71)}$1056	$^{(75)}$2298	$^{(72)}$4966	$^{118}0.16N^{1.1}$
138	Paravision (EverAI)	paravision	007	2021-02-01	529	235	^{213}4096	-	^{139}701	^{201}48	$^{(101)}$569	$^{(94)}$558	$^{(73)}$1086	$^{(72)}$2111	$^{(67)}$4254	$^{21}1.11N^{0.9}$
139	Paravision	paravision	009	2021-12-14	672	300	^{214}4100	-	^{109}631	^{209}82	$^{(197)}$3690	$^{(202)}$4230	$^{(171)}$8037	$^{(170)}$16532	$^{(166)}$31422	$^{95}1.62N^{1.0}$
140	Qnap Security	qnap	000	2021-07-28	182	15	^{113}2048	-	^{68}457	^{65}9	$^{(144)}$1231	$^{(168)}$1763	-	-	-	
141	Qnap Security	qnap	001	2021-12-09	191	13	^{122}2048	-	^{103}613	^{46}8	$^{(163)}$1666	$^{(156)}$1429	$^{(144)}$3472	$^{(146)}$7375	$^{(149)}$15159	$^{163}0.11N^{1.2}$
142	Qnap Security	qnap	002	2022-04-15	338	32	^{149}2048	-	^{176}822	^{143}17	$^{(130)}$958	$^{(143)}$1179	$^{(117)}$2312	$^{(116)}$4789	$^{(121)}$9791	$^{129}0.24N^{1.1}$
143	Quantasoft	quantasoft	1	2018-10-30	276	452	^{123}2048	k	^{47}385	^{31}6	$^{(220)}$15422	$^{(225)}$14858	$^{(186)}$14717	-	$^{(153)}$18323	
144	Rank One Computing	rankone	4	2018-10-09	0	101	^{1}85	k	^{3}36	^{35}7	$^{(24)}$101	$^{(24)}$101	$^{(19)}$190	-	-	$^{28}0.07N^{1.0}$
145	Rank One Computing	rankone	5	2018-10-24	0	101	^{5}133	k	^{4}92	^{36}7	$^{(29)}$140	$^{(29)}$144	$^{(24)}$266	$^{(23)}$525	$^{(22)}$1049	$^{25}0.11N^{1.0}$
146	Rank One Computing	rankone	006	2019-06-03	0	133	^{6}165	k	^{22}245	^{44}8	-	-	-	-	-	
147	Rank One Computing	rankone	007	2019-11-12	0	137	^{7}165	k	^{26}272	^{39}7	$^{(25)}$116	$^{(25)}$115	$^{(21)}$215	$^{(21)}$439	$^{(19)}$877	$^{52}0.07N^{1.0}$
148	Rank One Computing	rankone	009	2020-06-26	0	105	^{16}260	k	^{12}185	^{87}11	$^{(18)}$95	$^{(21)}$96	$^{(16)}$181	$^{(16)}$362	$^{(17)}$727	$^{38}0.06N^{1.0}$
149	Rank One Computing	rankone	010	2020-11-05	0	135	^{18}261	-	^{15}198	^{81}10	$^{(19)}$95	$^{(16)}$95	$^{(14)}$178	$^{(14)}$357	$^{(15)}$714	$^{34}0.06N^{1.0}$
150	Rank One Computing	rankone	011	2021-08-27	0	175	^{19}261	-	^{94}566	^{52}8	$^{(21)}$96	$^{(18)}$95	$^{(17)}$183	$^{(17)}$370	$^{(14)}$714	$^{46}0.06N^{1.0}$
151	Rank One Computing	rankone	012	2021-12-27	0	257	^{17}261	-	^{93}563	^{41}8	$^{(20)}$95	$^{(19)}$95	$^{(15)}$179	$^{(15)}$361	$^{(16)}$718	$^{37}0.06N^{1.0}$
152	Realnetworks Inc	realnetworks	2	2018-10-30	105	104	^{217}4104	k	^{21}241	^{173}28	$^{(173)}$2008	$^{(179)}$2048	$^{(153)}$4194	$^{(152)}$8642	$^{(148)}$15035	$^{65}1.08N^{1.0}$
153	Realnetworks Inc	realnetworks	003	2019-06-12	93	102	^{87}1848	k	^{10}173	^{99}13	$^{(141)}$1145	$^{(140)}$1132	$^{(112)}$2142	$^{(124)}$5241	$^{(125)}$10495	$^{133}0.21N^{1.1}$
154	Realnetworks Inc	realnetworks	004	2019-10-17	94	102	^{86}1848	1	^{9}171	^{86}11	$^{(140)}$1143	$^{(141)}$1137	$^{(114)}$2149	$^{(115)}$4740	$^{(117)}$9693	$^{113}0.36N^{1.0}$
155	Realnetworks Inc	realnetworks	005	2021-06-23	168	209	^{183}2056	-	^{33}332	^{58}9	$^{(162)}$1654	$^{(161)}$1616	$^{(138)}$3030	$^{(134)}$6068	$^{(134)}$12134	$^{43}1.01N^{1.0}$
156	Realnetworks Inc	realnetworks	006	2021-12-02	250	56	^{181}2056	-	^{37}348	^{47}8	$^{(94)}$543	$^{(91)}$531	$^{(69)}$996	$^{(70)}$1998	$^{(65)}$3991	$^{41}0.33N^{1.0}$

Notes	
1	Configuration size does not capture static data present in libraries. Libraries are included but the size also includes any ancillary libraries for image processing (e.g. openCV) or numerical computation (e.g. blas).
2	Finalization is the processing of converting N = 1600000 templates into a searchable data structure an operation which can be a simple copy, or the building of an index or tree, for example. The duration of the operation may be data dependent, and may not be linear in the number of input templates.
3	This multiplier expresses the increase in template size when k images are passed to the template generation function.
4	All durations are measured on Intel®Xeon®CPU E5-2630 v4 @ 2.20GHz processors. Estimates are made by wrapping the API function call in calls to std::chrono::high_resolution_clock which on the machine in (3) counts 1ns clock ticks. Precision is somewhat worse than that however.
5	Search durations are measured as in the prior note. The power-law model in the final column mostly fits the empirical results in Figure 136. However in certain cases the model is not correct and should not be used numerically.

Table 4: Summary of algorithms and properties included in this report. The blue superscripts give ranking for the quantity in that column. Missing search durations, denoted by "-", are absent because those runs were not executed, usually because we did not run on the larger galleries. Caution: The power-law model is sometimes an incorrect model. It is included here only to show broad sublinear behavior, which is flagged in green. The models should not be used for prediction.

This publication is available free of charge from: https://doi.org/10.6028/NIST.IR.8271

	DEVELOPER	SHORT	SEQ.	VALIDATION	CONFIG[1]	LIB[1]	TEMPLATE GENERATION			FINALIZE[2]	SEARCH DURATION[5] MILLISEC					
	FULL NAME	NAME	NUM.	DATE	DATA (MB)	DATA (MB)	SIZE (B)	MULT[3]	TIME (MS)[4]	TIME (S)	L=1	L=50	L=50	L=50	L=50	POWER LAW
										N=1.6M	N=1.6M	N=1.6M	N=3M	N=6M	N=12M	(μs)
157	Realnetworks Inc	realnetworks	007	2022-04-11	455	99	^{180}2056	-	^{110}634	^{144}17	$^{(122)}$815	$^{(122)}$812	$^{(97)}$1559	$^{(96)}$3159	$^{(92)}$6361	$^{109}0.27N^{1.0}$
158	Remark Holdings	remarkai	0	2018-10-30	187	847	^{140}2048	k	^{97}593	^{118}14	$^{(206)}$5685	$^{(210)}$5723	-	-	-	
159	Remark Holdings	remarkai	000	2019-06-12	234	1092	^{107}2048	k	^{117}650	^{98}12	$^{(207)}$5776	$^{(209)}$5703	$^{(177)}$11604	$^{(184)}$32133	$^{(183)}$91436	$^{179}0.05N^{1.3}$
160	Remark Holdings	remarkai	1	2018-10-30	187	847	^{115}2048	k	^{60}427	^{122}14	$^{(205)}$5680	$^{(211)}$5761	$^{(180)}$12475	$^{(182)}$28726	$^{(180)}$59618	$^{168}0.37N^{1.2}$
161	Rendip	rendip	000	2021-05-21	0	416	^{108}2048	-	^{204}890	^{68}9	$^{(48)}$249	$^{(69)}$368	$^{(56)}$697	$^{(56)}$1452	$^{(52)}$2926	$^{124}0.08N^{1.1}$
162	Reveal Media Ltd	revealmedia	000	2022-02-02	287	196	^{158}2052	-	^{46}383	^{75}10	$^{(177)}$2322	$^{(176)}$2019	$^{(152)}$3838	$^{(150)}$7816	$^{(152)}$16559	$^{98}0.78N^{1.0}$
163	SQIsoft	sqisoft	001	2021-12-20	271	377	^{176}2056	-	^{71}462	^{66}9	$^{(152)}$1310	$^{(151)}$1319	$^{(122)}$2456	$^{(118)}$4906	$^{(120)}$9755	$^{29}0.90N^{1.0}$
164	Samsung S1 Corp	s1	000	2021-06-03	257	196	^{203}4096	-	^{192}865	^{156}20	$^{(214)}$6715	$^{(219)}$6794	$^{(184)}$13032	$^{(180)}$26372	$^{(178)}$55723	$^{90}2.82N^{1.0}$
165	Samsung S1 Corp	s1	001	2021-11-01	240	198	^{96}2048	-	^{174}813	^{53}8	$^{(179)}$2415	$^{(188)}$2491	$^{(160)}$4718	$^{(158)}$9614	$^{(162)}$24472	$^{128}0.53N^{1.1}$
166	Samsung S1 Corp	s1	002	2022-05-04	244	93	^{106}2048	-	^{226}958	^{135}16	$^{(145)}$1234	$^{(147)}$1285	$^{(119)}$2411	$^{(117)}$4805	$^{(118)}$9705	$^{49}0.77N^{1.0}$
167	Scanovate Ltd	scanovate	000	2020-01-15	250	446	^{124}2048	-	^{141}705	^{120}14	$^{(156)}$1419	$^{(155)}$1412	$^{(137)}$3008	$^{(161)}$11616	$^{(132)}$12012	$^{169}0.10N^{1.2}$
168	Scanovate Ltd	scanovate	001	2020-09-10	250	446	^{92}2048	-	^{126}675	^{104}13	$^{(153)}$1321	$^{(152)}$1320	$^{(125)}$2502	$^{(121)}$5047	$^{(122)}$10163	$^{68}0.65N^{1.0}$
169	Sensetime Group	sensetime	0	2018-10-30	525	6	^{218}4104	k	^{137}693	^{194}41	$^{(88)}$498	$^{(87)}$501	$^{(81)}$1212	$^{(74)}$2281	$^{(74)}$5032	$^{139}0.09N^{1.1}$
170	Sensetime Group	sensetime	1	2018-10-30	525	6	^{216}4104	k	^{107}628	^{199}48	$^{(91)}$516	$^{(88)}$502	$^{(76)}$1146	$^{(76)}$2301	$^{(70)}$4765	$^{137}0.09N^{1.1}$
171	Sensetime Group	sensetime	002	2019-06-03	523	6	^{179}2056	k	^{100}603	^{149}18	$^{(67)}$359	$^{(70)}$370	$^{(105)}$1897	$^{(111)}$4508	$^{(113)}$9543	$^{189}0.00N^{1.5}$
172	Sensetime Group	sensetime	003	2019-12-02	769	76	^{177}2056	1	^{215}910	^{153}19	$^{(201)}$4885	$^{(206)}$4989	$^{(179)}$12325	$^{(176)}$24712	$^{(173)}$49445	$^{149}0.67N^{1.1}$
173	Sensetime Group	sensetime	004	2020-08-10	456	29	^{58}1032	-	^{134}690	^{97}12	$^{(184)}$2490	$^{(185)}$2477	$^{(158)}$4654	$^{(157)}$9402	$^{(160)}$19651	$^{70}1.22N^{1.0}$
174	Sensetime Group	sensetime	005	2020-12-17	631	39	^{59}1032	-	^{229}980	^{85}11	$^{(181)}$2459	$^{(200)}$3939	$^{(169)}$7398	$^{(167)}$14768	$^{(158)}$19016	$^{19}14.03N^{0.9}$
175	Sensetime Group	sensetime	006	2021-07-26	526	54	^{62}1032	-	^{217}929	^{40}7	$^{(178)}$2414	$^{(184)}$2422	$^{(156)}$4527	$^{(154)}$9128	$^{(154)}$18640	$^{59}1.35N^{1.0}$
176	Sensetime Group	sensetime	007	2022-01-15	526	37	^{60}1032	-	^{220}935	^{54}8	$^{(180)}$2432	$^{(183)}$2406	$^{(155)}$4513	$^{(153)}$8998	$^{(156)}$18796	$^{63}1.28N^{1.0}$
177	Shaman Software	shaman	6	2018-10-26	0	200	^{131}2048	k	^{142}706	^{119}14	$^{(104)}$603	$^{(103)}$612	-	-	-	
178	Shaman Software	shaman	7	2018-10-26	0	200	^{101}2048	k	^{143}707	^{121}14	$^{(103)}$602	$^{(104)}$614	$^{(77)}$1187	$^{(81)}$2448	$^{(77)}$5083	$^{94}0.25N^{1.0}$
179	Shanghai Yitu Technology	yitu	4	2018-10-30	2119	136	^{188}2070	1	^{208}897	^{197}45	$^{(150)}$1288	$^{(145)}$1203	$^{(121)}$2440	$^{(125)}$5241	$^{(116)}$9671	$^{89}0.52N^{1.0}$
180	Shanghai Yitu Technology	yitu	5	2018-10-30	2043	136	^{187}2070	1	^{188}853	^{196}44	$^{(146)}$1237	$^{(144)}$1199	$^{(126)}$2513	$^{(120)}$5013	$^{(115)}$9620	$^{85}0.55N^{1.0}$
181	Smilart	smilart	4	2018-10-30	65	89	^{27}512	k	^{8}167	^{20}4	$^{(221)}$16137	$^{(226)}$15633	-	-	-	
182	Smilart	smilart	5	2018-10-30	562	89	^{93}2048	k	^{65}450	^{117}14	-	-	-	-	-	
183	Staqu Technologies	staqu	000	2021-08-30	1018	690	^{205}4096	-	^{178}826	^{168}24	$^{(202)}$4950	$^{(205)}$4933	-	-	-	
184	Synesis	synesis	3	2018-10-30	237	150	^{202}4096	k	^{5}99	^{177}29	$^{(118)}$789	$^{(120)}$801	$^{(108)}$1941	$^{(102)}$3888	$^{(103)}$8810	$^{157}0.07N^{1.1}$
185	Synesis	synesis	003	2019-07-04	143	17	^{91}2048	k	^{18}211	^{94}12	$^{(90)}$507	$^{(89)}$502	$^{(116)}$2297	$^{(112)}$4564	$^{(111)}$9452	$^{184}0.00N^{1.4}$
186	Synesis	synesis	005	2020-09-08	494	24	^{215}4104	-	^{156}756	^{166}24	$^{(126)}$877	$^{(126)}$865	$^{(141)}$3182	$^{(114)}$4658	$^{(119)}$9750	$^{170}0.06N^{1.2}$
187	Tech5 SA	tech5	001	2019-08-19	1394	116	^{78}1536	k	^{203}887	^{74}10	$^{(70)}$383	$^{(117)}$766	$^{(132)}$2767	$^{(135)}$6149	$^{(88)}$6178	$^{148}0.12N^{1.1}$
188	Tech5 SA	tech5	002	2021-04-07	727	112	^{35}513	-	^{222}940	^{16}4	$^{(200)}$4682	$^{(217)}$6689	$^{(181)}$12541	$^{(177)}$25145	$^{(175)}$50239	$^{40}4.18N^{1.0}$
189	Tencent Deepsea Lab	deepsea	001	2019-07-29	250	323	^{100}2048	1	^{153}737	^{96}12	$^{(135)}$1021	$^{(135)}$1020	$^{(133)}$2774	$^{(131)}$5767	$^{(135)}$12341	$^{175}0.06N^{1.2}$
190	Tevian	tevian	5	2018-10-30	773	15	^{109}2048	1	^{54}405	^{126}15	$^{(75)}$405	$^{(77)}$408	$^{(61)}$854	$^{(64)}$1757	$^{(60)}$3380	$^{112}0.14N^{1.0}$
191	Tevian	tevian	006	2021-04-16	769	19	^{56}1032	-	^{98}597	^{73}10	$^{(60)}$295	$^{(60)}$295	$^{(46)}$578	$^{(45)}$1187	$^{(48)}$2741	$^{125}0.06N^{1.1}$
192	Tevian	tevian	007	2021-10-12	703	19	^{61}1032	-	^{163}777	^{24}4	$^{(61)}$297	$^{(61)}$298	$^{(47)}$579	$^{(44)}$1179	$^{(41)}$2418	$^{104}0.11N^{1.0}$
193	Thales	cogent	2	2018-10-30	681	39	^{66}1043	k	^{224}945	^{171}27	$^{(174)}$2017	$^{(181)}$2144	$^{(154)}$4298	$^{(151)}$8472	$^{(151)}$16429	$^{69}1.08N^{1.0}$
194	Thales	cogent	3	2018-10-30	681	39	^{65}1043	k	^{221}940	^{70}9	$^{(143)}$1230	$^{(150)}$1311	$^{(131)}$2687	$^{(126)}$5398	$^{(123)}$10184	$^{80}0.62N^{1.0}$
195	Thales	cogent	004	2021-02-10	1376	59	^{175}2053	-	^{225}947	^{111}14	$^{(189)}$2903	$^{(173)}$1911	$^{(145)}$3566	$^{(147)}$7498	$^{(150)}$16370	$^{111}0.64N^{1.0}$
196	Thales	cogent	005	2021-09-13	1043	56	^{67}1062	-	^{161}769	^{28}5	$^{(128)}$912	$^{(131)}$996	$^{(103)}$1872	$^{(101)}$3845	$^{(96)}$7555	$^{82}0.44N^{1.0}$
197	Thales	cogent	006	2022-05-14	508	70	^{44}550	-	^{184}843	^{42}8	$^{(102)}$587	$^{(123)}$820	$^{(98)}$1564	$^{(97)}$3173	$^{(100)}$8290	$^{132}0.16N^{1.1}$
198	TigerIT Americas LLC	tiger	2	2018-10-29	416	518	^{172}2052	k	^{70}461	^{130}15	$^{(169)}$1816	$^{(174)}$1921	$^{(151)}$3833	$^{(148)}$7526	$^{(146)}$14820	$^{87}0.83N^{1.0}$
199	TigerIT Americas LLC	tiger	3	2018-10-30	416	518	^{168}2052	k	^{69}461	^{228}37431	$^{(40)}$191	$^{(38)}$189	-	-	-	
200	Toshiba	toshiba	0	2018-10-30	961	105	^{83}1548	k	^{199}876	^{92}12	$^{(211)}$6153	$^{(213)}$6236	$^{(178)}$12221	$^{(178)}$25355	$^{(174)}$49448	$^{164}0.36N^{1.2}$
201	Toshiba	toshiba	1	2018-10-30	961	105	^{185}2060	k	^{198}875	^{229}44701	$^{(210)}$6007	$^{(215)}$6355	-	-	-	
202	Tripleize	aize	001	2021-08-06	262	150	^{128}2048	-	^{50}402	^{62}9	$^{(192)}$3087	$^{(195)}$3080	-	-	-	
203	Trueface.ai	trueface	000	2021-01-27	247	119	^{90}2000	-	^{38}363	^{102}13	$^{(50)}$271	$^{(66)}$327	$^{(50)}$614	$^{(48)}$1239	$^{(44)}$2678	$^{77}0.15N^{1.0}$
204	Veridas Digital Authentication Solutions S.L.	veridas	001	2021-03-05	347	875	^{156}2048	-	^{195}872	^{103}13	$^{(204)}$5493	$^{(208)}$5469	$^{(175)}$10350	$^{(173)}$20655	$^{(169)}$41264	$^{44}3.40N^{1.0}$
205	Veridas Digital Authentication Solutions S.L.	veridas	002	2021-07-06	347	870	^{98}2048	-	^{200}877	^{83}10	$^{(64)}$322	$^{(64)}$325	$^{(55)}$685	$^{(53)}$1365	$^{(47)}$2730	$^{119}0.09N^{1.1}$
206	Veridas Digital Authentication Solutions S.L.	veridas	003	2021-11-09	346	870	^{132}2048	-	^{193}867	^{56}9	$^{(83)}$440	$^{(65)}$327	$^{(57)}$699	$^{(54)}$1401	$^{(64)}$3954	$^{167}0.02N^{1.2}$
207	Vietnam Posts and Telecommunications Group	vnpt	001	2022-05-05	361	235	^{99}2048	-	^{206}892	^{157}20	$^{(121)}$813	$^{(121)}$804	$^{(95)}$1514	$^{(94)}$3037	$^{(86)}$6128	$^{42}0.50N^{1.0}$
208	Viettel Group	vts	000	2021-03-12	250	257	^{126}2048	-	^{80}492	^{214}2295	$^{(3)}$4	$^{(2)}$4	$^{(2)}$6	$^{(4)}$11	-	$^{13}0.61N^{0.6}$

Notes	
1	Configuration size does not capture static data present in libraries. Libraries are included but the size also includes any ancillary libraries for image processing (e.g. openCV) or numerical computation (e.g. blas).
2	Finalization is the processing of converting N = 1600000 templates into a searchable data structure an operation which can be a simple copy, or the building of an index or tree, for example. The duration of the operation may be data dependent, and may not be linear in the number of input templates.
3	This multiplier expresses the increase in template size when k images are passed to the template generation function.
4	All durations are measured on Intel®Xeon®CPU E5-2630 v4 @ 2.20GHz processors. Estimates are made by wrapping the API function call in calls to std::chrono::high_resolution_clock which on the machine in (3) counts 1ns clock ticks. Precision is somewhat worse than that however.
5	Search durations are measured as in the prior note. The power-law model in the final column mostly fits the empirical results in Figure 136. However in certain cases the model is not correct and should not be used numerically.

Table 5: Summary of algorithms and properties included in this report. The blue superscripts give ranking for the quantity in that column. Missing search durations, denoted by "-", are absent because those runs were not executed, usually because we did not run on the larger galleries. Caution: The power-law model is sometimes an incorrect model. It is included here only to show broad sublinear behavior, which is flagged in green. The models should not be used for prediction.

This publication is available free of charge from: https://doi.org/10.6028/NIST.IR.8271

	DEVELOPER	SHORT	SEQ.	VALIDATION	CONFIG[1]	LIB[1]	TEMPLATE GENERATION			FINALIZE[2]	SEARCH DURATION[5] MILLISEC					
	FULL NAME	NAME	NUM.	DATE	DATA (MB)	DATA (MB)	SIZE (B)	MULT[3]	TIME (MS)[4]	TIME (S)	L=1	L=50	L=50	L=50	L=50	POWER LAW
										N=1.6M	N=1.6M	N=1.6M	N=3M	N=6M	N=12M	(μs)
209	Viettel Group	vts	001	2021-07-16	352	600	[116]2048	-	[205]891	[162]21	(182)2477	(187)2487	(157)4644	(155)9313	(155)18713	[45]$1.53N^{1.0}$
210	Viettel Group	vts	002	2022-02-08	244	600	[133]2048	-	[210]903	[178]29	(183)2485	(186)2485	(159)4678	(156)9370	(157)18833	[50]$1.49N^{1.0}$
211	Vigilant Solutions	vigilant	5	2018-10-30	335	122	[80]1544	k	[158]762	[152]19	-	(166)1720	-	-	-	
212	Vigilant Solutions	vigilant	6	2018-10-30	337	122	[82]1544	k	[178]816	[160]21	-	(165)1713	-	-	-	
213	Vigilant Solutions	vigilantsolutions	007	2021-01-08	340	51	[79]1544	-	[105]616	[142]16	(155)1354	(154)1352	(135)2911	(133)5966	(129)11466	[131]$0.27N^{1.1}$
214	Vigilant Solutions	vigilantsolutions	008	2021-07-23	340	51	[81]1544	-	[52]403	[107]13	(138)1062	(137)1061	(118)2330	(129)5520	(112)9499	[153]$0.11N^{1.1}$
215	Visidon	visidon	1	2018-10-30	166	42	[159]2052	k	[122]667	[132]15	(198)4370	(204)4472	(172)8454	(171)17262	(167)34288	[62]$2.40N^{1.0}$
216	Visidon	vd	002	2021-05-18	248	42	[171]2052	-	[133]687	[57]9	(175)2089	(182)2336	-	-	-	
217	Visidon	vd	003	2021-10-12	497	43	[170]2052	-	[136]692	[48]8	(176)2095	(180)2082	-	-	-	
218	Visiob-Box	visionbox	000	2021-09-17	252	274	[184]2059	-	[78]481	[141]16	(78)422	(68)359	(62)855	(26)631	(37)2096	[17]$2.46N^{0.8}$
219	VisionLabs	visionlabs	6	2018-10-30	360	17	[26]512	1	[28]289	[225]20290	(15)36	(14)36	(12)39	(11)44	(9)53	[8]$3211.93N^{0.2}$
220	VisionLabs	visionlabs	7	2018-10-30	360	17	[34]512	1	[30]289	[227]34666	(16)63	(15)63	(13)72	(13)80	(11)115	[10]$2076.32N^{0.2}$
221	VisionLabs	visionlabs	008	2019-06-18	348	17	[30]512	1	[27]272	[223]12747	(10)23	(8)24	(7)26	(6)29	(5)33	[6]$2539.61N^{0.2}$
222	VisionLabs	visionlabs	009	2020-08-04	689	20	[28]512	-	[73]467	[224]13245	(11)23	(9)29	(9)34	(12)61	(12)145	[12]$8.88N^{0.6}$
223	VisionLabs	visionlabs	010	2021-02-05	1042	20	[29]512	-	[150]731	[219]11837	(8)21	(11)32	(10)36	(8)39	(6)43	[7]$3183.79N^{0.2}$
224	VisionLabs	visionlabs	011	2021-10-20	1042	20	[31]512	-	[152]735	[222]12255	(9)21	(7)23	(8)26	(7)34	(8)51	[11]$301.26N^{0.3}$
225	Vocord	vocord	5	2018-10-30	1035	185	[46]768	k	[165]780	[38]7	(34)158	(39)204	(30)383	(31)767	(26)1466	[47]$0.12N^{1.0}$
226	Vocord	vocord	6	2018-10-30	1035	185	[229]10240	k	[166]785	[213]243	(35)170	(42)216	-	-	-	
227	Xforward AI Technology	xforwardai	000	2020-07-24	236	171	[134]2048	-	[155]753	[109]13	(199)4603	(222)7647	(187)15723	(175)23900	(177)53729	[154]$0.56N^{1.1}$
228	Xforward AI Technology	xforwardai	001	2021-01-21	332	50	[105]2048	-	[128]677	[139]16	(209)5887	(203)4384	(173)8798	(172)18553	(172)48993	[161]$0.32N^{1.1}$
229	Xforward AI Technology	xforwardai	002	2021-05-24	691	50	[211]4096	-	[218]930	[150]18	(216)6957	(216)6400	(182)12659	(183)31077	(181)65158	[159]$0.52N^{1.1}$

Notes	
1	Configuration size does not capture static data present in libraries. Libraries are included but the size also includes any ancillary libraries for image processing (e.g. openCV) or numerical computation (e.g. blas).
2	Finalization is the processing of converting N = 1600000 templates into a searchable data structure an operation which can be a simple copy, or the building of an index or tree, for example. The duration of the operation may be data dependent, and may not be linear in the number of input templates.
3	This multiplier expresses the increase in template size when k images are passed to the template generation function.
4	All durations are measured on Intel®Xeon®CPU E5-2630 v4 @ 2.20GHz processors. Estimates are made by wrapping the API function call in calls to std::chrono::high_resolution_clock which on the machine in (3) counts 1ns clock ticks. Precision is somewhat worse than that however.
5	Search durations are measured as in the prior note. The power-law model in the final column mostly fits the empirical results in Figure 136. However in certain cases the model is not correct and should not be used numerically.

Table 6: Summary of algorithms and properties included in this report. The blue superscripts give ranking for the quantity in that column. Missing search durations, denoted by "-", are absent because those runs were not executed, usually because we did not run on the larger galleries. Caution: The power-law model is sometimes an incorrect model. It is included here only to show broad sublinear behavior, which is flagged in green. The models should not be used for prediction.

MISS RATES		INVESTIGATION, FNIR(N, R = 1, T = 0)								IDENTIFICATION, FNIR(N, R = L, T $\geq$ 0) FOR FPIR = 0.001							
#	ALGORITHM	(0, 2]	(2, 4]	(4, 6]	(6, 8]	(8, 10]	(10, 12]	(12, 14]	(14, 18]	(0, 2]	(2, 4]	(4, 6]	(6, 8]	(8, 10]	(10, 12]	(12, 14]	(14, 18]
1	3DIVI-005	^{98}0.0207	^{97}0.0304	^{97}0.0415	^{97}0.0533	^{97}0.0646	^{114}0.0735	^{114}0.0884	^{115}0.1148	^{101}0.1580	^{98}0.2316	^{98}0.3033	^{98}0.3740	^{98}0.4285	^{115}0.4742	^{116}0.5329	^{114}0.5975
2	ANKE-000	^{95}0.0162	^{95}0.0245	^{95}0.0333	^{95}0.0428	^{95}0.0515	^{112}0.0615	^{112}0.0780	^{111}0.1028	^{96}0.1132	^{96}0.1761	^{96}0.2402	^{96}0.3057	^{95}0.3640	^{112}0.4200	^{112}0.4928	^{112}0.5680
3	ANKE-002	^{49}0.0055	^{50}0.0074	^{50}0.0090	^{49}0.0103	^{48}0.0116	^{66}0.0135	^{65}0.0162	^{64}0.0202	^{54}0.0329	^{54}0.0560	^{56}0.0843	^{57}0.1169	^{57}0.1481	^{73}0.1820	^{74}0.2280	^{73}0.2831
4	AWARE-005	^{106}0.0328	^{106}0.0519	^{106}0.0712	^{104}0.0910	^{104}0.1078	^{121}0.1235	^{121}0.1457	^{121}0.1831	^{106}0.3605	^{107}0.4949	^{107}0.5948	^{107}0.6783	^{108}0.7393	^{125}0.7905	^{125}0.8408	^{126}0.8831
5	AWARE-006	^{110}0.0702	^{110}0.1110	^{110}0.1502	^{110}0.1899	^{110}0.2253	^{128}0.2614	^{127}0.3045	^{127}0.3659								
6	AYONIX-002	^{113}0.3360	^{114}0.4389	^{114}0.5144	^{114}0.5814	^{114}0.6340	^{131}0.6818	^{131}0.7297	^{132}0.7774	^{110}0.8288	^{111}0.9013	^{111}0.9375	^{111}0.9603	^{111}0.9744	^{129}0.9837	^{129}0.9893	^{129}0.9927
7	CAMVI-004	^{109}0.0623	^{109}0.0944	^{109}0.1243	^{109}0.1548	^{108}0.1812	^{125}0.2056	^{125}0.2344	^{123}0.2672	^{91}0.0810	^{91}0.1267	^{88}0.1721	^{88}0.2203	^{88}0.2619	^{103}0.3040	^{102}0.3543	^{98}0.4124
8	CAMVI-005	^{111}0.0849	^{111}0.1255	^{111}0.1631	^{111}0.1989	^{111}0.2298	^{127}0.2585	^{126}0.2915	^{126}0.3246								
9	CANON-001						^{25}0.0052	^{24}0.0057	^{19}0.0042						^{29}0.0491	^{29}0.0606	^{30}0.0826
10	CIB-000	^{14}0.0022	^{14}0.0030	^{15}0.0037	^{15}0.0044	^{17}0.0049	^{29}0.0057	^{29}0.0069	^{29}0.0062	^{25}0.0139	^{26}0.0240	^{27}0.0373	^{28}0.0525	^{28}0.0689	^{39}0.0859	^{40}0.1109	^{40}0.1454
11	CLEARVIEWAI-000	^{4}0.0017	^{4}0.0023	^{4}0.0028	^{9}0.0034	^{11}0.0039	^{19}0.0046	^{23}0.0056	^{24}0.0047	^{16}0.0066	^{18}0.0121	^{18}0.0194	^{19}0.0287	^{19}0.0385	^{30}0.0493	^{32}0.0662	^{32}0.0873
12	CLOUDWALK-HR-000	^{8}0.0019	^{7}0.0024	^{8}0.0029	^{6}0.0032	^{5}0.0032	^{5}0.0036	^{5}0.0041	^{3}0.0020	^{1}0.0029	^{1}0.0041	^{1}0.0054	^{1}0.0064	^{2}0.0073	^{4}0.0085	^{4}0.0102	^{4}0.0112
13	CLOUDWALK-MT-000						^{7}0.0037	^{2}0.0038	^{1}0.0013						^{1}0.0065	^{1}0.0072	^{1}0.0075
14	COGENT-000	^{90}0.0128	^{90}0.0184	^{93}0.0250	^{92}0.0327	^{92}0.0407	^{108}0.0488	^{107}0.0611	^{107}0.0794	^{77}0.0559	^{78}0.0923	^{76}0.1342	^{76}0.1812	^{75}0.2243	^{91}0.2675	^{90}0.3240	^{94}0.3992
15	COGENT-001	^{91}0.0128	^{91}0.0184	^{92}0.0250	^{93}0.0327	^{93}0.0407	^{109}0.0488	^{108}0.0611	^{106}0.0794	^{78}0.0559	^{79}0.0923	^{77}0.1342	^{77}0.1812	^{76}0.2243	^{92}0.2675	^{91}0.3240	^{95}0.3992
16	COGENT-002	^{69}0.0081	^{66}0.0105	^{63}0.0123	^{64}0.0137	^{62}0.0157	^{79}0.0175	^{77}0.0215	^{77}0.0280	^{69}0.0499	^{68}0.0827	^{67}0.1207	^{67}0.1639	^{67}0.2037	^{83}0.2432	^{84}0.2972	^{85}0.3638
17	COGENT-003	^{71}0.0082	^{67}0.0108	^{65}0.0128	^{67}0.0145	^{66}0.0168	^{85}0.0191	^{86}0.0239	^{83}0.0312	^{80}0.0582	^{80}0.0971	^{80}0.1417	^{80}0.1918	^{80}0.2380	^{98}0.2836	^{100}0.3440	^{101}0.4207
18	COGENT-004	^{59}0.0066	^{53}0.0080	^{45}0.0085	^{39}0.0080	^{31}0.0083	^{47}0.0092	^{48}0.0106	^{51}0.0130	^{63}0.0410	^{65}0.0720	^{65}0.1099	^{65}0.1539	^{64}0.1974	^{84}0.2443	^{87}0.3043	^{87}0.3757
19	COGENT-006						^{17}0.0045	^{15}0.0049	^{16}0.0038						^{24}0.0370	^{20}0.0448	^{20}0.0602
20	COGNITEC-000	^{105}0.0265	^{103}0.0423	^{103}0.0588	^{103}0.0757	^{102}0.0894	^{119}0.1014	^{119}0.1169	^{118}0.1381	^{100}0.1522	^{99}0.2330	^{99}0.3051	^{99}0.3751	^{99}0.4300	^{116}0.4779	^{115}0.5307	^{113}0.5913
21	COGNITEC-001	^{93}0.0149	^{94}0.0228	^{94}0.0312	^{94}0.0399	^{94}0.0479	^{111}0.0546	^{110}0.0656	^{108}0.0806	^{93}0.0963	^{93}0.1562	^{93}0.2157	^{93}0.2771	^{93}0.3287	^{110}0.3771	^{109}0.4343	^{108}0.4959
22	COGNITEC-002	^{77}0.0101	^{80}0.0138	^{81}0.0170	^{81}0.0201	^{81}0.0237	^{97}0.0264	^{95}0.0309	^{94}0.0389	^{72}0.0517	^{71}0.0879	^{72}0.1269	^{73}0.1707	^{71}0.2098	^{85}0.2463	^{83}0.2919	^{83}0.3535
23	COGNITEC-003	^{78}0.0104	^{81}0.0140	^{82}0.0174	^{82}0.0205	^{82}0.0238	^{98}0.0266	^{96}0.0311	^{96}0.0401	^{71}0.0504	^{70}0.0855	^{69}0.1235	^{69}0.1662	^{68}0.2045	^{82}0.2403	^{82}0.2854	^{81}0.3451
24	COGNITEC-004	^{64}0.0073	^{63}0.0099	^{62}0.0118	^{59}0.0130	^{59}0.0147	^{78}0.0163	^{74}0.0189	^{73}0.0239	^{53}0.0325	^{53}0.0548	^{52}0.0798	^{51}0.1074	^{50}0.1325	^{67}0.1591	^{64}0.1952	^{63}0.2414
25	COGNITEC-006						^{41}0.0081	^{39}0.0086	^{40}0.0090						^{36}0.0777	^{36}0.0926	^{36}0.1274
26	CUBOX-000	^{7}0.0019	^{5}0.0024	^{5}0.0028	^{4}0.0031	^{4}0.0032	^{6}0.0037	^{9}0.0044	^{9}0.0027	^{6}0.0039	^{6}0.0059	^{7}0.0083	^{8}0.0111	^{8}0.0141	^{13}0.0185	^{13}0.0252	^{13}0.0339
27	CYBERLINK-002	^{50}0.0055	^{45}0.0068	^{41}0.0075	^{35}0.0078	^{32}0.0084	^{48}0.0094	^{49}0.0107	^{47}0.0114	^{32}0.0180	^{33}0.0302	^{33}0.0460	^{32}0.0643	^{33}0.0837	^{48}0.1058	^{47}0.1370	^{47}0.1787
28	CYBERLINK-003	^{35}0.0041	^{34}0.0052	^{27}0.0057	^{25}0.0058	^{25}0.0061	^{38}0.0068	^{35}0.0078	^{37}0.0078	^{19}0.0109	^{19}0.0175	^{20}0.0259	^{21}0.0356	^{21}0.0468	^{33}0.0594	^{33}0.0787	^{34}0.1072
29	DAHUA-002	^{30}0.0035	^{28}0.0047	^{28}0.0058	^{27}0.0067	^{28}0.0074	^{42}0.0082	^{45}0.0100	^{44}0.0108	^{30}0.0169	^{32}0.0294	^{31}0.0449	^{30}0.0635	^{30}0.0817	^{45}0.1013	^{44}0.1291	^{43}0.1638
30	DAHUA-003	^{19}0.0026	^{19}0.0036	^{19}0.0043	^{20}0.0050	^{20}0.0055	^{31}0.0062	^{37}0.0080	^{32}0.0073	^{29}0.0160	^{30}0.0280	^{29}0.0432	^{29}0.0615	^{29}0.0794	^{43}0.0987	^{43}0.1270	^{41}0.1587
31	DEEPGLINT-001	^{17}0.0024	^{16}0.0032	^{14}0.0037	^{13}0.0040	^{13}0.0043	^{23}0.0049	^{25}0.0060	^{25}0.0052	^{12}0.0058	^{10}0.0087	^{11}0.0119	^{11}0.0155	^{11}0.0199	^{16}0.0249	^{16}0.0338	^{16}0.0463
32	DEEPSEA-001	^{70}0.0081	^{70}0.0116	^{73}0.0149	^{76}0.0182	^{76}0.0216	^{96}0.0260	^{98}0.0332	^{98}0.0432	^{66}0.0458	^{66}0.0752	^{64}0.1086	^{63}0.1460	^{63}0.1812	^{80}0.2186	^{80}0.2663	^{79}0.3213
33	DERMALOG-006	^{82}0.0113	^{82}0.0142	^{78}0.0163	^{77}0.0183	^{74}0.0200	^{90}0.0218	^{88}0.0251	^{86}0.0329	^{73}0.0545	^{73}0.0889	^{73}0.1271	^{72}0.1697	^{70}0.2090	^{87}0.2498	^{86}0.3028	^{86}0.3670
34	DERMALOG-007	^{88}0.0125	^{88}0.0170	^{88}0.0214	^{88}0.0264	^{87}0.0309	^{103}0.0356	^{104}0.0432	^{104}0.0579	^{92}0.0910	^{92}0.1453	^{92}0.2009	^{92}0.2602	^{92}0.3134	^{109}0.3649	^{108}0.4289	^{109}0.5007
35	DERMALOG-008	^{52}0.0057	^{52}0.0077	^{54}0.0095	^{54}0.0110	^{53}0.0128	^{72}0.0148	^{71}0.0180	^{72}0.0223	^{70}0.0501	^{69}0.0850	^{70}0.1247	^{71}0.1692	^{72}0.2105	^{88}0.2541	^{88}0.3102	^{88}0.3762
36	FUJITSULAB-001						^{46}0.0089	^{44}0.0098	^{46}0.0111						^{57}0.1403	^{56}0.1723	^{54}0.2165
37	GORILLA-002	^{100}0.0213	^{100}0.0359	^{101}0.0528	^{102}0.0716	^{103}0.0895	^{120}0.1088	^{120}0.1367	^{120}0.1765	^{103}0.1828	^{104}0.2787	^{104}0.3654	^{104}0.4485	^{104}0.5168	^{119}0.5823	^{119}0.6508	^{119}0.7180
38	GORILLA-005	^{38}0.0044	^{47}0.0070	^{58}0.0102	^{62}0.0136	^{67}0.0170	^{88}0.0204	^{91}0.0272	^{93}0.0373	^{79}0.0566	^{81}0.0973	^{82}0.1432	^{81}0.1937	^{81}0.2398	^{100}0.2862	^{99}0.3437	^{99}0.4150
39	GORILLA-007						^{57}0.0108	^{54}0.0128	^{52}0.0145						^{75}0.1862	^{73}0.2198	^{69}0.2716
40	IDEMIA-003	^{81}0.0110	^{86}0.0151	^{86}0.0196	^{85}0.0238	^{84}0.0281	^{101}0.0313	^{101}0.0368	^{100}0.0504	^{87}0.0717	^{86}0.1147	^{86}0.1614	^{86}0.2113	^{85}0.2553	^{102}0.2976	^{101}0.3537	^{102}0.4334
41	IDEMIA-004	^{80}0.0107	^{84}0.0148	^{85}0.0192	^{84}0.0233	^{83}0.0277	^{100}0.0312	^{100}0.0367	^{101}0.0512	^{58}0.0373	^{55}0.0587	^{54}0.0833	^{53}0.1100	^{52}0.1340	^{66}0.1580	^{63}0.1911	^{64}0.2482
42	IDEMIA-005	^{84}0.0118	^{87}0.0167	^{90}0.0218	^{89}0.0270	^{88}0.0317	^{104}0.0357	^{103}0.0425	^{103}0.0579	^{65}0.0440	^{64}0.0689	^{60}0.0964	^{59}0.1254	^{58}0.1513	^{72}0.1762	^{67}0.2113	^{67}0.2698
43	IDEMIA-006	^{87}0.0124	^{89}0.0171	^{89}0.0218	^{87}0.0263	^{86}0.0302	^{102}0.0321	^{99}0.0356	^{99}0.0471	^{62}0.0409	^{59}0.0620	^{57}0.0850	^{52}0.1097	^{49}0.1309	^{60}0.1486	^{58}0.1738	^{57}0.2200
44	IDEMIA-007	^{47}0.0050	^{48}0.0071	^{48}0.0089	^{50}0.0106	^{51}0.0124	^{68}0.0142	^{68}0.0171	^{70}0.0220	^{36}0.0202	^{36}0.0335	^{34}0.0491	^{33}0.0663	^{31}0.0825	^{44}0.0999	^{41}0.1240	^{44}0.1645

Table 7: **Accuracy for the FRVT 2018 mugshot sets under ageing**. *The second row shows the time lapse between gallery and subsequent probe images, in years. The first two columns identify the algorithm The next 8 values give rank-based FNIR with R = 1, T = 0 and FPIR = 1. All these are relevant to investigational uses where candidates from all searches would need human review. The second 8 values give threshold-based FNIR with T $\geq$ 0, FPIR = 0.001 and no rank criterion. The shaded cells indictate indicate the three most accurate algorithms for that elapsed time. The gallery size is 3068801. The total number of searches is 10951064.*

MISS RATES		INVESTIGATION, FNIR(N, R = 1, T = 0)								IDENTIFICATION, FNIR(N, R = L, T $\geq$ 0) FOR FPIR = 0.001							
#	ALGORITHM	(0, 2]	(2, 4]	(4, 6]	(6, 8]	(8, 10]	(10, 12]	(12, 14]	(14, 18]	(0, 2]	(2, 4]	(4, 6]	(6, 8]	(8, 10]	(10, 12]	(12, 14]	(14, 18]
45	IDEMIA-008	^{5}0.0018	^{6}0.0024	^{6}0.0029	^{5}0.0032	^{7}0.0035	^{9}0.0039	^{12}0.0046	^{12}0.0033	^{3}0.0034	^{3}0.0051	^{5}0.0069	^{5}0.0087	^{5}0.0102	^{8}0.0123	^{7}0.0146	^{7}0.0186
46	IDEMIA-009						^{11}0.0040	^{6}0.0042	^{6}0.0024						^{5}0.0094	^{5}0.0103	^{5}0.0123
47	IMAGUS-005	^{33}0.0039	^{33}0.0052	^{31}0.0061	^{29}0.0067	^{30}0.0077	^{45}0.0088	^{46}0.0103	^{45}0.0109	^{39}0.0212	^{39}0.0357	^{40}0.0539	^{40}0.0755	^{38}0.0967	^{53}0.1183	^{52}0.1485	^{50}0.1893
48	IMPERIAL-000	^{34}0.0040	^{35}0.0054	^{36}0.0067	^{38}0.0079	^{40}0.0093	^{58}0.0112	^{57}0.0139	^{59}0.0178	^{49}0.0286	^{51}0.0503	^{51}0.0779	^{54}0.1116	^{56}0.1455	^{74}0.1844	^{77}0.2341	^{76}0.2951
49	INCODE-003	^{94}0.0155	^{96}0.0247	^{96}0.0348	^{96}0.0463	^{96}0.0571	^{113}0.0674	^{113}0.0856	^{114}0.1114	^{102}0.1627	^{102}0.2507	^{102}0.3322	^{100}0.4122	^{100}0.4772	^{118}0.5368	^{118}0.6059	^{118}0.6766
50	INCODE-004	^{56}0.0061	^{59}0.0087	^{59}0.0110	^{61}0.0136	^{64}0.0161	^{81}0.0185	^{84}0.0236	^{82}0.0309	^{73}0.0532	^{74}0.0908	^{75}0.1334	^{75}0.1809	^{77}0.2245	^{93}0.2675	^{92}0.3249	^{91}0.3932
51	INNOVATRICS-004	^{114}0.3594	^{113}0.3629	^{113}0.3688	^{112}0.3754	^{112}0.3813	^{129}0.3870	^{129}0.3960	^{129}0.4135	^{107}0.4234	^{106}0.4642	^{106}0.5073	^{106}0.5522	^{105}0.5902	^{122}0.6274	^{120}0.6736	^{120}0.7253
52	INNOVATRICS-005	^{41}0.0046	^{41}0.0063	^{42}0.0078	^{45}0.0092	^{45}0.0106	^{60}0.0124	^{60}0.0149	^{60}0.0178	^{55}0.0343	^{56}0.0590	^{58}0.0886	^{58}0.1222	^{59}0.1544	^{77}0.1881	^{76}0.2321	^{74}0.2874
53	IREX-000	^{24}0.0031	^{24}0.0042	^{25}0.0051	^{26}0.0060	^{26}0.0068	^{40}0.0080	^{42}0.0095	^{43}0.0107	^{52}0.0313	^{52}0.0539	^{53}0.0815	^{56}0.1137	^{55}0.1442	^{71}0.1755	^{72}0.2181	^{70}0.2718
54	ISYSTEMS-002	^{76}0.0101	^{79}0.0135	^{80}0.0169	^{79}0.0197	^{80}0.0228	^{94}0.0256	^{94}0.0304	^{95}0.0398	^{90}0.0779	^{90}0.1258	^{91}0.1759	^{90}0.2299	^{90}0.2758	^{106}0.3204	^{106}0.3763	^{104}0.4401
55	ISYSTEMS-003	^{75}0.0089	^{69}0.0115	^{69}0.0139	^{69}0.0158	^{70}0.0177	^{87}0.0198	^{83}0.0234	^{80}0.0303	^{84}0.0647	^{84}0.1056	^{84}0.1502	^{84}0.1986	^{83}0.2402	^{96}0.2819	^{95}0.3351	^{93}0.3976
56	KEDACOM-001	^{83}0.0116	^{73}0.0130	^{67}0.0135	^{60}0.0133	^{57}0.0135	^{67}0.0141	^{61}0.0151	^{58}0.0176	^{41}0.0241	^{41}0.0360	^{39}0.0513	^{34}0.0689	^{34}0.0866	^{49}0.1060	^{45}0.1327	^{45}0.1694
57	LOOKMAN-003	^{86}0.0123	^{83}0.0144	^{77}0.0158	^{70}0.0168	^{71}0.0178	^{83}0.0188	^{76}0.0212	^{76}0.0260	^{64}0.0438	^{62}0.0687	^{61}0.0978	^{61}0.1296	^{60}0.1581	^{76}0.1879	^{75}0.2294	^{72}0.2756
58	LOOKMAN-005	^{85}0.0118	^{77}0.0134	^{70}0.0142	^{66}0.0144	^{61}0.0150	^{77}0.0160	^{69}0.0176	^{67}0.0213	^{51}0.0310	^{49}0.0480	^{46}0.0698	^{46}0.0954	^{46}0.1216	^{62}0.1491	^{62}0.1890	^{62}0.2381
59	MICROFOCUS-005	^{115}0.4269	^{115}0.5527	^{115}0.6355	^{116}0.7024	^{116}0.7503	^{133}0.7876	^{133}0.8234	^{134}0.8601	^{111}0.8338	^{112}0.9113	^{112}0.9468	^{112}0.9667	^{112}0.9771	^{128}0.9836	^{128}0.9880	^{128}0.9924
60	MICROSOFT-003	^{28}0.0034	^{32}0.0050	^{33}0.0064	^{36}0.0078	^{38}0.0092	^{54}0.0107	^{56}0.0135	^{57}0.0166	^{50}0.0288	^{50}0.0503	^{50}0.0763	^{50}0.1067	^{54}0.1359	^{69}0.1680	^{68}0.2116	^{66}0.2644
61	MICROSOFT-004	^{25}0.0032	^{27}0.0047	^{29}0.0060	^{32}0.0075	^{35}0.0087	^{51}0.0103	^{55}0.0131	^{55}0.0159	^{47}0.0268	^{48}0.0470	^{49}0.0716	^{48}0.1007	^{48}0.1291	^{68}0.1610	^{66}0.2052	^{65}0.2590
62	MICROSOFT-005	^{22}0.0031	^{29}0.0047	^{35}0.0066	^{43}0.0084	^{43}0.0103	^{64}0.0131	^{66}0.0164	^{62}0.0185	^{43}0.0243	^{44}0.0432	^{44}0.0658	^{44}0.0913	^{45}0.1172	^{59}0.1476	^{61}0.1874	^{59}0.2272
63	MICROSOFT-006	^{26}0.0032	^{31}0.0049	^{34}0.0065	^{42}0.0081	^{42}0.0096	^{59}0.0117	^{58}0.0144	^{56}0.0160	^{24}0.0134	^{24}0.0233	^{25}0.0346	^{23}0.0462	^{22}0.0578	^{35}0.0713	^{35}0.0903	^{35}0.1156
64	NEC-000	^{97}0.0195	^{99}0.0316	^{99}0.0445	^{99}0.0581	^{98}0.0699	^{116}0.0817	^{116}0.0998	^{116}0.1237	^{89}0.0759	^{89}0.1245	^{89}0.1729	^{89}0.2240	^{89}0.2671	^{105}0.3117	^{103}0.3639	^{103}0.4348
65	NEC-001	^{104}0.0246	^{102}0.0382	^{100}0.0524	^{100}0.0672	^{101}0.0793	^{118}0.0904	^{117}0.1076	^{117}0.1317	^{94}0.1019	^{94}0.1623	^{94}0.2214	^{94}0.2834	^{94}0.3341	^{111}0.3844	^{111}0.4440	^{110}0.5183
66	NEC-002	^{27}0.0033	^{22}0.0041	^{18}0.0043	^{16}0.0044	^{15}0.0045	^{22}0.0049	^{22}0.0056	^{18}0.0041	^{15}0.0066	^{11}0.0090	^{10}0.0111	^{10}0.0131	^{9}0.0149	^{11}0.0171	^{12}0.0207	^{12}0.0267
67	NEC-003	^{31}0.0036	^{26}0.0046	^{24}0.0051	^{24}0.0055	^{24}0.0059	^{33}0.0067	^{33}0.0077	^{35}0.0073	^{9}0.0056	^{9}0.0076	^{9}0.0091	^{7}0.0105	^{6}0.0119	^{10}0.0137	^{9}0.0162	^{9}0.0209
68	NEC-004	^{32}0.0039	^{25}0.0045	^{22}0.0047	^{18}0.0046	^{14}0.0044	^{21}0.0046	^{20}0.0052	^{15}0.0036	^{7}0.0046	^{5}0.0057	^{2}0.0063	^{2}0.0066	^{1}0.0069	^{2}0.0076	^{2}0.0090	^{2}0.0105
69	NEC-005						^{8}0.0037	^{4}0.0041	^{4}0.0020						^{3}0.0080	^{3}0.0091	^{3}0.0107
70	NEUROTECHNOLOGY-003	^{101}0.0234	^{101}0.0379	^{102}0.0549	^{101}0.0682	^{100}0.0720	^{115}0.0747	^{115}0.0886	^{113}0.1066	^{109}0.6802	^{109}0.8187	^{110}0.8920	^{110}0.9355	^{110}0.9594	^{127}0.9738	^{127}0.9828	^{127}0.9885
71	NEUROTECHNOLOGY-004	^{79}0.0104	^{78}0.0134	^{76}0.0156	^{73}0.0173	^{72}0.0195	^{89}0.0212	^{87}0.0245	^{84}0.0320	^{83}0.0642	^{82}0.1015	^{81}0.1426	^{79}0.1881	^{78}0.2299	^{94}0.2722	^{93}0.3269	^{92}0.3943
72	NEUROTECHNOLOGY-005	^{74}0.0089	^{71}0.0116	^{68}0.0136	^{68}0.0152	^{69}0.0173	^{86}0.0196	^{82}0.0233	^{81}0.0306	^{76}0.0556	^{76}0.0913	^{74}0.1315	^{74}0.1766	^{74}0.2192	^{90}0.2617	^{89}0.3174	^{89}0.3843
73	NEUROTECHNOLOGY-007	^{66}0.0078	^{65}0.0103	^{64}0.0124	^{65}0.0140	^{63}0.0161	^{80}0.0185	^{79}0.0225	^{78}0.0290	^{82}0.0641	^{85}0.1069	^{85}0.1546	^{85}0.2075	^{86}0.2572	^{104}0.3081	^{105}0.3713	^{105}0.4421
74	NEUROTECHNOLOGY-010						^{26}0.0053	^{26}0.0061	^{27}0.0053						^{40}0.0863	^{38}0.1050	^{38}0.1333
75	NOBLIS-002	^{112}0.1520	^{112}0.2419	^{112}0.3296	^{113}0.4114	^{113}0.4856	^{130}0.5528	^{130}0.6061	^{130}0.6532	^{113}0.9984	^{113}0.9996	^{113}0.9998	^{113}0.9999	^{113}0.9999	^{130}1.0000	^{133}1.0000	^{132}1.0000
76	NTECHLAB-003	^{65}0.0078	^{76}0.0131	^{87}0.0202	^{90}0.0295	^{91}0.0405	^{110}0.0543	^{111}0.0761	^{112}0.1035	^{68}0.0491	^{72}0.0881	^{79}0.1384	^{83}0.1985	^{87}0.2594	^{107}0.3270	^{107}0.4065	^{107}0.4891
77	NTECHLAB-004	^{62}0.0068	^{68}0.0110	^{79}0.0167	^{86}0.0239	^{89}0.0330	^{107}0.0447	^{109}0.0641	^{110}0.0891	^{60}0.0379	^{63}0.0688	^{66}0.1108	^{66}0.1629	^{73}0.2192	^{99}0.2846	^{104}0.3657	^{106}0.4524
78	NTECHLAB-006	^{51}0.0056	^{62}0.0095	^{72}0.0148	^{83}0.0218	^{85}0.0301	^{105}0.0413	^{106}0.0591	^{109}0.0814	^{56}0.0349	^{60}0.0636	^{63}0.1023	^{64}0.1506	^{66}0.2024	^{89}0.2617	^{96}0.3374	^{100}0.4185
79	NTECHLAB-007	^{37}0.0044	^{43}0.0066	^{49}0.0089	^{57}0.0118	^{60}0.0150	^{84}0.0189	^{89}0.0255	^{89}0.0342	^{45}0.0256	^{46}0.0450	^{48}0.0705	^{49}0.1012	^{51}0.1334	^{70}0.1692	^{69}0.2170	^{71}0.2752
80	NTECHLAB-008	^{18}0.0025	^{21}0.0038	^{26}0.0052	^{31}0.0074	^{44}0.0104	^{69}0.0146	^{85}0.0236	^{90}0.0348	^{26}0.0143	^{28}0.0267	^{32}0.0459	^{37}0.0733	^{40}0.1062	^{58}0.1469	^{65}0.2044	^{68}0.2698
81	NTECHLAB-009	^{13}0.0022	^{15}0.0031	^{16}0.0038	^{17}0.0045	^{19}0.0055	^{35}0.0067	^{40}0.0088	^{42}0.0100	^{18}0.0073	^{17}0.0117	^{17}0.0170	^{17}0.0238	^{18}0.0319	^{26}0.0419	^{27}0.0577	^{31}0.0833
82	NTECHLAB-011						^{28}0.0056	^{27}0.0066	^{33}0.0073						^{20}0.0351	^{21}0.0475	^{25}0.0724
83	PANGIAM-000						^{24}0.0051	^{21}0.0055	^{22}0.0046						^{32}0.0503	^{31}0.0617	^{29}0.0810
84	PARAVISION-002	^{53}0.0058	^{58}0.0083	^{60}0.0111	^{63}0.0137	^{65}0.0162	^{82}0.0187	^{81}0.0229	^{79}0.0295								
85	PARAVISION-003	^{44}0.0048	^{44}0.0067	^{51}0.0090	^{52}0.0109	^{54}0.0128	^{70}0.0148	^{70}0.0178	^{69}0.0219	^{57}0.0354	^{58}0.0618	^{59}0.0931	^{60}0.1290	^{61}0.1625	^{78}0.1964	^{78}0.2408	^{75}0.2924
86	PARAVISION-004	^{16}0.0024	^{17}0.0032	^{17}0.0040	^{19}0.0047	^{18}0.0053	^{30}0.0061	^{31}0.0073	^{31}0.0072	^{20}0.0118	^{23}0.0209	^{24}0.0327	^{24}0.0465	^{24}0.0613	^{37}0.0779	^{37}0.1008	^{37}0.1285
87	PARAVISION-005	^{12}0.0021	^{13}0.0028	^{13}0.0035	^{14}0.0041	^{16}0.0046	^{27}0.0054	^{28}0.0067	^{30}0.0070	^{11}0.0057	^{12}0.0093	^{12}0.0144	^{14}0.0207	^{15}0.0278	^{22}0.0368	^{24}0.0508	^{24}0.0715
88	PARAVISION-007	^{6}0.0019	^{8}0.0025	^{7}0.0029	^{8}0.0033	^{8}0.0036	^{14}0.0042	^{14}0.0049	^{11}0.0030	^{10}0.0057	^{13}0.0094	^{14}0.0144	^{13}0.0206	^{14}0.0275	^{21}0.0357	^{22}0.0485	^{21}0.0652

Table 8: **Accuracy for the FRVT 2018 mugshot sets under ageing**. *The second row shows the time lapse between gallery and subsequent probe images, in years. The first two columns identify the algorithm The next 8 values give rank-based FNIR with R = 1, T = 0 and FPIR = 1. All these are relevant to investigational uses where candidates from all searches would need human review. The second 8 values give threshold-based FNIR with T $\geq$ 0, FPIR = 0.001 and no rank criterion. The shaded cells indictate indicate the three most accurate algorithms for that elapsed time. The gallery size is 3068801. The total number of searches is 10951064.*

FNIR(N, R, T) = False neg. identification rate
FPIR(N, T) = False pos. identification rate
N = Num. enrolled subjects
R = Num. candidates examined
T = Threshold
T = 0 → Investigation
T > 0 → Identification

MISS RATES		INVESTIGATION, FNIR(N, R = 1, T = 0)								IDENTIFICATION, FNIR(N, R = L, T ≥ 0) FOR FPIR = 0.001							
#	ALGORITHM	(0, 2]	(2, 4]	(4, 6]	(6, 8]	(8, 10]	(10, 12]	(12, 14]	(14, 18]	(0, 2]	(2, 4]	(4, 6]	(6, 8]	(8, 10]	(10, 12]	(12, 14]	(14, 18]
89	PARAVISION-009						^{12}0.0041	^{10}0.0046	^{8}0.0026						^{18}0.0283	^{18}0.0371	^{18}0.0525
90	PIXELALL-002	^{72}0.0085	^{73}0.0119	^{71}0.0147	^{72}0.0172	^{73}0.0198	^{91}0.0225	^{90}0.0270	^{91}0.0349	^{97}0.1193	^{97}0.1900	^{97}0.2601	^{97}0.3332	^{97}0.3955	^{114}0.4565	^{114}0.5268	^{115}0.6030
91	PIXELALL-003	^{46}0.0050	^{42}0.0063	^{39}0.0072	^{34}0.0077	^{33}0.0085	^{49}0.0095	^{50}0.0113	^{48}0.0119	^{44}0.0248	^{43}0.0418	^{43}0.0622	^{43}0.0861	^{43}0.1104	^{55}0.1364	^{55}0.1723	^{55}0.2167
92	PIXELALL-004	^{45}0.0049	^{40}0.0063	^{40}0.0072	^{37}0.0079	^{36}0.0089	^{53}0.0103	^{53}0.0127	^{53}0.0146	^{38}0.0211	^{40}0.0360	^{42}0.0553	^{42}0.0792	^{39}0.1045	^{54}0.1317	^{54}0.1700	^{58}0.2246
93	PTAKURATSATU-000	^{54}0.0061	^{55}0.0082	^{55}0.0097	^{53}0.0109	^{49}0.0120	^{63}0.0131	^{59}0.0146	^{61}0.0180	^{59}0.0375	^{57}0.0596	^{55}0.0842	^{55}0.1116	^{53}0.1357	^{65}0.1553	^{59}0.1820	^{61}0.2326
94	RANKONE-002	^{99}0.0212	^{98}0.0313	^{98}0.0431	^{98}0.0562	^{99}0.0712	^{117}0.0881	^{118}0.1130	^{119}0.1543	^{95}0.1111	^{95}0.1707	^{95}0.2305	^{95}0.2968	^{96}0.3646	^{113}0.4345	^{113}0.5172	^{116}0.6110
95	RANKONE-004	^{108}0.0424	^{107}0.0643	^{107}0.0875	^{107}0.1127	^{107}0.1364	^{122}0.1579	^{122}0.1914	^{122}0.2378	^{104}0.1855	^{103}0.2681	^{103}0.3431	^{101}0.4155	^{101}0.4785	^{117}0.5350	^{117}0.5980	^{117}0.6722
96	RANKONE-005	^{92}0.0136	^{93}0.0192	^{91}0.0246	^{91}0.0303	^{90}0.0362	^{106}0.0422	^{105}0.0521	^{105}0.0694	^{81}0.0582	^{75}0.0910	^{71}0.1260	^{68}0.1645	^{65}0.2005	^{81}0.2353	^{81}0.2816	^{82}0.3522
97	RANKONE-007	^{67}0.0078	^{64}0.0099	^{61}0.0113	^{58}0.0123	^{58}0.0139	^{76}0.0156	^{75}0.0191	^{74}0.0242	^{42}0.0242	^{42}0.0376	^{41}0.0542	^{38}0.0737	^{37}0.0935	^{51}0.1130	^{49}0.1416	^{49}0.1811
98	RANKONE-009	^{48}0.0054	^{49}0.0072	^{46}0.0085	^{47}0.0098	^{47}0.0113	^{62}0.0130	^{67}0.0169	^{71}0.0220	^{37}0.0208	^{38}0.0345	^{37}0.0504	^{36}0.0706	^{36}0.0930	^{52}0.1174	^{53}0.1504	^{52}0.2002
99	RANKONE-010	^{42}0.0047	^{38}0.0061	^{38}0.0070	^{33}0.0076	^{34}0.0087	^{50}0.0098	^{51}0.0113	^{49}0.0120	^{31}0.0177	^{29}0.0269	^{26}0.0368	^{26}0.0479	^{23}0.0590	^{34}0.0688	^{34}0.0803	^{33}0.0991
100	RANKONE-011	^{23}0.0031	^{23}0.0041	^{23}0.0047	^{23}0.0053	^{22}0.0058	^{36}0.0067	^{32}0.0077	^{34}0.0073	^{23}0.0127	^{20}0.0194	^{21}0.0265	^{20}0.0345	^{20}0.0422	^{31}0.0499	^{30}0.0611	^{27}0.0756
101	RANKONE-012						^{32}0.0065	^{30}0.0069	^{26}0.0053						^{27}0.0460	^{25}0.0540	^{22}0.0672
102	REALNETWORKS-002	^{107}0.0381	^{108}0.0687	^{108}0.1062	^{108}0.1495	^{109}0.1963	^{126}0.2513	^{128}0.3206	^{128}0.3927	^{105}0.2153	^{105}0.3323	^{105}0.4444	^{105}0.5485	^{106}0.6355	^{123}0.7132	^{124}0.7855	^{124}0.8437
103	REALNETWORKS-003	^{103}0.0245	^{105}0.0437	^{105}0.0686	^{106}0.0975	^{106}0.1312	^{124}0.1719	^{124}0.2294	^{125}0.2907	^{98}0.1468	^{100}0.2370	^{101}0.3313	^{103}0.4269	^{103}0.5142	^{121}0.5979	^{122}0.6815	^{122}0.7567
104	REALNETWORKS-004	^{102}0.0244	^{104}0.0428	^{104}0.0663	^{105}0.0939	^{105}0.1251	^{123}0.1634	^{123}0.2170	^{124}0.2785	^{99}0.1484	^{101}0.2377	^{100}0.3303	^{102}0.4249	^{102}0.5106	^{120}0.5924	^{121}0.6758	^{121}0.7534
105	REALNETWORKS-006						^{39}0.0069	^{34}0.0077	^{38}0.0080						^{46}0.1022	^{42}0.1253	^{42}0.1622
106	S1-002						^{20}0.0046	^{17}0.0051	^{17}0.0038						^{28}0.0482	^{28}0.0597	^{28}0.0788
107	SCANOVATE-001	^{68}0.0079	^{72}0.0117	^{75}0.0151	^{78}0.0185	^{78}0.0221	^{95}0.0259	^{97}0.0321	^{97}0.0427	^{88}0.0727	^{88}0.1169	^{87}0.1650	^{87}0.2115	^{84}0.2528	^{101}0.2925	^{98}0.3437	^{97}0.4084
108	SENSETIME-002	^{96}0.0186	^{92}0.0191	^{84}0.0183	^{75}0.0179	^{68}0.0173	^{65}0.0133	^{41}0.0089	^{28}0.0059	^{40}0.0220	^{25}0.0236	^{19}0.0237	^{18}0.0240	^{12}0.0245	^{14}0.0219	^{11}0.0195	^{10}0.0222
109	SENSETIME-003	^{11}0.0021	^{12}0.0028	^{11}0.0031	^{7}0.0033	^{6}0.0035	^{10}0.0040	^{13}0.0047	^{13}0.0033	^{8}0.0046	^{8}0.0064	^{6}0.0076	^{4}0.0086	^{4}0.0101	^{7}0.0122	^{8}0.0155	^{8}0.0196
110	SENSETIME-004	^{3}0.0016	^{3}0.0022	^{3}0.0025	^{3}0.0028	^{3}0.0030	^{4}0.0035	^{8}0.0043	^{7}0.0025	^{4}0.0036	^{4}0.0052	^{3}0.0066	^{3}0.0081	^{3}0.0099	^{9}0.0126	^{10}0.0169	^{11}0.0230
111	SENSETIME-005	^{2}0.0015	^{2}0.0020	^{2}0.0024	^{2}0.0026	^{2}0.0029	^{3}0.0035	^{7}0.0043	^{10}0.0028	^{5}0.0036	^{7}0.0059	^{8}0.0089	^{9}0.0128	^{10}0.0177	^{15}0.0240	^{17}0.0345	^{17}0.0493
112	SENSETIME-006	^{1}0.0015	^{1}0.0019	^{1}0.0022	^{1}0.0025	^{1}0.0027	^{1}0.0033	^{3}0.0040	^{5}0.0021	^{2}0.0031	^{2}0.0049	^{4}0.0068	^{6}0.0097	^{7}0.0132	^{12}0.0184	^{14}0.0262	^{14}0.0359
113	SENSETIME-007						^{2}0.0035	^{1}0.0038	^{2}0.0015						^{6}0.0112	^{6}0.0140	^{6}0.0176
114	SIAT-002	^{117}0.8309	^{117}0.8310	^{117}0.8311	^{117}0.8306	^{117}0.8296	^{134}0.8302	^{134}0.8300	^{133}0.8301	^{112}0.8340	^{110}0.8368	^{109}0.8404	^{109}0.8445	^{109}0.8480	^{126}0.8532	^{126}0.8595	^{125}0.8691
115	SYNESIS-003	^{89}0.0125	^{85}0.0151	^{83}0.0174	^{80}0.0199	^{79}0.0223	^{92}0.0240	^{92}0.0279	^{87}0.0331	^{85}0.0658	^{83}0.1052	^{83}0.1483	^{82}0.1968	^{82}0.2399	^{97}0.2834	^{97}0.3405	^{96}0.4046
116	SYNESIS-005	^{40}0.0044	^{37}0.0058	^{37}0.0070	^{40}0.0080	^{37}0.0091	^{52}0.0103	^{52}0.0125	^{54}0.0152	^{46}0.0262	^{45}0.0444	^{45}0.0666	^{45}0.0923	^{44}0.1156	^{56}0.1399	^{57}0.1736	^{56}0.2185
117	TECH5-001	^{57}0.0061	^{61}0.0093	^{66}0.0128	^{71}0.0171	^{77}0.0221	^{99}0.0289	^{102}0.0412	^{102}0.0560	^{86}0.0660	^{87}0.1156	^{90}0.1733	^{91}0.2385	^{91}0.2998	^{108}0.3629	^{110}0.4424	^{111}0.5284
118	TOSHIBA-001	^{73}0.0086	^{74}0.0119	^{74}0.0150	^{74}0.0178	^{75}0.0209	^{93}0.0241	^{93}0.0292	^{92}0.0365								
119	TRUEFACE-000	^{36}0.0043	^{36}0.0057	^{30}0.0061	^{28}0.0067	^{27}0.0073	^{43}0.0084	^{43}0.0097	^{41}0.0099	^{35}0.0200	^{37}0.0338	^{38}0.0504	^{35}0.0705	^{35}0.0904	^{50}0.1112	^{48}0.1401	^{48}0.1792
120	VERIDAS-001	^{58}0.0063	^{56}0.0083	^{56}0.0099	^{56}0.0113	^{56}0.0132	^{71}0.0148	^{72}0.0184	^{68}0.0219	^{61}0.0403	^{61}0.0684	^{62}0.1012	^{62}0.1386	^{62}0.1741	^{79}0.2113	^{79}0.2611	^{80}0.3233
121	VISIONLABS-004	^{43}0.0048	^{46}0.0069	^{52}0.0091	^{55}0.0111	^{55}0.0130	^{74}0.0152	^{73}0.0187	^{75}0.0242	^{74}0.0540	^{77}0.0916	^{78}0.1358	^{78}0.1855	^{79}0.2303	^{95}0.2745	^{94}0.3312	^{90}0.3913
122	VISIONLABS-005	^{39}0.0044	^{39}0.0063	^{43}0.0081	^{46}0.0095	^{46}0.0109	^{61}0.0125	^{62}0.0151	^{63}0.0187	^{67}0.0479	^{67}0.0812	^{68}0.1212	^{70}0.1664	^{69}0.2078	^{86}0.2473	^{85}0.2999	^{84}0.3577
123	VISIONLABS-006	^{29}0.0035	^{30}0.0048	^{32}0.0061	^{30}0.0069	^{29}0.0077	^{44}0.0087	^{47}0.0105	^{50}0.0120	^{48}0.0273	^{47}0.0465	^{47}0.0702	^{47}0.0970	^{47}0.1228	^{61}0.1486	^{60}0.1847	^{60}0.2295
124	VISIONLABS-008	^{21}0.0028	^{20}0.0037	^{21}0.0047	^{22}0.0053	^{23}0.0058	^{34}0.0067	^{38}0.0081	^{39}0.0085	^{27}0.0143	^{27}0.0241	^{28}0.0373	^{27}0.0519	^{27}0.0677	^{38}0.0850	^{39}0.1104	^{39}0.1444
125	VISIONLABS-009	^{10}0.0020	^{10}0.0026	^{10}0.0030	^{10}0.0034	^{10}0.0038	^{16}0.0044	^{19}0.0052	^{21}0.0046	^{14}0.0065	^{15}0.0105	^{15}0.0156	^{15}0.0217	^{16}0.0289	^{23}0.0368	^{23}0.0499	^{23}0.0681
126	VISIONLABS-010	^{9}0.0020	^{9}0.0025	^{9}0.0030	^{11}0.0034	^{9}0.0036	^{15}0.0043	^{16}0.0051	^{23}0.0047	^{17}0.0069	^{16}0.0113	^{16}0.0170	^{16}0.0238	^{17}0.0316	^{25}0.0411	^{26}0.0557	^{26}0.0740
127	VISIONLABS-011						^{13}0.0042	^{11}0.0046	^{14}0.0036						^{17}0.0270	^{15}0.0337	^{15}0.0432
128	VTS-000	^{116}0.5878	^{116}0.6312	^{116}0.6602	^{115}0.6863	^{115}0.7073	^{132}0.7246	^{132}0.7458	^{131}0.7747	^{108}0.5929	^{108}0.6397	^{108}0.6729	^{108}0.7034	^{107}0.7279	^{124}0.7493	^{123}0.7739	^{123}0.8076
129	XFORWARDAI-000	^{20}0.0027	^{18}0.0034	^{20}0.0044	^{21}0.0052	^{21}0.0058	^{39}0.0067	^{36}0.0079	^{36}0.0076	^{28}0.0157	^{31}0.0281	^{30}0.0443	^{31}0.0635	^{32}0.0834	^{47}0.1050	^{46}0.1330	^{46}0.1714
130	XFORWARDAI-001	^{15}0.0023	^{11}0.0028	^{12}0.0034	^{12}0.0037	^{12}0.0039	^{18}0.0045	^{18}0.0052	^{20}0.0043	^{13}0.0060	^{14}0.0096	^{13}0.0144	^{12}0.0200	^{13}0.0260	^{19}0.0334	^{19}0.0435	^{19}0.0586
131	YITU-002	^{60}0.0066	^{57}0.0083	^{53}0.0094	^{48}0.0101	^{50}0.0121	^{73}0.0150	^{78}0.0223	^{85}0.0328	^{33}0.0189	^{34}0.0317	^{35}0.0494	^{39}0.0750	^{41}0.1066	^{63}0.1494	^{70}0.2171	^{77}0.2958
132	YITU-003	^{63}0.0072	^{60}0.0089	^{57}0.0100	^{51}0.0107	^{52}0.0125	^{75}0.0153	^{80}0.0226	^{88}0.0334	^{34}0.0194	^{35}0.0321	^{36}0.0500	^{41}0.0756	^{42}0.1071	^{64}0.1500	^{71}0.2177	^{78}0.2964

Table 9: **Accuracy for the FRVT 2018 mugshot sets under ageing**. *The second row shows the time lapse between gallery and subsequent probe images, in years. The first two columns identify the algorithm The next 8 values give rank-based FNIR with R = 1, T = 0 and FPIR = 1. All these are relevant to investigational uses where candidates from all searches would need human review. The second 8 values give threshold-based FNIR with T ≥ 0, FPIR = 0.001 and no rank criterion. The shaded cells indictate indicate the three most accurate algorithms for that elapsed time. The gallery size is 3068801. The total number of searches is 10951064.*

This publication is available free of charge from: https://doi.org/10.6028/NIST.IR.8271

MISS RATES		INVESTIGATION, FNIR(N, R = 1, T = 0)								IDENTIFICATION, FNIR(N, R = L, T $\geq$ 0) FOR FPIR = 0.001							
#	ALGORITHM	(0, 2]	(2, 4]	(4, 6]	(6, 8]	(8, 10]	(10, 12]	(12, 14]	(14, 18]	(0, 2]	(2, 4]	(4, 6]	(6, 8]	(8, 10]	(10, 12]	(12, 14]	(14, 18]
133	YITU-004	[55]0.0061	[51]0.0075	[44]0.0081	[41]0.0081	[39]0.0092	[55]0.0107	[64]0.0154	[66]0.0207	[22]0.0125	[22]0.0204	[23]0.0314	[25]0.0469	[26]0.0671	[42]0.0955	[51]0.1421	[53]0.2006
134	YITU-005	[61]0.0067	[54]0.0080	[47]0.0087	[44]0.0085	[41]0.0094	[56]0.0108	[63]0.0151	[65]0.0204	[21]0.0124	[21]0.0198	[22]0.0308	[22]0.0462	[25]0.0667	[41]0.0953	[50]0.1418	[51]0.1930

Table 10: **Accuracy for the FRVT 2018 mugshot sets under ageing**. *The second row shows the time lapse between gallery and subsequent probe images, in years. The first two columns identify the algorithm The next 8 values give rank-based FNIR with R = 1, T = 0 and FPIR = 1. All these are relevant to investigational uses where candidates from all searches would need human review. The second 8 values give threshold-based FNIR with T $\geq$ 0, FPIR = 0.001 and no rank criterion. The shaded cells indictate indicate the three most accurate algorithms for that elapsed time. The gallery size is 3068801. The total number of searches is 10951064.*

This publication is available free of charge from: https://doi.org/10.6028/NIST.IR.8271

#	ALGORITHM	INVESTIGATION MODE						IDENTIFICATION MODE						FAILURE TO EXTRACT					
		RANK ONE MISS RATE, FNIR(N, 0, 1)						HIGH T ⟶ FPIR = 0.001, FNIR(N, T, L)						FEATURES					
		N=1.6M						N=1.6M											
	GALLERY	MUGSHOT	MUGSHOT	MUGSHOT	VISA	BORDER	VISA	MUGSHOT	MUGSHOT	MUGSHOT	VISA	BORDER	VISA	MUGSHOT	MUGSHOT	MUGSHOT	VISA	BORDER	KIOSK
	PROBE	MUGSHOT	WEBCAM	PROFILE	BORDER	BOR¿10YR	KIOSK	MUGSHOT	WEBCAM	PROFILE	BORDER	BOR¿10YR	KIOSK	MUGSHOT	WEBCAM	PROFILE	BORDER	BOR¿10YR	KIOSK
1	20FACE-000	^{254}0.055	^{243}0.085	^{154}0.736	^{179}0.056	^{105}0.239	^{173}0.243	^{250}0.348	^{246}0.450	^{211}1.000	^{182}0.424	^{101}0.772	^{178}0.938	0.000	0.000	0.000		0.000	
2	3DIVI-003	^{263}0.083	^{260}0.206		^{192}0.141		^{197}0.474	^{259}0.400	^{260}0.626		^{194}0.605		^{159}0.821	0.002	0.005				
3	3DIVI-004	^{222}0.018	^{231}0.062		^{172}0.035		^{177}0.279	^{230}0.169	^{236}0.343		^{172}0.277		^{137}0.607	0.002	0.005				
4	3DIVI-005	^{223}0.018	^{230}0.062	^{201}0.930	^{211}0.821		^{178}0.279	^{227}0.166	^{234}0.339	^{148}0.996	^{200}0.864		^{136}0.597	0.002	0.005	0.442			
5	3DIVI-006	^{233}0.024	^{238}0.074		^{174}0.047		^{186}0.312	^{229}0.168	^{235}0.342		^{173}0.283		^{140}0.615	0.002	0.005				
6	ACER-000	^{200}0.011	^{194}0.036	^{181}0.827	^{159}0.025		^{161}0.209	^{220}0.146	^{213}0.246	^{101}0.981	^{167}0.201		^{123}0.490	0.000	0.000	0.042			
7	ACER-001	^{155}0.005	^{145}0.020	^{100}0.422	^{124}0.008	^{92}0.050	^{68}0.098	^{162}0.056	^{145}0.109	^{182}0.999	^{130}0.068	^{90}0.406	^{122}0.479	0.001	0.001	0.041		0.000	
8	AIZE-001	^{161}0.006	^{159}0.022	^{144}0.683	^{147}0.016	^{94}0.050	^{145}0.165	^{182}0.077	^{172}0.143	^{127}0.994	^{143}0.101	^{84}0.364	^{104}0.387	0.001	0.001	0.047		0.000	
9	ALCHERA-000	^{218}0.016	^{218}0.047	^{188}0.870	^{173}0.046		^{183}0.292	^{217}0.138	^{199}0.216	^{164}0.999	^{162}0.176		^{155}0.803	0.006	0.014	0.328			
10	ALCHERA-001	^{291}0.987	^{287}1.000		^{213}1.000		^{278}1.000	^{288}0.999	^{288}1.000		^{230}1.000		^{224}1.000	0.006	0.013	0.324			
11	ALCHERA-002	^{265}0.095	^{257}0.166	^{215}0.954	^{208}0.668		^{195}0.446	^{266}0.486	^{257}0.591	^{190}1.000	^{199}0.827		^{156}0.811	0.001	0.002	0.106			
12	ALCHERA-003	^{197}0.010	^{192}0.035	^{155}0.741	^{148}0.016		^{159}0.206	^{221}0.155	^{210}0.239	^{175}0.999	^{161}0.172		^{118}0.464	0.001	0.002	0.106			
13	ALCHERA-004	^{202}0.011	^{197}0.038	^{92}0.345	^{149}0.017	^{101}0.088	^{134}0.144	^{258}0.394	^{252}0.529	^{121}0.991	^{183}0.424	^{97}0.708	^{133}0.546	0.001	0.001	0.046		0.000	
14	ALLGOVISION-000	^{205}0.011	^{188}0.033	^{191}0.894	^{154}0.021		^{180}0.282	^{194}0.088	^{188}0.166	^{118}0.990	^{146}0.117		^{130}0.526	0.002	0.003	0.122			
15	ALLGOVISION-001	^{188}0.009	^{203}0.038	^{140}0.661	^{153}0.021		^{171}0.241	^{200}0.102	^{203}0.221	^{108}0.986	^{156}0.150		^{124}0.491	0.001	0.001	0.042			
16	ANKE-000	^{213}0.013	^{198}0.038	^{204}0.931	^{219}1.000		^{217}1.000	^{204}0.117	^{202}0.220	^{126}0.994	^{262}1.000		^{249}1.000	0.000	0.001	0.080			
17	ANKE-001	^{214}0.013	^{199}0.038	^{210}0.946	^{216}1.000		^{213}1.000	^{208}0.119	^{201}0.220	^{133}0.994	^{259}1.000		^{254}1.000	0.000	0.001	0.080			
18	ANKE-002	^{116}0.003	^{119}0.016	^{118}0.522	^{88}0.005		^{109}0.119	^{123}0.032	^{110}0.079	^{72}0.948	^{91}0.034		^{71}0.245	0.001	0.001	0.049			
19	AWARE-003	^{240}0.031	^{244}0.090	^{227}0.966	^{198}0.316		^{182}0.290	^{212}0.128	^{228}0.298	^{105}0.984	^{184}0.428		^{131}0.530	0.004	0.003	0.874			
20	AWARE-004	^{258}0.068	^{259}0.176	^{235}0.976	^{190}0.122		^{193}0.414	^{243}0.269	^{251}0.509	^{191}1.000	^{179}0.397		^{157}0.816	0.003	0.003	0.776			
21	AWARE-005	^{241}0.031	^{232}0.067	^{236}0.978	^{176}0.048		^{185}0.308	^{253}0.364	^{215}0.253	^{197}1.000	^{171}0.255		^{172}0.916	0.001	0.002	0.189			
22	AWARE-006	^{260}0.070	^{253}0.128	^{238}0.983	^{189}0.111		^{194}0.421	^{244}0.276	^{239}0.398	^{185}0.999	^{177}0.368		^{149}0.749	0.001	0.002	0.189			
23	AYONIX-000	^{284}0.450	^{282}0.685	^{247}0.996	^{206}0.607		^{209}0.867	^{276}0.811	^{276}0.939	^{154}0.998	^{204}0.954		^{186}0.982	0.010	0.031	0.939			
24	AYONIX-001	^{279}0.341	^{274}0.527	^{243}0.993	^{212}0.994		^{206}0.778	^{278}0.824	^{271}0.920	^{183}0.999	^{208}0.999		^{182}0.969	0.010	0.031	0.939			
25	AYONIX-002	^{280}0.341	^{275}0.527	^{242}0.993	^{202}0.464		^{205}0.778	^{277}0.824	^{272}0.920	^{181}0.999	^{201}0.915		^{183}0.969	0.010	0.031	0.939			
26	CAMVI-003	^{253}0.052	^{245}0.090	^{194}0.911	^{186}0.093		^{190}0.360	^{177}0.071	^{164}0.132	^{83}0.970	^{145}0.114		^{107}0.402	0.006	0.013	0.675			
27	CAMVI-004	^{251}0.047	^{239}0.077	^{157}0.744	^{185}0.072		^{184}0.296	^{178}0.072	^{166}0.136	^{179}0.999	^{142}0.100		^{153}0.787	0.000	0.000	0.000			
28	CAMVI-005	^{257}0.065	^{251}0.103	^{159}0.746	^{187}0.098		^{189}0.341	^{198}0.099	^{195}0.179	^{188}1.000	^{157}0.156		^{194}0.999	0.000	0.000	0.000			
29	CANON-001	^{14}0.001	^{4}0.006	^{28}0.088	^{16}0.001	^{14}0.007	^{14}0.062	^{33}0.005	^{23}0.023	^{17}0.365	^{21}0.008	^{24}0.068	^{30}0.139	0.001	0.000	0.042		0.000	
30	CANON-002	^{19}0.001	^{90}0.013	^{209}0.944	^{177}0.053	^{106}0.532	^{210}0.877	^{27}0.005	^{31}0.027	^{73}0.952	^{127}0.064	^{94}0.556	^{168}0.881	0.001	0.000	0.042		0.000	
31	CIB-000	^{44}0.002	^{22}0.008	^{33}0.100	^{29}0.002	^{37}0.011	^{22}0.069	^{59}0.012	^{57}0.045	^{204}1.000	^{51}0.017	^{43}0.141	^{169}0.894	0.000	0.000	0.000		0.000	
32	CLEARVIEWAI-000	^{13}0.001	^{11}0.007	^{7}0.062	^{15}0.001	^{10}0.006	^{7}0.056	^{35}0.006	^{27}0.025	^{88}0.974	^{22}0.008	^{19}0.057	^{82}0.268	0.000	0.000	0.037		0.000	
33	CLOUDWALK-HR-000	^{41}0.001	^{41}0.010	^{11}0.064	^{25}0.002	^{13}0.006	^{8}0.057	^{10}0.002	^{10}0.013	^{2}0.133	^{11}0.005	^{7}0.033	^{12}0.099	0.001	0.000	0.042		0.000	
34	CLOUDWALK-MT-000	^{61}0.002	^{60}0.011	^{3}0.057	^{5}0.001	^{3}0.004	^{2}0.051	^{9}0.002	^{9}0.013	^{1}0.109	^{1}0.002	^{1}0.018	^{1}0.072	0.001	0.000	0.042		0.000	
35	COGENT-000	^{199}0.010	^{216}0.046	^{226}0.965				^{153}0.053	^{169}0.140	^{139}0.995				0.000	0.000	0.000			
36	COGENT-001	^{198}0.010	^{215}0.046	^{225}0.965				^{152}0.053	^{168}0.140	^{138}0.995				0.000	0.000	0.000			
37	COGENT-002	^{131}0.004	^{147}0.020	^{199}0.925				^{139}0.044	^{135}0.098	^{153}0.998				0.000	0.000	0.000			
38	COGENT-003	^{133}0.004	^{152}0.021	^{208}0.939				^{144}0.046	^{129}0.095	^{155}0.998				0.000	0.000	0.000			
39	COGENT-004	^{80}0.002	^{85}0.013	^{198}0.922	^{77}0.004	^{60}0.019	^{102}0.113	^{124}0.033	^{63}0.051	^{151}0.997	^{63}0.022	^{39}0.126	^{116}0.456	0.000	0.000	0.000		0.000	
40	COGENT-005	^{55}0.002	^{49}0.010	^{39}0.126	^{30}0.002	^{35}0.010	^{110}0.120	^{44}0.009	^{46}0.037	^{114}0.989	^{38}0.011	^{29}0.082	^{170}0.905	0.000	0.000	0.000		0.000	
41	COGENT-006	^{25}0.001	^{15}0.007	^{18}0.067	^{8}0.001	^{20}0.007	^{77}0.101	^{24}0.004	^{24}0.023	^{12}0.238	^{15}0.006	^{91}0.422	^{26}0.130	0.000	0.000	0.041		0.000	
42	COGNITEC-000	^{235}0.025	^{227}0.059	^{223}0.964				^{225}0.161	^{229}0.303	^{122}0.992				0.003	0.002	0.924			
43	COGNITEC-001	^{206}0.012	^{190}0.034	^{217}0.958				^{199}0.102	^{207}0.230	^{232}1.000				0.003	0.002	0.924			
44	COGNITEC-002	^{162}0.006	^{175}0.025	^{212}0.949				^{155}0.053	^{194}0.178	^{203}1.000				0.003	0.002	0.924			
45	COGNITEC-003	^{166}0.006	^{174}0.025	^{203}0.930				^{151}0.053	^{186}0.162	^{206}1.000				0.004	0.002	0.878			
46	COGNITEC-004	^{124}0.003	^{118}0.016	^{178}0.813	^{139}0.013	^{97}0.057	^{133}0.143	^{122}0.031	^{133}0.097	^{115}0.990	^{129}0.068	^{82}0.316	^{84}0.288	0.002	0.001	0.635		0.006	

Table 11: **Miss rates by dataset:** *At left, rank 1 miss rates relevant to investigations; at right, with threshold set to target FPIR = 0.01 for higher volume, low prior, uses. Yellow indicates most accurate algorithm. Throughout blue superscripts indicate the rank of the algorithm for that column.*

This publication is available free of charge from: https://doi.org/10.6028/NIST.IR.8271

#	ALGORITHM	INVESTIGATION MODE						IDENTIFICATION MODE						FAILURE TO EXTRACT					
		RANK ONE MISS RATE, FNIR(N, 0, 1)						HIGH T ⟶ FPIR = 0.001, FNIR(N, T, L)						FEATURES					
		N=1.6M						N=1.6M											
	GALLERY	MUGSHOT	MUGSHOT	MUGSHOT	VISA	BORDER	VISA	MUGSHOT	MUGSHOT	MUGSHOT	VISA	BORDER	VISA	MUGSHOT	MUGSHOT	MUGSHOT	VISA	BORDER	KIOSK
	PROBE	MUGSHOT	WEBCAM	PROFILE	BORDER	BOR¿10YR	KIOSK	MUGSHOT	WEBCAM	PROFILE	BORDER	BOR¿10YR	KIOSK	MUGSHOT	WEBCAM	PROFILE	BORDER	BOR¿10YR	KIOSK
47	COGNITEC-005	^{52}0.002	^{47}0.010	^{151}0.713	^{155}0.021	^{89}0.037	^{104}0.115	^{46}0.010	^{53}0.041	^{280}1.000	^{101}0.041	^{52}0.157	^{52}0.179	0.002	0.001	0.614		0.017	
48	COGNITEC-006	^{48}0.002	^{38}0.010	^{148}0.703	^{115}0.007	^{70}0.024	^{97}0.111	^{41}0.008	^{49}0.040	^{289}1.000	^{79}0.030	^{58}0.171	^{144}0.681	0.002	0.001	0.568		0.003	
49	CUBOX-000	^{35}0.001	^{44}0.010	^{4}0.058	^{19}0.002	^{5}0.004	^{1}0.049	^{16}0.003	^{17}0.019	^{4}0.168	^{7}0.004	^{6}0.028	^{2}0.073	0.001	0.000	0.042		0.000	
50	CYBERLINK-000	^{135}0.004	^{144}0.020	^{152}0.717	^{118}0.007		^{126}0.134	^{163}0.056	^{149}0.116	^{142}0.995	^{126}0.063		^{98}0.339	0.001	0.001	0.063			
51	CYBERLINK-001	^{129}0.004	^{132}0.018	^{153}0.731	^{111}0.007		^{125}0.133	^{156}0.054	^{146}0.109	^{137}0.995	^{123}0.062		^{141}0.652	0.000	0.000	0.040			
52	CYBERLINK-002	^{109}0.003	^{72}0.012	^{132}0.577	^{71}0.004		^{90}0.107	^{69}0.015	^{72}0.053	^{113}0.988	^{67}0.024		^{85}0.288	0.001	0.000	0.042			
53	CYBERLINK-003	^{49}0.002	^{29}0.009	^{109}0.474	^{52}0.003	^{38}0.012	^{48}0.082	^{42}0.008	^{43}0.035	^{86}0.972	^{40}0.012	^{34}0.100	^{101}0.368	0.000	0.000	0.039		0.000	
54	CYBERLINK-004	^{54}0.002	^{68}0.011	^{101}0.423	^{49}0.003	^{36}0.011	^{81}0.104	^{39}0.007	^{44}0.036	^{217}1.000	^{42}0.013	^{35}0.109	^{181}0.954	0.000	0.000	0.011		0.000	
55	CYBERLINK-005	^{64}0.002	^{54}0.011	^{58}0.209	^{34}0.002	^{31}0.010	^{69}0.098	^{50}0.010	^{50}0.041	^{195}1.000	^{43}0.014	^{30}0.089	^{177}0.926	0.000	0.000	0.034		0.000	
56	DAHUA-000	^{192}0.009	^{177}0.026					^{190}0.086	^{165}0.135					0.004	0.003				
57	DAHUA-001	^{170}0.007	^{169}0.024	^{149}0.703				^{180}0.073	^{157}0.122	^{98}0.980				0.002	0.002	0.346			
58	DAHUA-002	^{70}0.002	^{71}0.012	^{81}0.304	^{47}0.003		^{50}0.084	^{70}0.015	^{59}0.046	^{37}0.638	^{48}0.017		^{42}0.159	0.001	0.000	0.099			
59	DAHUA-003	^{23}0.001	^{12}0.007	^{56}0.206	^{27}0.002	^{29}0.009	^{28}0.073	^{64}0.014	^{52}0.041	^{32}0.579	^{41}0.013	^{28}0.081	^{29}0.134	0.000	0.000	0.000		0.000	
60	DAHUA-004	^{12}0.001	^{16}0.008	^{43}0.144	^{20}0.002	^{17}0.007	^{20}0.069	^{38}0.007	^{29}0.026	^{26}0.485	^{28}0.008	^{15}0.051	^{22}0.113	0.000	0.000	0.000		0.000	
61	DAON-000	^{138}0.004	^{126}0.017	^{121}0.530	^{89}0.005	^{62}0.020	^{114}0.125	^{98}0.023	^{85}0.061	^{194}1.000	^{68}0.025	^{60}0.173	^{164}0.846	0.002	0.002	0.108		0.001	
62	DECATUR-000	^{86}0.002	^{70}0.011	^{64}0.229	^{81}0.004	^{59}0.019	^{93}0.109	^{101}0.023	^{91}0.066	^{42}0.675	^{72}0.027	^{59}0.173	^{69}0.239	0.001	0.000	0.044		0.001	
63	DEEPGLINT-001	^{39}0.001	^{10}0.007	^{54}0.200	^{40}0.002		^{29}0.073	^{20}0.003	^{11}0.014	^{187}1.000	^{16}0.006		^{41}0.159	0.000	0.000	0.038			
64	DEEPSEA-001	^{143}0.004	^{116}0.016	^{179}0.814	^{127}0.010		^{132}0.140	^{143}0.046	^{138}0.101	^{106}0.985	^{134}0.077		^{95}0.326	0.000	0.001	0.047			
65	DERMALOG-003	^{269}0.126	^{262}0.217		^{197}0.296		^{200}0.560	^{265}0.482	^{262}0.655		^{198}0.677		^{166}0.870	0.002	0.002	0.103			
66	DERMALOG-004	^{268}0.125	^{261}0.215	^{202}0.930	^{191}0.135		^{196}0.467	^{264}0.480	^{263}0.657	^{143}0.995	^{193}0.603		^{165}0.856	0.001	0.002	0.107			
67	DERMALOG-005	^{217}0.015	^{196}0.037	^{147}0.701	^{196}0.242		^{192}0.384	^{193}0.088	^{179}0.154	^{117}0.990	^{174}0.300		^{139}0.614	0.001	0.002	0.102			
68	DERMALOG-006	^{183}0.008	^{173}0.024	^{138}0.619	^{128}0.010		^{141}0.155	^{150}0.052	^{140}0.105	^{100}0.981	^{121}0.059		^{94}0.318	0.003	0.006	0.181			
69	DERMALOG-007	^{191}0.009	^{178}0.027	^{142}0.675	^{143}0.014		^{147}0.170	^{191}0.086	^{177}0.152	^{116}0.990	^{141}0.099		^{135}0.557	0.001	0.002	0.102			
70	DERMALOG-008	^{117}0.003	^{109}0.015	^{116}0.516	^{108}0.007	^{84}0.029	^{131}0.139	^{141}0.045	^{126}0.094	^{218}1.000	^{118}0.057	^{88}0.382	^{179}0.940	0.000	0.000	0.002		0.000	
71	DERMALOG-009	^{115}0.003	^{104}0.014	^{50}0.167	^{116}0.007	^{109}0.999	^{84}0.106	^{91}0.021	^{92}0.066	^{208}1.000	^{81}0.031	^{106}0.999	^{162}0.840	0.001	0.001	0.018		0.003	
72	DIGIDATA-000	^{287}0.590	^{276}0.548	^{192}0.895	^{207}0.642	^{107}0.707	^{208}0.813	^{270}0.610	^{256}0.577	^{131}0.994	^{196}0.646	^{102}0.789	^{160}0.824	0.002	0.001	0.070		0.001	
73	DILUSENSE-000	^{91}0.002	^{77}0.012	^{79}0.297	^{121}0.008	^{81}0.028	^{73}0.099	^{120}0.030	^{109}0.078	^{38}0.655	^{98}0.039	^{96}0.664	^{60}0.203	0.001	0.001	0.219		0.006	
74	EYEDEA-003	^{262}0.080	^{255}0.148	^{221}0.960	^{188}0.101		^{191}0.379	^{255}0.388	^{254}0.543	^{134}0.994	^{191}0.570		^{154}0.792	0.001	0.003	0.161			
75	F8-001	^{210}0.012		^{141}0.669	^{242}1.000		^{241}1.000	^{226}0.166		^{163}0.998				0.004	1.000	0.158			
76	FINCORE-000	^{201}0.011	^{191}0.034	^{165}0.767	^{166}0.032	^{102}0.117	^{156}0.191	^{216}0.134	^{200}0.217	^{200}1.000	^{163}0.187	^{95}0.598	^{117}0.458	0.000	0.001	0.043		0.000	
77	FUJITSULAB-000	^{92}0.002	^{97}0.014	^{104}0.440	^{73}0.004	^{65}0.023	^{70}0.098	^{92}0.021	^{78}0.056		^{65}0.024	^{61}0.177	^{70}0.240	0.000	0.001	0.016		0.000	
78	FUJITSULAB-001	^{72}0.002	^{89}0.013	^{106}0.455	^{78}0.004	^{73}0.026	^{86}0.106	^{82}0.018	^{80}0.058	^{123}0.992	^{66}0.024	^{98}0.739	^{73}0.247	0.000	0.003	0.150		0.002	
79	GLORY-000	^{273}0.178	^{268}0.320	^{246}0.994	^{195}0.228		^{202}0.678	^{254}0.367	^{255}0.547	^{136}0.995	^{186}0.453		^{161}0.839	0.011	0.013	0.985			
80	GLORY-001	^{270}0.127	^{265}0.267	^{241}0.992	^{194}0.178		^{201}0.594	^{246}0.305	^{253}0.537	^{124}0.993	^{181}0.408		^{158}0.819	0.011	0.013	0.988			
81	GORILLA-001	^{255}0.060	^{247}0.095	^{206}0.936	^{183}0.069		^{187}0.329	^{260}0.406	^{247}0.453	^{219}1.000	^{187}0.468		^{231}1.000	0.001	0.001	0.069			
82	GORILLA-002	^{229}0.020	^{212}0.044	^{161}0.753	^{160}0.027		^{166}0.214	^{233}0.188	^{222}0.268	^{226}1.000	^{170}0.250		^{198}1.000	0.001	0.001	0.069			
83	GORILLA-003	^{242}0.036	^{234}0.070	^{180}0.821	^{175}0.048		^{175}0.265	^{248}0.318	^{244}0.434	^{231}1.000	^{180}0.407		^{283}1.000	0.001	0.001	0.069			
84	GORILLA-004	^{167}0.006	^{170}0.024	^{146}0.697	^{132}0.012		^{144}0.162	^{196}0.089	^{185}0.160	^{75}0.959	^{151}0.135		^{113}0.438	0.000	0.001	0.042			
85	GORILLA-005	^{123}0.003	^{133}0.018	^{57}0.209	^{101}0.006		^{112}0.124	^{167}0.058	^{171}0.142	^{44}0.700	^{139}0.088		^{92}0.315	0.000	0.000	0.040			
86	GORILLA-006	^{60}0.002	^{74}0.012	^{37}0.122	^{60}0.003	^{55}0.018	^{83}0.105	^{113}0.027	^{120}0.089	^{30}0.531	^{73}0.028	^{56}0.166	^{63}0.218	0.000	0.000	0.041		0.000	
87	GORILLA-007	^{57}0.002	^{53}0.011	^{35}0.114	^{38}0.002	^{53}0.016	^{55}0.088	^{112}0.027	^{108}0.077	^{31}0.534	^{69}0.026	^{74}0.264	^{50}0.178	0.000	0.000	0.041		0.000	
88	GRIAULE-000	^{107}0.002	^{91}0.014	^{87}0.327	^{131}0.011	^{87}0.031	^{116}0.126	^{89}0.020	^{88}0.063	^{140}0.995	^{88}0.033	^{65}0.185	^{58}0.198	0.000	0.002	0.090		0.001	
89	HIK-003	^{207}0.012	^{181}0.027	^{145}0.689	^{135}0.012		^{138}0.151	^{201}0.103	^{181}0.158	^{81}0.969	^{154}0.142		^{115}0.445	0.000	0.000	0.048			
90	HIK-004	^{204}0.011	^{179}0.027	^{156}0.743	^{133}0.012		^{140}0.152	^{197}0.099	^{178}0.153	^{89}0.976	^{152}0.137		^{112}0.434	0.000	0.000	0.048			
91	HIK-005	^{148}0.005	^{121}0.017	^{123}0.535	^{113}0.007		^{96}0.111	^{136}0.044	^{107}0.077	^{184}0.999	^{128}0.068		^{132}0.541	0.000	0.000	0.000			
92	HIK-006	^{147}0.005	^{120}0.017	^{124}0.535				^{145}0.047	^{117}0.086	^{225}1.000				0.000	0.000	0.000			

Table 12: **Miss rates by dataset:** *At left, rank 1 miss rates relevant to investigations; at right, with threshold set to target FPIR = 0.01 for higher volume, low prior, uses. Yellow indicates most accurate algorithm. Throughout blue superscripts indicate the rank of the algorithm for that column.*

This publication is available free of charge from: https://doi.org/10.6028/NIST.IR.8271

#	ALGORITHM	INVESTIGATION MODE						IDENTIFICATION MODE						FAILURE TO EXTRACT					
		RANK ONE MISS RATE, FNIR(N, 0, 1)						HIGH T ⟶ FPIR = 0.001, FNIR(N, T, L)						FEATURES					
		N=1.6M						N=1.6M											
	GALLERY	MUGSHOT	MUGSHOT	MUGSHOT	VISA	BORDER	VISA	MUGSHOT	MUGSHOT	MUGSHOT	VISA	BORDER	VISA	MUGSHOT	MUGSHOT	MUGSHOT	VISA	BORDER	KIOSK
	PROBE	MUGSHOT	WEBCAM	PROFILE	BORDER	BOR¿10YR	KIOSK	MUGSHOT	WEBCAM	PROFILE	BORDER	BOR¿10YR	KIOSK	MUGSHOT	WEBCAM	PROFILE	BORDER	BOR¿10YR	KIOSK
93	HYPERVERGE-001	[32]0.001	[61]0.011	[17]0.067	[18]0.002	[15]0.007	[12]0.061	[25]0.004	[39]0.031	[9]0.220	[19]0.007	[17]0.053	[15]0.101	0.001	0.000	0.041		0.000	
94	HYPERVERGE-002	[29]0.001	[59]0.011	[8]0.063	[10]0.001	[12]0.006	[11]0.058	[21]0.004	[33]0.027	[8]0.210	[13]0.006	[14]0.048	[9]0.093	0.001	0.000	0.041		0.000	
95	HZAILU-000	[90]0.002	[88]0.013	[68]0.244	[53]0.003	[50]0.015	[58]0.090	[88]0.020	[64]0.051	[80]0.967	[57]0.020	[81]0.316	[36]0.153	0.001	0.001	0.054		0.001	
96	IDEMIA-003	[173]0.007	[189]0.034	[216]0.958	[151]0.018		[163]0.210	[146]0.047	[187]0.165		[148]0.123		[151]0.766	0.000	0.000	0.041			
97	IDEMIA-004	[169]0.007	[187]0.032	[211]0.947	[150]0.018		[162]0.210	[132]0.037	[153]0.118	[87]0.973	[147]0.123		[152]0.766	0.000	0.000	0.041			
98	IDEMIA-005	[182]0.008	[204]0.039	[214]0.954	[157]0.021		[167]0.217	[138]0.044	[176]0.150	[93]0.978	[149]0.130		[167]0.879	0.000	0.000	0.041			
99	IDEMIA-006	[195]0.010	[236]0.072	[229]0.969	[162]0.030		[174]0.253	[135]0.043	[205]0.226	[102]0.982	[155]0.144		[147]0.733	0.000	0.000	0.041			
100	IDEMIA-007	[108]0.003	[113]0.015	[268]1.000	[102]0.006	[88]0.036	[122]0.131	[81]0.018	[75]0.055	[262]1.000	[113]0.052	[63]0.182	[255]1.000	0.000	0.000	0.040		0.000	
101	IDEMIA-008	[11]0.001	[6]0.007	[25]0.079	[17]0.001	[18]0.007	[34]0.075	[8]0.002	[8]0.013	[7]0.204	[10]0.005	[11]0.036	[18]0.106	0.000	0.000	0.040		0.000	
102	IDEMIA-009	[4]0.001	[5]0.006	[13]0.065	[4]0.001	[8]0.005	[3]0.051	[2]0.002	[2]0.011	[3]0.141	[3]0.003	[5]0.027	[4]0.074	0.000	0.000	0.040		0.000	
103	IMAGUS-002	[276]0.220	[266]0.301	[240]0.988				[274]0.749	[268]0.816	[223]1.000				0.004	0.008	0.550			
104	IMAGUS-003	[281]0.356	[272]0.513	[244]0.993				[275]0.807	[270]0.909	[205]1.000				0.004	0.008	0.550			
105	IMAGUS-005	[76]0.002	[73]0.012	[84]0.319	[100]0.006	[63]0.022	[124]0.132	[85]0.018	[90]0.066	[59]0.838	[75]0.029	[55]0.161	[66]0.231	0.000	0.000	0.000		0.000	
106	IMAGUS-006	[81]0.002	[94]0.014	[78]0.293	[79]0.004	[61]0.019	[100]0.112	[87]0.019	[96]0.069	[67]0.897	[74]0.028	[54]0.161	[76]0.260	0.000	0.000	0.000		0.000	
107	IMAGUS-007	[83]0.002	[86]0.013	[85]0.321	[72]0.004	[64]0.022	[106]0.117	[100]0.023	[102]0.073	[65]0.893	[82]0.031	[57]0.169	[81]0.265	0.000	0.000	0.000		0.000	
108	IMAGUS-008	[264]0.086	[246]0.093	[82]0.305	[156]0.021	[100]0.081	[108]0.119	[283]0.974	[266]0.774	[145]0.996	[189]0.520	[107]1.000	[128]0.518	0.000	0.000	0.000		0.000	
109	IMPERIAL-000	[106]0.002	[110]0.015	[75]0.280	[85]0.004		[66]0.097	[106]0.026	[94]0.068	[167]0.999	[102]0.042		[72]0.245	0.000	0.000	0.000			
110	INCODE-000	[252]0.049	[249]0.100	[213]0.951				[247]0.310	[242]0.420	[159]0.998				0.001	0.004	0.173			
111	INCODE-001	[220]0.017	[217]0.046	[162]0.762				[236]0.212	[225]0.296	[221]1.000				0.001	0.004	0.173			
112	INCODE-002	[224]0.018	[219]0.048	[183]0.843				[232]0.184	[223]0.269	[125]0.993				0.000	0.001	0.066			
113	INCODE-003	[212]0.013	[206]0.040	[163]0.764				[228]0.167	[219]0.264	[180]0.999				0.000	0.001	0.066			
114	INCODE-004	[130]0.004	[130]0.017	[110]0.475	[125]0.008		[128]0.135	[159]0.054	[156]0.120	[135]0.995	[125]0.063		[90]0.313	0.000	0.001	0.066			
115	INCODE-005	[53]0.002	[66]0.011	[46]0.147	[41]0.002	[43]0.013	[43]0.079	[54]0.011	[55]0.043	[28]0.528	[50]0.017	[46]0.145	[39]0.155	0.000	0.000	0.042		0.000	
116	INNOVATRICS-002	[250]0.045	[237]0.074	[186]0.853				[241]0.234	[230]0.310	[212]1.000				0.000	0.001	0.046			
117	INNOVATRICS-003	[236]0.026	[222]0.055	[185]0.845				[237]0.221	[226]0.297	[193]1.000				0.000	0.001	0.046			
118	INNOVATRICS-004	[211]0.012	[208]0.040	[218]0.958				[214]0.132	[204]0.222	[97]0.980				0.000	0.001	0.046			
119	INNOVATRICS-005	[104]0.002	[103]0.014	[99]0.407	[87]0.005		[92]0.109	[125]0.034	[121]0.089	[60]0.846	[109]0.047		[74]0.251	0.000	0.001	0.041			
120	INNOVATRICS-007	[56]0.002	[65]0.011	[69]0.248	[44]0.002	[45]0.013	[37]0.077	[60]0.013	[65]0.051	[47]0.743	[49]0.017	[32]0.093	[37]0.154	0.000	0.001	0.041		0.000	
121	INTELLIVISION-001	[243]0.036	[250]0.102	[231]0.972	[180]0.057	[104]0.222	[188]0.333	[245]0.279	[240]0.404	[196]1.000	[175]0.328	[99]0.749	[145]0.685	0.001	0.000	0.044		0.000	
122	INTSYSMSU-000	[271]0.146	[168]0.023	[131]0.562	[184]0.072		[123]0.132	[286]0.998	[281]1.000	[192]1.000	[207]0.999		[195]0.999	0.000	0.000	0.050			
123	IREX-000	[144]0.004	[34]0.010	[143]0.681	[39]0.002	[39]0.012	[46]0.082	[117]0.028	[84]0.060	[74]0.957	[105]0.044	[80]0.302	[47]0.170	0.000	0.000	0.042		0.000	
124	ISYSTEMS-002	[168]0.006	[176]0.026	[184]0.844				[184]0.078	[160]0.126	[152]0.998				0.002	0.002	0.142			
125	ISYSTEMS-003	[156]0.005	[165]0.023	[168]0.791				[168]0.059	[144]0.107	[198]1.000				0.002	0.002	0.142			
126	KAKAO-000	[40]0.001	[52]0.011	[36]0.119	[43]0.002	[42]0.013	[39]0.078	[72]0.015	[77]0.056	[23]0.468	[54]0.019	[42]0.141	[40]0.158	0.000	0.000	0.041		0.000	
127	KEDACOM-001	[178]0.008	[193]0.036	[232]0.972	[168]0.034		[168]0.237	[99]0.023	[100]0.072	[110]0.986	[117]0.055		[88]0.305	0.000	0.000	0.000			
128	KNERON-000	[163]0.006	[180]0.027	[129]0.552	[161]0.028		[157]0.195							0.000	0.000	0.000			
129	KNERON-001	[239]0.030	[281]0.621	[67]0.237	[193]0.144	[103]0.207	[179]0.280							0.000	0.000	0.000		0.000	
130	LINE-000	[93]0.002	[95]0.014	[63]0.223	[93]0.005	[82]0.029	[87]0.107	[121]0.031	[130]0.095		[107]0.046	[77]0.278	[272]1.000	0.000	0.000	0.000		0.000	
131	LINE-001	[16]0.001	[14]0.007	[10]0.063	[24]0.002	[26]0.008	[54]0.085	[28]0.005	[30]0.027	[216]1.000	[33]0.009	[25]0.072	[267]1.000	0.000	0.000	0.000		0.000	
132	LOOKMAN-003	[187]0.009	[202]0.038		[171]0.035		[170]0.239	[137]0.044	[148]0.112		[138]0.084		[99]0.355	0.000	0.000				
133	LOOKMAN-004	[189]0.009	[205]0.039	[234]0.973				[140]0.045	[142]0.105	[90]0.977				0.000	0.000	0.000			
134	LOOKMAN-005	[181]0.008	[195]0.036	[233]0.972	[170]0.035		[169]0.237	[119]0.030	[116]0.086	[92]0.978	[124]0.062		[89]0.308	0.000	0.000	0.000			
135	MANTRA-000	[59]0.002	[45]0.010	[150]0.709	[110]0.007	[71]0.024	[98]0.112	[51]0.010	[51]0.041	[288]1.000	[76]0.029	[50]0.152	[197]1.000	0.002	0.001	0.591		0.003	
136	MEGVII-001	[208]0.012	[129]0.017		[271]1.000			[179]0.072	[134]0.097					0.002	0.000				
137	MEGVII-002	[209]0.012	[131]0.017	[105]0.450	[234]1.000			[183]0.077	[132]0.096	[162]0.998				0.002	0.000	0.033			
138	MICROFOCUS-003	[289]0.594	[285]0.781		[210]0.708		[212]0.907	[281]0.931	[280]0.979		[206]0.982		[190]0.991	0.001	0.005				

Table 13: **Miss rates by dataset:** *At left, rank 1 miss rates relevant to investigations; at right, with threshold set to target FPIR = 0.01 for higher volume, low prior, uses. Yellow indicates most accurate algorithm. Throughout blue superscripts indicate the rank of the algorithm for that column.*

This publication is available free of charge from: https://doi.org/10.6028/NIST.IR.8271

#	ALGORITHM	INVESTIGATION MODE						IDENTIFICATION MODE						FAILURE TO EXTRACT					
		RANK ONE MISS RATE, FNIR(N, 0, 1)						HIGH T → FPIR = 0.001, FNIR(N, T, L)						FEATURES					
		N=1.6M						N=1.6M											
	GALLERY	MUGSHOT	MUGSHOT	MUGSHOT	VISA	BORDER	VISA	MUGSHOT	MUGSHOT	MUGSHOT	VISA	BORDER	VISA	MUGSHOT	MUGSHOT	MUGSHOT	VISA	BORDER	KIOSK
	PROBE	MUGSHOT	WEBCAM	PROFILE	BORDER	BOR¿10YR	KIOSK	MUGSHOT	WEBCAM	PROFILE	BORDER	BOR¿10YR	KIOSK	MUGSHOT	WEBCAM	PROFILE	BORDER	BOR¿10YR	KIOSK
139	MICROFOCUS-004	^{286}0.576	^{284}0.758		^{209}0.701		^{211}0.904	^{287}0.999	^{278}0.975		^{205}0.974		^{188}0.989	0.001	0.005				
140	MICROFOCUS-005	^{282}0.424	^{279}0.601		^{204}0.494		^{204}0.777	^{279}0.835	^{274}0.928		^{203}0.935		^{187}0.985	0.001	0.005				
141	MICROFOCUS-006	^{283}0.427	^{278}0.583		^{203}0.490		^{207}0.782	^{284}0.978	^{273}0.923		^{202}0.923		^{184}0.971	0.001	0.005				
142	MICROSOFT-003	^{50}0.002	^{78}0.012		^{69}0.004		^{94}0.109	^{115}0.028	^{124}0.091		^{94}0.036		^{68}0.233	0.000	0.001				
143	MICROSOFT-004	^{42}0.001	^{76}0.012		^{63}0.004		^{95}0.109	^{107}0.026	^{118}0.087		^{89}0.033		^{64}0.222	0.000	0.001				
144	MICROSOFT-005	^{73}0.002	^{58}0.011	^{44}0.144	^{57}0.003		^{71}0.099	^{104}0.026	^{98}0.070	^{33}0.587	^{70}0.027		^{53}0.180	0.000	0.001	0.049			
145	MICROSOFT-006	^{79}0.002	^{69}0.011	^{48}0.150	^{67}0.004		^{74}0.100	^{55}0.012	^{45}0.037	^{18}0.386	^{85}0.032		^{49}0.178	0.000	0.001	0.049			
146	NEC-000	^{221}0.017	^{210}0.041	^{220}0.959	^{158}0.025		^{172}0.243	^{186}0.079	^{170}0.140	^{95}0.979			^{121}0.474	0.001	0.002	0.890			
147	NEC-001	^{230}0.021	^{223}0.056	^{228}0.967	^{167}0.033		^{176}0.277	^{203}0.106	^{197}0.197	^{109}0.986	^{150}0.133		^{120}0.468	0.005	0.003	0.934			
148	NEC-002	^{10}0.001	^{27}0.009	^{95}0.363	^{62}0.003		^{105}0.117	^{14}0.003	^{20}0.020	^{177}0.999	^{24}0.008		^{143}0.676	0.000	0.001	0.041			
149	NEC-003	^{30}0.001	^{42}0.010	^{94}0.352	^{66}0.004	^{41}0.013	^{111}0.120	^{12}0.002	^{16}0.017	^{56}0.824	^{27}0.008	^{12}0.036	^{142}0.668	0.000	0.001	0.041		0.001	
150	NEC-004	^{37}0.001	^{26}0.009	^{125}0.538	^{55}0.003	^{22}0.007	^{33}0.075	^{5}0.002	^{7}0.013	^{36}0.622	^{8}0.004	^{3}0.019	^{14}0.100	0.000	0.001	0.041		0.001	
151	NEC-005	^{21}0.001	^{17}0.008	^{26}0.081	^{23}0.002	^{7}0.005	^{30}0.073	^{3}0.002	^{3}0.012	^{41}0.673	^{5}0.003	^{2}0.019	^{11}0.099	0.000	0.001	0.040		0.001	
152	NEUROTECHNOLOGY-003	^{231}0.022	^{211}0.042	^{222}0.961				^{272}0.636	^{221}0.266	^{279}1.000				0.000	0.001	0.131			
153	NEUROTECHNOLOGY-004	^{158}0.006	^{143}0.020	^{230}0.970				^{173}0.063	^{150}0.117	^{130}0.994				0.000	0.001	0.131			
154	NEUROTECHNOLOGY-005	^{142}0.004	^{172}0.024	^{190}0.893				^{160}0.054	^{162}0.130	^{156}0.998				0.000	0.000	0.030			
155	NEUROTECHNOLOGY-006	^{225}0.018	^{214}0.045	^{136}0.606				^{242}0.249	^{241}0.418					0.000	0.000				
156	NEUROTECHNOLOGY-007	^{134}0.004	^{151}0.021	^{171}0.796	^{126}0.009		^{153}0.180	^{172}0.062	^{191}0.173	^{201}1.000	^{176}0.339		^{246}1.000	0.001	0.001	0.041			
157	NEUROTECHNOLOGY-008	^{89}0.002	^{102}0.014	^{107}0.457	^{74}0.004	^{67}0.023	^{76}0.101	^{154}0.053	^{112}0.080	^{222}1.000	^{93}0.035	^{79}0.293	^{59}0.203	0.000	0.001	0.052		0.001	
158	NEUROTECHNOLOGY-009	^{38}0.001	^{55}0.011	^{53}0.179	^{33}0.002	^{44}0.013	^{42}0.079	^{73}0.015	^{69}0.052	^{34}0.588	^{56}0.020	^{51}0.153	^{44}0.165	0.001	0.000	0.046		0.000	
159	NEUROTECHNOLOGY-010	^{24}0.001	^{33}0.009	^{20}0.070	^{12}0.001	^{21}0.007	^{19}0.068	^{49}0.010	^{47}0.037	^{14}0.277	^{36}0.010	^{27}0.075	^{25}0.126	0.000	0.000	0.041		0.000	
160	NEUROTECHNOLOGY-012	^{8}0.001	^{19}0.008	^{9}0.063	^{2}0.001	^{9}0.005	^{9}0.057	^{37}0.007	^{42}0.032	^{76}0.959	^{30}0.008	^{21}0.061	^{173}0.916	0.000	0.000	0.039		0.000	
161	NEWLAND-002	^{261}0.079	^{252}0.117	^{205}0.936				^{262}0.438	^{248}0.466	^{171}0.999				0.007	0.012	0.200			
162	NOBLIS-001	^{278}0.249	^{273}0.522	^{245}0.993				^{289}1.000	^{282}1.000	^{209}1.000				0.000	0.000	0.000			
163	NOBLIS-002	^{274}0.179	^{270}0.392	^{237}0.982				^{285}0.997	^{292}1.000	^{227}1.000				0.000	0.000	0.000			
164	NOTIONTAG-000	^{105}0.002	^{79}0.012	^{55}0.204	^{76}0.004	^{51}0.016	^{63}0.095	^{76}0.017	^{83}0.059	^{35}0.611	^{60}0.021	^{49}0.150	^{48}0.176	0.000	0.000	0.000		0.000	
165	NTECHLAB-003	^{164}0.006	^{162}0.023	^{112}0.504				^{158}0.054	^{151}0.118	^{58}0.837				0.000	0.000	0.040			
166	NTECHLAB-004	^{151}0.005	^{138}0.019	^{113}0.506	^{120}0.008		^{119}0.129	^{133}0.041	^{141}0.105	^{57}0.833	^{116}0.053		^{78}0.263	0.000	0.000	0.040			
167	NTECHLAB-005	^{149}0.005	^{134}0.018	^{96}0.367	^{123}0.008		^{107}0.118	^{134}0.042	^{139}0.102	^{50}0.771	^{132}0.073		^{86}0.294	0.000	0.000	0.040			
168	NTECHLAB-006	^{139}0.004	^{125}0.017	^{93}0.347	^{117}0.007		^{103}0.113	^{128}0.037	^{127}0.094	^{49}0.754	^{119}0.057		^{77}0.260	0.000	0.000	0.040			
169	NTECHLAB-007	^{110}0.003	^{80}0.012	^{86}0.326	^{84}0.004		^{88}0.107	^{103}0.026	^{93}0.067	^{48}0.750	^{86}0.032		^{65}0.223	0.000	0.000	0.042			
170	NTECHLAB-008	^{58}0.002	^{35}0.010	^{49}0.157	^{61}0.003		^{51}0.084	^{66}0.014	^{58}0.045	^{29}0.529	^{90}0.033		^{54}0.183	0.000	0.000	0.044			
171	NTECHLAB-009	^{26}0.001	^{20}0.008	^{41}0.138	^{31}0.002	^{46}0.013	^{32}0.074	^{30}0.005	^{22}0.022	^{20}0.430	^{44}0.015	^{36}0.109	^{32}0.142	0.000	0.000	0.041		0.001	
172	NTECHLAB-010	^{15}0.001	^{23}0.008	^{27}0.085	^{22}0.002	^{25}0.008	^{10}0.057	^{13}0.003	^{14}0.015	^{13}0.252	^{17}0.007	^{20}0.059	^{10}0.098	0.001	0.001	0.043		0.000	
173	NTECHLAB-011	^{9}0.001	^{8}0.007	^{21}0.072	^{14}0.001	^{24}0.007	^{4}0.051	^{17}0.003	^{13}0.015	^{10}0.228	^{32}0.009	^{26}0.074	^{7}0.091	0.000	0.000	0.040		0.000	
174	PANGIAM-000	^{22}0.001	^{18}0.008	^{23}0.074	^{26}0.002	^{23}0.007	^{17}0.065	^{36}0.006	^{37}0.030	^{16}0.318	^{35}0.009	^{41}0.136	^{17}0.105	0.000	0.001	0.044		0.001	
175	PARAVISION-000	^{226}0.019	^{201}0.038	^{122}0.534	^{201}0.423		^{199}0.529	^{195}0.089	^{189}0.170	^{173}0.999	^{188}0.470		^{176}0.926	0.000	0.000	0.000			
176	PARAVISION-001	^{132}0.004	^{148}0.020	^{88}0.329	^{200}0.414		^{198}0.484	^{147}0.049	^{161}0.128	^{165}0.999	^{185}0.444		^{148}0.739	0.000	0.000	0.000			
177	PARAVISION-002	^{137}0.004	^{155}0.022	^{90}0.335	^{145}0.015		^{149}0.175	^{148}0.050	^{154}0.119	^{103}0.983	^{135}0.080		^{125}0.497	0.000	0.000	0.032			
178	PARAVISION-003	^{122}0.003	^{140}0.019	^{70}0.252	^{146}0.015		^{146}0.167	^{126}0.035	^{131}0.096	^{132}0.994	^{120}0.058		^{87}0.296	0.000	0.000	0.032			
179	PARAVISION-004	^{51}0.002	^{48}0.010	^{34}0.104	^{98}0.006		^{99}0.112	^{53}0.010	^{48}0.038	^{213}1.000	^{52}0.018		^{171}0.908	0.000	0.000	0.032			
180	PARAVISION-005	^{46}0.002	^{37}0.010	^{24}0.079	^{112}0.007		^{85}0.106	^{23}0.004	^{25}0.024	^{96}0.980	^{37}0.011		^{27}0.132	0.000	0.000	0.038			
181	PARAVISION-007	^{18}0.001	^{21}0.008	^{14}0.066	^{91}0.005	^{32}0.010	^{75}0.101	^{22}0.004	^{26}0.025	^{220}1.000	^{31}0.009	^{37}0.113	^{225}1.000	0.000	0.000	0.000		0.000	
182	PARAVISION-009	^{7}0.001	^{13}0.007	^{15}0.067	^{11}0.001	^{4}0.004	^{5}0.054	^{15}0.003	^{18}0.019	^{46}0.735	^{4}0.003	^{8}0.033	^{3}0.073	0.000	0.001	0.025		0.000	
183	PIXELALL-002	^{146}0.005	^{158}0.022	^{176}0.810	^{130}0.011		^{154}0.187	^{202}0.105	^{238}0.388	^{215}1.000	^{192}0.602		^{264}1.000	0.000	0.000	0.000			
184	PIXELALL-003	^{87}0.002	^{101}0.014	^{115}0.515	^{107}0.006		^{137}0.151	^{95}0.022	^{101}0.073	^{189}1.000	^{97}0.037		^{134}0.554	0.000	0.000	0.000			

Table 14: **Miss rates by dataset:** *At left, rank 1 miss rates relevant to investigations; at right, with threshold set to target FPIR = 0.01 for higher volume, low prior, uses. Yellow indicates most accurate algorithm. Throughout blue superscripts indicate the rank of the algorithm for that column.*

FNIR(N, R, T) = False neg. identification rate
FPIR(N, T) = False pos. identification rate
N = Num. enrolled subjects
R = Num. candidates examined
T = Threshold
T = 0 → Investigation
T > 0 → Identification

This publication is available free of charge from: https://doi.org/10.6028/NIST.IR.8271

#	ALGORITHM	INVESTIGATION MODE						IDENTIFICATION MODE						FAILURE TO EXTRACT					
		RANK ONE MISS RATE, FNIR(N, 0, 1)						HIGH T → FPIR = 0.001, FNIR(N, T, L)						FEATURES					
		N=1.6M						N=1.6M											
	GALLERY	MUGSHOT	MUGSHOT	MUGSHOT	VISA	BORDER	VISA	MUGSHOT	MUGSHOT	MUGSHOT	VISA	BORDER	VISA	MUGSHOT	MUGSHOT	MUGSHOT	VISA	BORDER	KIOSK
	PROBE	MUGSHOT	WEBCAM	PROFILE	BORDER	BOR¿10YR	KIOSK	MUGSHOT	WEBCAM	PROFILE	BORDER	BOR¿10YR	KIOSK	MUGSHOT	WEBCAM	PROFILE	BORDER	BOR¿10YR	KIOSK
185	PIXELALL-004	^{84}0.002	^{107}0.015	^{119}0.523	^{95}0.005		^{139}0.152	^{84}0.018	^{111}0.079	^{207}1.000	^{111}0.051		^{191}0.994	0.000	0.000	0.000			
186	PIXELALL-005	^{74}0.002	^{57}0.011	^{72}0.264	^{134}0.012	^{78}0.028	^{135}0.146	^{57}0.012	^{62}0.050	^{210}1.000	^{71}0.027	^{67}0.203	^{196}1.000	0.000	0.000	0.000		0.000	
187	PTAKURATSATU-000	^{120}0.003	^{124}0.017	^{135}0.605	^{94}0.005	^{76}0.027	^{82}0.105	^{127}0.037	^{159}0.124	^{69}0.924	^{108}0.046	^{69}0.206	^{67}0.232	0.000	0.001	0.039		0.000	
188	QNAP-000	^{179}0.008	^{183}0.027	^{117}0.522	^{141}0.013	^{95}0.054	^{142}0.158	^{213}0.129	^{209}0.238	^{228}1.000	^{164}0.191	^{93}0.539	^{193}0.998	0.001	0.000	0.054		0.000	
189	QNAP-001	^{140}0.004	^{156}0.022	^{111}0.498	^{106}0.006	^{91}0.041	^{101}0.112	^{157}0.054	^{167}0.137	^{70}0.928	^{136}0.081	^{86}0.368	^{97}0.331	0.000	0.000	0.004		0.000	
190	QNAP-002	^{152}0.005	^{150}0.021	^{52}0.172	^{80}0.004	^{86}0.031	^{115}0.125	^{108}0.026	^{143}0.106	^{51}0.772	^{115}0.052	^{78}0.281	^{83}0.272	0.001	0.004	0.057		0.001	
191	QUANTASOFT-001	^{275}0.218	^{283}0.727					^{273}0.639						0.000	0.000				
192	RANKONE-002	^{228}0.019	^{235}0.071					^{207}0.118	^{217}0.261					0.000	0.000				
193	RANKONE-003	^{227}0.019	^{233}0.068					^{206}0.118	^{216}0.255					0.000	0.000				
194	RANKONE-004	^{249}0.041	^{254}0.141					^{234}0.193	^{243}0.426					0.000	0.000				
195	RANKONE-005	^{193}0.009	^{209}0.041	^{239}0.986				^{169}0.059	^{192}0.173	^{157}0.998				0.000	0.000	0.489			
196	RANKONE-006	^{154}0.005		^{173}0.797				^{129}0.037		^{91}0.977				0.002		0.167			
197	RANKONE-007	^{126}0.003	^{137}0.019	^{170}0.796				^{97}0.022	^{128}0.095	^{79}0.967				0.001	0.001	0.102			
198	RANKONE-009	^{100}0.002	^{82}0.013	^{126}0.549	^{97}0.006		^{127}0.134	^{79}0.018	^{105}0.076	^{82}0.969	^{122}0.062		^{96}0.328	0.000	0.000	0.000			
199	RANKONE-010	^{94}0.002	^{39}0.010	^{97}0.374	^{90}0.005	^{74}0.027	^{117}0.126	^{63}0.014	^{81}0.058	^{54}0.802	^{114}0.052	^{70}0.208	^{75}0.259	0.000	0.000	0.000		0.000	
200	RANKONE-011	^{43}0.002	^{67}0.011	^{62}0.223	^{65}0.004	^{58}0.019	^{49}0.082	^{43}0.009	^{60}0.048		^{96}0.037	^{62}0.182	^{185}0.977	0.000	0.000	0.000		0.000	
201	RANKONE-012	^{31}0.001	^{51}0.010	^{40}0.127	^{56}0.003	^{48}0.014	^{21}0.069	^{40}0.008	^{73}0.053		^{77}0.029	^{45}0.144	^{119}0.465	0.000	0.000	0.000		0.000	
202	REALNETWORKS-000	^{248}0.040	^{242}0.078					^{239}0.234	^{232}0.319					0.001	0.000				
203	REALNETWORKS-001	^{247}0.040	^{241}0.078					^{240}0.234	^{233}0.319					0.001	0.000				
204	REALNETWORKS-002	^{244}0.039	^{240}0.078					^{238}0.231	^{231}0.315					0.001	0.000				
205	REALNETWORKS-003	^{234}0.024	^{229}0.062	^{166}0.771	^{165}0.031		^{160}0.209	^{224}0.159	^{220}0.266	^{161}0.998	^{159}0.164		^{126}0.500	0.001	0.000	0.009			
206	REALNETWORKS-004	^{232}0.024	^{226}0.059	^{172}0.797	^{164}0.031		^{165}0.213	^{223}0.158	^{218}0.263	^{174}0.999	^{160}0.170		^{138}0.613	0.001	0.000	0.009			
207	REALNETWORKS-005	^{96}0.002	^{87}0.013	^{103}0.433	^{82}0.004	^{66}0.023	^{79}0.102	^{114}0.028	^{103}0.074	^{84}0.971	^{95}0.037	^{71}0.223	^{62}0.215	0.000	0.000	0.006		0.000	
208	REALNETWORKS-006	^{33}0.001	^{40}0.010	^{77}0.287	^{46}0.002	^{33}0.010	^{40}0.078	^{67}0.015	^{71}0.053	^{99}0.980	^{45}0.016	^{38}0.120	^{38}0.154	0.000	0.000	0.009		0.000	
209	REALNETWORKS-007	^{28}0.001	^{32}0.009	^{73}0.267	^{21}0.002	^{27}0.009	^{27}0.072	^{47}0.010	^{56}0.043	^{94}0.979	^{39}0.012	^{92}0.463	^{31}0.140	0.000	0.000	0.009		0.000	
210	REMARKAI-000	^{128}0.003	^{135}0.018	^{139}0.660	^{119}0.008		^{136}0.148	^{161}0.055	^{155}0.120	^{172}0.999	^{131}0.069		^{146}0.717	0.000	0.000	0.000			
211	REMARKAI-000	^{186}0.009	^{186}0.030					^{211}0.128	^{198}0.203					0.000	0.001				
212	REMARKAI-002	^{184}0.008	^{185}0.029	^{174}0.802				^{210}0.124	^{196}0.196	^{120}0.991				0.000	0.001	0.017			
213	RENDIP-000	^{47}0.002	^{108}0.015	^{102}0.424	^{103}0.006	^{77}0.028	^{52}0.084	^{56}0.012	^{82}0.059	^{66}0.894	^{61}0.022	^{64}0.185	^{45}0.167	0.000	0.000	0.041		0.000	
214	REVEALMEDIA-000	^{71}0.002	^{36}0.010	^{74}0.275	^{32}0.002	^{40}0.012	^{31}0.074	^{58}0.012	^{54}0.042	^{43}0.680	^{59}0.021	^{33}0.093	^{33}0.143	0.000	0.000	0.041		0.000	
215	S1-000	^{102}0.002	^{123}0.017	^{71}0.258	^{96}0.005	^{72}0.025	^{57}0.090	^{116}0.028	^{115}0.085	^{229}1.000	^{110}0.047	^{132}1.000	^{275}1.000	0.000	0.000	0.040		0.000	
216	S1-001	^{121}0.003	^{98}0.014	^{61}0.215	^{50}0.003	^{56}0.018	^{35}0.077	^{74}0.016	^{68}0.052	^{107}0.985	^{53}0.019	^{40}0.136	^{34}0.148	0.001	0.000	0.035		0.000	
217	S1-002	^{36}0.001	^{30}0.009	^{32}0.093	^{6}0.001	^{34}0.010	^{6}0.055	^{34}0.006	^{38}0.031	^{6}0.196	^{20}0.007	^{103}0.792	^{163}0.841	0.000	0.000	0.028		0.000	
218	SCANOVATE-000	^{153}0.005	^{213}0.045	^{130}0.560	^{169}0.035		^{164}0.211	^{176}0.067	^{212}0.240	^{64}0.893	^{168}0.215		^{106}0.400	0.000	0.001	0.057			
219	SCANOVATE-001	^{157}0.005	^{207}0.040	^{134}0.585	^{163}0.031		^{152}0.178	^{187}0.081	^{206}0.227	^{68}0.911	^{165}0.192		^{109}0.404	0.000	0.001	0.044			
220	SENSETIME-000	^{98}0.002	^{115}0.016	^{120}0.528				^{93}0.021	^{87}0.063	^{266}1.000				0.004	0.000	0.042			
221	SENSETIME-001	^{99}0.002	^{114}0.016					^{96}0.022	^{89}0.064					0.004	0.000				
222	SENSETIME-002	^{215}0.014	^{141}0.020	^{98}0.384	^{129}0.011		^{80}0.104	^{68}0.015	^{35}0.028	^{128}0.994	^{84}0.032		^{129}0.523	0.009	0.000	0.040			
223	SENSETIME-003	^{6}0.001	^{7}0.007	^{47}0.150	^{48}0.003		^{59}0.091	^{7}0.002	^{4}0.012	^{24}0.477	^{25}0.008		^{28}0.133	0.000	0.000	0.041			
224	SENSETIME-004	^{5}0.001	^{9}0.007	^{22}0.072	^{37}0.002		^{53}0.084	^{4}0.002	^{6}0.013	^{11}0.229	^{14}0.006		^{21}0.113	0.000	0.000	0.041			
225	SENSETIME-005	^{3}0.001	^{3}0.006	^{6}0.059	^{36}0.002	^{19}0.007	^{45}0.082	^{11}0.002	^{12}0.014	^{5}0.173	^{18}0.007	^{16}0.051	^{16}0.104	0.000	0.000	0.041		0.000	
226	SENSETIME-006	^{2}0.001	^{2}0.006	^{2}0.055	^{3}0.001	^{2}0.004	^{16}0.064	^{6}0.002	^{5}0.012	^{160}0.998	^{6}0.004	^{9}0.034	^{8}0.093	0.000	0.000	0.025		0.000	
227	SENSETIME-007	^{1}0.001	^{1}0.006	^{1}0.052	^{1}0.001	^{1}0.003	^{13}0.062	^{1}0.001	^{1}0.009	^{178}0.999	^{2}0.003	^{4}0.024	^{5}0.085	0.000	0.000	0.025		0.000	
228	SHAMAN-003	^{266}0.124	^{258}0.172					^{263}0.451	^{258}0.597					0.020	0.011				
229	SHAMAN-004	^{277}0.222	^{267}0.319					^{271}0.615	^{265}0.754					0.020	0.011				
230	SHAMAN-006	^{246}0.040	^{225}0.058	^{207}0.938				^{218}0.141	^{208}0.237	^{85}0.972				0.020	0.011	0.869			

Table 15: **Miss rates by dataset:** *At left, rank 1 miss rates relevant to investigations; at right, with threshold set to target FPIR = 0.01 for higher volume, low prior, uses. Yellow indicates most accurate algorithm. Throughout blue superscripts indicate the rank of the algorithm for that column.*

This publication is available free of charge from: https://doi.org/10.6028/NIST.IR.8271

#	ALGORITHM	INVESTIGATION MODE						IDENTIFICATION MODE						FAILURE TO EXTRACT					
		RANK ONE MISS RATE, FNIR(N, 0, 1)						HIGH T → FPIR = 0.001, FNIR(N, T, L)						FEATURES					
		N=1.6M						N=1.6M											
	GALLERY	MUGSHOT	MUGSHOT	MUGSHOT	VISA	BORDER	VISA	MUGSHOT	MUGSHOT	MUGSHOT	VISA	BORDER	VISA	MUGSHOT	MUGSHOT	MUGSHOT	VISA	BORDER	KIOSK
	PROBE	MUGSHOT	WEBCAM	PROFILE	BORDER	BOR¿10YR	KIOSK	MUGSHOT	WEBCAM	PROFILE	BORDER	BOR¿10YR	KIOSK	MUGSHOT	WEBCAM	PROFILE	BORDER	BOR¿10YR	KIOSK
231	SHAMAN-007	^{245}0.040	^{224}0.057					^{219}0.141	^{211}0.240					0.020	0.010				
232	SIAT-001	^{65}0.002	^{269}0.333		^{83}0.004		^{72}0.099	^{77}0.018	^{237}0.365		^{80}0.031			0.000	0.000				
233	SIAT-002	^{67}0.002	^{271}0.446		^{199}0.348		^{78}0.102	^{94}0.022	^{249}0.478		^{178}0.372		^{175}0.923	0.000	0.000				
234	SMILART-004	^{290}0.965	^{286}0.974					^{282}0.968	^{279}0.976					0.011	0.013				
235	SMILART-005													0.011	0.013				
236	SQISOFT-001	^{141}0.004	^{139}0.019	^{76}0.282	^{92}0.005	^{75}0.027	^{67}0.097	^{215}0.132	^{214}0.252	^{52}0.797	^{100}0.040	^{83}0.317	^{111}0.420	0.000	0.000	0.039		0.000	
237	STAQU-000	^{175}0.007	^{146}0.020	^{137}0.613	^{152}0.020	^{96}0.055	^{143}0.159	^{170}0.062	^{243}0.443	^{199}1.000	^{190}0.535	^{104}0.961	^{263}1.000	0.000	0.000	0.000		0.000	
238	SYNESIS-003	^{272}0.170	^{263}0.235					^{268}0.582	^{261}0.646					0.006	0.015				
239	SYNESIS-003	^{219}0.016	^{166}0.023	^{182}0.827	^{137}0.013		^{129}0.136	^{174}0.065	^{158}0.123	^{77}0.960	^{133}0.075		^{91}0.314	0.000	0.001	0.063			
240	SYNESIS-005	^{185}0.009	^{83}0.013	^{158}0.744	^{59}0.003		^{60}0.092	^{102}0.025	^{99}0.072	^{104}0.984	^{87}0.032		^{61}0.214	0.001	0.000	0.135			
241	TECH5-001	^{136}0.004	^{122}0.017	^{133}0.584	^{109}0.007		^{89}0.107	^{164}0.057	^{275}0.935	^{230}1.000	^{169}0.244		^{192}0.994	0.000	0.000	0.006			
242	TECH5-002	^{111}0.003	^{56}0.011	^{83}0.312	^{58}0.003	^{83}0.029	^{56}0.089	^{111}0.027	^{97}0.070	^{55}0.805	^{99}0.039	^{68}0.205	^{114}0.440	0.001	0.000	0.041		0.000	
243	TEVIAN-003	^{216}0.015	^{220}0.052					^{231}0.177	^{227}0.298					0.001	0.002				
244	TEVIAN-004	^{203}0.011	^{200}0.038					^{205}0.117	^{193}0.176					0.001	0.002				
245	TEVIAN-005	^{176}0.007	^{184}0.028	^{108}0.467				^{192}0.087	^{173}0.144	^{78}0.962				0.001	0.002	0.116			
246	TEVIAN-006	^{103}0.002	^{63}0.011	^{38}0.123	^{51}0.003	^{47}0.013	^{25}0.071	^{48}0.010	^{40}0.032	^{19}0.425	^{46}0.016	^{31}0.093	^{180}0.951	0.001	0.000	0.062		0.000	
247	TEVIAN-007	^{63}0.002	^{31}0.009	^{31}0.093	^{28}0.002	^{30}0.009	^{18}0.067	^{32}0.005	^{21}0.022	^{15}0.301	^{34}0.009	^{23}0.065	^{23}0.122	0.000	0.000	0.062		0.000	
248	TIGER-000	^{256}0.062	^{248}0.095					^{257}0.390	^{250}0.500					0.000	0.000				
249	TIGER-002	^{159}0.006	^{163}0.023	^{114}0.514				^{188}0.086	^{182}0.158	^{169}0.999				0.000	0.000	0.056			
250	TIGER-003	^{160}0.006	^{164}0.023					^{189}0.086	^{183}0.158					0.000	0.000				
251	TONGYITRANS-000	^{171}0.007	^{160}0.022					^{181}0.074	^{147}0.112					0.003	0.001				
252	TONGYITRANS-001	^{172}0.007	^{161}0.022					^{175}0.066	^{137}0.101					0.003	0.001				
253	TOSHIBA-000	^{145}0.004	^{153}0.022	^{164}0.766				^{171}0.062	^{152}0.118	^{141}0.995				0.000	0.000	0.070			
254	TOSHIBA-001	^{150}0.005	^{157}0.022					^{166}0.058	^{125}0.092					0.000	0.000				
255	TRUEFACE-000	^{125}0.003	^{92}0.014	^{65}0.230	^{114}0.007	^{69}0.024	^{61}0.092	^{83}0.018	^{86}0.062	^{61}0.882	^{78}0.030	^{66}0.194	^{56}0.188	0.001	0.001	0.047		0.003	
256	VD-000	^{283}0.474	^{277}0.551					^{280}0.917	^{277}0.946					0.011	0.013				
257	VD-001	^{238}0.028	^{221}0.053					^{235}0.201	^{224}0.281					0.005	0.001				
258	VD-002	^{194}0.010	^{182}0.027	^{189}0.893	^{140}0.013	^{93}0.050	^{150}0.176	^{185}0.079	^{175}0.148	^{144}0.996	^{140}0.095	^{85}0.367	^{102}0.372	0.004	0.003	0.156		0.002	
259	VD-003	^{177}0.008	^{154}0.022	^{167}0.773	^{122}0.008	^{85}0.030	^{130}0.137	^{142}0.046	^{136}0.100	^{170}0.999	^{112}0.051	^{73}0.244	^{93}0.315	0.003	0.003	0.144		0.002	
260	VERIDAS-001	^{114}0.003	^{99}0.014	^{127}0.550	^{104}0.006	^{79}0.028	^{120}0.131	^{131}0.037	^{114}0.082	^{112}0.987	^{104}0.044	^{75}0.266	^{80}0.264	0.000	0.002	0.093		0.001	
261	VERIDAS-002	^{113}0.003	^{100}0.014	^{128}0.550	^{105}0.006	^{80}0.028	^{121}0.131	^{130}0.037	^{113}0.082	^{111}0.987	^{103}0.044	^{76}0.266	^{79}0.264	0.000	0.002	0.093		0.001	
262	VERIDAS-003	^{66}0.002	^{62}0.011	^{80}0.297	^{73}0.004	^{52}0.016	^{91}0.108	^{75}0.017	^{76}0.055	^{149}0.997	^{55}0.020	^{48}0.150	^{51}0.178	0.000	0.002	0.093		0.001	
263	VIGILANTSOLUTIONS-003	^{259}0.069	^{256}0.151	^{219}0.958				^{261}0.408	^{264}0.660	^{166}0.999				0.000	0.001	0.127			
264	VIGILANTSOLUTIONS-004	^{267}0.125	^{264}0.244	^{224}0.965				^{267}0.549	^{269}0.817	^{147}0.996				0.000	0.001	0.127			
265	VIGILANTSOLUTIONS-005	^{190}0.009		^{196}0.920				^{256}0.388		^{214}1.000				0.000	0.001	0.127			
266	VIGILANTSOLUTIONS-006	^{196}0.010		^{197}0.921				^{251}0.353		^{224}1.000				0.000	0.001	0.127			
267	VIGILANTSOLUTIONS-007	^{127}0.003	^{127}0.017	^{200}0.925	^{138}0.013	^{98}0.068	^{148}0.175	^{118}0.028	^{119}0.088	^{146}0.996	^{137}0.081	^{87}0.371	^{105}0.391	0.000	0.001	0.127		0.001	
268	VIGILANTSOLUTIONS-008	^{119}0.003	^{128}0.017	^{195}0.913	^{142}0.014	^{99}0.072	^{151}0.178	^{90}0.021	^{106}0.077	^{168}0.999	^{144}0.104	^{89}0.398	^{127}0.511	0.000	0.001	0.127		0.001	
269	VISIONBOX-000	^{75}0.002	^{64}0.011	^{160}0.752	^{86}0.005	^{54}0.017	^{41}0.078	^{80}0.018	^{79}0.057	^{119}0.990	^{64}0.023	^{47}0.146	^{43}0.162	0.000	0.001	0.043		0.001	
270	VISIONLABS-004	^{112}0.003	^{142}0.020	^{91}0.343				^{165}0.058	^{184}0.159	^{63}0.890				0.001	0.001	0.046			
271	VISIONLABS-005	^{101}0.002	^{136}0.019	^{89}0.334				^{149}0.050	^{174}0.147	^{62}0.888				0.001	0.001	0.046			
272	VISIONLABS-006	^{68}0.002	^{112}0.015	^{60}0.211	^{68}0.004		^{65}0.096	^{110}0.027	^{123}0.090	^{39}0.672				0.001	0.001	0.051			
273	VISIONLABS-007	^{62}0.002	^{111}0.015	^{59}0.211	^{64}0.004		^{64}0.095	^{109}0.027	^{122}0.090	^{40}0.672	^{83}0.031		^{55}0.185	0.001	0.001	0.051			
274	VISIONLABS-008	^{82}0.002	^{93}0.014	^{42}0.141	^{35}0.002		^{44}0.081	^{61}0.013	^{67}0.051	^{25}0.481	^{47}0.017		^{35}0.151	0.001	0.000	0.075			
275	VISIONLABS-009	^{17}0.001	^{25}0.008	^{30}0.091	^{13}0.001		^{24}0.071	^{26}0.005	^{28}0.025	^{53}0.799	^{29}0.008		^{20}0.113	0.000	0.000	0.060			
276	VISIONLABS-010	^{34}0.001	^{50}0.010	^{19}0.069	^{9}0.001	^{11}0.006	^{23}0.069	^{31}0.005	^{34}0.027		^{23}0.008	^{18}0.055	^{19}0.109	0.000	0.000	0.040		0.000	

Table 16: **Miss rates by dataset:** *At left, rank 1 miss rates relevant to investigations; at right, with threshold set to target FPIR = 0.01 for higher volume, low prior, uses. Yellow indicates most accurate algorithm. Throughout blue superscripts indicate the rank of the algorithm for that column.*

This publication is available free of charge from: https://doi.org/10.6028/NIST.IR.8271

#	ALGORITHM	INVESTIGATION MODE						IDENTIFICATION MODE						FAILURE TO EXTRACT					
		RANK ONE MISS RATE, FNIR(N, 0, 1)						HIGH T ⟶ FPIR = 0.001, FNIR(N, T, L)						FEATURES					
		N=1.6M						N=1.6M											
	GALLERY	MUGSHOT	MUGSHOT	MUGSHOT	VISA	BORDER	VISA	MUGSHOT	MUGSHOT	MUGSHOT	VISA	BORDER	VISA	MUGSHOT	MUGSHOT	MUGSHOT	VISA	BORDER	KIOSK
	PROBE	MUGSHOT	WEBCAM	PROFILE	BORDER	BOR¿10YR	KIOSK	MUGSHOT	WEBCAM	PROFILE	BORDER	BOR¿10YR	KIOSK	MUGSHOT	WEBCAM	PROFILE	BORDER	BOR¿10YR	KIOSK
277	VISIONLABS-011	^{20}0.001	^{28}0.009	^{12}0.064	^{7}0.001	^{6}0.004	^{15}0.063	^{19}0.003	^{19}0.020		^{9}0.004	^{10}0.034	^{6}0.090	0.000	0.000	0.032		0.000	
278	VNPT-001	^{88}0.002	^{105}0.014	^{45}0.145	^{45}0.002	^{68}0.023	^{26}0.071	^{65}0.014	^{95}0.068	^{45}0.718	^{92}0.035	^{105}0.990	^{100}0.362	0.001	0.000	0.042		0.000	
279	VOCORD-003	^{165}0.006	^{171}0.024	^{175}0.804	^{182}0.061		^{155}0.188	^{209}0.122	^{180}0.155	^{158}0.998	^{158}0.157		^{108}0.404	0.001	0.011	0.425			
280	VOCORD-004	^{180}0.008	^{149}0.021	^{169}0.792	^{136}0.012		^{118}0.127	^{252}0.355	^{190}0.173	^{202}1.000	^{166}0.193		^{189}0.991	0.000	0.000	0.000			
281	VOCORD-005	^{174}0.007	^{167}0.023	^{177}0.812	^{178}0.055		^{158}0.206	^{222}0.158	^{163}0.130	^{150}0.997	^{153}0.138		^{103}0.381	0.001	0.009	0.554			
282	VOCORD-006	^{293}1.000	^{290}1.000	^{263}1.000	^{218}1.000		^{218}1.000	^{293}1.000	^{286}1.000	^{259}1.000	^{260}1.000		^{252}1.000	0.001	0.009	0.554			
283	VTS-000	^{288}0.594	^{280}0.608	^{193}0.909	^{205}0.607	^{108}0.724	^{203}0.739	^{269}0.598	^{259}0.619	^{176}0.999	^{195}0.613	^{100}0.760	^{150}0.761	0.000	0.001	0.047		0.000	
284	VTS-001	^{45}0.002	^{43}0.010	^{51}0.167	^{99}0.006	^{57}0.018	^{38}0.077	^{62}0.013	^{66}0.051	^{129}0.994	^{62}0.022	^{44}0.141	^{57}0.192	0.000	0.000	0.040		0.000	
285	VTS-002	^{77}0.002	^{84}0.013	^{66}0.233	^{144}0.014	^{90}0.038	^{113}0.125	^{105}0.026	^{104}0.075	^{186}1.000	^{106}0.045	^{72}0.231	^{110}0.417	0.000	0.000	0.029		0.000	
286	XFORWARDAI-000	^{95}0.002	^{96}0.014	^{29}0.089	^{70}0.004	^{49}0.015	^{62}0.094	^{71}0.015	^{74}0.053	^{21}0.440	^{58}0.021	^{53}0.159	^{46}0.169	0.000	0.000	0.000		0.000	
287	XFORWARDAI-001	^{85}0.002	^{81}0.013	^{16}0.067	^{54}0.003	^{28}0.009	^{47}0.082	^{29}0.005	^{36}0.028	^{22}0.448	^{26}0.008	^{22}0.062	^{24}0.123	0.000	0.000	0.000		0.000	
288	XFORWARDAI-002	^{78}0.002	^{75}0.012	^{5}0.059	^{42}0.002	^{16}0.007	^{36}0.077	^{18}0.003	^{15}0.016	^{27}0.525	^{12}0.005	^{13}0.041	^{13}0.099	0.000	0.000	0.000		0.000	
289	YISHENG-001	^{237}0.027	^{228}0.060		^{181}0.058		^{181}0.287	^{249}0.346	^{267}0.808		^{197}0.666		^{174}0.919	0.002	0.005				
290	YITU-002	^{69}0.002	^{46}0.010					^{78}0.018	^{61}0.049					0.000	0.000				
291	YITU-003	^{118}0.003	^{117}0.016					^{86}0.019	^{70}0.052					0.003	0.001				
292	YITU-004	^{27}0.001	^{24}0.008	^{187}0.866				^{45}0.010	^{32}0.027	^{71}0.936				0.000	0.000	0.000			
293	YITU-005	^{97}0.002	^{106}0.014					^{52}0.010	^{41}0.032					0.003	0.001				

Table 17: **Miss rates by dataset:** *At left, rank 1 miss rates relevant to investigations; at right, with threshold set to target FPIR = 0.01 for higher volume, low prior, uses. Yellow indicates most accurate algorithm. Throughout blue superscripts indicate the rank of the algorithm for that column.*

MISSES BELOW THRESHOLD, T		ENROL MOST RECENT				
FNIR(N, T> 0, R >L)		DATASET: FRVT 2018 MUGSHOTS				
#	ALGORITHM	N=0.64M	N=1.6M	N=3.0M	N=6.0M	N=12.0M
1	3DIVI-005	^{227}0.1358	^{227}0.1664	^{200}0.1915	^{191}0.2370	^{183}0.3054
2	ACER-000	^{221}0.1185	^{220}0.1455	^{194}0.1714	^{184}0.2074	^{176}0.2537
3	ALCHERA-003	^{219}0.1176	^{221}0.1553	^{196}0.1853	^{192}0.2409	^{191}0.3553
4	ALLGOVISION-000	^{193}0.0688	^{194}0.0881	^{177}0.1084	^{169}0.1389	^{156}0.2129
5	ALLGOVISION-001	^{199}0.0785	^{200}0.1017	^{184}0.1218	^{176}0.1584	^{163}0.2273
6	ANKE-000	^{206}0.0942	^{204}0.1169	^{189}0.1404	^{181}0.1776	^{177}0.2559
7	ANKE-002	^{123}0.0229	^{123}0.0318	^{124}0.0406	^{118}0.0605	^{104}0.1466
8	AWARE-003	^{216}0.1098	^{212}0.1283	^{190}0.1447	^{179}0.1768	^{168}0.2364
9	AWARE-005	^{255}0.3389	^{253}0.3643	^{207}0.3993	^{200}0.4526	^{175}0.2531
10	AYONIX-002	^{277}0.7862	^{277}0.8242	^{213}0.8508	^{205}0.8704	^{199}0.8939
11	CAMVI-004	^{149}0.0367	^{178}0.0716	^{172}0.0983	^{194}0.2508	^{180}0.2701
12	CANON-001	^{33}0.0039	^{33}0.0054	^{33}0.0074	^{30}0.0158	^{38}0.0924
13	CANON-002	^{28}0.0036	^{27}0.0047	^{28}0.0061	^{24}0.0124	^{24}0.0808
14	CIB-000	^{56}0.0086	^{59}0.0125	^{59}0.0160	^{64}0.0303	^{80}0.1251
15	CLEARVIEWAI-000	^{35}0.0040	^{35}0.0058	^{35}0.0078	^{31}0.0159	^{41}0.0971
16	CLOUDWALK-HR-000	^{10}0.0019	^{10}0.0020	^{8}0.0023	^{13}0.0072	^{17}0.0701
17	CLOUDWALK-MT-000	^{11}0.0019	^{9}0.0020	^{7}0.0022	^{5}0.0049	^{9}0.0466
18	COGENT-000	^{167}0.0430	^{153}0.0527	^{153}0.0695	^{155}0.1133	^{145}0.1960
19	COGENT-001	^{168}0.0430	^{152}0.0527	^{154}0.0695	^{154}0.1133	^{144}0.1960
20	COGENT-002	^{135}0.0322	^{139}0.0444	^{139}0.0610	^{152}0.1116	^{158}0.2180
21	COGENT-003	^{136}0.0328	^{144}0.0463	^{151}0.0683	^{162}0.1294	^{170}0.2445
22	COGENT-004	^{120}0.0210	^{124}0.0331	^{134}0.0527	^{157}0.1138	^{155}0.2119
23	COGENT-005	^{45}0.0064	^{44}0.0091	^{44}0.0123	^{63}0.0303	^{76}0.1233
24	COGENT-006	^{24}0.0032	^{24}0.0044	^{24}0.0057	^{22}0.0120	^{26}0.0830
25	COGNITEC-000	^{229}0.1377	^{225}0.1606	^{199}0.1870	^{186}0.2176	^{182}0.2831
26	COGNITEC-001	^{201}0.0807	^{199}0.1017	^{183}0.1214	^{172}0.1513	^{161}0.2238
27	COGNITEC-002	^{160}0.0406	^{155}0.0531	^{147}0.0666	^{140}0.0935	^{140}0.1874
28	COGNITEC-003	^{157}0.0400	^{151}0.0526	^{142}0.0650	^{135}0.0895	^{133}0.1772
29	COGNITEC-004	^{122}0.0222	^{122}0.0313	^{120}0.0388	^{110}0.0540	^{58}0.1103
30	COGNITEC-005	^{44}0.0063	^{46}0.0096	^{52}0.0144	^{57}0.0287	^{40}0.0967
31	COGNITEC-006	^{40}0.0053	^{41}0.0077	^{43}0.0117	^{45}0.0254	^{34}0.0919
32	CYBERLINK-000	^{162}0.0414	^{163}0.0565	^{158}0.0707	^{148}0.1031	^{151}0.2050
33	CYBERLINK-001	^{153}0.0392	^{156}0.0536	^{152}0.0695	^{145}0.0973	^{134}0.1794
34	CYBERLINK-002	^{66}0.0105	^{69}0.0148	^{74}0.0202	^{85}0.0399	^{81}0.1255
35	CYBERLINK-003	^{41}0.0056	^{42}0.0077	^{39}0.0100	^{41}0.0235	^{77}0.1237
36	CYBERLINK-004	^{39}0.0051	^{39}0.0071	^{41}0.0102	^{35}0.0199	^{84}0.1269
37	CYBERLINK-005	^{47}0.0067	^{50}0.0099	^{50}0.0138	^{82}0.0394	^{118}0.1566
38	DAHUA-001	^{182}0.0569	^{180}0.0727	^{166}0.0878	^{158}0.1148	^{139}0.1867
39	DAHUA-002	^{71}0.0108	^{70}0.0151	^{69}0.0191	^{59}0.0291	^{69}0.1153
40	DAHUA-003	^{63}0.0100	^{64}0.0139	^{65}0.0180	^{60}0.0296	^{63}0.1130
41	DAHUA-004	^{38}0.0048	^{38}0.0069	^{37}0.0090	^{33}0.0164	^{27}0.0853
42	DAON-000	^{98}0.0161	^{98}0.0226	^{100}0.0293	^{117}0.0562	^{127}0.1702
43	DECATUR-000	^{100}0.0173	^{101}0.0229	^{101}0.0305	^{95}0.0464	^{101}0.1433
44	DEEPGLINT-001	^{20}0.0027	^{20}0.0033	^{19}0.0043	^{23}0.0121	^{37}0.0922
45	DEEPSEA-001	^{145}0.0347	^{143}0.0462	^{138}0.0586	^{133}0.0802	^{129}0.1708
46	DERMALOG-005	^{197}0.0700	^{193}0.0880	^{179}0.1144	^{175}0.1578	^{171}0.2451
47	DERMALOG-006	^{154}0.0395	^{150}0.0517	^{143}0.0659	^{144}0.0973	^{132}0.1745
48	DERMALOG-007	^{194}0.0691	^{191}0.0863	^{178}0.1107	^{171}0.1504	^{166}0.2299
49	DERMALOG-008	^{141}0.0338	^{141}0.0455	^{141}0.0626	^{149}0.1060	^{164}0.2276
50	DERMALOG-009	^{91}0.0148	^{91}0.0206	^{92}0.0268	^{89}0.0416	^{95}0.1374
51	DILUSENSE-000	^{119}0.0208	^{120}0.0305	^{118}0.0377	^{114}0.0543	^{99}0.1429
52	FUJITSULAB-000	^{92}0.0148	^{92}0.0206	^{96}0.0277	^{112}0.0541	^{131}0.1739
53	FUJITSULAB-001	^{76}0.0126	^{82}0.0182	^{87}0.0251	^{121}0.0646	^{152}0.2079
54	GORILLA-002	^{233}0.1539	^{233}0.1880	^{203}0.2184	^{195}0.2596	^{190}0.3398
55	GORILLA-004	^{196}0.0699	^{196}0.0892	^{175}0.1048	^{167}0.1370	^{148}0.1969
56	GORILLA-005	^{172}0.0453	^{167}0.0583	^{157}0.0704	^{146}0.0974	^{105}0.1474
57	GORILLA-006	^{113}0.0196	^{113}0.0275	^{106}0.0331	^{103}0.0516	^{61}0.1113
58	GORILLA-007	^{110}0.0190	^{112}0.0271	^{112}0.0348	^{106}0.0520	^{62}0.1129
59	GRIAULE-000	^{88}0.0145	^{89}0.0201	^{88}0.0253	^{87}0.0407	^{102}0.1440
60	HIK-003	^{202}0.0828	^{201}0.1028	^{182}0.1202	^{174}0.1525	^{173}0.2480
61	HIK-004	^{200}0.0796	^{197}0.0988	^{180}0.1147	^{170}0.1474	^{174}0.2483
62	HIK-005	^{133}0.0312	^{136}0.0436	^{137}0.0560	^{137}0.0911	^{157}0.2129
63	HYPERVERGE-001	^{25}0.0033	^{25}0.0045	^{25}0.0059	^{19}0.0117	^{29}0.0872
64	HYPERVERGE-002	^{21}0.0028	^{21}0.0037	^{21}0.0046	^{10}0.0064	^{1}0.0064
65	HZAILU-000	^{87}0.0143	^{88}0.0197	^{89}0.0255	^{88}0.0411	^{72}0.1174
66	IDEMIA-003	^{143}0.0346	^{146}0.0471	^{167}0.0892	^{197}0.2789	^{194}0.4311
67	IDEMIA-004	^{132}0.0300	^{132}0.0373	^{126}0.0447	^{119}0.0617	^{126}0.1635
68	IDEMIA-005	^{148}0.0360	^{138}0.0440	^{135}0.0537	^{132}0.0764	^{141}0.1915
69	IDEMIA-006	^{146}0.0351	^{135}0.0433	^{133}0.0525	^{129}0.0734	^{159}0.2201
70	IDEMIA-007	^{83}0.0136	^{81}0.0181	^{76}0.0228	^{75}0.0357	^{98}0.1402
71	IDEMIA-008	^{8}0.0016	^{8}0.0019	^{10}0.0024	^{6}0.0053	^{10}0.0470
72	IDEMIA-009	^{2}0.0013	^{2}0.0016	^{2}0.0018	^{9}0.0061	^{13}0.0550

Table 18: **Identification-mode: Effect of N on FNIR at high threshold.** *Values are threshold-based miss rates i.e.* FNIR *at* FPIR = *0.001 for five enrollment population sizes, N. The right six columns apply for enrollment of one image. Missing entries usually apply because another algorithm from the same developer was run instead. Some developers are missing because less accurate algorithms were not run on galleries with $N \geq 3\,000\,000$. Throughout blue superscripts indicate the rank of the algorithm for that column.*

This publication is available free of charge from: https://doi.org/10.6028/NIST.IR.8271

This publication is available free of charge from: https://doi.org/10.6028/NIST.IR.8271

MISSES BELOW THRESHOLD, T		ENROL MOST RECENT				
FNIR(N, T> 0, R >L)		DATASET: FRVT 2018 MUGSHOTS				
#	ALGORITHM	N=0.64M	N=1.6M	N=3.0M	N=6.0M	N=12.0M
73	IMAGUS-005	^{84}0.0137	^{85}0.0185	^{82}0.0237	^{77}0.0368	^{54}0.1067
74	IMAGUS-006	^{85}0.0137	^{87}0.0190	^{85}0.0244	^{83}0.0396	^{70}0.1159
75	IMAGUS-007	^{96}0.0160	^{100}0.0228	^{98}0.0284	^{92}0.0444	^{73}0.1179
76	IMPERIAL-000	^{106}0.0187	^{106}0.0259	^{116}0.0358	^{128}0.0733	^{135}0.1794
77	INCODE-003	^{226}0.1324	^{228}0.1672	^{201}0.1961	^{189}0.2345	^{185}0.3123
78	INCODE-004	^{158}0.0403	^{159}0.0538	^{146}0.0662	^{139}0.0917	^{123}0.1619
79	INCODE-005	^{54}0.0083	^{54}0.0113	^{53}0.0145	^{42}0.0247	^{32}0.0912
80	INNOVATRICS-007	^{60}0.0093	^{60}0.0125	^{58}0.0159	^{47}0.0259	^{55}0.1092
81	INTSYSMSU-000	^{288}0.9982	^{286}0.9984	^{217}0.9985	^{208}0.9987	^{203}0.9988
82	IREX-000	^{111}0.0190	^{117}0.0280	^{121}0.0391	^{124}0.0677	^{108}0.1479
83	ISYSTEMS-002	^{184}0.0584	^{184}0.0783	^{171}0.0973	^{168}0.1373	^{165}0.2295
84	ISYSTEMS-003	^{170}0.0438	^{168}0.0590	^{164}0.0807	^{160}0.1259	^{167}0.2357
85	KAKAO-000	^{72}0.0109	^{72}0.0151	^{71}0.0196	^{70}0.0324	^{44}0.1010
86	KEDACOM-001	^{102}0.0181	^{99}0.0227	^{90}0.0265	^{91}0.0422	^{92}0.1340
87	LOOKMAN-003	^{144}0.0346	^{137}0.0437	^{131}0.0514	^{127}0.0724	^{124}0.1620
88	LOOKMAN-005	^{124}0.0240	^{119}0.0301	^{115}0.0356	^{102}0.0512	^{91}0.1334
89	MANTRA-000	^{46}0.0065	^{51}0.0101	^{54}0.0151	^{65}0.0308	^{48}0.1035
90	MEGVII-001	^{180}0.0562	^{179}0.0722	^{165}0.0872	^{164}0.1309	^{181}0.2713
91	MICROFOCUS-005	^{285}0.9732	^{279}0.8354	^{214}0.8555	^{206}0.8755	^{200}0.8954
92	MICROSOFT-003	^{114}0.0198	^{115}0.0278	^{114}0.0356	^{109}0.0538	^{114}0.1539
93	MICROSOFT-004	^{105}0.0185	^{107}0.0259	^{107}0.0333	^{104}0.0517	^{112}0.1510
94	MICROSOFT-005	^{103}0.0181	^{104}0.0256	^{104}0.0320	^{101}0.0512	^{110}0.1491
95	MICROSOFT-006	^{59}0.0091	^{55}0.0120	^{60}0.0162	^{62}0.0301	^{109}0.1482
96	NEC-000	^{188}0.0637	^{186}0.0789	^{170}0.0933	^{159}0.1163	^{143}0.1941
97	NEC-001	^{203}0.0863	^{203}0.1055	^{185}0.1249	^{173}0.1519	^{162}0.2253
98	NEC-002	^{14}0.0020	^{14}0.0026	^{14}0.0033	^{26}0.0135	^{15}0.0653
99	NEC-003	^{15}0.0021	^{12}0.0024	^{11}0.0028	^{8}0.0059	^{12}0.0540
100	NEC-004	^{9}0.0017	^{5}0.0018	^{4}0.0020	^{2}0.0037	^{4}0.0329
101	NEC-005	^{4}0.0015	^{3}0.0017	^{3}0.0019	^{11}0.0065	^{2}0.0307
102	NEUROTECHNOLOGY-003	^{271}0.5698	^{272}0.6362	^{212}0.7035	^{204}0.7602	^{198}0.8224
103	NEUROTECHNOLOGY-004	^{174}0.0466	^{173}0.0629	^{159}0.0779	^{156}0.1135	^{154}0.2102
104	NEUROTECHNOLOGY-005	^{155}0.0396	^{160}0.0538	^{149}0.0675	^{143}0.0950	^{147}0.1966
105	NEUROTECHNOLOGY-007	^{169}0.0436	^{172}0.0623	^{161}0.0802	^{165}0.1320	^{169}0.2393
106	NEUROTECHNOLOGY-008	^{142}0.0339	^{154}0.0530	^{168}0.0893	^{180}0.1769	^{188}0.3288
107	NEUROTECHNOLOGY-009	^{70}0.0108	^{73}0.0152	^{72}0.0196	^{68}0.0324	^{57}0.1102
108	NEUROTECHNOLOGY-010	^{50}0.0069	^{49}0.0099	^{51}0.0138	^{94}0.0449	^{130}0.1727
109	NEUROTECHNOLOGY-012	^{37}0.0047	^{37}0.0068	^{38}0.0097	^{51}0.0265	^{94}0.1343
110	NOTIONTAG-000	^{77}0.0128	^{76}0.0175	^{77}0.0228	^{76}0.0357	^{85}0.1270
111	NTECHLAB-003	^{164}0.0421	^{158}0.0537	^{148}0.0674	^{136}0.0907	^{120}0.1582
112	NTECHLAB-004	^{134}0.0312	^{133}0.0405	^{132}0.0519	^{126}0.0722	^{111}0.1503
113	NTECHLAB-005	^{138}0.0334	^{134}0.0424	^{136}0.0537	^{131}0.0760	^{117}0.1543
114	NTECHLAB-006	^{130}0.0288	^{128}0.0367	^{129}0.0471	^{123}0.0670	^{113}0.1523
115	NTECHLAB-007	^{107}0.0188	^{103}0.0256	^{102}0.0317	^{100}0.0495	^{90}0.1306
116	NTECHLAB-008	^{69}0.0107	^{66}0.0145	^{67}0.0187	^{56}0.0286	^{43}0.0995
117	NTECHLAB-009	^{30}0.0037	^{30}0.0049	^{29}0.0062	^{25}0.0125	^{20}0.0735
118	NTECHLAB-010	^{12}0.0020	^{13}0.0025	^{12}0.0030	^{15}0.0077	^{19}0.0710
119	NTECHLAB-011	^{16}0.0022	^{17}0.0030	^{18}0.0038	^{14}0.0075	^{14}0.0625
120	PANGIAM-000	^{36}0.0042	^{36}0.0060	^{36}0.0080	^{32}0.0160	^{30}0.0876
121	PARAVISION-003	^{126}0.0260	^{126}0.0351	^{127}0.0447	^{122}0.0657	^{125}0.1630
122	PARAVISION-004	^{51}0.0074	^{53}0.0101	^{49}0.0136	^{52}0.0267	^{82}0.1256
123	PARAVISION-005	^{23}0.0032	^{23}0.0041	^{23}0.0057	^{34}0.0174	^{49}0.1037
124	PARAVISION-007	^{22}0.0030	^{22}0.0040	^{22}0.0055	^{36}0.0211	^{56}0.1097
125	PARAVISION-009	^{13}0.0020	^{15}0.0026	^{17}0.0038	^{18}0.0098	^{28}0.0857
126	PIXELALL-002	^{198}0.0716	^{202}0.1052	^{192}0.1475	^{193}0.2489	^{193}0.3904
127	PIXELALL-003	^{95}0.0158	^{95}0.0218	^{99}0.0288	^{96}0.0474	^{67}0.1138
128	PIXELALL-004	^{79}0.0129	^{84}0.0183	^{86}0.0245	^{78}0.0378	^{96}0.1375
129	PIXELALL-005	^{57}0.0087	^{57}0.0121	^{62}0.0171	^{44}0.0250	^{51}0.1052
130	PTAKURATSATU-000	^{127}0.0275	^{127}0.0366	^{128}0.0458	^{107}0.0523	^{11}0.0523
131	QNAP-001	^{159}0.0404	^{157}0.0536	^{145}0.0661	^{138}0.0916	^{121}0.1595
132	QNAP-002	^{115}0.0200	^{108}0.0265	^{105}0.0327	^{98}0.0490	^{93}0.1341
133	QUANTASOFT-001	^{273}0.6387	^{273}0.6387	^{211}0.6387		^{196}0.6387
134	RANKONE-002	^{211}0.0973	^{207}0.1175	^{187}0.1359	^{177}0.1718	^{178}0.2613
135	RANKONE-003	^{212}0.0973	^{206}0.1175	^{186}0.1359	^{178}0.1718	^{179}0.2613
136	RANKONE-005	^{175}0.0473	^{169}0.0592	^{155}0.0700	^{141}0.0944	^{149}0.1998
137	RANKONE-007	^{99}0.0168	^{97}0.0222	^{91}0.0266	^{80}0.0381	^{64}0.1132
138	RANKONE-009	^{80}0.0132	^{79}0.0177	^{79}0.0230	^{72}0.0344	^{36}0.0921
139	RANKONE-010	^{67}0.0106	^{63}0.0136	^{63}0.0174	^{50}0.0265	^{22}0.0785
140	RANKONE-011	^{43}0.0063	^{43}0.0087	^{42}0.0115	^{53}0.0269	^{66}0.1135
141	RANKONE-012	^{42}0.0058	^{40}0.0077	^{40}0.0100	^{37}0.0220	^{60}0.1111
142	REALNETWORKS-002	^{239}0.1943	^{238}0.2314	^{206}0.2656	^{199}0.3134	^{187}0.3208
143	REALNETWORKS-003	^{225}0.1300	^{224}0.1594	^{198}0.1858	^{187}0.2246	^{184}0.3076
144	REALNETWORKS-004	^{224}0.1279	^{223}0.1581	^{197}0.1857	^{188}0.2329	^{186}0.3179

Table 19: **Identification-mode: Effect of N on FNIR at high threshold.** *Values are threshold-based miss rates i.e.* FNIR *at* FPIR *= 0.001 for five enrollment population sizes, N. The right six columns apply for enrollment of one image. Missing entries usually apply because another algorithm from the same developer was run instead. Some developers are missing because less accurate algorithms were not run on galleries with $N \geq 3\,000\,000$. Throughout blue superscripts indicate the rank of the algorithm for that column.*

This publication is available free of charge from: https://doi.org/10.6028/NIST.IR.8271

MISSES BELOW THRESHOLD, T		ENROL MOST RECENT				
FNIR(N, T> 0, R >L)		DATASET: FRVT 2018 MUGSHOTS				
#	ALGORITHM	N=0.64M	N=1.6M	N=3.0M	N=6.0M	N=12.0M
145	REALNETWORKS-005	[116]0.0202	[114]0.0277	[113]0.0355	[116]0.0560	[100]0.1431
146	REALNETWORKS-006	[62]0.0097	[67]0.0145	[66]0.0182	[66]0.0308	[42]0.0991
147	REALNETWORKS-007	[49]0.0068	[47]0.0097	[45]0.0125	[39]0.0233	[33]0.0917
148	REMARKAI-000	[161]0.0406	[161]0.0552	[150]0.0676	[147]0.1028	[150]0.2003
149	RENDIP-000	[55]0.0085	[56]0.0121	[56]0.0156	[55]0.0277	[74]0.1182
150	REVEALMEDIA-000	[58]0.0090	[58]0.0122	[57]0.0158	[54]0.0277	[45]0.1019
151	S1-000	[118]0.0204	[116]0.0279	[119]0.0382	[120]0.0630	[128]0.1707
152	S1-001	[73]0.0115	[74]0.0156	[73]0.0199	[81]0.0392	[83]0.1256
153	S1-002	[34]0.0040	[34]0.0056	[34]0.0077	[49]0.0264	[87]0.1285
154	SCANOVATE-000	[176]0.0498	[176]0.0667	[162]0.0804	[151]0.1097	[59]0.1109
155	SCANOVATE-001	[187]0.0630	[187]0.0815	[173]0.0993	[161]0.1292	[146]0.1960
156	SENSETIME-000	[94]0.0158	[93]0.0208	[94]0.0270	[84]0.0398	[75]0.1232
157	SENSETIME-001	[97]0.0161	[96]0.0219	[97]0.0277	[90]0.0420	[88]0.1304
158	SENSETIME-002	[89]0.0146	[68]0.0148	[55]0.0153	[40]0.0234	[16]0.0657
159	SENSETIME-003	[6]0.0016	[7]0.0018	[6]0.0021	[7]0.0054	[7]0.0451
160	SENSETIME-004	[5]0.0015	[4]0.0018	[5]0.0021	[3]0.0040	[5]0.0354
161	SENSETIME-005	[7]0.0016	[11]0.0022	[13]0.0031	[17]0.0089	[8]0.0454
162	SENSETIME-006	[3]0.0014	[6]0.0018	[9]0.0023	[4]0.0047	[6]0.0372
163	SENSETIME-007	[1]0.0012	[1]0.0014	[1]0.0016	[1]0.0036	[3]0.0316
164	SHAMAN-007	[223]0.1212	[219]0.1413	[193]0.1587	[182]0.1879	[172]0.2460
165	SIAT-001	[82]0.0136	[77]0.0176	[80]0.0230	[71]0.0344	[47]0.1035
166	SIAT-002	[93]0.0154	[94]0.0216	[95]0.0273	[86]0.0404	[86]0.1283
167	SQISOFT-001	[204]0.0921	[215]0.1322	[195]0.1781	[190]0.2348	[201]0.9271
168	SYNESIS-003	[269]0.5341	[268]0.5821	[210]0.6113	[203]0.6479	[197]0.6822
169	SYNESIS-003	[177]0.0499	[174]0.0652	[163]0.0804	[150]0.1095	[142]0.1916
170	SYNESIS-005	[101]0.0181	[102]0.0248	[103]0.0319	[105]0.0518	[119]0.1580
171	TECH5-001	[163]0.0420	[164]0.0574	[169]0.0911	[185]0.2106	[192]0.3725
172	TECH5-002	[112]0.0194	[111]0.0269	[111]0.0346	[108]0.0537	[122]0.1607
173	TEVIAN-005	[195]0.0692	[192]0.0873	[176]0.1066	[163]0.1301	[137]0.1840
174	TEVIAN-006	[53]0.0078	[48]0.0098	[47]0.0130	[48]0.0261	[89]0.1305
175	TEVIAN-007	[32]0.0038	[32]0.0052	[30]0.0065	[29]0.0154	[39]0.0957
176	TIGER-002	[190]0.0647	[188]0.0861	[174]0.1036	[166]0.1332	[160]0.2231
177	TOSHIBA-000	[173]0.0460	[171]0.0620	[160]0.0780	[153]0.1117	[153]0.2082
178	TRUEFACE-000	[81]0.0134	[83]0.0182	[83]0.0238	[79]0.0380	[97]0.1385
179	VD-001	[235]0.1642	[235]0.2015	[205]0.2351	[196]0.2736	[189]0.3293
180	VERIDAS-001	[128]0.0278	[131]0.0373	[130]0.0491	[130]0.0753	[115]0.1541
181	VERIDAS-002	[129]0.0278	[130]0.0373	[117]0.0373	[99]0.0491	[21]0.0753
182	VERIDAS-003	[74]0.0117	[75]0.0166	[75]0.0219	[93]0.0446	[116]0.1543
183	VIGILANTSOLUTIONS-008	[90]0.0146	[90]0.0205	[93]0.0269	[92]0.0489	[71]0.1164
184	VISIONBOX-000	[75]0.0122	[80]0.0177	[84]0.0239		[202]0.9538
185	VISIONLABS-004	[166]0.0427	[165]0.0578	[156]0.0703	[142]0.0949	[138]0.1853
186	VISIONLABS-005	[151]0.0369	[149]0.0502	[140]0.0626	[134]0.0847	[136]0.1815
187	VISIONLABS-006	[109]0.0188	[110]0.0267	[109]0.0336	[113]0.0542	[106]0.1478
188	VISIONLABS-007	[108]0.0188	[109]0.0266	[108]0.0335	[111]0.0540	[107]0.1479
189	VISIONLABS-008	[61]0.0096	[61]0.0131	[61]0.0166	[58]0.0291	[79]0.1247
190	VISIONLABS-009	[27]0.0034	[26]0.0046	[26]0.0060	[27]0.0140	[31]0.0881
191	VISIONLABS-010	[31]0.0038	[31]0.0051	[32]0.0070	[28]0.0149	[35]0.0920
192	VISIONLABS-011	[18]0.0025	[19]0.0033	[20]0.0044	[21]0.0120	[25]0.0825
193	VNPT-001	[65]0.0104	[65]0.0143	[68]0.0190	[61]0.0296	[46]0.1028
194	VOCORD-005	[220]0.1179	[222]0.1577	[202]0.2183	[198]0.3122	[195]0.4490
195	VTS-001	[64]0.0102	[62]0.0133	[64]0.0175	[67]0.0322	[78]0.1243
196	VTS-002	[104]0.0185	[105]0.0259	[110]0.0344	[115]0.0549	[103]0.1447
197	XFORWARDAI-000	[68]0.0107	[71]0.0151	[70]0.0195	[69]0.0324	[52]0.1057
198	XFORWARDAI-001	[29]0.0037	[29]0.0049	[27]0.0060	[20]0.0120	[23]0.0800
199	XFORWARDAI-002	[19]0.0026	[18]0.0030	[16]0.0035	[16]0.0078	[18]0.0706
200	YITU-002	[78]0.0129	[78]0.0177	[78]0.0228	[73]0.0345	[65]0.1133
201	YITU-003	[86]0.0138	[86]0.0185	[81]0.0236	[74]0.0353	[68]0.1148
202	YITU-004	[48]0.0067	[45]0.0096	[46]0.0129	[38]0.0232	[50]0.1046
203	YITU-005	[52]0.0074	[52]0.0101	[48]0.0135	[46]0.0255	[53]0.1057

Table 20: **Identification-mode: Effect of N on FNIR at high threshold.** *Values are threshold-based miss rates i.e.* FNIR *at* FPIR = *0.001 for five enrollment population sizes, N. The right six columns apply for enrollment of one image. Missing entries usually apply because another algorithm from the same developer was run instead. Some developers are missing because less accurate algorithms were not run on galleries with* $N \geq 3\,000\,000$. *Throughout blue superscripts indicate the rank of the algorithm for that column.*

MISSES AT GIVEN RANK		ENROL MOST RECENT											
FNIR(N, T= 0, R)		RANK 1						RANK 50					
#	ALGORITHM	N=0.64M	N=1.6M	N=3.0M	N=6.0M	N=12.0M	aN^b	N=0.64M	N=1.6M	N=3.0M	N=6.0M	N=12.0M	aN^b
1	3DIVI-005	^{225}0.0137	^{223}0.0176	^{193}0.0210	^{187}0.0253	^{182}0.0302	^{146}0.0004 N$^{0.271}$ ^{164}	^{206}0.0040	^{206}0.0049	^{183}0.0057	^{179}0.0068	^{174}0.0081	^{48}0.0002 N$^{0.240}$ ^{169}
2	ACER-000	^{194}0.0081	^{200}0.0106	^{181}0.0128	^{179}0.0157	^{174}0.0195	^{61}0.0001 N$^{0.299}$ ^{188}	^{153}0.0020	^{171}0.0026	^{160}0.0031	^{160}0.0037	^{156}0.0045	^{19}0.0000 N$^{0.284}$ ^{182}
3	ALCHERA-003	^{190}0.0079	^{197}0.0104	^{179}0.0123	^{178}0.0147	^{173}0.0180	^{92}0.0002 N$^{0.278}$ ^{175}	^{187}0.0027	^{185}0.0032	^{166}0.0035	^{163}0.0042	^{157}0.0048	^{52}0.0002 N$^{0.199}$ ^{159}
4	ALLGOVISION-000	^{208}0.0101	^{205}0.0114	^{180}0.0127	^{177}0.0145	^{172}0.0166	^{179}0.0010 N$^{0.171}$ ^{100}	^{226}0.0063	^{222}0.0067	^{188}0.0071	^{182}0.0075	^{173}0.0081	^{185}0.0020 N$^{0.086}$ ^{117}
5	ALLGOVISION-001	^{182}0.0069	^{188}0.0090	^{174}0.0107	^{172}0.0128	^{169}0.0157	^{78}0.0002 N$^{0.277}$ ^{173}	^{174}0.0023	^{175}0.0027	^{161}0.0031	^{155}0.0036	^{152}0.0043	^{41}0.0001 N$^{0.211}$ ^{164}
6	ANKE-000	^{211}0.0102	^{213}0.0132	^{189}0.0155	^{184}0.0188	^{178}0.0225	^{128}0.0003 N$^{0.270}$ ^{163}	^{196}0.0032	^{198}0.0040	^{179}0.0046	^{172}0.0056	^{165}0.0066	^{40}0.0001 N$^{0.247}$ ^{171}
7	ANKE-002	^{116}0.0024	^{116}0.0028	^{116}0.0032	^{112}0.0037	^{107}0.0043	^{71}0.0002 N$^{0.203}$ ^{117}	^{125}0.0016	^{125}0.0017	^{118}0.0017	^{108}0.0018	^{103}0.0019	^{106}0.0006 N$^{0.067}$ ^{105}
8	AWARE-003	^{242}0.0238	^{240}0.0306	^{204}0.0361	^{198}0.0431	^{195}0.0506	^{175}0.0008 N$^{0.258}$ ^{158}	^{220}0.0055	^{228}0.0075	^{198}0.0092	^{193}0.0113	^{192}0.0143	^{30}0.0001 N$^{0.323}$ ^{192}
9	AWARE-005	^{243}0.0245	^{241}0.0311	^{205}0.0366	^{199}0.0434	^{186}0.0312	^{196}0.0056 N$^{0.118}$ ^{56}	^{224}0.0062	^{234}0.0082	^{200}0.0101	^{196}0.0128	^{176}0.0089	^{130}0.0007 N$^{0.169}$ ^{154}
10	AYONIX-002	^{279}0.2935	^{280}0.3414	^{215}0.3736	^{209}0.4101	^{201}0.4465	^{201}0.0440 N$^{0.143}$ ^{73}	^{278}0.0950	^{280}0.1274	^{215}0.1524	^{206}0.1828	^{200}0.2150	^{187}0.0023 N$^{0.279}$ ^{180}
11	CAMVI-004	^{218}0.0124	^{251}0.0468	^{209}0.0719	^{206}0.2363	^{200}0.2367	^{3}0.0000 N$^{1.055}$ ^{202}	^{250}0.0117	^{265}0.0464	^{211}0.0715	^{207}0.2361	^{201}0.2364	^{3}0.0000 N$^{1.071}$ ^{202}
12	CANON-001	^{15}0.0011	^{14}0.0011	^{14}0.0012	^{16}0.0013	^{14}0.0014	^{107}0.0002 N$^{0.113}$ ^{49}	^{18}0.0009	^{18}0.0009	^{18}0.0009	^{19}0.0009	^{18}0.0010	^{105}0.0006 N$^{0.026}$ ^{50}
13	CANON-002	^{18}0.0011	^{19}0.0012	^{22}0.0013	^{22}0.0014	^{21}0.0016	^{70}0.0002 N$^{0.142}$ ^{72}	^{19}0.0009	^{16}0.0009	^{16}0.0009	^{14}0.0009	^{14}0.0009	^{131}0.0007 N$^{0.015}$ ^{26}
14	CIB-000	^{48}0.0014	^{44}0.0015	^{44}0.0017	^{48}0.0019	^{163}0.0131	^{4}0.0000 N$^{0.635}$ ^{201}	^{59}0.0012	^{53}0.0012	^{50}0.0012	^{49}0.0012	^{188}0.0122	^{4}0.0000 N$^{0.647}$ ^{201}
15	CLEARVIEWAI-000	^{12}0.0010	^{13}0.0011	^{15}0.0012	^{17}0.0013	^{18}0.0015	^{83}0.0002 N$^{0.129}$ ^{65}	^{21}0.0009	^{17}0.0009	^{17}0.0009	^{17}0.0009	^{16}0.0010	^{120}0.0007 N$^{0.019}$ ^{40}
16	CLOUDWALK-HR-000	^{53}0.0015	^{41}0.0015	^{38}0.0015	^{32}0.0016	^{26}0.0017	^{171}0.0007 N$^{0.054}$ ^{11}	^{111}0.0014	^{97}0.0014	^{87}0.0014	^{80}0.0014	^{62}0.0014	^{168}0.0012 N$^{0.012}$ ^{18}
17	CLOUDWALK-MT-000	^{79}0.0018	^{61}0.0018	^{53}0.0018	^{44}0.0019	^{36}0.0020	^{180}0.0011 N$^{0.036}$ ^{6}	^{138}0.0018	^{133}0.0018	^{122}0.0018	^{105}0.0018	^{91}0.0018	^{182}0.0017 N$^{0.002}$ ^{4}
18	COGENT-000	^{210}0.0101	^{199}0.0105	^{176}0.0109	^{167}0.0115	^{160}0.0125	^{194}0.0038 N$^{0.071}$ ^{17}	^{163}0.0021	^{164}0.0024	^{156}0.0028	^{158}0.0036	^{179}0.0095	^{8}0.0000 N$^{0.466}$ ^{198}
19	COGENT-001	^{209}0.0101	^{198}0.0105	^{175}0.0109	^{165}0.0115	^{161}0.0125	^{193}0.0038 N$^{0.071}$ ^{18}	^{162}0.0021	^{163}0.0024	^{155}0.0028	^{157}0.0036	^{180}0.0095	^{9}0.0000 N$^{0.466}$ ^{197}
20	COGENT-002	^{128}0.0029	^{131}0.0036	^{129}0.0041	^{127}0.0049	^{123}0.0059	^{43}0.0001 N$^{0.244}$ ^{150}	^{107}0.0014	^{115}0.0015	^{112}0.0017	^{115}0.0019	^{115}0.0021	^{53}0.0002 N$^{0.144}$ ^{148}
21	COGENT-003	^{134}0.0031	^{133}0.0038	^{134}0.0043	^{130}0.0051	^{127}0.0060	^{57}0.0001 N$^{0.230}$ ^{139}	^{119}0.0015	^{128}0.0017	^{131}0.0018	^{127}0.0020	^{121}0.0022	^{58}0.0002 N$^{0.143}$ ^{147}
22	COGENT-004	^{81}0.0018	^{80}0.0020	^{78}0.0022	^{77}0.0025	^{69}0.0028	^{98}0.0002 N$^{0.159}$ ^{89}	^{100}0.0013	^{95}0.0014	^{91}0.0014	^{85}0.0015	^{75}0.0015	^{113}0.0007 N$^{0.050}$ ^{84}
23	COGENT-005	^{61}0.0016	^{55}0.0017	^{54}0.0018	^{51}0.0020	^{45}0.0021	^{145}0.0004 N$^{0.108}$ ^{44}	^{101}0.0013	^{87}0.0013	^{80}0.0014	^{69}0.0014	^{61}0.0014	^{165}0.0011 N$^{0.017}$ ^{31}
24	COGENT-006	^{27}0.0012	^{25}0.0012	^{23}0.0013	^{20}0.0014	^{19}0.0015	^{144}0.0004 N$^{0.088}$ ^{31}	^{43}0.0011	^{42}0.0011	^{38}0.0011	^{31}0.0011	^{28}0.0011	^{143}0.0008 N$^{0.019}$ ^{38}
25	COGNITEC-000	^{236}0.0195	^{235}0.0252	^{201}0.0297	^{196}0.0352	^{190}0.0417	^{168}0.0006 N$^{0.259}$ ^{159}	^{216}0.0050	^{220}0.0065	^{195}0.0077	^{192}0.0097	^{187}0.0122	^{37}0.0001 N$^{0.305}$ ^{186}
26	COGNITEC-001	^{204}0.0090	^{206}0.0117	^{186}0.0139	^{182}0.0166	^{176}0.0199	^{118}0.0002 N$^{0.271}$ ^{166}	^{192}0.0030	^{191}0.0034	^{175}0.0040	^{171}0.0046	^{161}0.0054	^{51}0.0002 N$^{0.207}$ ^{163}
27	COGNITEC-002	^{164}0.0048	^{162}0.0057	^{154}0.0067	^{148}0.0079	^{147}0.0094	^{100}0.0002 N$^{0.232}$ ^{141}	^{176}0.0024	^{172}0.0026	^{158}0.0028	^{150}0.0030	^{140}0.0034	^{88}0.0005 N$^{0.117}$ ^{134}
28	COGNITEC-003	^{167}0.0053	^{166}0.0062	^{157}0.0072	^{154}0.0085	^{150}0.0100	^{125}0.0003 N$^{0.222}$ ^{130}	^{189}0.0028	^{183}0.0030	^{163}0.0032	^{153}0.0035	^{146}0.0037	^{138}0.0008 N$^{0.097}$ ^{125}
29	COGNITEC-004	^{123}0.0027	^{124}0.0032	^{124}0.0037	^{122}0.0045	^{120}0.0056	^{33}0.0001 N$^{0.253}$ ^{156}	^{96}0.0013	^{98}0.0014	^{100}0.0015	^{100}0.0017	^{97}0.0019	^{62}0.0002 N$^{0.123}$ ^{139}
30	COGNITEC-005	^{50}0.0014	^{52}0.0016	^{56}0.0018	^{54}0.0021	^{55}0.0024	^{62}0.0001 N$^{0.169}$ ^{97}	^{49}0.0011	^{49}0.0011	^{46}0.0012	^{45}0.0012	^{37}0.0012	^{111}0.0007 N$^{0.037}$ ^{64}
31	COGNITEC-006	^{46}0.0014	^{48}0.0016	^{45}0.0017	^{47}0.0019	^{47}0.0022	^{81}0.0002 N$^{0.154}$ ^{81}	^{50}0.0011	^{48}0.0011	^{45}0.0012	^{41}0.0012	^{40}0.0012	^{112}0.0007 N$^{0.036}$ ^{63}
32	CYBERLINK-000	^{140}0.0034	^{135}0.0040	^{137}0.0046	^{133}0.0054	^{129}0.0063	^{94}0.0002 N$^{0.209}$ ^{123}	^{159}0.0021	^{154}0.0022	^{147}0.0023	^{143}0.0025	^{134}0.0027	^{102}0.0006 N$^{0.092}$ ^{122}
33	CYBERLINK-001	^{131}0.0030	^{129}0.0035	^{131}0.0042	^{129}0.0050	^{126}0.0060	^{44}0.0001 N$^{0.243}$ ^{149}	^{129}0.0016	^{132}0.0017	^{125}0.0018	^{122}0.0020	^{118}0.0022	^{74}0.0004 N$^{0.109}$ ^{129}
34	CYBERLINK-002	^{115}0.0024	^{109}0.0026	^{107}0.0028	^{101}0.0031	^{91}0.0035	^{161}0.0005 N$^{0.121}$ ^{58}	^{155}0.0020	^{149}0.0021	^{142}0.0021	^{135}0.0022	^{120}0.0022	^{172}0.0012 N$^{0.036}$ ^{62}
35	CYBERLINK-003	^{51}0.0015	^{49}0.0016	^{46}0.0017	^{40}0.0018	^{37}0.0020	^{138}0.0003 N$^{0.110}$ ^{46}	^{52}0.0011	^{51}0.0012	^{49}0.0012	^{48}0.0012	^{43}0.0013	^{98}0.0006 N$^{0.047}$ ^{80}
36	CYBERLINK-004	^{64}0.0016	^{54}0.0017	^{52}0.0018	^{43}0.0019	^{40}0.0021	^{162}0.0005 N$^{0.085}$ ^{30}	^{108}0.0014	^{99}0.0014	^{89}0.0014	^{81}0.0014	^{69}0.0015	^{164}0.0010 N$^{0.022}$ ^{44}
37	CYBERLINK-005	^{74}0.0017	^{64}0.0018	^{59}0.0019	^{56}0.0021	^{50}0.0023	^{154}0.0004 N$^{0.099}$ ^{39}	^{113}0.0014	^{101}0.0014	^{98}0.0015	^{88}0.0015	^{74}0.0015	^{153}0.0009 N$^{0.032}$ ^{59}
38	DAHUA-001	^{168}0.0053	^{170}0.0067	^{161}0.0079	^{159}0.0093	^{154}0.0112	^{80}0.0002 N$^{0.256}$ ^{157}	^{186}0.0027	^{178}0.0029	^{162}0.0031	^{152}0.0034	^{148}0.0038	^{94}0.0005 N$^{0.121}$ ^{137}
39	DAHUA-002	^{71}0.0017	^{70}0.0018	^{71}0.0021	^{65}0.0023	^{62}0.0027	^{93}0.0002 N$^{0.156}$ ^{83}	^{87}0.0013	^{86}0.0013	^{83}0.0014	^{75}0.0014	^{67}0.0015	^{125}0.0007 N$^{0.043}$ ^{76}
40	DAHUA-003	^{14}0.0010	^{23}0.0012	^{26}0.0014	^{30}0.0016	^{33}0.0018	^{24}0.0001 N$^{0.199}$ ^{114}	^{14}0.0009	^{12}0.0009	^{12}0.0009	^{13}0.0009	^{12}0.0009	^{100}0.0006 N$^{0.027}$ ^{51}
41	DAHUA-004	^{13}0.0010	^{12}0.0011	^{12}0.0012	^{12}0.0013	^{15}0.0014	^{104}0.0002 N$^{0.113}$ ^{52}	^{16}0.0009	^{14}0.0009	^{15}0.0009	^{16}0.0009	^{13}0.0009	^{108}0.0006 N$^{0.023}$ ^{45}
42	DAON-000	^{151}0.0039	^{138}0.0041	^{132}0.0043	^{121}0.0045	^{117}0.0049	^{183}0.0014 N$^{0.077}$ ^{21}	^{202}0.0036	^{194}0.0036	^{171}0.0036	^{159}0.0037	^{145}0.0037	^{189}0.0030 N$^{0.013}$ ^{21}
43	DECATUR-000	^{83}0.0018	^{86}0.0021	^{88}0.0024	^{86}0.0028	^{85}0.0033	^{50}0.0001 N$^{0.201}$ ^{116}	^{80}0.0013	^{80}0.0013	^{78}0.0013	^{82}0.0014	^{77}0.0016	^{85}0.0005 N$^{0.072}$ ^{108}
44	DEEPGLINT-001	^{45}0.0014	^{39}0.0014	^{36}0.0015	^{34}0.0016	^{32}0.0018	^{150}0.0004 N$^{0.089}$ ^{32}	^{90}0.0013	^{74}0.0013	^{71}0.0013	^{65}0.0013	^{54}0.0013	^{162}0.0010 N$^{0.017}$ ^{30}
45	DEEPSEA-001	^{139}0.0033	^{143}0.0043	^{143}0.0052	^{141}0.0065	^{139}0.0081	^{18}0.0001 N$^{0.311}$ ^{191}	^{77}0.0012	^{92}0.0014	^{104}0.0015	^{102}0.0017	^{104}0.0020	^{44}0.0001 N$^{0.157}$ ^{152}
46	DERMALOG-005	^{217}0.0114	^{217}0.0149	^{191}0.0201	^{192}0.0289	^{193}0.0447	^{8}0.0000 N$^{0.470}$ ^{200}	^{244}0.0094	^{245}0.0122	^{206}0.0171	^{200}0.0254	^{196}0.0406	^{10}0.0000 N$^{0.505}$ ^{199}
47	DERMALOG-006	^{185}0.0075	^{183}0.0081	^{169}0.0086	^{160}0.0093	^{151}0.0104	^{188}0.0017 N$^{0.109}$ ^{45}	^{225}0.0062	^{219}0.0063	^{186}0.0064	^{178}0.0065	^{166}0.0068	^{194}0.0043 N$^{0.028}$ ^{54}
48	DERMALOG-007	^{192}0.0080	^{191}0.0092	^{173}0.0102	^{170}0.0118	^{165}0.0140	^{166}0.0006 N$^{0.190}$ ^{111}	^{218}0.0051	^{213}0.0054	^{182}0.0056	^{173}0.0058	^{164}0.0063	^{186}0.0020 N$^{0.068}$ ^{106}
49	DERMALOG-008	^{114}0.0024	^{117}0.0029	^{118}0.0034	^{116}0.0040	^{115}0.0048	^{38}0.0001 N$^{0.239}$ ^{146}	^{118}0.0015	^{113}0.0015	^{110}0.0016	^{103}0.0017	^{99}0.0019	^{80}0.0004 N$^{0.088}$ ^{118}
50	DERMALOG-009	^{120}0.0026	^{115}0.0028	^{111}0.0030	^{105}0.0033	^{94}0.0037	^{163}0.0005 N$^{0.121}$ ^{59}	^{164}0.0022	^{156}0.0022	^{145}0.0022	^{137}0.0023	^{124}0.0024	^{177}0.0015 N$^{0.028}$ ^{55}
51	DILUSENSE-000	^{88}0.0019	^{91}0.0022	^{91}0.0025	^{87}0.0028	^{87}0.0033	^{66}0.0002 N$^{0.187}$ ^{108}	^{70}0.0012	^{64}0.0013	^{66}0.0013	^{70}0.0014	^{64}0.0014	^{93}0.0005 N$^{0.062}$ ^{100}
52	FUJITSULAB-000	^{89}0.0019	^{92}0.0022	^{96}0.0025	^{95}0.0029	^{86}0.0033	^{63}0.0001 N$^{0.190}$ ^{110}	^{98}0.0013	^{90}0.0014	^{88}0.0014	^{84}0.0015	^{81}0.0016	^{97}0.0006 N$^{0.059}$ ^{94}
53	FUJITSULAB-001	^{72}0.0017	^{72}0.0019	^{72}0.0021	^{66}0.0023	^{60}0.0026	^{108}0.0002 N$^{0.149}$ ^{77}	^{99}0.0013	^{93}0.0014	^{86}0.0014	^{83}0.0015	^{72}0.0015	^{126}0.0007 N$^{0.045}$ ^{77}
54	GORILLA-002	^{227}0.0147	^{229}0.0197	^{197}0.0238	^{191}0.0288	^{187}0.0351	^{131}0.0003 N$^{0.295}$ ^{184}	^{195}0.0032	^{200}0.0041	^{181}0.0049	^{176}0.0062	^{172}0.0080	^{20}0.0000 N$^{0.315}$ ^{189}
55	GORILLA-004	^{165}0.0048	^{167}0.0063	^{159}0.0075	^{158}0.0091	^{156}0.0114	^{39}0.0001 N$^{0.292}$ ^{182}	^{123}0.0015	^{135}0.0018	^{143}0.0021	^{141}0.0025	^{139}0.0029	^{32}0.0001 N$^{0.222}$ ^{166}
56	GORILLA-005	^{119}0.0026	^{123}0.0032	^{126}0.0038	^{124}0.0046	^{121}0.0056	^{21}0.0001 N$^{0.271}$ ^{168}	^{74}0.0012	^{75}0.0013	^{85}0.0014	^{95}0.0016	^{92}0.0018	^{60}0.0002 N$^{0.127}$ ^{141}
57	GORILLA-006	^{54}0.0015	^{60}0.0017	^{69}0.0020	^{71}0.0024	^{72}0.0029	^{22}0.0001 N$^{0.226}$ ^{136}	^{42}0.0010	^{43}0.0011	^{44}0.0011	^{39}0.0012	^{39}0.0012	^{89}0.0005 N$^{0.056}$ ^{90}
58	GORILLA-007	^{44}0.0014	^{57}0.0017	^{60}0.0019	^{69}0.0023	^{70}0.0028	^{20}0.0001 N$^{0.241}$ ^{148}	^{40}0.0010	^{39}0.0011	^{35}0.0011	^{34}0.0011	^{34}0.0012	^{96}0.0006 N$^{0.043}$ ^{74}
59	GRIAULE-000	^{109}0.0022	^{107}0.0025	^{105}0.0028	^{99}0.0030	^{92}0.0035	^{130}0.0003 N$^{0.152}$ ^{80}	^{128}0.0016	^{123}0.0017	^{124}0.0018	^{111}0.0018	^{100}0.0019	^{117}0.0007 N$^{0.062}$ ^{98}
60	HIK-003	^{205}0.0091	^{207}0.0117	^{187}0.0140	^{183}0.0169	^{177}0.0203	^{110}0.0002 N$^{0.274}$ ^{171}	^{175}0.0024	^{182}0.0030	^{170}0.0036	^{168}0.0044	^{160}0.0053	^{25}0.0001 N$^{0.278}$ ^{179}
61	HIK-004	^{203}0.0088	^{204}0.0113	^{184}0.0134	^{180}0.0163	^{175}0.0195	^{113}0.0002 N$^{0.271}$ ^{169}	^{178}0.0024	^{179}0.0030	^{167}0.0035	^{164}0.0042	^{159}0.0052	^{31}0.0001 N$^{0.259}$ ^{176}
62	HIK-005	^{145}0.0036	^{148}0.0046	^{146}0.0053	^{140}0.0065	^{138}0.0081	^{35}0.0001 N$^{0.274}$ ^{170}	^{68}0.0012	^{108}0.0015	^{109}0.0016	^{114}0.0019	^{117}0.0022	^{35}0.0001 N$^{0.202}$ ^{161}
63	HYPERVERGE-001	^{36}0.0013	^{32}0.0014	^{29}0.0014	^{26}0.0015	^{25}0.0017	^{151}0.0004 N$^{0.084}$ ^{26}	^{89}0.0013	^{77}0.0013	^{68}0.0013	^{56}0.0013	^{45}0.0013	^{171}0.0012 N$^{0.004}$ ^{9}
64	HYPERVERGE-002	^{37}0.0013	^{29}0.0014	^{28}0.0014	^{24}0.0015	^{16}0.0015	^{177}0.0009 N$^{0.031}$ ^{4}	^{83}0.0013	^{70}0.0013	^{65}0.0013	^{55}0.0013	^{44}0.0013	^{169}0.0012 N$^{0.006}$ ^{11}
65	HZAILU-000	^{91}0.0019	^{90}0.0022	^{90}0.0025	^{88}0.0028	^{88}0.0033	^{72}0.0002 N$^{0.185}$ ^{107}	^{115}0.0014	^{102}0.0014	^{97}0.0015	^{89}0.0015	^{78}0.0016	^{155}0.0009 N$^{0.032}$ ^{60}
66	IDEMIA-003	^{170}0.0054	^{173}0.0069	^{166}0.0084	^{163}0.0101	^{159}0.0122	^{52}0.0001 N$^{0.281}$ ^{177}	^{170}0.0023	^{176}0.0027	^{159}0.0031	^{156}0.0036	^{150}0.0041	^{45}0.0002 N$^{0.201}$ ^{160}
67	IDEMIA-004	^{173}0.0054	^{169}0.0066	^{163}0.0079	^{164}0.0097	^{158}0.0117	^{59}0.0001 N$^{0.270}$ ^{162}	^{145}0.0018	^{150}0.0021	^{152}0.0025	^{149}0.0030	^{144}0.0036	^{29}0.0001 N$^{0.241}$ ^{170}
68	IDEMIA-005	^{178}0.0064	^{182}0.0081	^{171}0.0097	^{169}0.0118	^{166}0.0143	^{67}0.0002 N$^{0.277}$ ^{174}	^{169}0.0022	^{181}0.0030	^{169}0.0036	^{169}0.0044	^{162}0.0055	^{17}0.0000 N$^{0.300}$ ^{185}
69	IDEMIA-006	^{187}0.0076	^{195}0.0096	^{178}0.0113	^{174}0.0135	^{171}0.0161	^{114}0.0002 N$^{0.259}$ ^{160}	^{188}0.0028	^{195}0.0037	^{178}0.0046	^{174}0.0059	^{170}0.0076	^{15}0.0000 N$^{0.341}$ ^{194}
70	IDEMIA-007	^{100}0.0021	^{108}0.0026	^{110}0.0030	^{107}0.0036	^{108}0.0044	^{25}0.0001 N$^{0.250}$ ^{154}	^{48}0.0011	^{55}0.0012	^{58}0.0012	^{72}0.0014	^{73}0.0015	^{63}0.0002 N$^{0.110}$ ^{131}
71	IDEMIA-008	^{8}0.0010	^{11}0.0011	^{11}0.0011	^{11}0.0013	^{11}0.0014	^{89}0.0002 N$^{0.121}$ ^{60}	^{17}0.0009	^{15}0.0009	^{13}0.0009	^{15}0.0009	^{11}0.0009	^{124}0.0007 N$^{0.016}$ ^{28}
72	IDEMIA-009	^{4}0.0009	^{4}0.0010	^{5}0.0010	^{4}0.0011	^{5}0.0012	^{120}0.0002 N$^{0.097}$ ^{37}	^{13}0.0008	^{10}0.0009	^{9}0.0009	^{10}0.0009	^{6}0.0009	^{139}0.0008 N$^{0.007}$ ^{12}

Table 21: **Investigation-mode: Effect of N on FNIR on recent images** *For five enrollment population sizes, N, with T = 0 and FPIR = 1. The left five columns are rank 1 miss rates The right five columns are rank 50 miss rates Missing entries usually apply because another algorithm from the same developer was run instead. Some developers are missing because less accurate algorithms were not run on galleries with $N > 1\,600\,000$. Throughout blue superscripts indicate the rank of the algorithm for that column, and yellow highlighting indicates the most accurate value. Caution: The Power-low models are mostly intended to draw attention to the kind of behavior, not as a model to be used for prediction.*

This publication is available free of charge from: https://doi.org/10.6028/NIST.IR.8271

MISSES AT GIVEN RANK		ENROL MOST RECENT											
FNIR(N, T= 0, R)		RANK 1						RANK 50					
#	ALGORITHM	N=0.64M	N=1.6M	N=3.0M	N=6.0M	N=12.0M	aN^b	N=0.64M	N=1.6M	N=3.0M	N=6.0M	N=12.0M	aN^b
73	IMAGUS-005	^{80}0.0018	^{76}0.0019	^{76}0.0022	^{76}0.0025	^{67}0.0028	^{97}0.0002 N$^{0.158}$ ^{88}	^{81}0.0013	^{88}0.0013	^{81}0.0014	^{79}0.0014	^{79}0.0016	^{92}0.0005 N$^{0.066}$ ^{104}
74	IMAGUS-006	^{82}0.0018	^{81}0.0020	^{77}0.0022	^{74}0.0025	^{71}0.0029	^{102}0.0002 N$^{0.156}$ ^{82}	^{106}0.0014	^{104}0.0014	^{99}0.0015	^{87}0.0015	^{83}0.0016	^{123}0.0007 N$^{0.049}$ ^{83}
75	IMAGUS-007	^{77}0.0017	^{83}0.0020	^{82}0.0022	^{81}0.0026	^{75}0.0030	^{56}0.0001 N$^{0.189}$ ^{109}	^{65}0.0012	^{67}0.0013	^{63}0.0013	^{59}0.0013	^{66}0.0015	^{91}0.0005 N$^{0.064}$ ^{102}
76	IMPERIAL-000	^{107}0.0022	^{106}0.0024	^{103}0.0027	^{100}0.0030	^{93}0.0035	^{124}0.0003 N$^{0.157}$ ^{84}	^{132}0.0016	^{127}0.0017	^{119}0.0017	^{107}0.0018	^{95}0.0018	^{156}0.0009 N$^{0.041}$ ^{71}
77	INCODE-003	^{207}0.0098	^{212}0.0129	^{188}0.0154	^{185}0.0191	^{179}0.0233	^{88}0.0002 N$^{0.296}$ ^{185}	^{177}0.0024	^{184}0.0031	^{173}0.0036	^{170}0.0046	^{163}0.0056	^{23}0.0001 N$^{0.285}$ ^{183}
78	INCODE-004	^{129}0.0029	^{130}0.0035	^{130}0.0041	^{128}0.0049	^{125}0.0060	^{42}0.0001 N$^{0.244}$ ^{151}	^{143}0.0018	^{138}0.0019	^{137}0.0020	^{132}0.0021	^{119}0.0022	^{104}0.0006 N$^{0.077}$ ^{112}
79	INCODE-005	^{56}0.0015	^{53}0.0017	^{51}0.0018	^{52}0.0020	^{52}0.0023	^{109}0.0002 N$^{0.140}$ ^{70}	^{73}0.0012	^{66}0.0013	^{64}0.0013	^{64}0.0013	^{59}0.0014	^{122}0.0007 N$^{0.041}$ ^{68}
80	INNOVATRICS-007	^{62}0.0016	^{56}0.0017	^{58}0.0019	^{55}0.0021	^{56}0.0024	^{106}0.0002 N$^{0.143}$ ^{75}	^{71}0.0012	^{63}0.0012	^{60}0.0013	^{57}0.0013	^{52}0.0013	^{128}0.0007 N$^{0.037}$ ^{65}
81	INTSYSMSU-000	^{271}0.1395	^{271}0.1457	^{211}0.1498	^{203}0.1544	^{197}0.1591	^{203}0.0768 N$^{0.045}$ ^{8}	^{280}0.1098	^{278}0.1163	^{214}0.1206	^{205}0.1252	^{199}0.1296	^{203}0.0519 N$^{0.056}$ ^{91}
82	IREX-000	^{155}0.0043	^{144}0.0044	^{135}0.0044	^{123}0.0046	^{114}0.0048	^{190}0.0028 N$^{0.032}$ ^{5}	^{211}0.0043	^{202}0.0043	^{177}0.0043	^{166}0.0043	^{151}0.0043	^{193}0.0042 N$^{0.002}$ ^{5}
83	ISYSTEMS-002	^{169}0.0053	^{168}0.0064	^{158}0.0072	^{152}0.0083	^{148}0.0096	^{141}0.0003 N$^{0.204}$ ^{119}	^{198}0.0033	^{192}0.0034	^{168}0.0036	^{161}0.0038	^{149}0.0041	^{173}0.0013 N$^{0.071}$ ^{107}
84	ISYSTEMS-003	^{159}0.0046	^{156}0.0052	^{147}0.0057	^{142}0.0066	^{136}0.0076	^{153}0.0004 N$^{0.174}$ ^{102}	^{194}0.0031	^{188}0.0033	^{164}0.0034	^{154}0.0035	^{147}0.0037	^{174}0.0013 N$^{0.063}$ ^{101}
85	KAKAO-000	^{32}0.0013	^{40}0.0015	^{42}0.0016	^{46}0.0019	^{49}0.0022	^{37}0.0001 N$^{0.192}$ ^{113}	^{25}0.0009	^{25}0.0010	^{24}0.0010	^{25}0.0010	^{25}0.0011	^{84}0.0005 N$^{0.050}$ ^{85}
86	KEDACOM-001	^{188}0.0076	^{178}0.0077	^{162}0.0079	^{151}0.0083	^{141}0.0087	^{195}0.0040 N$^{0.047}$ ^{9}	^{231}0.0071	^{224}0.0072	^{192}0.0072	^{180}0.0073	^{167}0.0073	^{198}0.0063 N$^{0.009}$ ^{15}
87	KNERON-000	^{163}0.0048	^{163}0.0059	^{155}0.0067	^{149}0.0079	^{146}0.0093	^{111}0.0002 N$^{0.226}$ ^{135}	^{213}0.0048	^{215}0.0059	^{187}0.0067	^{185}0.0079	^{178}0.0093	^{61}0.0002 N$^{0.226}$ ^{167}
88	LOOKMAN-003	^{196}0.0083	^{187}0.0088	^{170}0.0091	^{162}0.0096	^{152}0.0104	^{191}0.0030 N$^{0.076}$ ^{20}	^{235}0.0072	^{227}0.0074	^{194}0.0075	^{183}0.0076	^{171}0.0077	^{196}0.0054 N$^{0.022}$ ^{43}
89	LOOKMAN-005	^{189}0.0078	^{181}0.0080	^{165}0.0083	^{155}0.0086	^{144}0.0092	^{192}0.0038 N$^{0.053}$ ^{10}	^{233}0.0072	^{225}0.0072	^{193}0.0073	^{181}0.0073	^{165}0.0074	^{197}0.0060 N$^{0.013}$ ^{23}
90	MANTRA-000	^{57}0.0015	^{59}0.0017	^{61}0.0019	^{60}0.0022	^{58}0.0025	^{65}0.0002 N$^{0.171}$ ^{99}	^{64}0.0012	^{57}0.0012	^{55}0.0012	^{52}0.0013	^{47}0.0013	^{110}0.0007 N$^{0.042}$ ^{72}
91	MEGVII-001	^{213}0.0105	^{208}0.0118	^{182}0.0128	^{176}0.0142	^{170}0.0161	^{185}0.0015 N$^{0.143}$ ^{74}	^{237}0.0077	^{233}0.0080	^{196}0.0082	^{190}0.0086	^{177}0.0089	^{192}0.0040 N$^{0.048}$ ^{82}
92	MICROFOCUS-005	^{282}0.3700	^{282}0.4242	^{216}0.4610	^{208}0.5000	^{202}0.5391	^{202}0.0674 N$^{0.128}$ ^{64}	^{283}0.1300	^{283}0.1724	^{216}0.2046	^{208}0.2425	^{202}0.2810	^{191}0.0040 N$^{0.263}$ ^{177}
93	MICROSOFT-003	^{30}0.0013	^{50}0.0016	^{57}0.0018	^{63}0.0022	^{68}0.0028	^{14}0.0000 N$^{0.271}$ ^{167}	^{2}0.0006	^{2}0.0006	^{3}0.0007	^{7}0.0008	^{9}0.0009	^{28}0.0001 N$^{0.158}$ ^{153}
94	MICROSOFT-004	^{28}0.0012	^{42}0.0015	^{50}0.0018	^{59}0.0021	^{66}0.0028	^{13}0.0000 N$^{0.281}$ ^{176}	^{1}0.0006	^{1}0.0006	^{1}0.0007	^{1}0.0007	^{9}0.0009	^{38}0.0001 N$^{0.139}$ ^{145}
95	MICROSOFT-005	^{55}0.0015	^{73}0.0019	^{85}0.0023	^{97}0.0030	^{98}0.0037	^{9}0.0000 N$^{0.320}$ ^{193}	^{3}0.0006	^{3}0.0006	^{2}0.0007	^{2}0.0008	^{7}0.0009	^{39}0.0001 N$^{0.136}$ ^{144}
96	MICROSOFT-006	^{59}0.0016	^{79}0.0020	^{94}0.0025	^{98}0.0030	^{101}0.0038	^{12}0.0000 N$^{0.305}$ ^{189}	^{4}0.0006	^{4}0.0007	^{4}0.0007	^{9}0.0009	^{22}0.0010	^{22}0.0000 N$^{0.184}$ ^{156}
97	NEC-000	^{221}0.0131	^{221}0.0170	^{192}0.0203	^{186}0.0244	^{181}0.0294	^{137}0.0003 N$^{0.276}$ ^{172}	^{191}0.0029	^{197}0.0038	^{180}0.0048	^{175}0.0059	^{169}0.0074	^{16}0.0000 N$^{0.319}$ ^{190}
98	NEC-001	^{233}0.0180	^{230}0.0209	^{196}0.0233	^{190}0.0266	^{183}0.0304	^{187}0.0016 N$^{0.179}$ ^{104}	^{248}0.0109	^{241}0.0113	^{201}0.0116	^{194}0.0121	^{189}0.0129	^{195}0.0051 N$^{0.056}$ ^{89}
99	NEC-002	^{5}0.0009	^{10}0.0010	^{10}0.0011	^{9}0.0012	^{7}0.0013	^{96}0.0002 N$^{0.113}$ ^{51}	^{5}0.0008	^{5}0.0008	^{5}0.0008	^{4}0.0008	^{4}0.0008	^{83}0.0005 N$^{0.038}$ ^{66}
100	NEC-003	^{34}0.0013	^{30}0.0014	^{30}0.0015	^{27}0.0016	^{23}0.0016	^{155}0.0005 N$^{0.079}$ ^{22}	^{61}0.0012	^{54}0.0012	^{51}0.0012	^{46}0.0012	^{41}0.0012	^{152}0.0009 N$^{0.019}$ ^{39}
101	NEC-004	^{42}0.0014	^{37}0.0014	^{32}0.0015	^{28}0.0016	^{24}0.0017	^{167}0.0006 N$^{0.059}$ ^{13}	^{85}0.0013	^{73}0.0013	^{70}0.0013	^{67}0.0013	^{50}0.0013	^{163}0.0010 N$^{0.016}$ ^{29}
102	NEC-005	^{25}0.0011	^{21}0.0012	^{18}0.0012	^{14}0.0013	^{12}0.0014	^{157}0.0005 N$^{0.066}$ ^{15}	^{45}0.0011	^{41}0.0011	^{36}0.0011	^{32}0.0011	^{27}0.0011	^{151}0.0009 N$^{0.013}$ ^{22}
103	NEUROTECHNOLOGY-003	^{232}0.0179	^{231}0.0225	^{198}0.0263	^{193}0.0306	^{188}0.0361	^{174}0.0007 N$^{0.239}$ ^{147}	^{210}0.0042	^{214}0.0057	^{191}0.0072	^{191}0.0090	^{186}0.0112	^{21}0.0000 N$^{0.334}$ ^{193}
104	NEUROTECHNOLOGY-004	^{160}0.0046	^{158}0.0056	^{153}0.0064	^{147}0.0074	^{142}0.0088	^{119}0.0002 N$^{0.220}$ ^{129}	^{166}0.0022	^{165}0.0025	^{157}0.0028	^{151}0.0031	^{142}0.0034	^{65}0.0003 N$^{0.154}$ ^{150}
105	NEUROTECHNOLOGY-005	^{144}0.0035	^{142}0.0043	^{140}0.0049	^{136}0.0057	^{131}0.0068	^{84}0.0002 N$^{0.223}$ ^{132}	^{161}0.0021	^{159}0.0023	^{150}0.0024	^{144}0.0025	^{136}0.0028	^{103}0.0006 N$^{0.092}$ ^{123}
106	NEUROTECHNOLOGY-007	^{137}0.0032	^{134}0.0039	^{136}0.0044	^{131}0.0052	^{128}0.0062	^{74}0.0002 N$^{0.222}$ ^{131}	^{156}0.0020	^{152}0.0022	^{146}0.0023	^{138}0.0024	^{129}0.0026	^{129}0.0007 N$^{0.076}$ ^{111}
107	NEUROTECHNOLOGY-008	^{85}0.0019	^{89}0.0022	^{89}0.0025	^{93}0.0029	^{89}0.0034	^{45}0.0001 N$^{0.205}$ ^{121}	^{95}0.0013	^{82}0.0013	^{79}0.0013	^{74}0.0014	^{68}0.0015	^{127}0.0007 N$^{0.043}$ ^{73}
108	NEUROTECHNOLOGY-009	^{35}0.0013	^{38}0.0014	^{39}0.0016	^{41}0.0018	^{41}0.0021	^{60}0.0001 N$^{0.162}$ ^{91}	^{46}0.0011	^{44}0.0011	^{42}0.0011	^{38}0.0012	^{35}0.0012	^{134}0.0007 N$^{0.029}$ ^{56}
109	NEUROTECHNOLOGY-010	^{23}0.0011	^{24}0.0012	^{24}0.0013	^{23}0.0015	^{22}0.0016	^{99}0.0002 N$^{0.125}$ ^{62}	^{36}0.0010	^{32}0.0010	^{28}0.0010	^{24}0.0010	^{23}0.0011	^{145}0.0008 N$^{0.014}$ ^{24}
110	NEUROTECHNOLOGY-012	^{11}0.0010	^{8}0.0010	^{7}0.0011	^{7}0.0012	^{9}0.0013	^{117}0.0002 N$^{0.102}$ ^{41}	^{27}0.0009	^{23}0.0009	^{19}0.0009	^{18}0.0009	^{17}0.0010	^{144}0.0008 N$^{0.009}$ ^{14}
111	NOTIONTAG-000	^{113}0.0023	^{105}0.0024	^{99}0.0026	^{91}0.0029	^{81}0.0032	^{156}0.0005 N$^{0.117}$ ^{54}	^{149}0.0019	^{145}0.0019	^{139}0.0020	^{128}0.0020	^{114}0.0021	^{175}0.0013 N$^{0.027}$ ^{52}
112	NTECHLAB-003	^{161}0.0046	^{164}0.0062	^{160}0.0076	^{161}0.0094	^{155}0.0114	^{26}0.0001 N$^{0.310}$ ^{190}	^{92}0.0013	^{119}0.0016	^{129}0.0018	^{134}0.0022	^{130}0.0026	^{24}0.0001 N$^{0.237}$ ^{168}
113	NTECHLAB-004	^{147}0.0037	^{151}0.0048	^{148}0.0058	^{144}0.0071	^{140}0.0085	^{28}0.0001 N$^{0.291}$ ^{181}	^{54}0.0011	^{85}0.0013	^{103}0.0015	^{101}0.0017	^{112}0.0021	^{34}0.0001 N$^{0.198}$ ^{158}
114	NTECHLAB-005	^{141}0.0035	^{149}0.0047	^{149}0.0058	^{145}0.0073	^{145}0.0092	^{16}0.0000 N$^{0.334}$ ^{196}	^{10}0.0008	^{38}0.0011	^{54}0.0012	^{92}0.0015	^{101}0.0019	^{11}0.0000 N$^{0.283}$ ^{181}
115	NTECHLAB-006	^{130}0.0030	^{139}0.0041	^{141}0.0050	^{138}0.0062	^{137}0.0078	^{15}0.0000 N$^{0.326}$ ^{195}	^{6}0.0008	^{19}0.0009	^{39}0.0011	^{54}0.0013	^{84}0.0016	^{13}0.0000 N$^{0.253}$ ^{172}
116	NTECHLAB-007	^{104}0.0022	^{110}0.0027	^{112}0.0031	^{111}0.0037	^{109}0.0044	^{30}0.0001 N$^{0.245}$ ^{152}	^{53}0.0011	^{58}0.0012	^{62}0.0013	^{76}0.0014	^{76}0.0015	^{64}0.0003 N$^{0.109}$ ^{130}
117	NTECHLAB-008	^{49}0.0014	^{58}0.0017	^{64}0.0020	^{72}0.0024	^{63}0.0027	^{23}0.0001 N$^{0.224}$ ^{134}	^{35}0.0010	^{36}0.0010	^{34}0.0011	^{37}0.0011	^{36}0.0012	^{77}0.0004 N$^{0.065}$ ^{103}
118	NTECHLAB-009	^{26}0.0012	^{26}0.0013	^{25}0.0014	^{25}0.0015	^{28}0.0018	^{82}0.0002 N$^{0.140}$ ^{69}	^{26}0.0009	^{24}0.0009	^{23}0.0010	^{22}0.0010	^{21}0.0010	^{95}0.0005 N$^{0.041}$ ^{69}
119	NTECHLAB-010	^{16}0.0011	^{15}0.0011	^{13}0.0012	^{13}0.0013	^{13}0.0014	^{133}0.0003 N$^{0.091}$ ^{34}	^{37}0.0010	^{34}0.0010	^{27}0.0010	^{23}0.0010	^{20}0.0010	^{157}0.0009 N$^{0.005}$ ^{10}
120	NTECHLAB-011	^{10}0.0010	^{9}0.0010	^{8}0.0011	^{8}0.0012	^{8}0.0013	^{115}0.0002 N$^{0.103}$ ^{42}	^{15}0.0009	^{13}0.0009	^{14}0.0009	^{12}0.0009	^{10}0.0009	^{118}0.0007 N$^{0.017}$ ^{32}
121	PANGIAM-000	^{24}0.0011	^{22}0.0012	^{21}0.0013	^{18}0.0014	^{20}0.0016	^{105}0.0002 N$^{0.118}$ ^{57}	^{34}0.0010	^{35}0.0010	^{30}0.0010	^{27}0.0011	^{26}0.0011	^{115}0.0007 N$^{0.027}$ ^{53}
122	PARAVISION-003	^{122}0.0026	^{122}0.0031	^{121}0.0035	^{118}0.0042	^{116}0.0048	^{68}0.0002 N$^{0.210}$ ^{124}	^{131}0.0016	^{131}0.0017	^{128}0.0018	^{124}0.0020	^{113}0.0021	^{86}0.0005 N$^{0.089}$ ^{119}
123	PARAVISION-004	^{58}0.0015	^{51}0.0016	^{49}0.0017	^{45}0.0019	^{43}0.0021	^{139}0.0003 N$^{0.111}$ ^{47}	^{88}0.0013	^{79}0.0013	^{72}0.0013	^{62}0.0013	^{57}0.0014	^{161}0.0010 N$^{0.020}$ ^{42}
124	PARAVISION-005	^{52}0.0015	^{46}0.0015	^{41}0.0016	^{38}0.0018	^{34}0.0019	^{149}0.0004 N$^{0.094}$ ^{36}	^{94}0.0013	^{83}0.0013	^{75}0.0013	^{66}0.0013	^{56}0.0014	^{166}0.0011 N$^{0.015}$ ^{25}
125	PARAVISION-007	^{22}0.0011	^{18}0.0012	^{19}0.0012	^{15}0.0013	^{17}0.0015	^{135}0.0003 N$^{0.091}$ ^{33}	^{38}0.0010	^{30}0.0010	^{25}0.0010	^{26}0.0010	^{24}0.0011	^{141}0.0008 N$^{0.018}$ ^{36}
126	PARAVISION-009	^{9}0.0010	^{7}0.0010	^{9}0.0011	^{10}0.0012	^{10}0.0014	^{91}0.0002 N$^{0.118}$ ^{55}	^{22}0.0009	^{21}0.0009	^{22}0.0009	^{21}0.0010	^{19}0.0010	^{99}0.0006 N$^{0.032}$ ^{58}
127	PIXELALL-002	^{149}0.0037	^{146}0.0045	^{144}0.0052	^{139}0.0062	^{135}0.0075	^{64}0.0002 N$^{0.238}$ ^{145}	^{136}0.0017	^{144}0.0019	^{141}0.0021	^{139}0.0024	^{131}0.0027	^{57}0.0002 N$^{0.154}$ ^{151}
128	PIXELALL-003	^{87}0.0019	^{87}0.0021	^{87}0.0024	^{84}0.0028	^{83}0.0032	^{75}0.0002 N$^{0.182}$ ^{106}	^{105}0.0014	^{100}0.0014	^{92}0.0014	^{86}0.0015	^{80}0.0016	^{136}0.0007 N$^{0.045}$ ^{78}
129	PIXELALL-004	^{73}0.0017	^{84}0.0020	^{84}0.0023	^{79}0.0026	^{76}0.0030	^{54}0.0001 N$^{0.192}$ ^{112}	^{91}0.0013	^{89}0.0013	^{84}0.0014	^{78}0.0014	^{70}0.0015	^{116}0.0007 N$^{0.046}$ ^{79}
130	PIXELALL-005	^{78}0.0018	^{74}0.0019	^{65}0.0020	^{58}0.0021	^{54}0.0024	^{159}0.0005 N$^{0.098}$ ^{38}	^{122}0.0015	^{118}0.0016	^{108}0.0016	^{96}0.0016	^{86}0.0016	^{170}0.0012 N$^{0.018}$ ^{34}
131	PTAKURATSATU-000	^{118}0.0025	^{120}0.0030	^{123}0.0036	^{115}0.0040	^{103}0.0040	^{129}0.0003 N$^{0.167}$ ^{95}	^{121}0.0015	^{120}0.0016	^{132}0.0018	^{121}0.0020	^{105}0.0020	^{78}0.0004 N$^{0.096}$ ^{124}
132	QNAP-001	^{142}0.0035	^{140}0.0041	^{138}0.0047	^{132}0.0054	^{130}0.0063	^{116}0.0002 N$^{0.200}$ ^{115}	^{167}0.0022	^{162}0.0023	^{151}0.0024	^{145}0.0025	^{135}0.0028	^{146}0.0008 N$^{0.072}$ ^{109}
133	QNAP-002	^{162}0.0047	^{152}0.0049	^{142}0.0052	^{134}0.0054	^{124}0.0059	^{186}0.0016 N$^{0.079}$ ^{23}	^{209}0.0041	^{201}0.0042	^{176}0.0042	^{167}0.0043	^{154}0.0044	^{190}0.0032 N$^{0.019}$ ^{41}
134	QUANTASOFT-001	^{278}0.2177	^{275}0.2177	^{214}0.2177		^{198}0.2177	^{204}0.2177 N$^{0.000}$ ^{1}	^{281}0.1116	^{277}0.1116	^{213}0.1116		^{198}0.1116	^{204}0.1116 N$^{-0.000}$ ^{1}
135	RANKONE-002	^{228}0.0155	^{228}0.0194	^{194}0.0224	^{188}0.0262	^{185}0.0304	^{173}0.0007 N$^{0.230}$ ^{137}	^{214}0.0048	^{217}0.0060	^{190}0.0071	^{188}0.0085	^{183}0.0102	^{46}0.0002 N$^{0.254}$ ^{175}
136	RANKONE-003	^{229}0.0155	^{227}0.0194	^{195}0.0224	^{189}0.0262	^{184}0.0304	^{172}0.0007 N$^{0.230}$ ^{138}	^{215}0.0048	^{218}0.0060	^{189}0.0071	^{189}0.0085	^{184}0.0102	^{47}0.0002 N$^{0.254}$ ^{174}
137	RANKONE-005	^{186}0.0075	^{193}0.0094	^{177}0.0110	^{173}0.0132	^{168}0.0156	^{122}0.0003 N$^{0.251}$ ^{155}	^{185}0.0026	^{186}0.0032	^{172}0.0036	^{165}0.0043	^{158}0.0050	^{42}0.0001 N$^{0.221}$ ^{165}
138	RANKONE-007	^{127}0.0028	^{126}0.0034	^{125}0.0038	^{120}0.0045	^{119}0.0053	^{77}0.0002 N$^{0.211}$ ^{125}	^{120}0.0015	^{124}0.0017	^{126}0.0018	^{118}0.0019	^{116}0.0021	^{67}0.0003 N$^{0.123}$ ^{138}
139	RANKONE-009	^{93}0.0020	^{100}0.0024	^{102}0.0027	^{103}0.0032	^{100}0.0038	^{41}0.0001 N$^{0.219}$ ^{128}	^{102}0.0013	^{96}0.0014	^{95}0.0015	^{90}0.0015	^{82}0.0016	^{101}0.0006 N$^{0.059}$ ^{95}
140	RANKONE-010	^{97}0.0020	^{94}0.0022	^{93}0.0025	^{92}0.0029	^{84}0.0032	^{103}0.0002 N$^{0.164}$ ^{94}	^{114}0.0014	^{106}0.0015	^{101}0.0015	^{94}0.0016	^{88}0.0017	^{107}0.0006 N$^{0.058}$ ^{93}
141	RANKONE-011	^{40}0.0014	^{43}0.0015	^{43}0.0017	^{42}0.0018	^{44}0.0021	^{85}0.0002 N$^{0.150}$ ^{79}	^{55}0.0011	^{50}0.0012	^{48}0.0012	^{42}0.0012	^{38}0.0012	^{148}0.0008 N$^{0.023}$ ^{46}
142	RANKONE-012	^{31}0.0013	^{31}0.0014	^{37}0.0015	^{35}0.0017	^{35}0.0020	^{86}0.0002 N$^{0.144}$ ^{76}	^{47}0.0011	^{47}0.0011	^{43}0.0011	^{36}0.0011	^{31}0.0012	^{150}0.0009 N$^{0.016}$ ^{27}
143	REALNETWORKS-002	^{248}0.0299	^{244}0.0393	^{207}0.0470	^{201}0.0562	^{196}0.0580	^{182}0.0013 N$^{0.236}$ ^{144}	^{219}0.0054	^{229}0.0076	^{199}0.0097	^{195}0.0126	^{190}0.0132	^{33}0.0001 N$^{0.320}$ ^{191}
144	REALNETWORKS-003	^{234}0.0183	^{234}0.0242	^{200}0.0291	^{195}0.0352	^{192}0.0423	^{148}0.0004 N$^{0.287}$ ^{180}	^{208}0.0041	^{210}0.0054	^{185}0.0064	^{186}0.0080	^{182}0.0101	^{27}0.0001 N$^{0.307}$ ^{187}

Table 22: **Investigation-mode: Effect of N on FNIR on recent images** *For five enrollment population sizes, N, with T = 0 and FPIR = 1. The left five columns are rank 1 miss rates The right five columns are rank 50 miss rates Missing entries usually apply because another algorithm from the same developer was run instead. Some developers are missing because less accurate algorithms were not run on galleries with $N > 1\,600\,000$. Throughout blue superscripts indicate the rank of the algorithm for that column, and yellow highlighting indicates the most accurate value. Caution: The Power-low models are mostly intended to draw attention to the kind of behavior, not as a model to be used for prediction.*

This publication is available free of charge from: https://doi.org/10.6028/NIST.IR.8271

MISSES AT GIVEN RANK		ENROL MOST RECENT											
FNIR(N, T= 0, R)		RANK 1						RANK 50					
#	ALGORITHM	N=0.64M	N=1.6M	N=3.0M	N=6.0M	N=12.0M	aN^b	N=0.64M	N=1.6M	N=3.0M	N=6.0M	N=12.0M	aN^b
145	REALNETWORKS-004	^{231}0.0175	^{232}0.0236	^{199}0.0284	^{194}0.0347	^{189}0.0416	^{140}0.0003 N$^{0.295}$ ^{183}	^{205}0.0040	^{207}0.0050	^{184}0.0061	^{184}0.0078	^{181}0.0099	^{26}0.0001 N$^{0.315}$ ^{188}
146	REALNETWORKS-005	^{94}0.0020	^{96}0.0023	^{100}0.0026	^{96}0.0030	^{95}0.0037	^{49}0.0001 N$^{0.207}$ ^{122}	^{60}0.0012	^{59}0.0012	^{69}0.0013	^{73}0.0014	^{65}0.0015	^{76}0.0004 N$^{0.081}$ ^{114}
147	REALNETWORKS-006	^{33}0.0013	^{33}0.0014	^{40}0.0016	^{39}0.0018	^{38}0.0021	^{58}0.0001 N$^{0.163}$ ^{93}	^{31}0.0010	^{29}0.0010	^{31}0.0010	^{33}0.0011	^{32}0.0012	^{29}0.0004 N$^{0.060}$ ^{97}
148	REALNETWORKS-007	^{29}0.0013	^{28}0.0013	^{27}0.0014	^{29}0.0016	^{30}0.0018	^{112}0.0002 N$^{0.124}$ ^{61}	^{29}0.0010	^{26}0.0010	^{29}0.0010	^{29}0.0011	^{29}0.0011	^{81}0.0004 N$^{0.057}$ ^{92}
149	REMARKAI-000	^{125}0.0027	^{128}0.0034	^{128}0.0040	^{126}0.0048	^{122}0.0058	^{32}0.0001 N$^{0.260}$ ^{161}	^{116}0.0014	^{117}0.0015	^{111}0.0016	^{106}0.0018	^{106}0.0020	^{69}0.0003 N$^{0.108}$ ^{127}
150	RENDIP-000	^{47}0.0014	^{47}0.0015	^{48}0.0017	^{49}0.0019	^{48}0.0022	^{76}0.0002 N$^{0.158}$ ^{86}	^{57}0.0012	^{56}0.0012	^{53}0.0012	^{47}0.0012	^{42}0.0013	^{147}0.0008 N$^{0.025}$ ^{48}
151	REVEALMEDIA-000	^{70}0.0017	^{71}0.0019	^{63}0.0020	^{64}0.0023	^{57}0.0025	^{126}0.0003 N$^{0.134}$ ^{66}	^{66}0.0012	^{62}0.0012	^{57}0.0012	^{53}0.0013	^{46}0.0013	^{137}0.0007 N$^{0.035}$ ^{61}
152	S1-000	^{99}0.0021	^{102}0.0024	^{106}0.0028	^{104}0.0032	^{99}0.0037	^{55}0.0001 N$^{0.203}$ ^{118}	^{117}0.0014	^{112}0.0015	^{105}0.0015	^{98}0.0016	^{90}0.0017	^{114}0.0007 N$^{0.055}$ ^{88}
153	S1-001	^{135}0.0031	^{121}0.0031	^{119}0.0034	^{108}0.0036	^{104}0.0040	^{176}0.0009 N$^{0.092}$ ^{35}	^{171}0.0023	^{161}0.0023	^{148}0.0024	^{140}0.0024	^{128}0.0025	^{181}0.0017 N$^{0.023}$ ^{47}
154	S1-002	^{41}0.0014	^{36}0.0014	^{33}0.0015	^{33}0.0016	^{29}0.0018	^{152}0.0004 N$^{0.085}$ ^{27}	^{93}0.0013	^{84}0.0013	^{73}0.0013	^{60}0.0013	^{51}0.0013	^{167}0.0011 N$^{0.011}$ ^{17}
155	SCANOVATE-000	^{150}0.0038	^{153}0.0050	^{151}0.0059	^{146}0.0073	^{134}0.0073	^{79}0.0002 N$^{0.235}$ ^{143}	^{110}0.0014	^{116}0.0015	^{116}0.0017	^{129}0.0020	^{110}0.0020	^{55}0.0002 N$^{0.142}$ ^{146}
156	SCANOVATE-001	^{153}0.0041	^{157}0.0053	^{152}0.0064	^{150}0.0079	^{149}0.0098	^{27}0.0001 N$^{0.299}$ ^{186}	^{103}0.0013	^{114}0.0015	^{117}0.0017	^{130}0.0021	^{127}0.0024	^{36}0.0001 N$^{0.207}$ ^{162}
157	SENSETIME-000	^{105}0.0022	^{98}0.0023	^{98}0.0026	^{90}0.0028	^{82}0.0032	^{142}0.0003 N$^{0.135}$ ^{67}	^{133}0.0016	^{130}0.0017	^{123}0.0018	^{112}0.0018	^{108}0.0020	^{133}0.0007 N$^{0.060}$ ^{96}
158	SENSETIME-001	^{103}0.0022	^{99}0.0023	^{95}0.0025	^{94}0.0029	^{96}0.0037	^{90}0.0002 N$^{0.177}$ ^{103}	^{130}0.0016	^{121}0.0016	^{115}0.0017	^{109}0.0018	^{125}0.0024	^{66}0.0003 N$^{0.125}$ ^{140}
159	SENSETIME-002	^{224}0.0136	^{215}0.0137	^{185}0.0137	^{175}0.0138	^{164}0.0139	^{199}0.0124 N$^{0.007}$ ^{2}	^{254}0.0136	^{247}0.0136	^{203}0.0136	^{197}0.0136	^{191}0.0136	^{200}0.0135 N$^{0.001}$ ^{3}
160	SENSETIME-003	^{7}0.0010	^{6}0.0010	^{6}0.0010	^{6}0.0011	^{6}0.0012	^{132}0.0003 N$^{0.085}$ ^{29}	^{24}0.0009	^{22}0.0009	^{20}0.0009	^{20}0.0010	^{15}0.0010	^{140}0.0008 N$^{0.013}$ ^{20}
161	SENSETIME-004	^{6}0.0010	^{5}0.0010	^{4}0.0010	^{5}0.0011	^{4}0.0012	^{134}0.0003 N$^{0.081}$ ^{24}	^{11}0.0008	^{9}0.0009	^{10}0.0009	^{8}0.0009	^{8}0.0009	^{109}0.0007 N$^{0.018}$ ^{37}
162	SENSETIME-005	^{2}0.0008	^{3}0.0009	^{3}0.0009	^{3}0.0010	^{3}0.0011	^{123}0.0003 N$^{0.085}$ ^{28}	^{7}0.0008	^{6}0.0008	^{6}0.0008	^{3}0.0008	^{1}0.0008	^{142}0.0008 N$^{0.002}$ ^{6}
163	SENSETIME-006	^{3}0.0008	^{2}0.0009	^{2}0.0009	^{2}0.0010	^{2}0.0010	^{136}0.0003 N$^{0.069}$ ^{16}	^{9}0.0008	^{8}0.0008	^{8}0.0008	^{6}0.0008	^{3}0.0008	^{121}0.0007 N$^{0.011}$ ^{16}
164	SENSETIME-007	^{1}0.0008	^{1}0.0008	^{1}0.0009	^{1}0.0009	^{1}0.0010	^{143}0.0004 N$^{0.061}$ ^{14}	^{8}0.0008	^{7}0.0008	^{7}0.0008	^{5}0.0008	^{2}0.0008	^{132}0.0007 N$^{0.008}$ ^{13}
165	SHAMAN-007	^{252}0.0371	^{245}0.0396	^{206}0.0416	^{200}0.0443	^{194}0.0473	^{198}0.0122 N$^{0.083}$ ^{25}	^{267}0.0308	^{261}0.0314	^{209}0.0319	^{201}0.0326	^{195}0.0337	^{201}0.0207 N$^{0.029}$ ^{57}
166	SIAT-001	^{67}0.0017	^{65}0.0018	^{67}0.0020	^{67}0.0023	^{64}0.0027	^{69}0.0002 N$^{0.173}$ ^{101}	^{41}0.0010	^{45}0.0011	^{47}0.0012	^{50}0.0013	^{49}0.0013	^{70}0.0003 N$^{0.085}$ ^{116}
167	SIAT-002	^{66}0.0016	^{67}0.0018	^{70}0.0020	^{68}0.0023	^{61}0.0027	^{73}0.0002 N$^{0.171}$ ^{98}	^{56}0.0011	^{60}0.0012	^{61}0.0013	^{61}0.0013	^{58}0.0014	^{90}0.0005 N$^{0.062}$ ^{99}
168	SQISOFT-001	^{126}0.0028	^{141}0.0042	^{150}0.0059	^{153}0.0084	^{203}0.9207	^{2}0.0000 N$^{1.674}$ ^{203}	^{30}0.0010	^{37}0.0010	^{40}0.0011	^{44}0.0012	^{203}0.9198	^{2}0.0000 N$^{1.883}$ ^{203}
169	SYNESIS-003	^{272}0.1456	^{272}0.1700	^{212}0.1876	^{204}0.2088	^{199}0.2317	^{200}0.0177 N$^{0.158}$ ^{87}	^{274}0.0828	^{274}0.0869	^{212}0.0920	^{204}0.0998	^{197}0.1104	^{202}0.0218 N$^{0.098}$ ^{126}
170	SYNESIS-003	^{230}0.0161	^{219}0.0162	^{190}0.0163	^{181}0.0165	^{180}0.0254	^{189}0.0027 N$^{0.127}$ ^{63}	^{257}0.0160	^{252}0.0160	^{205}0.0160	^{199}0.0160	^{194}0.0245	^{158}0.0009 N$^{0.192}$ ^{157}
171	SYNESIS-005	^{199}0.0085	^{185}0.0085	^{168}0.0085	^{156}0.0086	^{143}0.0088	^{197}0.0072 N$^{0.012}$ ^{3}	^{241}0.0085	^{235}0.0085	^{197}0.0085	^{187}0.0085	^{175}0.0085	^{199}0.0085 N$^{0.000}$ ^{2}
172	TECH5-001	^{136}0.0032	^{136}0.0040	^{139}0.0047	^{135}0.0057	^{133}0.0071	^{31}0.0001 N$^{0.271}$ ^{165}	^{124}0.0016	^{126}0.0017	^{127}0.0018	^{120}0.0020	^{122}0.0023	^{68}0.0003 N$^{0.119}$ ^{135}
173	TECH5-002	^{95}0.0020	^{111}0.0027	^{114}0.0031	^{110}0.0037	^{113}0.0047	^{17}0.0000 N$^{0.285}$ ^{179}	^{20}0.0009	^{28}0.0010	^{37}0.0011	^{40}0.0012	^{48}0.0013	^{49}0.0002 N$^{0.127}$ ^{142}
174	TEVIAN-005	^{174}0.0056	^{176}0.0073	^{167}0.0084	^{166}0.0105	^{162}0.0130	^{53}0.0001 N$^{0.283}$ ^{178}	^{152}0.0020	^{158}0.0023	^{153}0.0025	^{147}0.0028	^{141}0.0034	^{50}0.0002 N$^{0.178}$ ^{155}
175	TEVIAN-006	^{112}0.0023	^{103}0.0024	^{101}0.0026	^{85}0.0028	^{79}0.0031	^{165}0.0005 N$^{0.106}$ ^{43}	^{126}0.0016	^{122}0.0017	^{114}0.0017	^{104}0.0017	^{94}0.0018	^{154}0.0009 N$^{0.041}$ ^{70}
176	TEVIAN-007	^{75}0.0017	^{63}0.0018	^{55}0.0018	^{53}0.0020	^{42}0.0021	^{169}0.0006 N$^{0.073}$ ^{19}	^{78}0.0013	^{69}0.0013	^{67}0.0013	^{63}0.0013	^{55}0.0013	^{149}0.0009 N$^{0.026}$ ^{49}
177	TIGER-002	^{156}0.0044	^{159}0.0056	^{156}0.0068	^{157}0.0086	^{153}0.0105	^{29}0.0001 N$^{0.299}$ ^{187}	^{84}0.0013	^{110}0.0015	^{121}0.0018	^{131}0.0021	^{132}0.0027	^{18}0.0000 N$^{0.253}$ ^{173}
178	TOSHIBA-000	^{143}0.0035	^{145}0.0045	^{145}0.0052	^{137}0.0061	^{167}0.0154	^{6}0.0000 N$^{0.449}$ ^{199}	^{127}0.0016	^{137}0.0018	^{136}0.0019	^{133}0.0021	^{185}0.0105	^{5}0.0000 N$^{0.539}$ ^{200}
179	TRUEFACE-000	^{133}0.0031	^{125}0.0033	^{122}0.0035	^{114}0.0039	^{106}0.0043	^{170}0.0006 N$^{0.115}$ ^{53}	^{182}0.0025	^{168}0.0026	^{154}0.0026	^{146}0.0027	^{137}0.0028	^{179}0.0015 N$^{0.038}$ ^{67}
180	VD-001	^{241}0.0230	^{238}0.0276	^{202}0.0315	^{197}0.0363	^{191}0.0418	^{184}0.0015 N$^{0.204}$ ^{120}	^{251}0.0120	^{246}0.0130	^{204}0.0140	^{198}0.0154	^{193}0.0170	^{188}0.0024 N$^{0.120}$ ^{136}
181	VERIDAS-001	^{111}0.0023	^{114}0.0028	^{115}0.0032	^{113}0.0037	^{110}0.0045	^{40}0.0001 N$^{0.231}$ ^{140}	^{112}0.0014	^{107}0.0015	^{102}0.0015	^{99}0.0016	^{93}0.0018	^{82}0.0005 N$^{0.083}$ ^{115}
182	VERIDAS-002	^{110}0.0023	^{113}0.0028	^{104}0.0028	^{102}0.0032	^{97}0.0037	^{127}0.0003 N$^{0.158}$ ^{85}	^{109}0.0014	^{105}0.0015	^{94}0.0015	^{91}0.0015	^{85}0.0016	^{135}0.0007 N$^{0.047}$ ^{81}
183	VERIDAS-003	^{68}0.0017	^{66}0.0018	^{62}0.0020	^{62}0.0022	^{59}0.0026	^{101}0.0002 N$^{0.150}$ ^{78}	^{82}0.0013	^{78}0.0013	^{74}0.0013	^{68}0.0014	^{63}0.0014	^{119}0.0007 N$^{0.043}$ ^{75}
184	VIGILANTSOLUTIONS-008	^{117}0.0025	^{119}0.0029	^{120}0.0034	^{117}0.0040	^{111}0.0047	^{51}0.0001 N$^{0.224}$ ^{133}	^{58}0.0012	^{71}0.0013	^{90}0.0014	^{93}0.0015	^{89}0.0017	^{54}0.0002 N$^{0.130}$ ^{143}
185	VISIONBOX-000	^{76}0.0017	^{75}0.0019	^{29}0.0022	^{220}1.0000	^{204}0.9526	^{1}0.0000 N$^{2.570}$ ^{204}	^{75}0.0012	^{68}0.0013	^{77}0.0013	^{210}1.0000	^{204}0.9525	^{1}0.0000 N$^{2.719}$ ^{204}
186	VISIONLABS-004	^{106}0.0022	^{112}0.0027	^{117}0.0032	^{119}0.0044	^{132}0.0070	^{7}0.0000 N$^{0.387}$ ^{197}	^{76}0.0012	^{94}0.0014	^{113}0.0017	^{142}0.0025	^{155}0.0045	^{6}0.0000 N$^{0.435}$ ^{196}
187	VISIONLABS-005	^{92}0.0020	^{101}0.0024	^{109}0.0029	^{109}0.0037	^{118}0.0051	^{11}0.0000 N$^{0.322}$ ^{194}	^{72}0.0012	^{76}0.0013	^{107}0.0016	^{119}0.0019	^{138}0.0029	^{12}0.0000 N$^{0.298}$ ^{184}
188	VISIONLABS-006	^{65}0.0016	^{68}0.0018	^{80}0.0022	^{89}0.0028	^{105}0.0041	^{10}0.0000 N$^{0.314}$ ^{192}	^{67}0.0012	^{72}0.0013	^{96}0.0015	^{113}0.0019	^{133}0.0027	^{14}0.0000 N$^{0.275}$ ^{178}
189	VISIONLABS-007	^{63}0.0016	^{62}0.0018	^{66}0.0020	^{70}0.0023	^{90}0.0034	^{19}0.0001 N$^{0.248}$ ^{153}	^{63}0.0012	^{61}0.0012	^{59}0.0013	^{58}0.0013	^{107}0.0020	^{43}0.0001 N$^{0.152}$ ^{149}
190	VISIONLABS-008	^{84}0.0019	^{82}0.0020	^{75}0.0021	^{78}0.0025	^{77}0.0030	^{87}0.0002 N$^{0.169}$ ^{96}	^{134}0.0016	^{127}0.0017	^{120}0.0017	^{123}0.0020	^{123}0.0023	^{71}0.0003 N$^{0.114}$ ^{132}
191	VISIONLABS-009	^{19}0.0011	^{17}0.0011	^{17}0.0012	^{19}0.0014	^{27}0.0017	^{47}0.0001 N$^{0.160}$ ^{90}	^{33}0.0010	^{27}0.0010	^{28}0.0010	^{35}0.0011	^{60}0.0014	^{59}0.0002 N$^{0.109}$ ^{128}
192	VISIONLABS-010	^{39}0.0014	^{34}0.0014	^{34}0.0015	^{36}0.0017	^{39}0.0021	^{95}0.0002 N$^{0.137}$ ^{68}	^{79}0.0013	^{65}0.0013	^{76}0.0013	^{77}0.0014	^{87}0.0017	^{73}0.0004 N$^{0.090}$ ^{121}
193	VISIONLABS-011	^{20}0.0011	^{20}0.0012	^{20}0.0013	^{21}0.0014	^{31}0.0018	^{46}0.0001 N$^{0.162}$ ^{92}	^{39}0.0010	^{40}0.0011	^{41}0.0011	^{43}0.0012	^{71}0.0015	^{56}0.0002 N$^{0.114}$ ^{133}
194	VNPT-001	^{98}0.0020	^{88}0.0022	^{83}0.0023	^{75}0.0025	^{65}0.0028	^{164}0.0005 N$^{0.101}$ ^{40}	^{140}0.0018	^{134}0.0018	^{130}0.0018	^{110}0.0018	^{96}0.0019	^{176}0.0014 N$^{0.018}$ ^{33}
195	VOCORD-005	^{175}0.0060	^{174}0.0070	^{164}0.0082	^{163}0.0097	^{157}0.0117	^{121}0.0003 N$^{0.232}$ ^{142}	^{199}0.0033	^{193}0.0035	^{174}0.0037	^{162}0.0040	^{153}0.0043	^{159}0.0010 N$^{0.090}$ ^{120}
196	VTS-001	^{38}0.0014	^{45}0.0015	^{47}0.0017	^{50}0.0019	^{51}0.0023	^{48}0.0001 N$^{0.179}$ ^{105}	^{32}0.0010	^{31}0.0010	^{32}0.0010	^{28}0.0011	^{30}0.0011	^{87}0.0005 N$^{0.051}$ ^{86}
197	VTS-002	^{69}0.0017	^{77}0.0019	^{81}0.0022	^{80}0.0026	^{80}0.0032	^{36}0.0001 N$^{0.215}$ ^{127}	^{44}0.0011	^{46}0.0011	^{52}0.0012	^{51}0.0013	^{53}0.0013	^{75}0.0004 N$^{0.079}$ ^{113}
198	XFORWARDAI-000	^{102}0.0021	^{95}0.0023	^{86}0.0024	^{82}0.0027	^{73}0.0029	^{158}0.0005 N$^{0.111}$ ^{48}	^{150}0.0019	^{143}0.0019	^{135}0.0019	^{125}0.0020	^{109}0.0020	^{178}0.0015 N$^{0.018}$ ^{35}
199	XFORWARDAI-001	^{96}0.0020	^{85}0.0020	^{73}0.0021	^{61}0.0022	^{53}0.0024	^{178}0.0009 N$^{0.055}$ ^{12}	^{148}0.0019	^{142}0.0019	^{134}0.0019	^{117}0.0019	^{102}0.0019	^{184}0.0018 N$^{0.004}$ ^{8}
200	XFORWARDAI-002	^{90}0.0019	^{78}0.0020	^{68}0.0020	^{57}0.0021	^{46}0.0022	^{181}0.0011 N$^{0.038}$ ^{7}	^{147}0.0019	^{141}0.0019	^{133}0.0019	^{116}0.0019	^{98}0.0019	^{183}0.0018 N$^{0.003}$ ^{7}
201	YITU-002	^{60}0.0016	^{69}0.0018	^{74}0.0021	^{73}0.0024	^{74}0.0029	^{34}0.0001 N$^{0.213}$ ^{126}	^{28}0.0009	^{33}0.0010	^{33}0.0010	^{30}0.0011	^{33}0.0012	^{72}0.0004 N$^{0.073}$ ^{110}
202	YITU-003	^{121}0.0026	^{118}0.0029	^{113}0.0031	^{106}0.0035	^{102}0.0039	^{147}0.0004 N$^{0.141}$ ^{71}	^{157}0.0020	^{151}0.0021	^{144}0.0022	^{136}0.0023	^{126}0.0024	^{160}0.0010 N$^{0.054}$ ^{87}
203	YITU-004	^{21}0.0011	^{27}0.0013	^{35}0.0015	^{37}0.0017	^{112}0.0047	^{5}0.0000 N$^{0.438}$ ^{198}	^{12}0.0008	^{11}0.0009	^{11}0.0009	^{11}0.0009	^{143}0.0036	^{7}0.0000 N$^{0.395}$ ^{195}
204	YITU-005	^{108}0.0022	^{97}0.0023	^{92}0.0025	^{83}0.0027	^{78}0.0031	^{160}0.0005 N$^{0.113}$ ^{50}	^{151}0.0020	^{146}0.0020	^{140}0.0020	^{126}0.0020	^{111}0.0020	^{180}0.0017 N$^{0.012}$ ^{19}

Table 23: **Investigation-mode: Effect of N on FNIR on recent images** *For five enrollment population sizes, N, with T = 0 and FPIR = 1. The left five columns are rank 1 miss rates The right five columns are rank 50 miss rates Missing entries usually apply because another algorithm from the same developer was run instead. Some developers are missing because less accurate algorithms were not run on galleries with $N > 1\,600\,000$. Throughout blue superscripts indicate the rank of the algorithm for that column, and yellow highlighting indicates the most accurate value. Caution: The Power-low models are mostly intended to draw attention to the kind of behavior, not as a model to be used for prediction.*

This publication is available free of charge from: https://doi.org/10.6028/NIST.IR.8271

MISSES OUTSIDE RANK R		RESOURCE USAGE		ENROL MOST RECENT, N = 1.6M					
FNIR(N, T=0, R)		TEMPLATE		FRVT 2018 MUGSHOTS					
#	ALGORITHM	BYTES	MSEC	R=1	R=5	R=10	R=20	R=50	WORK-10
1	20FACE-000	^{205}2048	^{57}247	^{254}0.0552	^{248}0.0269	^{247}0.0198	^{244}0.0146	^{238}0.0099	^{249}1.275
2	3DIVI-003	^{63}512	^{158}625	^{263}0.0833	^{258}0.0444	^{258}0.0349	^{254}0.0270	^{254}0.0191	^{259}1.447
3	3DIVI-004	^{275}4096	^{159}628	^{222}0.0175	^{215}0.0091	^{213}0.0075	^{210}0.0061	^{205}0.0049	^{219}1.092
4	3DIVI-005	^{269}4096	^{167}653	^{223}0.0176	^{216}0.0091	^{211}0.0074	^{209}0.0061	^{206}0.0049	^{220}1.092
5	3DIVI-006	^{71}528	^{166}653	^{233}0.0240	^{240}0.0171	^{243}0.0160	^{245}0.0154	^{250}0.0148	^{238}1.162
6	ACER-000	^{54}512	^{47}201	^{200}0.0106	^{184}0.0051	^{180}0.0041	^{178}0.0034	^{171}0.0026	^{185}1.053
7	ACER-001	^{151}2048	^{38}184	^{155}0.0051	^{157}0.0032	^{156}0.0028	^{155}0.0025	^{155}0.0022	^{156}1.031
8	AIZE-001	^{158}2048	^{97}403	^{161}0.0056	^{161}0.0037	^{166}0.0033	^{167}0.0030	^{174}0.0027	^{162}1.035
9	ALCHERA-000	^{159}2048	^{61}263	^{218}0.0161	^{227}0.0124	^{232}0.0117	^{237}0.0111	^{240}0.0105	^{226}1.116
10	ALCHERA-001	^{157}2048	^{23}66	^{291}0.9869	^{291}0.9782	^{291}0.9735	^{291}0.9679	^{290}0.9590	^{291}9.811
11	ALCHERA-002	^{146}2048	^{31}115	^{265}0.0949	^{263}0.0555	^{261}0.0443	^{261}0.0354	^{256}0.0254	^{263}1.544
12	ALCHERA-003	^{171}2048	^{142}548	^{197}0.0104	^{187}0.0054	^{187}0.0045	^{186}0.0038	^{185}0.0032	^{189}1.055
13	ALCHERA-004	^{177}2048	^{258}854	^{202}0.0110	^{183}0.0049	^{175}0.0038	^{170}0.0032	^{167}0.0025	^{183}1.051
14	ALLGOVISION-000	^{188}2048	^{102}425	^{205}0.0114	^{210}0.0084	^{216}0.0078	^{217}0.0073	^{222}0.0067	^{210}1.079
15	ALLGOVISION-001	^{181}2048	^{229}792	^{188}0.0090	^{181}0.0048	^{179}0.0040	^{177}0.0033	^{175}0.0027	^{181}1.048
16	ANKE-000	^{244}2072	^{109}431	^{213}0.0132	^{201}0.0073	^{200}0.0060	^{199}0.0050	^{198}0.0040	^{206}1.072
17	ANKE-001	^{243}2072	^{111}433	^{214}0.0132	^{202}0.0073	^{202}0.0061	^{200}0.0050	^{199}0.0040	^{207}1.073
18	ANKE-002	^{232}2056	^{162}641	^{116}0.0028	^{116}0.0020	^{115}0.0018	^{121}0.0018	^{125}0.0017	^{117}1.019
19	AWARE-003	^{245}2076	^{203}716	^{240}0.0306	^{237}0.0162	^{234}0.0127	^{231}0.0100	^{228}0.0075	^{239}1.163
20	AWARE-004	^{19}92	^{200}712	^{258}0.0679	^{255}0.0348	^{252}0.0274	^{252}0.0208	^{249}0.0145	^{255}1.354
21	AWARE-005	^{257}3100	^{236}827	^{241}0.0311	^{238}0.0167	^{236}0.0134	^{233}0.0107	^{234}0.0082	^{240}1.167
22	AWARE-006	^{20}124	^{233}818	^{260}0.0697	^{257}0.0369	^{253}0.0288	^{253}0.0223	^{251}0.0158	^{257}1.371
23	AYONIX-000	^{101}1036	^{18}10	^{284}0.4505	^{285}0.3540	^{285}0.3176	^{285}0.2834	^{285}0.2381	^{285}4.288
24	AYONIX-001	^{100}1036	^{20}12	^{279}0.3414	^{279}0.2338	^{279}0.1977	^{280}0.1652	^{279}0.1274	^{279}3.226
25	AYONIX-002	^{102}1036	^{19}11	^{280}0.3414	^{280}0.2338	^{280}0.1977	^{279}0.1652	^{280}0.1274	^{280}3.226
26	CAMVI-003	^{85}1024	^{196}707	^{253}0.0520	^{262}0.0517	^{263}0.0517	^{266}0.0517	^{266}0.0517	^{261}1.466
27	CAMVI-004	^{87}1024	^{205}718	^{251}0.0468	^{260}0.0465	^{262}0.0465	^{263}0.0464	^{265}0.0464	^{258}1.419
28	CAMVI-005	^{89}1024	^{220}769	^{257}0.0652	^{264}0.0648	^{268}0.0648	^{269}0.0648	^{271}0.0647	^{264}1.584
29	CANON-001	^{264}4096	^{266}893	^{14}0.0011	^{21}0.0010	^{20}0.0010	^{18}0.0009	^{18}0.0009	^{17}1.009
30	CANON-002	^{14}0	^{17}6	^{19}0.0012	^{17}0.0010	^{15}0.0009	^{15}0.0009	^{16}0.0009	^{14}1.009
31	CIB-000	^{291}8196	^{175}674	^{44}0.0015	^{51}0.0013	^{48}0.0012	^{49}0.0012	^{53}0.0012	^{50}1.012
32	CLEARVIEWAI-000	^{265}4096	^{217}765	^{13}0.0011	^{20}0.0010	^{21}0.0010	^{17}0.0009	^{17}0.0009	^{15}1.009
33	CLOUDWALK-HR-000	^{140}2048	^{273}908	^{41}0.0015	^{70}0.0014	^{77}0.0014	^{88}0.0014	^{97}0.0014	^{64}1.013
34	CLOUDWALK-MT-000	^{169}2048	^{257}870	^{61}0.0018	^{97}0.0018	^{107}0.0018	^{116}0.0018	^{133}0.0018	^{93}1.016
35	COGENT-000	^{67}525	^{143}551	^{199}0.0105	^{221}0.0096	^{225}0.0095	^{172}0.0032	^{164}0.0024	^{216}1.088
36	COGENT-001	^{68}525	^{144}552	^{198}0.0105	^{220}0.0096	^{226}0.0095	^{171}0.0032	^{163}0.0024	^{217}1.088
37	COGENT-002	^{104}1043	^{291}987	^{131}0.0036	^{126}0.0022	^{124}0.0020	^{119}0.0018	^{115}0.0015	^{127}1.021
38	COGENT-003	^{103}1043	^{288}960	^{133}0.0038	^{137}0.0024	^{133}0.0021	^{135}0.0019	^{128}0.0017	^{135}1.023
39	COGENT-004	^{229}2053	^{285}952	^{80}0.0020	^{83}0.0016	^{84}0.0015	^{92}0.0015	^{95}0.0014	^{81}1.015
40	COGENT-005	^{105}1062	^{223}774	^{55}0.0017	^{67}0.0014	^{69}0.0014	^{79}0.0014	^{87}0.0013	^{67}1.013
41	COGENT-006	^{9}0	^{3}0	^{25}0.0012	^{32}0.0011	^{32}0.0011	^{36}0.0011	^{42}0.0011	^{30}1.010
42	COGNITEC-000	^{219}2052	^{36}176	^{235}0.0252	^{233}0.0136	^{231}0.0107	^{230}0.0085	^{220}0.0065	^{234}1.136
43	COGNITEC-001	^{224}2052	^{48}202	^{206}0.0117	^{193}0.0062	^{193}0.0051	^{194}0.0042	^{191}0.0034	^{194}1.062
44	COGNITEC-002	^{227}2052	^{53}227	^{162}0.0057	^{160}0.0037	^{161}0.0032	^{162}0.0029	^{172}0.0026	^{161}1.035
45	COGNITEC-003	^{221}2052	^{71}297	^{166}0.0062	^{169}0.0040	^{170}0.0036	^{176}0.0033	^{183}0.0030	^{168}1.039
46	COGNITEC-004	^{225}2052	^{44}192	^{124}0.0032	^{119}0.0020	^{109}0.0018	^{102}0.0015	^{98}0.0014	^{121}1.020
47	COGNITEC-005	^{208}2052	^{85}367	^{52}0.0016	^{45}0.0013	^{45}0.0012	^{45}0.0012	^{49}0.0011	^{45}1.012
48	COGNITEC-006	^{213}2052	^{119}463	^{48}0.0016	^{44}0.0013	^{42}0.0012	^{44}0.0012	^{48}0.0011	^{42}1.012
49	CUBOX-000	^{149}2048	^{277}918	^{35}0.0014	^{60}0.0014	^{70}0.0014	^{80}0.0014	^{91}0.0014	^{55}1.012
50	CYBERLINK-000	^{222}2052	^{190}699	^{135}0.0040	^{147}0.0028	^{151}0.0026	^{154}0.0024	^{154}0.0022	^{146}1.027
51	CYBERLINK-001	^{207}2052	^{110}433	^{129}0.0035	^{132}0.0023	^{131}0.0021	^{126}0.0018	^{132}0.0017	^{130}1.022
52	CYBERLINK-002	^{285}4140	^{212}738	^{109}0.0026	^{128}0.0023	^{137}0.0022	^{145}0.0021	^{149}0.0021	^{125}1.021
53	CYBERLINK-003	^{289}6212	^{189}696	^{49}0.0016	^{49}0.0013	^{50}0.0013	^{50}0.0012	^{51}0.0012	^{52}1.012
54	CYBERLINK-004	^{288}6212	^{213}738	^{54}0.0017	^{74}0.0015	^{83}0.0015	^{89}0.0014	^{99}0.0014	^{71}1.014
55	CYBERLINK-005	^{287}6212	^{214}739	^{64}0.0018	^{84}0.0016	^{90}0.0015	^{98}0.0015	^{101}0.0014	^{78}1.015
56	DAHUA-000	^{134}2048	^{91}378	^{192}0.0093	^{197}0.0066	^{201}0.0061	^{207}0.0057	^{211}0.0054	^{195}1.062
57	DAHUA-001	^{194}2048	^{87}371	^{170}0.0067	^{170}0.0040	^{169}0.0036	^{174}0.0033	^{178}0.0029	^{170}1.040
58	DAHUA-002	^{187}2048	^{191}699	^{70}0.0018	^{72}0.0015	^{79}0.0014	^{84}0.0014	^{86}0.0013	^{72}1.014
59	DAHUA-003	^{180}2048	^{208}725	^{23}0.0012	^{14}0.0010	^{12}0.0009	^{12}0.0009	^{12}0.0009	^{13}1.009
60	DAHUA-004	^{204}2048	^{216}759	^{12}0.0011	^{11}0.0010	^{14}0.0009	^{14}0.0009	^{14}0.0009	^{12}1.009
61	DAON-000	^{238}2069	^{149}584	^{138}0.0041	^{162}0.0038	^{173}0.0037	^{183}0.0037	^{194}0.0036	^{158}1.034
62	DECATUR-000	^{216}2052	^{260}874	^{86}0.0021	^{85}0.0016	^{87}0.0015	^{86}0.0014	^{80}0.0013	^{85}1.015
63	DEEPGLINT-001	^{263}4096	^{180}687	^{39}0.0014	^{57}0.0014	^{59}0.0013	^{67}0.0013	^{74}0.0013	^{54}1.012
64	DEEPSEA-001	^{170}2048	^{226}780	^{143}0.0043	^{127}0.0022	^{112}0.0018	^{107}0.0016	^{92}0.0014	^{131}1.022
65	DERMALOG-003	^{24}128	^{51}211	^{269}0.1259	^{268}0.0744	^{266}0.0603	^{265}0.0480	^{264}0.0347	^{268}1.731
66	DERMALOG-004	^{22}128	^{49}208	^{268}0.1251	^{267}0.0739	^{265}0.0598	^{264}0.0475	^{263}0.0343	^{267}1.727
67	DERMALOG-005	^{21}128	^{136}532	^{217}0.0149	^{230}0.0129	^{233}0.0125	^{239}0.0123	^{245}0.0122	^{227}1.118
68	DERMALOG-006	^{34}256	^{134}514	^{183}0.0081	^{200}0.0069	^{203}0.0066	^{211}0.0065	^{219}0.0063	^{198}1.063
69	DERMALOG-007	^{23}128	^{104}413	^{191}0.0092	^{198}0.0066	^{199}0.0060	^{206}0.0057	^{213}0.0054	^{196}1.062
70	DERMALOG-008	^{61}512	^{86}370	^{117}0.0029	^{115}0.0020	^{111}0.0018	^{110}0.0017	^{113}0.0015	^{116}1.019
71	DERMALOG-009	^{55}512	^{82}347	^{115}0.0028	^{135}0.0024	^{144}0.0023	^{148}0.0023	^{156}0.0022	^{129}1.022
72	DIGIDATA-000	^{16}0	^{15}2	^{287}0.5897	^{288}0.5892	^{288}0.5891	^{288}0.5891	^{288}0.5891	^{288}6.303

Table 24: **Rank-based accuracy for the FRVT 2018 mugshot sets**. *In columns 3 and 4 are template size and template generation duration. Thereafter values are rank-based FNIR with T = 0 and FPIR = 1. This is appropriate to investigational uses but not those with higher volumes where candidates from all searches would need review. The next column is a workload statistic, a small value shows an algorithm front-loads mates into the first 10 candidates. Throughout, blue superscripts indicate the rank of the algorithm for that column, and the best value is highlighted in yellow.*

This publication is available free of charge from: https://doi.org/10.6028/NIST.IR.8271

MISSES OUTSIDE RANK R		RESOURCE USAGE		ENROL MOST RECENT, N = 1.6M					
FNIR(N, T=0, R)		TEMPLATE		FRVT 2018 MUGSHOTS					
#	ALGORITHM	BYTES	MSEC	R=1	R=5	R=10	R=20	R=50	WORK-10
73	DILUSENSE-000	^{2}0	^{7}2	^{91}0.0022	^{81}0.0015	^{75}0.0014	^{75}0.0013	^{64}0.0013	^{82}1.015
74	EYEDEA-003	^{99}1036	^{92}385	^{262}0.0800	^{259}0.0451	^{259}0.0362	^{258}0.0289	^{255}0.0211	^{260}1.448
75	F8-001	^{192}2048	^{249}851	^{210}0.0120	^{222}0.0105	^{229}0.0102	^{232}0.0100	^{237}0.0099	^{222}1.096
76	FINCORE-000	^{183}2048	^{124}477	^{201}0.0108	^{186}0.0052	^{182}0.0042	^{180}0.0034	^{173}0.0026	^{187}1.054
77	FUJITSULAB-000	^{95}1032	^{284}950	^{92}0.0022	^{90}0.0016	^{92}0.0015	^{91}0.0015	^{90}0.0014	^{90}1.015
78	FUJITSULAB-001	^{8}0	^{5}1	^{72}0.0019	^{79}0.0015	^{88}0.0015	^{85}0.0014	^{93}0.0014	^{75}1.014
79	GLORY-000	^{49}418	^{32}160	^{273}0.1781	^{275}0.1391	^{275}0.1266	^{275}0.1154	^{275}0.1007	^{274}2.298
80	GLORY-001	^{128}1726	^{99}405	^{270}0.1268	^{270}0.0967	^{270}0.0869	^{271}0.0778	^{272}0.0673	^{270}1.903
81	GORILLA-001	^{247}2156	^{34}169	^{255}0.0603	^{250}0.0304	^{249}0.0230	^{249}0.0174	^{242}0.0117	^{250}1.309
82	GORILLA-002	^{109}1132	^{80}341	^{229}0.0197	^{217}0.0092	^{207}0.0070	^{202}0.0054	^{200}0.0041	^{221}1.096
83	GORILLA-003	^{248}2156	^{147}563	^{242}0.0361	^{235}0.0146	^{230}0.0106	^{224}0.0078	^{212}0.0054	^{237}1.158
84	GORILLA-004	^{249}2192	^{95}395	^{167}0.0063	^{156}0.0032	^{152}0.0026	^{149}0.0023	^{135}0.0018	^{157}1.033
85	GORILLA-005	^{290}6288	^{127}483	^{123}0.0032	^{104}0.0019	^{102}0.0017	^{94}0.0015	^{75}0.0013	^{114}1.018
86	GORILLA-006	^{292}8336	^{219}768	^{60}0.0017	^{43}0.0013	^{41}0.0012	^{42}0.0012	^{43}0.0011	^{48}1.012
87	GORILLA-007	^{4}0	^{16}6	^{57}0.0017	^{39}0.0012	^{39}0.0012	^{35}0.0011	^{39}0.0011	^{40}1.012
88	GRIAULE-000	^{217}2052	^{106}419	^{107}0.0025	^{113}0.0020	^{117}0.0019	^{122}0.0018	^{123}0.0017	^{111}1.018
89	HIK-003	^{116}1408	^{160}633	^{207}0.0117	^{192}0.0060	^{191}0.0048	^{191}0.0039	^{182}0.0030	^{193}1.061
90	HIK-004	^{110}1152	^{132}510	^{204}0.0113	^{191}0.0059	^{190}0.0047	^{184}0.0037	^{179}0.0030	^{192}1.060
91	HIK-005	^{117}1408	^{157}619	^{148}0.0046	^{139}0.0025	^{127}0.0020	^{113}0.0017	^{108}0.0015	^{140}1.025
92	HIK-006	^{115}1408	^{153}610	^{147}0.0046	^{140}0.0025	^{128}0.0020	^{112}0.0017	^{109}0.0015	^{141}1.025
93	HYPERVERGE-001	^{83}1024	^{248}846	^{32}0.0014	^{46}0.0013	^{56}0.0013	^{62}0.0013	^{77}0.0013	^{44}1.012
94	HYPERVERGE-002	^{3}0	^{4}1	^{29}0.0014	^{47}0.0013	^{55}0.0013	^{61}0.0013	^{70}0.0013	^{43}1.012
95	HZAILU-000	^{17}0	^{6}1	^{90}0.0022	^{88}0.0016	^{93}0.0015	^{96}0.0015	^{102}0.0014	^{88}1.015
96	IDEMIA-003	^{70}528	^{181}689	^{173}0.0069	^{177}0.0045	^{177}0.0039	^{179}0.0034	^{176}0.0027	^{174}1.043
97	IDEMIA-004	^{69}528	^{173}669	^{169}0.0066	^{166}0.0038	^{162}0.0032	^{161}0.0027	^{150}0.0021	^{164}1.038
98	IDEMIA-005	^{47}352	^{87}374	^{182}0.0081	^{175}0.0044	^{171}0.0036	^{173}0.0032	^{181}0.0030	^{177}1.044
99	IDEMIA-006	^{48}352	^{88}373	^{195}0.0096	^{185}0.0052	^{183}0.0042	^{190}0.0039	^{195}0.0037	^{184}1.052
100	IDEMIA-007	^{80}860	^{231}807	^{108}0.0026	^{86}0.0016	^{76}0.0014	^{60}0.0013	^{55}0.0012	^{91}1.015
101	IDEMIA-008	^{46}300	^{114}451	^{11}0.0011	^{10}0.0009	^{13}0.0009	^{16}0.0009	^{15}0.0009	^{8}1.009
102	IDEMIA-009	^{6}0	^{1}0	^{4}0.0010	^{4}0.0009	^{7}0.0009	^{9}0.0009	^{10}0.0009	^{4}1.008
103	IMAGUS-002	^{50}512	^{24}76	^{276}0.2203	^{274}0.1342	^{273}0.1090	^{272}0.0871	^{270}0.0632	^{275}2.308
104	IMAGUS-003	^{58}512	^{22}57	^{281}0.3559	^{281}0.2491	^{281}0.2132	^{281}0.1791	^{281}0.1397	^{281}3.363
105	IMAGUS-005	^{162}2048	^{228}788	^{76}0.0019	^{87}0.0016	^{85}0.0015	^{83}0.0014	^{88}0.0013	^{83}1.015
106	IMAGUS-006	^{143}2048	^{271}905	^{81}0.0020	^{92}0.0016	^{94}0.0015	^{95}0.0015	^{104}0.0014	^{86}1.015
107	IMAGUS-007	^{152}2048	^{150}590	^{83}0.0020	^{75}0.0015	^{72}0.0014	^{63}0.0013	^{67}0.0013	^{73}1.014
108	IMAGUS-008	^{15}0	^{14}2	^{264}0.0860	^{265}0.0701	^{267}0.0646	^{267}0.0590	^{267}0.0518	^{265}1.648
109	IMPERIAL-000	^{179}2048	^{169}654	^{106}0.0024	^{106}0.0019	^{113}0.0018	^{120}0.0018	^{127}0.0017	^{106}1.018
110	INCODE-000	^{84}1024	^{41}190	^{252}0.0489	^{247}0.0261	^{248}0.0204	^{246}0.0160	^{243}0.0117	^{247}1.262
111	INCODE-001	^{164}2048	^{183}690	^{220}0.0166	^{211}0.0084	^{205}0.0067	^{204}0.0055	^{203}0.0043	^{212}1.086
112	INCODE-002	^{190}2048	^{68}291	^{224}0.0178	^{214}0.0090	^{208}0.0070	^{205}0.0056	^{204}0.0043	^{218}1.092
113	INCODE-003	^{184}2048	^{193}704	^{212}0.0129	^{196}0.0064	^{194}0.0051	^{192}0.0040	^{184}0.0031	^{200}1.066
114	INCODE-004	^{144}2048	^{131}508	^{130}0.0035	^{133}0.0024	^{135}0.0021	^{138}0.0020	^{138}0.0019	^{132}1.023
115	INCODE-005	^{167}2048	^{130}500	^{53}0.0017	^{59}0.0014	^{67}0.0014	^{64}0.0013	^{66}0.0013	^{59}1.013
116	INNOVATRICS-002	^{73}530	^{59}255	^{250}0.0451	^{252}0.0342	^{255}0.0322	^{257}0.0308	^{259}0.0297	^{254}1.321
117	INNOVATRICS-003	^{72}530	^{58}255	^{236}0.0263	^{228}0.0126	^{224}0.0095	^{219}0.0074	^{209}0.0053	^{231}1.129
118	INNOVATRICS-004	^{106}1076	^{101}406	^{211}0.0123	^{195}0.0063	^{192}0.0050	^{193}0.0040	^{187}0.0032	^{199}1.064
119	INNOVATRICS-005	^{75}538	^{245}842	^{104}0.0024	^{100}0.0018	^{103}0.0017	^{105}0.0016	^{103}0.0014	^{100}1.017
120	INNOVATRICS-007	^{74}538	^{227}785	^{56}0.0017	^{65}0.0014	^{60}0.0013	^{57}0.0013	^{63}0.0012	^{62}1.013
121	INTELLIVISION-001	^{12}0	^{12}2	^{243}0.0365	^{245}0.0199	^{241}0.0160	^{240}0.0126	^{236}0.0095	^{243}1.199
122	INTSYSMSU-000	^{202}2048	^{177}675	^{271}0.1457	^{273}0.1320	^{276}0.1272	^{276}0.1225	^{278}0.1163	^{273}2.203
123	IREX-000	^{256}3080	^{293}2379	^{144}0.0044	^{171}0.0043	^{185}0.0043	^{196}0.0043	^{202}0.0043	^{169}1.039
124	ISYSTEMS-002	^{141}2048	^{76}316	^{168}0.0064	^{172}0.0043	^{178}0.0039	^{182}0.0037	^{192}0.0034	^{173}1.041
125	ISYSTEMS-003	^{139}2048	^{251}856	^{156}0.0052	^{167}0.0039	^{172}0.0036	^{181}0.0034	^{188}0.0033	^{163}1.037
126	KAKAO-000	^{228}2052	^{243}840	^{40}0.0015	^{29}0.0011	^{29}0.0011	^{24}0.0010	^{25}0.0010	^{31}1.010
127	KEDACOM-001	^{44}292	^{138}537	^{178}0.0077	^{203}0.0074	^{209}0.0073	^{216}0.0072	^{224}0.0072	^{201}1.067
128	KNERON-000	^{201}2048	^{135}530	^{163}0.0059	^{190}0.0059	^{198}0.0059	^{208}0.0059	^{215}0.0059	^{186}1.053
129	KNERON-001	^{154}2048	^{123}468	^{239}0.0295	^{249}0.0295	^{254}0.0295	^{256}0.0295	^{258}0.0295	^{248}1.266
130	LINE-000	^{200}2048	^{126}482	^{93}0.0022	^{80}0.0015	^{71}0.0014	^{55}0.0013	^{52}0.0012	^{80}1.015
131	LINE-001	^{172}2048	^{274}910	^{16}0.0011	^{19}0.0010	^{22}0.0010	^{21}0.0009	^{20}0.0009	^{18}1.009
132	LOOKMAN-003	^{45}292	^{81}342	^{187}0.0088	^{207}0.0078	^{215}0.0076	^{221}0.0075	^{227}0.0074	^{204}1.071
133	LOOKMAN-004	^{78}548	^{77}325	^{189}0.0091	^{208}0.0079	^{214}0.0076	^{220}0.0075	^{226}0.0073	^{205}1.072
134	LOOKMAN-005	^{77}548	^{133}514	^{181}0.0080	^{205}0.0075	^{212}0.0074	^{218}0.0073	^{225}0.0072	^{202}1.068
135	MANTRA-000	^{212}2052	^{102}412	^{59}0.0017	^{53}0.0013	^{54}0.0013	^{54}0.0012	^{57}0.0012	^{57}1.013
136	MEGVII-001	^{262}4096	^{165}652	^{208}0.0118	^{218}0.0093	^{218}0.0087	^{228}0.0084	^{233}0.0080	^{213}1.086
137	MEGVII-002	^{268}4096	^{171}656	^{209}0.0118	^{219}0.0093	^{220}0.0088	^{227}0.0084	^{232}0.0080	^{214}1.087
138	MICROFOCUS-003	^{38}256	^{64}269	^{289}0.5942	^{287}0.4692	^{287}0.4204	^{287}0.3724	^{287}0.3095	^{287}5.361
139	MICROFOCUS-004	^{30}256	^{65}270	^{286}0.5763	^{286}0.4519	^{286}0.4026	^{286}0.3560	^{286}0.2957	^{286}5.199
140	MICROFOCUS-005	^{35}256	^{63}266	^{282}0.4242	^{282}0.3028	^{282}0.2606	^{282}0.2209	^{283}0.1724	^{282}3.861
141	MICROFOCUS-006	^{37}256	^{62}265	^{283}0.4268	^{283}0.3049	^{283}0.2623	^{284}0.2233	^{284}0.1746	^{283}3.880
142	MICROSOFT-003	^{86}1024	^{98}404	^{50}0.0016	^{18}0.0010	^{8}0.0009	^{3}0.0008	^{2}0.0006	^{21}1.009
143	MICROSOFT-004	^{168}2048	^{225}773	^{42}0.0015	^{9}0.0009	^{1}0.0008	^{1}0.0007	^{1}0.0006	^{19}1.009
144	MICROSOFT-005	^{88}1024	^{174}673	^{73}0.0019	^{12}0.0010	^{6}0.0008	^{2}0.0008	^{3}0.0006	^{25}1.010

Table 25: **Rank-based accuracy for the FRVT 2018 mugshot sets**. *In columns 3 and 4 are template size and template generation duration. Thereafter values are rank-based FNIR with T = 0 and FPIR = 1. This is appropriate to investigational uses but not those with higher volumes where candidates from all searches would need review. The next column is a workload statistic, a small value shows an algorithm front-loads mates into the first 10 candidates. Throughout, blue superscripts indicate the rank of the algorithm for that column, and the best value is highlighted in yellow.*

This publication is available free of charge from: https://doi.org/10.6028/NIST.IR.8271

MISSES OUTSIDE RANK R		RESOURCE USAGE		ENROL MOST RECENT, N = 1.6M					
FNIR(N, T=0, R)		TEMPLATE		FRVT 2018 MUGSHOTS					
#	ALGORITHM	BYTES	MSEC	R=1	R=5	R=10	R=20	R=50	WORK-10
145	MICROSOFT-006	^{90}1024	^{188}695	^{79}0.0020	^{31}0.0011	^{16}0.0010	^{4}0.0008	^{4}0.0007	^{36}1.011
146	NEC-000	^{254}2592	^{25}82	^{221}0.0170	^{213}0.0086	^{204}0.0066	^{201}0.0052	^{197}0.0038	^{215}1.087
147	NEC-001	^{255}2592	^{26}88	^{230}0.0209	^{234}0.0141	^{235}0.0128	^{238}0.0119	^{241}0.0113	^{233}1.135
148	NEC-002	^{126}1616	^{168}653	^{10}0.0010	^{5}0.0009	^{5}0.0008	^{6}0.0008	^{5}0.0008	^{5}1.008
149	NEC-003	^{127}1712	^{184}690	^{30}0.0014	^{42}0.0012	^{44}0.0012	^{52}0.0012	^{54}0.0012	^{38}1.011
150	NEC-004	^{107}1104	^{290}967	^{37}0.0014	^{55}0.0013	^{66}0.0013	^{66}0.0013	^{73}0.0013	^{53}1.012
151	NEC-005	^{108}1104	^{289}964	^{21}0.0012	^{30}0.0011	^{33}0.0011	^{37}0.0011	^{41}0.0011	^{29}1.010
152	NEUROTECHNOLOGY-003	^{137}2048	^{141}547	^{231}0.0225	^{229}0.0126	^{227}0.0100	^{225}0.0078	^{214}0.0057	^{230}1.125
153	NEUROTECHNOLOGY-004	^{193}2048	^{140}543	^{158}0.0056	^{159}0.0036	^{164}0.0032	^{166}0.0029	^{165}0.0025	^{160}1.035
154	NEUROTECHNOLOGY-005	^{31}256	^{103}412	^{142}0.0043	^{149}0.0029	^{153}0.0027	^{153}0.0024	^{159}0.0023	^{150}1.028
155	NEUROTECHNOLOGY-006	^{32}256	^{215}746	^{225}0.0180	^{209}0.0079	^{197}0.0059	^{197}0.0046	^{189}0.0033	^{211}1.083
156	NEUROTECHNOLOGY-007	^{36}256	^{35}169	^{134}0.0039	^{144}0.0027	^{149}0.0025	^{150}0.0023	^{152}0.0022	^{142}1.026
157	NEUROTECHNOLOGY-008	^{66}514	^{230}804	^{89}0.0022	^{76}0.0015	^{80}0.0014	^{81}0.0014	^{82}0.0013	^{79}1.015
158	NEUROTECHNOLOGY-009	^{65}513	^{179}686	^{38}0.0014	^{38}0.0012	^{40}0.0012	^{41}0.0011	^{44}0.0011	^{37}1.011
159	NEUROTECHNOLOGY-010	^{39}256	^{172}663	^{24}0.0012	^{23}0.0011	^{25}0.0010	^{25}0.0010	^{32}0.0010	^{24}1.010
160	NEUROTECHNOLOGY-012	^{10}0	^{2}0	^{8}0.0010	^{16}0.0010	^{19}0.0010	^{19}0.0009	^{23}0.0009	^{11}1.009
161	NEWLAND-002	^{142}2048	^{256}868	^{261}0.0786	^{261}0.0480	^{260}0.0397	^{260}0.0332	^{257}0.0263	^{262}1.468
162	NOBLIS-001	^{196}2048	^{50}211	^{278}0.2492	^{278}0.1772	^{278}0.1542	^{278}0.1339	^{276}0.1112	^{278}2.679
163	NOBLIS-002	^{286}6144	^{137}535	^{274}0.1794	^{271}0.1108	^{271}0.0903	^{270}0.0722	^{269}0.0535	^{271}2.077
164	NOTIONTAG-000	^{246}2120	^{118}461	^{105}0.0024	^{123}0.0021	^{130}0.0021	^{141}0.0020	^{145}0.0019	^{119}1.019
165	NTECHLAB-003	^{259}3484	^{239}831	^{164}0.0062	^{152}0.0029	^{145}0.0023	^{136}0.0019	^{119}0.0016	^{155}1.030
166	NTECHLAB-004	^{260}3484	^{278}929	^{151}0.0048	^{130}0.0023	^{118}0.0019	^{109}0.0016	^{85}0.0013	^{138}1.024
167	NTECHLAB-005	^{131}1940	^{204}717	^{149}0.0047	^{125}0.0022	^{106}0.0017	^{70}0.0013	^{38}0.0011	^{133}1.023
168	NTECHLAB-006	^{132}1940	^{244}841	^{139}0.0041	^{105}0.0019	^{86}0.0015	^{48}0.0012	^{19}0.0009	^{120}1.019
169	NTECHLAB-007	^{258}3348	^{242}834	^{110}0.0027	^{93}0.0017	^{78}0.0014	^{74}0.0013	^{58}0.0012	^{95}1.016
170	NTECHLAB-008	^{113}1300	^{145}562	^{58}0.0017	^{37}0.0012	^{38}0.0012	^{38}0.0011	^{36}0.0010	^{41}1.012
171	NTECHLAB-009	^{114}1300	^{269}900	^{26}0.0013	^{25}0.0011	^{24}0.0010	^{23}0.0010	^{24}0.0009	^{27}1.010
172	NTECHLAB-010	^{111}1280	^{261}875	^{15}0.0011	^{22}0.0010	^{23}0.0010	^{26}0.0010	^{34}0.0010	^{20}1.009
173	NTECHLAB-011	^{112}1280	^{254}865	^{9}0.0010	^{7}0.0009	^{11}0.0009	^{13}0.0009	^{13}0.0009	^{7}1.008
174	PANGIAM-000	^{13}0	^{11}2	^{22}0.0012	^{26}0.0011	^{28}0.0011	^{29}0.0010	^{35}0.0010	^{26}1.010
175	PARAVISION-000	^{173}2048	^{113}438	^{226}0.0188	^{239}0.0171	^{245}0.0167	^{248}0.0165	^{253}0.0164	^{236}1.156
176	PARAVISION-001	^{182}2048	^{151}590	^{132}0.0038	^{136}0.0024	^{136}0.0022	^{142}0.0020	^{139}0.0019	^{136}1.023
177	PARAVISION-002	^{195}2048	^{90}377	^{137}0.0040	^{141}0.0025	^{141}0.0022	^{144}0.0021	^{140}0.0019	^{139}1.025
178	PARAVISION-003	^{135}2048	^{210}735	^{122}0.0031	^{124}0.0022	^{129}0.0020	^{131}0.0019	^{131}0.0017	^{124}1.021
179	PARAVISION-004	^{267}4096	^{207}720	^{51}0.0016	^{61}0.0014	^{63}0.0013	^{72}0.0013	^{79}0.0013	^{61}1.013
180	PARAVISION-005	^{274}4096	^{252}858	^{46}0.0015	^{58}0.0014	^{64}0.0013	^{73}0.0013	^{83}0.0013	^{56}1.013
181	PARAVISION-007	^{266}4096	^{194}706	^{18}0.0012	^{27}0.0011	^{27}0.0010	^{28}0.0010	^{30}0.0010	^{23}1.010
182	PARAVISION-009	^{276}4100	^{161}638	^{7}0.0010	^{13}0.0010	^{17}0.0010	^{22}0.0009	^{21}0.0009	^{9}1.009
183	PIXELALL-002	^{251}2560	^{43}198	^{146}0.0045	^{150}0.0029	^{150}0.0025	^{147}0.0022	^{144}0.0019	^{151}1.028
184	PIXELALL-003	^{252}2560	^{206}719	^{87}0.0021	^{89}0.0016	^{91}0.0015	^{90}0.0014	^{100}0.0014	^{89}1.015
185	PIXELALL-004	^{250}2560	^{115}453	^{84}0.0020	^{78}0.0015	^{82}0.0015	^{87}0.0014	^{89}0.0013	^{77}1.014
186	PIXELALL-005	^{253}2560	^{247}845	^{74}0.0019	^{94}0.0017	^{97}0.0016	^{108}0.0016	^{118}0.0016	^{87}1.015
187	PTAKURATSATU-000	^{76}538	^{275}910	^{120}0.0030	^{122}0.0021	^{123}0.0019	^{118}0.0018	^{120}0.0016	^{122}1.020
188	QNAP-000	^{199}2048	^{116}457	^{179}0.0078	^{173}0.0044	^{174}0.0037	^{175}0.0033	^{177}0.0028	^{175}1.043
189	QNAP-001	^{150}2048	^{154}615	^{140}0.0041	^{151}0.0029	^{154}0.0027	^{156}0.0025	^{162}0.0023	^{148}1.028
190	QNAP-002	^{7}0	^{10}2	^{152}0.0049	^{174}0.0044	^{186}0.0043	^{195}0.0043	^{201}0.0042	^{171}1.040
191	QUANTASOFT-001	^{192}2048	^{96}396	^{275}0.2177	^{277}0.1643	^{277}0.1468	^{277}0.1312	^{277}0.1116	^{277}2.539
192	RANKONE-002	^{27}133	^{29}113	^{228}0.0194	^{223}0.0112	^{222}0.0093	^{223}0.0077	^{217}0.0060	^{223}1.111
193	RANKONE-003	^{26}133	^{30}114	^{227}0.0194	^{224}0.0112	^{223}0.0093	^{222}0.0077	^{218}0.0060	^{224}1.111
194	RANKONE-004	^{18}85	^{21}36	^{249}0.0415	^{246}0.0226	^{246}0.0177	^{242}0.0141	^{239}0.0102	^{246}1.225
195	RANKONE-005	^{25}133	^{27}94	^{193}0.0094	^{188}0.0054	^{188}0.0046	^{189}0.0039	^{186}0.0032	^{188}1.054
196	RANKONE-006	^{29}165	^{60}261	^{154}0.0050	^{155}0.0030	^{155}0.0027	^{151}0.0024	^{148}0.0021	^{154}1.030
197	RANKONE-007	^{28}165	^{67}278	^{126}0.0034	^{131}0.0023	^{132}0.0021	^{127}0.0018	^{124}0.0017	^{128}1.022
198	RANKONE-009	^{40}260	^{43}191	^{100}0.0024	^{91}0.0016	^{95}0.0015	^{97}0.0015	^{96}0.0014	^{92}1.015
199	RANKONE-010	^{41}261	^{46}200	^{94}0.0022	^{98}0.0018	^{99}0.0016	^{103}0.0015	^{106}0.0015	^{97}1.016
200	RANKONE-011	^{42}261	^{148}567	^{43}0.0015	^{41}0.0012	^{43}0.0012	^{46}0.0012	^{50}0.0012	^{39}1.011
201	RANKONE-012	^{43}261	^{146}563	^{31}0.0014	^{35}0.0012	^{36}0.0011	^{40}0.0011	^{47}0.0011	^{33}1.011
202	REALNETWORKS-000	^{277}4100	^{55}244	^{248}0.0402	^{243}0.0195	^{239}0.0149	^{236}0.0111	^{230}0.0077	^{244}1.201
203	REALNETWORKS-001	^{282}4104	^{54}243	^{247}0.0402	^{244}0.0195	^{240}0.0149	^{235}0.0111	^{231}0.0077	^{245}1.201
204	REALNETWORKS-002	^{281}4104	^{56}245	^{244}0.0393	^{242}0.0189	^{238}0.0142	^{234}0.0108	^{229}0.0076	^{242}1.195
205	REALNETWORKS-003	^{130}1848	^{37}178	^{234}0.0242	^{226}0.0117	^{221}0.0090	^{215}0.0070	^{210}0.0054	^{228}1.120
206	REALNETWORKS-004	^{129}1848	^{39}185	^{232}0.0236	^{225}0.0112	^{219}0.0087	^{213}0.0068	^{207}0.0050	^{225}1.116
207	REALNETWORKS-005	^{230}2056	^{78}337	^{96}0.0023	^{82}0.0016	^{73}0.0014	^{77}0.0013	^{59}0.0012	^{84}1.015
208	REALNETWORKS-006	^{233}2056	^{83}350	^{33}0.0014	^{36}0.0012	^{35}0.0011	^{32}0.0011	^{29}0.0010	^{34}1.011
209	REALNETWORKS-007	^{5}0	^{9}2	^{28}0.0013	^{33}0.0012	^{31}0.0011	^{30}0.0011	^{26}0.0010	^{32}1.011
210	REMARKAI-000	^{136}2048	^{185}691	^{128}0.0034	^{121}0.0021	^{116}0.0019	^{111}0.0017	^{117}0.0015	^{123}1.020
211	REMARKAI-000	^{174}2048	^{155}615	^{186}0.0086	^{176}0.0044	^{167}0.0036	^{169}0.0031	^{166}0.0025	^{178}1.045
212	REMARKAI-002	^{161}2048	^{112}434	^{184}0.0081	^{168}0.0040	^{159}0.0031	^{157}0.0026	^{147}0.0021	^{172}1.041
213	RENDIP-000	^{176}2048	^{267}894	^{47}0.0015	^{50}0.0013	^{47}0.0012	^{51}0.0012	^{56}0.0012	^{49}1.012
214	REVEALMEDIA-000	^{214}2052	^{93}385	^{71}0.0019	^{52}0.0013	^{57}0.0013	^{58}0.0013	^{62}0.0012	^{60}1.013
215	S1-000	^{273}4096	^{255}865	^{102}0.0024	^{96}0.0018	^{100}0.0017	^{106}0.0016	^{112}0.0015	^{99}1.017
216	S1-001	^{198}2048	^{232}814	^{121}0.0031	^{138}0.0025	^{148}0.0024	^{152}0.0024	^{161}0.0023	^{134}1.023

Table 26: **Rank-based accuracy for the FRVT 2018 mugshot sets**. *In columns 3 and 4 are template size and template generation duration. Thereafter values are rank-based FNIR with T = 0 and FPIR = 1. This is appropriate to investigational uses but not those with higher volumes where candidates from all searches would need review. The next column is a workload statistic, a small value shows an algorithm front-loads mates into the first 10 candidates. Throughout, blue superscripts indicate the rank of the algorithm for that column, and the best value is highlighted in yellow.*

This publication is available free of charge from: https://doi.org/10.6028/NIST.IR.8271

MISSES OUTSIDE RANK R		RESOURCE USAGE		ENROL MOST RECENT, N = 1.6M					
FNIR(N, T=0, R)		TEMPLATE		FRVT 2018 MUGSHOTS					
#	ALGORITHM	BYTES	MSEC	R=1	R=5	R=10	R=20	R=50	WORK-10
217	S1-002	^{1}0	^{8}2	^{36}0.0014	^{54}0.0013	^{61}0.0013	^{71}0.0013	^{84}0.0013	^{51}1.012
218	SCANOVATE-000	^{155}2048	^{199}712	^{153}0.0050	^{143}0.0026	^{138}0.0022	^{125}0.0018	^{116}0.0015	^{145}1.026
219	SCANOVATE-001	^{185}2048	^{176}675	^{157}0.0053	^{145}0.0027	^{142}0.0022	^{128}0.0018	^{114}0.0015	^{149}1.028
220	SENSETIME-000	^{229}4104	^{202}715	^{98}0.0023	^{117}0.0020	^{121}0.0019	^{123}0.0018	^{130}0.0017	^{112}1.018
221	SENSETIME-001	^{278}4104	^{170}656	^{99}0.0023	^{114}0.0020	^{119}0.0019	^{115}0.0017	^{121}0.0016	^{109}1.018
222	SENSETIME-002	^{234}2056	^{164}650	^{215}0.0137	^{232}0.0136	^{237}0.0136	^{241}0.0136	^{247}0.0136	^{229}1.122
223	SENSETIME-003	^{231}2056	^{282}940	^{6}0.0010	^{15}0.0010	^{18}0.0010	^{20}0.0009	^{22}0.0009	^{10}1.009
224	SENSETIME-004	^{97}1032	^{198}710	^{5}0.0010	^{6}0.0009	^{9}0.0009	^{10}0.0009	^{9}0.0009	^{6}1.008
225	SENSETIME-005	^{96}1032	^{292}1007	^{3}0.0009	^{2}0.0008	^{2}0.0008	^{5}0.0008	^{6}0.0008	^{2}1.008
226	SENSETIME-006	^{92}1032	^{286}956	^{2}0.0009	^{3}0.0008	^{4}0.0008	^{8}0.0008	^{8}0.0008	^{3}1.008
227	SENSETIME-007	^{93}1032	^{287}958	^{1}0.0008	^{1}0.0008	^{3}0.0008	^{7}0.0008	^{7}0.0008	^{1}1.007
228	SHAMAN-003	^{191}2048	^{192}704	^{266}0.1243	^{269}0.0823	^{269}0.0708	^{268}0.0616	^{268}0.0518	^{269}1.789
229	SHAMAN-004	^{166}2048	^{163}642	^{277}0.2221	^{276}0.1473	^{274}0.1241	^{274}0.1049	^{273}0.0825	^{276}2.411
230	SHAMAN-006	^{206}2048	^{195}706	^{246}0.0398	^{254}0.0344	^{257}0.0332	^{259}0.0323	^{262}0.0315	^{253}1.316
231	SHAMAN-007	^{156}2048	^{197}709	^{245}0.0396	^{253}0.0342	^{256}0.0331	^{258}0.0322	^{261}0.0314	^{251}1.315
232	SIAT-001	^{226}2052	^{246}842	^{65}0.0018	^{63}0.0014	^{52}0.0013	^{47}0.0012	^{45}0.0011	^{63}1.013
233	SIAT-002	^{211}2052	^{272}906	^{67}0.0018	^{62}0.0014	^{65}0.0013	^{65}0.0013	^{60}0.0012	^{66}1.013
234	SMILART-004	^{60}512	^{33}167	^{290}0.9648	^{290}0.9641	^{290}0.9640	^{290}0.9639	^{291}0.9638	^{290}9.678
235	SMILART-005	^{160}2048	^{122}464						^{293}10.000
236	SQISOFT-001	^{235}2056	^{117}460	^{141}0.0042	^{69}0.0014	^{49}0.0013	^{43}0.0012	^{37}0.0010	^{96}1.016
237	STAQU-000	^{271}4096	^{237}827	^{175}0.0071	^{193}0.0060	^{195}0.0057	^{203}0.0055	^{208}0.0053	^{190}1.056
238	SYNESIS-003	^{272}4096	^{28}103	^{272}0.1700	^{272}0.1172	^{272}0.1047	^{273}0.0953	^{274}0.0869	^{272}2.120
239	SYNESIS-003	^{203}2048	^{52}215	^{219}0.0162	^{236}0.0160	^{242}0.0160	^{247}0.0160	^{252}0.0160	^{235}1.144
240	SYNESIS-005	^{280}4104	^{221}772	^{185}0.0085	^{212}0.0085	^{217}0.0085	^{229}0.0085	^{235}0.0085	^{209}1.076
241	TECH5-001	^{118}1536	^{268}898	^{136}0.0040	^{134}0.0024	^{134}0.0021	^{129}0.0018	^{126}0.0017	^{137}1.024
242	TECH5-002	^{64}513	^{283}941	^{111}0.0027	^{68}0.0014	^{46}0.0012	^{39}0.0011	^{28}0.0010	^{76}1.014
243	TEVIAN-003	^{175}2048	^{74}300	^{216}0.0147	^{204}0.0074	^{196}0.0059	^{198}0.0047	^{196}0.0037	^{208}1.075
244	TEVIAN-004	^{165}2048	^{72}299	^{203}0.0113	^{189}0.0057	^{189}0.0047	^{185}0.0037	^{180}0.0030	^{191}1.058
245	TEVIAN-005	^{153}2048	^{105}416	^{176}0.0073	^{165}0.0038	^{160}0.0031	^{160}0.0027	^{158}0.0023	^{167}1.038
246	TEVIAN-006	^{98}1032	^{152}599	^{103}0.0024	^{101}0.0018	^{108}0.0018	^{114}0.0017	^{122}0.0017	^{101}1.017
247	TEVIAN-007	^{94}1032	^{225}779	^{63}0.0018	^{56}0.0014	^{62}0.0013	^{68}0.0013	^{69}0.0013	^{58}1.013
248	TIGER-000	^{220}2052	^{108}428	^{256}0.0616	^{251}0.0310	^{250}0.0236	^{250}0.0178	^{244}0.0120	^{252}1.315
249	TIGER-002	^{215}2052	^{121}464	^{159}0.0056	^{153}0.0029	^{147}0.0024	^{130}0.0019	^{110}0.0015	^{152}1.030
250	TIGER-003	^{209}2052	^{120}464	^{160}0.0056	^{154}0.0029	^{146}0.0024	^{132}0.0019	^{111}0.0015	^{153}1.030
251	TONGYITRANS-000	^{242}2070	^{42}190	^{171}0.0069	^{163}0.0038	^{165}0.0032	^{164}0.0029	^{169}0.0026	^{165}1.038
252	TONGYITRANS-001	^{240}2070	^{40}189	^{172}0.0069	^{164}0.0038	^{163}0.0032	^{165}0.0029	^{170}0.0026	^{166}1.038
253	TOSHIBA-000	^{125}1548	^{279}930	^{145}0.0045	^{142}0.0026	^{140}0.0022	^{139}0.0020	^{139}0.0018	^{143}1.026
254	TOSHIBA-001	^{237}2060	^{280}931	^{150}0.0048	^{146}0.0027	^{143}0.0023	^{143}0.0020	^{136}0.0018	^{147}1.027
255	TRUEFACE-000	^{133}2000	^{84}365	^{125}0.0033	^{148}0.0028	^{157}0.0028	^{159}0.0026	^{168}0.0026	^{144}1.026
256	VD-000	^{91}1028	^{79}337	^{285}0.4737	^{284}0.3204	^{284}0.2695	^{283}0.2215	^{282}0.1678	^{284}4.058
257	VD-001	^{218}2052	^{187}695	^{238}0.0276	^{241}0.0181	^{244}0.0162	^{243}0.0146	^{246}0.0130	^{241}1.174
258	VD-002	^{223}2052	^{182}689	^{194}0.0095	^{206}0.0077	^{210}0.0073	^{214}0.0070	^{223}0.0068	^{203}1.071
259	VD-003	^{210}2052	^{186}693	^{177}0.0076	^{199}0.0069	^{206}0.0067	^{212}0.0066	^{221}0.0066	^{197}1.063
260	VERIDAS-001	^{189}2048	^{263}885	^{114}0.0028	^{110}0.0019	^{105}0.0017	^{104}0.0015	^{107}0.0015	^{110}1.018
261	VERIDAS-002	^{186}2048	^{264}888	^{113}0.0028	^{109}0.0019	^{101}0.0017	^{101}0.0015	^{105}0.0015	^{108}1.018
262	VERIDAS-003	^{138}2048	^{262}877	^{66}0.0018	^{73}0.0015	^{74}0.0014	^{76}0.0013	^{78}0.0013	^{70}1.014
263	VIGILANTSOLUTIONS-003	^{120}1544	^{240}832	^{259}0.0694	^{256}0.0349	^{251}0.0262	^{251}0.0201	^{248}0.0140	^{256}1.355
264	VIGILANTSOLUTIONS-004	^{122}1544	^{238}830	^{267}0.1249	^{266}0.0706	^{264}0.0557	^{262}0.0434	^{260}0.0305	^{266}1.699
265	VIGILANTSOLUTIONS-005	^{121}1544	^{224}778	^{190}0.0092	^{178}0.0045	^{168}0.0036	^{163}0.0029	^{153}0.0022	^{179}1.046
266	VIGILANTSOLUTIONS-006	^{119}1544	^{241}834	^{196}0.0099	^{180}0.0048	^{176}0.0038	^{168}0.0030	^{157}0.0022	^{182}1.049
267	VIGILANTSOLUTIONS-007	^{123}1544	^{156}618	^{127}0.0034	^{112}0.0020	^{104}0.0017	^{100}0.0015	^{81}0.0013	^{118}1.019
268	VIGILANTSOLUTIONS-008	^{124}1544	^{100}405	^{119}0.0029	^{103}0.0018	^{96}0.0016	^{93}0.0015	^{71}0.0013	^{107}1.018
269	VISIONBOX-000	^{236}2059	^{125}482	^{75}0.0019	^{77}0.0015	^{81}0.0014	^{78}0.0013	^{68}0.0013	^{74}1.014
270	VISIONLABS-004	^{33}256	^{75}315	^{112}0.0027	^{99}0.0018	^{98}0.0016	^{99}0.0015	^{94}0.0014	^{103}1.017
271	VISIONLABS-005	^{51}512	^{73}300	^{101}0.0024	^{95}0.0017	^{89}0.0015	^{82}0.0014	^{76}0.0013	^{94}1.016
272	VISIONLABS-006	^{56}512	^{69}292	^{68}0.0018	^{71}0.0015	^{68}0.0014	^{69}0.0013	^{72}0.0013	^{69}1.014
273	VISIONLABS-007	^{53}512	^{70}293	^{62}0.0018	^{66}0.0014	^{58}0.0013	^{56}0.0013	^{61}0.0012	^{65}1.013
274	VISIONLABS-008	^{59}512	^{66}277	^{82}0.0020	^{102}0.0018	^{110}0.0018	^{117}0.0018	^{129}0.0017	^{98}1.017
275	VISIONLABS-009	^{52}512	^{129}494	^{17}0.0011	^{24}0.0011	^{26}0.0010	^{27}0.0010	^{27}0.0010	^{22}1.010
276	VISIONLABS-010	^{62}512	^{209}732	^{34}0.0014	^{48}0.0013	^{53}0.0013	^{59}0.0013	^{65}0.0013	^{47}1.012
277	VISIONLABS-011	^{57}512	^{211}736	^{20}0.0012	^{28}0.0011	^{34}0.0011	^{33}0.0011	^{40}0.0011	^{28}1.010
278	VNPT-001	^{11}0	^{13}2	^{88}0.0022	^{107}0.0019	^{114}0.0018	^{124}0.0018	^{134}0.0018	^{104}1.017
279	VOCORD-003	^{81}896	^{201}714	^{165}0.0062	^{158}0.0035	^{158}0.0030	^{158}0.0026	^{160}0.0023	^{159}1.035
280	VOCORD-004	^{82}896	^{139}538	^{180}0.0079	^{182}0.0049	^{184}0.0043	^{188}0.0038	^{190}0.0034	^{180}1.048
281	VOCORD-005	^{79}768	^{234}822	^{174}0.0070	^{179}0.0046	^{181}0.0041	^{187}0.0038	^{193}0.0035	^{176}1.044
282	VOCORD-006	^{293}10240	^{235}825	^{293}1.0000	^{292}1.0000	^{292}1.0000	^{292}1.0000	^{292}1.0000	^{292}10.000
283	VTS-000	^{163}2048	^{128}492	^{288}0.5937	^{289}0.5936	^{289}0.5936	^{289}0.5936	^{289}0.5936	^{289}6.343
284	VTS-001	^{147}2048	^{265}891	^{45}0.0015	^{34}0.0012	^{30}0.0011	^{31}0.0011	^{31}0.0010	^{35}1.011
285	VTS-002	^{178}2048	^{270}903	^{77}0.0019	^{64}0.0014	^{51}0.0013	^{53}0.0012	^{46}0.0011	^{68}1.013
286	XFORWARDAI-000	^{145}2048	^{218}768	^{95}0.0023	^{118}0.0020	^{125}0.0020	^{137}0.0019	^{143}0.0019	^{113}1.018
287	XFORWARDAI-001	^{148}2048	^{178}681	^{85}0.0020	^{111}0.0019	^{122}0.0019	^{134}0.0019	^{142}0.0019	^{105}1.018
288	XFORWARDAI-002	^{270}4096	^{281}935	^{78}0.0020	^{108}0.0019	^{120}0.0019	^{133}0.0019	^{141}0.0019	^{102}1.017

Table 27: **Rank-based accuracy for the FRVT 2018 mugshot sets**. *In columns 3 and 4 are template size and template generation duration. Thereafter values are rank-based FNIR with T = 0 and FPIR = 1. This is appropriate to investigational uses but not those with higher volumes where candidates from all searches would need review. The next column is a workload statistic, a small value shows an algorithm front-loads mates into the first 10 candidates. Throughout, blue superscripts indicate the rank of the algorithm for that column, and the best value is highlighted in yellow.*

This publication is available free of charge from: https://doi.org/10.6028/NIST.IR.8271

This publication is available free of charge from: https://doi.org/10.6028/NIST.IR.8271

MISSES OUTSIDE RANK R		RESOURCE USAGE		ENROL MOST RECENT, N = 1.6M					
FNIR(N, T=0, R)		TEMPLATE		FRVT 2018 MUGSHOTS					
#	ALGORITHM	BYTES	MSEC	R=1	R=5	R=10	R=20	R=50	WORK-10
289	YISHENG-001	^{261}3704	^{94}387	^{237}0.0265	^{231}0.0130	^{228}0.0102	^{226}0.0080	^{216}0.0059	^{232}1.134
290	YITU-002	^{284}4138	^{258}870	^{69}0.0018	^{40}0.0012	^{37}0.0011	^{34}0.0011	^{33}0.0010	^{46}1.012
291	YITU-003	^{283}4138	^{259}871	^{118}0.0029	^{129}0.0023	^{139}0.0022	^{146}0.0021	^{151}0.0021	^{126}1.021
292	YITU-004	^{239}2070	^{276}910	^{27}0.0013	^{8}0.0009	^{10}0.0009	^{11}0.0009	^{11}0.0009	^{16}1.009
293	YITU-005	^{241}2070	^{253}861	^{97}0.0023	^{120}0.0021	^{126}0.0020	^{140}0.0020	^{146}0.0020	^{115}1.019

Table 28: **Rank-based accuracy for the FRVT 2018 mugshot sets**. *In columns 3 and 4 are template size and template generation duration. Thereafter values are rank-based FNIR with T = 0 and FPIR = 1. This is appropriate to investigational uses but not those with higher volumes where candidates from all searches would need review. The next column is a workload statistic, a small value shows an algorithm front-loads mates into the first 10 candidates. Throughout, blue superscripts indicate the rank of the algorithm for that column, and the best value is highlighted in yellow.*

This publication is available free of charge from: https://doi.org/10.6028/NIST.IR.8271

MISSES BELOW THRESHOLD, T		ENROL RECENT MUGSHOT, N = 1.6M									ENROL APPLICATION PORTRAIT, N = 1.6M					
		ENROL: MUGSHOT			ENROL: MUGSHOT			ENROL: MUGSHOT			ENROL: VISA		ENROL: BORDER		ENROL: VISA	
		PROBE: MUGSHOT			PROBE: WEBCAM			PROBE: PROFILE			PROBE: BORDER		PROBE: BORDER 10+YR		PROBE: KIOSK	
#	ALGORITHM	FPIR=0.0003	FPIR=0.001	FPIR=0.01	FPIR=0.0003	FPIR=0.001	FPIR=0.01	FPIR=0.0003	FPIR=0.001	FPIR=0.01	FPIR=0.001	FPIR=0.01	FPIR=0.001	FPIR=0.01	FPIR=0.001	FPIR=0.01
1	20FACE-000	^{241}0.462	^{250}0.348	^{257}0.230	^{253}0.763	^{246}0.450	^{246}0.301	^{210}1.000	^{211}1.000	^{226}1.000	^{182}0.424	^{182}0.255	^{101}0.772	^{105}0.599	^{178}0.938	^{189}0.836
2	3DIVI-003	^{243}0.482	^{259}0.400	^{263}0.282	^{248}0.685	^{260}0.626	^{262}0.497				^{194}0.605	^{194}0.445			^{159}0.821	^{178}0.717
3	3DIVI-004	^{214}0.256	^{230}0.169	^{234}0.093	^{218}0.400	^{236}0.343	^{240}0.237				^{172}0.277	^{176}0.172			^{137}0.607	^{159}0.485
4	3DIVI-005	^{213}0.255	^{227}0.166	^{233}0.093	^{217}0.395	^{234}0.339	^{239}0.234	^{143}0.998	^{148}0.996	^{160}0.990	^{200}0.864	^{202}0.846			^{136}0.597	^{158}0.484
5	3DIVI-006	^{212}0.253	^{229}0.168	^{236}0.096	^{221}0.403	^{235}0.342	^{241}0.238				^{173}0.283	^{177}0.174			^{140}0.615	^{160}0.490
6	ACER-000	^{198}0.208	^{220}0.146	^{223}0.074	^{202}0.300	^{213}0.246	^{215}0.157	^{92}0.987	^{101}0.981	^{125}0.955	^{167}0.201	^{172}0.114			^{123}0.490	^{144}0.363
7	ACER-001	^{144}0.109	^{162}0.056	^{166}0.026	^{138}0.136	^{145}0.109	^{148}0.069	^{171}1.000	^{182}0.999	^{205}0.998	^{130}0.068	^{129}0.036	^{90}0.406	^{95}0.250	^{122}0.479	^{98}0.206
8	AIZE-001	^{155}0.127	^{182}0.077	^{180}0.034	^{168}0.187	^{172}0.143	^{171}0.087	^{116}0.995	^{127}0.994	^{150}0.983	^{143}0.101	^{144}0.052	^{84}0.364	^{90}0.216	^{104}0.387	^{128}0.289
9	ALCHERA-000	^{205}0.231	^{217}0.138	^{218}0.070	^{191}0.259	^{199}0.216	^{209}0.146	^{153}0.999	^{164}0.999	^{188}0.996	^{162}0.176	^{170}0.111			^{155}0.803	^{154}0.456
10	ALCHERA-001	^{288}1.000	^{288}0.999	^{290}0.999	^{282}1.000	^{288}1.000	^{291}1.000				^{230}1.000	^{269}1.000			^{224}1.000	^{249}1.000
11	ALCHERA-002	^{266}0.807	^{266}0.486	^{266}0.302	^{247}0.685	^{257}0.591	^{257}0.442	^{190}1.000	^{190}1.000	^{210}0.999	^{199}0.827	^{199}0.770			^{156}0.811	^{175}0.705
12	ALCHERA-003	^{237}0.450	^{221}0.155	^{219}0.070	^{203}0.304	^{210}0.239	^{214}0.152	^{184}1.000	^{175}0.999	^{193}0.997	^{161}0.172	^{163}0.097			^{118}0.464	^{143}0.362
13	ALCHERA-004	^{248}0.520	^{258}0.394	^{256}0.211	^{244}0.642	^{252}0.529	^{251}0.327	^{117}0.995	^{121}0.991	^{87}0.813	^{183}0.424	^{180}0.232	^{97}0.708	^{100}0.515	^{133}0.546	^{152}0.398
14	ALLGOVISION-000	^{164}0.138	^{194}0.088	^{200}0.045	^{179}0.202	^{188}0.166	^{195}0.106	^{103}0.993	^{118}0.990	^{149}0.982	^{146}0.117	^{151}0.066			^{130}0.526	^{151}0.396
15	ALLGOVISION-001	^{173}0.155	^{200}0.102	^{206}0.053	^{196}0.275	^{203}0.221	^{208}0.141	^{107}0.993	^{108}0.986	^{108}0.933	^{156}0.150	^{159}0.081			^{124}0.491	^{150}0.389
16	ANKE-000	^{184}0.184	^{204}0.117	^{215}0.063	^{190}0.256	^{202}0.220	^{212}0.151	^{113}0.995	^{126}0.994	^{158}0.990	^{262}1.000	^{243}1.000			^{249}1.000	^{260}1.000
17	ANKE-001	^{182}0.183	^{208}0.119	^{216}0.063	^{189}0.256	^{201}0.220	^{213}0.151	^{119}0.995	^{133}0.994	^{169}0.992	^{259}1.000	^{239}1.000			^{254}1.000	^{265}1.000
18	ANKE-002	^{108}0.062	^{123}0.032	^{122}0.014	^{104}0.103	^{110}0.079	^{112}0.050	^{71}0.975	^{72}0.948	^{83}0.795	^{91}0.034	^{94}0.018			^{71}0.245	^{92}0.190
19	AWARE-003	^{181}0.174	^{212}0.128	^{226}0.082	^{213}0.351	^{228}0.298	^{233}0.204	^{89}0.987	^{105}0.984	^{144}0.977	^{184}0.428	^{188}0.378			^{131}0.530	^{153}0.443
20	AWARE-004	^{229}0.355	^{243}0.269	^{252}0.175	^{240}0.619	^{251}0.509	^{255}0.375	^{187}1.000	^{191}1.000	^{212}0.999	^{179}0.397	^{184}0.279			^{157}0.816	^{170}0.631
21	AWARE-005	^{254}0.608	^{253}0.364	^{228}0.085	^{208}0.342	^{215}0.253	^{217}0.163	^{182}1.000	^{197}1.000	^{213}0.999	^{171}0.255	^{174}0.122			^{172}0.916	^{177}0.714
22	AWARE-006	^{242}0.475	^{244}0.276	^{253}0.175	^{230}0.466	^{239}0.398	^{244}0.283	^{168}1.000	^{185}0.999	^{206}0.999	^{177}0.368	^{181}0.254			^{149}0.749	^{167}0.623
23	AYONIX-000	^{269}0.846	^{276}0.811	^{282}0.724	^{266}0.956	^{276}0.939	^{278}0.892	^{144}0.998	^{154}0.998	^{185}0.995	^{204}0.954	^{204}0.891			^{186}0.982	^{196}0.959
24	AYONIX-001	^{270}0.875	^{278}0.824	^{280}0.701	^{261}0.946	^{271}0.920	^{274}0.845	^{179}1.000	^{183}0.999	^{190}0.996	^{208}0.999	^{208}0.998			^{182}0.969	^{192}0.926
25	AYONIX-002	^{271}0.876	^{277}0.824	^{281}0.702	^{262}0.946	^{272}0.920	^{273}0.845	^{180}1.000	^{181}0.999	^{189}0.996	^{201}0.915	^{200}0.821			^{183}0.969	^{193}0.926
26	CAMVI-003	^{133}0.094	^{177}0.071	^{211}0.058	^{148}0.152	^{164}0.132	^{196}0.108	^{77}0.979	^{83}0.970	^{114}0.940	^{145}0.114	^{164}0.100			^{107}0.402	^{147}0.377
27	CAMVI-004	^{142}0.107	^{178}0.072	^{209}0.054	^{186}0.240	^{166}0.136	^{185}0.100	^{169}1.000	^{179}0.999	^{196}0.998	^{142}0.100	^{158}0.081			^{153}0.787	^{161}0.507
28	CAMVI-005	^{165}0.139	^{198}0.099	^{225}0.076	^{227}0.451	^{195}0.179	^{203}0.132	^{176}1.000	^{188}1.000	^{203}0.998	^{157}0.156	^{171}0.112			^{194}0.999	^{202}0.983
29	CANON-001	^{27}0.012	^{33}0.005	^{33}0.002	^{23}0.031	^{23}0.023	^{23}0.015	^{26}0.633	^{17}0.365	^{26}0.217	^{21}0.008	^{23}0.004	^{24}0.068	^{27}0.034	^{30}0.139	^{21}0.092
30	CANON-002	^{19}0.010	^{27}0.005	^{27}0.002	^{28}0.034	^{31}0.027	^{38}0.020	^{66}0.956	^{73}0.952	^{118}0.947	^{127}0.064	^{146}0.056	^{94}0.556	^{103}0.542	^{168}0.881	^{191}0.878
31	CIB-000	^{78}0.044	^{59}0.012	^{54}0.005	^{75}0.077	^{57}0.045	^{53}0.025	^{198}1.000	^{204}1.000	^{222}1.000	^{51}0.017	^{43}0.008	^{43}0.141	^{43}0.068	^{169}0.894	^{162}0.521
32	CLEARVIEWAI-000	^{29}0.013	^{35}0.006	^{31}0.002	^{33}0.036	^{27}0.025	^{27}0.016	^{156}0.999	^{88}0.974	^{14}0.149	^{22}0.008	^{17}0.004	^{19}0.057	^{19}0.027	^{82}0.268	^{12}0.080
33	CLOUDWALK-HR-000	^{8}0.004	^{10}0.002	^{14}0.002	^{8}0.015	^{10}0.013	^{13}0.012	^{2}0.188	^{2}0.133	^{4}0.095	^{11}0.005	^{11}0.003	^{7}0.033	^{10}0.018	^{12}0.099	^{7}0.075
34	CLOUDWALK-MT-000	^{4}0.003	^{9}0.002	^{17}0.002	^{5}0.015	^{9}0.013	^{15}0.012	^{1}0.169	^{1}0.109	^{1}0.077	^{1}0.002	^{3}0.002	^{1}0.018	^{1}0.009	^{1}0.072	^{3}0.063
35	COGENT-000	^{168}0.143	^{153}0.053	^{171}0.029	^{160}0.175	^{169}0.140	^{187}0.100	^{124}0.996	^{139}0.995	^{165}0.991						
36	COGENT-001	^{169}0.143	^{152}0.053	^{172}0.029	^{159}0.175	^{168}0.140	^{189}0.100	^{123}0.996	^{138}0.995	^{166}0.991						
37	COGENT-002	^{178}0.159	^{139}0.044	^{133}0.017	^{124}0.124	^{135}0.098	^{139}0.063	^{148}0.998	^{153}0.998	^{175}0.994						
38	COGENT-003	^{196}0.203	^{144}0.046	^{127}0.016	^{122}0.121	^{129}0.095	^{136}0.061	^{149}0.999	^{155}0.998	^{184}0.995						
39	COGENT-004	^{200}0.209	^{124}0.033	^{64}0.006	^{62}0.067	^{63}0.051	^{66}0.031	^{142}0.998	^{151}0.997	^{186}0.995	^{63}0.022	^{65}0.012	^{39}0.126	^{46}0.072	^{116}0.456	^{83}0.178
40	COGENT-005	^{93}0.050	^{44}0.009	^{46}0.004	^{43}0.050	^{46}0.037	^{48}0.023	^{121}0.996	^{114}0.989	^{33}0.323	^{38}0.011	^{37}0.006	^{29}0.082	^{33}0.043	^{120}0.905	^{94}0.202
41	COGENT-006	^{23}0.010	^{24}0.004	^{24}0.002	^{26}0.033	^{24}0.023	^{24}0.015	^{13}0.383	^{12}0.238	^{11}0.145	^{15}0.006	^{14}0.003	^{91}0.422	^{21}0.028	^{26}0.130	^{40}0.120
42	COGNITEC-000	^{203}0.226	^{225}0.161	^{235}0.095	^{225}0.439	^{229}0.303	^{231}0.200	^{120}0.996	^{122}0.992	^{133}0.971						
43	COGNITEC-001	^{194}0.192	^{199}0.102	^{207}0.053	^{277}0.997	^{207}0.230	^{205}0.135	^{259}1.000	^{232}1.000	^{129}0.965						
44	COGNITEC-002	^{151}0.122	^{155}0.053	^{161}0.025	^{274}0.990	^{194}0.178	^{192}0.101	^{270}1.000	^{203}1.000	^{126}0.956						
45	COGNITEC-003	^{137}0.099	^{151}0.053	^{163}0.025	^{183}0.222	^{186}0.162	^{186}0.100	^{282}1.000	^{206}1.000	^{117}0.946						
46	COGNITEC-004	^{101}0.055	^{122}0.031	^{123}0.014	^{127}0.127	^{133}0.097	^{128}0.058	^{115}0.995	^{115}0.990	^{103}0.919	^{129}0.068	^{130}0.038	^{82}0.316	^{89}0.196	^{84}0.288	^{105}0.218

Table 29: **Threshold-based accuracy**. *Values are FNIR(N, T, L) with N = 1.6 million with thresholds set to produce FPIR = 0.0003, 0.001, and 0.01 in non-mate searches. Throughout blue superscripts indicate the rank of the algorithm for that column. Caution: The Power-low models are mostly intended to draw attention to the kind of behavior, not as a model to be used for prediction.*

This publication is available free of charge from: https://doi.org/10.6028/NIST.IR.8271

MISSES BELOW THRESHOLD, T		ENROL RECENT MUGSHOT, N = 1.6M									ENROL APPLICATION PORTRAIT, N = 1.6M					
		ENROL: MUGSHOT			ENROL: MUGSHOT			ENROL: MUGSHOT			ENROL: VISA		ENROL: BORDER		ENROL: VISA	
		PROBE: MUGSHOT			PROBE: WEBCAM			PROBE: PROFILE			PROBE: BORDER		PROBE: BORDER 10+YR		PROBE: KIOSK	
#	ALGORITHM	FPIR=0.0003	FPIR=0.001	FPIR=0.01	FPIR=0.0003	FPIR=0.001	FPIR=0.01	FPIR=0.0003	FPIR=0.001	FPIR=0.01	FPIR=0.001	FPIR=0.01	FPIR=0.001	FPIR=0.01	FPIR=0.001	FPIR=0.01
47	COGNITEC-005	^{102}0.055	^{46}0.010	^{43}0.004	^{50}0.058	^{53}0.041	^{45}0.022	^{241}1.000	^{280}1.000	^{97}0.878	^{101}0.041	^{116}0.028	^{52}0.157	^{61}0.092	^{52}0.179	^{62}0.145
48	COGNITEC-006	^{56}0.029	^{41}0.008	^{40}0.003	^{56}0.065	^{49}0.040	^{42}0.022	^{250}1.000	^{289}1.000	^{207}0.999	^{79}0.030	^{74}0.013	^{58}0.171	^{54}0.081	^{144}0.681	^{102}0.214
49	CUBOX-000	^{11}0.005	^{16}0.003	^{19}0.002	^{17}0.022	^{17}0.019	^{19}0.014	^{6}0.276	^{4}0.168	^{7}0.104	^{7}0.004	^{8}0.003	^{6}0.028	^{6}0.014	^{2}0.073	^{2}0.062
50	CYBERLINK-000	^{163}0.137	^{163}0.056	^{153}0.023	^{154}0.162	^{149}0.116	^{151}0.070	^{136}0.997	^{142}0.995	^{148}0.981	^{126}0.063	^{124}0.032			^{98}0.339	^{112}0.232
51	CYBERLINK-001	^{134}0.096	^{156}0.054	^{151}0.022	^{141}0.138	^{146}0.109	^{144}0.067	^{134}0.997	^{137}0.995	^{151}0.984	^{123}0.062	^{120}0.031			^{141}0.652	^{114}0.239
52	CYBERLINK-002	^{70}0.038	^{69}0.015	^{69}0.006	^{65}0.068	^{72}0.053	^{71}0.032	^{109}0.994	^{113}0.988	^{127}0.957	^{67}0.024	^{68}0.013			^{85}0.288	^{72}0.157
53	CYBERLINK-003	^{82}0.045	^{42}0.008	^{42}0.004	^{38}0.045	^{43}0.035	^{40}0.021	^{110}0.995	^{86}0.972	^{91}0.845	^{40}0.012	^{41}0.007	^{34}0.100	^{36}0.051	^{101}0.368	^{42}0.120
54	CYBERLINK-004	^{192}0.188	^{39}0.007	^{39}0.003	^{54}0.063	^{44}0.036	^{44}0.022	^{223}1.000	^{217}1.000	^{215}0.999	^{42}0.013	^{40}0.007	^{35}0.109	^{34}0.050	^{181}0.954	^{131}0.291
55	CYBERLINK-005	^{199}0.208	^{50}0.010	^{49}0.004	^{45}0.054	^{50}0.041	^{55}0.026	^{192}1.000	^{195}1.000	^{98}0.888	^{43}0.014	^{42}0.007	^{30}0.089	^{31}0.043	^{177}0.926	^{122}0.266
56	DAHUA-000	^{157}0.128	^{190}0.086	^{197}0.045	^{163}0.179	^{165}0.135	^{169}0.083									
57	DAHUA-001	^{141}0.106	^{180}0.073	^{184}0.037	^{147}0.151	^{157}0.122	^{160}0.075	^{91}0.987	^{98}0.980	^{109}0.933						
58	DAHUA-002	^{50}0.026	^{70}0.015	^{67}0.006	^{51}0.060	^{59}0.046	^{60}0.029	^{31}0.681	^{37}0.638	^{52}0.522	^{48}0.017	^{47}0.008			^{42}0.159	^{46}0.125
59	DAHUA-003	^{48}0.025	^{64}0.014	^{58}0.005	^{44}0.054	^{52}0.041	^{51}0.024	^{27}0.647	^{32}0.579	^{43}0.447	^{41}0.013	^{39}0.006	^{28}0.081	^{32}0.043	^{29}0.134	^{31}0.109
60	DAHUA-004	^{31}0.014	^{38}0.007	^{38}0.003	^{27}0.033	^{29}0.026	^{28}0.016	^{18}0.552	^{26}0.485	^{35}0.345	^{28}0.008	^{26}0.004	^{15}0.051	^{17}0.027	^{22}0.113	^{24}0.094
61	DAON-000	^{161}0.135	^{98}0.023	^{97}0.009	^{79}0.079	^{85}0.061	^{88}0.039	^{191}1.000	^{194}1.000	^{202}0.998	^{68}0.025	^{69}0.013	^{60}0.173	^{60}0.091	^{164}0.846	^{80}0.172
62	DECATUR-000	^{75}0.043	^{101}0.023	^{101}0.010	^{84}0.085	^{91}0.066	^{90}0.040	^{34}0.757	^{42}0.675	^{48}0.509	^{72}0.027	^{78}0.014	^{59}0.173	^{67}0.098	^{69}0.239	^{70}0.156
63	DEEPGLINT-001	^{21}0.010	^{20}0.003	^{20}0.002	^{11}0.018	^{11}0.014	^{8}0.010	^{206}1.000	^{187}1.000	^{47}0.503	^{16}0.006	^{25}0.004			^{41}0.159	^{25}0.097
64	DEEPSEA-001	^{120}0.073	^{143}0.046	^{149}0.022	^{130}0.129	^{138}0.101	^{131}0.059	^{95}0.988	^{106}0.985	^{138}0.973	^{134}0.077	^{135}0.041			^{95}0.326	^{117}0.251
65	DERMALOG-003	^{250}0.550	^{265}0.482	^{269}0.360	^{251}0.715	^{262}0.655	^{266}0.526				^{198}0.677	^{196}0.554			^{166}0.870	^{185}0.791
66	DERMALOG-004	^{252}0.554	^{264}0.480	^{268}0.358	^{250}0.711	^{263}0.657	^{264}0.526	^{128}0.997	^{143}0.995	^{168}0.991	^{193}0.603	^{195}0.458			^{165}0.856	^{181}0.751
67	DERMALOG-005	^{193}0.189	^{193}0.088	^{192}0.043	^{175}0.201	^{179}0.154	^{182}0.096	^{125}0.996	^{117}0.990	^{121}0.950	^{174}0.300	^{183}0.267			^{139}0.614	^{155}0.459
68	DERMALOG-006	^{136}0.098	^{150}0.052	^{165}0.026	^{140}0.137	^{140}0.105	^{143}0.067	^{96}0.989	^{100}0.981	^{110}0.933	^{121}0.059	^{122}0.031			^{94}0.318	^{110}0.230
69	DERMALOG-007	^{190}0.188	^{191}0.086	^{190}0.040	^{174}0.200	^{177}0.152	^{179}0.093	^{126}0.996	^{116}0.990	^{120}0.950	^{141}0.099	^{143}0.052			^{135}0.557	^{135}0.299
70	DERMALOG-008	^{217}0.268	^{141}0.045	^{132}0.017	^{184}0.231	^{126}0.094	^{123}0.054	^{220}1.000	^{218}1.000	^{223}1.000	^{118}0.057	^{111}0.025	^{88}0.382	^{86}0.158	^{179}0.940	^{173}0.678
71	DERMALOG-009	^{74}0.041	^{91}0.021	^{93}0.009	^{86}0.086	^{92}0.066	^{93}0.040	^{193}1.000	^{208}1.000	^{220}1.000	^{81}0.031	^{85}0.016	^{106}0.999	^{108}0.999	^{162}0.840	^{106}0.222
72	DIGIDATA-000	^{255}0.620	^{270}0.610	^{278}0.598	^{238}0.588	^{256}0.577	^{267}0.560	^{158}0.999	^{131}0.994	^{116}0.942	^{196}0.646	^{198}0.643	^{102}0.789	^{106}0.722	^{160}0.824	^{187}0.816
73	DILUSENSE-000	^{96}0.053	^{120}0.030	^{118}0.012	^{100}0.100	^{109}0.078	^{109}0.047	^{45}0.852	^{38}0.655	^{45}0.488	^{98}0.039	^{106}0.022	^{96}0.664	^{93}0.242	^{60}0.203	^{69}0.154
74	EYEDEA-003	^{247}0.509	^{255}0.388	^{261}0.265	^{242}0.625	^{254}0.543	^{256}0.404	^{129}0.997	^{134}0.994	^{157}0.990	^{191}0.570	^{190}0.392			^{154}0.792	^{172}0.658
75	F8-001	^{239}0.458	^{226}0.166	^{181}0.036				^{155}0.999	^{163}0.998	^{187}0.995						
76	FINCORE-000	^{189}0.187	^{216}0.134	^{222}0.071	^{195}0.267	^{200}0.217	^{206}0.140	^{185}1.000	^{200}1.000	^{180}0.995	^{163}0.187	^{169}0.108	^{95}0.598	^{99}0.418	^{117}0.458	^{140}0.349
77	FUJITSULAB-000	^{209}0.246	^{92}0.021	^{89}0.008	^{68}0.070	^{78}0.056	^{81}0.035				^{65}0.024	^{73}0.013	^{61}0.177	^{65}0.093	^{70}0.240	^{71}0.156
78	FUJITSULAB-001	^{258}0.655	^{82}0.018	^{73}0.007	^{111}0.112	^{80}0.058	^{73}0.033	^{122}0.996	^{123}0.992	^{115}0.940	^{66}0.024	^{63}0.011	^{98}0.739	^{98}0.310	^{73}0.247	^{65}0.146
79	GLORY-000	^{236}0.441	^{254}0.367	^{265}0.295	^{237}0.586	^{255}0.547	^{260}0.470	^{112}0.995	^{136}0.995	^{172}0.993	^{186}0.453	^{189}0.381			^{161}0.839	^{186}0.795
80	GLORY-001	^{228}0.355	^{246}0.305	^{258}0.236	^{236}0.582	^{253}0.537	^{258}0.448	^{108}0.994	^{124}0.993	^{162}0.991	^{181}0.408	^{186}0.336			^{158}0.819	^{182}0.753
81	GORILLA-001	^{264}0.747	^{260}0.406	^{259}0.246	^{239}0.590	^{247}0.453	^{249}0.314	^{197}1.000	^{219}1.000	^{238}1.000	^{187}0.468	^{185}0.299			^{231}1.000	^{176}0.710
82	GORILLA-002	^{216}0.266	^{233}0.188	^{240}0.106	^{210}0.342	^{222}0.268	^{223}0.170	^{207}1.000	^{226}1.000	^{173}0.993	^{170}0.250	^{175}0.137			^{198}1.000	^{157}0.466
83	GORILLA-003	^{262}0.694	^{248}0.318	^{250}0.157	^{246}0.684	^{244}0.434	^{242}0.247	^{258}1.000	^{231}1.000	^{228}1.000	^{180}0.407	^{178}0.213			^{283}1.000	^{164}0.562
84	GORILLA-004	^{160}0.135	^{196}0.089	^{193}0.043	^{176}0.202	^{185}0.160	^{190}0.101	^{67}0.972	^{75}0.959	^{100}0.903	^{151}0.135	^{155}0.072			^{113}0.438	^{137}0.309
85	GORILLA-005	^{130}0.086	^{167}0.058	^{167}0.026	^{162}0.179	^{171}0.142	^{173}0.088	^{37}0.770	^{44}0.700	^{56}0.553	^{139}0.088	^{134}0.040			^{92}0.315	^{107}0.223
86	GORILLA-006	^{80}0.046	^{113}0.027	^{108}0.011	^{117}0.118	^{120}0.089	^{119}0.053	^{22}0.602	^{30}0.531	^{37}0.369	^{73}0.028	^{71}0.013	^{56}0.166	^{64}0.093	^{63}0.218	^{68}0.154
87	GORILLA-007	^{83}0.046	^{112}0.027	^{106}0.010	^{101}0.101	^{108}0.077	^{104}0.045	^{25}0.626	^{31}0.534	^{38}0.369	^{69}0.026	^{64}0.012	^{74}0.264	^{70}0.108	^{50}0.178	^{57}0.138
88	GRIAULE-000	^{77}0.044	^{89}0.020	^{91}0.009	^{82}0.082	^{88}0.063	^{87}0.038	^{137}0.997	^{140}0.995	^{122}0.952	^{88}0.033	^{102}0.020	^{65}0.185	^{69}0.107	^{58}0.198	^{76}0.166
89	HIK-003	^{179}0.159	^{201}0.103	^{210}0.057	^{171}0.190	^{181}0.158	^{194}0.105	^{29}0.980	^{81}0.969	^{105}0.925	^{154}0.142	^{157}0.080			^{115}0.445	^{142}0.359
90	HIK-004	^{175}0.156	^{197}0.099	^{208}0.054	^{166}0.182	^{178}0.153	^{191}0.101	^{85}0.983	^{89}0.976	^{119}0.947	^{152}0.137	^{156}0.077			^{112}0.434	^{141}0.353
91	HIK-005	^{139}0.102	^{136}0.044	^{137}0.019	^{96}0.098	^{107}0.077	^{111}0.048	^{174}1.000	^{184}0.999	^{198}0.998	^{128}0.068	^{127}0.036			^{132}0.541	^{119}0.258
92	HIK-006	^{167}0.142	^{145}0.047	^{140}0.020	^{109}0.111	^{117}0.086	^{117}0.052	^{205}1.000	^{225}1.000	^{217}0.999						

Table 30: **Threshold-based accuracy**. *Values are FNIR(N, T, L) with N = 1.6 million with thresholds set to produce FPIR = 0.0003, 0.001, and 0.01 in non-mate searches. Throughout blue superscripts indicate the rank of the algorithm for that column. Caution: The Power-low models are mostly intended to draw attention to the kind of behavior, not as a model to be used for prediction.*

This publication is available free of charge from: https://doi.org/10.6028/NIST.IR.8271

MISSES BELOW THRESHOLD, T		ENROL RECENT MUGSHOT, N = 1.6M									ENROL APPLICATION PORTRAIT, N = 1.6M					
		ENROL: MUGSHOT			ENROL: MUGSHOT			ENROL: MUGSHOT			ENROL: VISA		ENROL: BORDER		ENROL: VISA	
		PROBE: MUGSHOT			PROBE: WEBCAM			PROBE: PROFILE			PROBE: BORDER		PROBE: BORDER 10+YR		PROBE: KIOSK	
#	ALGORITHM	FPIR=0.0003	FPIR=0.001	FPIR=0.01	FPIR=0.0003	FPIR=0.001	FPIR=0.01	FPIR=0.0003	FPIR=0.001	FPIR=0.01	FPIR=0.001	FPIR=0.01	FPIR=0.001	FPIR=0.01	FPIR=0.001	FPIR=0.01
93	HYPERVERGE-001	^{18}0.009	^{25}0.004	^{28}0.002	^{34}0.039	^{39}0.031	^{39}0.020	^{5}0.275	^{9}0.220	^{12}0.146	^{19}0.007	^{22}0.004	^{17}0.053	^{20}0.027	^{15}0.101	^{13}0.083
94	HYPERVERGE-002	^{17}0.008	^{21}0.004	^{22}0.002	^{29}0.034	^{33}0.027	^{33}0.018	^{8}0.278	^{8}0.210	^{8}0.131	^{13}0.006	^{10}0.003	^{14}0.048	^{14}0.023	^{9}0.093	^{9}0.077
95	HZAILU-000	^{63}0.035	^{88}0.020	^{92}0.009	^{55}0.064	^{64}0.051	^{65}0.031	^{83}0.983	^{80}0.967	^{88}0.813	^{57}0.020	^{53}0.010	^{81}0.316	^{50}0.077	^{36}0.153	^{45}0.120
96	IDEMIA-003	^{251}0.552	^{146}0.047	^{144}0.021	^{286}1.000	^{187}0.165	^{164}0.079			^{280}1.000	^{148}0.123	^{148}0.061			^{151}0.766	^{168}0.630
97	IDEMIA-004	^{100}0.055	^{132}0.037	^{143}0.021	^{143}0.144	^{153}0.118	^{163}0.079	^{74}0.976	^{87}0.973	^{130}0.968	^{147}0.123	^{147}0.061			^{152}0.766	^{169}0.630
98	IDEMIA-005	^{115}0.066	^{138}0.044	^{164}0.026	^{165}0.181	^{176}0.150	^{193}0.102	^{78}0.979	^{93}0.978	^{136}0.973	^{149}0.130	^{153}0.070			^{167}0.879	^{179}0.743
99	IDEMIA-006	^{113}0.065	^{135}0.043	^{162}0.025	^{194}0.266	^{205}0.226	^{216}0.161	^{88}0.984	^{102}0.982	^{147}0.980	^{155}0.144	^{161}0.090			^{147}0.733	^{163}0.531
100	IDEMIA-007	^{66}0.035	^{81}0.018	^{84}0.008	^{73}0.073	^{75}0.055	^{74}0.033	^{286}1.000	^{262}1.000	^{249}1.000	^{113}0.052	^{108}0.022	^{63}0.182	^{71}0.109	^{255}1.000	^{200}0.982
101	IDEMIA-008	^{6}0.004	^{8}0.002	^{9}0.001	^{10}0.016	^{8}0.013	^{5}0.009	^{7}0.276	^{7}0.204	^{9}0.136	^{10}0.005	^{9}0.003	^{11}0.036	^{12}0.019	^{18}0.106	^{20}0.092
102	IDEMIA-009	^{5}0.004	^{2}0.002	^{3}0.001	^{2}0.012	^{2}0.011	^{2}0.008	^{3}0.202	^{3}0.141	^{5}0.099	^{3}0.003	^{4}0.002	^{5}0.027	^{5}0.013	^{4}0.074	^{4}0.064
103	IMAGUS-002	^{274}0.908	^{274}0.749	^{276}0.564	^{260}0.944	^{268}0.816	^{270}0.645	^{203}1.000	^{223}1.000	^{229}1.000						
104	IMAGUS-003	^{273}0.898	^{275}0.807	^{279}0.669	^{265}0.954	^{270}0.909	^{272}0.809	^{214}1.000	^{205}1.000	^{224}1.000						
105	IMAGUS-005	^{63}0.034	^{85}0.018	^{85}0.008	^{87}0.088	^{90}0.066	^{91}0.040	^{55}0.926	^{59}0.838	^{67}0.647	^{75}0.029	^{86}0.016	^{55}0.161	^{66}0.094	^{66}0.231	^{90}0.189
106	IMAGUS-006	^{71}0.039	^{87}0.019	^{86}0.008	^{91}0.093	^{96}0.069	^{99}0.042	^{81}0.980	^{67}0.897	^{61}0.621	^{74}0.028	^{80}0.015	^{54}0.161	^{62}0.092	^{76}0.260	^{86}0.181
107	IMAGUS-007	^{76}0.044	^{100}0.023	^{100}0.010	^{99}0.100	^{102}0.073	^{103}0.045	^{68}0.973	^{65}0.893	^{68}0.651	^{82}0.031	^{83}0.016	^{57}0.169	^{68}0.098	^{81}0.265	^{85}0.181
108	IMAGUS-008	^{283}0.995	^{283}0.974	^{275}0.523	^{267}0.958	^{266}0.774	^{245}0.285	^{177}1.000	^{145}0.996	^{73}0.700	^{189}0.520	^{154}0.071	^{107}1.000	^{102}0.540	^{128}0.518	^{115}0.246
109	IMPERIAL-000	^{172}0.154	^{106}0.026	^{96}0.009	^{89}0.089	^{94}0.068	^{96}0.041	^{217}1.000	^{167}0.999	^{179}0.995	^{102}0.042	^{103}0.020			^{72}0.245	^{77}0.168
110	INCODE-000	^{235}0.423	^{247}0.310	^{254}0.199	^{232}0.486	^{242}0.420	^{248}0.304	^{178}1.000	^{159}0.998	^{177}0.994						
111	INCODE-001	^{224}0.319	^{236}0.212	^{241}0.112	^{212}0.348	^{225}0.296	^{229}0.198	^{199}1.000	^{221}1.000	^{221}1.000						
112	INCODE-002	^{221}0.285	^{232}0.184	^{239}0.100	^{206}0.333	^{223}0.269	^{225}0.176	^{139}0.998	^{125}0.993	^{143}0.976						
113	INCODE-003	^{222}0.286	^{228}0.167	^{227}0.084	^{216}0.372	^{219}0.264	^{219}0.164	^{188}1.000	^{180}0.999	^{191}0.996						
114	INCODE-004	^{138}0.099	^{159}0.054	^{155}0.023	^{156}0.167	^{156}0.120	^{152}0.070	^{135}0.997	^{135}0.995	^{107}0.929	^{125}0.063	^{121}0.031			^{90}0.313	^{108}0.226
115	INCODE-005	^{38}0.021	^{54}0.011	^{52}0.005	^{47}0.055	^{55}0.043	^{56}0.026	^{24}0.614	^{28}0.528	^{39}0.372	^{50}0.017	^{50}0.009	^{46}0.145	^{47}0.073	^{39}0.155	^{35}0.116
116	INNOVATRICS-002	^{233}0.379	^{241}0.234	^{249}0.139	^{220}0.403	^{230}0.310	^{235}0.209	^{211}1.000	^{212}1.000	^{219}0.999						
117	INNOVATRICS-003	^{223}0.297	^{237}0.221	^{245}0.132	^{214}0.351	^{226}0.297	^{232}0.203	^{186}1.000	^{193}1.000	^{201}0.998						
118	INNOVATRICS-004	^{187}0.184	^{214}0.132	^{224}0.074	^{192}0.262	^{204}0.222	^{210}0.149	^{87}0.984	^{97}0.980	^{135}0.973						
119	INNOVATRICS-005	^{104}0.057	^{125}0.034	^{124}0.014	^{113}0.114	^{121}0.089	^{118}0.052	^{49}0.890	^{60}0.846	^{74}0.723	^{109}0.047	^{107}0.022			^{74}0.251	^{87}0.182
120	INNOVATRICS-007	^{43}0.024	^{60}0.013	^{59}0.005	^{57}0.065	^{65}0.051	^{67}0.032	^{41}0.806	^{47}0.743	^{57}0.567	^{49}0.017	^{51}0.009	^{32}0.093	^{38}0.053	^{37}0.154	^{44}0.120
121	INTELLIVISION-001	^{246}0.508	^{245}0.279	^{251}0.158	^{229}0.459	^{240}0.404	^{247}0.302	^{195}1.000	^{196}1.000	^{216}0.999	^{175}0.328	^{179}0.219	^{99}0.749	^{104}0.598	^{145}0.685	^{165}0.562
122	INTSYSMSU-000	^{284}0.999	^{286}0.998	^{288}0.990	^{279}1.000	^{281}1.000	^{282}0.998	^{183}1.000	^{192}1.000	^{197}0.998	^{207}0.999	^{207}0.989			^{195}0.999	^{204}0.988
123	IREX-000	^{117}0.068	^{117}0.028	^{83}0.008	^{98}0.099	^{84}0.060	^{69}0.032	^{94}0.988	^{74}0.957	^{72}0.680	^{105}0.044	^{60}0.011	^{80}0.302	^{40}0.062	^{47}0.170	^{55}0.135
124	ISYSTEMS-002	^{174}0.155	^{184}0.078	^{177}0.032	^{152}0.161	^{160}0.126	^{166}0.080	^{146}0.998	^{152}0.998	^{171}0.993						
125	ISYSTEMS-003	^{197}0.204	^{168}0.059	^{158}0.024	^{137}0.135	^{144}0.107	^{146}0.068	^{194}1.000	^{198}1.000	^{195}0.997						
126	KAKAO-000	^{54}0.028	^{72}0.015	^{71}0.006	^{71}0.071	^{77}0.056	^{79}0.034	^{17}0.539	^{23}0.468	^{34}0.327	^{54}0.019	^{52}0.010	^{42}0.141	^{48}0.075	^{40}0.158	^{43}0.120
127	KEDACOM-001	^{73}0.041	^{99}0.023	^{121}0.013	^{94}0.096	^{100}0.072	^{122}0.054	^{97}0.989	^{110}0.986	^{139}0.973	^{117}0.055	^{137}0.043			^{88}0.305	^{121}0.264
128	KNERON-000			^{179}0.033			^{184}0.099									
129	KNERON-001			^{204}0.052												
130	LINE-000	^{109}0.062	^{121}0.031	^{119}0.012	^{134}0.132	^{130}0.095	^{124}0.054			^{234}1.000	^{107}0.046	^{104}0.021	^{77}0.278	^{84}0.151	^{222}1.000	^{123}0.268
131	LINE-001	^{57}0.030	^{28}0.005	^{23}0.002	^{58}0.066	^{30}0.027	^{26}0.015	^{216}1.000	^{216}1.000	^{230}1.000	^{33}0.009	^{24}0.004	^{25}0.072	^{28}0.034	^{267}1.000	^{190}0.858
132	LOOKMAN-003	^{114}0.066	^{137}0.044	^{160}0.025	^{133}0.131	^{148}0.112	^{167}0.082				^{138}0.084	^{149}0.061			^{99}0.355	^{136}0.304
133	LOOKMAN-004	^{121}0.074	^{140}0.045	^{156}0.024	^{123}0.123	^{142}0.105	^{158}0.075	^{76}0.979	^{90}0.977	^{141}0.974						
134	LOOKMAN-005	^{92}0.050	^{119}0.030	^{130}0.017	^{102}0.102	^{116}0.086	^{140}0.063	^{80}0.980	^{92}0.978	^{137}0.973	^{124}0.062	^{139}0.047			^{89}0.308	^{125}0.273
135	MANTRA-000	^{116}0.066	^{51}0.010	^{44}0.004	^{52}0.063	^{51}0.041	^{43}0.022	^{249}1.000	^{288}1.000	^{214}0.999	^{76}0.029	^{75}0.014	^{50}0.152	^{55}0.081	^{197}1.000	^{66}0.151
136	MEGVII-001	^{201}0.210	^{179}0.072	^{183}0.037	^{119}0.119	^{134}0.097	^{133}0.061									
137	MEGVII-002	^{215}0.258	^{183}0.077	^{185}0.037	^{120}0.120	^{132}0.096	^{130}0.059	^{154}0.999	^{162}0.998	^{96}0.872						
138	MICROFOCUS-003	^{277}0.958	^{281}0.931	^{285}0.866	^{273}0.988	^{280}0.979	^{280}0.948				^{206}0.982	^{206}0.945			^{190}0.991	^{199}0.977

Table 31: **Threshold-based accuracy**. *Values are FNIR(N, T, L) with N = 1.6 million with thresholds set to produce FPIR = 0.0003, 0.001, and 0.01 in non-mate searches. Throughout blue superscripts indicate the rank of the algorithm for that column. Caution: The Power-low models are mostly intended to draw attention to the kind of behavior, not as a model to be used for prediction.*

This publication is available free of charge from: https://doi.org/10.6028/NIST.IR.8271

MISSES BELOW THRESHOLD, T		ENROL RECENT MUGSHOT, N = 1.6M									ENROL APPLICATION PORTRAIT, N = 1.6M					
		ENROL: MUGSHOT			ENROL: MUGSHOT			ENROL: MUGSHOT			ENROL: VISA		ENROL: BORDER		ENROL: VISA	
		PROBE: MUGSHOT			PROBE: WEBCAM			PROBE: PROFILE			PROBE: BORDER		PROBE: BORDER 10+YR		PROBE: KIOSK	
#	ALGORITHM	FPIR=0.0003	FPIR=0.001	FPIR=0.01	FPIR=0.0003	FPIR=0.001	FPIR=0.01	FPIR=0.0003	FPIR=0.001	FPIR=0.01	FPIR=0.001	FPIR=0.01	FPIR=0.001	FPIR=0.01	FPIR=0.001	FPIR=0.01
139	MICROFOCUS-004	^{286}0.999	^{287}0.999	^{291}0.999	^{272}0.984	^{278}0.975	^{279}0.940				^{205}0.974	^{205}0.935			^{188}0.989	^{198}0.976
140	MICROFOCUS-005	^{272}0.883	^{279}0.835	^{283}0.736	^{264}0.951	^{274}0.928	^{276}0.865				^{203}0.935	^{203}0.848			^{187}0.985	^{197}0.965
141	MICROFOCUS-006	^{281}0.983	^{284}0.978	^{286}0.963	^{263}0.950	^{273}0.923	^{275}0.858				^{202}0.923	^{201}0.843			^{184}0.971	^{194}0.939
142	MICROSOFT-003	^{90}0.049	^{115}0.028	^{113}0.012	^{114}0.117	^{124}0.091	^{127}0.056				^{94}0.036	^{100}0.019			^{68}0.233	^{82}0.176
143	MICROSOFT-004	^{85}0.046	^{107}0.026	^{107}0.011	^{110}0.111	^{118}0.087	^{121}0.053				^{89}0.033	^{95}0.018			^{64}0.222	^{79}0.170
144	MICROSOFT-005	^{87}0.047	^{104}0.026	^{104}0.010	^{90}0.090	^{98}0.070	^{97}0.041	^{165}0.999	^{33}0.587	^{36}0.354	^{70}0.027	^{72}0.013			^{53}0.180	^{54}0.134
145	MICROSOFT-006	^{47}0.025	^{55}0.012	^{66}0.006	^{41}0.048	^{45}0.037	^{52}0.024	^{14}0.452	^{18}0.386	^{28}0.281	^{85}0.032	^{81}0.015			^{49}0.178	^{56}0.138
146	NEC-000	^{147}0.113	^{186}0.079	^{201}0.047	^{157}0.171	^{170}0.140	^{177}0.093	^{84}0.983	^{95}0.979	^{132}0.969					^{121}0.474	^{148}0.377
147	NEC-001	^{171}0.148	^{203}0.106	^{214}0.060	^{185}0.238	^{197}0.197	^{204}0.133	^{98}0.991	^{109}0.986	^{134}0.972	^{150}0.133	^{160}0.082			^{120}0.468	^{149}0.378
148	NEC-002	^{34}0.018	^{14}0.003	^{12}0.002	^{22}0.029	^{20}0.020	^{17}0.013	^{172}1.000	^{177}0.999	^{181}0.995	^{24}0.008	^{35}0.005			^{143}0.676	^{132}0.292
149	NEC-003	^{10}0.005	^{12}0.002	^{16}0.002	^{16}0.021	^{16}0.017	^{16}0.013	^{51}0.902	^{56}0.824	^{64}0.628	^{27}0.008	^{36}0.006	^{12}0.036	^{13}0.023	^{142}0.668	^{120}0.261
150	NEC-004	^{1}0.003	^{5}0.002	^{11}0.002	^{7}0.015	^{7}0.013	^{10}0.010	^{28}0.654	^{36}0.622	^{58}0.575	^{8}0.004	^{15}0.004	^{3}0.019	^{4}0.012	^{14}0.100	^{16}0.088
151	NEC-005	^{15}0.007	^{3}0.002	^{8}0.001	^{3}0.014	^{3}0.012	^{6}0.009	^{50}0.901	^{41}0.673	^{21}0.177	^{5}0.003	^{6}0.002	^{2}0.019	^{2}0.011	^{11}0.099	^{15}0.087
152	NEUROTECHNOLOGY-003	^{285}0.999	^{272}0.636	^{238}0.099	^{254}0.773	^{221}0.266	^{218}0.164	^{240}1.000	^{279}1.000	^{270}1.000						
153	NEUROTECHNOLOGY-004	^{149}0.120	^{173}0.063	^{169}0.028	^{144}0.146	^{150}0.117	^{154}0.073	^{127}0.996	^{130}0.994	^{159}0.990						
154	NEUROTECHNOLOGY-005	^{148}0.117	^{160}0.054	^{150}0.022	^{188}0.252	^{162}0.130	^{157}0.074	^{151}0.999	^{156}0.998	^{156}0.989						
155	NEUROTECHNOLOGY-006	^{282}0.987	^{242}0.249	^{243}0.121	^{285}1.000	^{241}0.418	^{234}0.206									
156	NEUROTECHNOLOGY-007	^{211}0.252	^{172}0.062	^{147}0.021	^{276}0.996	^{191}0.173	^{145}0.068	^{218}1.000	^{201}1.000	^{194}0.997	^{176}0.339	^{128}0.036			^{246}1.000	^{205}0.989
157	NEUROTECHNOLOGY-008	^{265}0.797	^{154}0.053	^{117}0.012	^{108}0.110	^{112}0.080	^{108}0.047	^{202}1.000	^{222}1.000	^{236}1.000	^{93}0.035	^{91}0.017	^{79}0.293	^{82}0.149	^{59}0.203	^{67}0.152
158	NEUROTECHNOLOGY-009	^{51}0.027	^{73}0.015	^{65}0.006	^{60}0.066	^{69}0.052	^{68}0.032	^{29}0.661	^{34}0.588	^{42}0.436	^{56}0.020	^{55}0.010	^{51}0.153	^{57}0.082	^{44}0.165	^{50}0.129
159	NEUROTECHNOLOGY-010	^{226}0.346	^{49}0.010	^{41}0.003	^{40}0.047	^{47}0.037	^{49}0.023	^{12}0.377	^{14}0.277	^{19}0.170	^{36}0.010	^{30}0.005	^{27}0.075	^{30}0.039	^{25}0.126	^{26}0.097
160	NEUROTECHNOLOGY-012	^{132}0.092	^{37}0.007	^{30}0.002	^{39}0.045	^{42}0.032	^{36}0.019	^{189}1.000	^{76}0.959	^{13}0.149	^{30}0.008	^{18}0.004	^{21}0.061	^{22}0.028	^{173}0.916	^{17}0.088
161	NEWLAND-002	^{249}0.523	^{262}0.438	^{264}0.294	^{233}0.535	^{248}0.466	^{252}0.335	^{161}0.999	^{171}0.999	^{200}0.998						
162	NOBLIS-001	^{289}1.000	^{289}1.000	^{289}0.991	^{290}1.000	^{282}1.000	^{286}1.000	^{209}1.000	^{209}1.000	^{232}1.000						
163	NOBLIS-002	^{287}1.000	^{285}0.997	^{273}0.488	^{287}1.000	^{292}1.000	^{288}1.000	^{208}1.000	^{227}1.000	^{237}1.000						
164	NOTIONTAG-000	^{61}0.032	^{76}0.017	^{81}0.007	^{74}0.076	^{83}0.059	^{85}0.036	^{30}0.671	^{33}0.611	^{44}0.467	^{60}0.021	^{62}0.011	^{49}0.150	^{58}0.084	^{48}0.176	^{58}0.140
165	NTECHLAB-003	^{124}0.080	^{158}0.054	^{170}0.028	^{145}0.148	^{151}0.118	^{159}0.075	^{47}0.873	^{58}0.837	^{81}0.752						
166	NTECHLAB-004	^{111}0.063	^{133}0.041	^{145}0.021	^{132}0.131	^{141}0.105	^{142}0.065	^{46}0.868	^{57}0.833	^{79}0.746	^{116}0.053	^{119}0.030			^{78}0.263	^{104}0.214
167	NTECHLAB-005	^{110}0.062	^{134}0.042	^{146}0.021	^{131}0.130	^{139}0.102	^{141}0.063	^{42}0.816	^{50}0.771	^{70}0.661	^{132}0.073	^{132}0.039			^{86}0.294	^{109}0.227
168	NTECHLAB-006	^{103}0.056	^{128}0.037	^{135}0.018	^{121}0.121	^{127}0.094	^{129}0.059	^{40}0.802	^{49}0.754	^{65}0.635	^{119}0.057	^{123}0.032			^{77}0.260	^{100}0.207
169	NTECHLAB-007	^{72}0.040	^{103}0.026	^{114}0.012	^{83}0.085	^{93}0.067	^{95}0.041	^{39}0.796	^{48}0.750	^{66}0.642	^{86}0.032	^{92}0.017			^{65}0.223	^{81}0.176
170	NTECHLAB-008	^{45}0.024	^{66}0.014	^{74}0.007	^{49}0.057	^{58}0.045	^{61}0.029	^{21}0.601	^{29}0.529	^{41}0.391	^{90}0.033	^{96}0.018			^{54}0.183	^{59}0.140
171	NTECHLAB-009	^{20}0.010	^{30}0.005	^{35}0.003	^{21}0.028	^{22}0.022	^{21}0.014	^{16}0.522	^{20}0.430	^{30}0.311	^{44}0.015	^{45}0.008	^{36}0.109	^{39}0.061	^{32}0.142	^{32}0.114
172	NTECHLAB-010	^{12}0.005	^{13}0.003	^{10}0.002	^{13}0.018	^{14}0.015	^{12}0.011	^{11}0.334	^{13}0.252	^{18}0.169	^{17}0.007	^{21}0.004	^{20}0.059	^{24}0.031	^{10}0.098	^{8}0.077
173	NTECHLAB-011	^{13}0.006	^{17}0.003	^{13}0.002	^{12}0.018	^{13}0.015	^{11}0.010	^{9}0.291	^{10}0.228	^{16}0.150	^{32}0.009	^{28}0.004	^{26}0.074	^{29}0.038	^{7}0.091	^{6}0.075
174	PANGIAM-000	^{30}0.014	^{36}0.006	^{34}0.003	^{36}0.039	^{37}0.030	^{34}0.018	^{70}0.974	^{16}0.318	^{20}0.175	^{35}0.009	^{29}0.005	^{41}0.136	^{26}0.033	^{17}0.105	^{14}0.083
175	PARAVISION-000	^{220}0.278	^{195}0.089	^{199}0.045	^{226}0.447	^{189}0.170	^{188}0.100	^{215}1.000	^{173}0.999	^{192}0.997	^{188}0.470	^{193}0.443			^{176}0.926	^{184}0.779
176	PARAVISION-001	^{166}0.140	^{147}0.049	^{142}0.020	^{180}0.207	^{161}0.128	^{156}0.074	^{219}1.000	^{165}0.999	^{176}0.994	^{185}0.444	^{192}0.428			^{148}0.739	^{166}0.573
177	PARAVISION-002	^{129}0.085	^{148}0.050	^{152}0.022	^{149}0.152	^{154}0.119	^{161}0.076	^{101}0.992	^{103}0.983	^{80}0.748	^{135}0.080	^{138}0.043			^{125}0.497	^{124}0.268
178	PARAVISION-003	^{112}0.063	^{126}0.035	^{126}0.016	^{126}0.124	^{131}0.096	^{132}0.060	^{133}0.997	^{132}0.994	^{75}0.733	^{120}0.058	^{126}0.034			^{87}0.296	^{111}0.232
179	PARAVISION-004	^{46}0.025	^{53}0.010	^{51}0.004	^{42}0.049	^{48}0.038	^{50}0.024	^{212}1.000	^{213}1.000	^{85}0.797	^{52}0.018	^{58}0.011			^{171}0.908	^{101}0.211
180	PARAVISION-005	^{33}0.014	^{23}0.004	^{26}0.002	^{24}0.031	^{25}0.024	^{29}0.016	^{131}0.997	^{96}0.980	^{22}0.181	^{37}0.011	^{46}0.008			^{27}0.132	^{41}0.120
181	PARAVISION-007	^{88}0.048	^{22}0.004	^{18}0.002	^{234}0.560	^{26}0.025	^{25}0.015	^{200}1.000	^{220}1.000	^{239}1.000	^{31}0.009	^{38}0.006	^{37}0.113	^{16}0.024	^{225}1.000	^{239}1.000
182	PARAVISION-009	^{16}0.007	^{15}0.003	^{7}0.001	^{19}0.026	^{18}0.019	^{14}0.012	^{38}0.778	^{46}0.735	^{55}0.550	^{4}0.003	^{2}0.002	^{8}0.033	^{7}0.015	^{3}0.073	^{1}0.061
183	PIXELALL-002	^{259}0.664	^{202}0.105	^{173}0.030	^{269}0.974	^{238}0.388	^{168}0.083		^{215}1.000	^{227}1.000	^{192}0.602	^{141}0.047			^{264}1.000	^{207}1.000
184	PIXELALL-003	^{89}0.049	^{95}0.022	^{94}0.009	^{103}0.102	^{101}0.073	^{100}0.043		^{189}1.000	^{199}0.998	^{97}0.037	^{101}0.020			^{134}0.554	^{118}0.255

Table 32: **Threshold-based accuracy**. *Values are FNIR(N, T, L) with N = 1.6 million with thresholds set to produce FPIR = 0.0003, 0.001, and 0.01 in non-mate searches. Throughout blue superscripts indicate the rank of the algorithm for that column. Caution: The Power-low models are mostly intended to draw attention to the kind of behavior, not as a model to be used for prediction.*

FNIR(N, R, T) = False neg. identification rate
FPIR(N, T) = False pos. identification rate
N = Num. enrolled subjects
R = Num. candidates examined
T = Threshold
T = 0 → Investigation
T > 0 → Identification

This publication is available free of charge from: https://doi.org/10.6028/NIST.IR.8271

MISSES BELOW THRESHOLD, T		ENROL RECENT MUGSHOT, N = 1.6M									ENROL APPLICATION PORTRAIT, N = 1.6M					
		ENROL: MUGSHOT			ENROL: MUGSHOT			ENROL: MUGSHOT			ENROL: VISA		ENROL: BORDER		ENROL: VISA	
		PROBE: MUGSHOT			PROBE: WEBCAM			PROBE: PROFILE			PROBE: BORDER		PROBE: BORDER 10+YR		PROBE: KIOSK	
#	ALGORITHM	FPIR=0.0003	FPIR=0.001	FPIR=0.01	FPIR=0.0003	FPIR=0.001	FPIR=0.01	FPIR=0.0003	FPIR=0.001	FPIR=0.01	FPIR=0.001	FPIR=0.01	FPIR=0.001	FPIR=0.01	FPIR=0.001	FPIR=0.01
185	PIXELALL-004	^{150}0.120	^{84}0.018	^{78}0.007	^{255}0.783	^{111}0.079	^{86}0.037		^{207}1.000	^{209}0.999	^{111}0.051	^{82}0.015			^{191}0.994	^{195}0.942
186	PIXELALL-005	^{123}0.079	^{57}0.012	^{53}0.005	^{228}0.456	^{62}0.050	^{58}0.027		^{210}1.000	^{218}0.999	^{71}0.027	^{88}0.017	^{67}0.203	^{44}0.071	^{196}1.000	^{201}0.983
187	PTAKURATSATU-000	^{105}0.057	^{129}0.037	^{131}0.017	^{155}0.165	^{159}0.124	^{153}0.071	^{63}0.947	^{69}0.924	^{94}0.868	^{108}0.046	^{105}0.022	^{69}0.206	^{75}0.120	^{67}0.232	^{84}0.179
188	QNAP-000	^{280}0.972	^{213}0.129	^{205}0.052	^{278}0.998	^{209}0.238	^{199}0.117	^{222}1.000	^{228}1.000	^{233}1.000	^{164}0.191	^{152}0.068	^{93}0.539	^{97}0.263	^{193}0.998	^{203}0.985
189	QNAP-001	^{128}0.083	^{157}0.054	^{159}0.024	^{161}0.176	^{167}0.137	^{170}0.085	^{59}0.943	^{70}0.928	^{95}0.870	^{136}0.081	^{136}0.041	^{86}0.368	^{92}0.227	^{97}0.331	^{116}0.248
190	QNAP-002	^{81}0.045	^{108}0.026	^{120}0.013	^{139}0.136	^{143}0.106	^{147}0.068	^{43}0.820	^{51}0.772	^{62}0.622	^{115}0.052	^{112}0.025	^{78}0.281	^{87}0.171	^{83}0.272	^{103}0.214
191	QUANTASOFT-001	^{263}0.713	^{273}0.639	^{274}0.493												
192	RANKONE-002	^{185}0.184	^{207}0.118	^{220}0.071	^{204}0.308	^{217}0.261	^{228}0.190									
193	RANKONE-003	^{186}0.184	^{206}0.118	^{221}0.071	^{201}0.300	^{216}0.255	^{226}0.187									
194	RANKONE-004	^{210}0.250	^{234}0.193	^{244}0.124	^{231}0.482	^{243}0.426	^{250}0.324									
195	RANKONE-005	^{135}0.096	^{169}0.059	^{178}0.033	^{181}0.212	^{192}0.173	^{200}0.119	^{162}0.999	^{157}0.998	^{178}0.994						
196	RANKONE-006	^{107}0.061	^{129}0.037	^{138}0.020				^{90}0.987	^{91}0.977	^{111}0.937						
197	RANKONE-007	^{62}0.034	^{97}0.022	^{110}0.011	^{118}0.118	^{128}0.095	^{135}0.061	^{73}0.975	^{79}0.967	^{104}0.924						
198	RANKONE-009	^{58}0.031	^{79}0.018	^{88}0.008	^{95}0.098	^{105}0.076	^{102}0.045	^{82}0.983	^{82}0.969	^{93}0.859	^{122}0.062	^{118}0.029			^{96}0.328	^{99}0.206
199	RANKONE-010	^{40}0.023	^{63}0.014	^{79}0.007	^{76}0.077	^{81}0.058	^{84}0.036	^{52}0.905	^{54}0.802	^{69}0.652	^{114}0.052	^{115}0.027	^{70}0.208	^{74}0.119	^{75}0.259	^{93}0.194
200	RANKONE-011	^{145}0.109	^{43}0.009	^{48}0.004	^{80}0.079	^{60}0.048	^{62}0.029				^{96}0.037	^{93}0.017	^{62}0.182	^{63}0.092	^{185}0.977	^{156}0.465
201	RANKONE-012	^{37}0.020	^{40}0.008	^{45}0.004	^{72}0.072	^{73}0.053	^{63}0.030				^{77}0.029	^{77}0.014	^{45}0.144	^{45}0.072	^{119}0.465	^{49}0.128
202	REALNETWORKS-000	^{231}0.374	^{239}0.234	^{247}0.138	^{224}0.433	^{232}0.319	^{236}0.209									
203	REALNETWORKS-001	^{232}0.374	^{240}0.234	^{248}0.138	^{223}0.433	^{233}0.319	^{237}0.209									
204	REALNETWORKS-002	^{230}0.370	^{238}0.231	^{246}0.137	^{222}0.416	^{231}0.315	^{238}0.209									
205	REALNETWORKS-003	^{218}0.273	^{224}0.159	^{230}0.090	^{209}0.342	^{220}0.266	^{224}0.172	^{159}0.999	^{161}0.998	^{153}0.987	^{159}0.164	^{165}0.103			^{126}0.500	^{145}0.364
206	REALNETWORKS-004	^{208}0.242	^{223}0.158	^{229}0.090	^{215}0.353	^{218}0.263	^{221}0.169	^{175}1.000	^{174}0.999	^{170}0.992	^{160}0.170	^{166}0.103			^{138}0.613	^{146}0.370
207	REALNETWORKS-005	^{95}0.052	^{114}0.028	^{116}0.012	^{93}0.094	^{103}0.074	^{107}0.047	^{86}0.984	^{84}0.971	^{99}0.896	^{95}0.037	^{89}0.017	^{71}0.223	^{77}0.123	^{62}0.215	^{75}0.165
208	REALNETWORKS-006	^{49}0.025	^{67}0.015	^{62}0.006	^{66}0.068	^{71}0.053	^{72}0.032	^{102}0.993	^{99}0.980	^{90}0.838	^{45}0.016	^{48}0.008	^{38}0.120	^{41}0.063	^{38}0.154	^{34}0.116
209	REALNETWORKS-007	^{36}0.019	^{47}0.010	^{47}0.004	^{48}0.057	^{56}0.043	^{57}0.027	^{99}0.992	^{94}0.979	^{92}0.855	^{39}0.012	^{34}0.005	^{92}0.463	^{42}0.063	^{31}0.140	^{28}0.100
210	REMARKAI-000	^{154}0.125	^{161}0.055	^{154}0.023	^{158}0.173	^{155}0.120	^{150}0.070	^{167}0.999	^{172}0.999	^{182}0.995	^{131}0.069	^{125}0.033			^{146}0.717	^{138}0.315
211	REMARKAI-000	^{195}0.197	^{211}0.128	^{213}0.059	^{193}0.263	^{198}0.203	^{202}0.123									
212	REMARKAI-002	^{191}0.188	^{210}0.124	^{212}0.059	^{187}0.248	^{196}0.196	^{201}0.122	^{106}0.993	^{120}0.991	^{146}0.980						
213	RENDIP-000	^{41}0.023	^{56}0.012	^{57}0.005	^{170}0.189	^{82}0.059	^{78}0.034	^{62}0.945	^{66}0.894	^{78}0.744	^{61}0.022	^{70}0.013	^{64}0.185	^{59}0.089	^{45}0.167	^{51}0.130
214	REVEALMEDIA-000	^{42}0.024	^{58}0.012	^{61}0.006	^{46}0.054	^{54}0.042	^{54}0.025	^{33}0.755	^{43}0.680	^{54}0.539	^{59}0.021	^{59}0.011	^{33}0.093	^{37}0.051	^{33}0.143	^{37}0.118
215	S1-000	^{162}0.137	^{116}0.028	^{109}0.011	^{129}0.129	^{115}0.085	^{110}0.048	^{221}1.000	^{229}1.000	^{59}0.596	^{110}0.047	^{97}0.018	^{132}1.000	^{76}0.123	^{275}1.000	^{171}0.632
216	S1-001	^{99}0.054	^{74}0.016	^{76}0.007	^{59}0.066	^{68}0.052	^{77}0.033	^{100}0.992	^{107}0.985	^{123}0.952	^{53}0.019	^{54}0.010	^{40}0.136	^{49}0.075	^{34}0.148	^{38}0.119
217	S1-002	^{106}0.060	^{34}0.006	^{32}0.002	^{85}0.085	^{38}0.031	^{32}0.018	^{54}0.924	^{6}0.196	^{3}0.095	^{20}0.007	^{12}0.003	^{103}0.792	^{85}0.151	^{163}0.841	^{61}0.144
218	SCANOVATE-000	^{140}0.103	^{176}0.067	^{174}0.030	^{200}0.296	^{212}0.240	^{211}0.150	^{57}0.931	^{64}0.893	^{86}0.803	^{168}0.215	^{173}0.118			^{106}0.400	^{134}0.299
219	SCANOVATE-001	^{156}0.128	^{187}0.081	^{186}0.037	^{199}0.281	^{206}0.227	^{207}0.140	^{58}0.935	^{68}0.911	^{89}0.834	^{165}0.192	^{167}0.103			^{109}0.404	^{130}0.290
220	SENSETIME-000	^{67}0.036	^{93}0.021	^{95}0.009	^{77}0.078	^{87}0.063	^{92}0.040	^{227}1.000	^{266}1.000	^{154}0.988						
221	SENSETIME-001	^{65}0.036	^{96}0.022	^{99}0.010	^{81}0.080	^{89}0.064	^{98}0.041									
222	SENSETIME-002	^{69}0.037	^{68}0.015	^{125}0.014	^{125}0.124	^{35}0.028	^{47}0.023	^{130}0.997	^{128}0.994	^{145}0.979	^{84}0.032	^{90}0.017			^{129}0.523	^{74}0.160
223	SENSETIME-003	^{7}0.004	^{7}0.002	^{6}0.001	^{4}0.014	^{4}0.012	^{4}0.009	^{23}0.607	^{24}0.477	^{31}0.311	^{25}0.008	^{33}0.005			^{28}0.133	^{33}0.115
224	SENSETIME-004	^{3}0.003	^{4}0.002	^{5}0.001	^{6}0.015	^{6}0.013	^{9}0.010	^{10}0.301	^{11}0.229	^{15}0.149	^{14}0.006	^{16}0.004			^{21}0.113	^{27}0.100
225	SENSETIME-005	^{24}0.011	^{11}0.002	^{4}0.001	^{14}0.018	^{12}0.014	^{7}0.010	^{4}0.259	^{5}0.173	^{6}0.103	^{18}0.007	^{19}0.004	^{16}0.051	^{15}0.023	^{16}0.104	^{22}0.093
226	SENSETIME-006	^{9}0.005	^{6}0.002	^{2}0.001	^{9}0.016	^{5}0.012	^{3}0.009	^{150}0.999	^{160}0.998	^{71}0.680	^{6}0.004	^{5}0.002	^{9}0.034	^{8}0.016	^{8}0.093	^{11}0.079
227	SENSETIME-007	^{2}0.003	^{1}0.001	^{1}0.001	^{1}0.012	^{1}0.009	^{1}0.007	^{173}1.000	^{178}0.999	^{53}0.538	^{2}0.003	^{1}0.001	^{4}0.024	^{3}0.011	^{5}0.085	^{5}0.074
228	SHAMAN-003	^{245}0.506	^{263}0.451	^{267}0.347	^{245}0.650	^{258}0.597	^{261}0.472									
229	SHAMAN-004	^{260}0.679	^{271}0.615	^{272}0.488	^{256}0.812	^{265}0.754	^{269}0.639									
230	SHAMAN-006	^{188}0.185	^{218}0.141	^{232}0.092	^{197}0.278	^{208}0.237	^{220}0.168	^{75}0.978	^{85}0.972	^{128}0.960						

Table 33: **Threshold-based accuracy**. *Values are FNIR(N, T, L) with N = 1.6 million with thresholds set to produce FPIR = 0.0003, 0.001, and 0.01 in non-mate searches. Throughout blue superscripts indicate the rank of the algorithm for that column. Caution: The Power-low models are mostly intended to draw attention to the kind of behavior, not as a model to be used for prediction.*

This publication is available free of charge from: https://doi.org/10.6028/NIST.IR.8271

MISSES BELOW THRESHOLD, T		ENROL RECENT MUGSHOT, N = 1.6M									ENROL APPLICATION PORTRAIT, N = 1.6M					
		ENROL: MUGSHOT			ENROL: MUGSHOT			ENROL: MUGSHOT			ENROL: VISA		ENROL: BORDER		ENROL: VISA	
		PROBE: MUGSHOT			PROBE: WEBCAM			PROBE: PROFILE			PROBE: BORDER		PROBE: BORDER 10+YR		PROBE: KIOSK	
#	ALGORITHM	FPIR=0.0003	FPIR=0.001	FPIR=0.01	FPIR=0.0003	FPIR=0.001	FPIR=0.01	FPIR=0.0003	FPIR=0.001	FPIR=0.01	FPIR=0.001	FPIR=0.01	FPIR=0.001	FPIR=0.01	FPIR=0.001	FPIR=0.01
231	SHAMAN-007	^{183}0.183	^{219}0.141	^{231}0.092	^{198}0.280	^{211}0.240	^{222}0.169									
232	SIAT-001	^{159}0.132	^{77}0.018	^{75}0.007	^{243}0.641	^{237}0.365	^{253}0.348				^{80}0.031	^{76}0.014				
233	SIAT-002	^{234}0.417	^{94}0.022	^{80}0.007	^{259}0.942	^{249}0.478	^{259}0.460				^{178}0.372	^{187}0.356			^{175}0.923	^{78}0.169
234	SMILART-004	^{279}0.970	^{282}0.968	^{287}0.965	^{270}0.977	^{279}0.976	^{281}0.973									
235	SMILART-005															
236	SQISOFT-001	^{204}0.226	^{215}0.132	^{196}0.044	^{207}0.340	^{214}0.252	^{197}0.111	^{65}0.956	^{52}0.797	^{60}0.608	^{100}0.040	^{99}0.019	^{83}0.317	^{83}0.150	^{111}0.420	^{91}0.189
237	STAQU-000	^{225}0.334	^{170}0.062	^{148}0.022	^{257}0.848	^{245}0.443	^{134}0.061	^{196}1.000	^{199}1.000	^{211}0.999	^{190}0.535	^{133}0.039	^{104}0.961	^{88}0.183	^{265}1.000	^{206}0.999
238	SYNESIS-003	^{257}0.648	^{268}0.582	^{271}0.443	^{249}0.708	^{261}0.646	^{263}0.524									
239	SYNESIS-003	^{146}0.111	^{174}0.065	^{175}0.032	^{150}0.155	^{158}0.123	^{162}0.078	^{69}0.973	^{77}0.960	^{101}0.911	^{133}0.075	^{131}0.039			^{91}0.314	^{113}0.235
240	SYNESIS-005	^{91}0.050	^{102}0.025	^{112}0.011	^{88}0.088	^{99}0.072	^{101}0.043	^{114}0.995	^{104}0.984	^{82}0.795	^{87}0.032	^{84}0.016			^{61}0.214	^{73}0.158
241	TECH5-001	^{267}0.807	^{164}0.057	^{134}0.018	^{275}0.994	^{275}0.935	^{126}0.055	^{276}1.000	^{230}1.000	^{225}1.000	^{169}0.244	^{117}0.028			^{192}0.994	^{188}0.817
242	TECH5-002	^{98}0.053	^{111}0.027	^{115}0.012	^{92}0.094	^{97}0.070	^{94}0.040	^{48}0.874	^{55}0.805	^{63}0.627	^{99}0.039	^{98}0.019	^{68}0.205	^{72}0.111	^{114}0.440	^{88}0.182
243	TEVIAN-003	^{207}0.239	^{231}0.177	^{237}0.096	^{211}0.346	^{227}0.298	^{230}0.198									
244	TEVIAN-004	^{180}0.170	^{205}0.117	^{217}0.063	^{182}0.216	^{193}0.176	^{198}0.115									
245	TEVIAN-005	^{158}0.129	^{192}0.087	^{198}0.045	^{164}0.180	^{173}0.144	^{174}0.089	^{93}0.988	^{78}0.962	^{84}0.796						
246	TEVIAN-006	^{44}0.024	^{48}0.010	^{56}0.005	^{37}0.041	^{40}0.032	^{41}0.021	^{19}0.562	^{19}0.425	^{29}0.291	^{46}0.016	^{49}0.009	^{31}0.093	^{35}0.050	^{180}0.951	^{36}0.117
247	TEVIAN-007	^{25}0.011	^{32}0.005	^{36}0.003	^{20}0.028	^{21}0.022	^{22}0.015	^{15}0.504	^{15}0.301	^{23}0.183	^{34}0.009	^{31}0.005	^{23}0.065	^{25}0.033	^{23}0.122	^{30}0.102
248	TIGER-000	^{240}0.462	^{257}0.390	^{260}0.261	^{235}0.565	^{250}0.500	^{254}0.366									
249	TIGER-002	^{177}0.158	^{188}0.086	^{189}0.039	^{177}0.202	^{182}0.158	^{181}0.095	^{166}0.999	^{169}0.999	^{142}0.975						
250	TIGER-003	^{176}0.158	^{189}0.086	^{188}0.039	^{178}0.202	^{183}0.158	^{180}0.095									
251	TONGYITRANS-000	^{143}0.107	^{181}0.074	^{187}0.038	^{142}0.141	^{147}0.112	^{149}0.069									
252	TONGYITRANS-001	^{153}0.124	^{175}0.066	^{176}0.032	^{128}0.128	^{137}0.101	^{138}0.062									
253	TOSHIBA-000	^{152}0.123	^{171}0.062	^{168}0.027	^{146}0.150	^{152}0.118	^{155}0.074	^{132}0.997	^{141}0.995	^{155}0.988						
254	TOSHIBA-001	^{202}0.225	^{166}0.058	^{136}0.019	^{136}0.133	^{125}0.092	^{125}0.054									
255	TRUEFACE-000	^{84}0.046	^{83}0.018	^{87}0.008	^{78}0.079	^{86}0.062	^{89}0.039	^{118}0.995	^{61}0.882	^{46}0.499	^{78}0.030	^{87}0.016	^{66}0.194	^{73}0.111	^{56}0.188	^{63}0.145
256	VD-000	^{276}0.950	^{280}0.917	^{284}0.827	^{268}0.968	^{277}0.946	^{277}0.871									
257	VD-001	^{219}0.278	^{235}0.201	^{242}0.116	^{205}0.331	^{224}0.281	^{227}0.188									
258	VD-002	^{170}0.144	^{185}0.079	^{182}0.036	^{169}0.188	^{175}0.148	^{175}0.092	^{141}0.998	^{144}0.996	^{152}0.987	^{140}0.095	^{142}0.048	^{85}0.367	^{91}0.220	^{102}0.372	^{126}0.280
259	VD-003	^{206}0.234	^{142}0.046	^{139}0.020	^{135}0.133	^{136}0.100	^{137}0.061	^{164}0.999	^{170}0.999	^{174}0.994	^{112}0.051	^{114}0.027	^{73}0.244	^{78}0.133	^{93}0.315	^{95}0.203
260	VERIDAS-001	^{125}0.080	^{131}0.037	^{129}0.016	^{106}0.106	^{114}0.082	^{114}0.051	^{105}0.993	^{112}0.987	^{112}0.938	^{104}0.044	^{109}0.023	^{75}0.266	^{80}0.146	^{80}0.264	^{96}0.204
261	VERIDAS-002	^{126}0.080	^{130}0.037	^{128}0.016	^{107}0.106	^{113}0.082	^{113}0.051	^{104}0.993	^{111}0.987	^{113}0.938	^{103}0.044	^{110}0.023	^{76}0.266	^{81}0.146	^{79}0.264	^{97}0.204
262	VERIDAS-003	^{118}0.072	^{75}0.017	^{68}0.006	^{69}0.071	^{76}0.055	^{75}0.033	^{147}0.998	^{149}0.997	^{106}0.927	^{55}0.020	^{57}0.011	^{48}0.150	^{51}0.078	^{51}0.178	^{60}0.142
263	VIGILANTSOLUTIONS-003	^{244}0.482	^{261}0.408	^{262}0.282	^{252}0.730	^{264}0.660	^{265}0.526	^{160}0.999	^{166}0.999	^{183}0.995						
264	VIGILANTSOLUTIONS-004	^{256}0.624	^{267}0.549	^{270}0.422	^{258}0.858	^{269}0.817	^{271}0.709	^{145}0.998	^{147}0.996	^{164}0.991						
265	VIGILANTSOLUTIONS-005	^{275}0.936	^{256}0.388	^{191}0.043				^{213}1.000	^{214}1.000	^{231}1.000						
266	VIGILANTSOLUTIONS-006	^{278}0.959	^{251}0.353	^{194}0.043				^{204}1.000	^{224}1.000	^{235}1.000						
267	VIGILANTSOLUTIONS-007	^{122}0.076	^{118}0.028	^{111}0.011	^{112}0.113	^{119}0.088	^{120}0.053	^{138}0.997	^{146}0.996	^{167}0.991	^{137}0.081	^{140}0.047	^{87}0.371	^{94}0.242	^{105}0.391	^{133}0.295
268	VIGILANTSOLUTIONS-008	^{94}0.051	^{90}0.021	^{98}0.010	^{105}0.105	^{106}0.077	^{105}0.046	^{170}1.000	^{168}0.999	^{163}0.991	^{144}0.104	^{145}0.054	^{89}0.398	^{96}0.259	^{127}0.511	^{139}0.316
269	VISIONBOX-000	^{119}0.073	^{80}0.018	^{77}0.007	^{70}0.071	^{79}0.057	^{82}0.035	^{111}0.995	^{119}0.990	^{140}0.974	^{64}0.023	^{66}0.012	^{47}0.146	^{53}0.081	^{43}0.162	^{47}0.126
270	VISIONLABS-004	^{131}0.091	^{165}0.058	^{157}0.024	^{173}0.199	^{184}0.159	^{183}0.097	^{60}0.944	^{63}0.890	^{77}0.742						
271	VISIONLABS-005	^{127}0.080	^{149}0.050	^{141}0.020	^{167}0.183	^{174}0.147	^{172}0.087	^{61}0.945	^{62}0.888	^{76}0.736						
272	VISIONLABS-006	^{80}0.044	^{110}0.027	^{103}0.010	^{116}0.117	^{123}0.090	^{116}0.051	^{35}0.764	^{39}0.672	^{51}0.511						
273	VISIONLABS-007	^{79}0.044	^{109}0.027	^{102}0.010	^{115}0.117	^{122}0.090	^{115}0.051	^{36}0.764	^{40}0.672	^{50}0.511	^{83}0.031	^{79}0.014			^{55}0.185	^{64}0.145
274	VISIONLABS-008	^{53}0.028	^{61}0.013	^{60}0.006	^{64}0.068	^{67}0.051	^{70}0.032	^{20}0.574	^{25}0.481	^{32}0.317	^{47}0.017	^{44}0.008			^{35}0.151	^{39}0.119
275	VISIONLABS-009	^{28}0.012	^{26}0.005	^{21}0.002	^{25}0.032	^{28}0.025	^{30}0.017	^{56}0.930	^{53}0.799	^{25}0.196	^{29}0.008	^{27}0.004			^{20}0.113	^{23}0.093
276	VISIONLABS-010	^{32}0.014	^{31}0.005	^{29}0.002	^{30}0.034	^{34}0.027	^{35}0.019			^{17}0.169	^{23}0.008	^{20}0.004	^{18}0.055	^{18}0.027	^{19}0.109	^{19}0.089

Table 34: **Threshold-based accuracy**. *Values are FNIR(N, T, L) with N = 1.6 million with thresholds set to produce FPIR = 0.0003, 0.001, and 0.01 in non-mate searches. Throughout blue superscripts indicate the rank of the algorithm for that column. Caution: The Power-low models are mostly intended to draw attention to the kind of behavior, not as a model to be used for prediction.*

This publication is available free of charge from: https://doi.org/10.6028/NIST.IR.8271

MISSES BELOW THRESHOLD, T		ENROL RECENT MUGSHOT, N = 1.6M									ENROL APPLICATION PORTRAIT, N = 1.6M					
		ENROL: MUGSHOT			ENROL: MUGSHOT			ENROL: MUGSHOT			ENROL: VISA		ENROL: BORDER		ENROL: VISA	
		PROBE: MUGSHOT			PROBE: WEBCAM			PROBE: PROFILE			PROBE: BORDER		PROBE: BORDER 10+YR		PROBE: KIOSK	
#	ALGORITHM	FPIR=0.0003	FPIR=0.001	FPIR=0.01	FPIR=0.0003	FPIR=0.001	FPIR=0.01	FPIR=0.0003	FPIR=0.001	FPIR=0.01	FPIR=0.001	FPIR=0.01	FPIR=0.001	FPIR=0.01	FPIR=0.001	FPIR=0.01
277	VISIONLABS-011	^{26}0.011	^{19}0.003	^{15}0.002	^{18}0.024	^{19}0.020	^{20}0.014			^{24}0.194	^{9}0.004	^{7}0.002	^{10}0.034	^{9}0.017	^{6}0.090	^{10}0.079
278	VNPT-001	^{52}0.027	^{65}0.014	^{70}0.006	^{151}0.158	^{95}0.068	^{83}0.036	^{53}0.922	^{45}0.718	^{40}0.373	^{92}0.035	^{61}0.011	^{105}0.990	^{101}0.537	^{100}0.362	^{53}0.134
279	VOCORD-003	^{227}0.354	^{209}0.122	^{202}0.048	^{172}0.195	^{180}0.155	^{178}0.093	^{152}0.999	^{158}0.998	^{161}0.991	^{158}0.157	^{168}0.105			^{108}0.404	^{129}0.289
280	VOCORD-004	^{268}0.826	^{252}0.355	^{203}0.051	^{219}0.401	^{190}0.173	^{176}0.093	^{201}1.000	^{202}1.000	^{208}0.999	^{166}0.193	^{150}0.065			^{189}0.991	^{183}0.776
281	VOCORD-005	^{261}0.689	^{222}0.158	^{195}0.044	^{153}0.161	^{163}0.130	^{165}0.080	^{157}0.999	^{150}0.997	^{131}0.968	^{153}0.138	^{162}0.090			^{103}0.381	^{127}0.287
282	VOCORD-006	^{290}1.000	^{293}1.000	^{292}1.000	^{293}1.000	^{286}1.000	^{283}1.000	^{291}1.000	^{259}1.000	^{246}1.000	^{260}1.000	^{244}1.000			^{252}1.000	^{263}1.000
283	VTS-000	^{253}0.605	^{269}0.598	^{277}0.595	^{241}0.624	^{259}0.619	^{268}0.613	^{163}0.999	^{176}0.999	^{204}0.998	^{195}0.613	^{197}0.609	^{100}0.760	^{107}0.739	^{150}0.761	^{180}0.749
284	VTS-001	^{64}0.035	^{62}0.013	^{63}0.006	^{63}0.067	^{66}0.051	^{64}0.031	^{140}0.998	^{129}0.994	^{49}0.510	^{62}0.022	^{67}0.012	^{44}0.141	^{52}0.079	^{57}0.192	^{48}0.126
285	VTS-002	^{97}0.053	^{105}0.026	^{105}0.010	^{97}0.098	^{104}0.075	^{106}0.046	^{181}1.000	^{186}1.000	^{124}0.953	^{106}0.045	^{113}0.026	^{22}0.231	^{79}0.133	^{110}0.417	^{89}0.187
286	XFORWARDAI-000	^{55}0.029	^{71}0.015	^{72}0.006	^{67}0.070	^{74}0.053	^{80}0.034	^{32}0.698	^{21}0.440	^{27}0.250	^{58}0.021	^{56}0.011	^{53}0.159	^{56}0.082	^{46}0.169	^{52}0.134
287	XFORWARDAI-001	^{22}0.010	^{29}0.005	^{37}0.003	^{32}0.036	^{36}0.028	^{37}0.020	^{44}0.838	^{22}0.448	^{10}0.143	^{26}0.008	^{32}0.005	^{22}0.062	^{23}0.030	^{24}0.123	^{29}0.102
288	XFORWARDAI-002	^{14}0.007	^{18}0.003	^{25}0.002	^{15}0.018	^{15}0.016	^{18}0.014	^{72}0.975	^{27}0.525	^{2}0.095	^{12}0.005	^{13}0.003	^{13}0.041	^{11}0.018	^{13}0.099	^{18}0.089
289	YISHENG-001	^{238}0.452	^{249}0.346	^{255}0.206	^{271}0.983	^{267}0.808	^{243}0.269				^{197}0.666	^{191}0.396			^{174}0.919	^{174}0.695
290	YITU-002	^{59}0.031	^{78}0.018	^{82}0.008	^{53}0.063	^{61}0.049	^{59}0.028									
291	YITU-003	^{60}0.032	^{86}0.019	^{90}0.009	^{61}0.067	^{70}0.052	^{76}0.033									
292	YITU-004	^{35}0.019	^{45}0.010	^{50}0.004	^{31}0.035	^{32}0.027	^{31}0.017	^{64}0.948	^{71}0.936	^{102}0.913						
293	YITU-005	^{39}0.022	^{52}0.010	^{55}0.005	^{35}0.039	^{41}0.032	^{46}0.023									

Table 35: **Threshold-based accuracy**. *Values are FNIR(N, T, L) with N = 1.6 million with thresholds set to produce FPIR = 0.0003, 0.001, and 0.01 in non-mate searches. Throughout blue superscripts indicate the rank of the algorithm for that column. Caution: The Power-low models are mostly intended to draw attention to the kind of behavior, not as a model to be used for prediction.*

Appendices

Appendix A Accuracy on large-population FRVT 2018 mugshots

This publication is available free of charge from: https://doi.org/10.6028/NIST.IR.8271

2022/06/13	FNIR(N, R, T) =	False neg. identification rate	N = Num. enrolled subjects	T = Threshold	$T = 0 \rightarrow$ Investigation
18:09:57	FPIR(N, T) =	False pos. identification rate	R = Num. candidates examined		$T > 0 \rightarrow$ Identification

This publication is available free of charge from: https://doi.org/10.6028/NIST.IR.8271

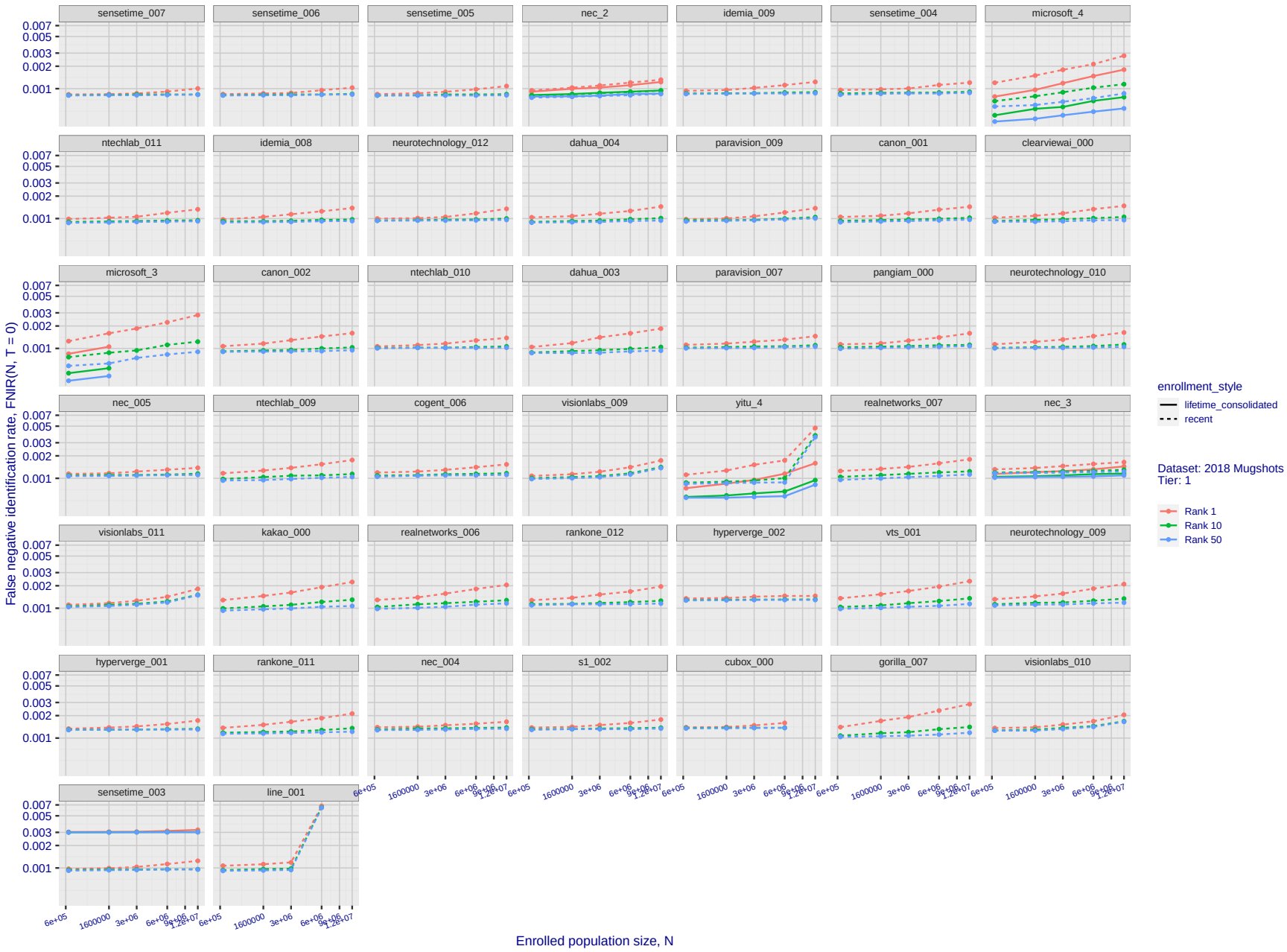

Figure 20: **[FRVT-2018 Mugshot Dataset] Rank-based identification miss rates vs. number of enrolled subjects**. *The figure shows false negative identification rates, FNIR(N, R), across various gallery sizes and ranks 1, 10 and 50. The threshold is set to zero, so this metric rewards even weak scoring rank 1 mates. This also means FPIR = 1, so any search without an enrolled mate will return non-mated candidates. For clarity, results are sorted and reported into tiers spanning multiple pages, the tiering criteria being rank 1 hit rate on a gallery size of 640 000.*

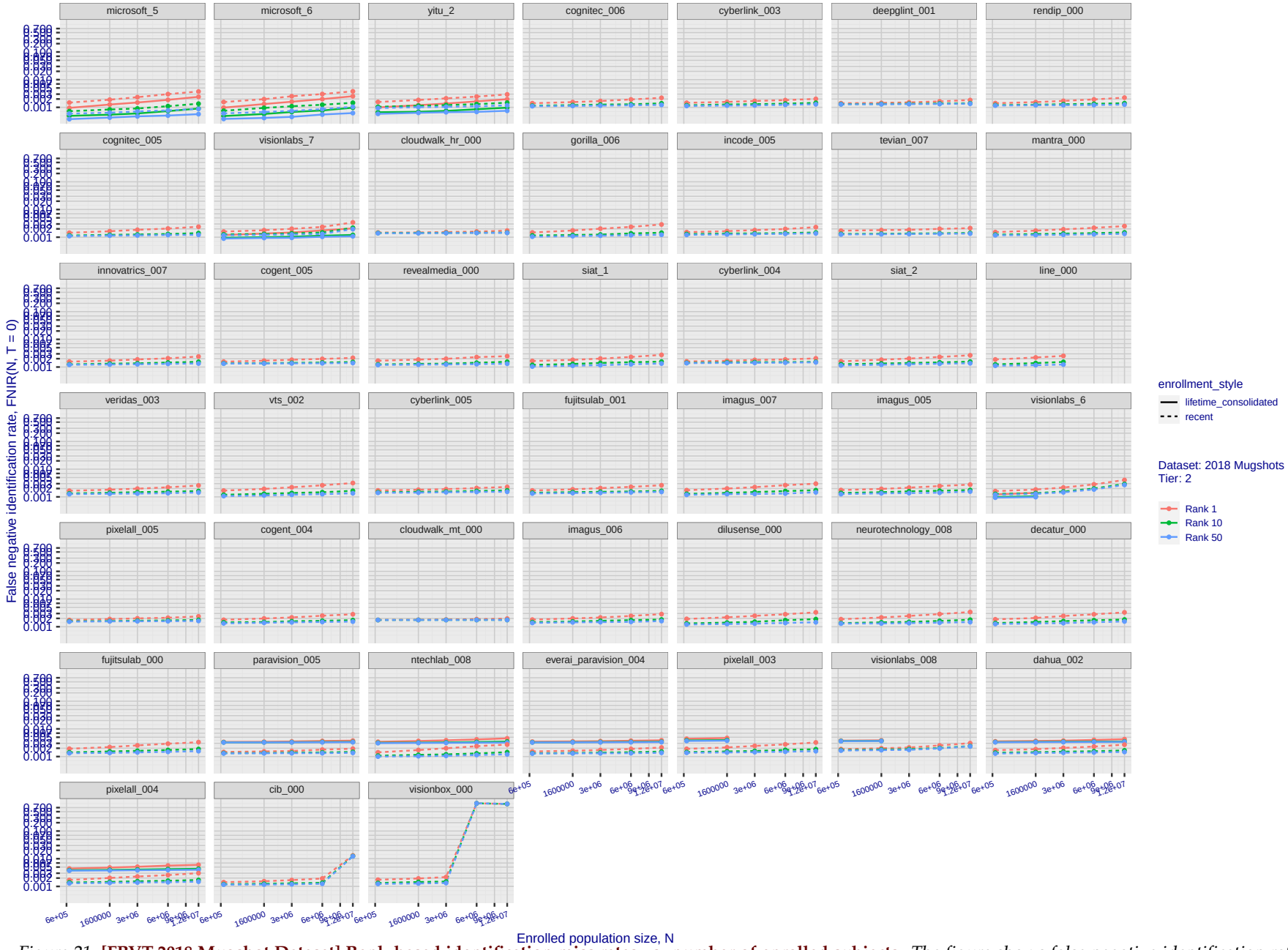

Figure 21: **[FRVT-2018 Mugshot Dataset] Rank-based identification miss rates vs. number of enrolled subjects**. *The figure shows false negative identification rates, FNIR(N, R), across various gallery sizes and ranks 1, 10 and 50. The threshold is set to zero, so this metric rewards even weak scoring rank 1 mates. This also means FPIR = 1, so any search without an enrolled mate will return non-mated candidates. For clarity, results are sorted and reported into tiers spanning multiple pages, the tiering criteria being rank 1 hit rate on a gallery size of 640 000.*

This publication is available free of charge from: https://doi.org/10.6028/NIST.IR.8271

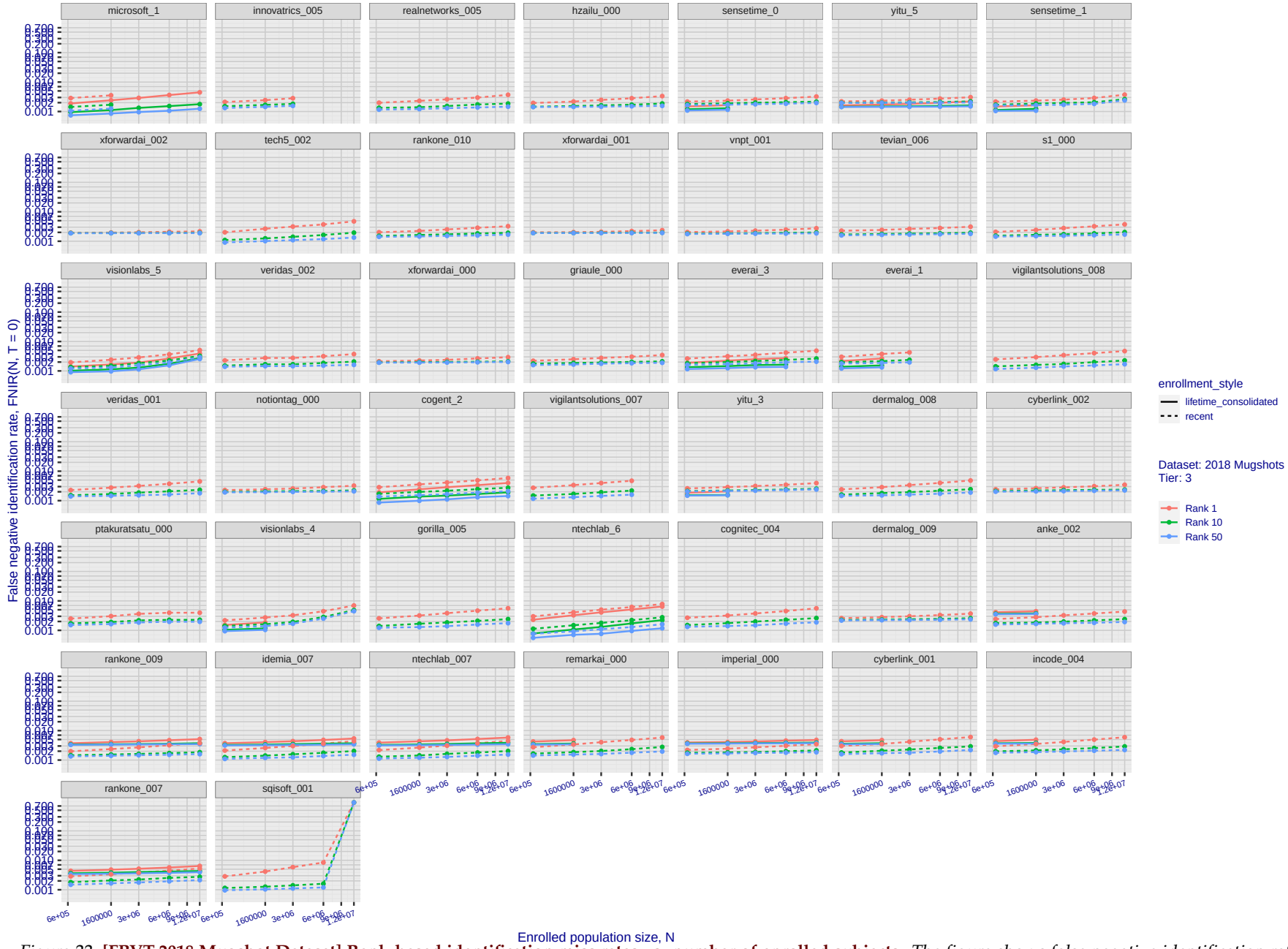

Figure 22: **[FRVT-2018 Mugshot Dataset] Rank-based identification miss rates vs. number of enrolled subjects**. *The figure shows false negative identification rates, FNIR(N, R), across various gallery sizes and ranks 1, 10 and 50. The threshold is set to zero, so this metric rewards even weak scoring rank 1 mates. This also means FPIR = 1, so any search without an enrolled mate will return non-mated candidates. For clarity, results are sorted and reported into tiers spanning multiple pages, the tiering criteria being rank 1 hit rate on a gallery size of 640 000.*

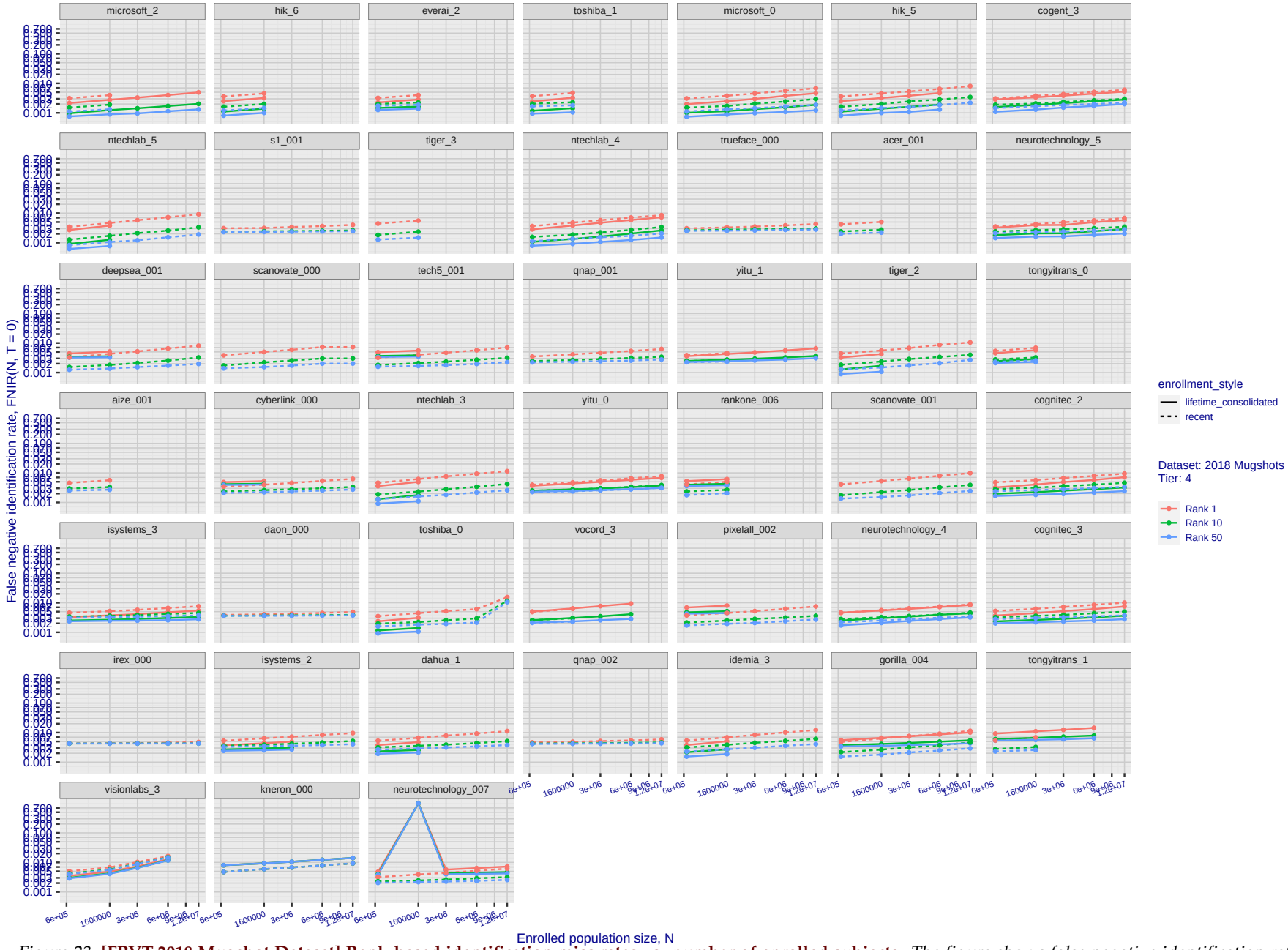

Figure 23: **[FRVT-2018 Mugshot Dataset] Rank-based identification miss rates vs. number of enrolled subjects**. *The figure shows false negative identification rates, FNIR(N, R), across various gallery sizes and ranks 1, 10 and 50. The threshold is set to zero, so this metric rewards even weak scoring rank 1 mates. This also means FPIR = 1, so any search without an enrolled mate will return non-mated candidates. For clarity, results are sorted and reported into tiers spanning multiple pages, the tiering criteria being rank 1 hit rate on a gallery size of 640 000.*

This publication is available free of charge from: https://doi.org/10.6028/NIST.IR.8271

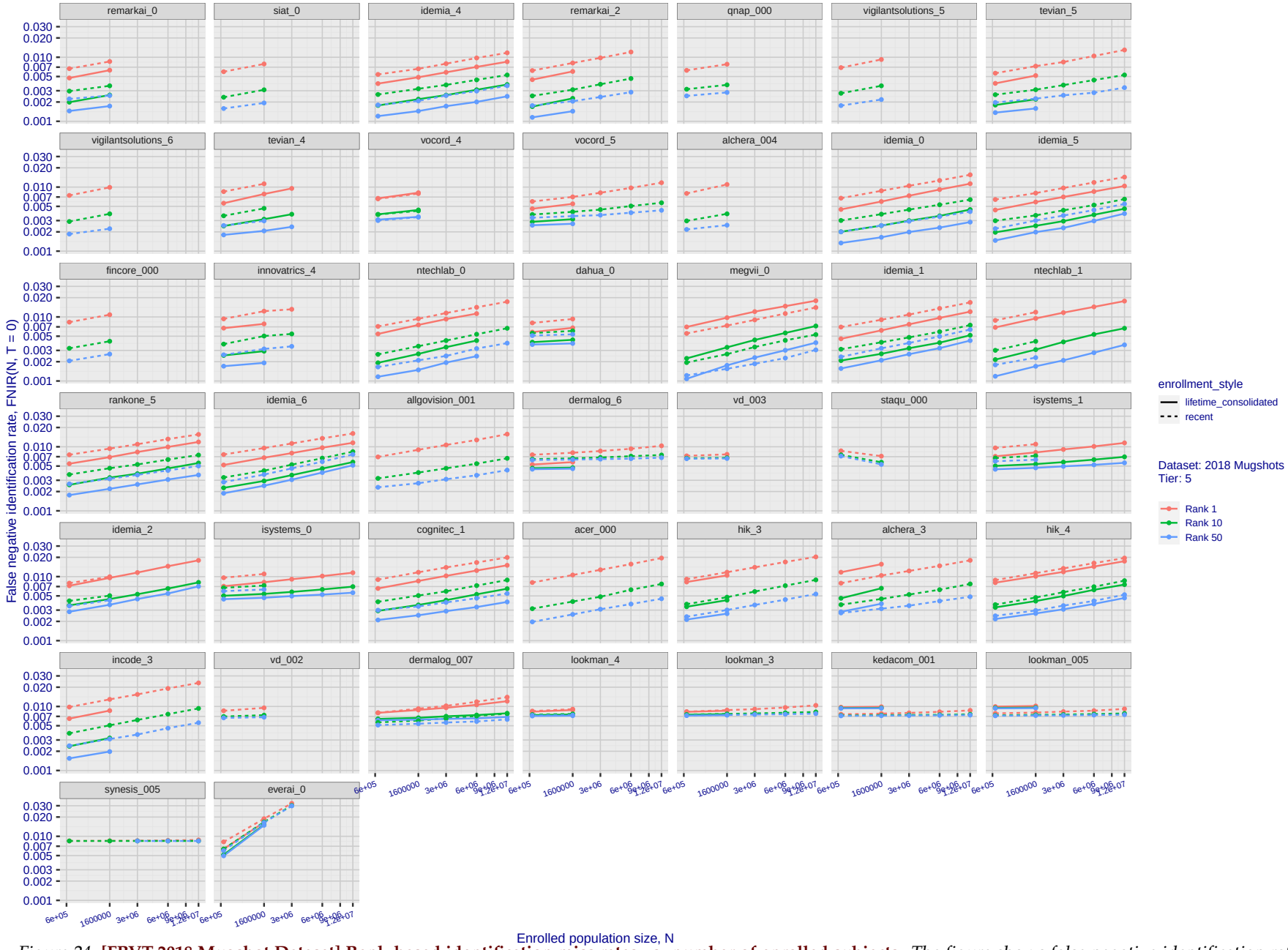

Figure 24: **[FRVT-2018 Mugshot Dataset] Rank-based identification miss rates vs. number of enrolled subjects**. *The figure shows false negative identification rates, FNIR(N, R), across various gallery sizes and ranks 1, 10 and 50. The threshold is set to zero, so this metric rewards even weak scoring rank 1 mates. This also means FPIR = 1, so any search without an enrolled mate will return non-mated candidates. For clarity, results are sorted and reported into tiers spanning multiple pages, the tiering criteria being rank 1 hit rate on a gallery size of 640 000.*

This publication is available free of charge from: https://doi.org/10.6028/NIST.IR.8271

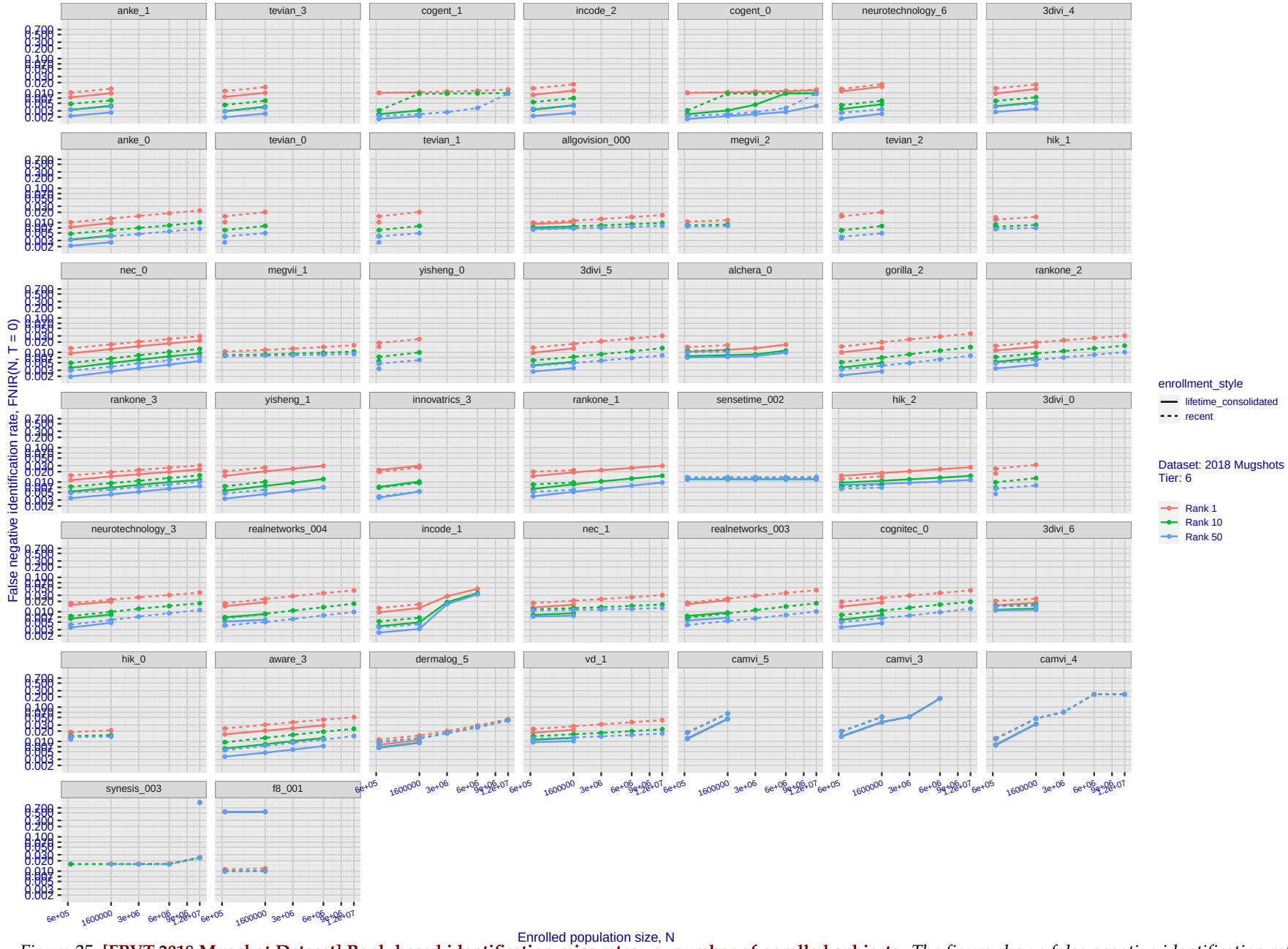

Figure 25: **[FRVT-2018 Mugshot Dataset] Rank-based identification miss rates vs. number of enrolled subjects**. *The figure shows false negative identification rates, FNIR(N, R), across various gallery sizes and ranks 1, 10 and 50. The threshold is set to zero, so this metric rewards even weak scoring rank 1 mates. This also means FPIR = 1, so any search without an enrolled mate will return non-mated candidates. For clarity, results are sorted and reported into tiers spanning multiple pages, the tiering criteria being rank 1 hit rate on a gallery size of 640 000.*

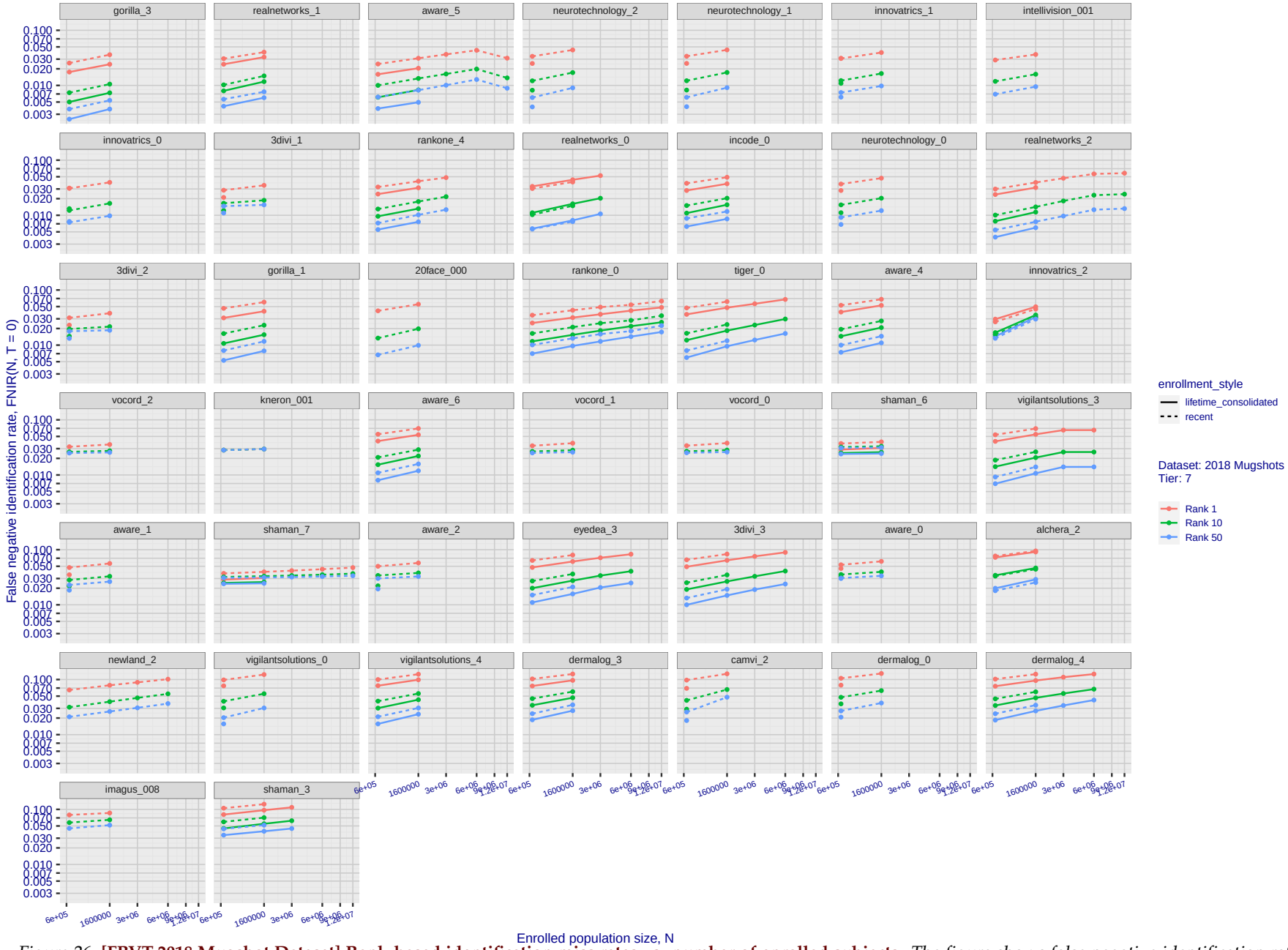

Figure 26: **[FRVT-2018 Mugshot Dataset] Rank-based identification miss rates vs. number of enrolled subjects**. *The figure shows false negative identification rates, FNIR(N, R), across various gallery sizes and ranks 1, 10 and 50. The threshold is set to zero, so this metric rewards even weak scoring rank 1 mates. This also means FPIR = 1, so any search without an enrolled mate will return non-mated candidates. For clarity, results are sorted and reported into tiers spanning multiple pages, the tiering criteria being rank 1 hit rate on a gallery size of 640 000.*

This publication is available free of charge from: https://doi.org/10.6028/NIST.IR.8271

2022/06/13
18:09:57

FNIR(N, R, T) = False neg. identification rate
FPIR(N, T) = False pos. identification rate

N = Num. enrolled subjects
R = Num. candidates examined

T = Threshold

T = 0 → Investigation
T > 0 → Identification

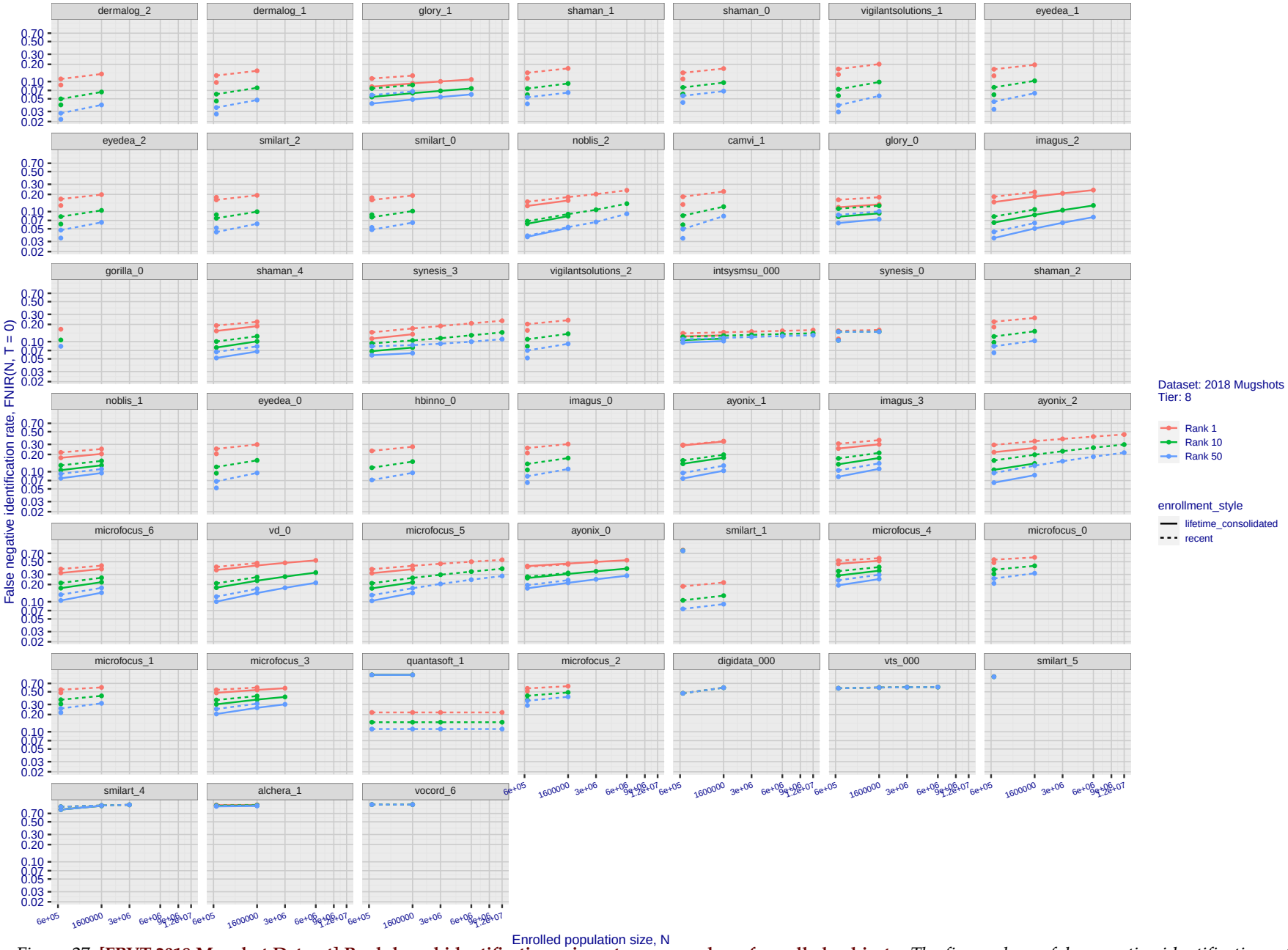

Figure 27: **[FRVT-2018 Mugshot Dataset] Rank-based identification miss rates vs. number of enrolled subjects**. *The figure shows false negative identification rates, FNIR(N, R), across various gallery sizes and ranks 1, 10 and 50. The threshold is set to zero, so this metric rewards even weak scoring rank 1 mates. This also means FPIR = 1, so any search without an enrolled mate will return non-mated candidates. For clarity, results are sorted and reported into tiers spanning multiple pages, the tiering criteria being rank 1 hit rate on a gallery size of 640 000.*

2022/06/13	FNIR(N, R, T) =	False neg. identification rate	N = Num. enrolled subjects	T = Threshold	$T = 0 \rightarrow$ Investigation
18:09:57	FPIR(N, T) =	False pos. identification rate	R = Num. candidates examined		$T > 0 \rightarrow$ Identification

This publication is available free of charge from: https://doi.org/10.6028/NIST.IR.8271

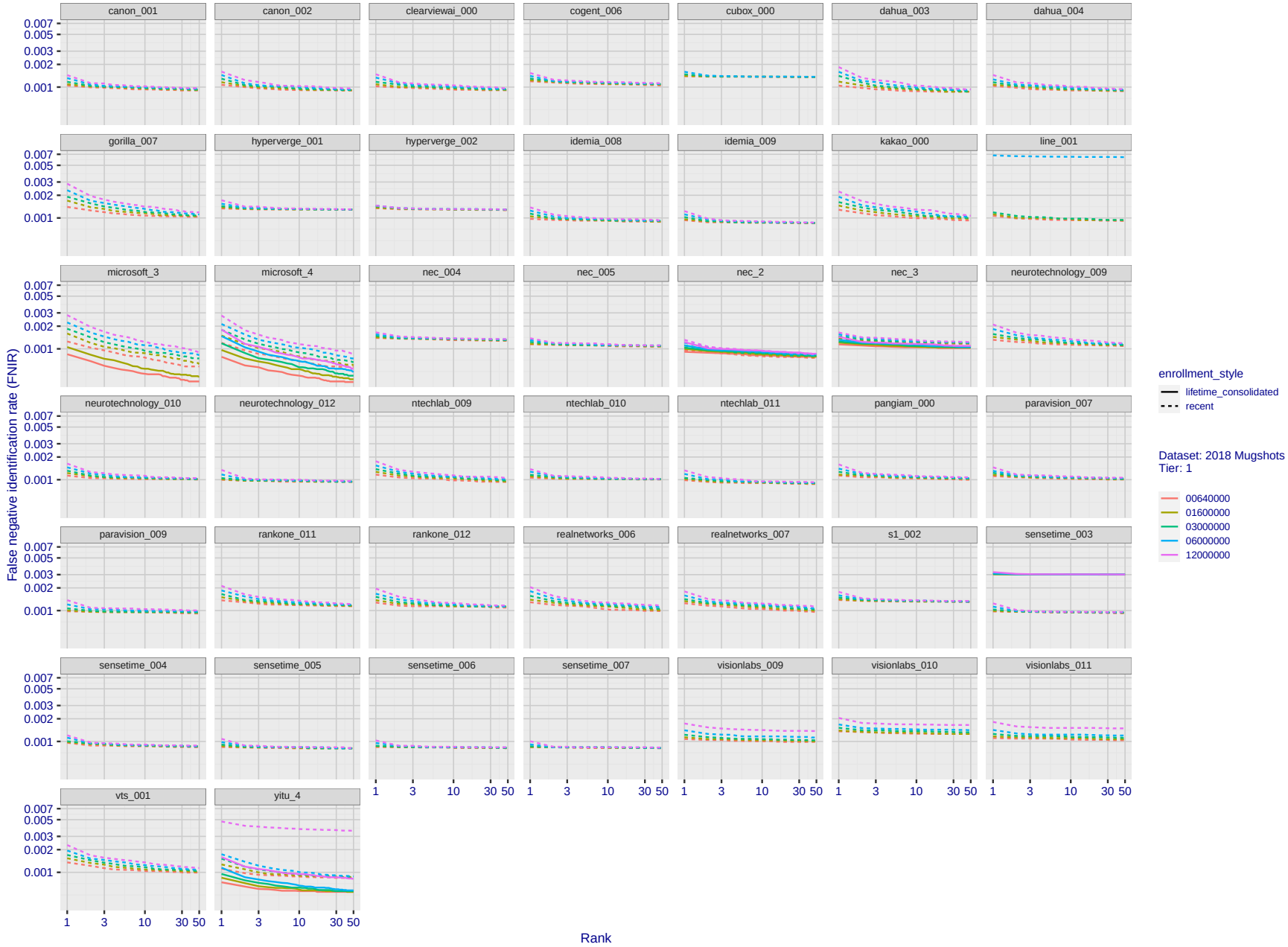

Figure 28: **[FRVT-2018 Mugshot Dataset] Rank-based identification miss rates vs. rank**. *The figure shows false negative identification rates (FNIR) for ranks up to 50. This metric is appropriate to investigational applications where human reviewers will adjudicate sorted candidate lists. Note that with threshold set to zero, FPIR = 1, i.e. any search without an enrolled mate will return non-mated candidates. Results are sorted and reported into tiers for clarity, with the tiering criteria being rank 1 hit rate on a gallery size of N = 640 000 subjects.*

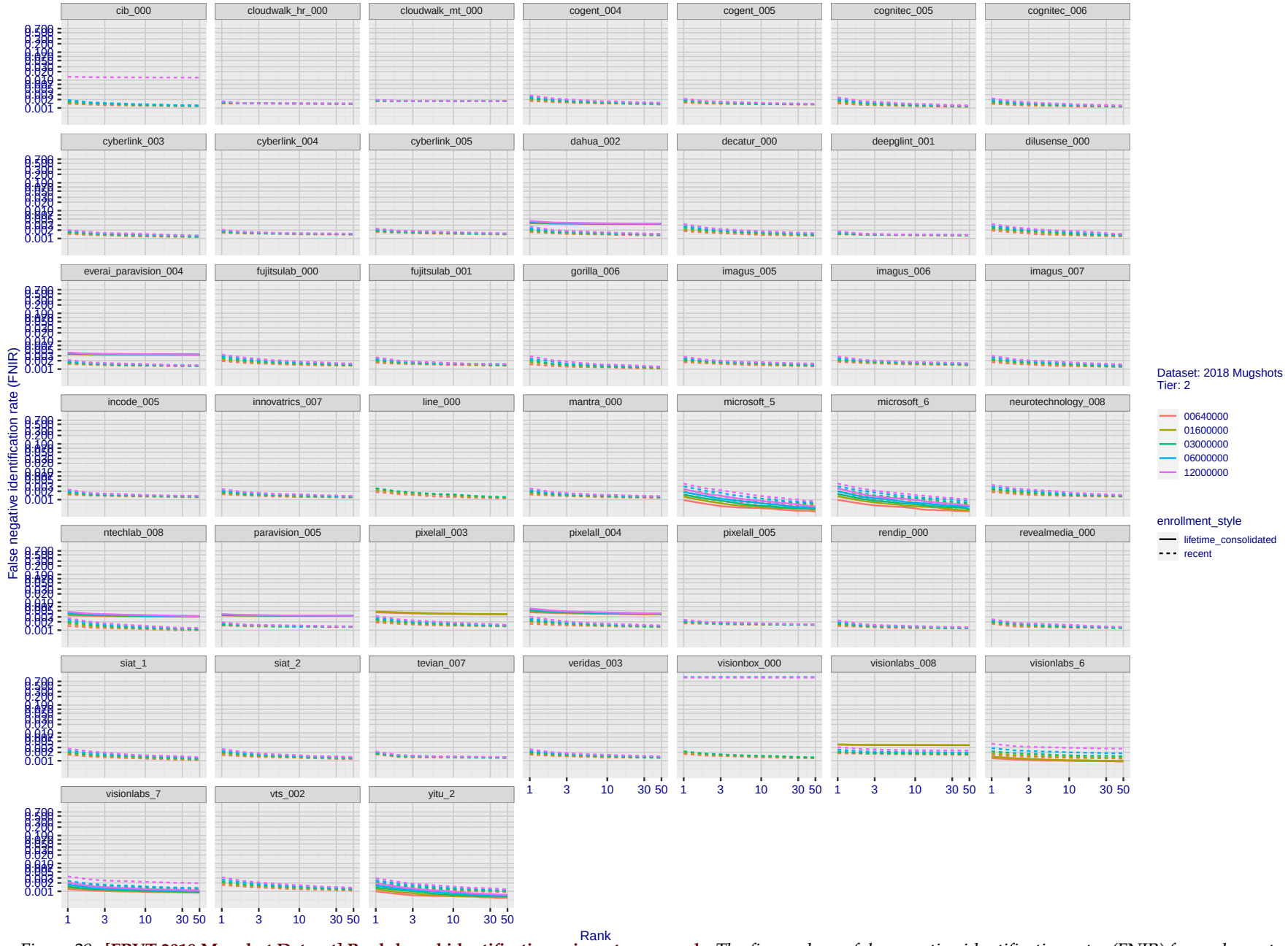

Figure 29: **[FRVT-2018 Mugshot Dataset] Rank-based identification miss rates vs. rank**. *The figure shows false negative identification rates (FNIR) for ranks up to 50. This metric is appropriate to investigational applications where human reviewers will adjudicate sorted candidate lists. Note that with threshold set to zero, FPIR = 1, i.e. any search without an enrolled mate will return non-mated candidates. Results are sorted and reported into tiers for clarity, with the tiering criteria being rank 1 hit rate on a gallery size of N = 640 000 subjects.*

This publication is available free of charge from: https://doi.org/10.6028/NIST.IR.8271

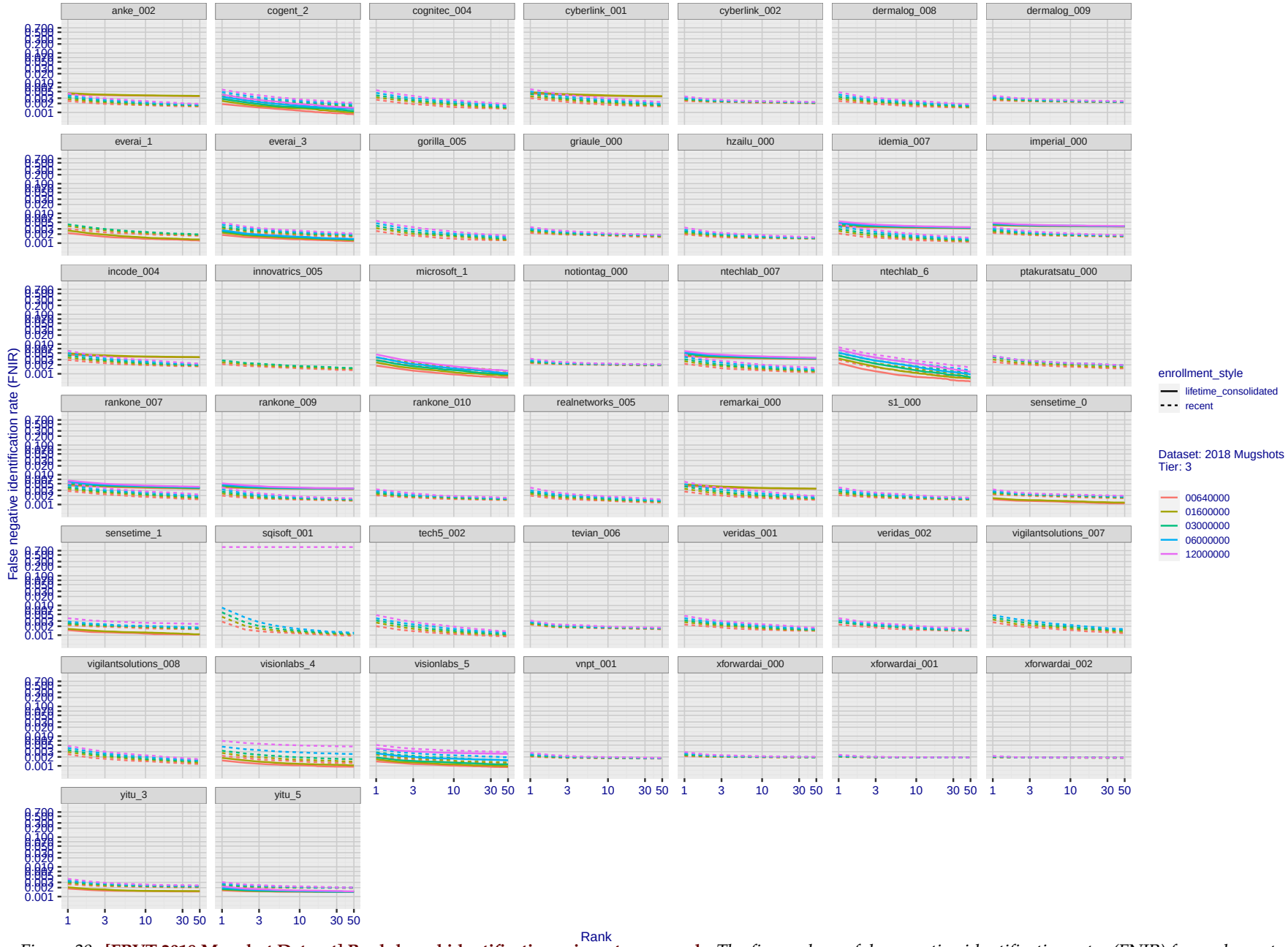

Figure 30: **[FRVT-2018 Mugshot Dataset] Rank-based identification miss rates vs. rank**. *The figure shows false negative identification rates (FNIR) for ranks up to 50. This metric is appropriate to investigational applications where human reviewers will adjudicate sorted candidate lists. Note that with threshold set to zero, FPIR = 1, i.e. any search without an enrolled mate will return non-mated candidates. Results are sorted and reported into tiers for clarity, with the tiering criteria being rank 1 hit rate on a gallery size of N = 640 000 subjects.*

This publication is available free of charge from: https://doi.org/10.6028/NIST.IR.8271

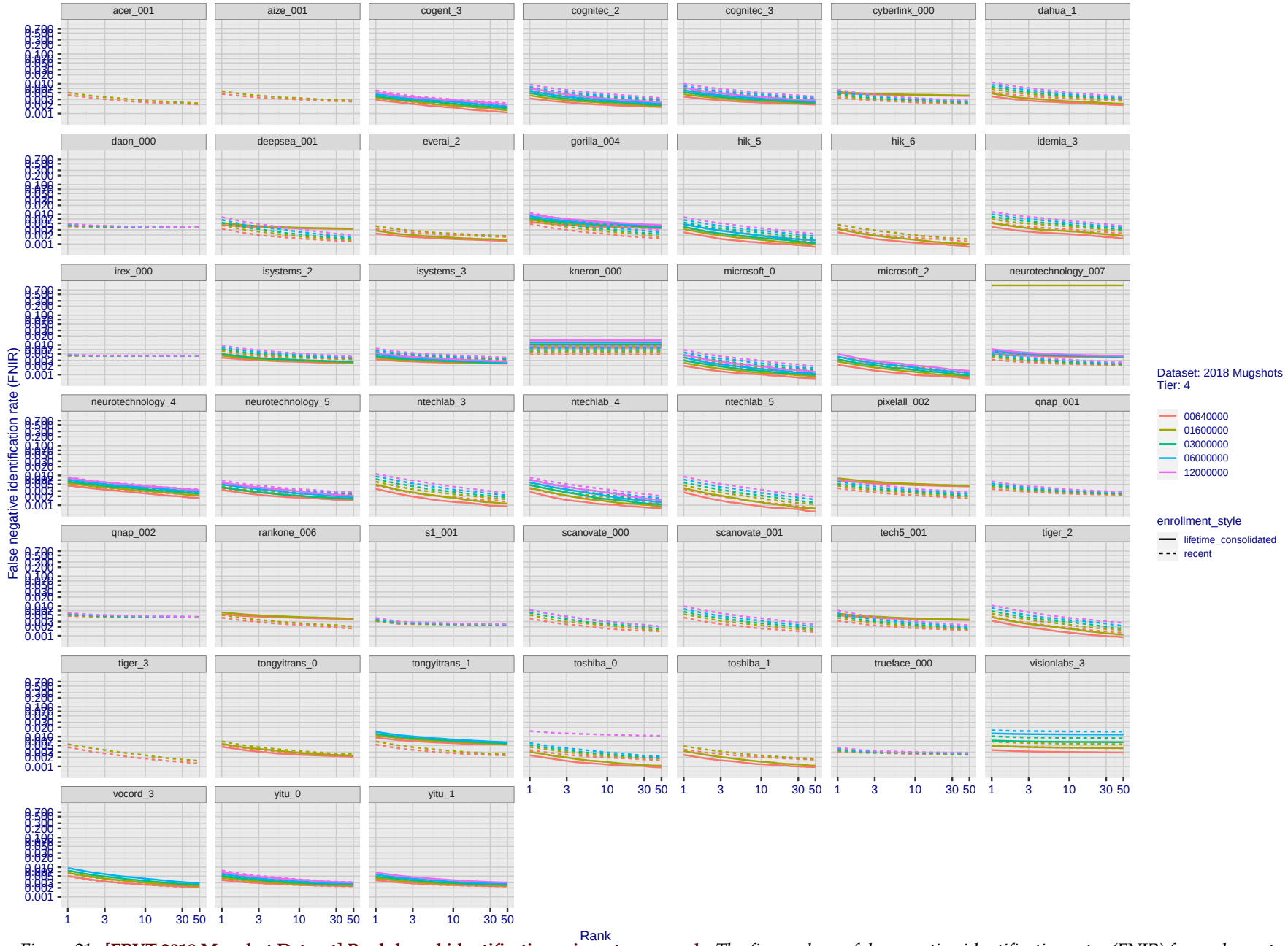

Figure 31: **[FRVT-2018 Mugshot Dataset] Rank-based identification miss rates vs. rank**. *The figure shows false negative identification rates (FNIR) for ranks up to 50. This metric is appropriate to investigational applications where human reviewers will adjudicate sorted candidate lists. Note that with threshold set to zero, FPIR = 1, i.e. any search without an enrolled mate will return non-mated candidates. Results are sorted and reported into tiers for clarity, with the tiering criteria being rank 1 hit rate on a gallery size of N = 640 000 subjects.*

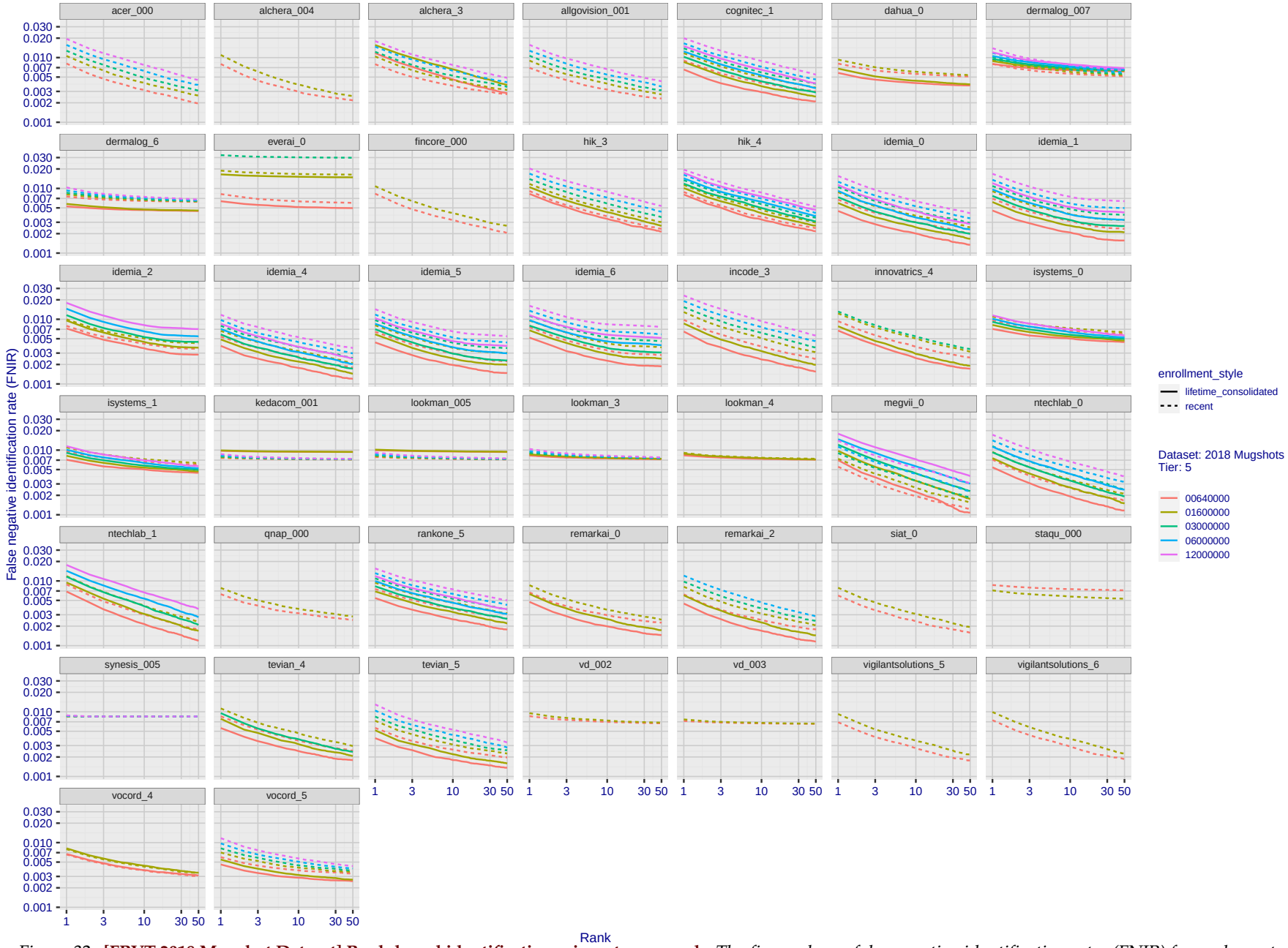

Figure 32: **[FRVT-2018 Mugshot Dataset] Rank-based identification miss rates vs. rank**. *The figure shows false negative identification rates (FNIR) for ranks up to 50. This metric is appropriate to investigational applications where human reviewers will adjudicate sorted candidate lists. Note that with threshold set to zero, FPIR = 1, i.e. any search without an enrolled mate will return non-mated candidates. Results are sorted and reported into tiers for clarity, with the tiering criteria being rank 1 hit rate on a gallery size of N = 640 000 subjects.*

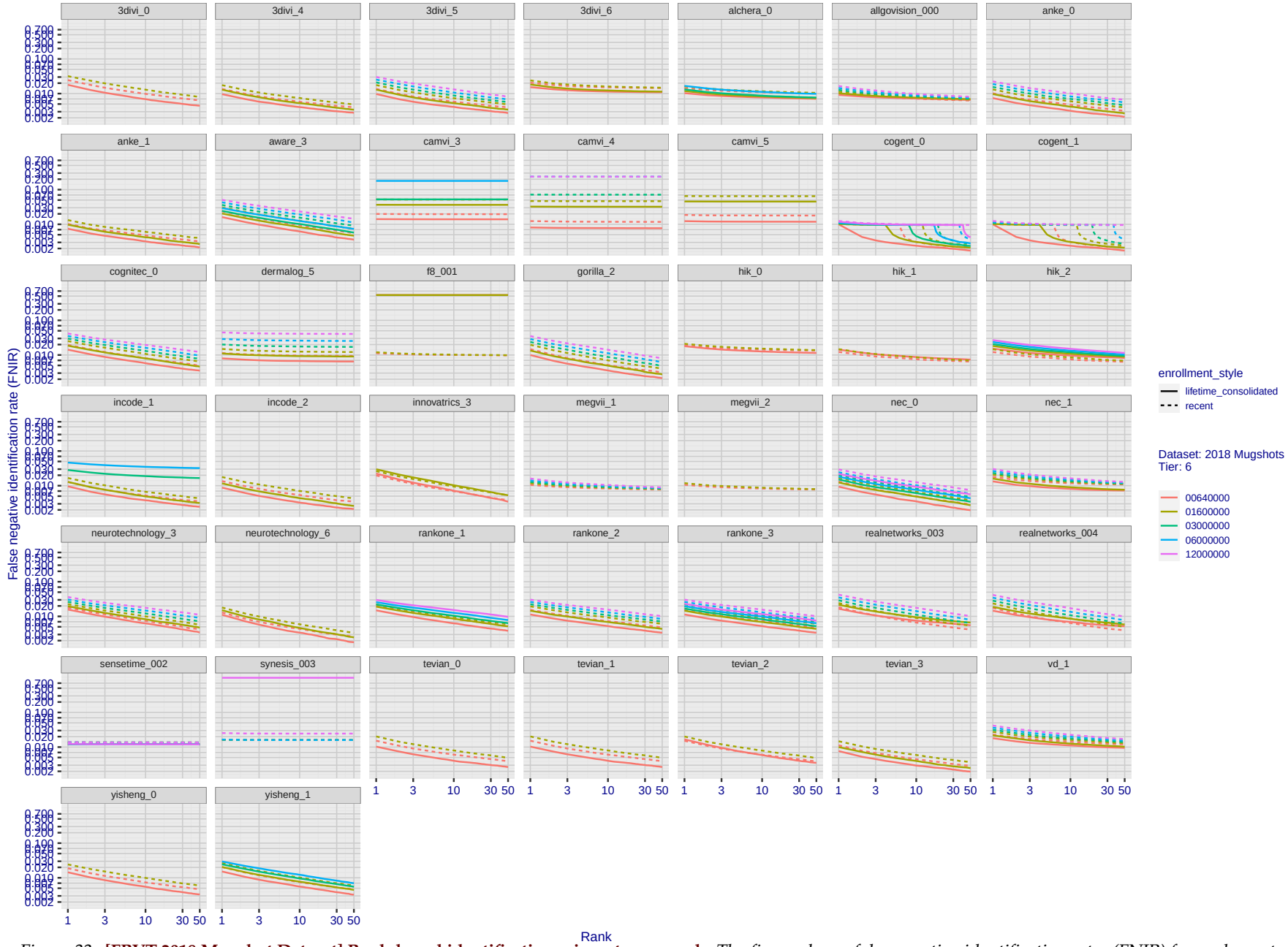

Figure 33: **[FRVT-2018 Mugshot Dataset] Rank-based identification miss rates vs. rank**. *The figure shows false negative identification rates (FNIR) for ranks up to 50. This metric is appropriate to investigational applications where human reviewers will adjudicate sorted candidate lists. Note that with threshold set to zero, FPIR = 1, i.e. any search without an enrolled mate will return non-mated candidates. Results are sorted and reported into tiers for clarity, with the tiering criteria being rank 1 hit rate on a gallery size of N = 640 000 subjects.*

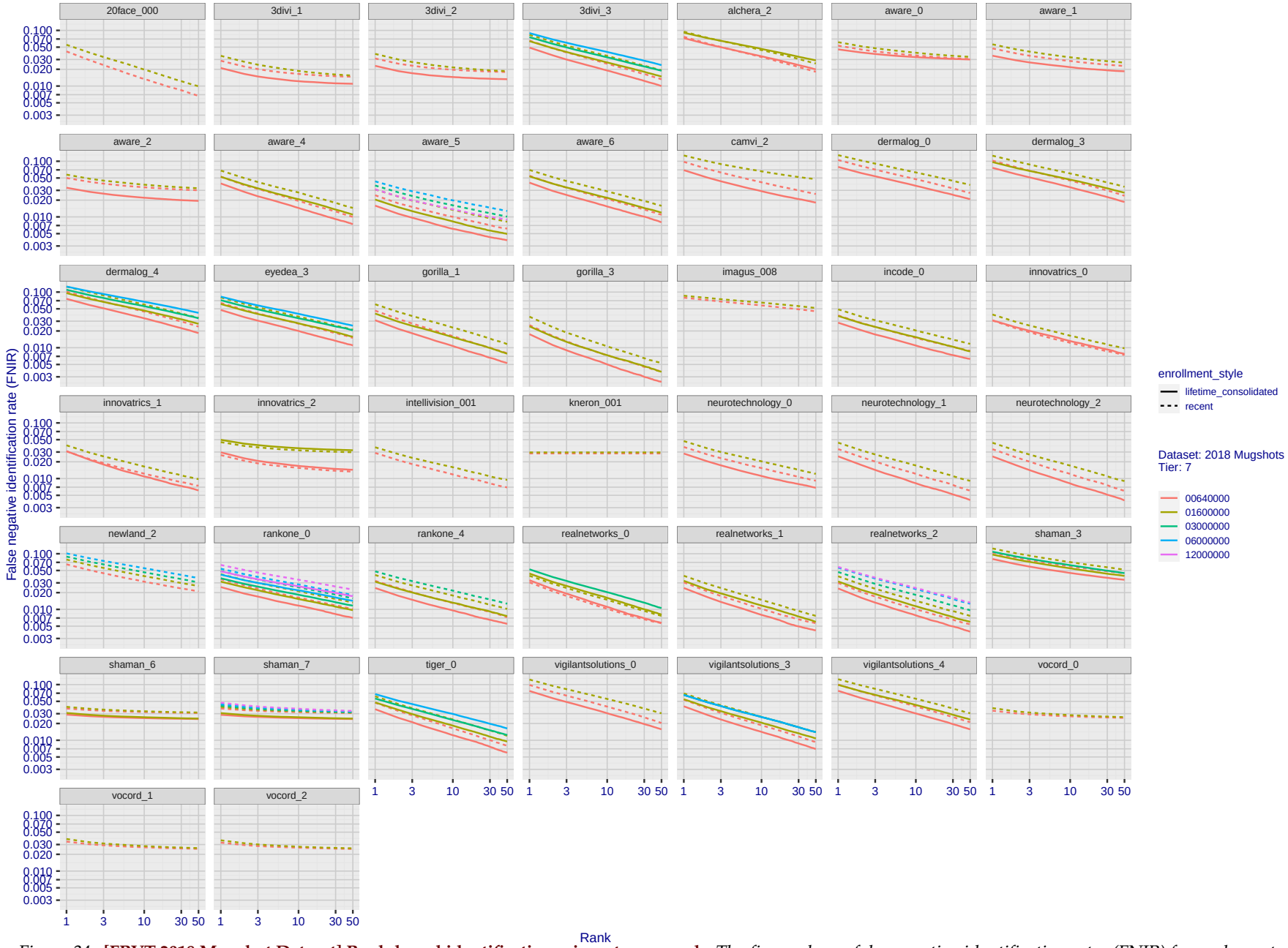

Figure 34: **[FRVT-2018 Mugshot Dataset] Rank-based identification miss rates vs. rank**. *The figure shows false negative identification rates (FNIR) for ranks up to 50. This metric is appropriate to investigational applications where human reviewers will adjudicate sorted candidate lists. Note that with threshold set to zero, FPIR = 1, i.e. any search without an enrolled mate will return non-mated candidates. Results are sorted and reported into tiers for clarity, with the tiering criteria being rank 1 hit rate on a gallery size of N = 640 000 subjects.*

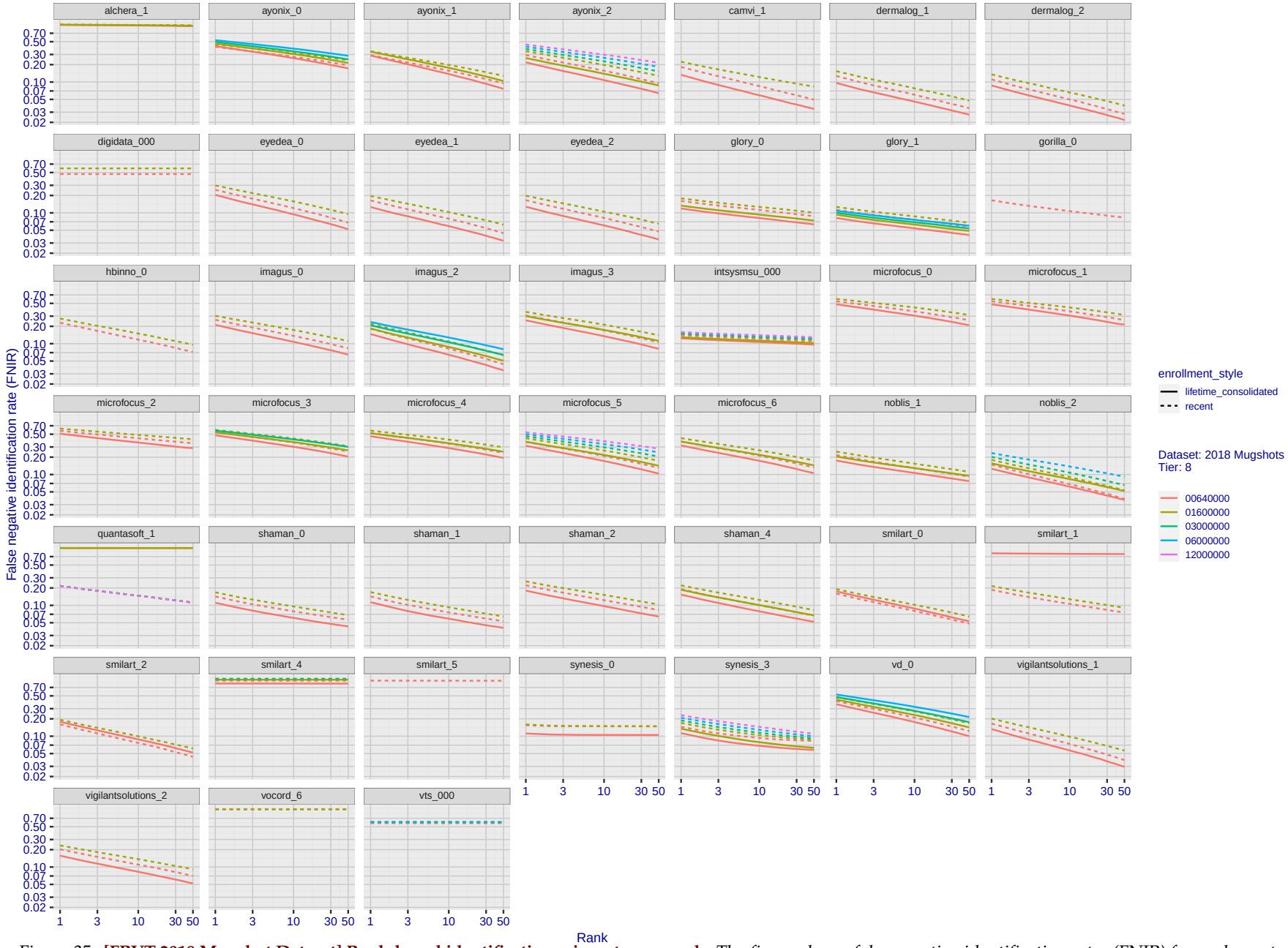

Figure 35: **[FRVT-2018 Mugshot Dataset] Rank-based identification miss rates vs. rank**. *The figure shows false negative identification rates (FNIR) for ranks up to 50. This metric is appropriate to investigational applications where human reviewers will adjudicate sorted candidate lists. Note that with threshold set to zero, FPIR = 1, i.e. any search without an enrolled mate will return non-mated candidates. Results are sorted and reported into tiers for clarity, with the tiering criteria being rank 1 hit rate on a gallery size of N = 640 000 subjects.*

2022/06/13	FNIR(N, R, T) =	False neg. identification rate	N = Num. enrolled subjects	T = Threshold	$T = 0 \rightarrow$ Investigation
18:09:57	FPIR(N, T) =	False pos. identification rate	R = Num. candidates examined		$T > 0 \rightarrow$ Identification

This publication is available free of charge from: https://doi.org/10.6028/NIST.IR.8271

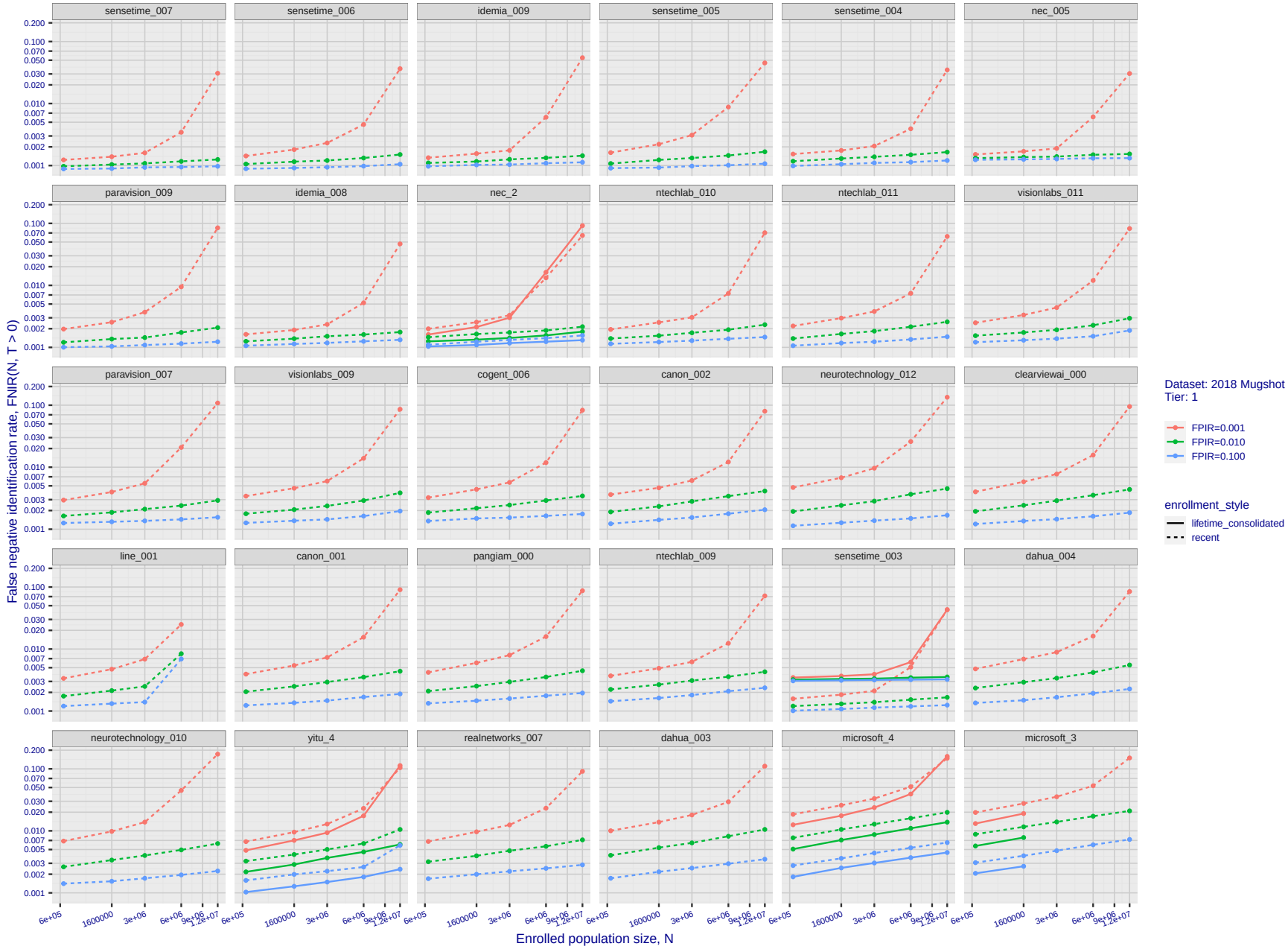

FNIR(N, R, T) = False neg. identification rate
FPIR(N, T) = False pos. identification rate
N = Num. enrolled subjects
R = Num. candidates examined
T = Threshold
T = 0 → Investigation
T > 0 → Identification

Figure 36: **[FRVT-2018 Mugshot Dataset] Threshold-based identification miss rates vs. number of enrolled subjects**. *The figure shows FNIR(N, T) across various gallery sizes when the threshold is set to achieve the given FPIRs. The rank criterion is irrelevant at high thresholds as mates are always at rank 1. The results are computed from the trials listed in rows 1-10 of Table 1. Less accurate algorithms were not run on large N, so results are missing. For clarity, results are sorted and reported into tiers spanning multiple pages. The tiering criteria is complicated: First paging by FNIR(N_b, 1, 0), then sorting by median FNIR(N_b, T), N_b = 640 000.*

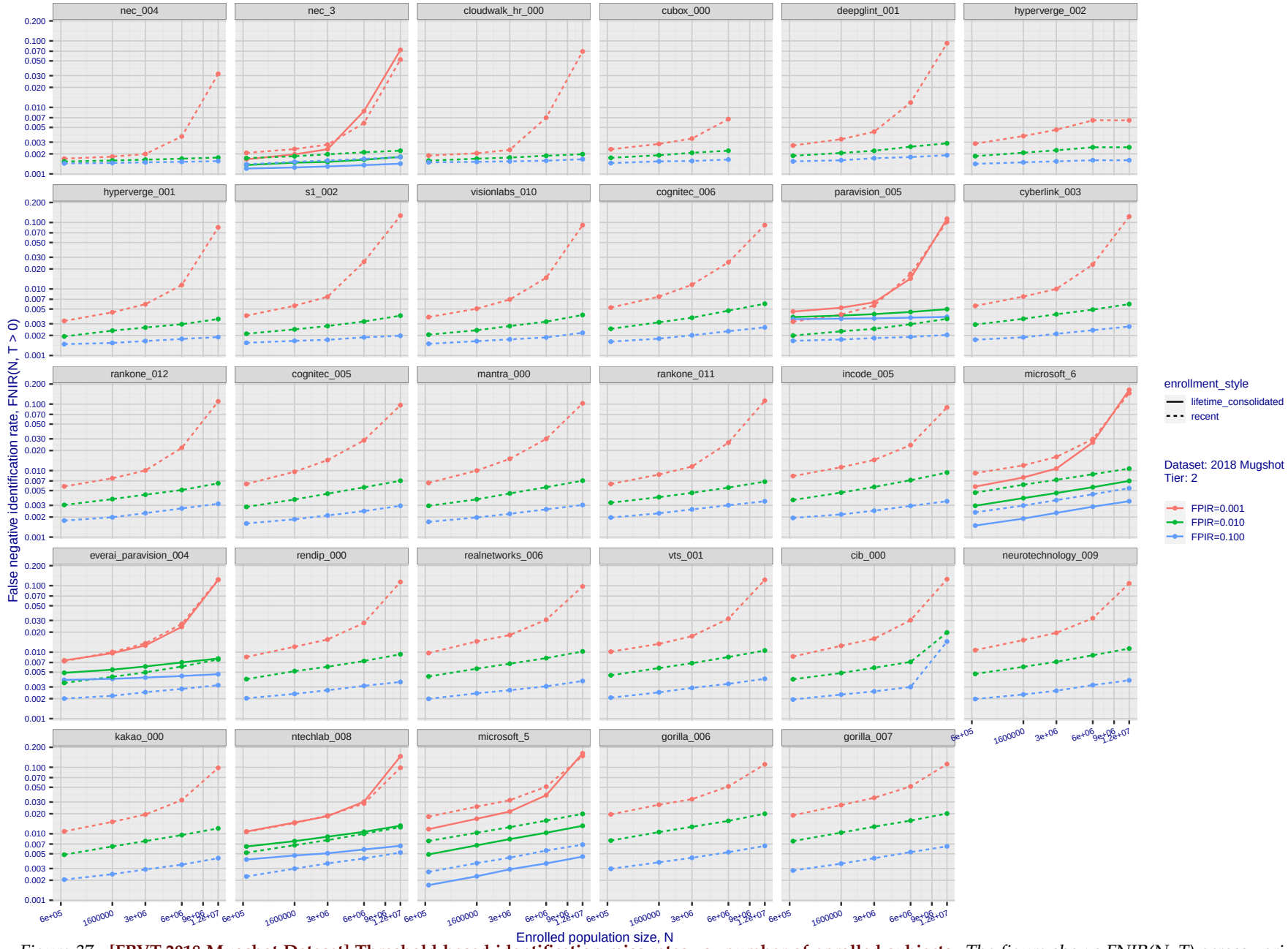

Figure 37: **[FRVT-2018 Mugshot Dataset] Threshold-based identification miss rates vs. number of enrolled subjects**. *The figure shows FNIR(N, T) across various gallery sizes when the threshold is set to achieve the given FPIRs. The rank criterion is irrelevant at high thresholds as mates are always at rank 1. The results are computed from the trials listed in rows 1-10 of Table 1. Less accurate algorithms were not run on large N, so results are missing. For clarity, results are sorted and reported into tiers spanning multiple pages. The tiering criteria is complicated: First paging by FNIR(N_b, 1, 0), then sorting by median FNIR(N_b, T), N_b = 640 000.*

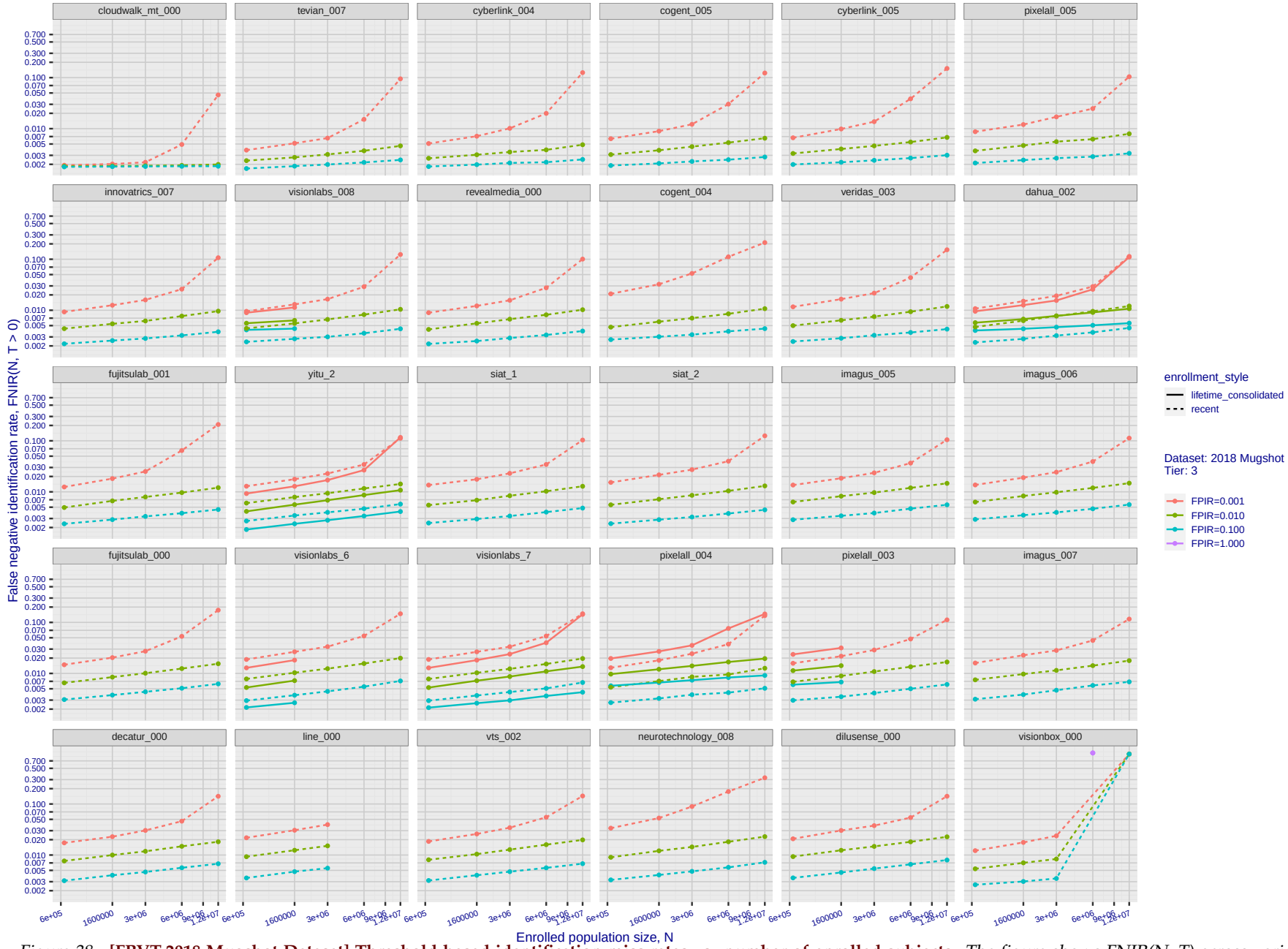

Figure 38: **[FRVT-2018 Mugshot Dataset] Threshold-based identification miss rates vs. number of enrolled subjects**. *The figure shows FNIR(N, T) across various gallery sizes when the threshold is set to achieve the given FPIRs. The rank criterion is irrelevant at high thresholds as mates are always at rank 1. The results are computed from the trials listed in rows 1-10 of Table 1. Less accurate algorithms were not run on large N, so results are missing. For clarity, results are sorted and reported into tiers spanning multiple pages. The tiering criteria is complicated: First paging by FNIR(N_b, 1, 0), then sorting by median FNIR(N_b, T), N_b = 640 000.*

This publication is available free of charge from: https://doi.org/10.6028/NIST.IR.8271

2022/06/13
18:09:57

FNIR(N, R, T) = False neg. identification rate
FPIR(N, T) = False pos. identification rate
N = Num. enrolled subjects
R = Num. candidates examined
T = Threshold
T = 0 → Investigation
T > 0 → Identification

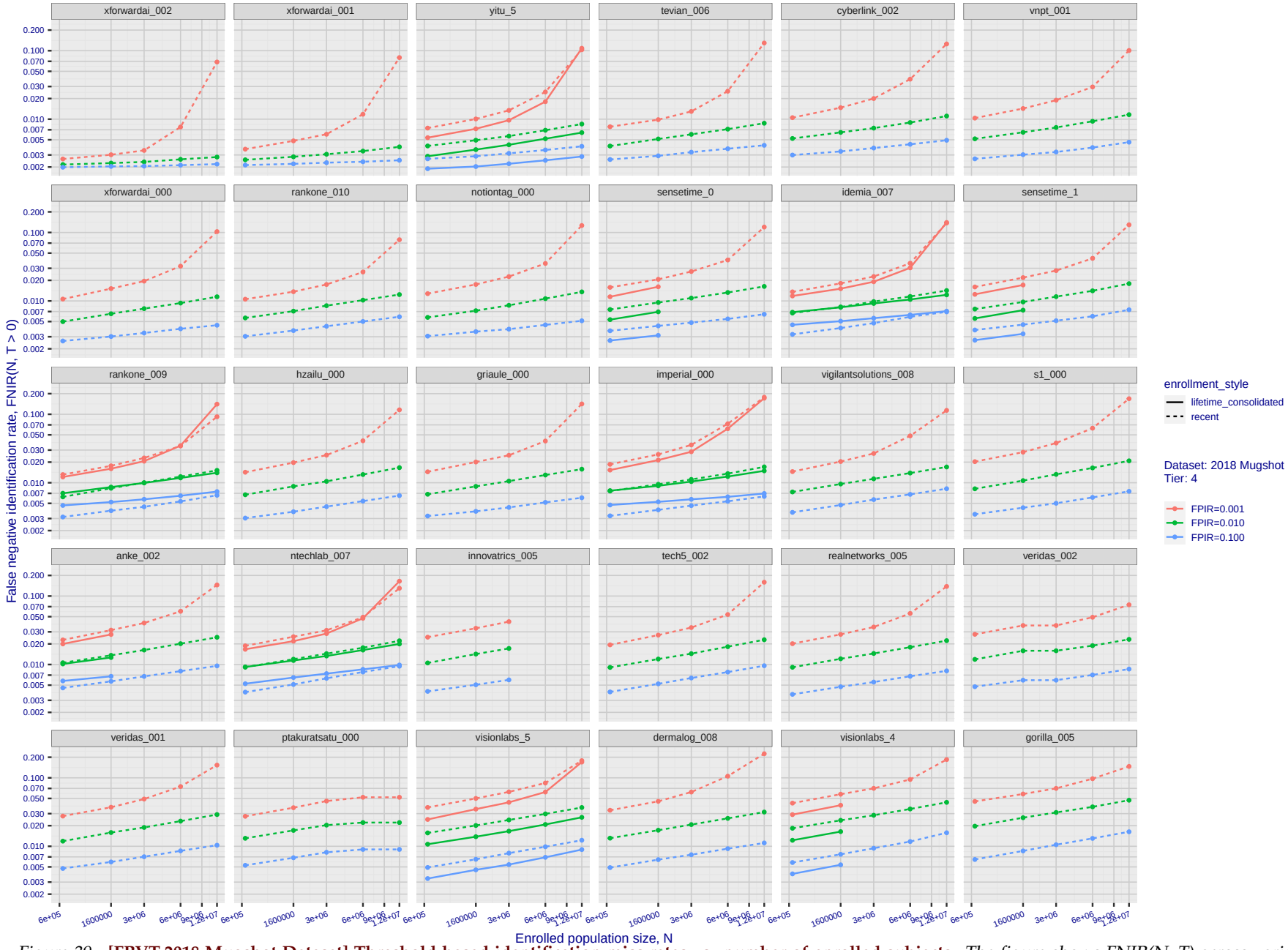

Figure 39: **[FRVT-2018 Mugshot Dataset] Threshold-based identification miss rates vs. number of enrolled subjects**. *The figure shows FNIR(N, T) across various gallery sizes when the threshold is set to achieve the given FPIRs. The rank criterion is irrelevant at high thresholds as mates are always at rank 1. The results are computed from the trials listed in rows 1-10 of Table 1. Less accurate algorithms were not run on large N, so results are missing. For clarity, results are sorted and reported into tiers spanning multiple pages. The tiering criteria is complicated: First paging by FNIR(N_b, 1, 0), then sorting by median FNIR(N_b, T), N_b = 640 000.*

This publication is available free of charge from: https://doi.org/10.6028/NIST.IR.8271

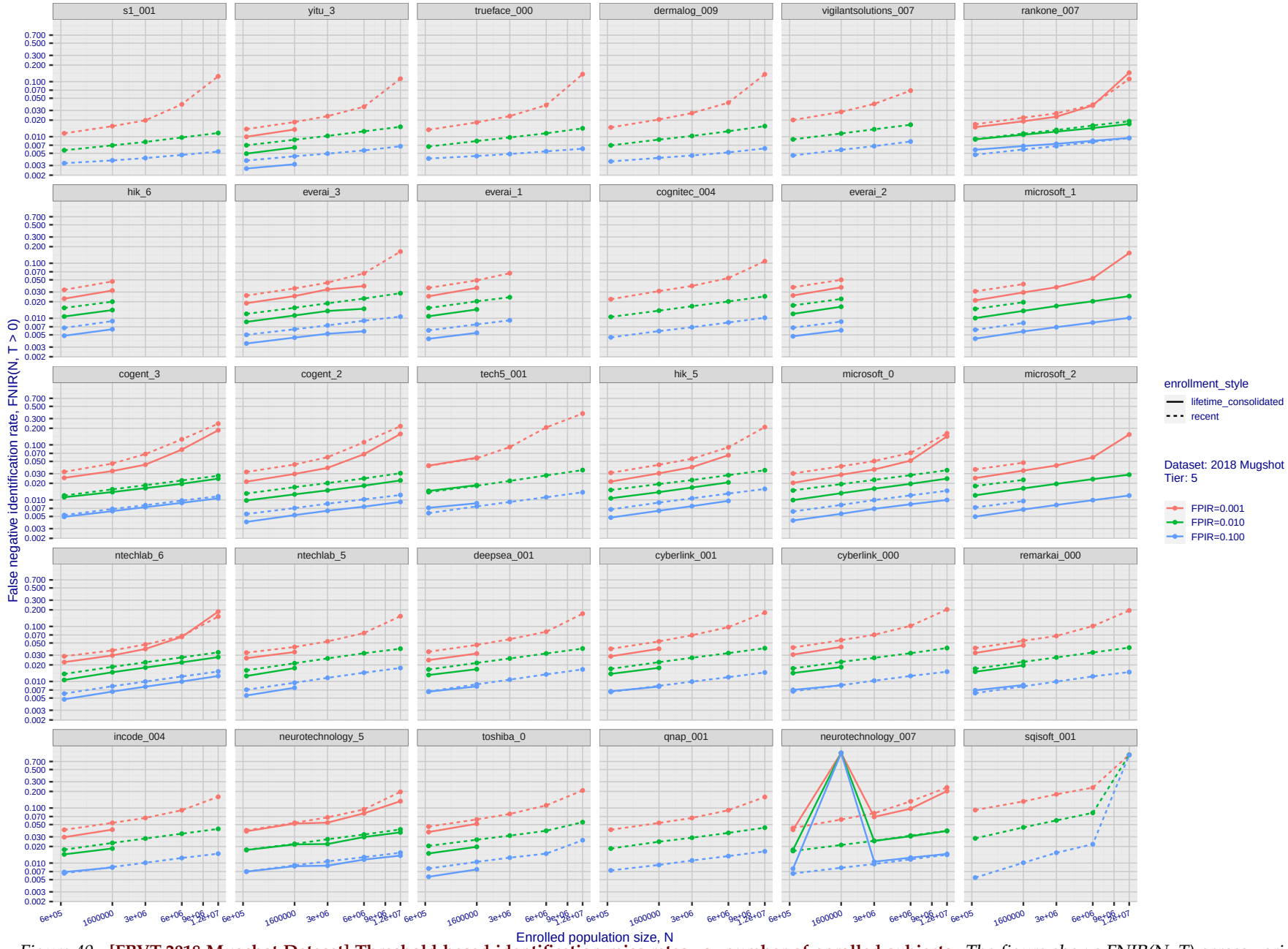

Figure 40: **[FRVT-2018 Mugshot Dataset] Threshold-based identification miss rates vs. number of enrolled subjects**. *The figure shows FNIR(N, T) across various gallery sizes when the threshold is set to achieve the given FPIRs. The rank criterion is irrelevant at high thresholds as mates are always at rank 1. The results are computed from the trials listed in rows 1-10 of Table 1. Less accurate algorithms were not run on large N, so results are missing. For clarity, results are sorted and reported into tiers spanning multiple pages. The tiering criteria is complicated: First paging by FNIR(N_b, 1, 0), then sorting by median FNIR(N_b, T), N_b = 640 000.*

This publication is available free of charge from: https://doi.org/10.6028/NIST.IR.8271

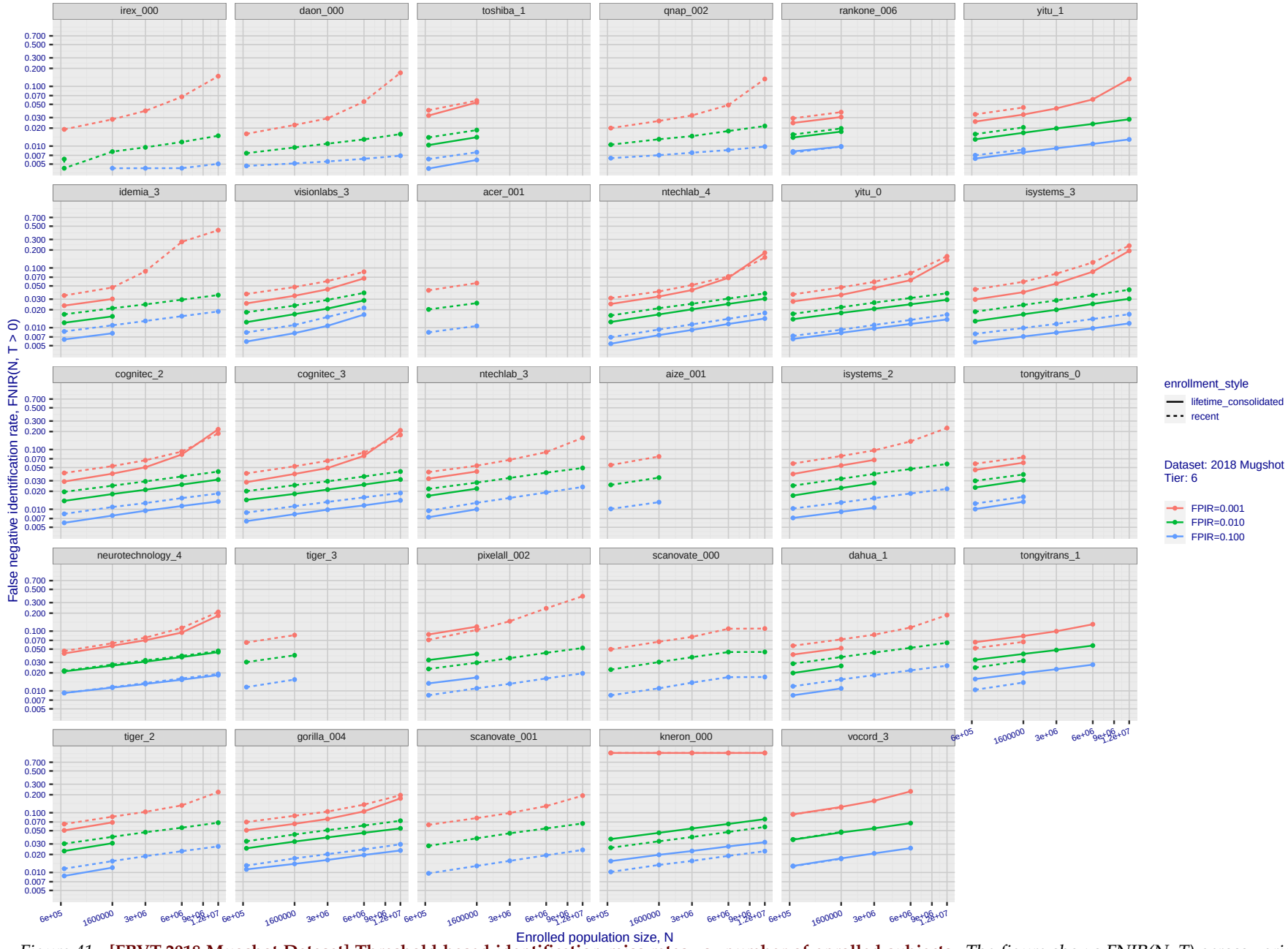

Figure 41: **[FRVT-2018 Mugshot Dataset] Threshold-based identification miss rates vs. number of enrolled subjects**. *The figure shows FNIR(N, T) across various gallery sizes when the threshold is set to achieve the given FPIRs. The rank criterion is irrelevant at high thresholds as mates are always at rank 1. The results are computed from the trials listed in rows 1-10 of Table 1. Less accurate algorithms were not run on large N, so results are missing. For clarity, results are sorted and reported into tiers spanning multiple pages. The tiering criteria is complicated: First paging by FNIR(N_b, 1, 0), then sorting by median FNIR(N_b, T), N_b = 640 000.*

This publication is available free of charge from: https://doi.org/10.6028/NIST.IR.8271

2022/06/13
18:09:57

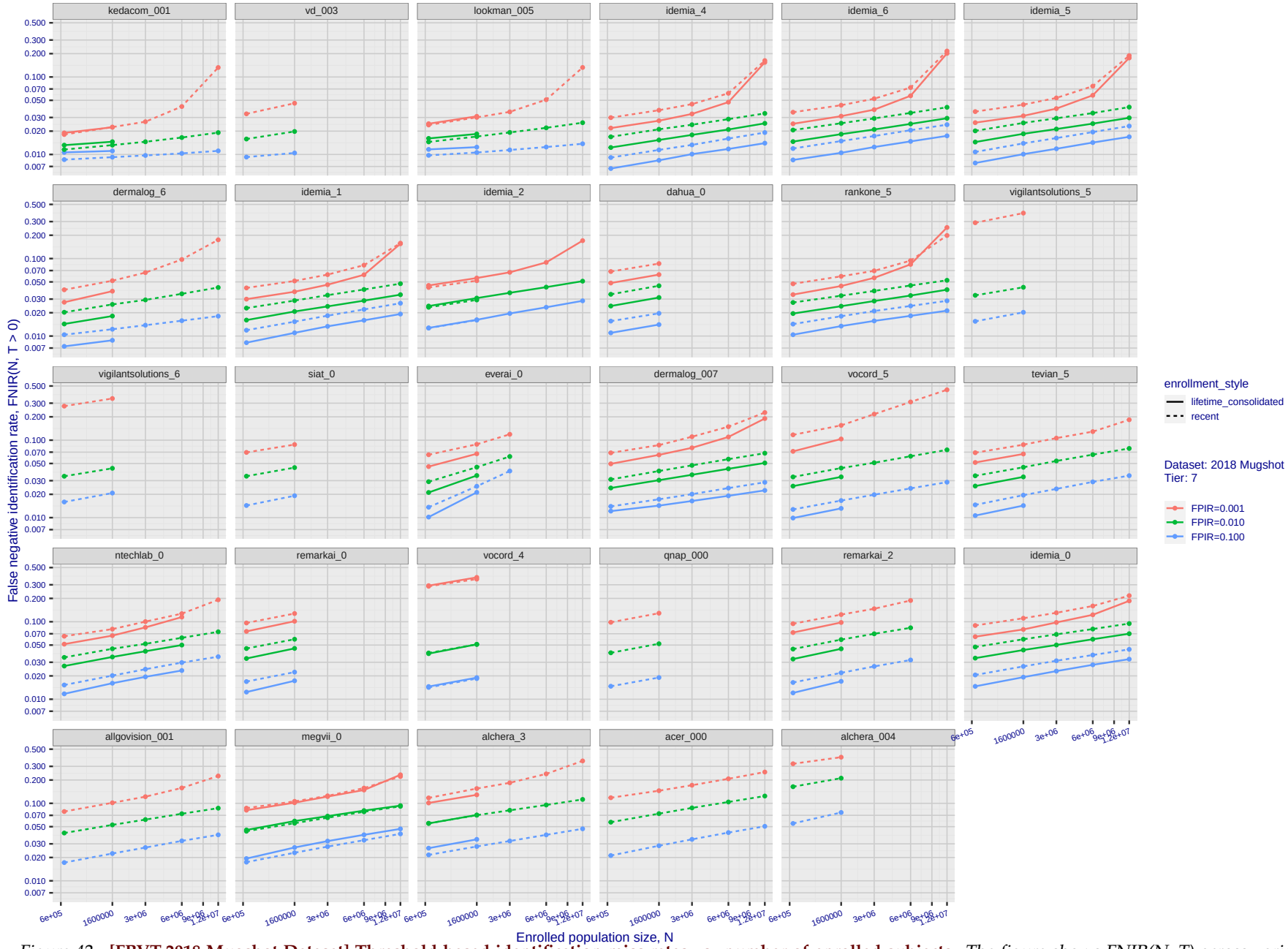

Figure 42: **[FRVT-2018 Mugshot Dataset] Threshold-based identification miss rates vs. number of enrolled subjects**. *The figure shows FNIR(N, T) across various gallery sizes when the threshold is set to achieve the given FPIRs. The rank criterion is irrelevant at high thresholds as mates are always at rank 1. The results are computed from the trials listed in rows 1-10 of Table 1. Less accurate algorithms were not run on large N, so results are missing. For clarity, results are sorted and reported into tiers spanning multiple pages. The tiering criteria is complicated: First paging by FNIR(N_b, 1, 0), then sorting by median FNIR(N_b, T), N_b = 640 000.*

FNIR(N, R, T) = False neg. identification rate
FPIR(N, T) = False pos. identification rate
N = Num. enrolled subjects
R = Num. candidates examined
T = Threshold
T = 0 → Investigation
T > 0 → Identification

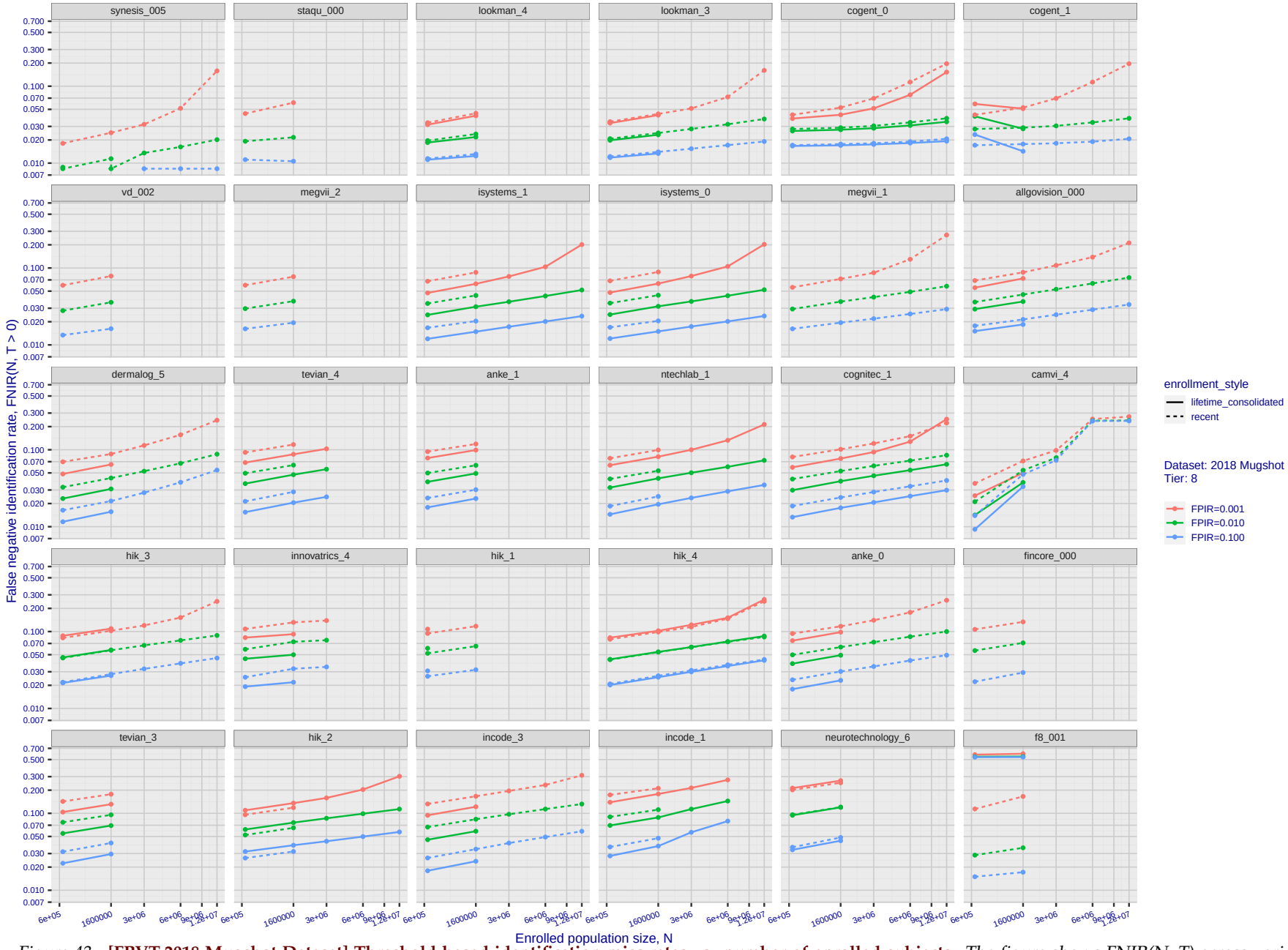

Figure 43: **[FRVT-2018 Mugshot Dataset] Threshold-based identification miss rates vs. number of enrolled subjects**. *The figure shows FNIR(N, T) across various gallery sizes when the threshold is set to achieve the given FPIRs. The rank criterion is irrelevant at high thresholds as mates are always at rank 1. The results are computed from the trials listed in rows 1-10 of Table 1. Less accurate algorithms were not run on large N, so results are missing. For clarity, results are sorted and reported into tiers spanning multiple pages. The tiering criteria is complicated: First paging by FNIR(N_b, 1, 0), then sorting by median FNIR(N_b, T), N_b = 640 000.*

This publication is available free of charge from: https://doi.org/10.6028/NIST.IR.8271

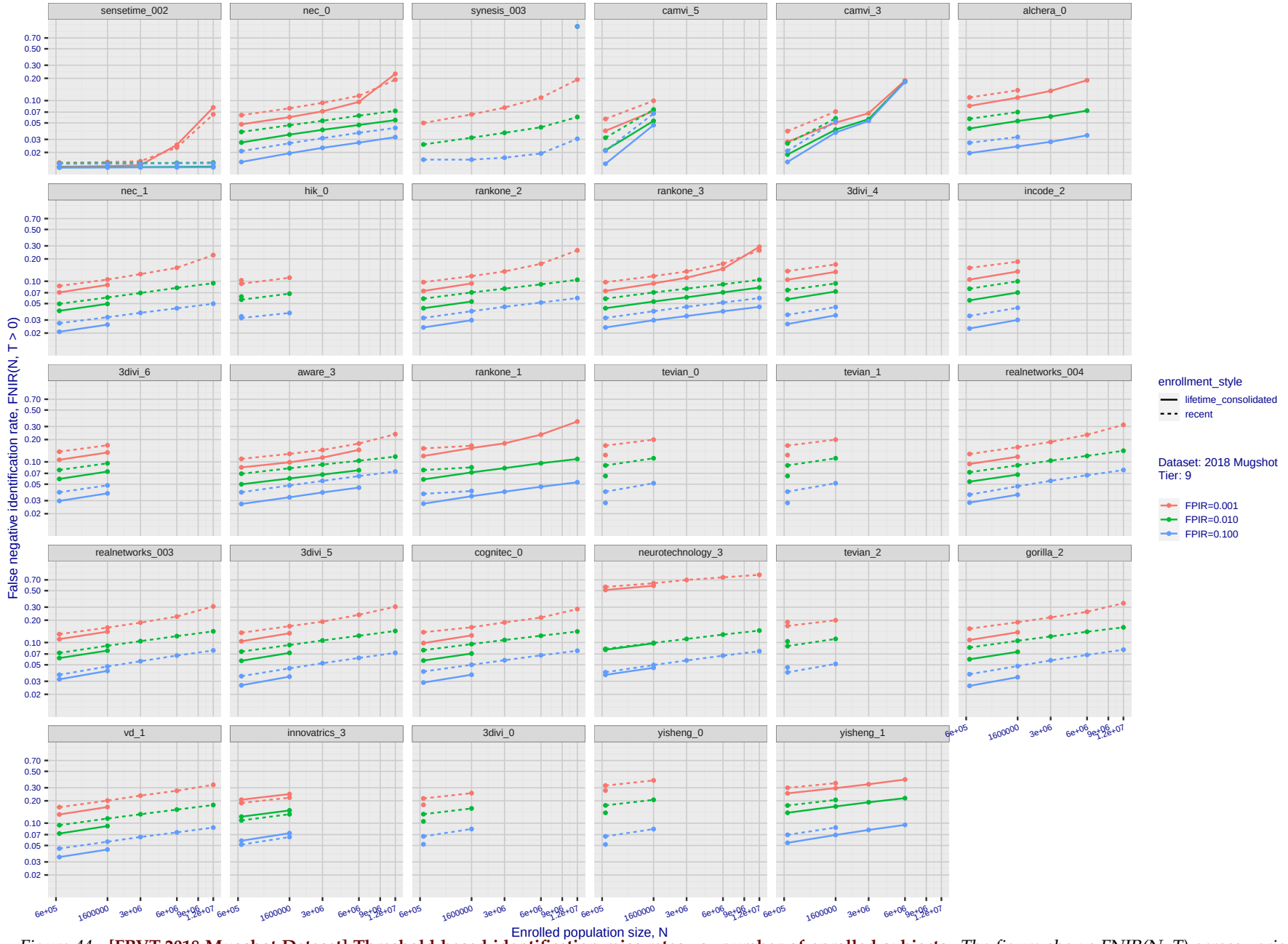

Figure 44: **[FRVT-2018 Mugshot Dataset] Threshold-based identification miss rates vs. number of enrolled subjects**. *The figure shows FNIR(N, T) across various gallery sizes when the threshold is set to achieve the given FPIRs. The rank criterion is irrelevant at high thresholds as mates are always at rank 1. The results are computed from the trials listed in rows 1-10 of Table 1. Less accurate algorithms were not run on large N, so results are missing. For clarity, results are sorted and reported into tiers spanning multiple pages. The tiering criteria is complicated: First paging by FNIR(N_b, 1, 0), then sorting by median FNIR(N_b, T), N_b = 640 000.*

This publication is available free of charge from: https://doi.org/10.6028/NIST.IR.8271

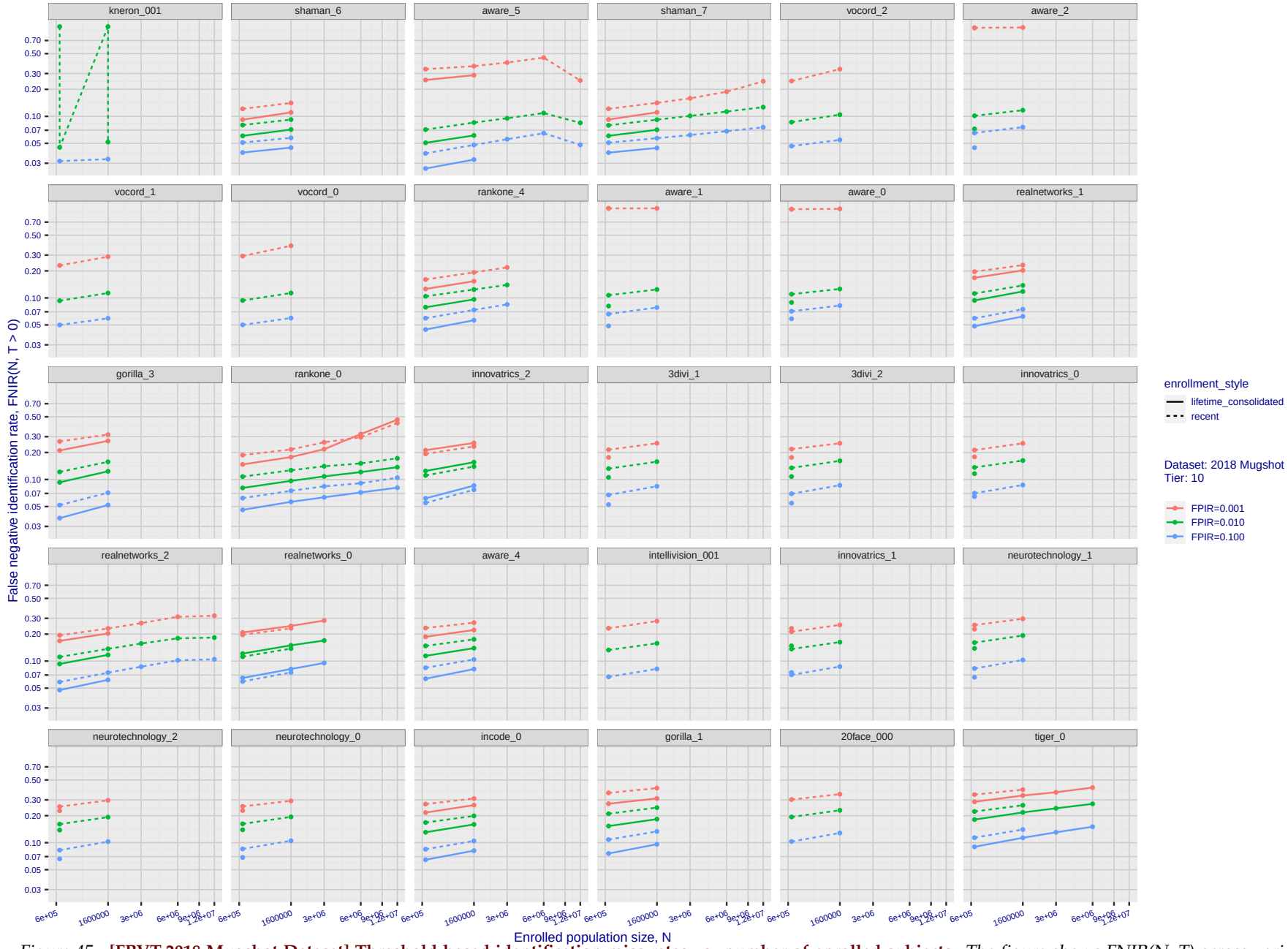

Figure 45: **[FRVT-2018 Mugshot Dataset] Threshold-based identification miss rates vs. number of enrolled subjects**. *The figure shows FNIR(N, T) across various gallery sizes when the threshold is set to achieve the given FPIRs. The rank criterion is irrelevant at high thresholds as mates are always at rank 1. The results are computed from the trials listed in rows 1-10 of Table 1. Less accurate algorithms were not run on large N, so results are missing. For clarity, results are sorted and reported into tiers spanning multiple pages. The tiering criteria is complicated: First paging by FNIR(N_b, 1, 0), then sorting by median FNIR(N_b, T), N_b = 640 000.*

This publication is available free of charge from: https://doi.org/10.6028/NIST.IR.8271

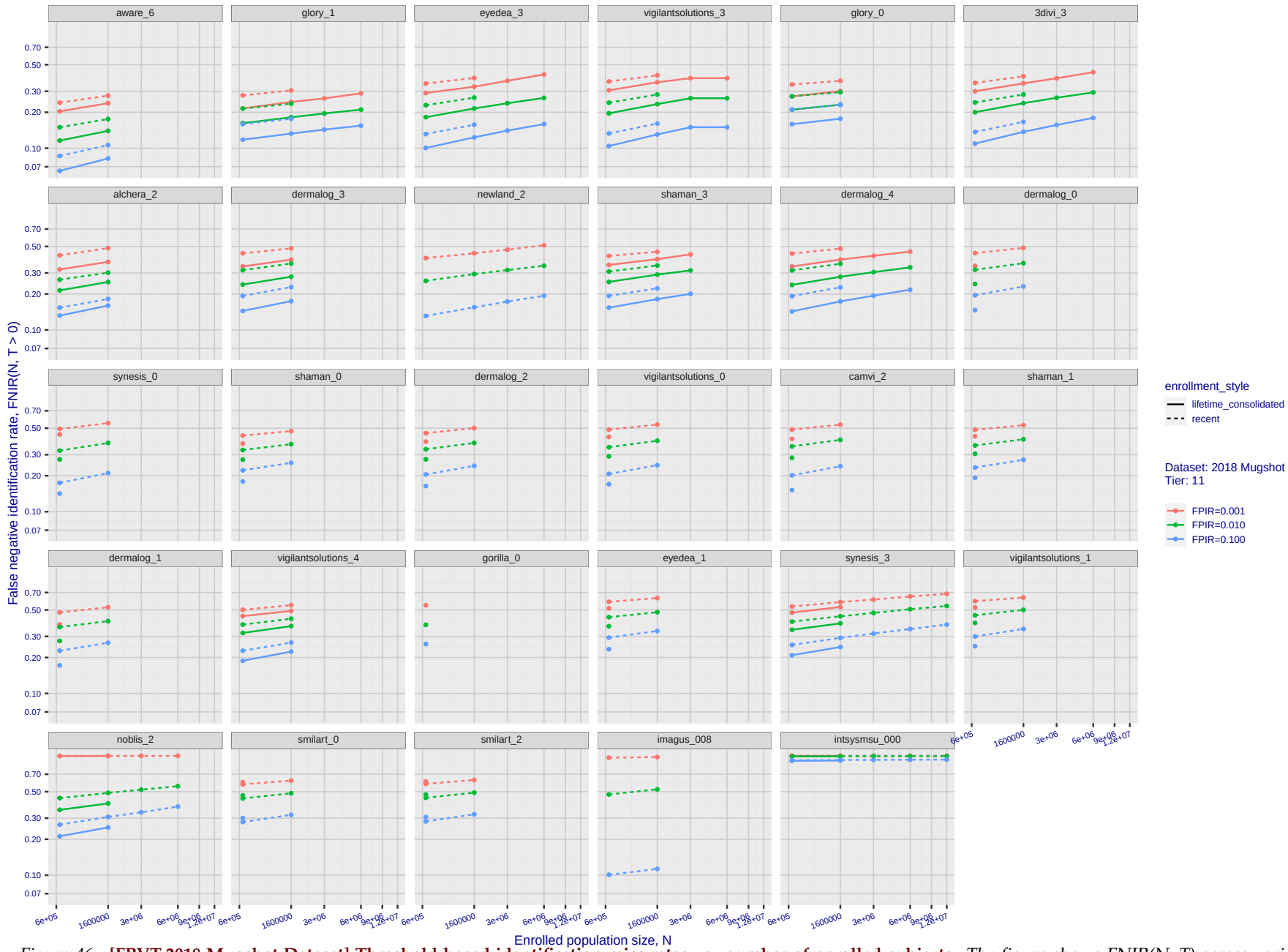

Figure 46: **[FRVT-2018 Mugshot Dataset] Threshold-based identification miss rates vs. number of enrolled subjects**. *The figure shows FNIR(N, T) across various gallery sizes when the threshold is set to achieve the given FPIRs. The rank criterion is irrelevant at high thresholds as mates are always at rank 1. The results are computed from the trials listed in rows 1-10 of Table 1. Less accurate algorithms were not run on large N, so results are missing. For clarity, results are sorted and reported into tiers spanning multiple pages. The tiering criteria is complicated: First paging by FNIR(N_b, 1, 0), then sorting by median FNIR(N_b, T), N_b = 640 000.*

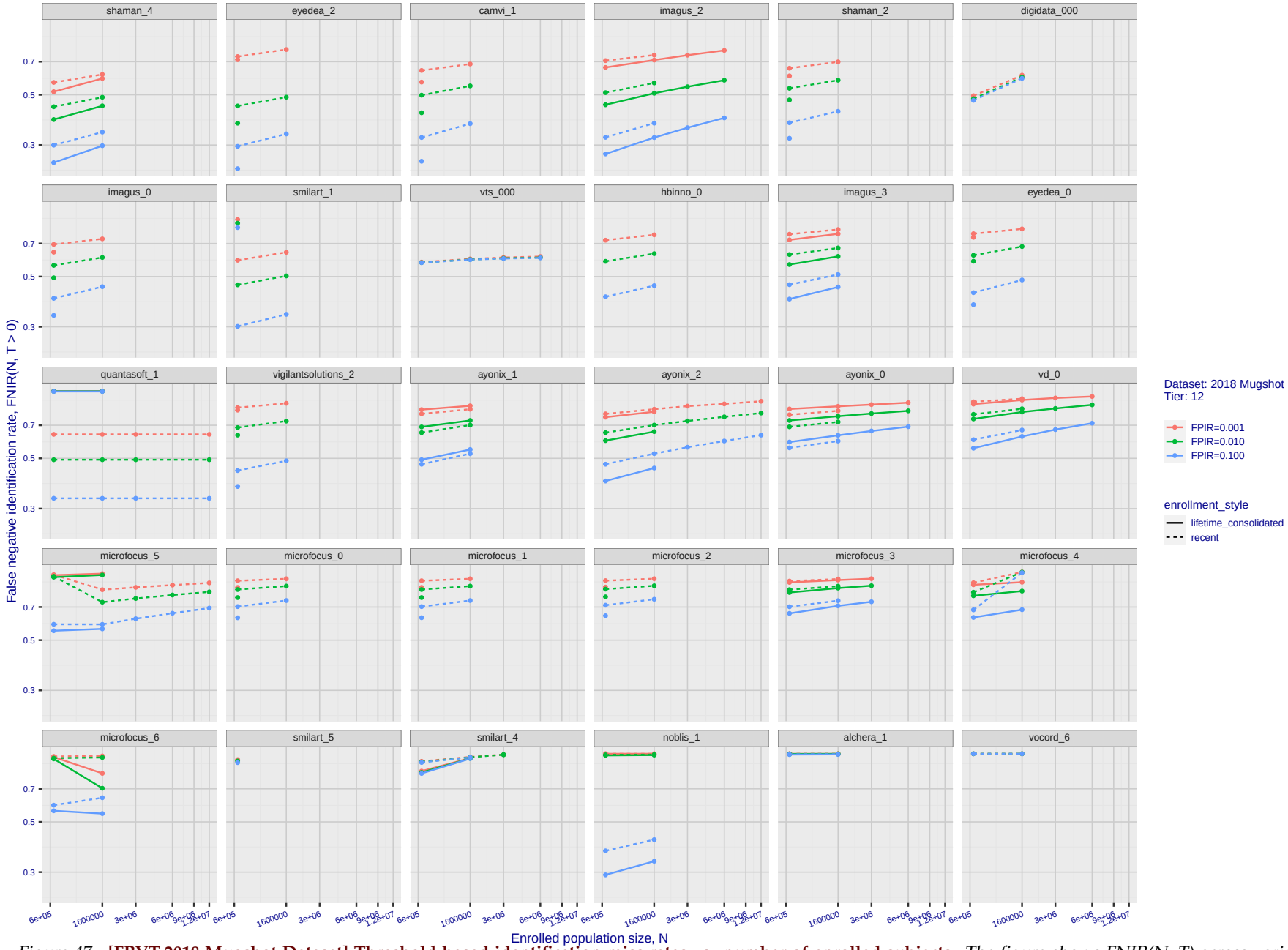

Figure 47: **[FRVT-2018 Mugshot Dataset] Threshold-based identification miss rates vs. number of enrolled subjects**. *The figure shows FNIR(N, T) across various gallery sizes when the threshold is set to achieve the given FPIRs. The rank criterion is irrelevant at high thresholds as mates are always at rank 1. The results are computed from the trials listed in rows 1-10 of Table 1. Less accurate algorithms were not run on large N, so results are missing. For clarity, results are sorted and reported into tiers spanning multiple pages. The tiering criteria is complicated: First paging by FNIR(N_b, 1, 0), then sorting by median FNIR(N_b, T), N_b = 640 000.*

2022/06/13	FNIR(N, R, T) =	False neg. identification rate	N = Num. enrolled subjects	T = Threshold	$T = 0 \rightarrow$ Investigation
18:09:57	FPIR(N, T) =	False pos. identification rate	R = Num. candidates examined		$T > 0 \rightarrow$ Identification

This publication is available free of charge from: https://doi.org/10.6028/NIST.IR.8271

This publication is available free of charge from: https://doi.org/10.6028/NIST.IR.8271

2022/06/13 18:09:57

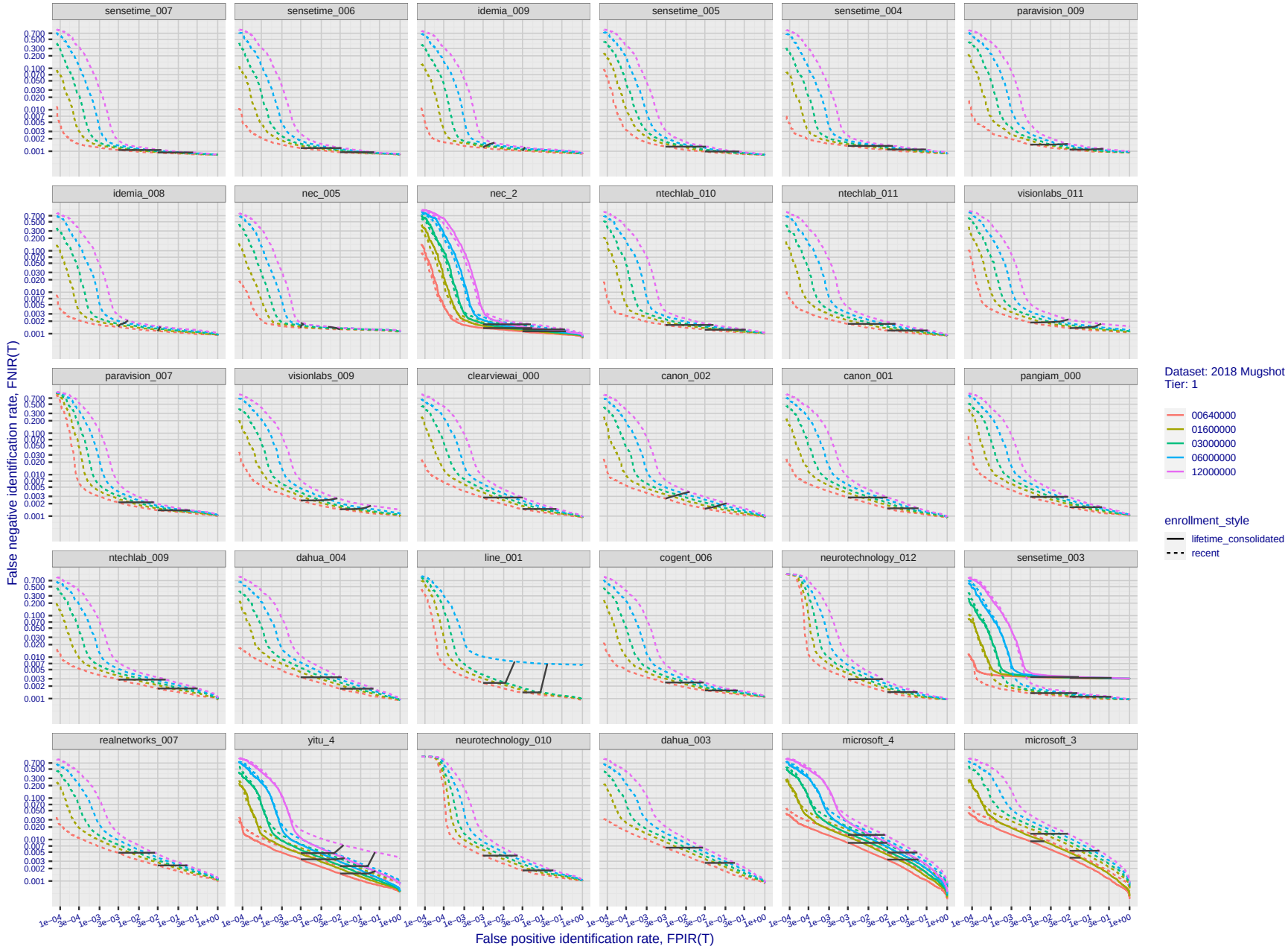

FNIR(N, R, T) = False neg. identification rate
FPIR(N, T) = False pos. identification rate
N = Num. enrolled subjects
R = Num. candidates examined
T = Threshold
T = 0 → Investigation
T > 0 → Identification

Figure 48: **[FRVT-2018 Mugshot Dataset] Identification miss rates vs. false positive rates**. *The figure shows miss rates FNIR(N, L, T) as a function of FPIR(N, T), with N ranging from 640 000 to 12 000 000 as noted in rows 1-10 of Table 1. These error tradeoff characteristics are useful for applications where a threshold must be elevated to limit false positives, such as when human reviewer labor is not matched to the volume of searches. Dark lines join points of equal threshold: If horizontal, FPIR(T) rises with N, and mate scores are independent of N. Other algorithms adjust scores in an attempt to make FPIR independent of N.*

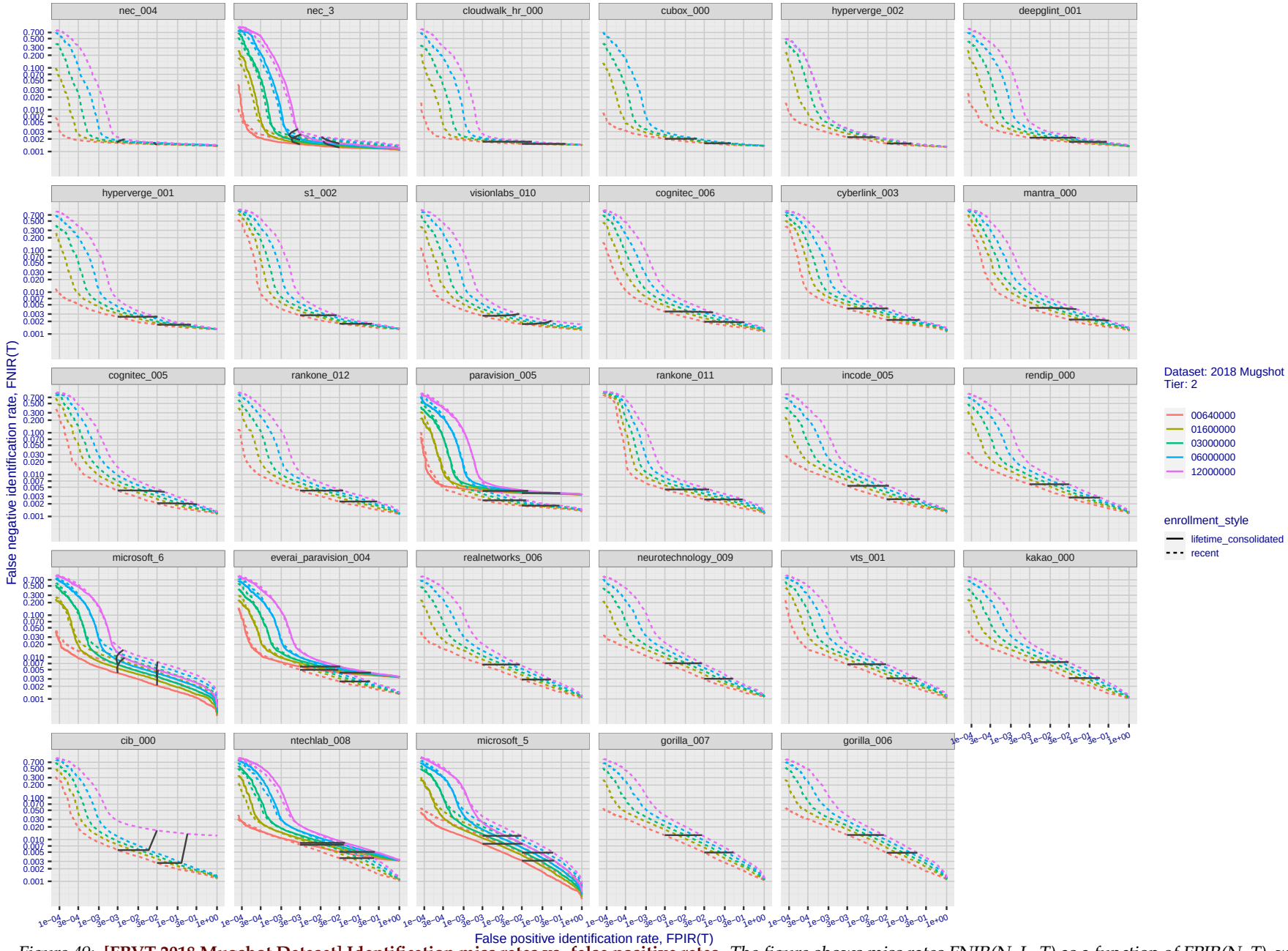

FNIR(N, R, T) = False neg. identification rate
FPIR(N, T) = False pos. identification rate
N = Num. enrolled subjects
R = Num. candidates examined
T = Threshold
T = 0 → Investigation
T > 0 → Identification

Figure 49: **[FRVT-2018 Mugshot Dataset] Identification miss rates vs. false positive rates**. *The figure shows miss rates FNIR(N, L, T) as a function of FPIR(N, T), with N ranging from 640 000 to 12 000 000 as noted in rows 1-10 of Table 1. These error tradeoff characteristics are useful for applications where a threshold must be elevated to limit false positives, such as when human reviewer labor is not matched to the volume of searches. Dark lines join points of equal threshold: If horizontal, FPIR(T) rises with N, and mate scores are independent of N. Other algorithms adjust scores in an attempt to make FPIR independent of N.*

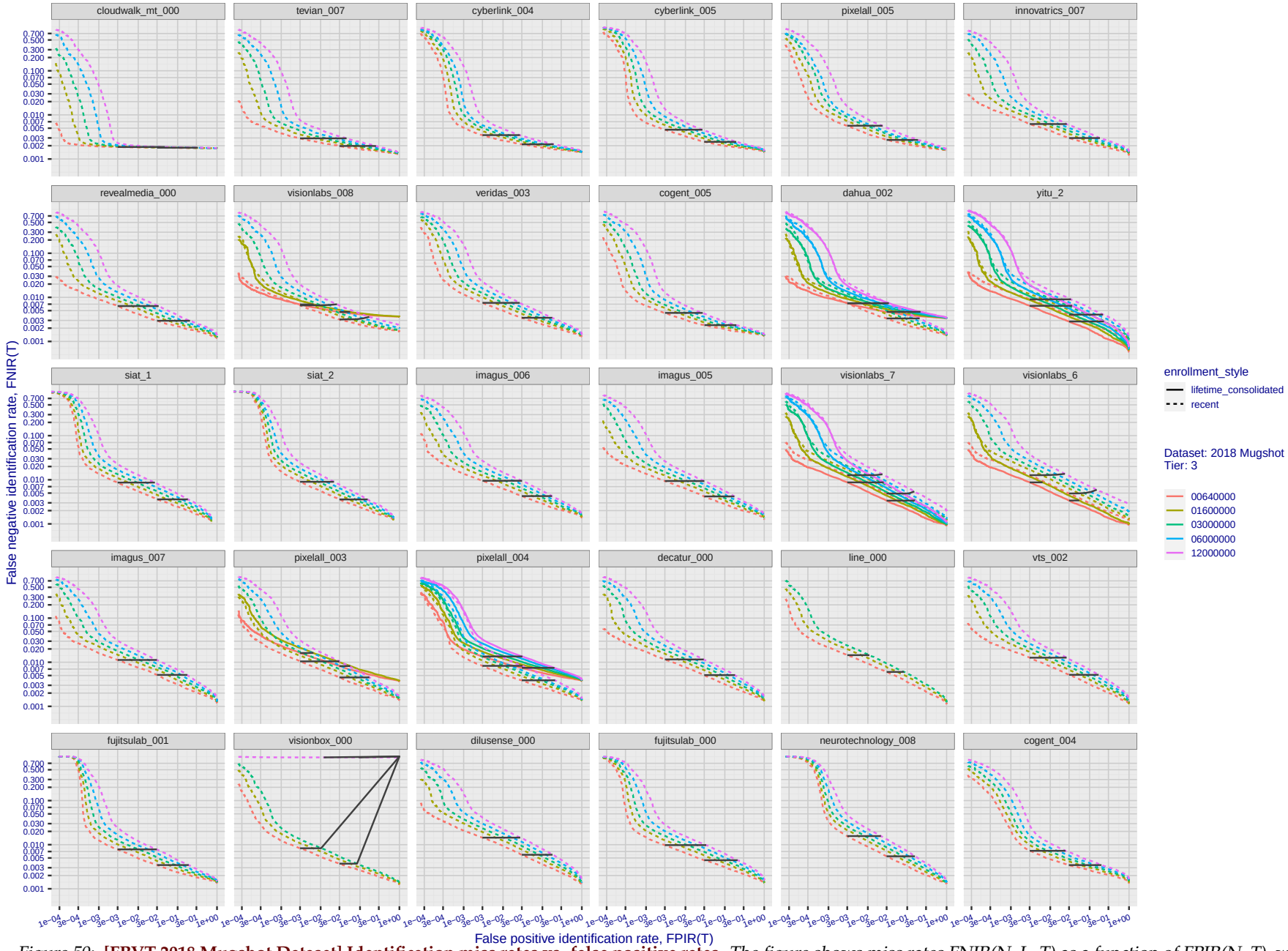

Figure 50: **[FRVT-2018 Mugshot Dataset] Identification miss rates vs. false positive rates**. *The figure shows miss rates FNIR(N, L, T) as a function of FPIR(N, T), with N ranging from 640 000 to 12 000 000 as noted in rows 1-10 of Table 1. These error tradeoff characteristics are useful for applications where a threshold must be elevated to limit false positives, such as when human reviewer labor is not matched to the volume of searches. Dark lines join points of equal threshold: If horizontal, FPIR(T) rises with N, and mate scores are independent of N. Other algorithms adjust scores in an attempt to make FPIR independent of N.*

This publication is available free of charge from: https://doi.org/10.6028/NIST.IR.8271

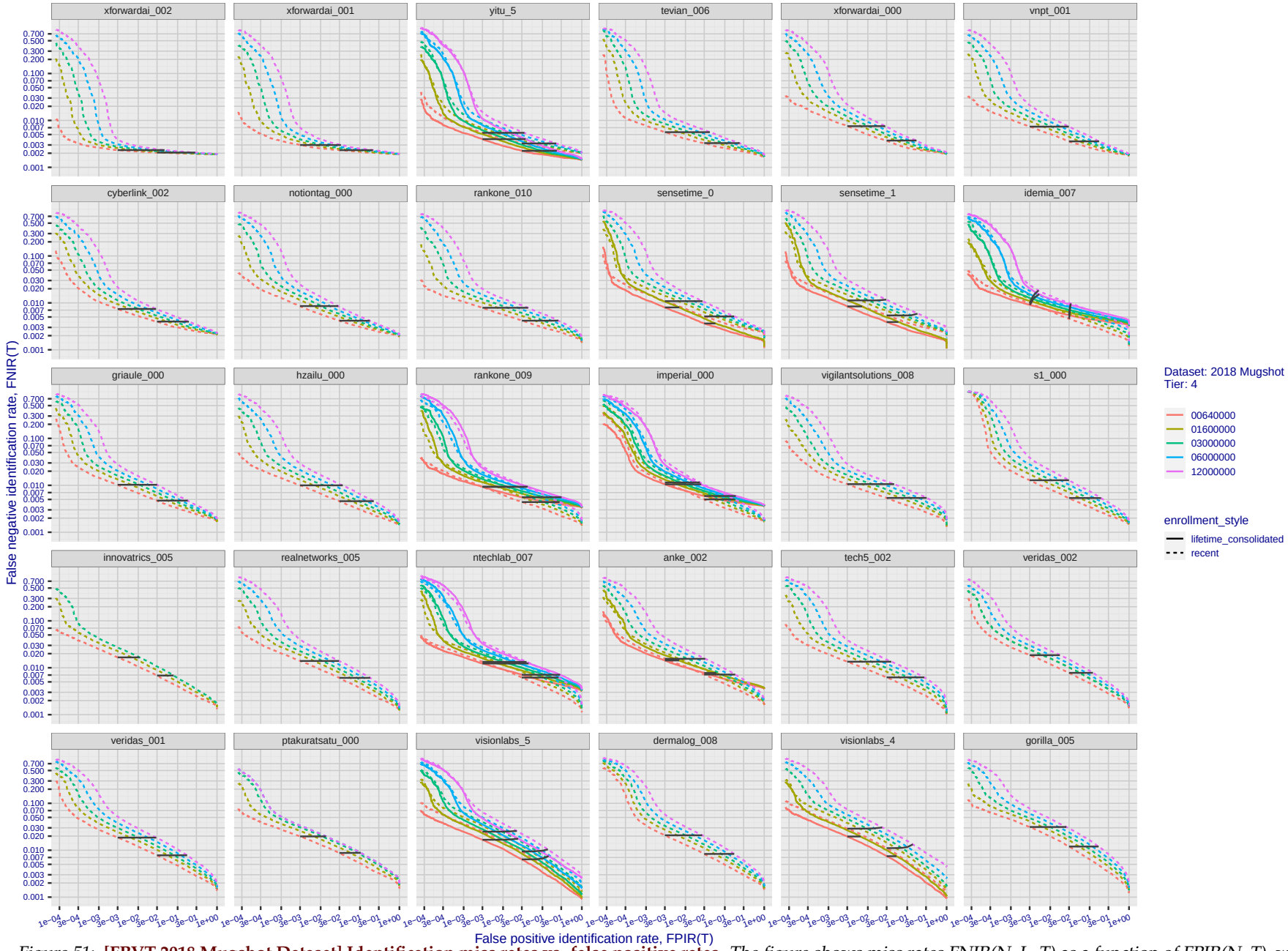

Figure 51: **[FRVT-2018 Mugshot Dataset] Identification miss rates vs. false positive rates**. *The figure shows miss rates FNIR(N, L, T) as a function of FPIR(N, T), with N ranging from 640 000 to 12 000 000 as noted in rows 1-10 of Table 1. These error tradeoff characteristics are useful for applications where a threshold must be elevated to limit false positives, such as when human reviewer labor is not matched to the volume of searches. Dark lines join points of equal threshold: If horizontal, FPIR(T) rises with N, and mate scores are independent of N. Other algorithms adjust scores in an attempt to make FPIR independent of N.*

This publication is available free of charge from: https://doi.org/10.6028/NIST.IR.8271

2022/06/13
18:09:57

FNIR(N, R, T) = False neg. identification rate
FPIR(N, T) = False pos. identification rate
N = Num. enrolled subjects
R = Num. candidates examined
T = Threshold
T = 0 → Investigation
T > 0 → Identification

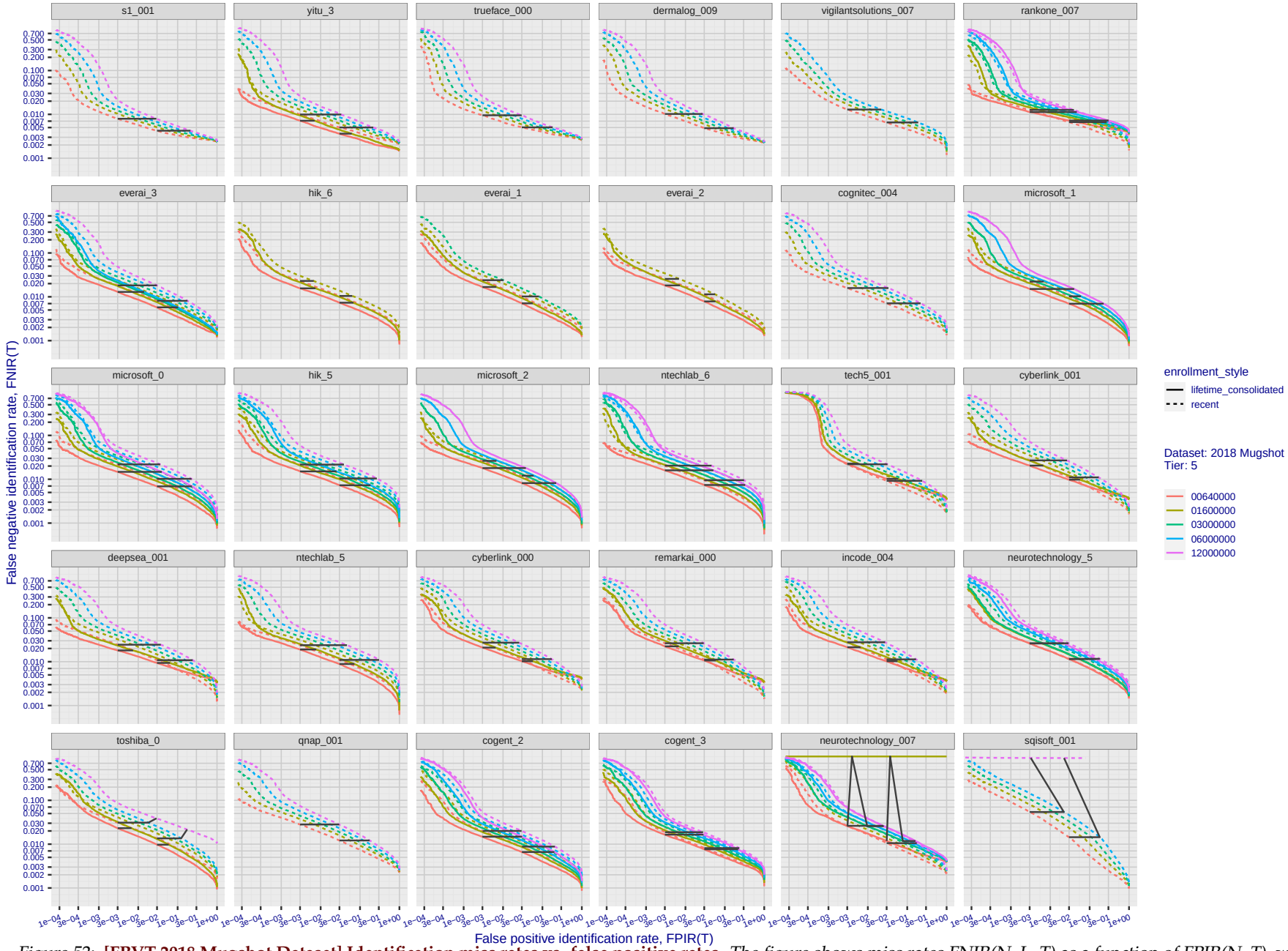

Figure 52: **[FRVT-2018 Mugshot Dataset] Identification miss rates vs. false positive rates**. *The figure shows miss rates FNIR(N, L, T) as a function of FPIR(N, T), with N ranging from 640 000 to 12 000 000 as noted in rows 1-10 of Table 1. These error tradeoff characteristics are useful for applications where a threshold must be elevated to limit false positives, such as when human reviewer labor is not matched to the volume of searches. Dark lines join points of equal threshold: If horizontal, FPIR(T) rises with N, and mate scores are independent of N. Other algorithms adjust scores in an attempt to make FPIR independent of N.*

This publication is available free of charge from: https://doi.org/10.6028/NIST.IR.8271

2022/06/13
18:09:57

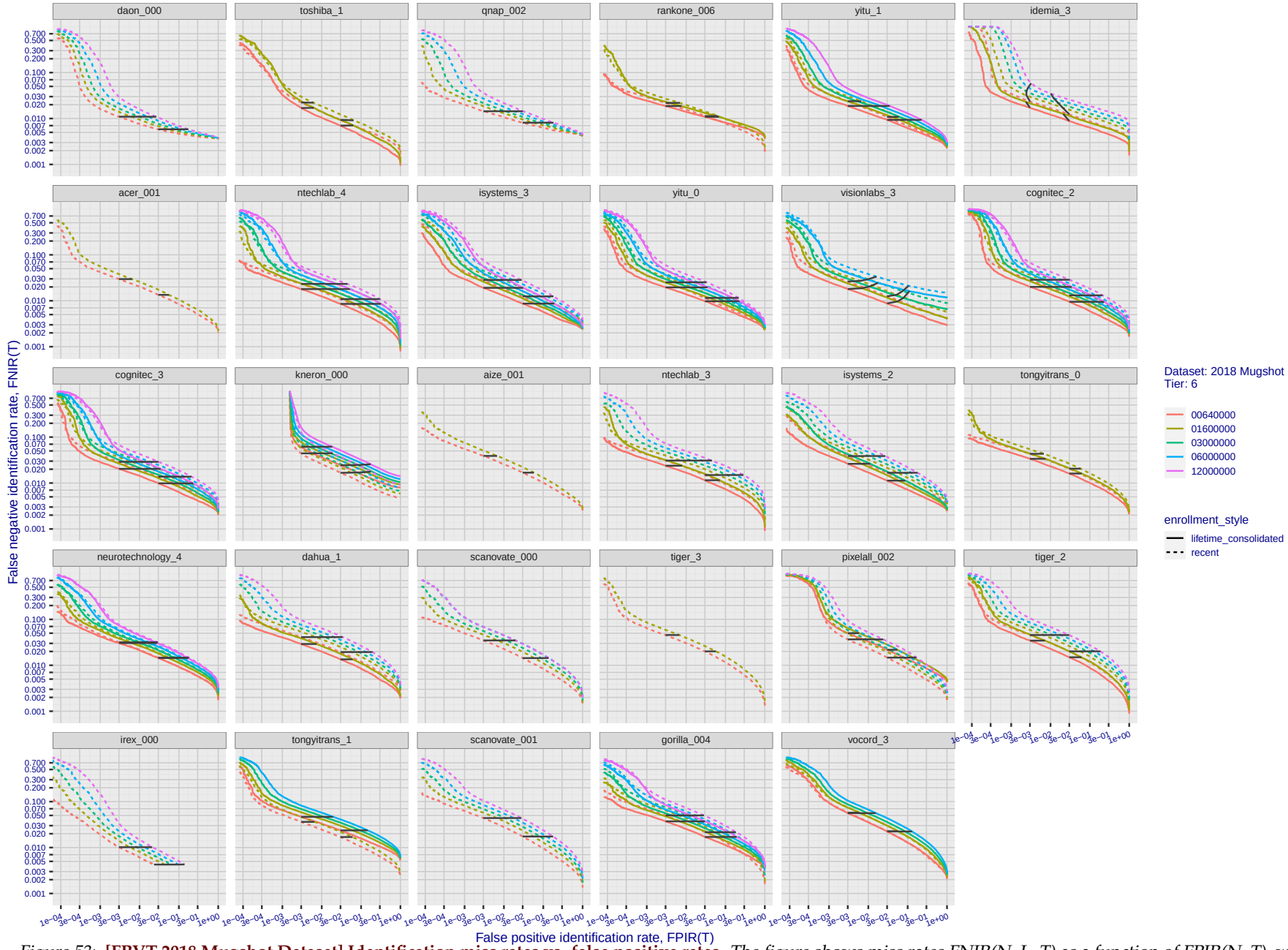

FNIR(N, R, T) = False neg. identification rate
FPIR(N, T) = False pos. identification rate
N = Num. enrolled subjects
R = Num. candidates examined
T = Threshold
T = 0 → Investigation
T > 0 → Identification

Figure 53: **[FRVT-2018 Mugshot Dataset] Identification miss rates vs. false positive rates**. *The figure shows miss rates FNIR(N, L, T) as a function of FPIR(N, T), with N ranging from 640 000 to 12 000 000 as noted in rows 1-10 of Table 1. These error tradeoff characteristics are useful for applications where a threshold must be elevated to limit false positives, such as when human reviewer labor is not matched to the volume of searches. Dark lines join points of equal threshold: If horizontal, FPIR(T) rises with N, and mate scores are independent of N. Other algorithms adjust scores in an attempt to make FPIR independent of N.*

This publication is available free of charge from: https://doi.org/10.6028/NIST.IR.8271

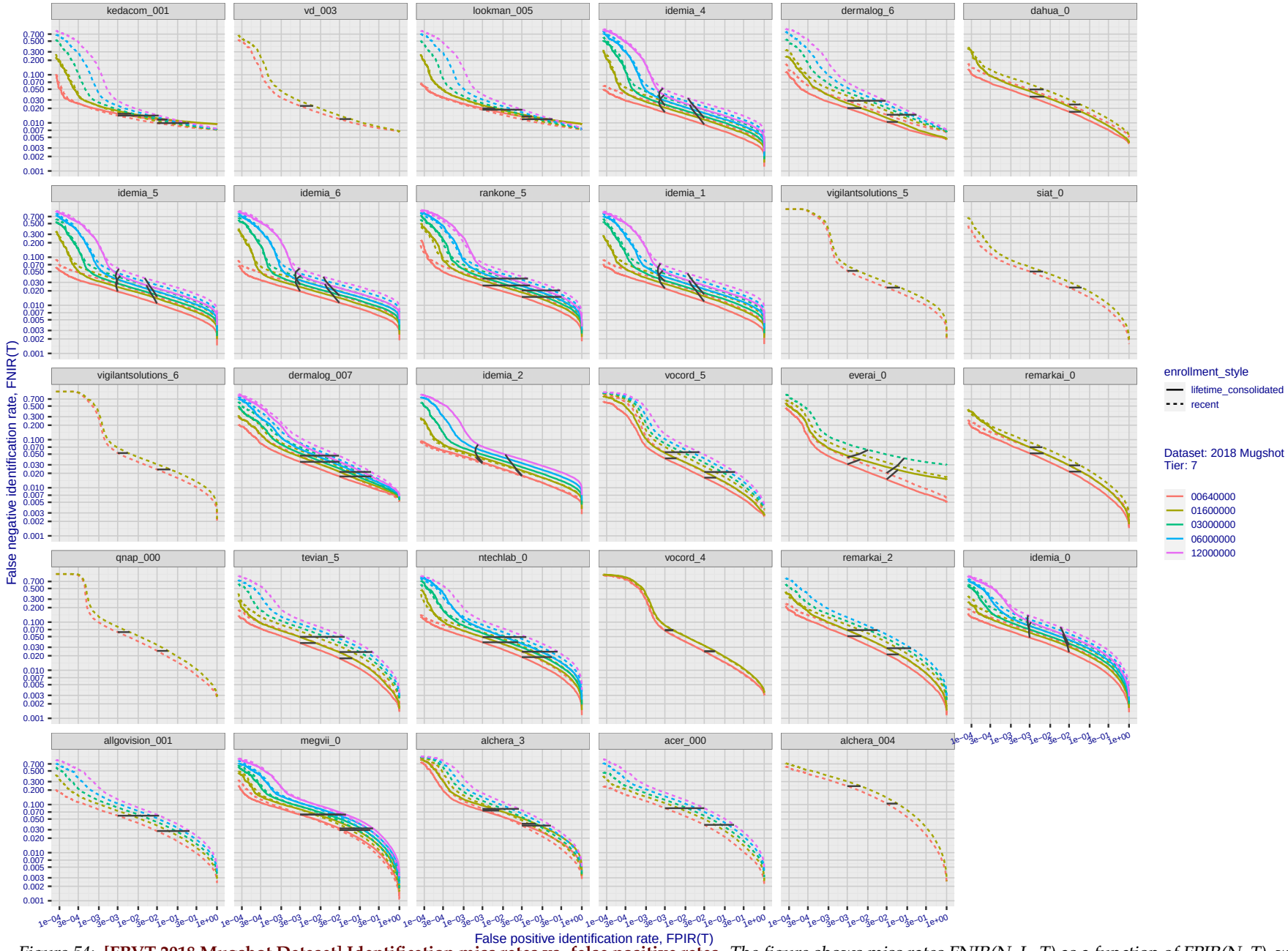

Figure 54: **[FRVT-2018 Mugshot Dataset] Identification miss rates vs. false positive rates**. *The figure shows miss rates FNIR(N, L, T) as a function of FPIR(N, T), with N ranging from 640 000 to 12 000 000 as noted in rows 1-10 of Table 1. These error tradeoff characteristics are useful for applications where a threshold must be elevated to limit false positives, such as when human reviewer labor is not matched to the volume of searches. Dark lines join points of equal threshold: If horizontal, FPIR(T) rises with N, and mate scores are independent of N. Other algorithms adjust scores in an attempt to make FPIR independent of N.*

This publication is available free of charge from: https://doi.org/10.6028/NIST.IR.8271

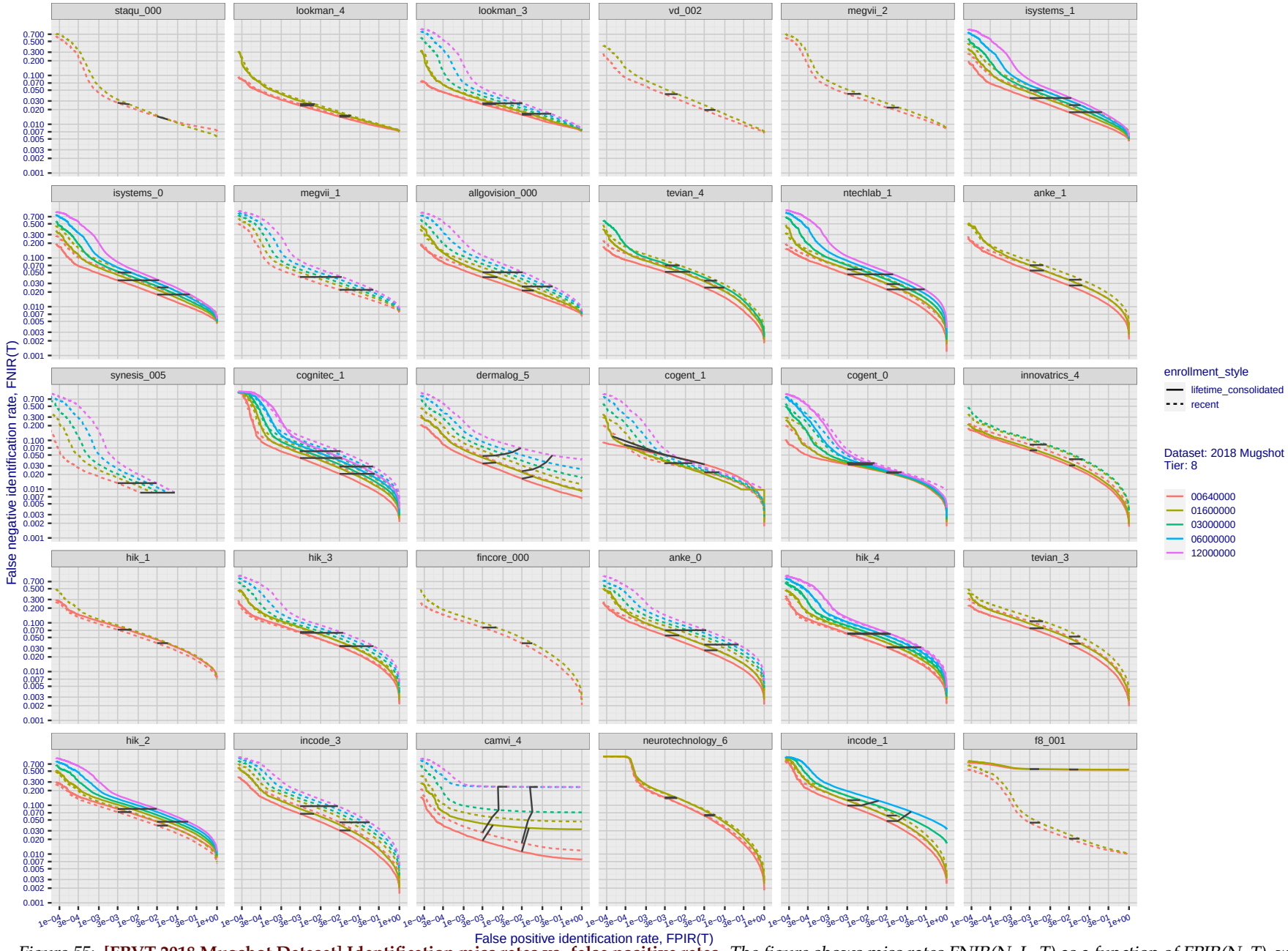

Figure 55: **[FRVT-2018 Mugshot Dataset] Identification miss rates vs. false positive rates**. *The figure shows miss rates FNIR(N, L, T) as a function of FPIR(N, T), with N ranging from 640 000 to 12 000 000 as noted in rows 1-10 of Table 1. These error tradeoff characteristics are useful for applications where a threshold must be elevated to limit false positives, such as when human reviewer labor is not matched to the volume of searches. Dark lines join points of equal threshold: If horizontal, FPIR(T) rises with N, and mate scores are independent of N. Other algorithms adjust scores in an attempt to make FPIR independent of N.*

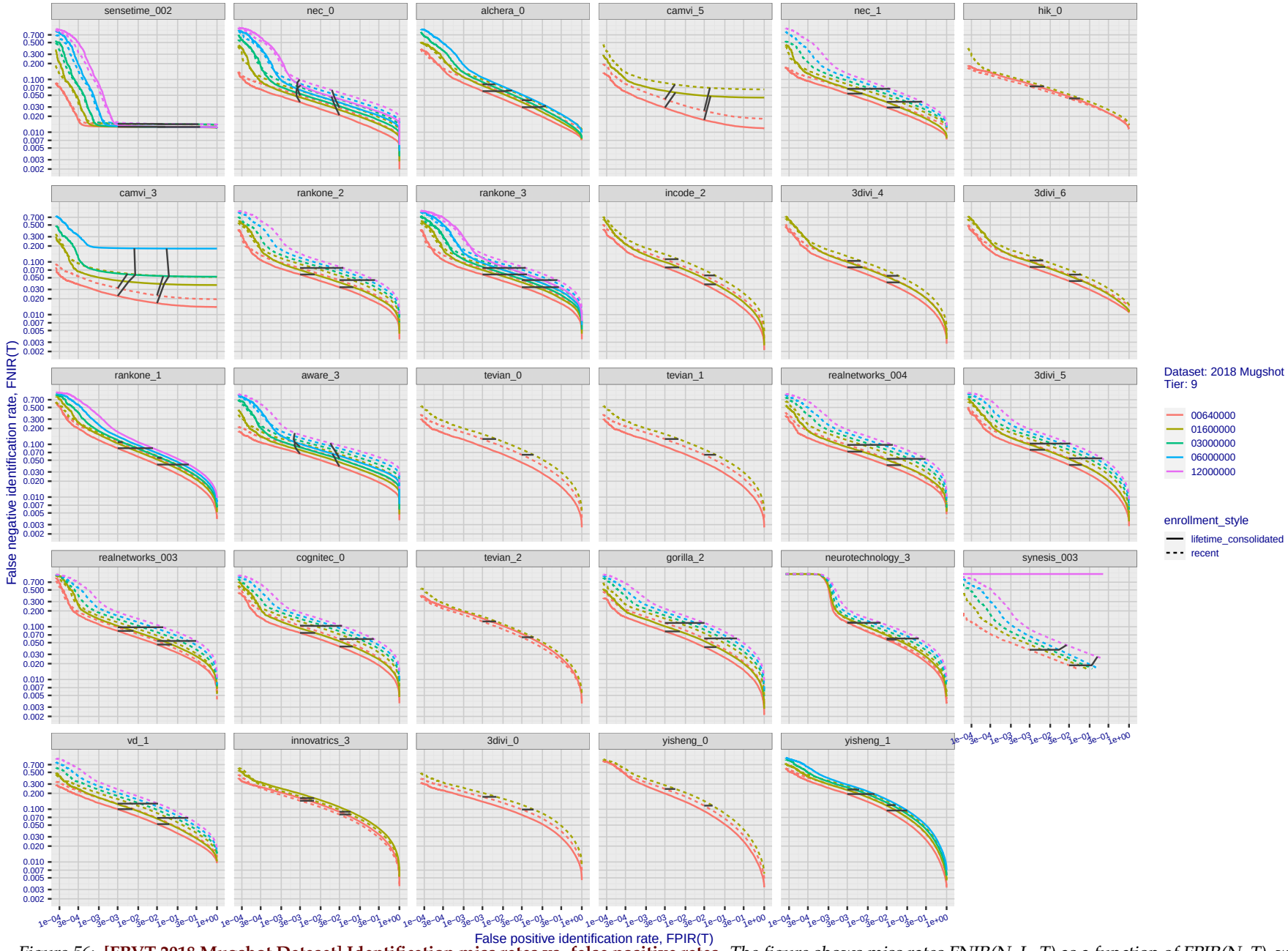

Figure 56: **[FRVT-2018 Mugshot Dataset] Identification miss rates vs. false positive rates**. *The figure shows miss rates FNIR(N, L, T) as a function of FPIR(N, T), with N ranging from 640 000 to 12 000 000 as noted in rows 1-10 of Table 1. These error tradeoff characteristics are useful for applications where a threshold must be elevated to limit false positives, such as when human reviewer labor is not matched to the volume of searches. Dark lines join points of equal threshold: If horizontal, FPIR(T) rises with N, and mate scores are independent of N. Other algorithms adjust scores in an attempt to make FPIR independent of N.*

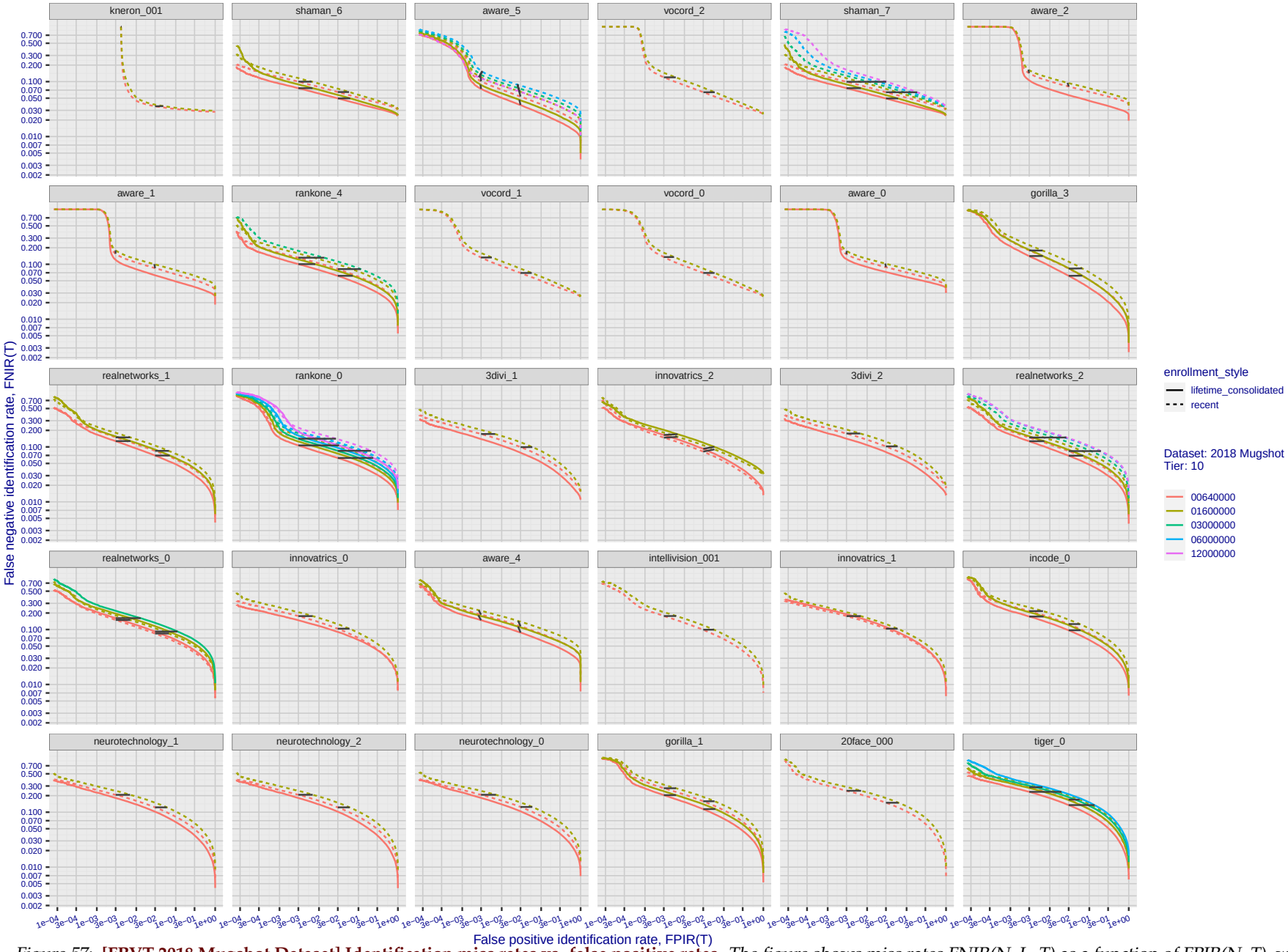

Figure 57: **[FRVT-2018 Mugshot Dataset] Identification miss rates vs. false positive rates**. *The figure shows miss rates FNIR(N, L, T) as a function of FPIR(N, T), with N ranging from 640 000 to 12 000 000 as noted in rows 1-10 of Table 1. These error tradeoff characteristics are useful for applications where a threshold must be elevated to limit false positives, such as when human reviewer labor is not matched to the volume of searches. Dark lines join points of equal threshold: If horizontal, FPIR(T) rises with N, and mate scores are independent of N. Other algorithms adjust scores in an attempt to make FPIR independent of N.*

This publication is available free of charge from: https://doi.org/10.6028/NIST.IR.8271

2022/06/13
18:09:57

FNIR(N, R, T) = False neg. identification rate
FPIR(N, T) = False pos. identification rate
N = Num. enrolled subjects
R = Num. candidates examined
T = Threshold
T = 0 → Investigation
T > 0 → Identification

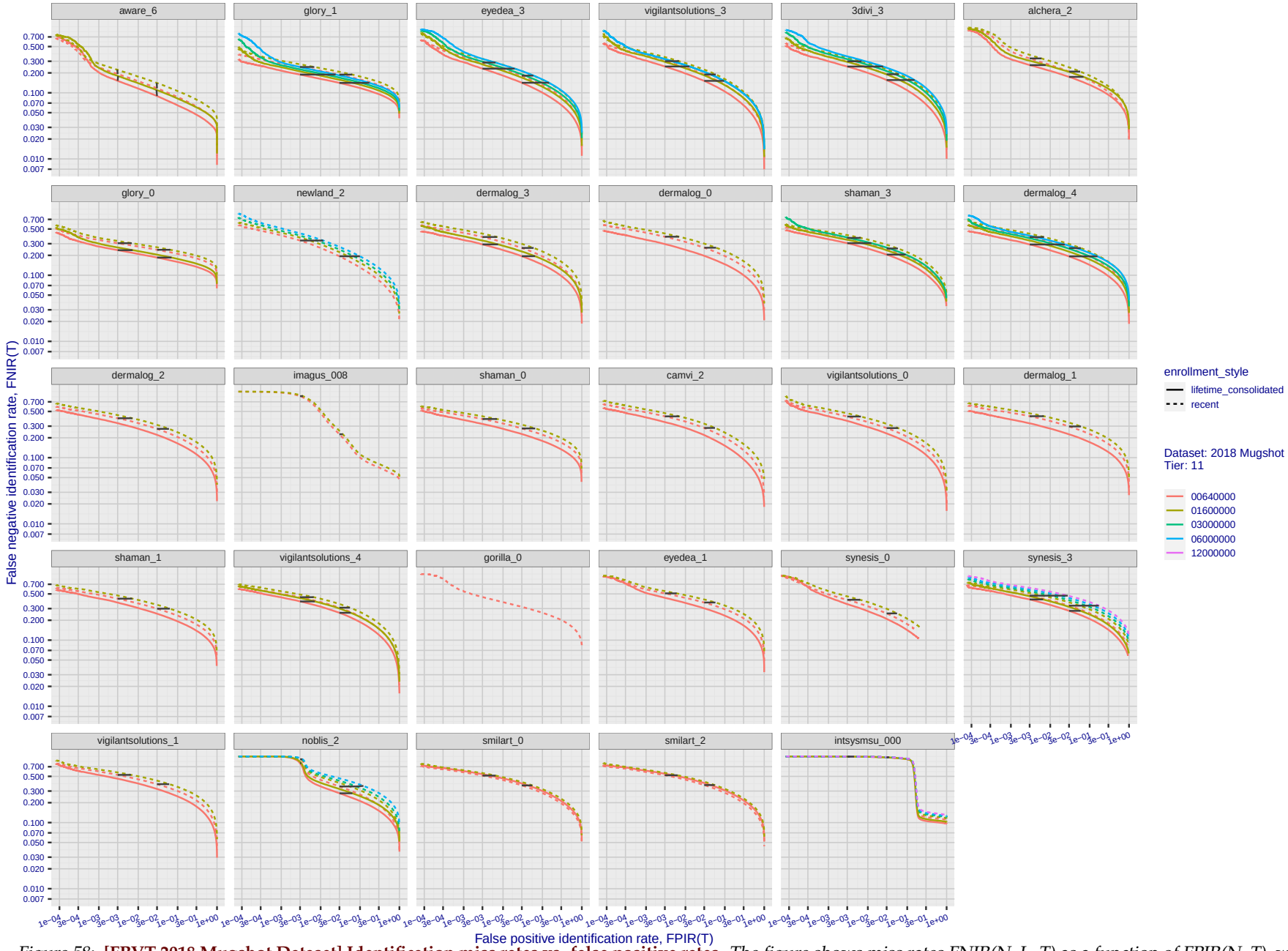

Figure 58: **[FRVT-2018 Mugshot Dataset] Identification miss rates vs. false positive rates**. *The figure shows miss rates FNIR(N, L, T) as a function of FPIR(N, T), with N ranging from 640 000 to 12 000 000 as noted in rows 1-10 of Table 1. These error tradeoff characteristics are useful for applications where a threshold must be elevated to limit false positives, such as when human reviewer labor is not matched to the volume of searches. Dark lines join points of equal threshold: If horizontal, FPIR(T) rises with N, and mate scores are independent of N. Other algorithms adjust scores in an attempt to make FPIR independent of N.*

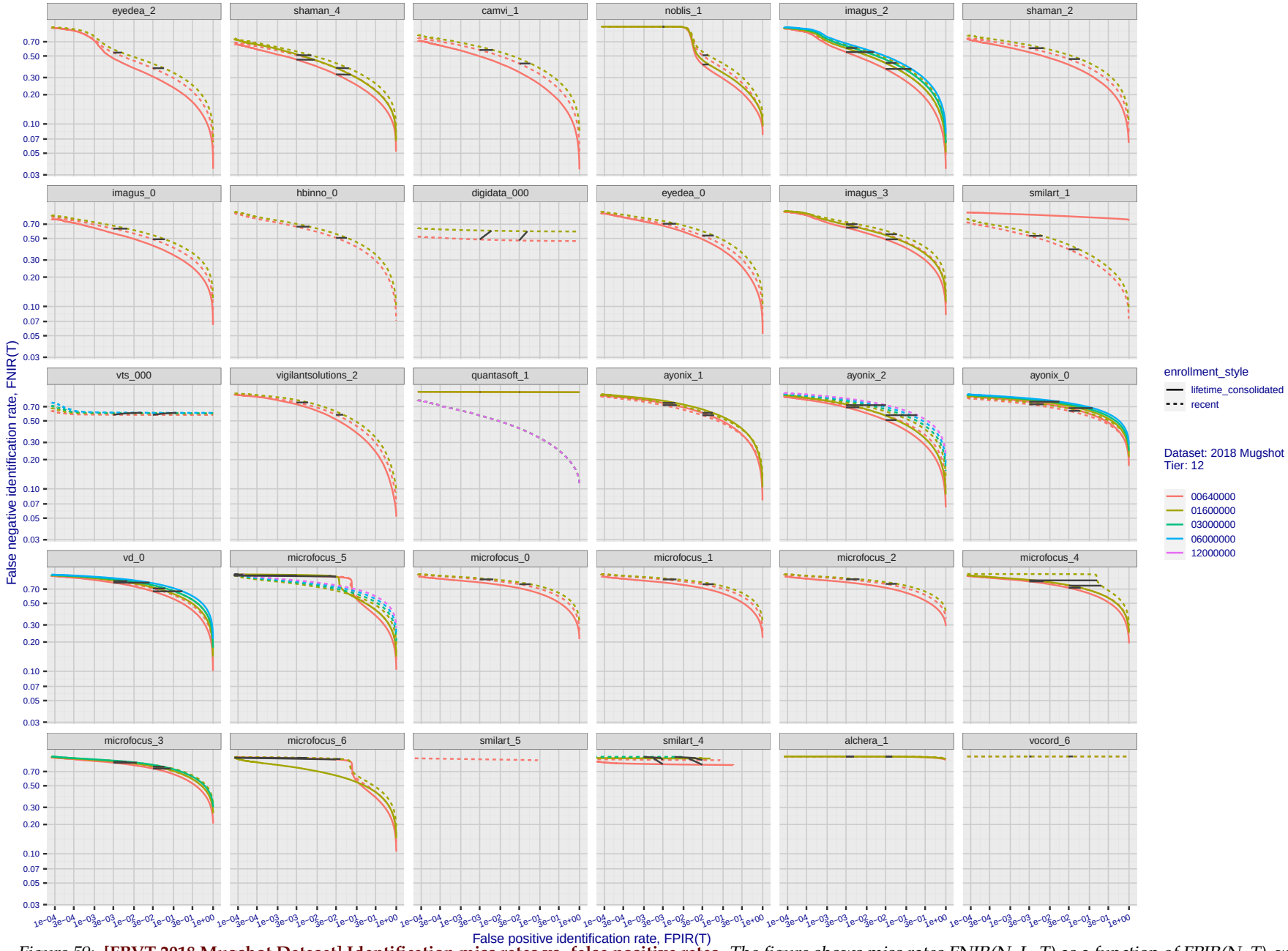

Figure 59: **[FRVT-2018 Mugshot Dataset] Identification miss rates vs. false positive rates**. *The figure shows miss rates FNIR(N, L, T) as a function of FPIR(N, T), with N ranging from 640 000 to 12 000 000 as noted in rows 1-10 of Table 1. These error tradeoff characteristics are useful for applications where a threshold must be elevated to limit false positives, such as when human reviewer labor is not matched to the volume of searches. Dark lines join points of equal threshold: If horizontal, FPIR(T) rises with N, and mate scores are independent of N. Other algorithms adjust scores in an attempt to make FPIR independent of N.*

Appendix B Effect of time-lapse: Accuracy after face ageing

This publication is available free of charge from: https://doi.org/10.6028/NIST.IR.8271

This publication is available free of charge from: https://doi.org/10.6028/NIST.IR.8271

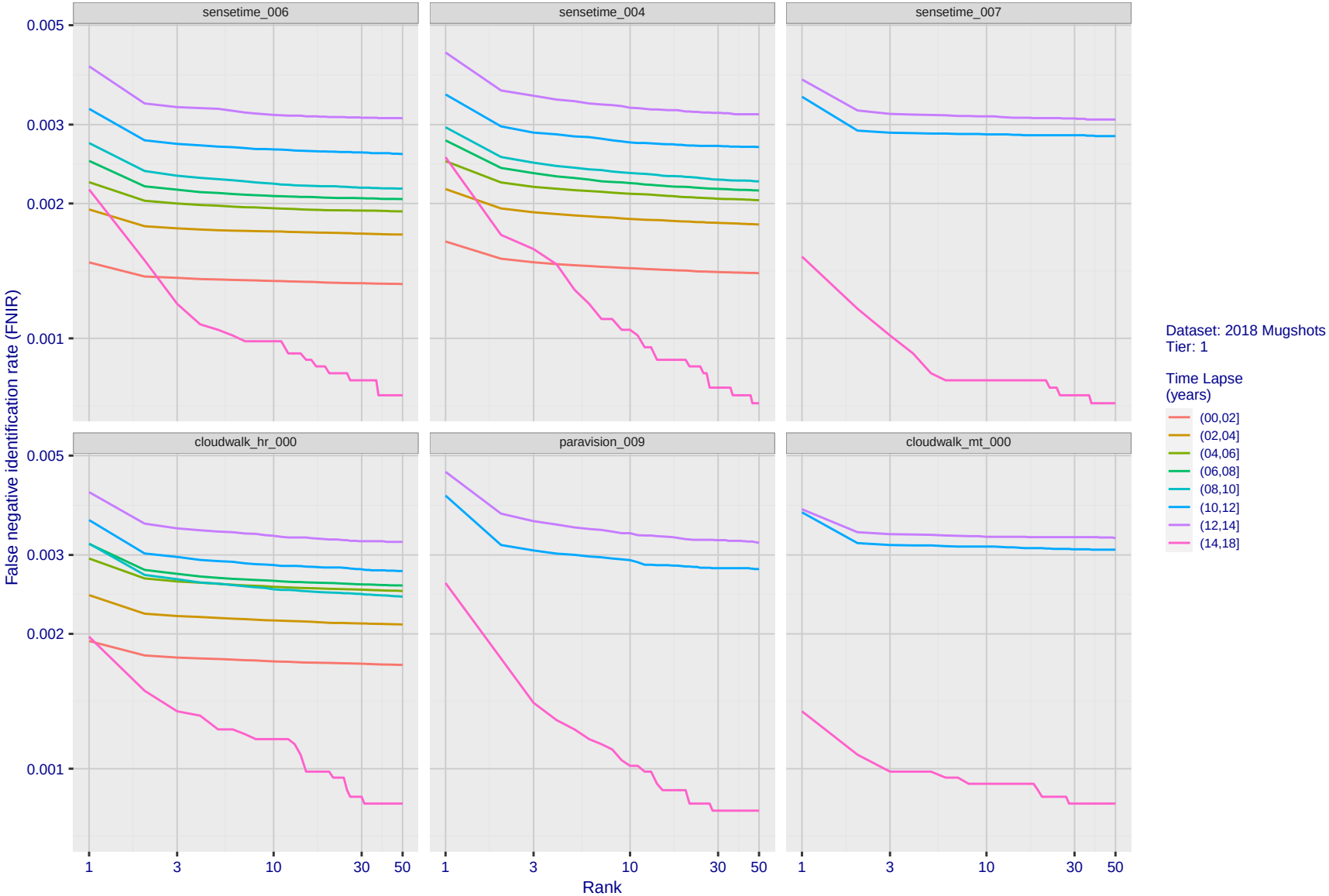

Figure 60: **[FRVT-2018 Mugshot Ageing Dataset] Identification miss rates vs. rank by time-elapsed**. *The oldest image of each individual is enrolled. Thereafter, all more recent images are searched. Miss rates are computed over all searches noted in row 17 of Table 1 and binned by number of years between search and initial enrollment.*

This publication is available free of charge from: https://doi.org/10.6028/NIST.IR.8271

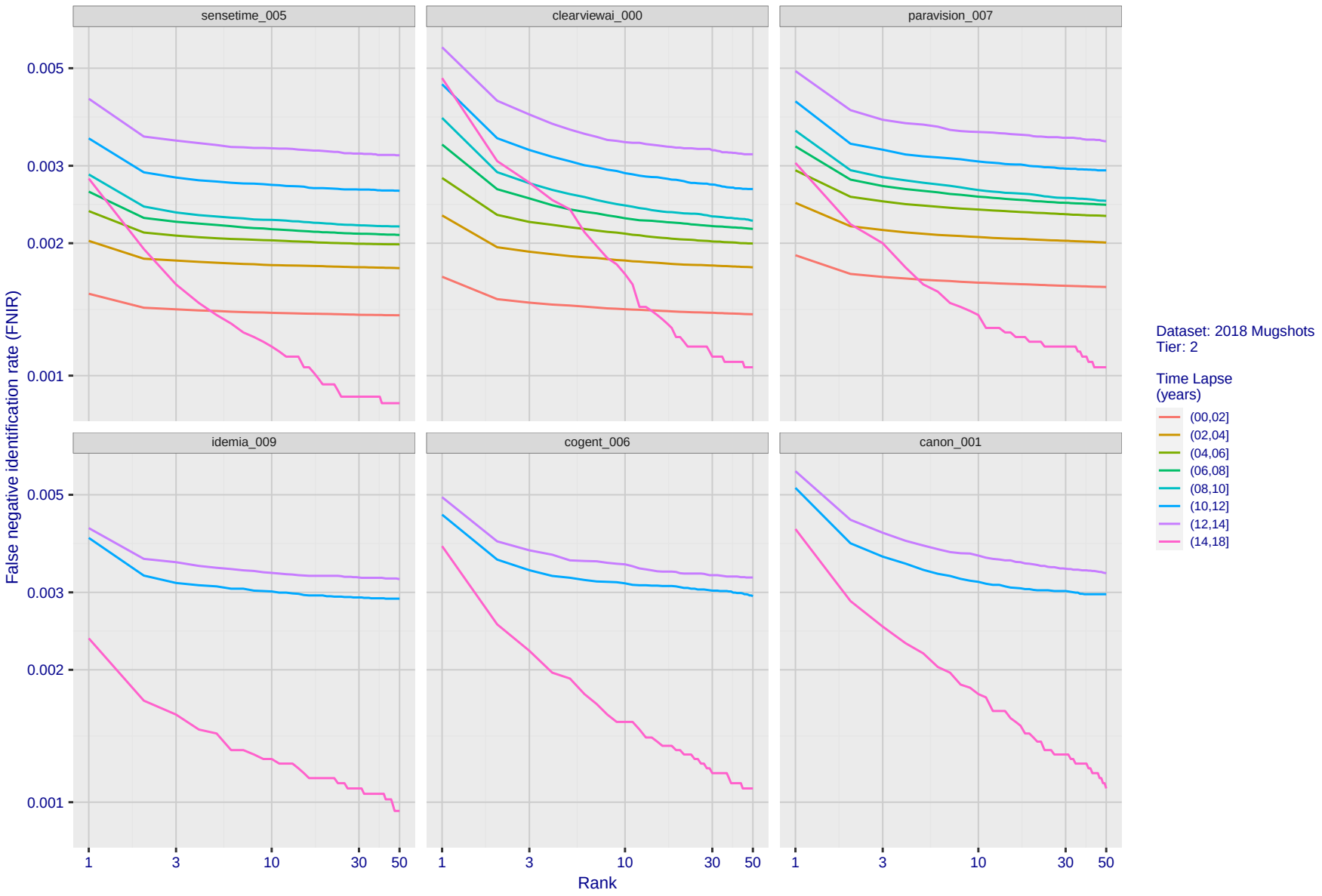

Figure 61: **[FRVT-2018 Mugshot Ageing Dataset] Identification miss rates vs. rank by time-elapsed**. *The oldest image of each individual is enrolled. Thereafter, all more recent images are searched. Miss rates are computed over all searches noted in row 17 of Table 1 and binned by number of years between search and initial enrollment.*

This publication is available free of charge from: https://doi.org/10.6028/NIST.IR.8271

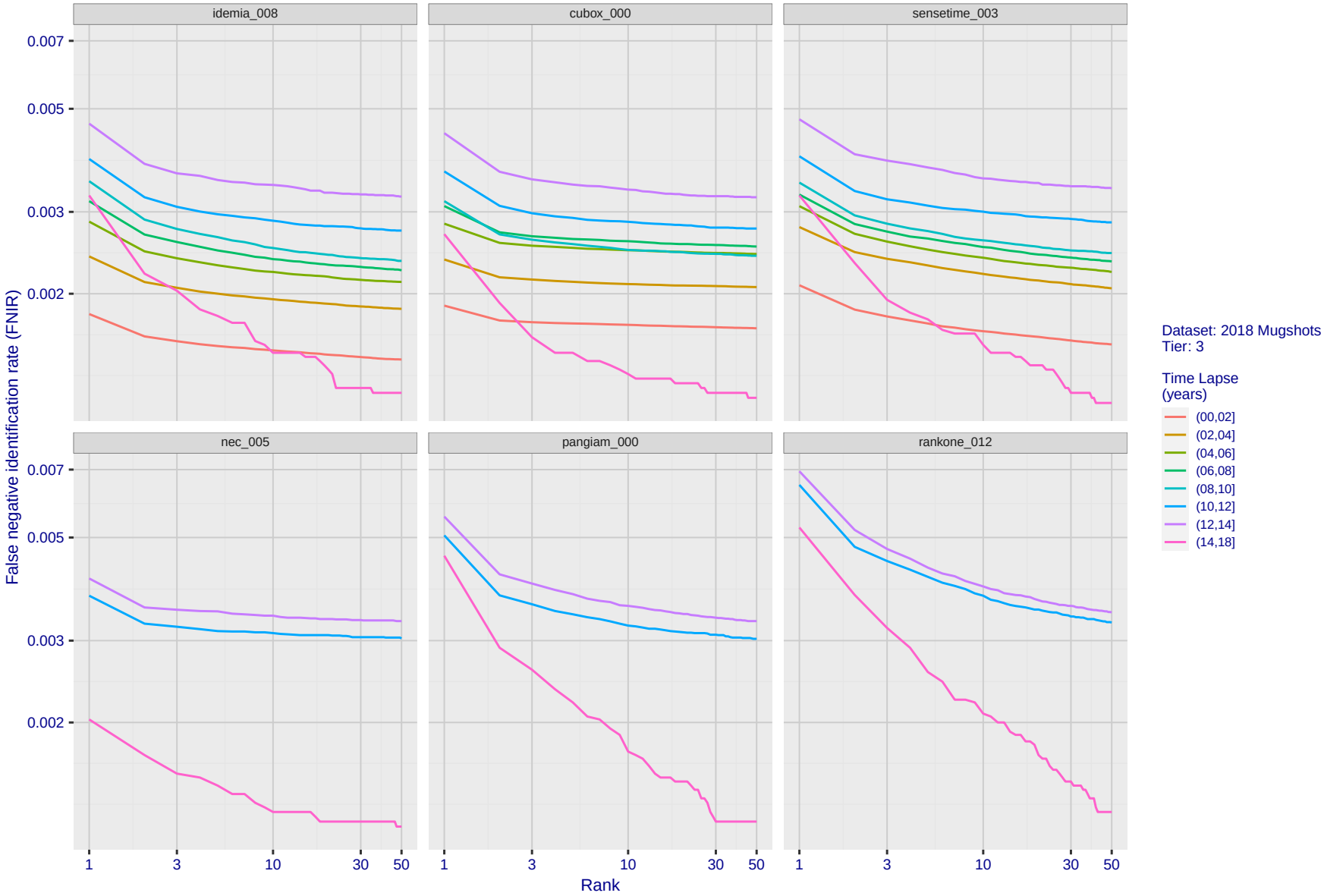

Figure 62: **[FRVT-2018 Mugshot Ageing Dataset] Identification miss rates vs. rank by time-elapsed**. *The oldest image of each individual is enrolled. Thereafter, all more recent images are searched. Miss rates are computed over all searches noted in row 17 of Table 1 and binned by number of years between search and initial enrollment.*

This publication is available free of charge from: https://doi.org/10.6028/NIST.IR.8271

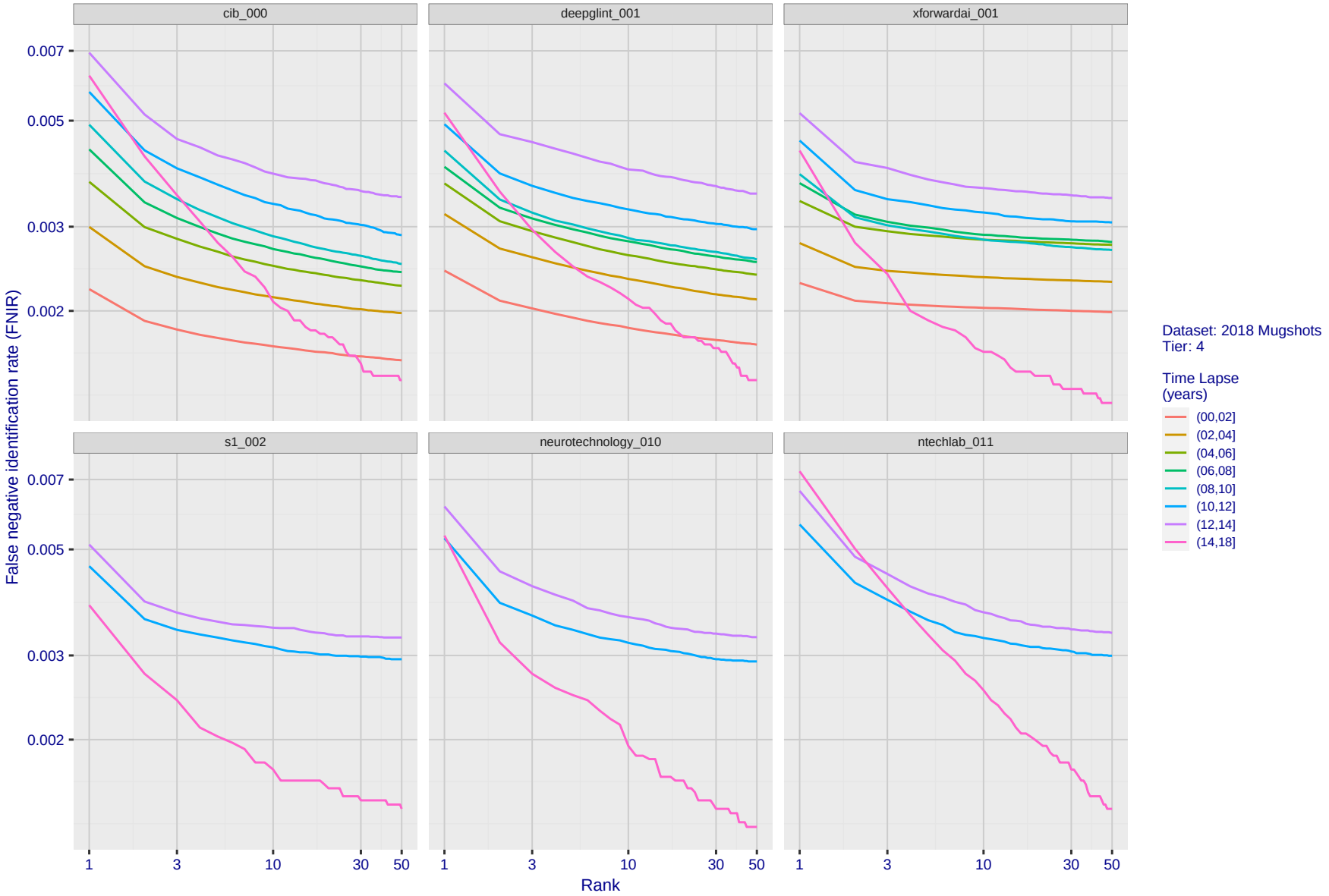

Figure 63: **[FRVT-2018 Mugshot Ageing Dataset] Identification miss rates vs. rank by time-elapsed**. *The oldest image of each individual is enrolled. Thereafter, all more recent images are searched. Miss rates are computed over all searches noted in row 17 of Table 1 and binned by number of years between search and initial enrollment.*

This publication is available free of charge from: https://doi.org/10.6028/NIST.IR.8271

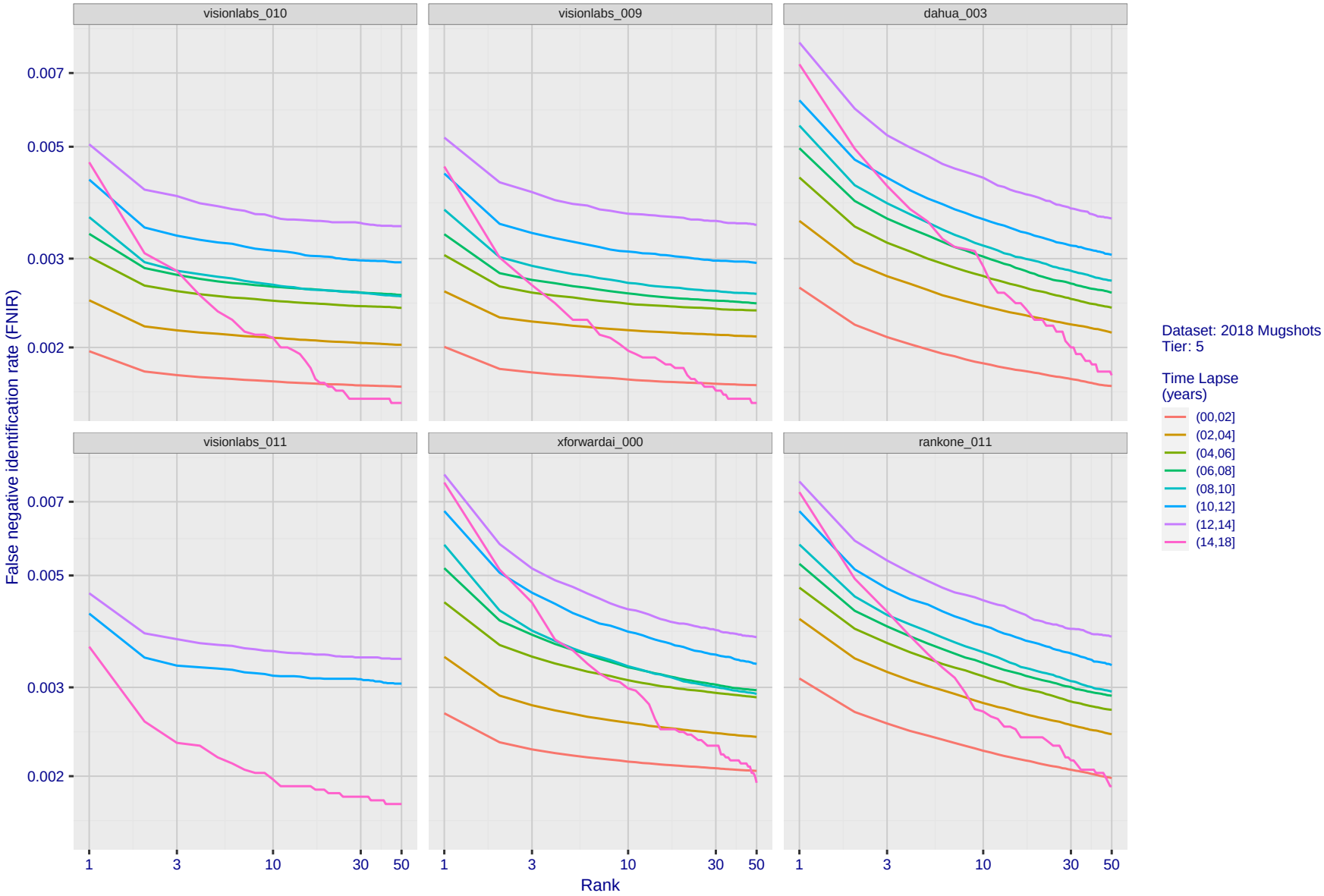

Figure 64: **[FRVT-2018 Mugshot Ageing Dataset] Identification miss rates vs. rank by time-elapsed**. *The oldest image of each individual is enrolled. Thereafter, all more recent images are searched. Miss rates are computed over all searches noted in row 17 of Table 1 and binned by number of years between search and initial enrollment.*

This publication is available free of charge from: https://doi.org/10.6028/NIST.IR.8271

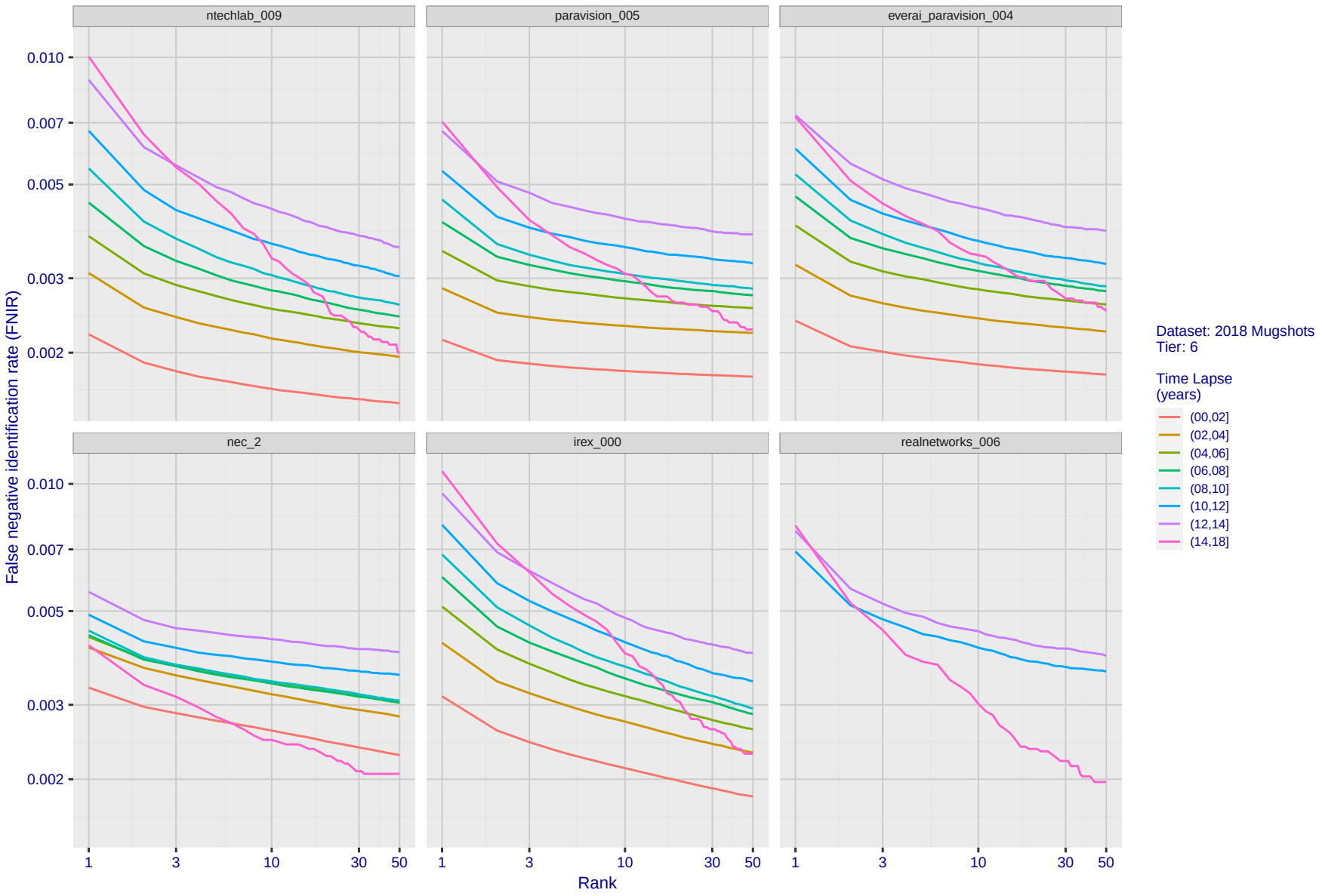

Figure 65: **[FRVT-2018 Mugshot Ageing Dataset] Identification miss rates vs. rank by time-elapsed**. *The oldest image of each individual is enrolled. Thereafter, all more recent images are searched. Miss rates are computed over all searches noted in row 17 of Table 1 and binned by number of years between search and initial enrollment.*

This publication is available free of charge from: https://doi.org/10.6028/NIST.IR.8271

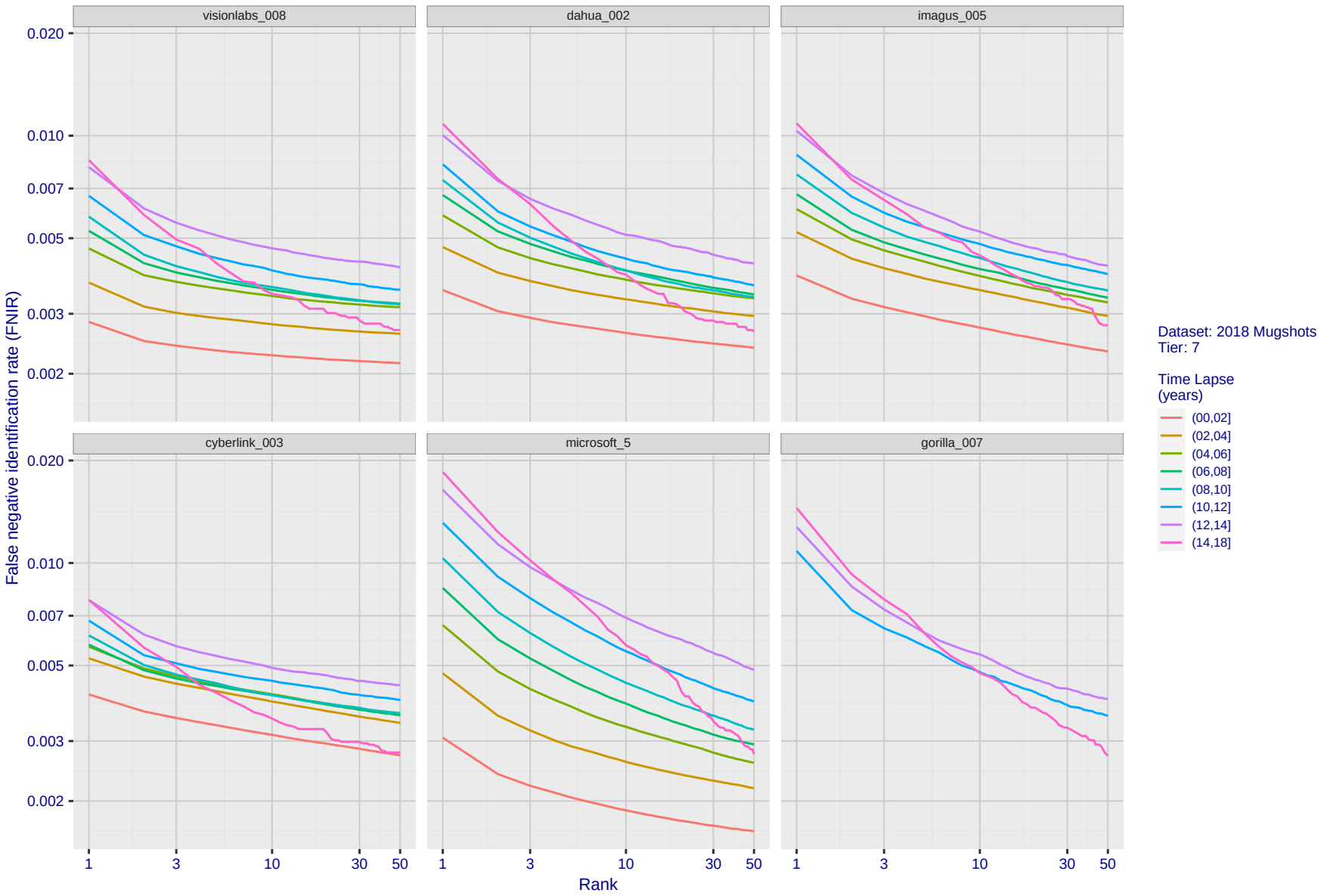

Figure 66: **[FRVT-2018 Mugshot Ageing Dataset] Identification miss rates vs. rank by time-elapsed**. *The oldest image of each individual is enrolled. Thereafter, all more recent images are searched. Miss rates are computed over all searches noted in row 17 of Table 1 and binned by number of years between search and initial enrollment.*

This publication is available free of charge from: https://doi.org/10.6028/NIST.IR.8271

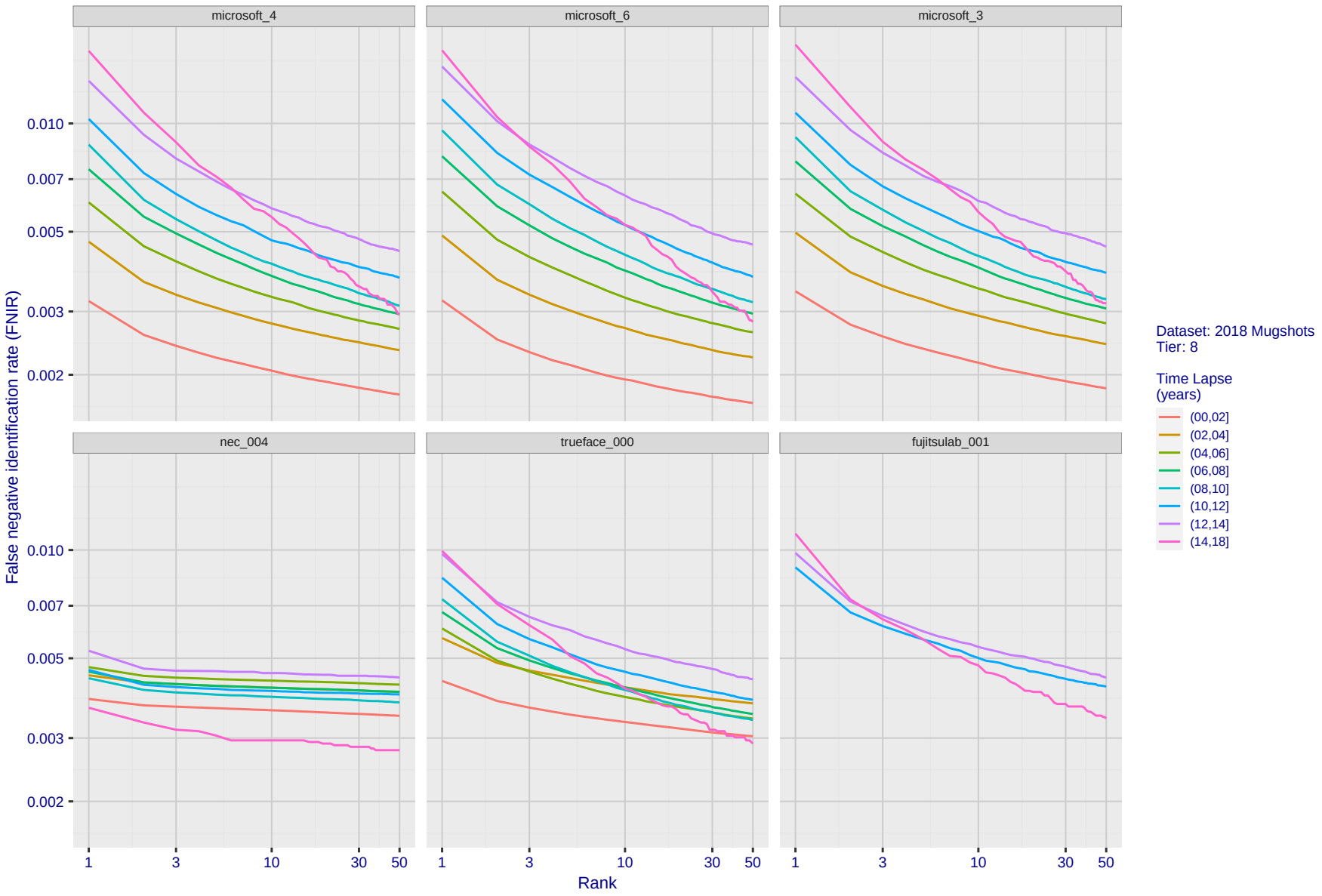

Figure 67: **[FRVT-2018 Mugshot Ageing Dataset] Identification miss rates vs. rank by time-elapsed**. *The oldest image of each individual is enrolled. Thereafter, all more recent images are searched. Miss rates are computed over all searches noted in row 17 of Table 1 and binned by number of years between search and initial enrollment.*

This publication is available free of charge from: https://doi.org/10.6028/NIST.IR.8271

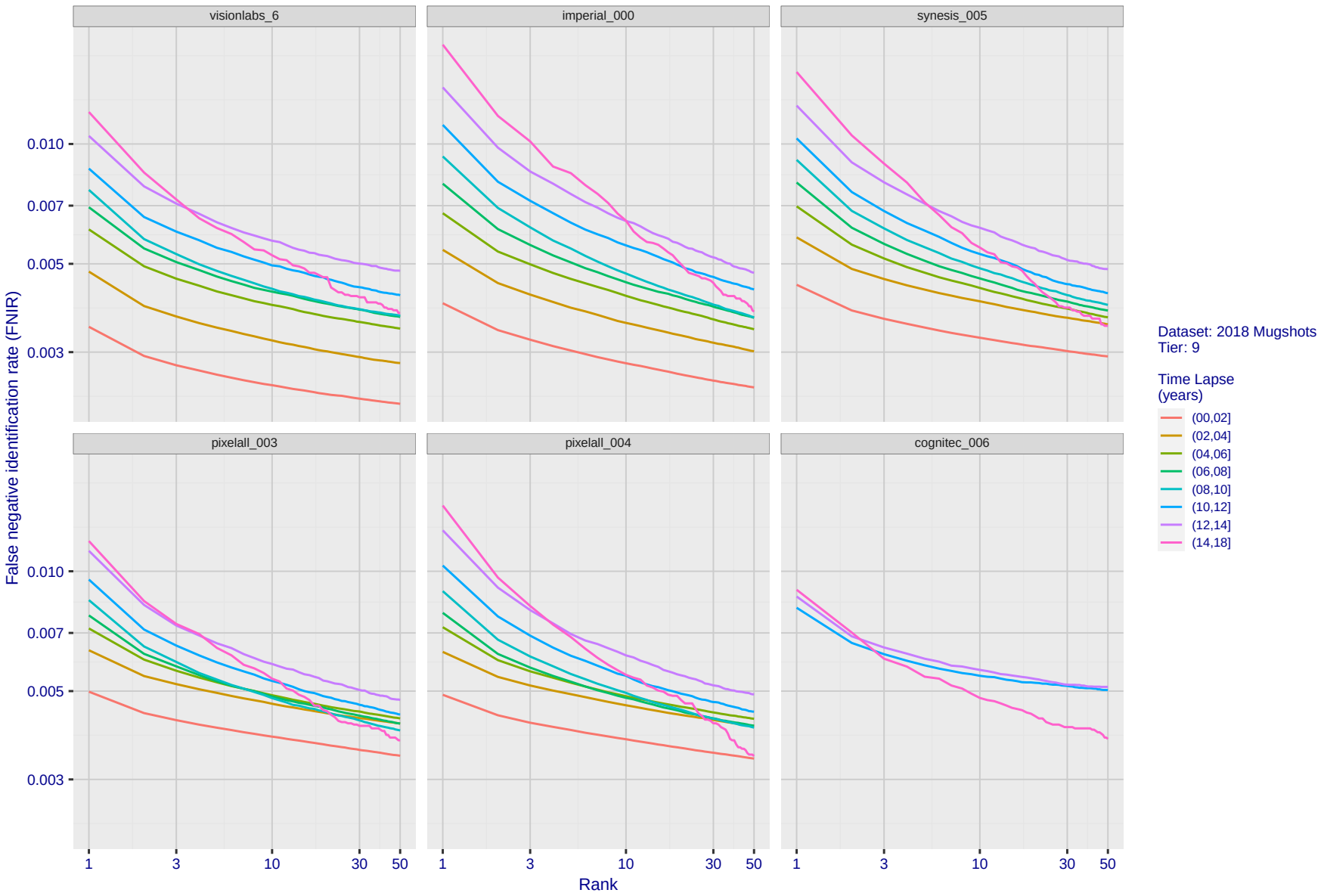

Figure 68: **[FRVT-2018 Mugshot Ageing Dataset] Identification miss rates vs. rank by time-elapsed**. *The oldest image of each individual is enrolled. Thereafter, all more recent images are searched. Miss rates are computed over all searches noted in row 17 of Table 1 and binned by number of years between search and initial enrollment.*

This publication is available free of charge from: https://doi.org/10.6028/NIST.IR.8271

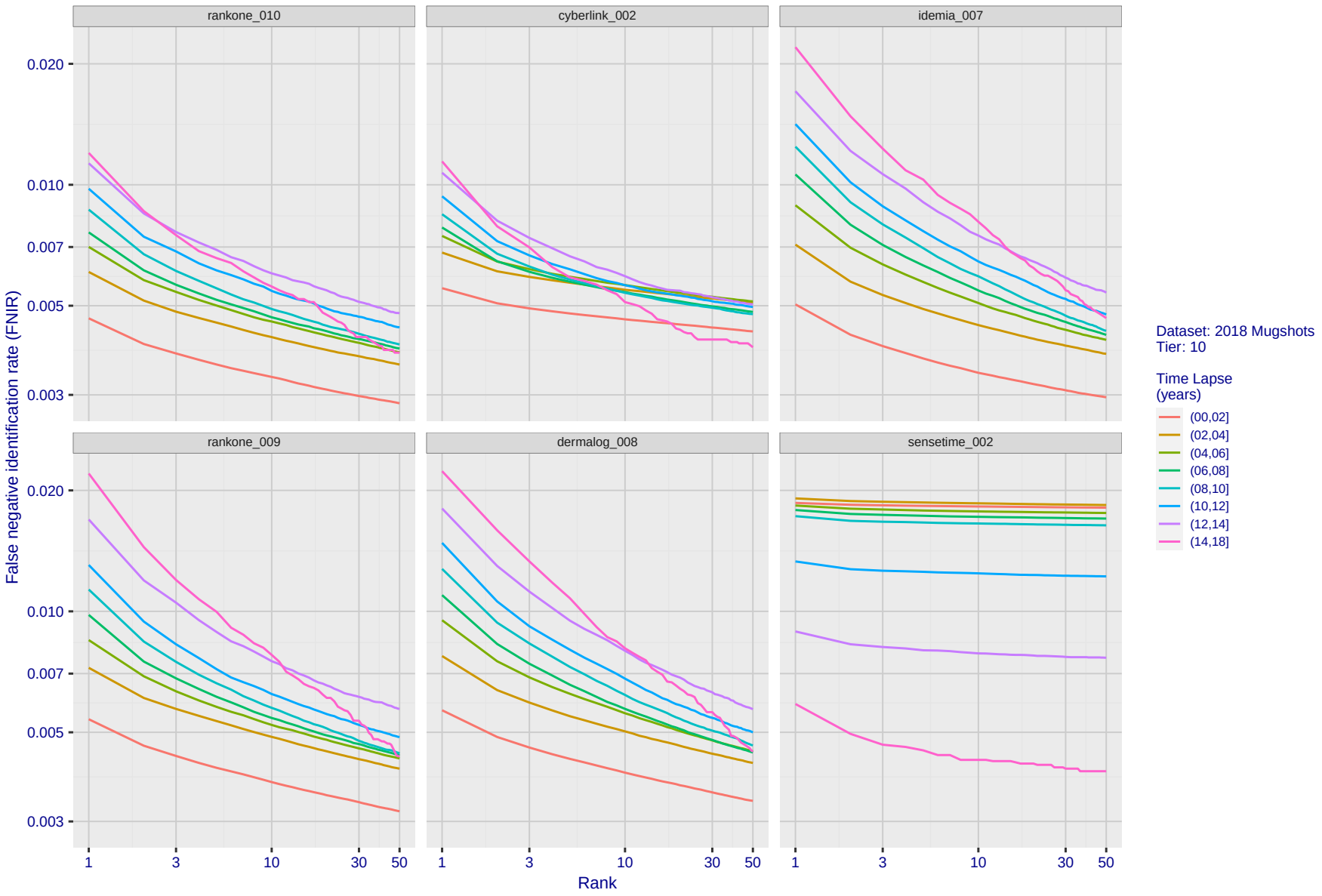

Figure 69: **[FRVT-2018 Mugshot Ageing Dataset] Identification miss rates vs. rank by time-elapsed**. *The oldest image of each individual is enrolled. Thereafter, all more recent images are searched. Miss rates are computed over all searches noted in row 17 of Table 1 and binned by number of years between search and initial enrollment.*

This publication is available free of charge from: https://doi.org/10.6028/NIST.IR.8271

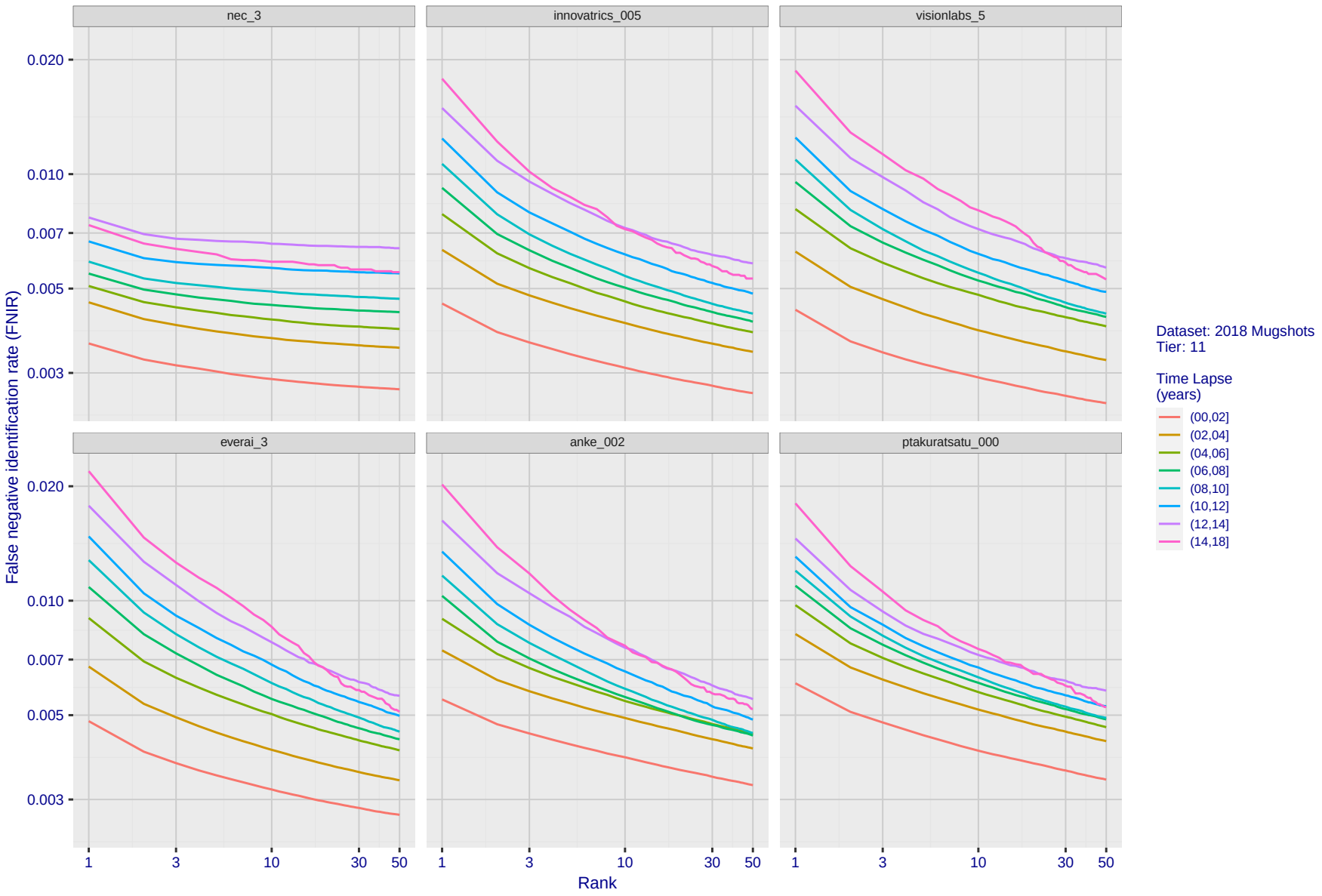

Figure 70: **[FRVT-2018 Mugshot Ageing Dataset] Identification miss rates vs. rank by time-elapsed**. *The oldest image of each individual is enrolled. Thereafter, all more recent images are searched. Miss rates are computed over all searches noted in row 17 of Table 1 and binned by number of years between search and initial enrollment.*

This publication is available free of charge from: https://doi.org/10.6028/NIST.IR.8271

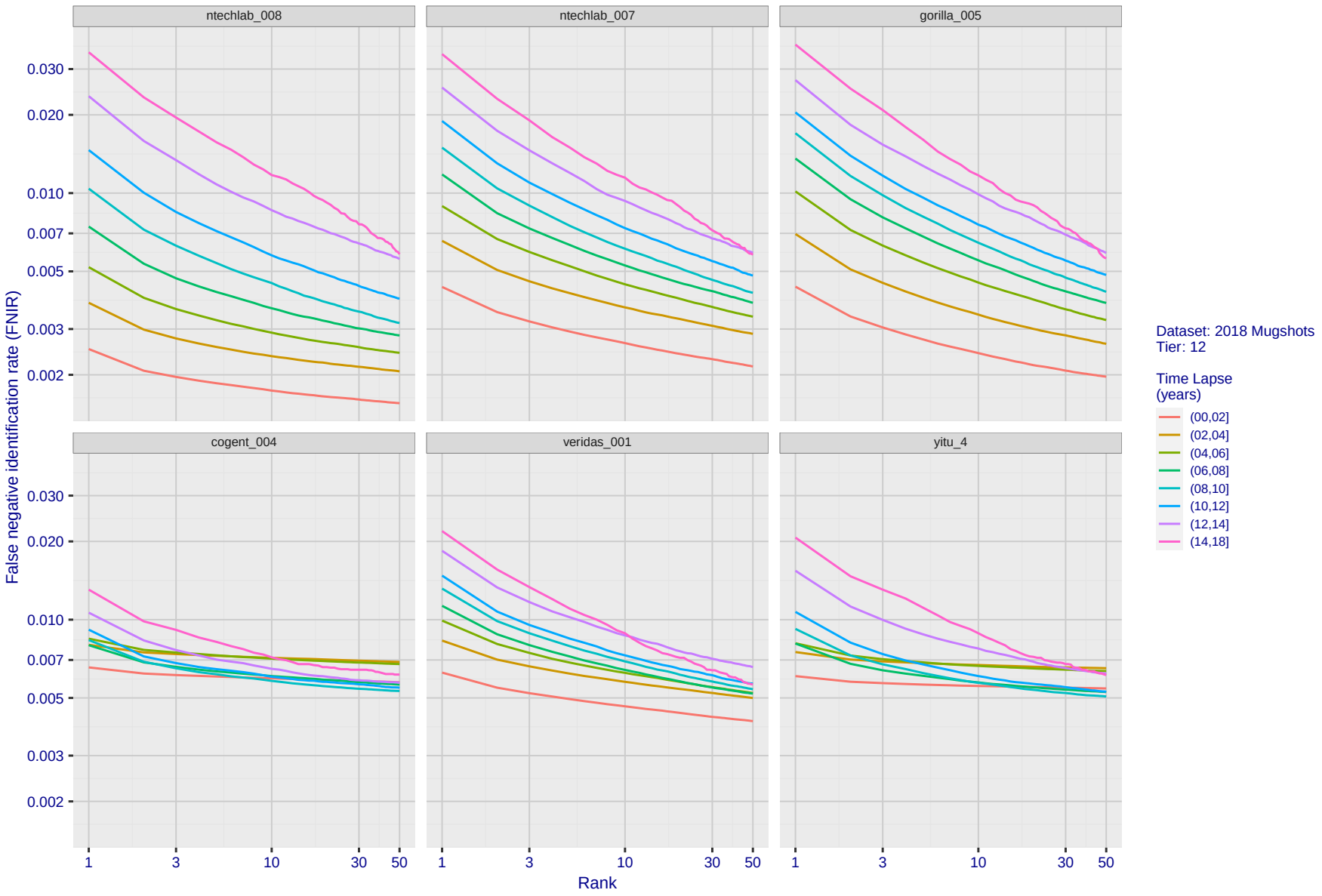

Figure 71: **[FRVT-2018 Mugshot Ageing Dataset] Identification miss rates vs. rank by time-elapsed**. *The oldest image of each individual is enrolled. Thereafter, all more recent images are searched. Miss rates are computed over all searches noted in row 17 of Table 1 and binned by number of years between search and initial enrollment.*

This publication is available free of charge from: https://doi.org/10.6028/NIST.IR.8271

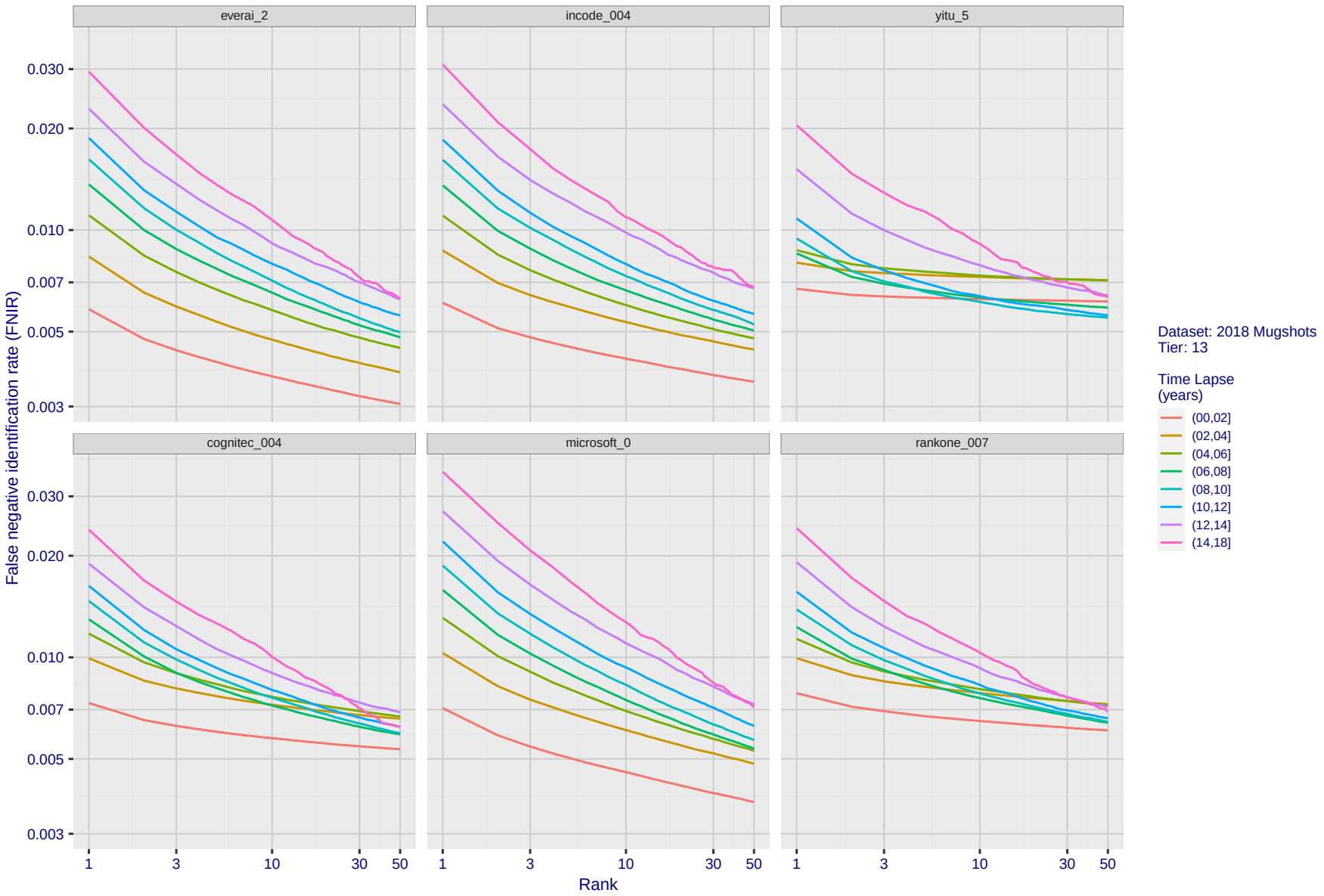

Figure 72: **[FRVT-2018 Mugshot Ageing Dataset] Identification miss rates vs. rank by time-elapsed**. *The oldest image of each individual is enrolled. Thereafter, all more recent images are searched. Miss rates are computed over all searches noted in row 17 of Table 1 and binned by number of years between search and initial enrollment.*

This publication is available free of charge from: https://doi.org/10.6028/NIST.IR.8271

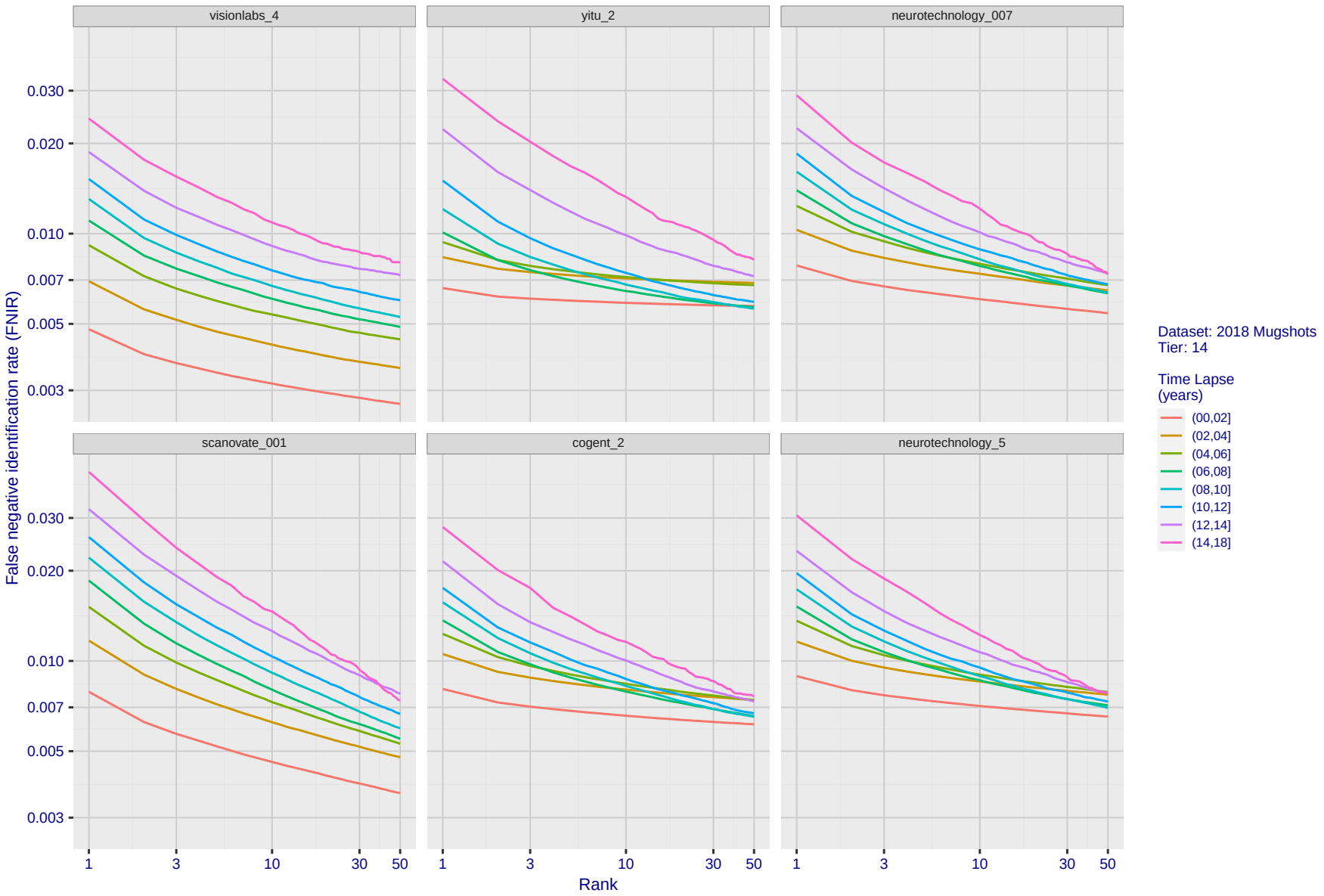

Figure 73: **[FRVT-2018 Mugshot Ageing Dataset] Identification miss rates vs. rank by time-elapsed**. *The oldest image of each individual is enrolled. Thereafter, all more recent images are searched. Miss rates are computed over all searches noted in row 17 of Table 1 and binned by number of years between search and initial enrollment.*

This publication is available free of charge from: https://doi.org/10.6028/NIST.IR.8271

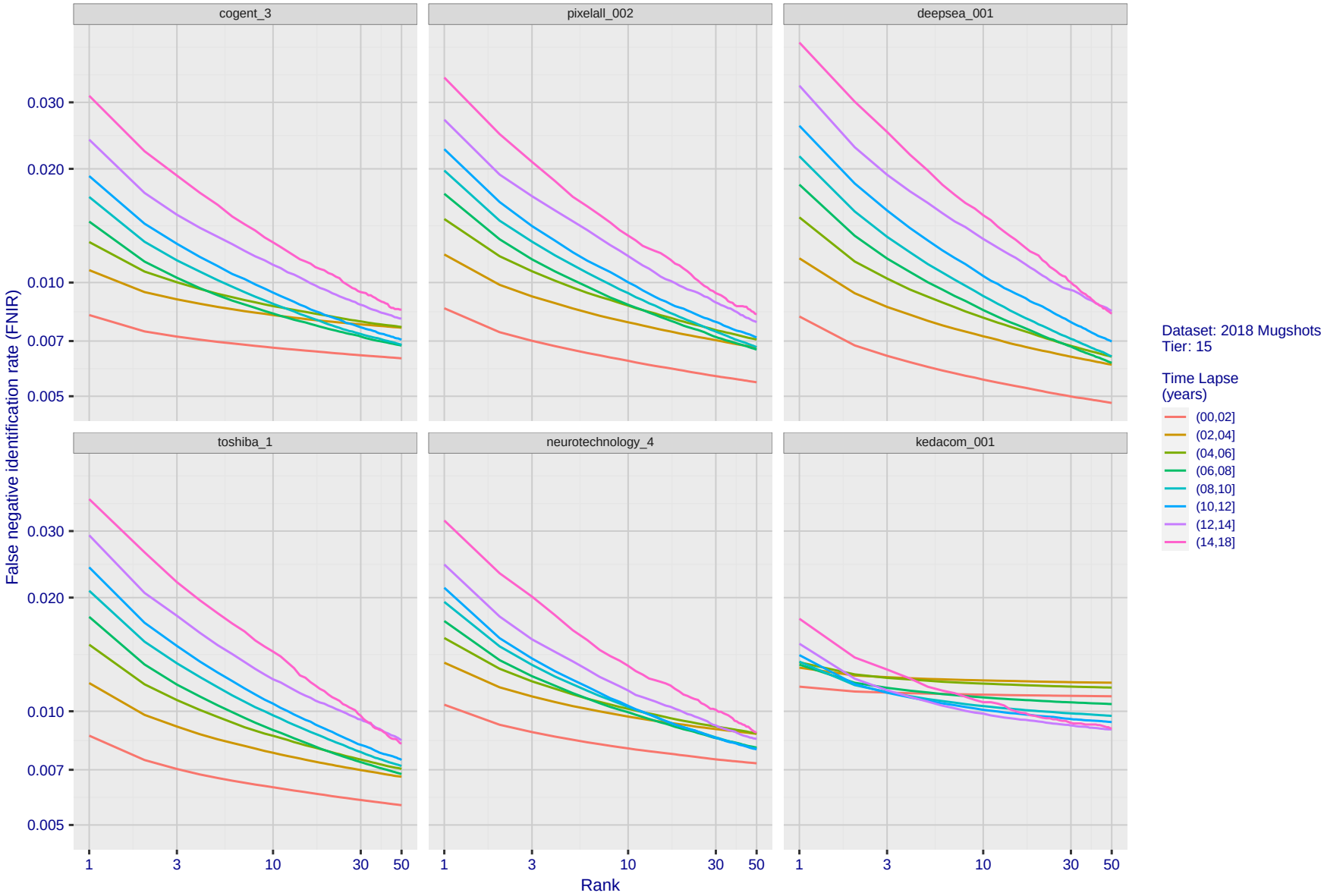

Figure 74: **[FRVT-2018 Mugshot Ageing Dataset] Identification miss rates vs. rank by time-elapsed**. *The oldest image of each individual is enrolled. Thereafter, all more recent images are searched. Miss rates are computed over all searches noted in row 17 of Table 1 and binned by number of years between search and initial enrollment.*

This publication is available free of charge from: https://doi.org/10.6028/NIST.IR.8271

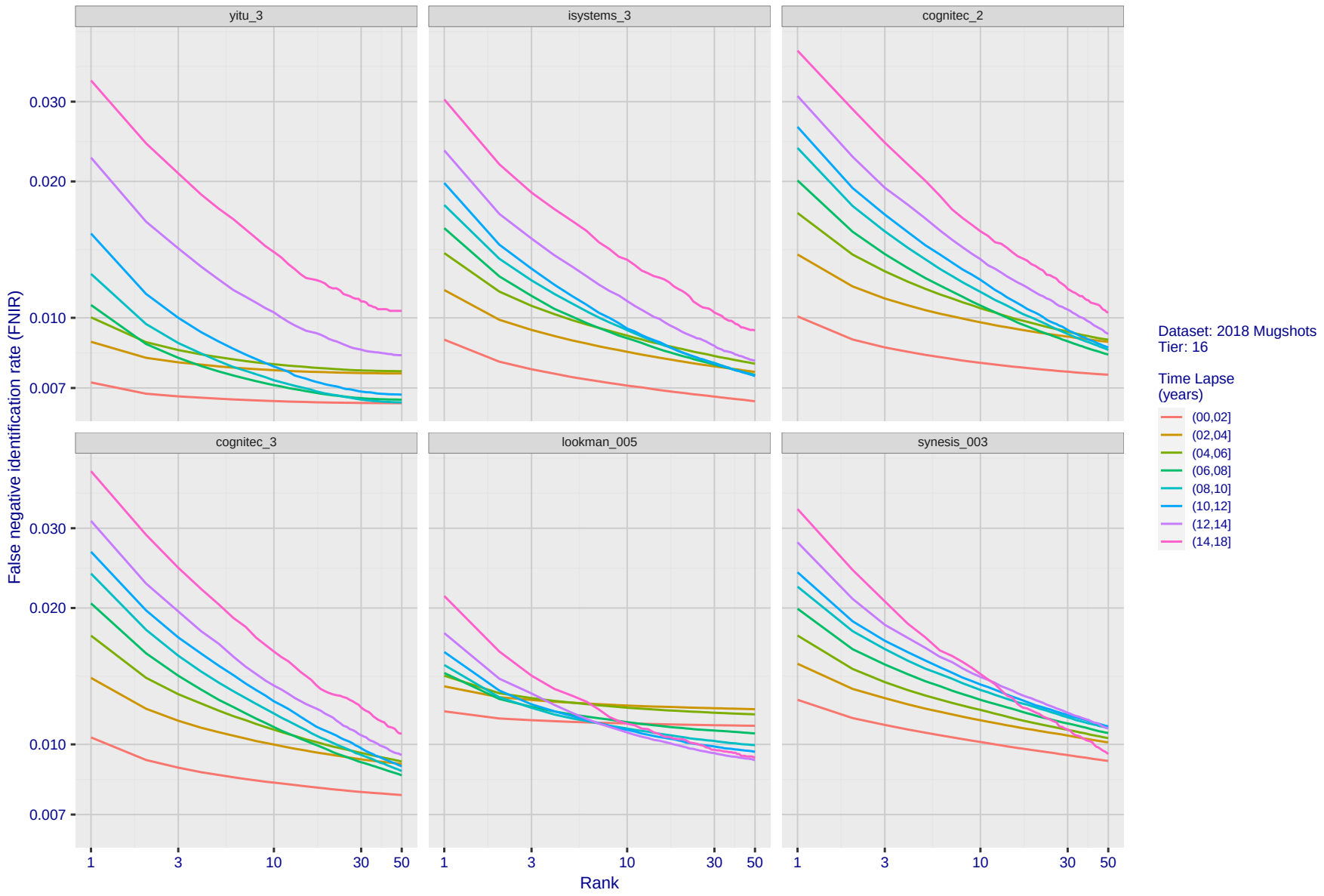

Figure 75: **[FRVT-2018 Mugshot Ageing Dataset] Identification miss rates vs. rank by time-elapsed**. *The oldest image of each individual is enrolled. Thereafter, all more recent images are searched. Miss rates are computed over all searches noted in row 17 of Table 1 and binned by number of years between search and initial enrollment.*

This publication is available free of charge from: https://doi.org/10.6028/NIST.IR.8271

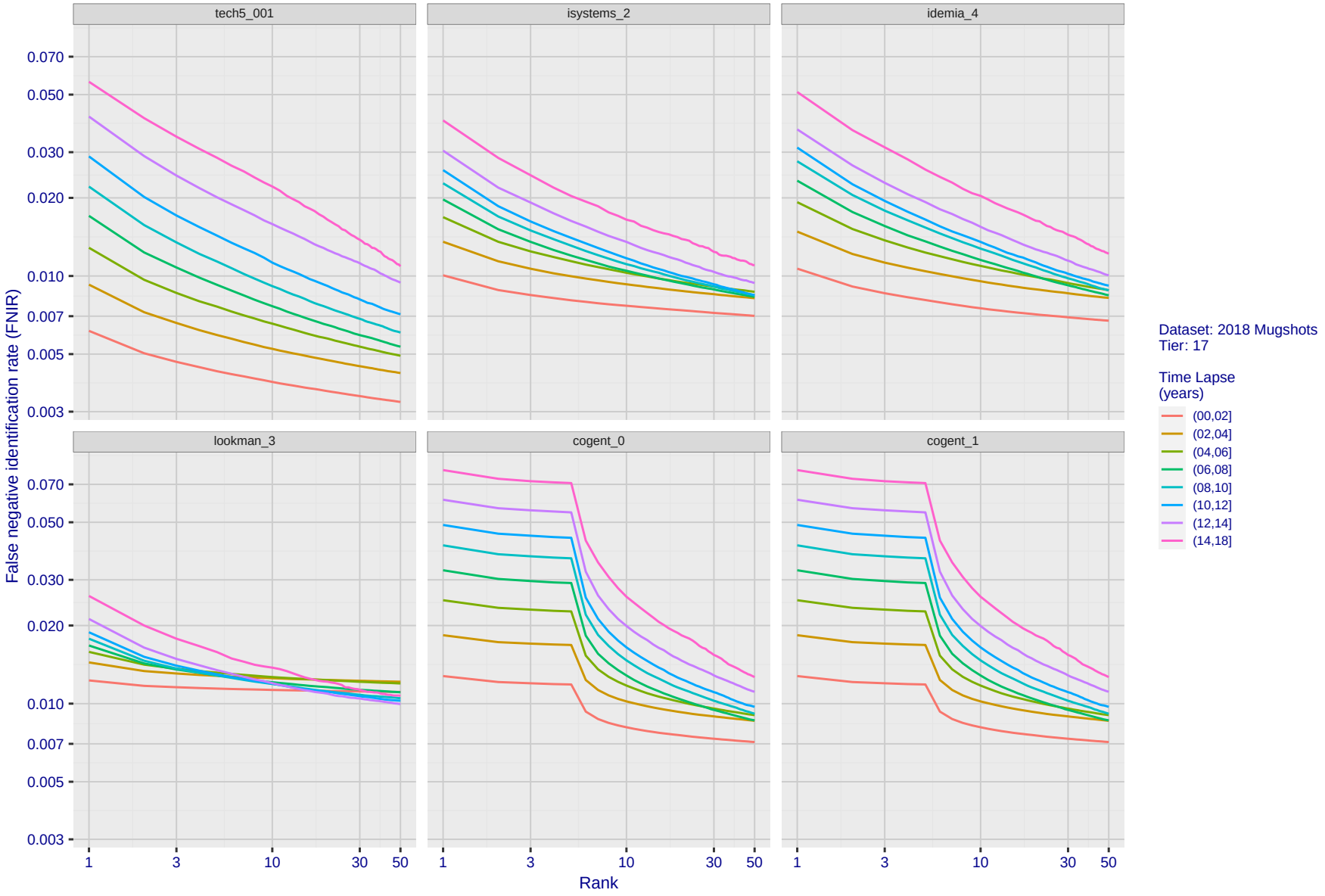

Figure 76: **[FRVT-2018 Mugshot Ageing Dataset] Identification miss rates vs. rank by time-elapsed**. *The oldest image of each individual is enrolled. Thereafter, all more recent images are searched. Miss rates are computed over all searches noted in row 17 of Table 1 and binned by number of years between search and initial enrollment.*

This publication is available free of charge from: https://doi.org/10.6028/NIST.IR.8271

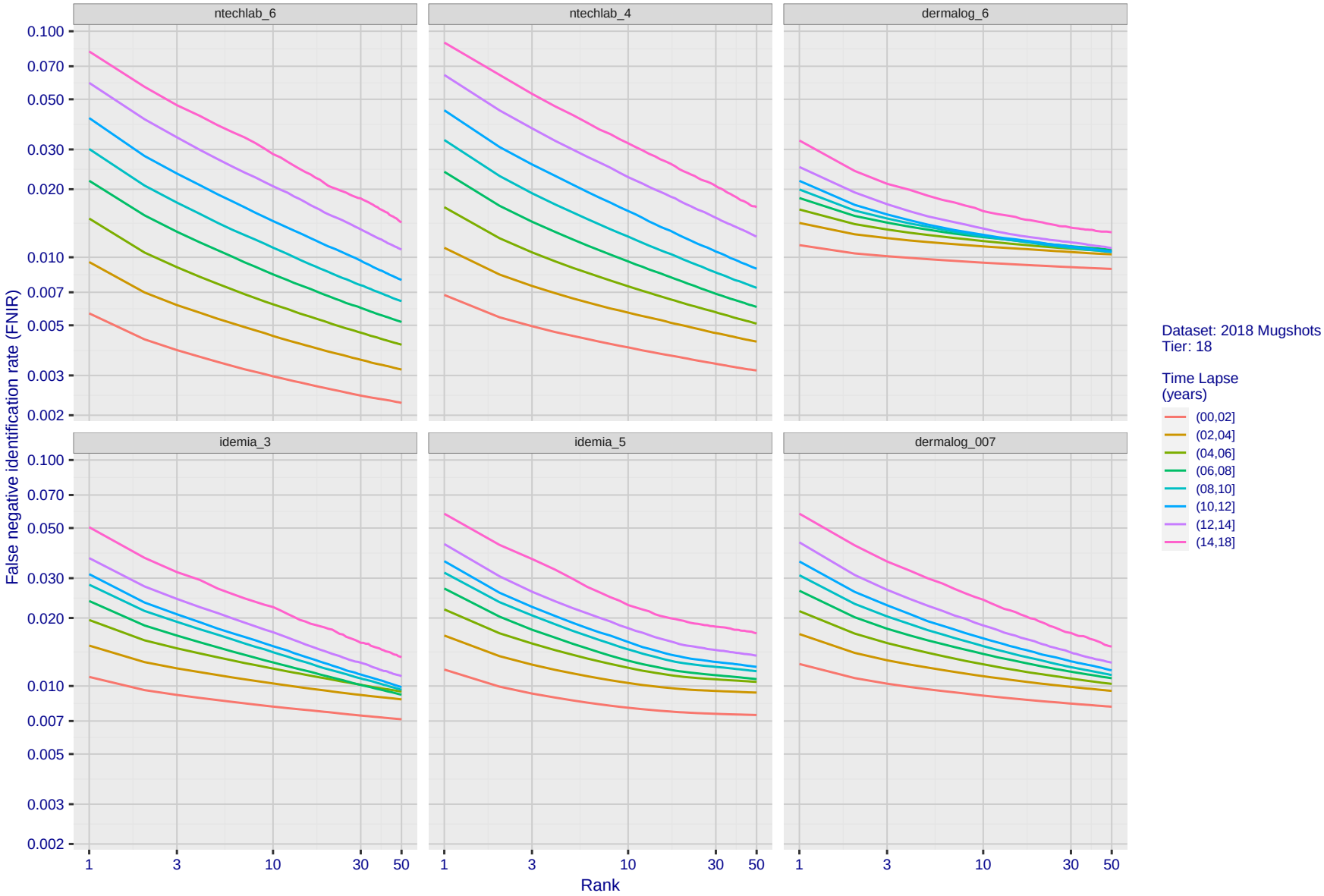

Figure 77: **[FRVT-2018 Mugshot Ageing Dataset] Identification miss rates vs. rank by time-elapsed**. *The oldest image of each individual is enrolled. Thereafter, all more recent images are searched. Miss rates are computed over all searches noted in row 17 of Table 1 and binned by number of years between search and initial enrollment.*

This publication is available free of charge from: https://doi.org/10.6028/NIST.IR.8271

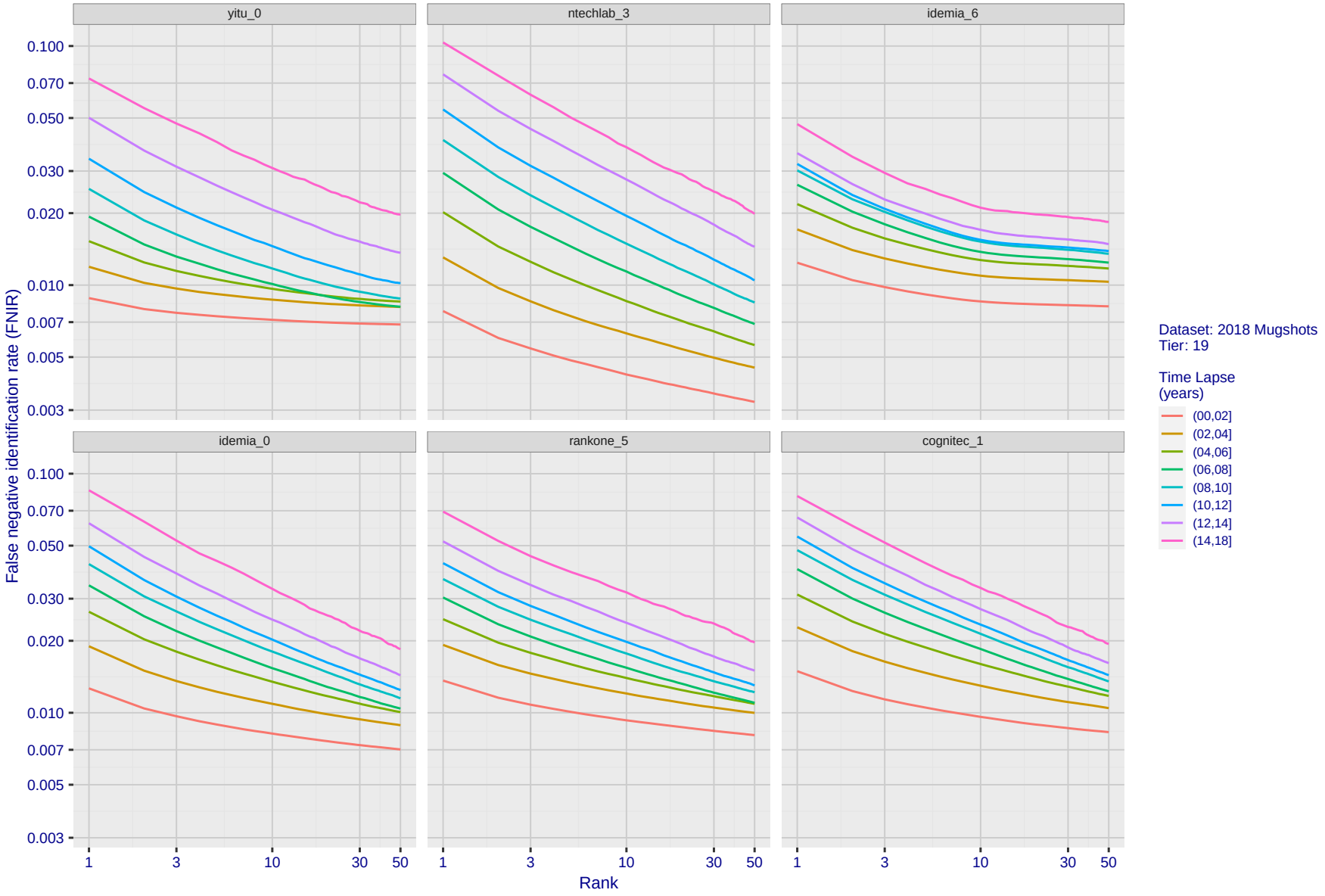

Figure 78: **[FRVT-2018 Mugshot Ageing Dataset] Identification miss rates vs. rank by time-elapsed**. *The oldest image of each individual is enrolled. Thereafter, all more recent images are searched. Miss rates are computed over all searches noted in row 17 of Table 1 and binned by number of years between search and initial enrollment.*

This publication is available free of charge from: https://doi.org/10.6028/NIST.IR.8271

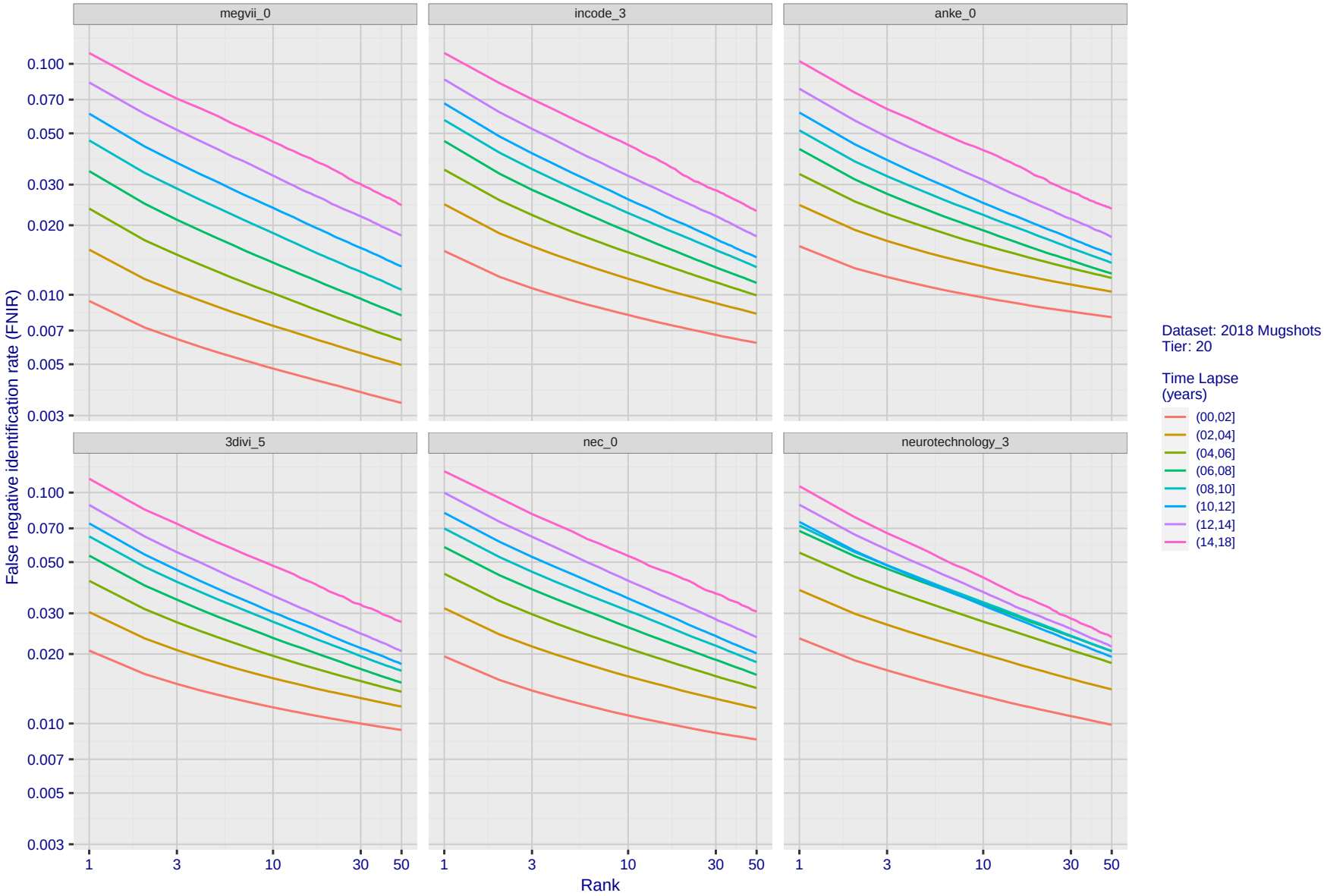

Figure 79: **[FRVT-2018 Mugshot Ageing Dataset] Identification miss rates vs. rank by time-elapsed**. *The oldest image of each individual is enrolled. Thereafter, all more recent images are searched. Miss rates are computed over all searches noted in row 17 of Table 1 and binned by number of years between search and initial enrollment.*

This publication is available free of charge from: https://doi.org/10.6028/NIST.IR.8271

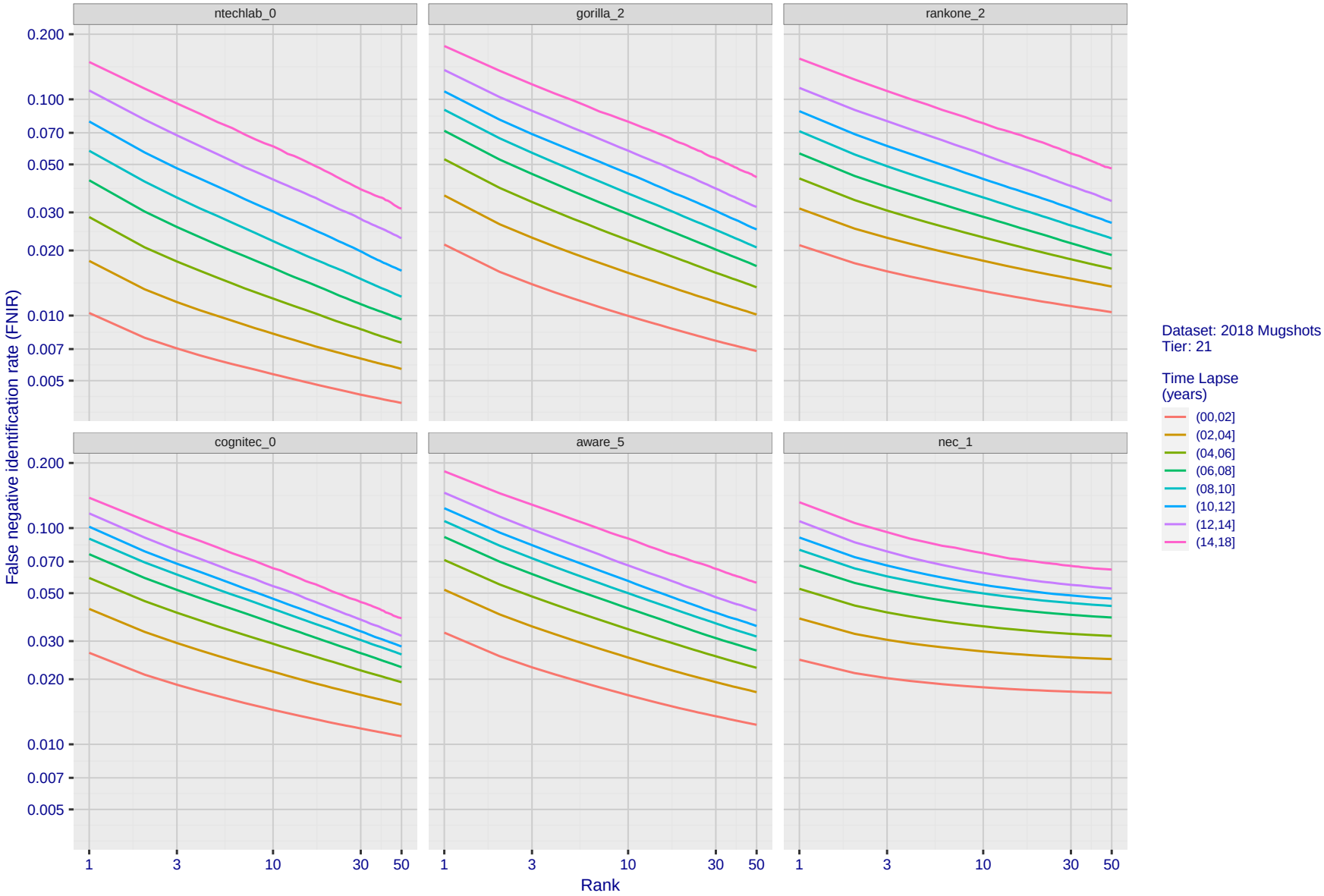

Figure 80: **[FRVT-2018 Mugshot Ageing Dataset] Identification miss rates vs. rank by time-elapsed**. *The oldest image of each individual is enrolled. Thereafter, all more recent images are searched. Miss rates are computed over all searches noted in row 17 of Table 1 and binned by number of years between search and initial enrollment.*

This publication is available free of charge from: https://doi.org/10.6028/NIST.IR.8271

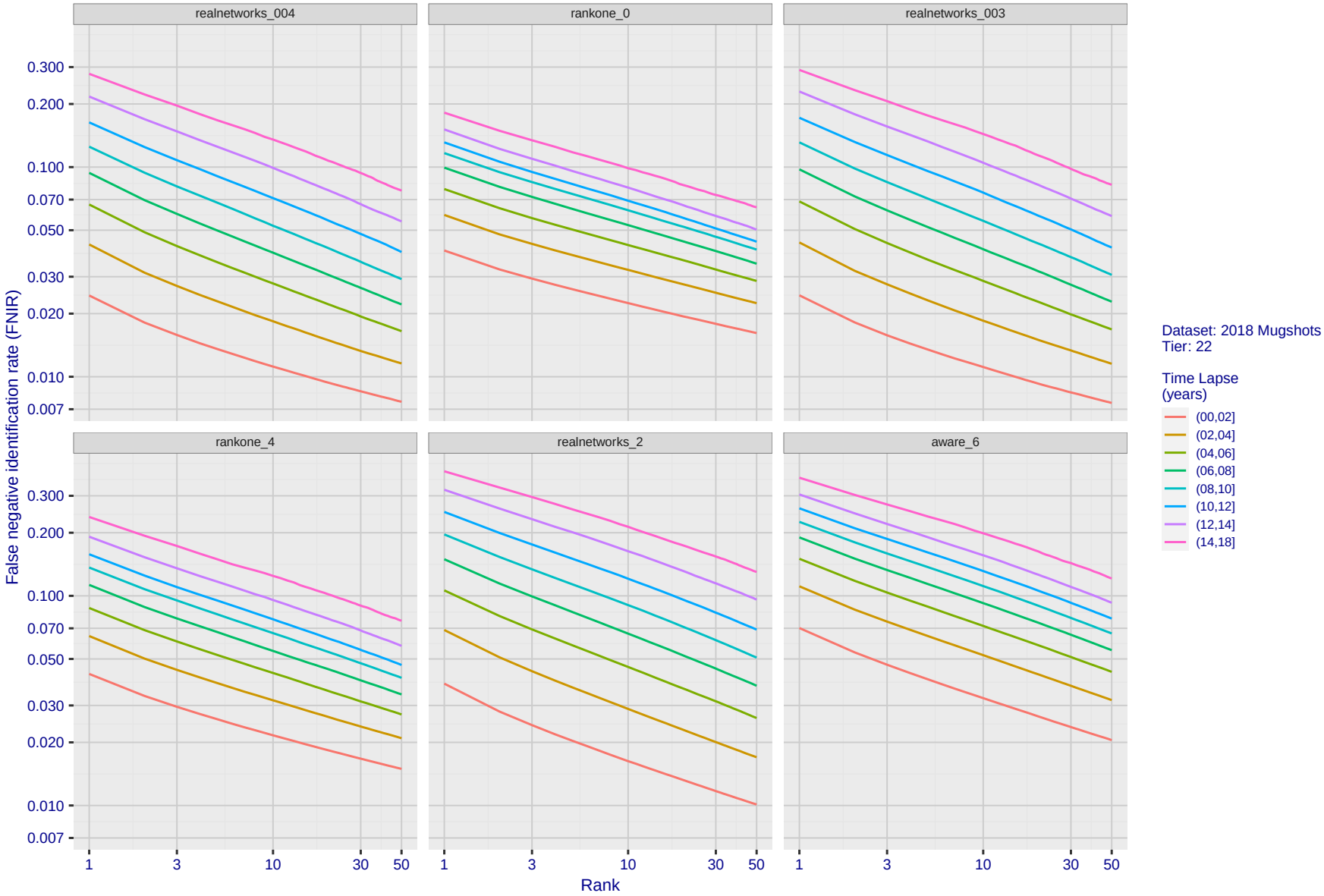

Figure 81: **[FRVT-2018 Mugshot Ageing Dataset] Identification miss rates vs. rank by time-elapsed**. *The oldest image of each individual is enrolled. Thereafter, all more recent images are searched. Miss rates are computed over all searches noted in row 17 of Table 1 and binned by number of years between search and initial enrollment.*

This publication is available free of charge from: https://doi.org/10.6028/NIST.IR.8271

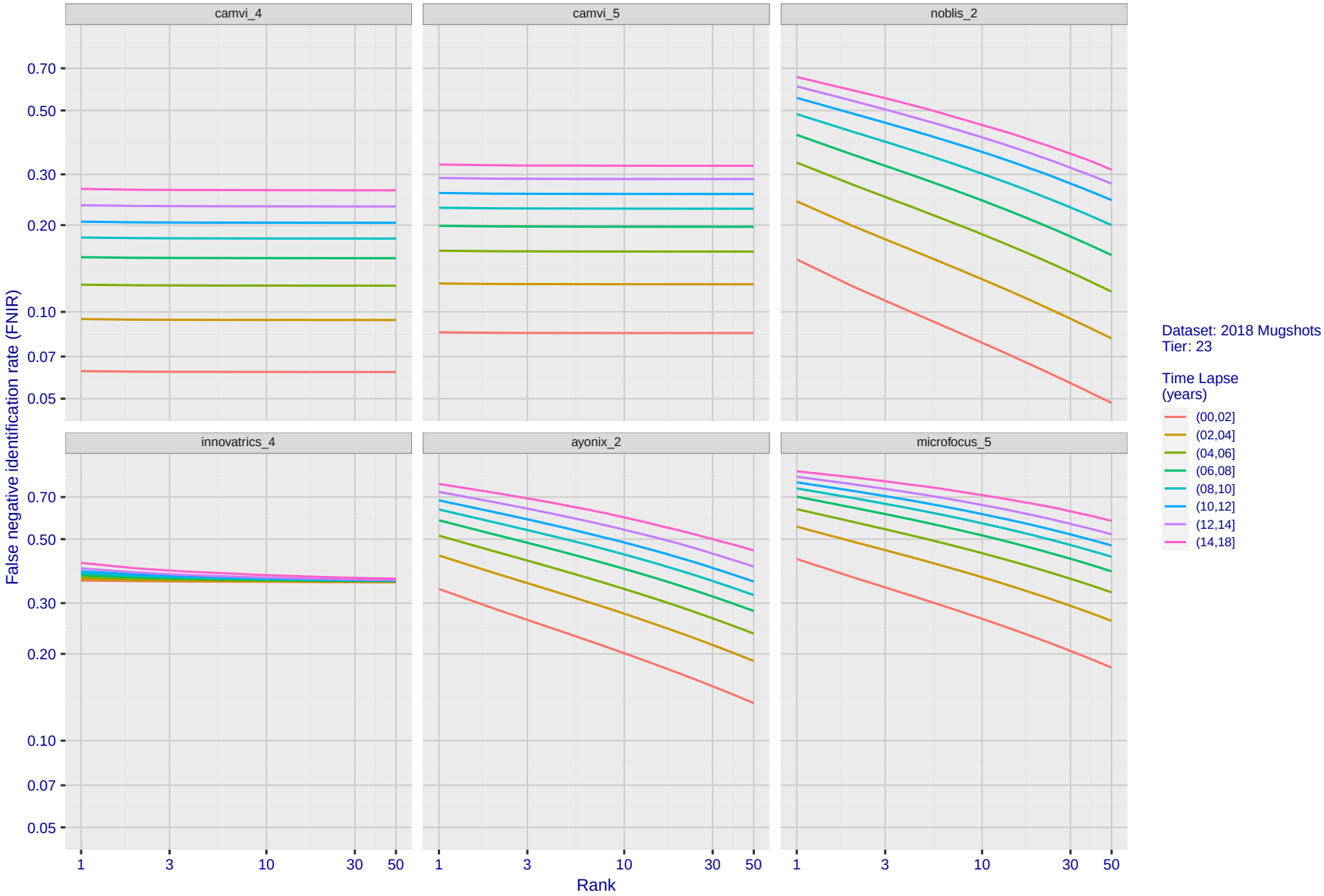

Figure 82: **[FRVT-2018 Mugshot Ageing Dataset] Identification miss rates vs. rank by time-elapsed**. *The oldest image of each individual is enrolled. Thereafter, all more recent images are searched. Miss rates are computed over all searches noted in row 17 of Table 1 and binned by number of years between search and initial enrollment.*

This publication is available free of charge from: https://doi.org/10.6028/NIST.IR.8271

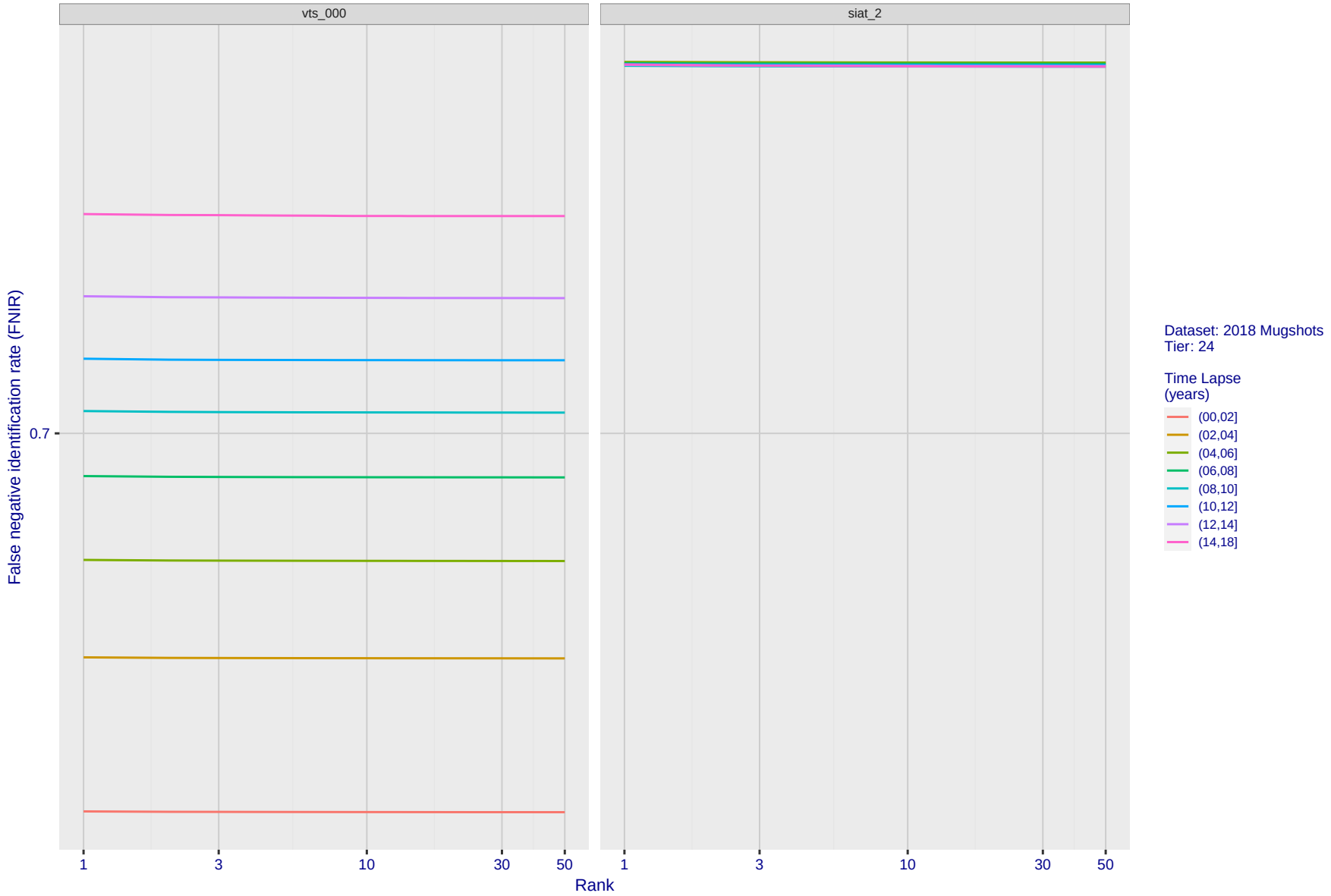

Figure 83: **[FRVT-2018 Mugshot Ageing Dataset] Identification miss rates vs. rank by time-elapsed**. *The oldest image of each individual is enrolled. Thereafter, all more recent images are searched. Miss rates are computed over all searches noted in row 17 of Table 1 and binned by number of years between search and initial enrollment.*

2022/06/13	FNIR(N, R, T) =	False neg. identification rate	N = Num. enrolled subjects	T = Threshold	$T = 0 \rightarrow$ Investigation
18:09:57	FPIR(N, T) =	False pos. identification rate	R = Num. candidates examined		$T > 0 \rightarrow$ Identification

This publication is available free of charge from: https://doi.org/10.6028/NIST.IR.8271

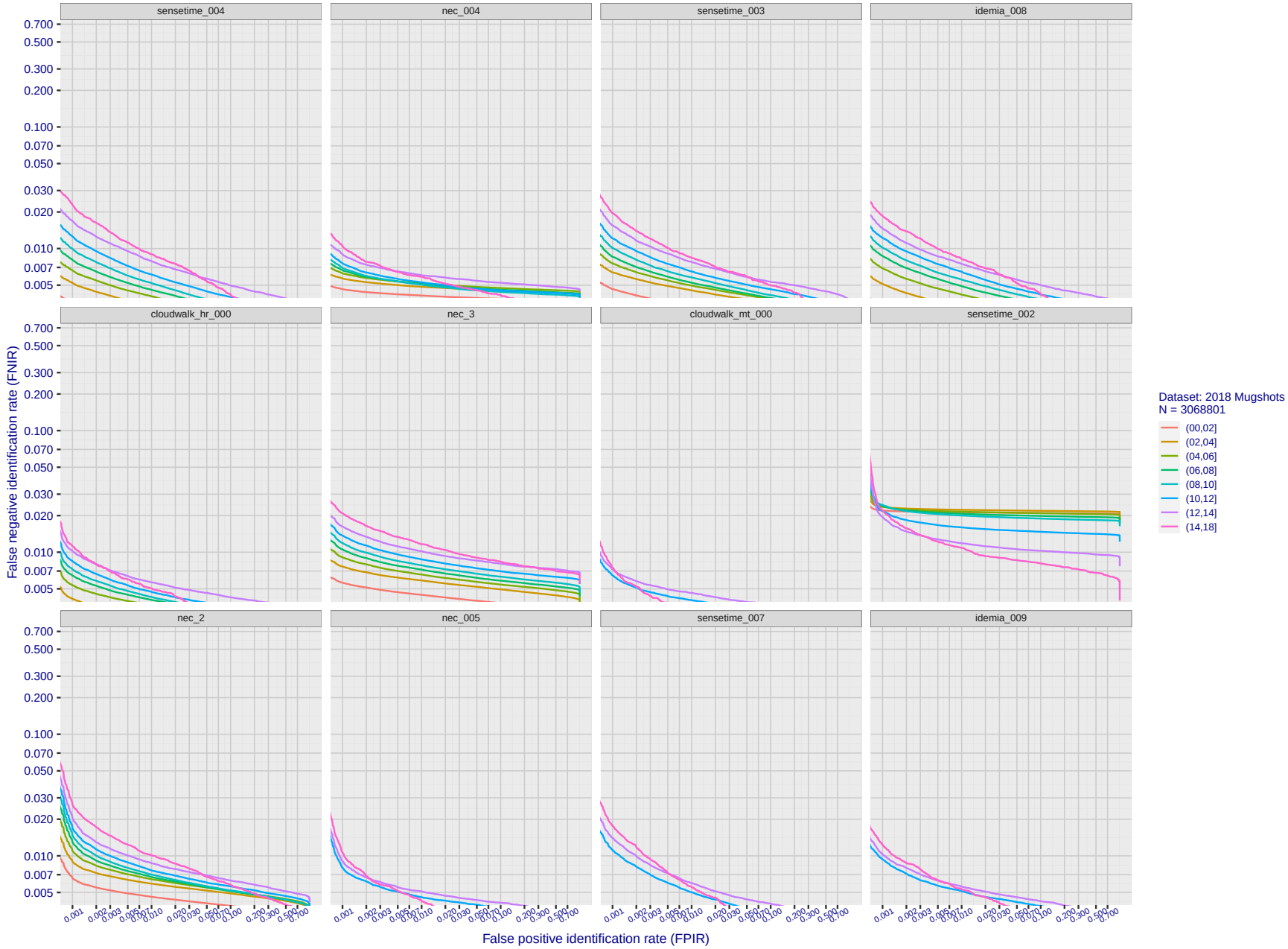

Figure 84: **[FRVT-2018 Mugshot Ageing Dataset] Identification miss rates vs. FPIR by time-elapsed**. *The oldest image of each individual is enrolled. Thereafter, all more recent images are searched. Miss rates are computed over all searches noted in row 17 of Table 1 and binned by number of years between search and initial enrollment. FPIR is computed from the same FRVT 2018 non-mates noted in row 3 of Table 1 with N = 3 000 000.*

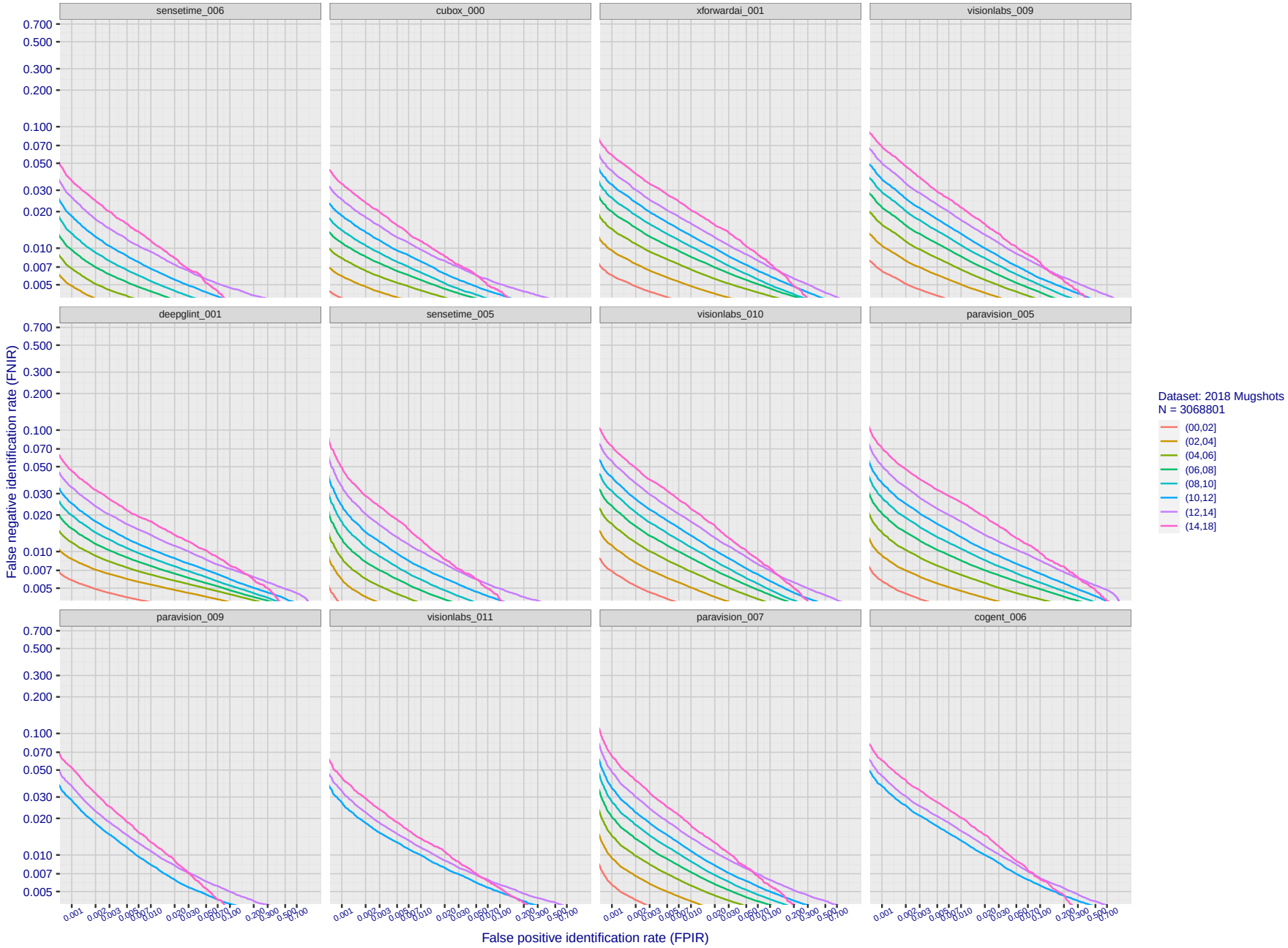

Figure 85: **[FRVT-2018 Mugshot Ageing Dataset] Identification miss rates vs. FPIR by time-elapsed**. *The oldest image of each individual is enrolled. Thereafter, all more recent images are searched. Miss rates are computed over all searches noted in row 17 of Table 1 and binned by number of years between search and initial enrollment. FPIR is computed from the same FRVT 2018 non-mates noted in row 3 of Table 1 with N = 3 000 000.*

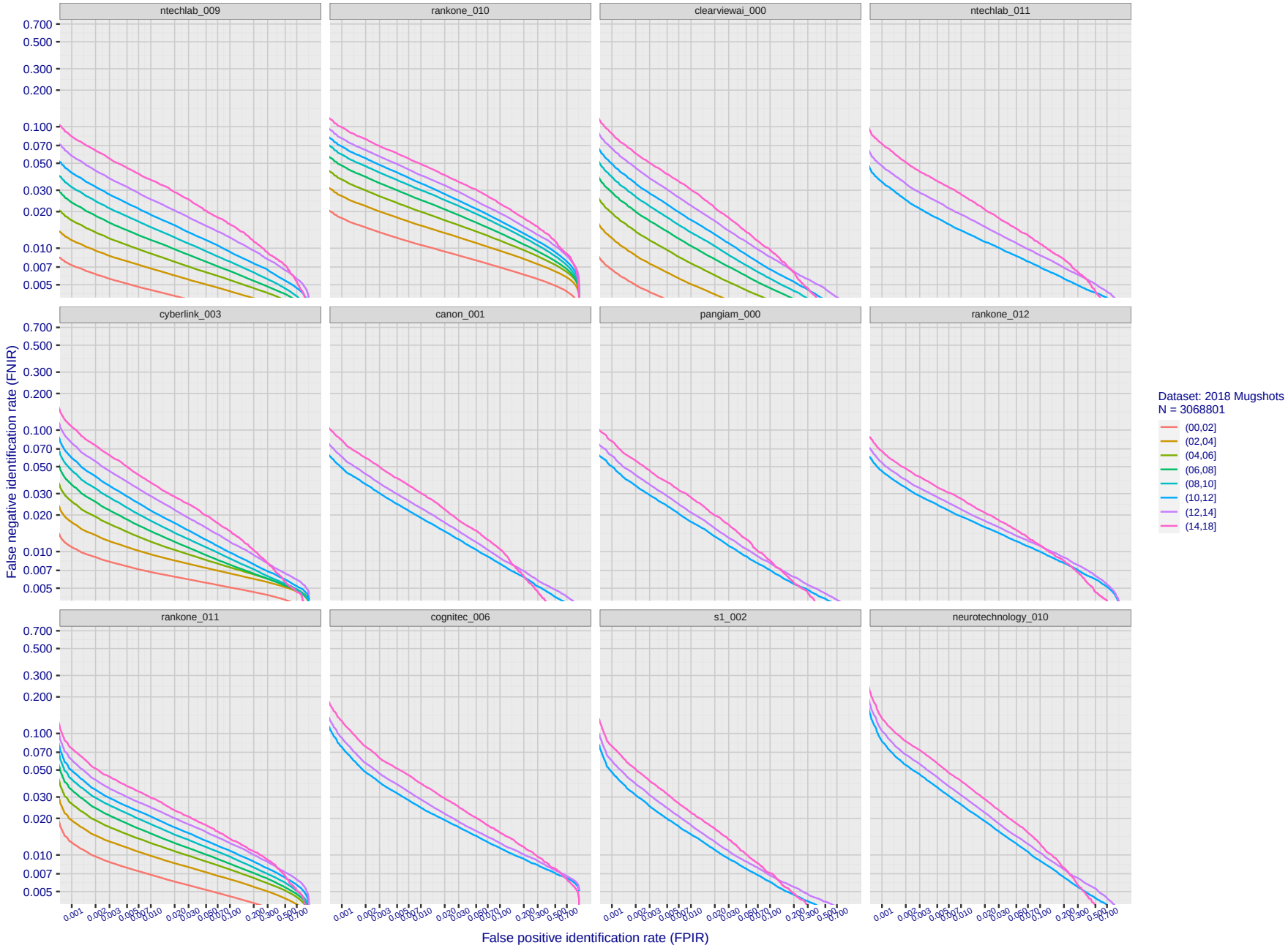

Figure 86: **[FRVT-2018 Mugshot Ageing Dataset] Identification miss rates vs. FPIR by time-elapsed**. *The oldest image of each individual is enrolled. Thereafter, all more recent images are searched. Miss rates are computed over all searches noted in row 17 of Table 1 and binned by number of years between search and initial enrollment. FPIR is computed from the same FRVT 2018 non-mates noted in row 3 of Table 1 with N = 3 000 000.*

This publication is available free of charge from: https://doi.org/10.6028/NIST.IR.8271

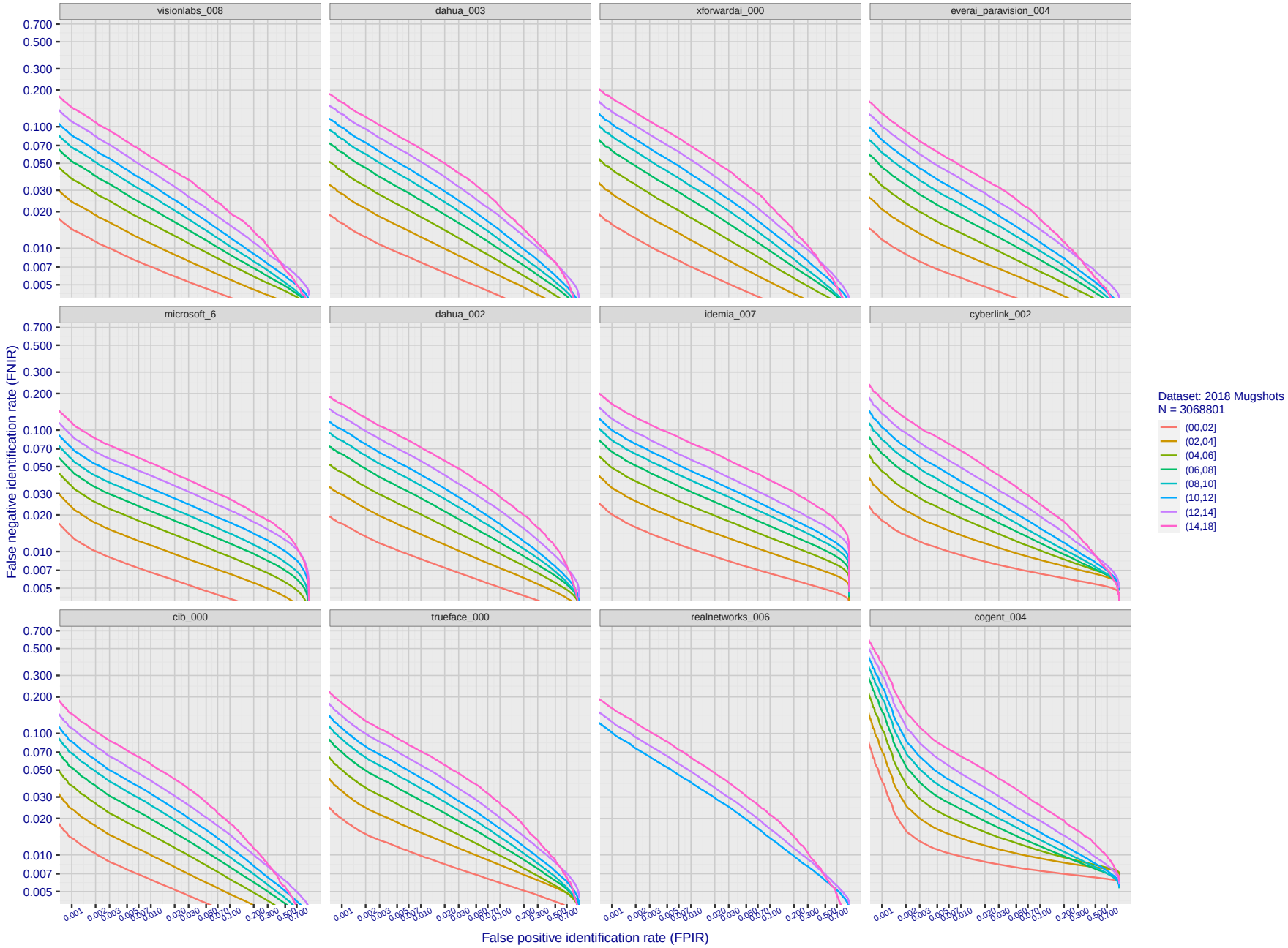

Figure 87: **[FRVT-2018 Mugshot Ageing Dataset] Identification miss rates vs. FPIR by time-elapsed**. *The oldest image of each individual is enrolled. Thereafter, all more recent images are searched. Miss rates are computed over all searches noted in row 17 of Table 1 and binned by number of years between search and initial enrollment. FPIR is computed from the same FRVT 2018 non-mates noted in row 3 of Table 1 with N = 3 000 000.*

This publication is available free of charge from: https://doi.org/10.6028/NIST.IR.8271

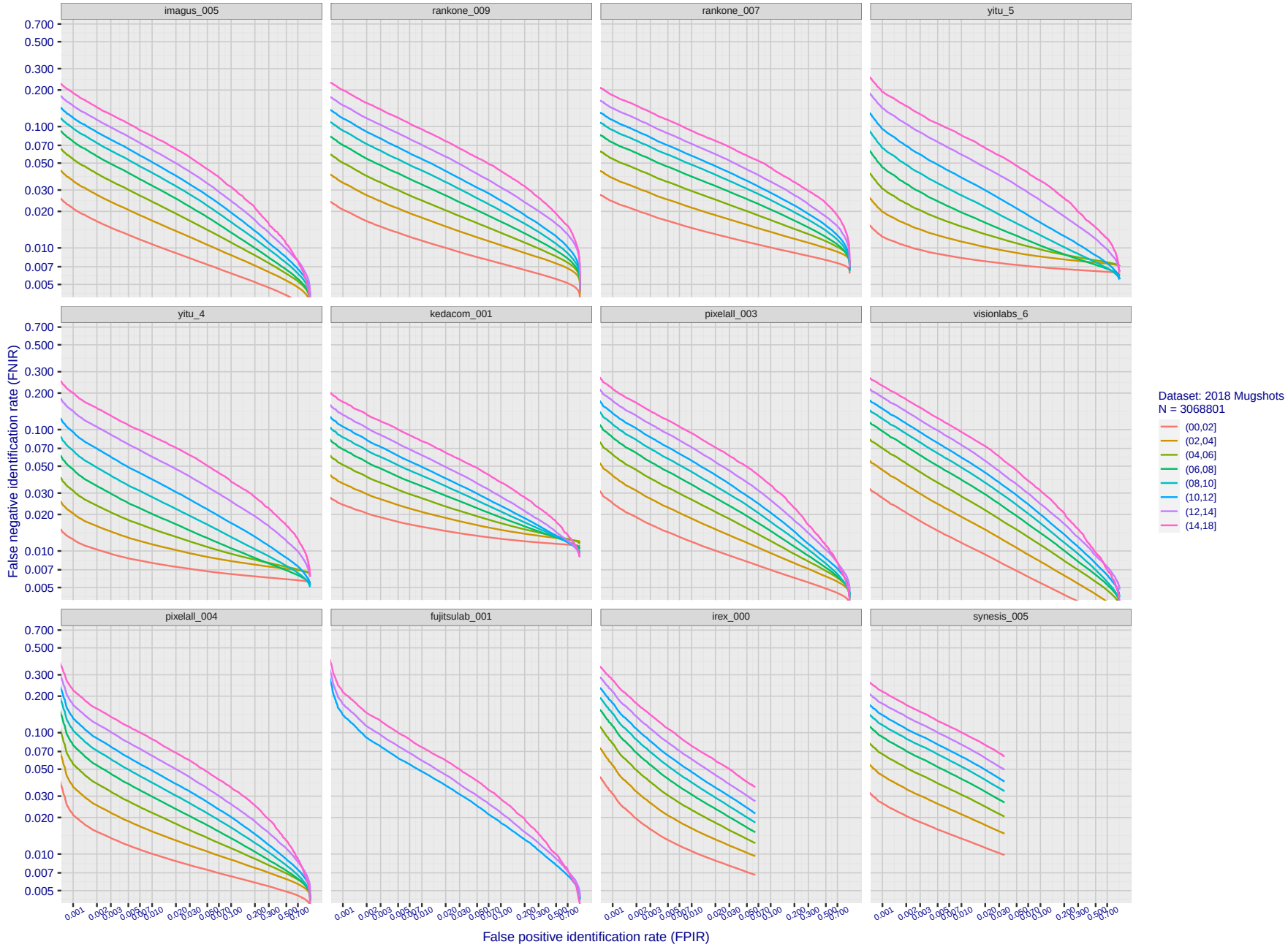

Figure 88: **[FRVT-2018 Mugshot Ageing Dataset] Identification miss rates vs. FPIR by time-elapsed**. *The oldest image of each individual is enrolled. Thereafter, all more recent images are searched. Miss rates are computed over all searches noted in row 17 of Table 1 and binned by number of years between search and initial enrollment. FPIR is computed from the same FRVT 2018 non-mates noted in row 3 of Table 1 with N = 3 000 000.*

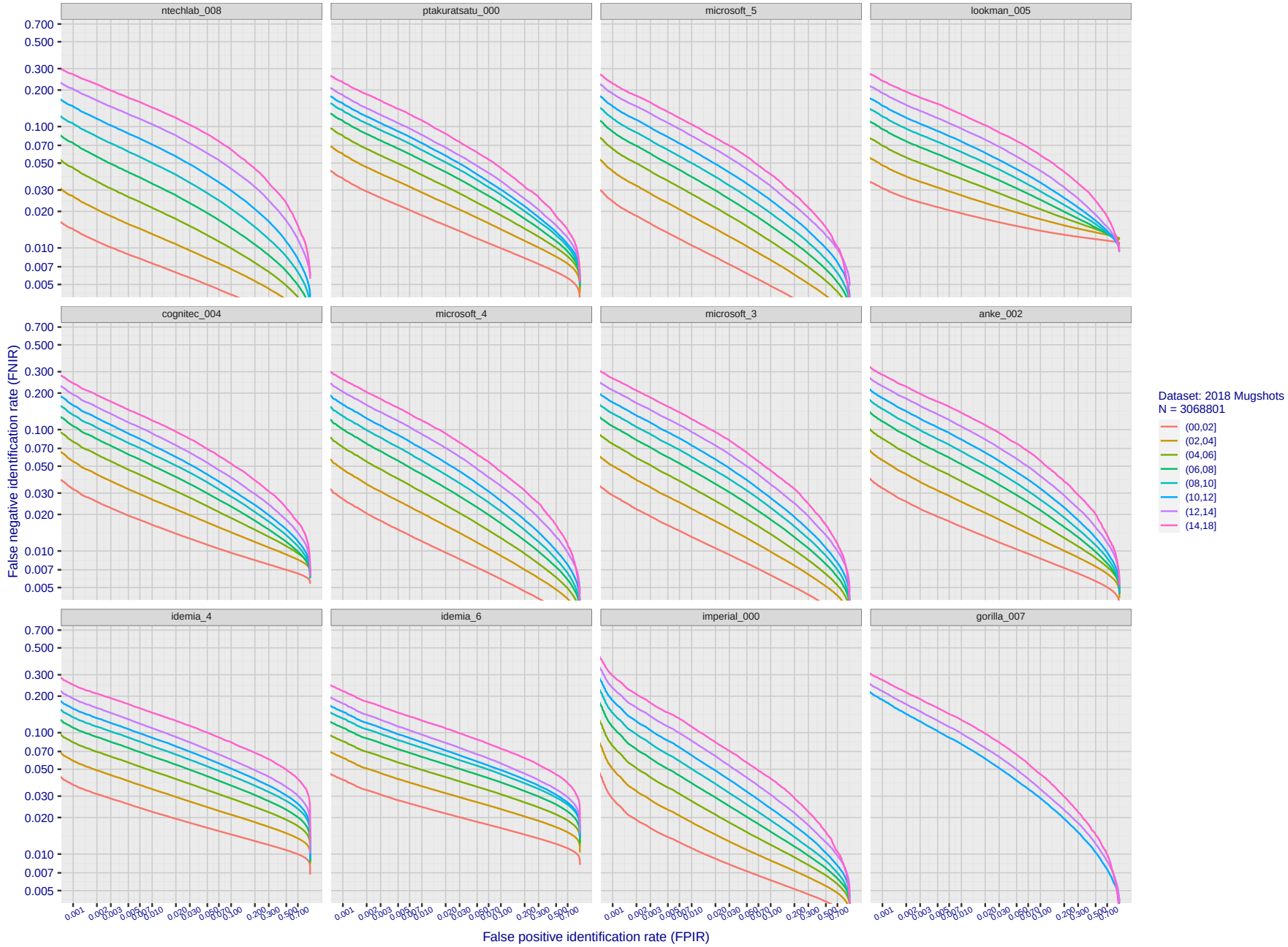

Figure 89: **[FRVT-2018 Mugshot Ageing Dataset] Identification miss rates vs. FPIR by time-elapsed**. *The oldest image of each individual is enrolled. Thereafter, all more recent images are searched. Miss rates are computed over all searches noted in row 17 of Table 1 and binned by number of years between search and initial enrollment. FPIR is computed from the same FRVT 2018 non-mates noted in row 3 of Table 1 with N = 3 000 000.*

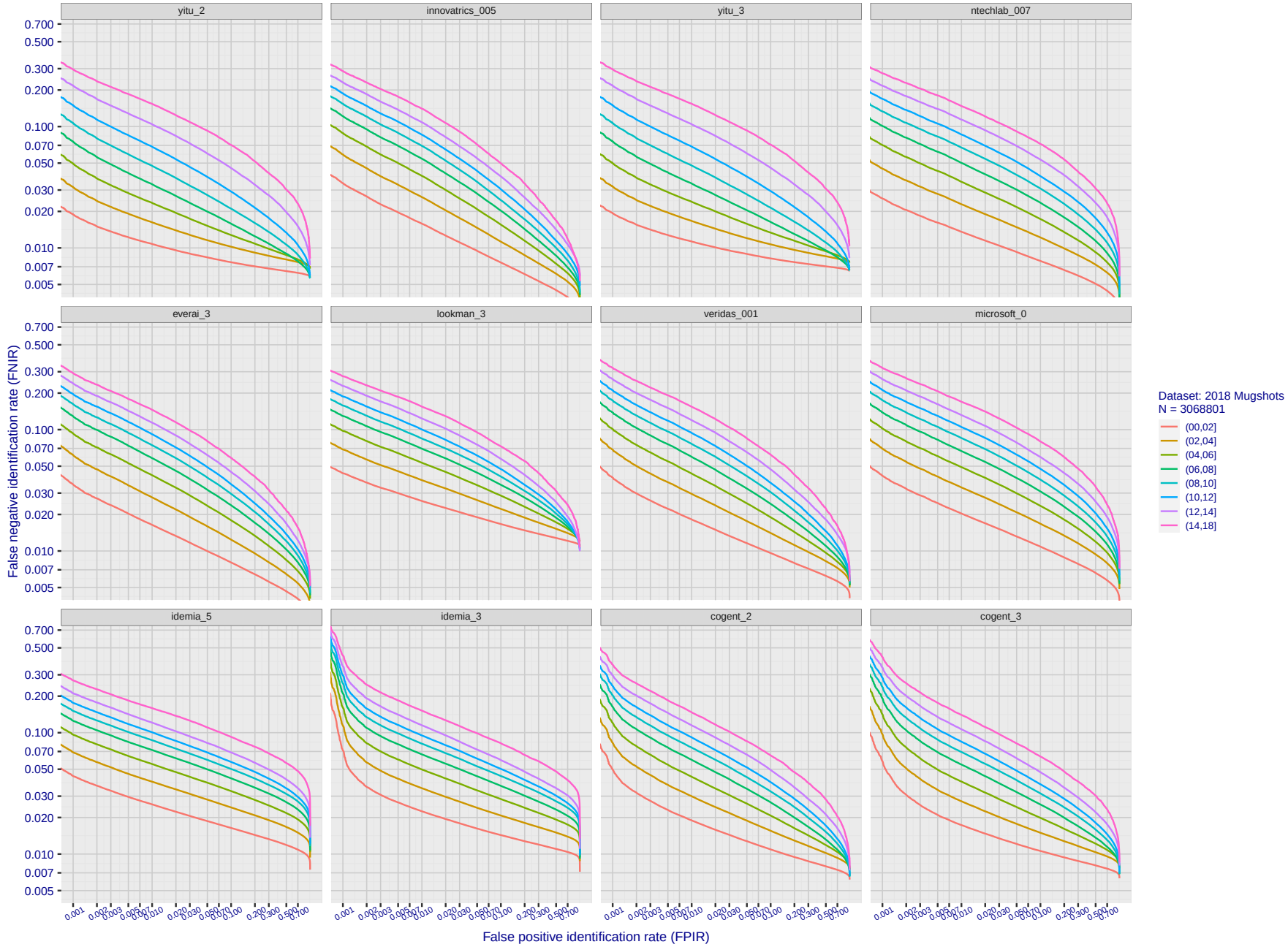

Figure 90: **[FRVT-2018 Mugshot Ageing Dataset] Identification miss rates vs. FPIR by time-elapsed**. *The oldest image of each individual is enrolled. Thereafter, all more recent images are searched. Miss rates are computed over all searches noted in row 17 of Table 1 and binned by number of years between search and initial enrollment. FPIR is computed from the same FRVT 2018 non-mates noted in row 3 of Table 1 with N = 3 000 000.*

This publication is available free of charge from: https://doi.org/10.6028/NIST.IR.8271

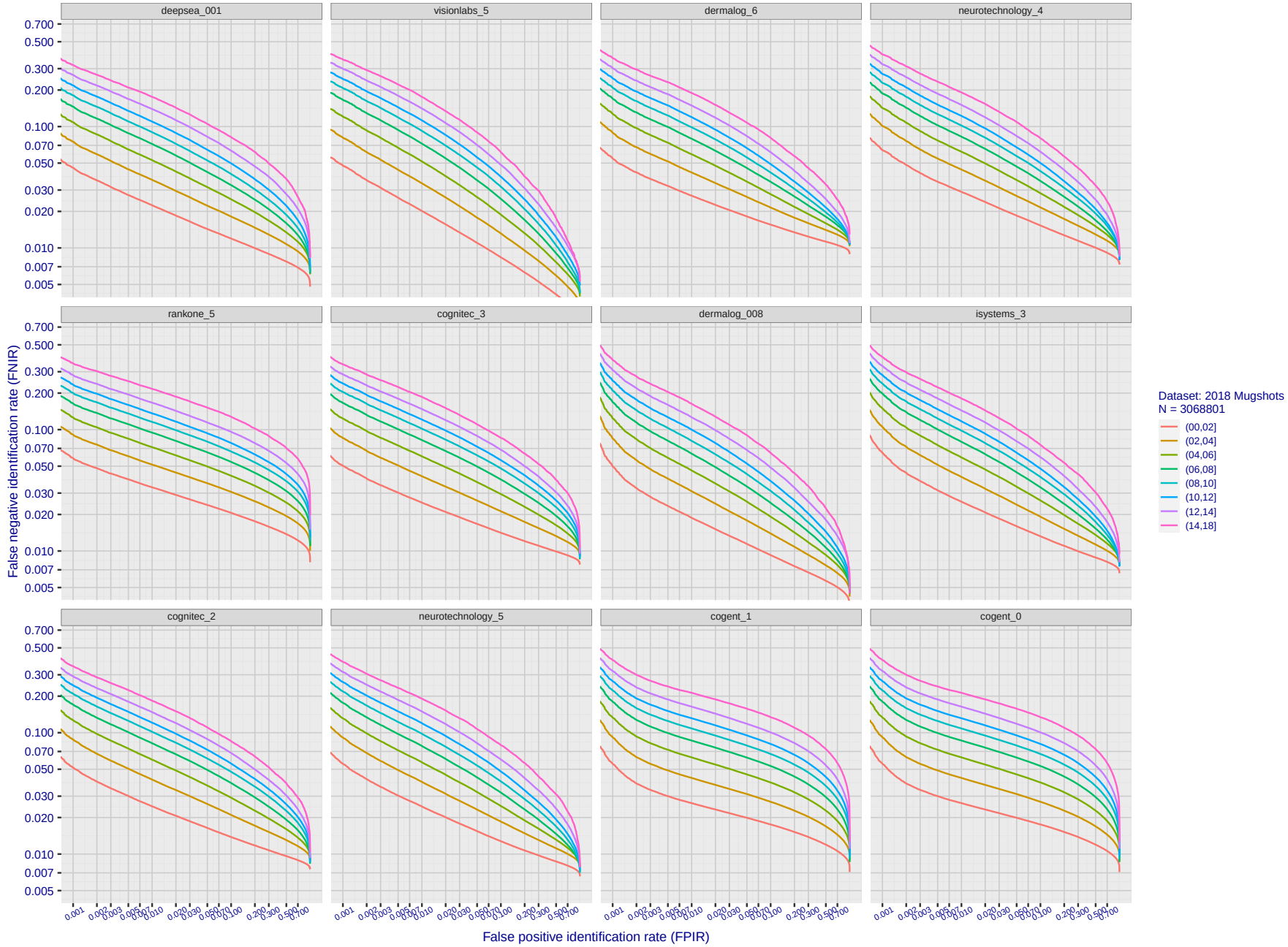

Figure 91: **[FRVT-2018 Mugshot Ageing Dataset] Identification miss rates vs. FPIR by time-elapsed**. *The oldest image of each individual is enrolled. Thereafter, all more recent images are searched. Miss rates are computed over all searches noted in row 17 of Table 1 and binned by number of years between search and initial enrollment. FPIR is computed from the same FRVT 2018 non-mates noted in row 3 of Table 1 with N = 3 000 000.*

This publication is available free of charge from: https://doi.org/10.6028/NIST.IR.8271

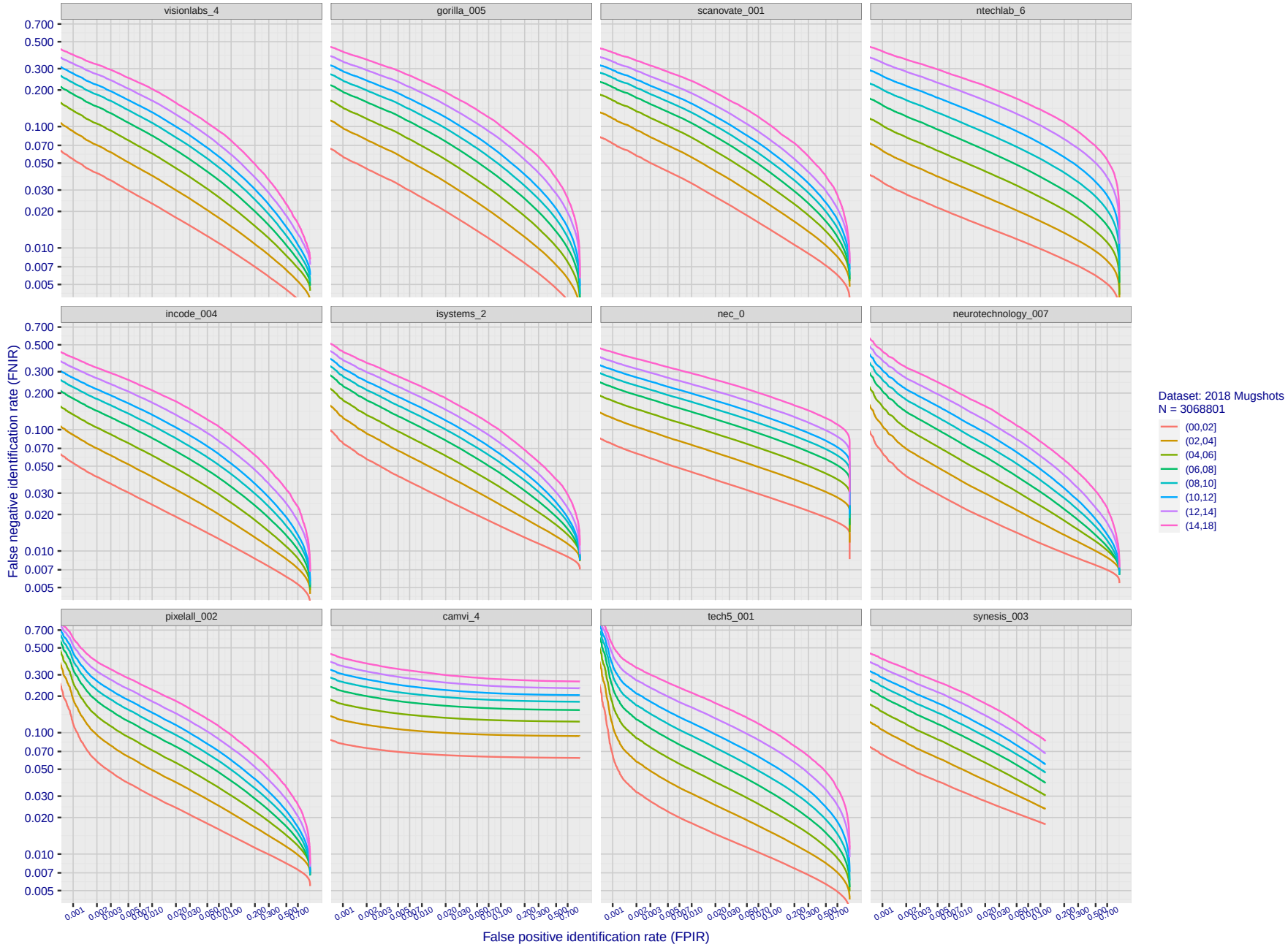

Figure 92: **[FRVT-2018 Mugshot Ageing Dataset] Identification miss rates vs. FPIR by time-elapsed**. *The oldest image of each individual is enrolled. Thereafter, all more recent images are searched. Miss rates are computed over all searches noted in row 17 of Table 1 and binned by number of years between search and initial enrollment. FPIR is computed from the same FRVT 2018 non-mates noted in row 3 of Table 1 with N = 3 000 000.*

This publication is available free of charge from: https://doi.org/10.6028/NIST.IR.8271

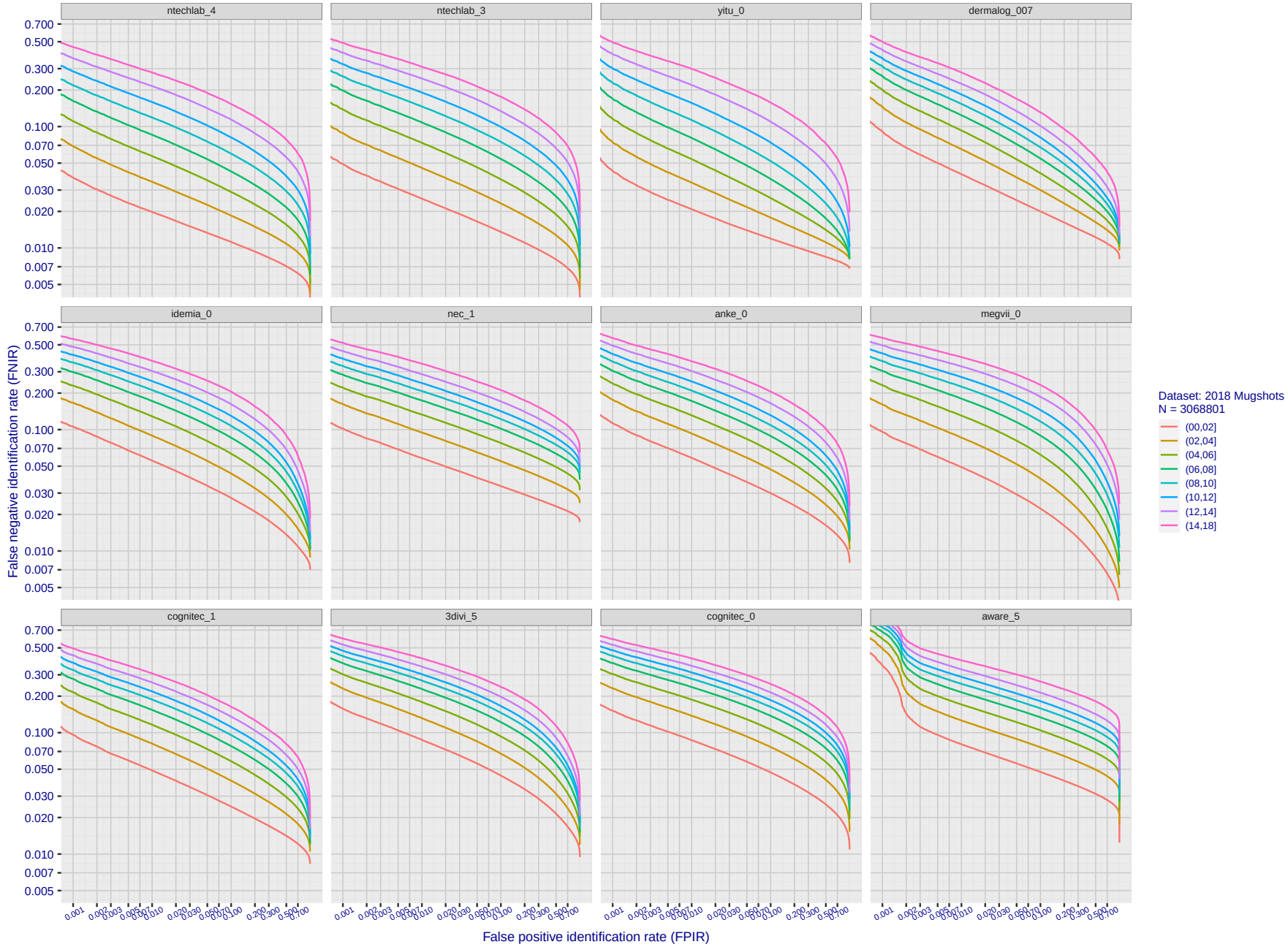

Figure 93: **[FRVT-2018 Mugshot Ageing Dataset] Identification miss rates vs. FPIR by time-elapsed**. *The oldest image of each individual is enrolled. Thereafter, all more recent images are searched. Miss rates are computed over all searches noted in row 17 of Table 1 and binned by number of years between search and initial enrollment. FPIR is computed from the same FRVT 2018 non-mates noted in row 3 of Table 1 with N = 3 000 000.*

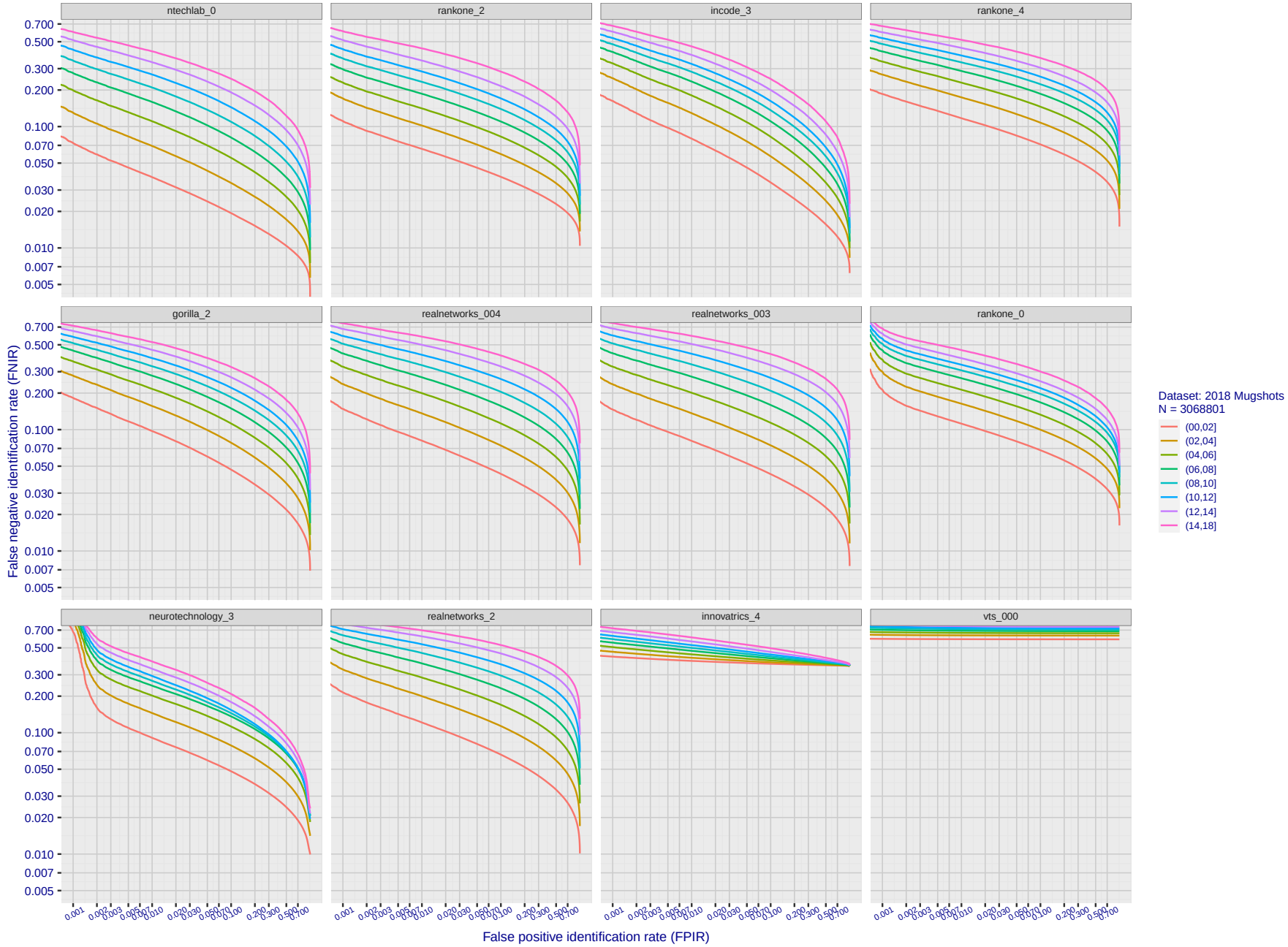

Figure 94: **[FRVT-2018 Mugshot Ageing Dataset] Identification miss rates vs. FPIR by time-elapsed**. *The oldest image of each individual is enrolled. Thereafter, all more recent images are searched. Miss rates are computed over all searches noted in row 17 of Table 1 and binned by number of years between search and initial enrollment. FPIR is computed from the same FRVT 2018 non-mates noted in row 3 of Table 1 with N = 3 000 000.*

This publication is available free of charge from: https://doi.org/10.6028/NIST.IR.8271

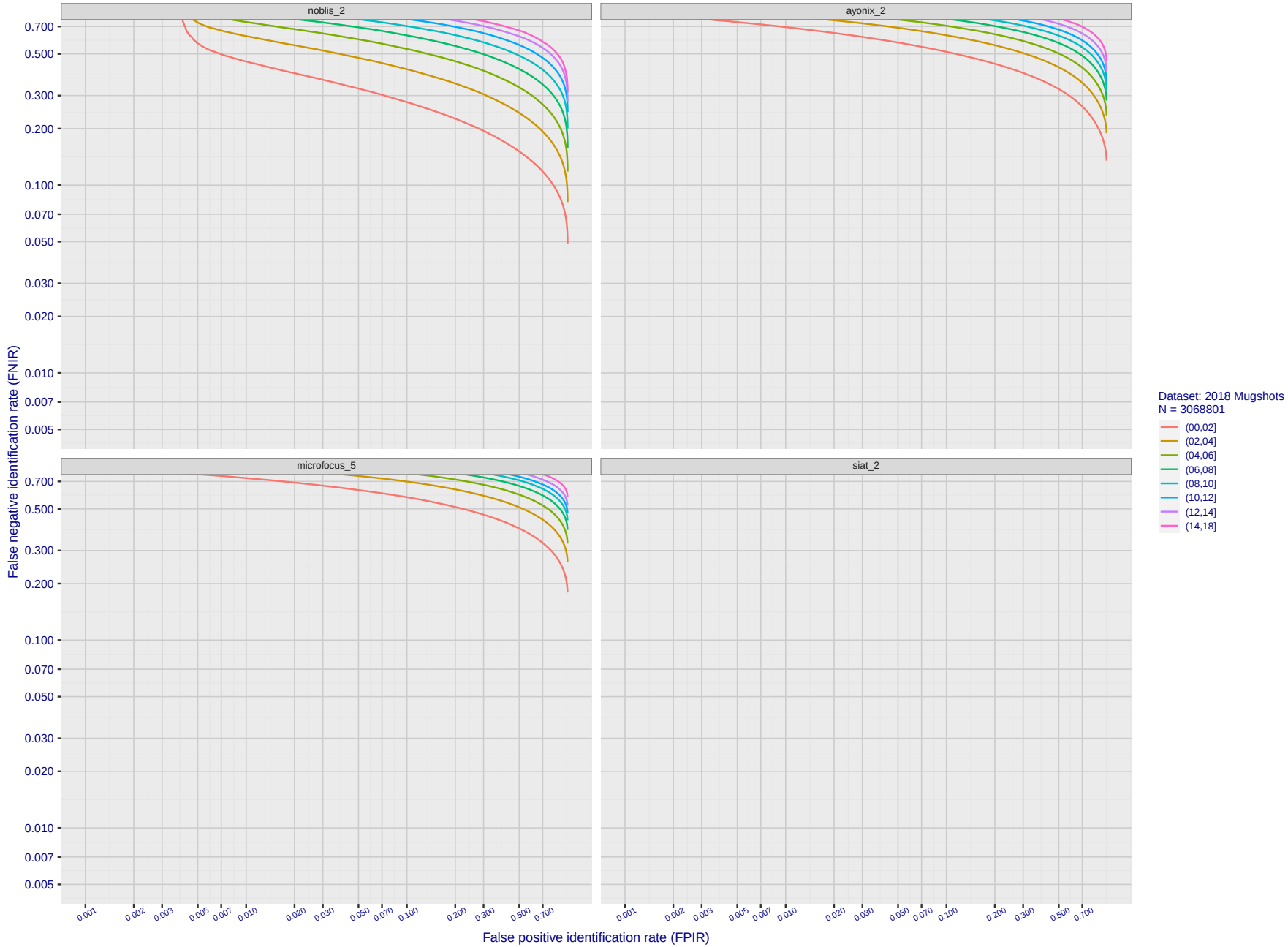

Figure 95: **[FRVT-2018 Mugshot Ageing Dataset] Identification miss rates vs. FPIR by time-elapsed**. *The oldest image of each individual is enrolled. Thereafter, all more recent images are searched. Miss rates are computed over all searches noted in row 17 of Table 1 and binned by number of years between search and initial enrollment. FPIR is computed from the same FRVT 2018 non-mates noted in row 3 of Table 1 with N = 3 000 000.*

2022/06/13	FNIR(N, R, T) =	False neg. identification rate	N = Num. enrolled subjects	T = Threshold	$T = 0 \rightarrow$ Investigation
18:09:57	FPIR(N, T) =	False pos. identification rate	R = Num. candidates examined		$T > 0 \rightarrow$ Identification

This publication is available free of charge from: https://doi.org/10.6028/NIST.IR.8271

This publication is available free of charge from: https://doi.org/10.6028/NIST.IR.8271

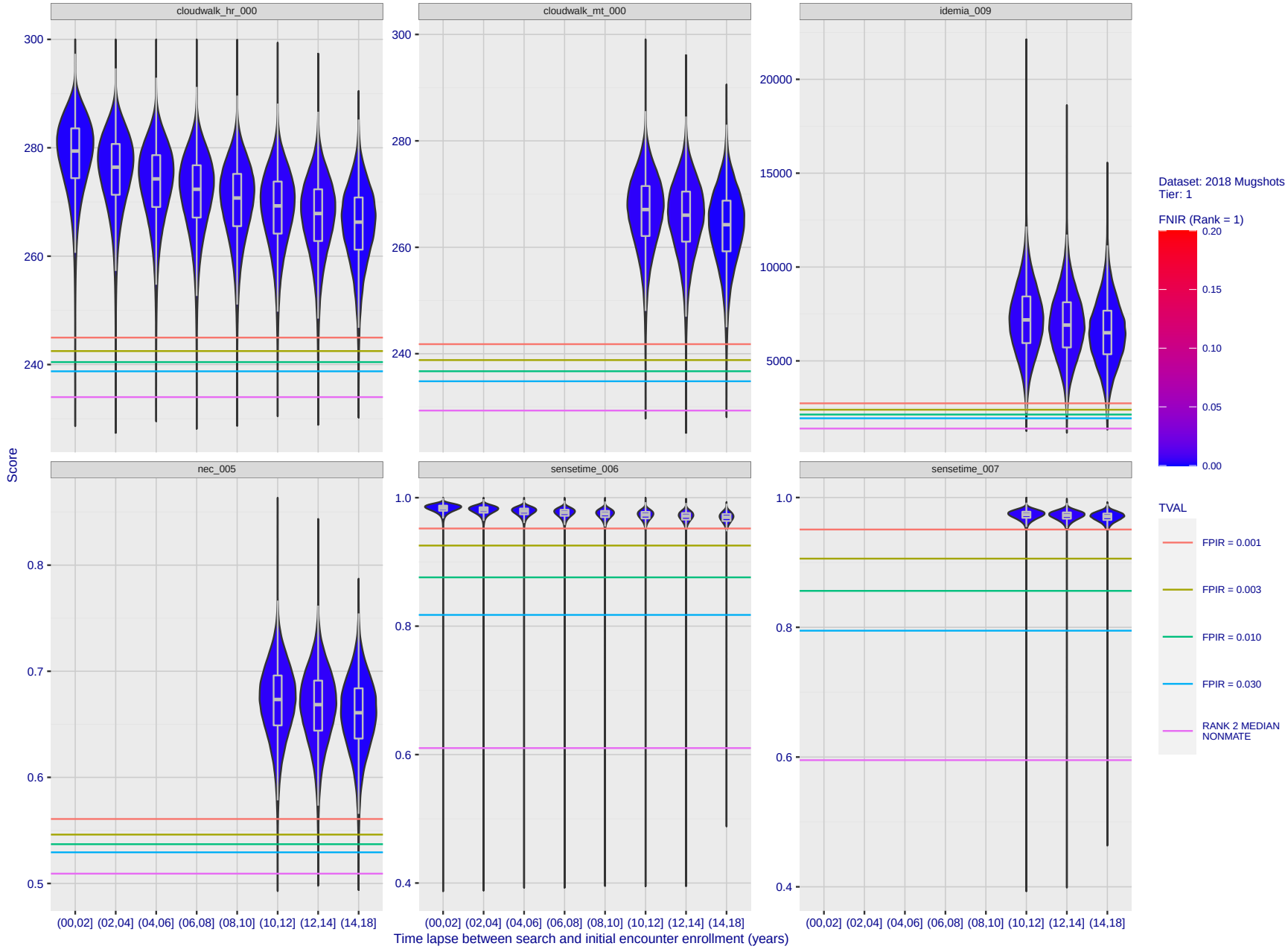

Figure 96: **[FRVT-2018 Mugshot Ageing Dataset] Native mate scores vs. time-elapsed**. *The oldest image of each individual is enrolled. Thereafter, all more recent images are searched. Mated score distributions are computed over all searches noted in row 17 of Table 1 binned by number of years between search and initial enrollment.*

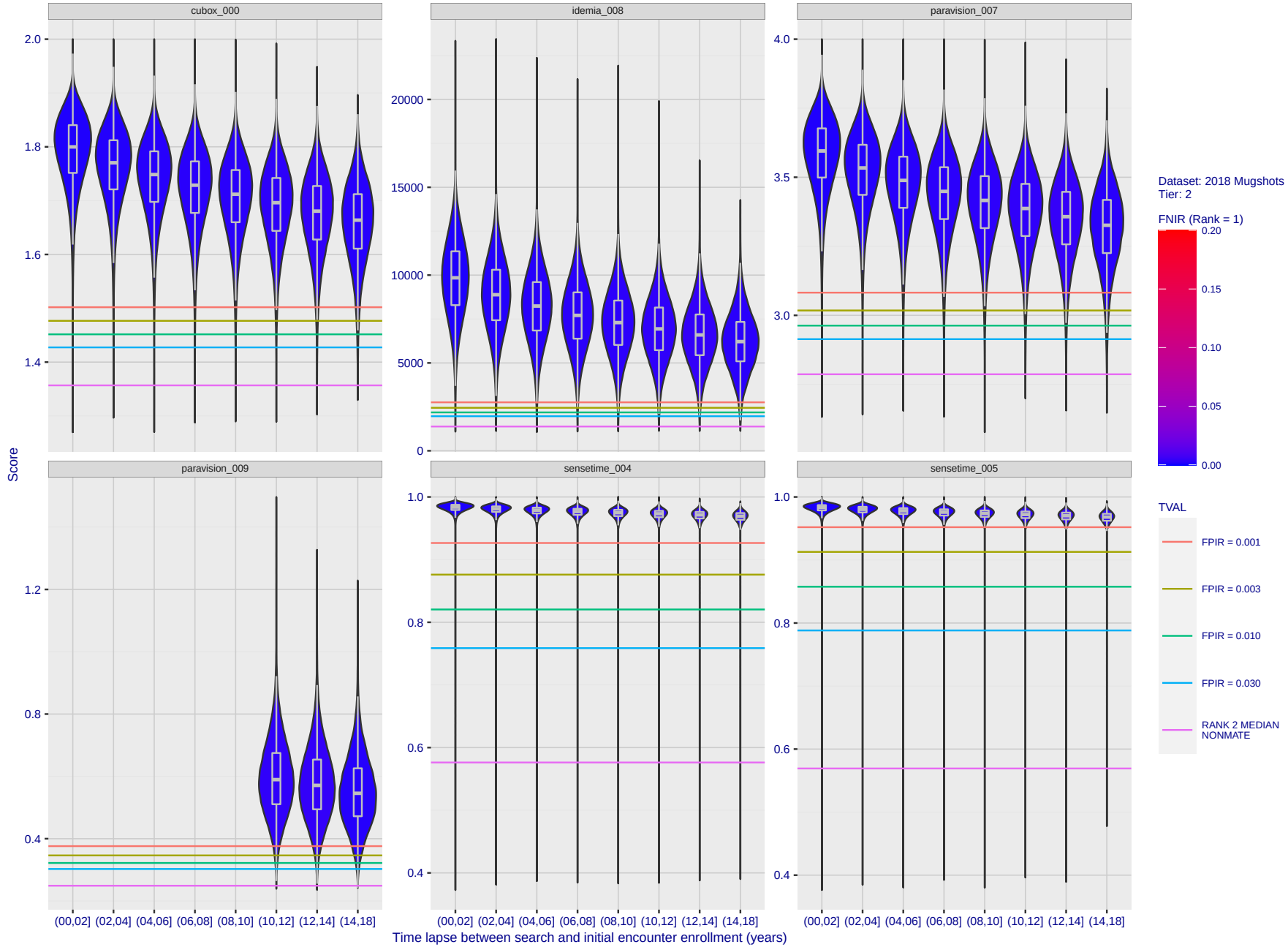

Figure 97: **[FRVT-2018 Mugshot Ageing Dataset] Native mate scores vs. time-elapsed**. *The oldest image of each individual is enrolled. Thereafter, all more recent images are searched. Mated score distributions are computed over all searches noted in row 17 of Table 1 binned by number of years between search and initial enrollment.*

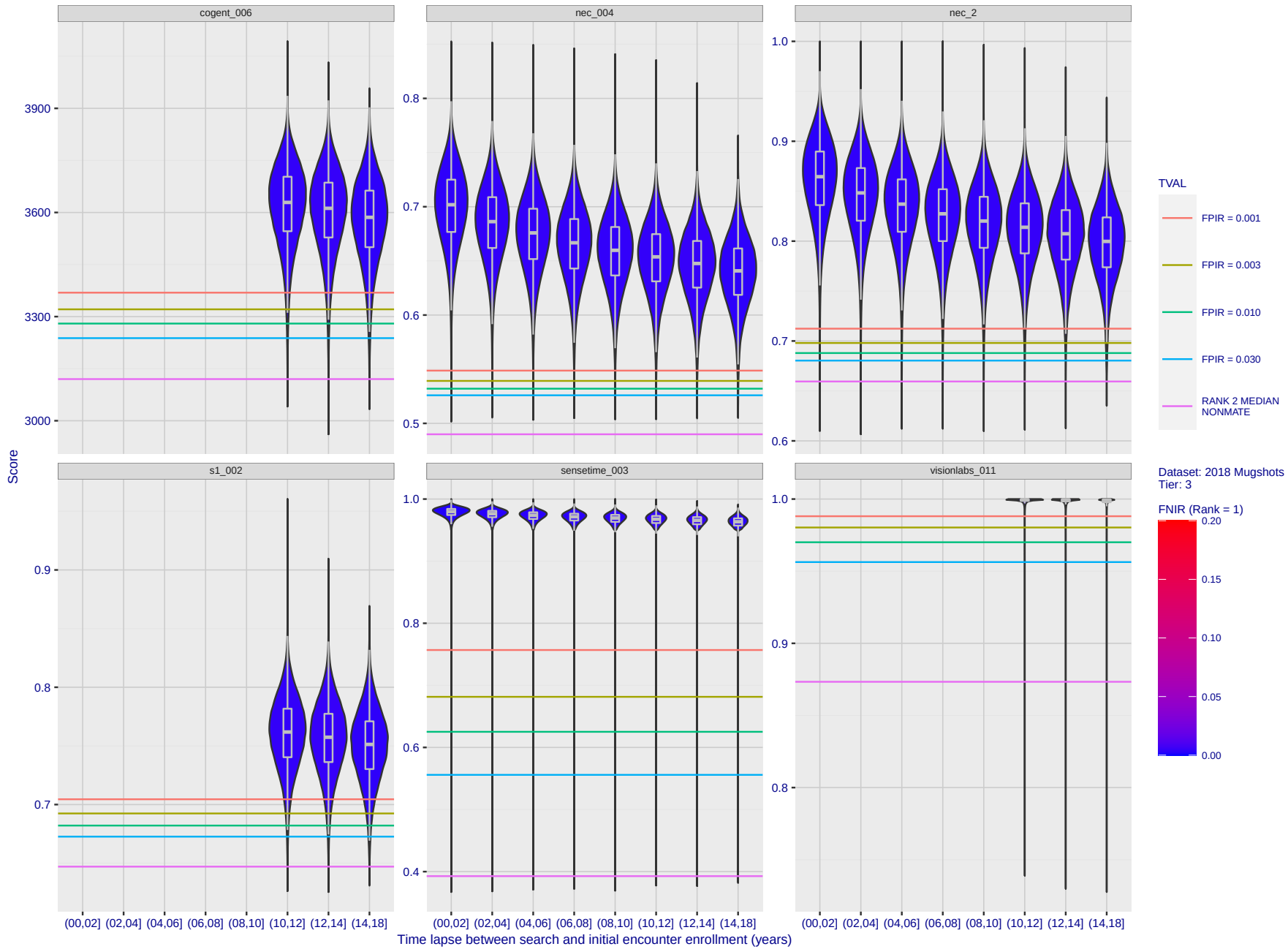

Figure 98: **[FRVT-2018 Mugshot Ageing Dataset] Native mate scores vs. time-elapsed**. *The oldest image of each individual is enrolled. Thereafter, all more recent images are searched. Mated score distributions are computed over all searches noted in row 17 of Table 1 binned by number of years between search and initial enrollment.*

This publication is available free of charge from: https://doi.org/10.6028/NIST.IR.8271

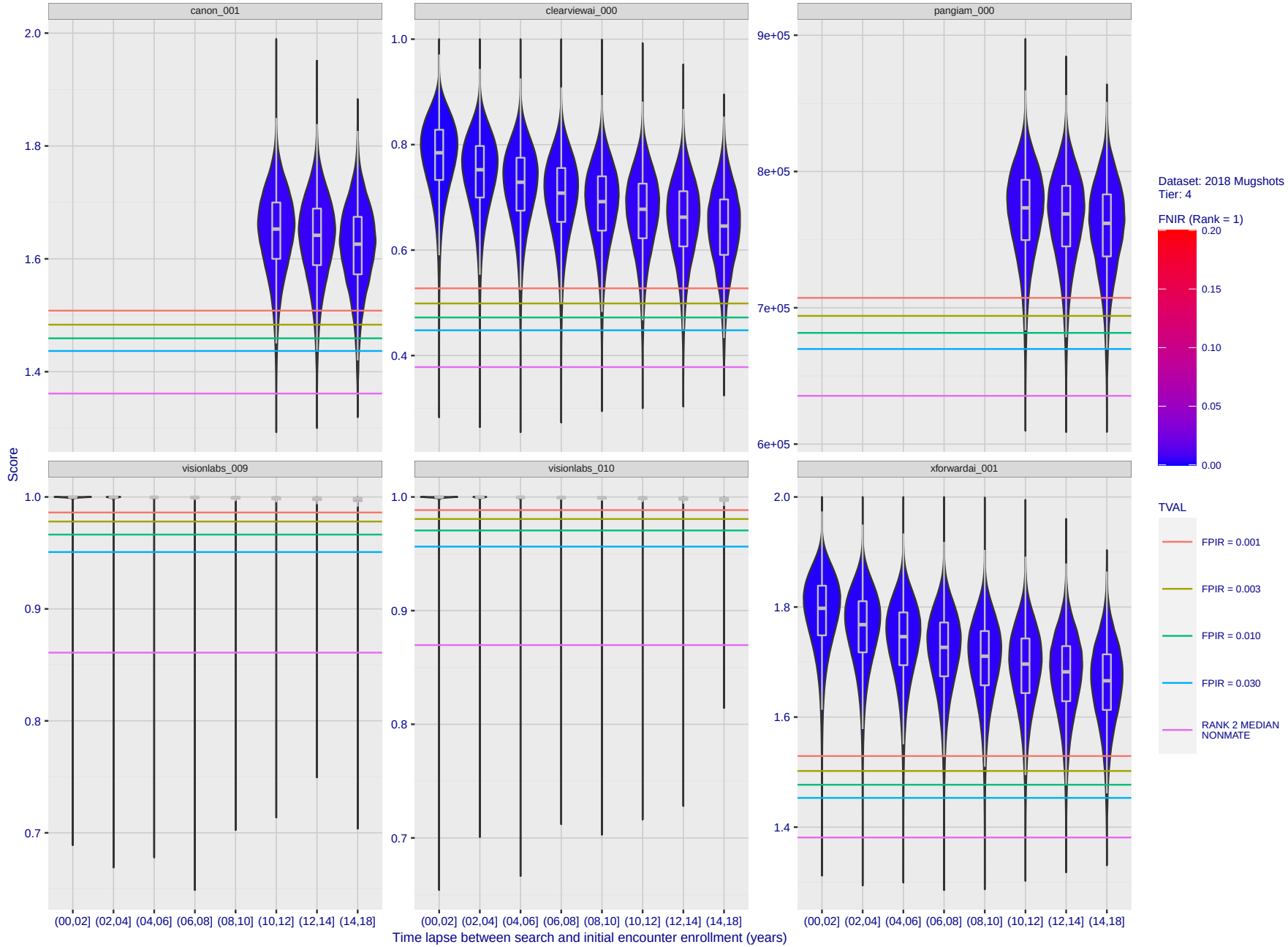

Figure 99: **[FRVT-2018 Mugshot Ageing Dataset] Native mate scores vs. time-elapsed**. *The oldest image of each individual is enrolled. Thereafter, all more recent images are searched. Mated score distributions are computed over all searches noted in row 17 of Table 1 binned by number of years between search and initial enrollment.*

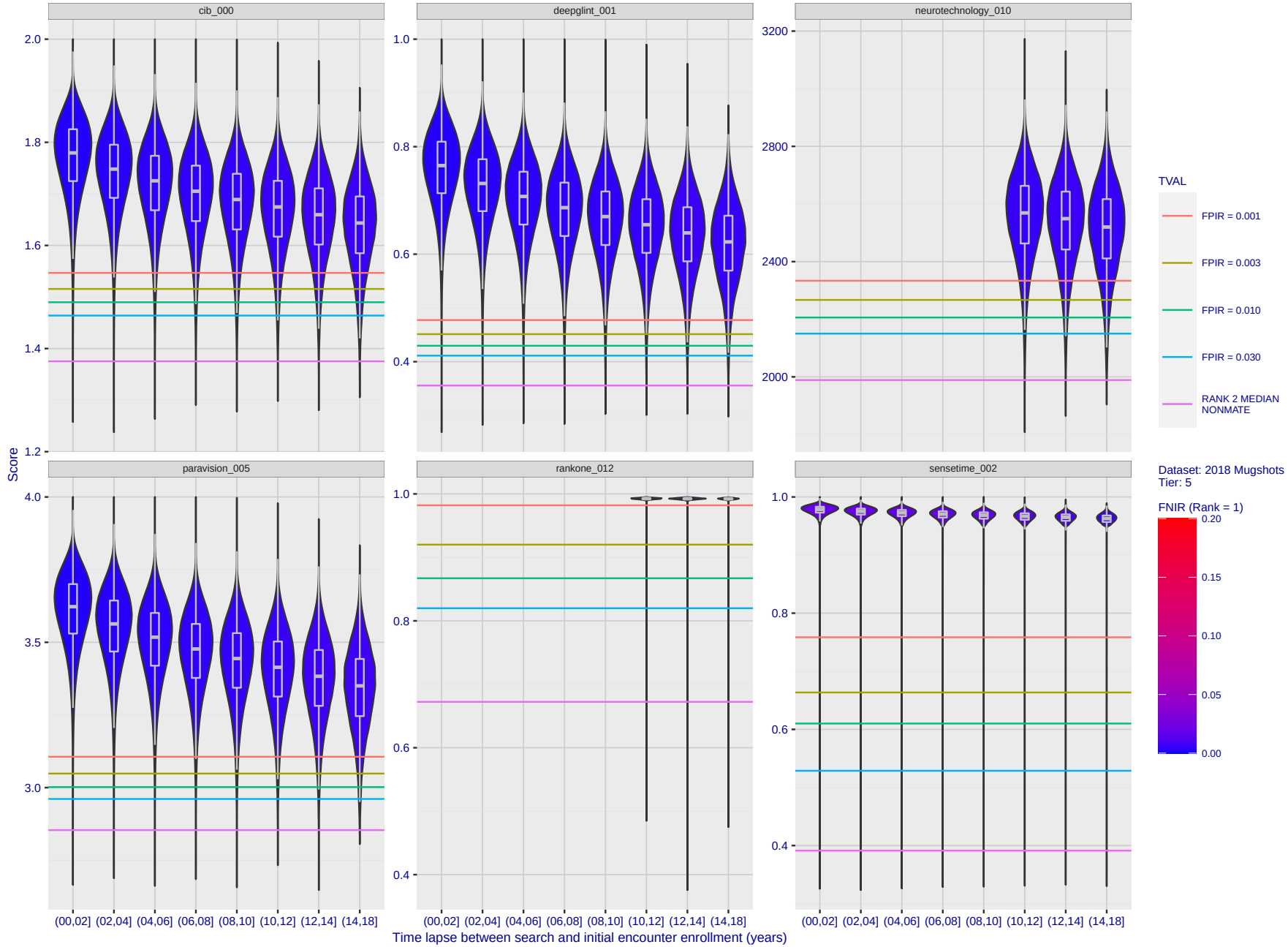

Figure 100: **[FRVT-2018 Mugshot Ageing Dataset] Native mate scores vs. time-elapsed**. *The oldest image of each individual is enrolled. Thereafter, all more recent images are searched. Mated score distributions are computed over all searches noted in row 17 of Table 1 binned by number of years between search and initial enrollment.*

This publication is available free of charge from: https://doi.org/10.6028/NIST.IR.8271

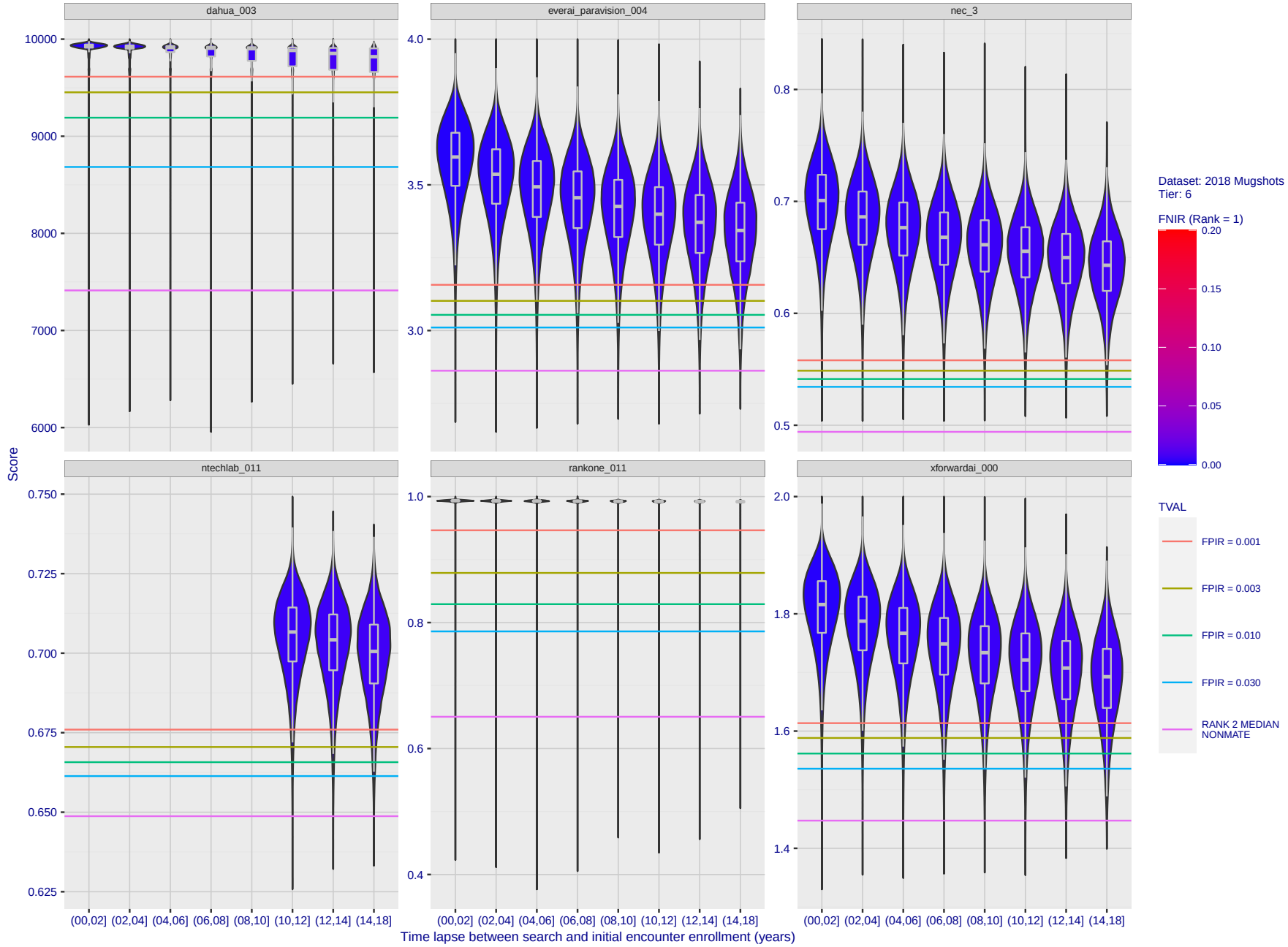

Figure 101: **[FRVT-2018 Mugshot Ageing Dataset] Native mate scores vs. time-elapsed**. *The oldest image of each individual is enrolled. Thereafter, all more recent images are searched. Mated score distributions are computed over all searches noted in row 17 of Table 1 binned by number of years between search and initial enrollment.*

This publication is available free of charge from: https://doi.org/10.6028/NIST.IR.8271

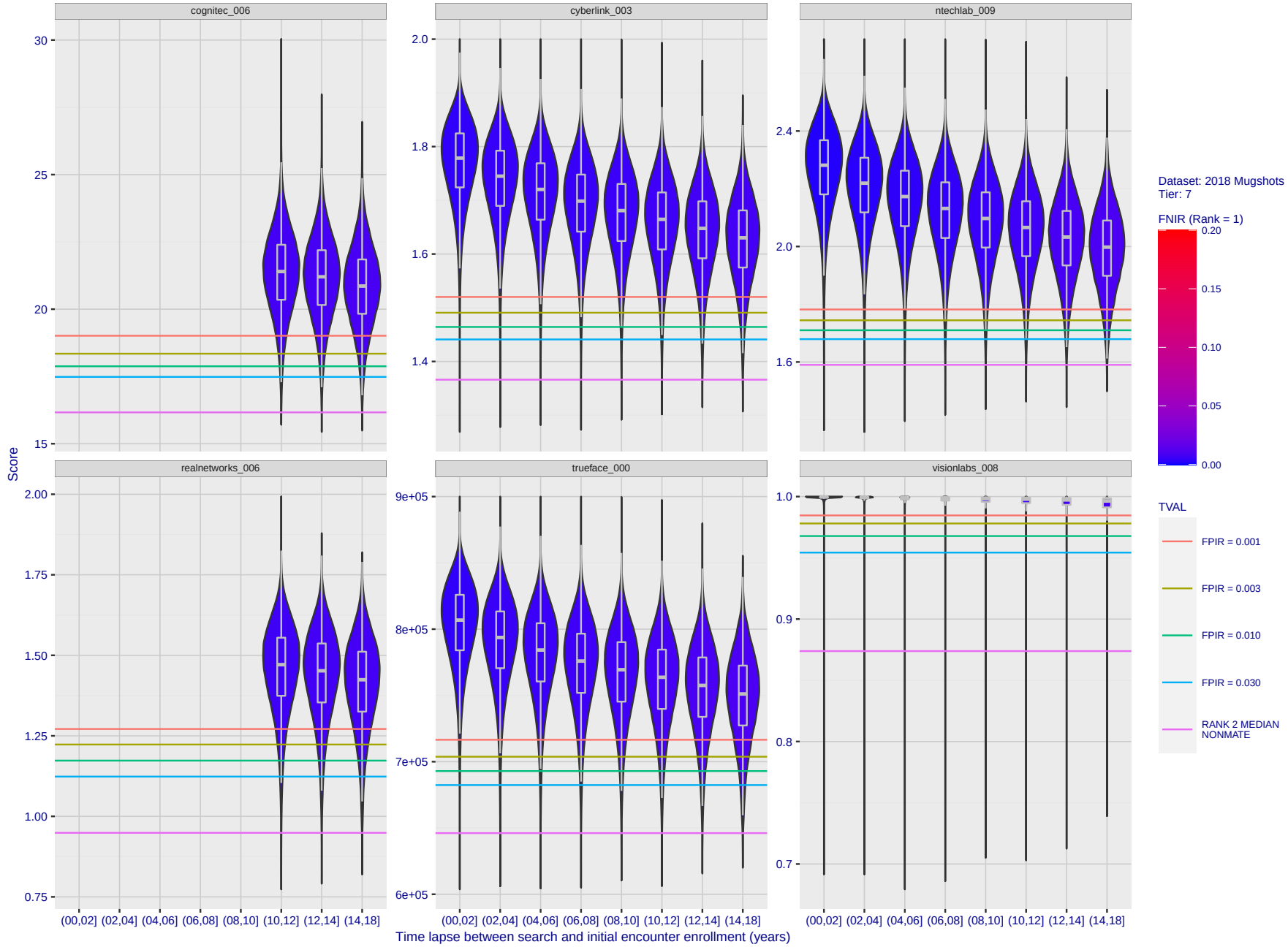

Figure 102: **[FRVT-2018 Mugshot Ageing Dataset] Native mate scores vs. time-elapsed**. *The oldest image of each individual is enrolled. Thereafter, all more recent images are searched. Mated score distributions are computed over all searches noted in row 17 of Table 1 binned by number of years between search and initial enrollment.*

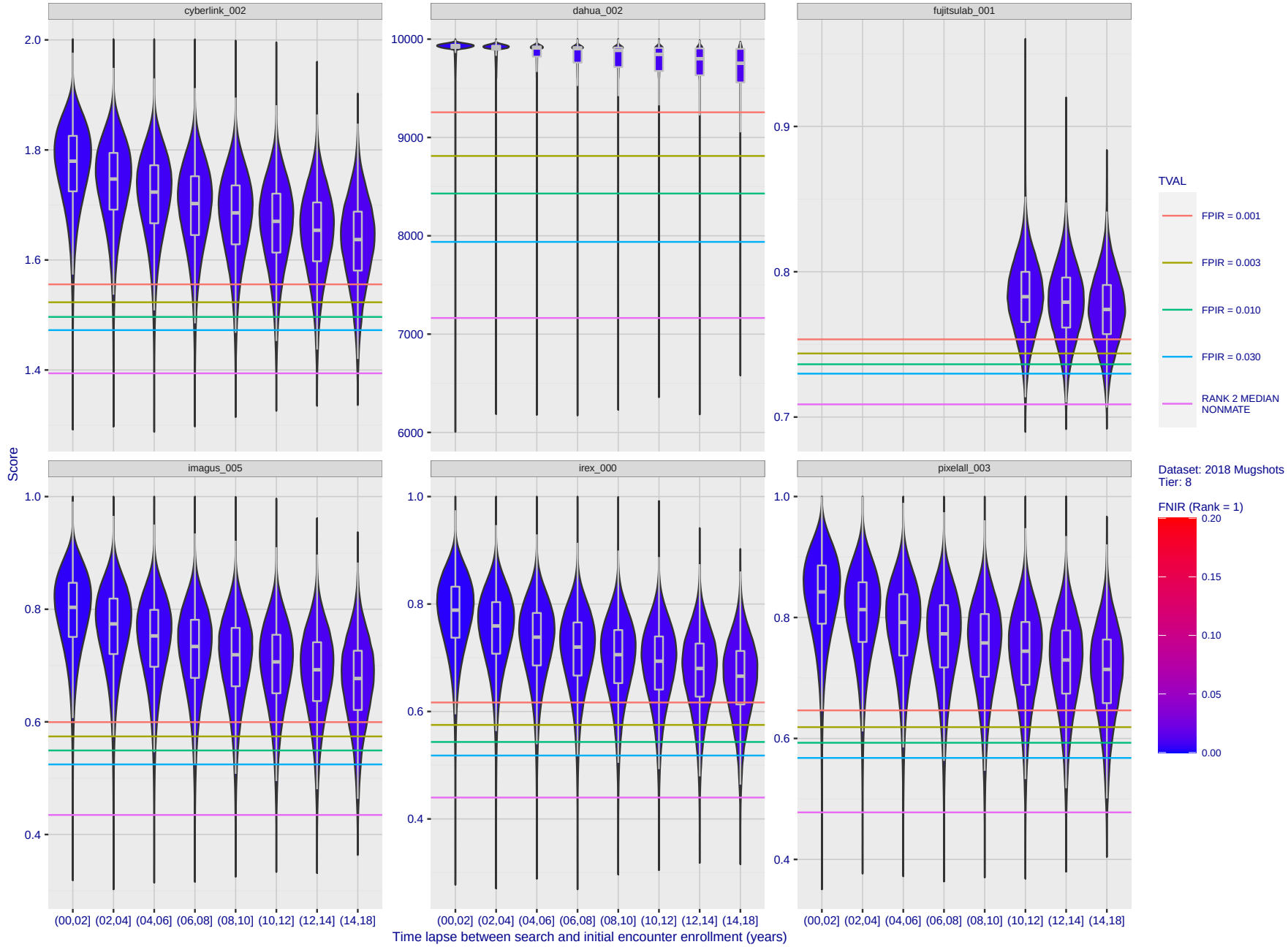

Figure 103: **[FRVT-2018 Mugshot Ageing Dataset] Native mate scores vs. time-elapsed**. *The oldest image of each individual is enrolled. Thereafter, all more recent images are searched. Mated score distributions are computed over all searches noted in row 17 of Table 1 binned by number of years between search and initial enrollment.*

This publication is available free of charge from: https://doi.org/10.6028/NIST.IR.8271

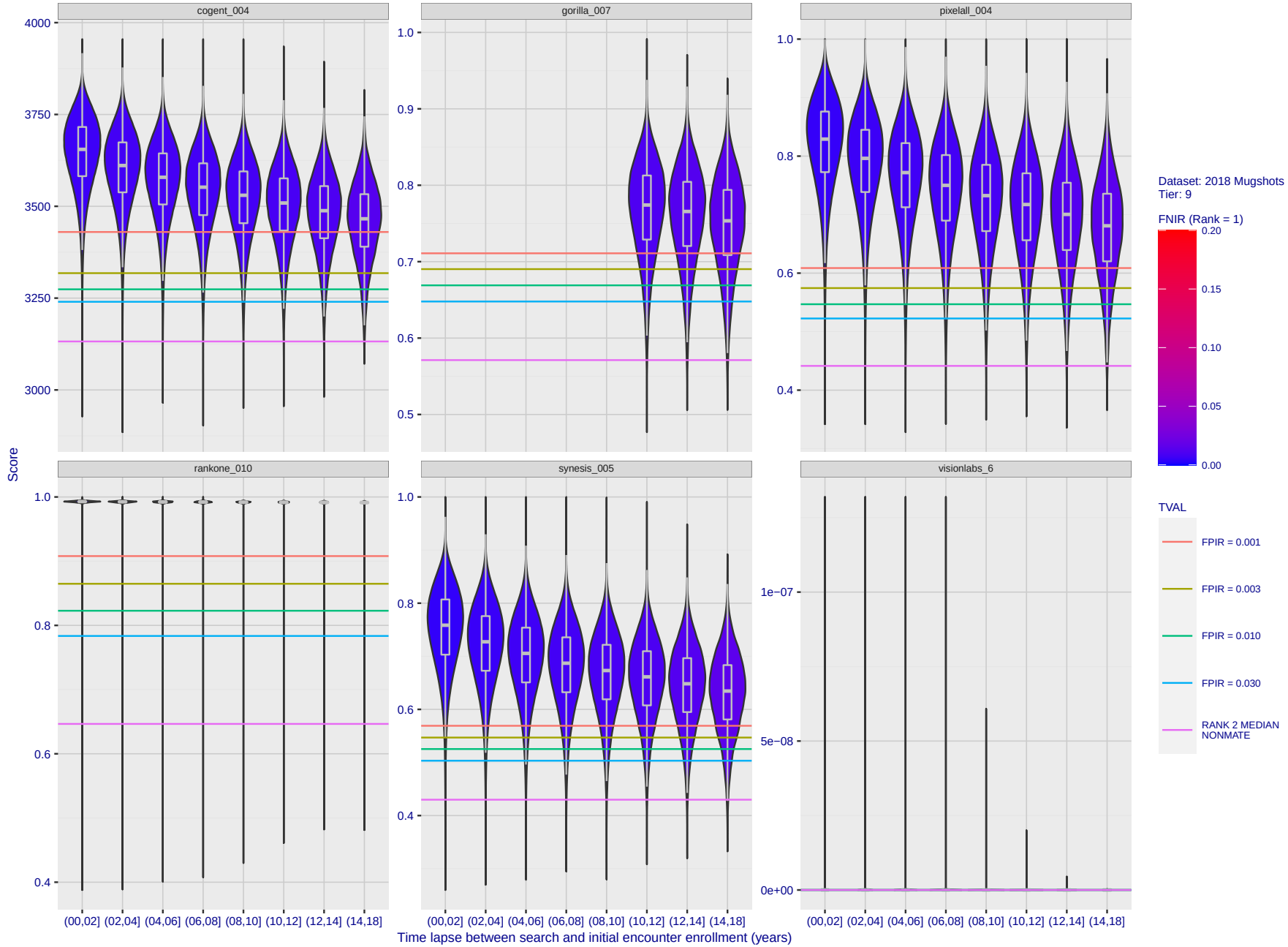

Figure 104: **[FRVT-2018 Mugshot Ageing Dataset] Native mate scores vs. time-elapsed**. *The oldest image of each individual is enrolled. Thereafter, all more recent images are searched. Mated score distributions are computed over all searches noted in row 17 of Table 1 binned by number of years between search and initial enrollment.*

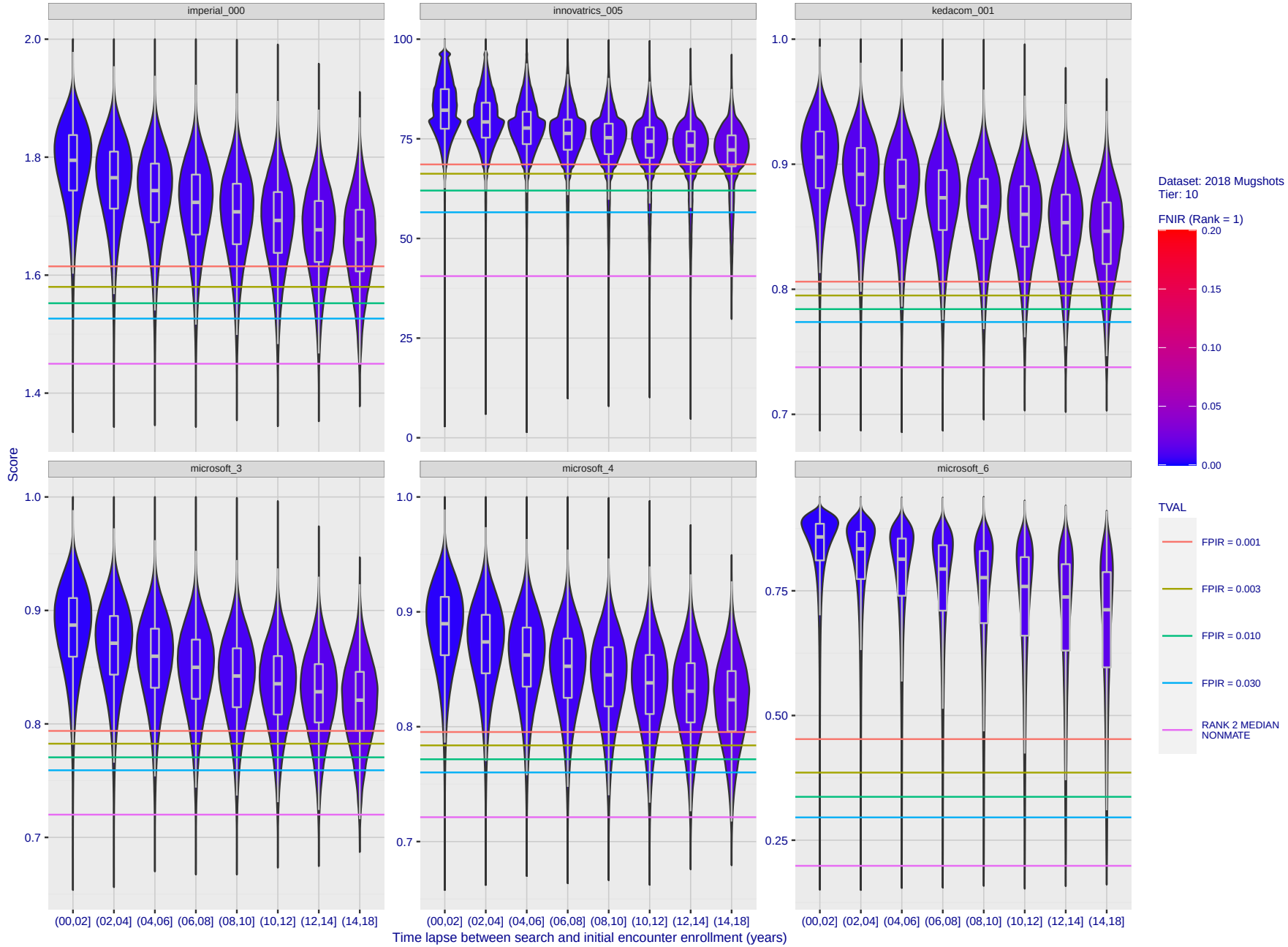

Figure 105: **[FRVT-2018 Mugshot Ageing Dataset] Native mate scores vs. time-elapsed**. *The oldest image of each individual is enrolled. Thereafter, all more recent images are searched. Mated score distributions are computed over all searches noted in row 17 of Table 1 binned by number of years between search and initial enrollment.*

This publication is available free of charge from: https://doi.org/10.6028/NIST.IR.8271

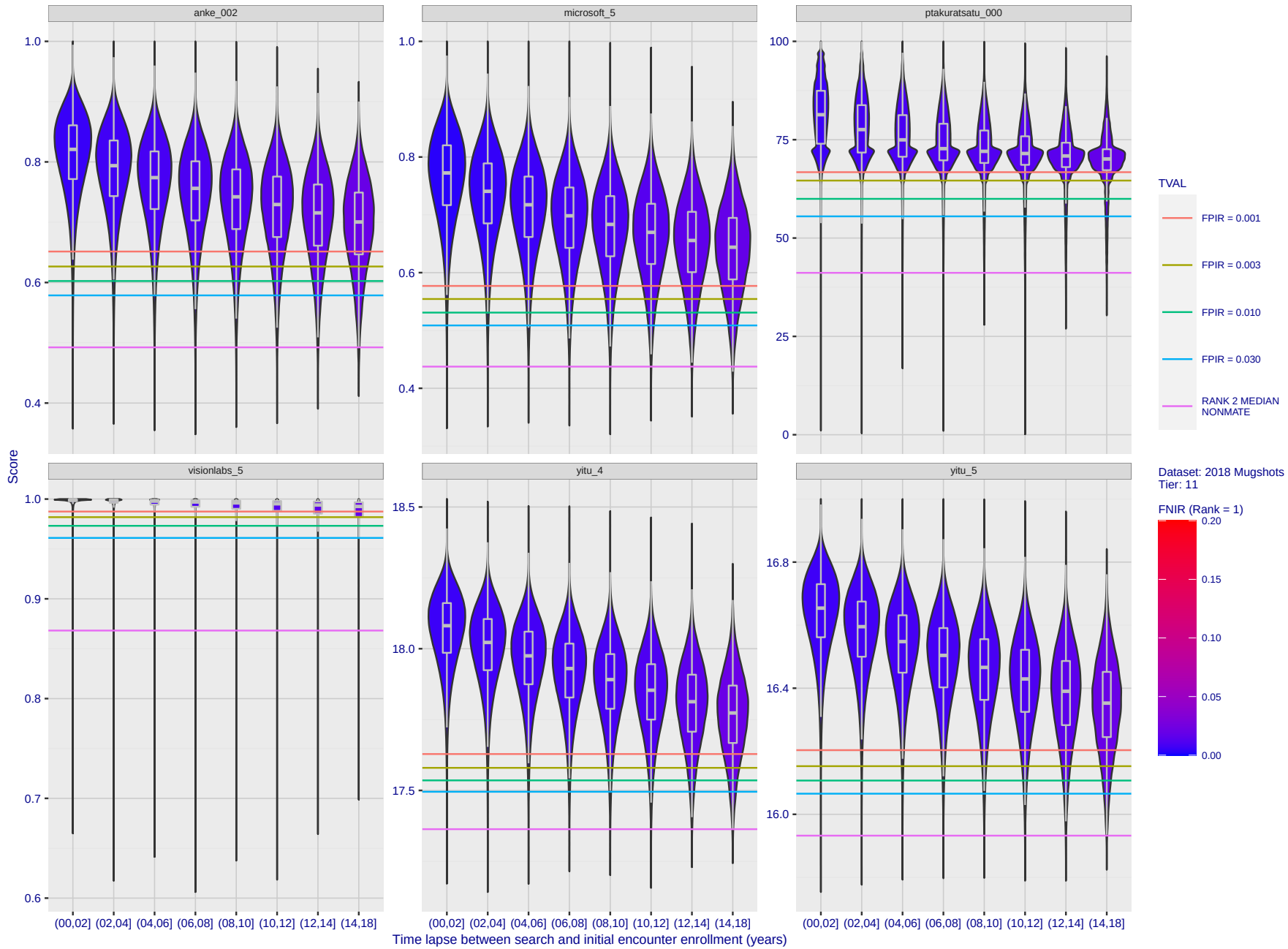

Figure 106: **[FRVT-2018 Mugshot Ageing Dataset] Native mate scores vs. time-elapsed**. *The oldest image of each individual is enrolled. Thereafter, all more recent images are searched. Mated score distributions are computed over all searches noted in row 17 of Table 1 binned by number of years between search and initial enrollment.*

This publication is available free of charge from: https://doi.org/10.6028/NIST.IR.8271

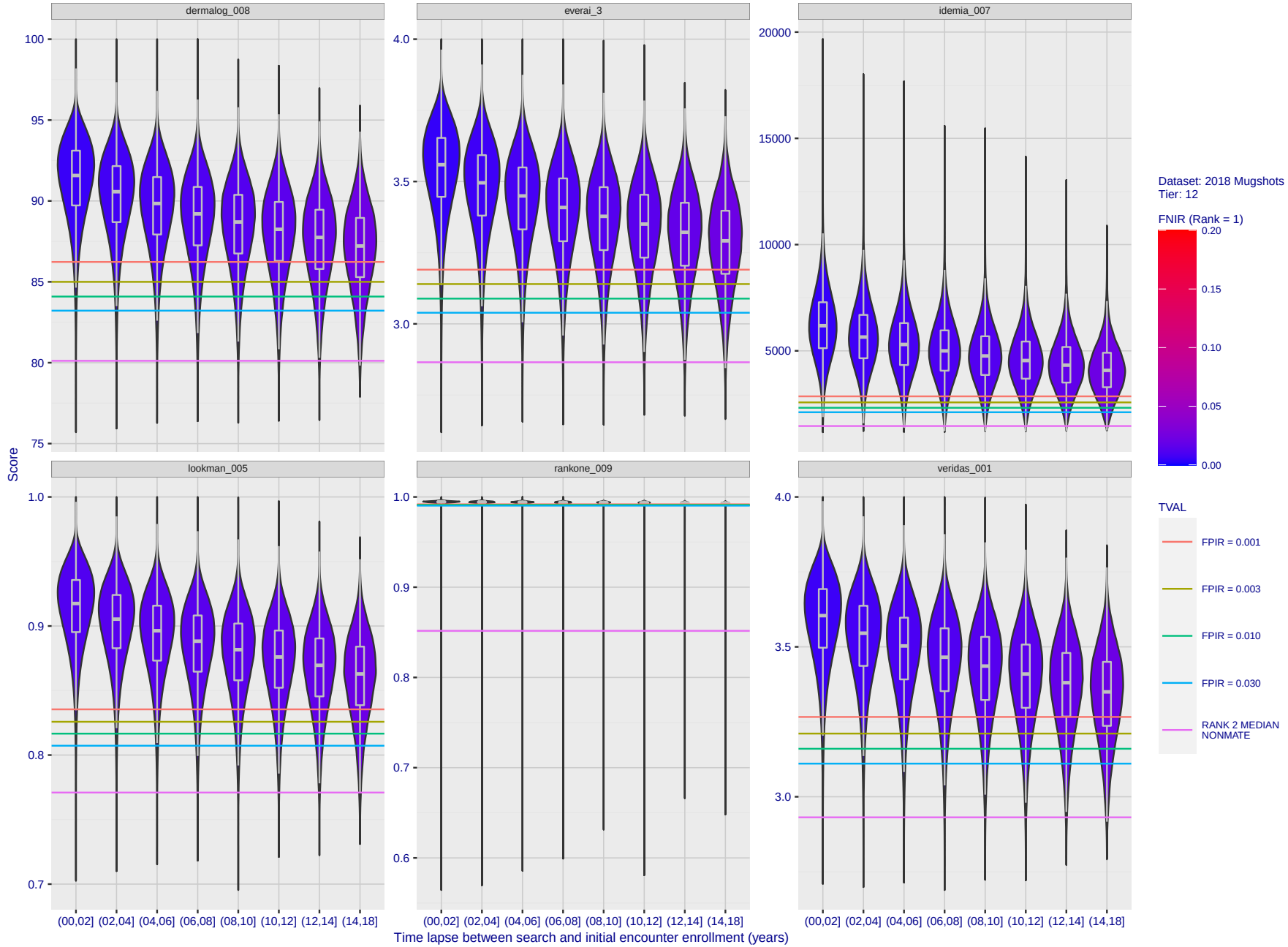

Figure 107: **[FRVT-2018 Mugshot Ageing Dataset] Native mate scores vs. time-elapsed**. *The oldest image of each individual is enrolled. Thereafter, all more recent images are searched. Mated score distributions are computed over all searches noted in row 17 of Table 1 binned by number of years between search and initial enrollment.*

This publication is available free of charge from: https://doi.org/10.6028/NIST.IR.8271

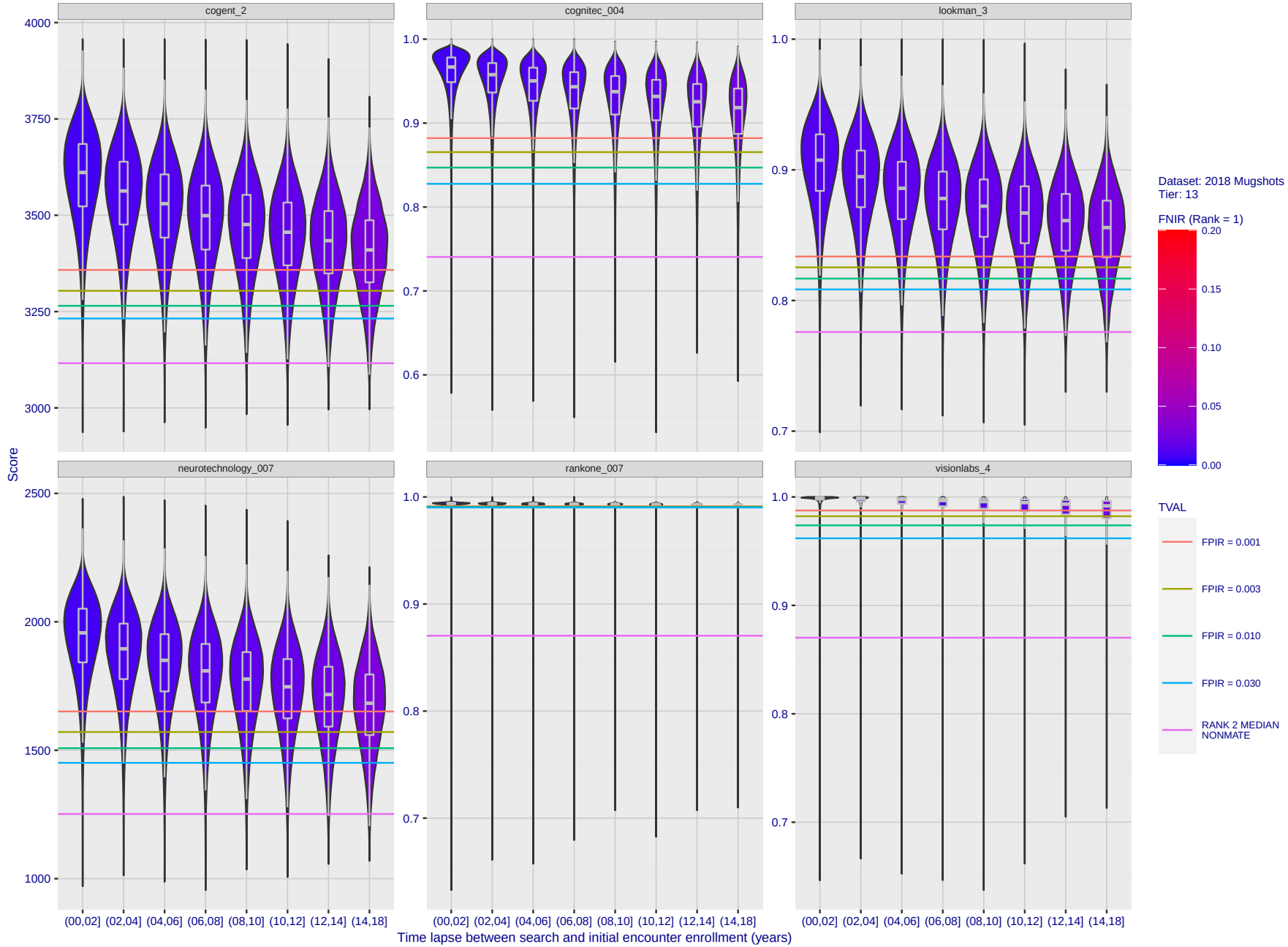

Figure 108: **[FRVT-2018 Mugshot Ageing Dataset] Native mate scores vs. time-elapsed**. *The oldest image of each individual is enrolled. Thereafter, all more recent images are searched. Mated score distributions are computed over all searches noted in row 17 of Table 1 binned by number of years between search and initial enrollment.*

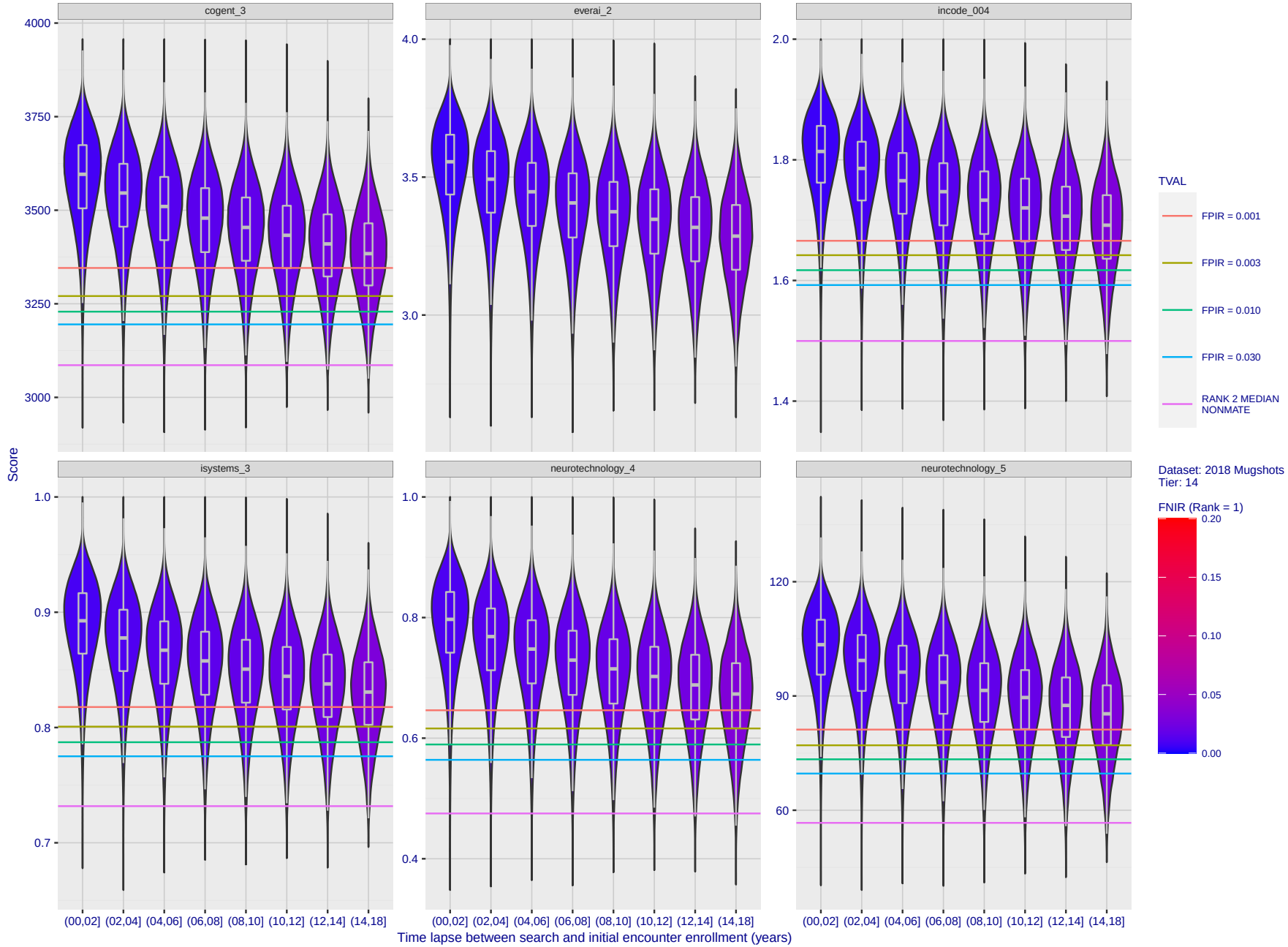

Figure 109: **[FRVT-2018 Mugshot Ageing Dataset] Native mate scores vs. time-elapsed**. *The oldest image of each individual is enrolled. Thereafter, all more recent images are searched. Mated score distributions are computed over all searches noted in row 17 of Table 1 binned by number of years between search and initial enrollment.*

This publication is available free of charge from: https://doi.org/10.6028/NIST.IR.8271

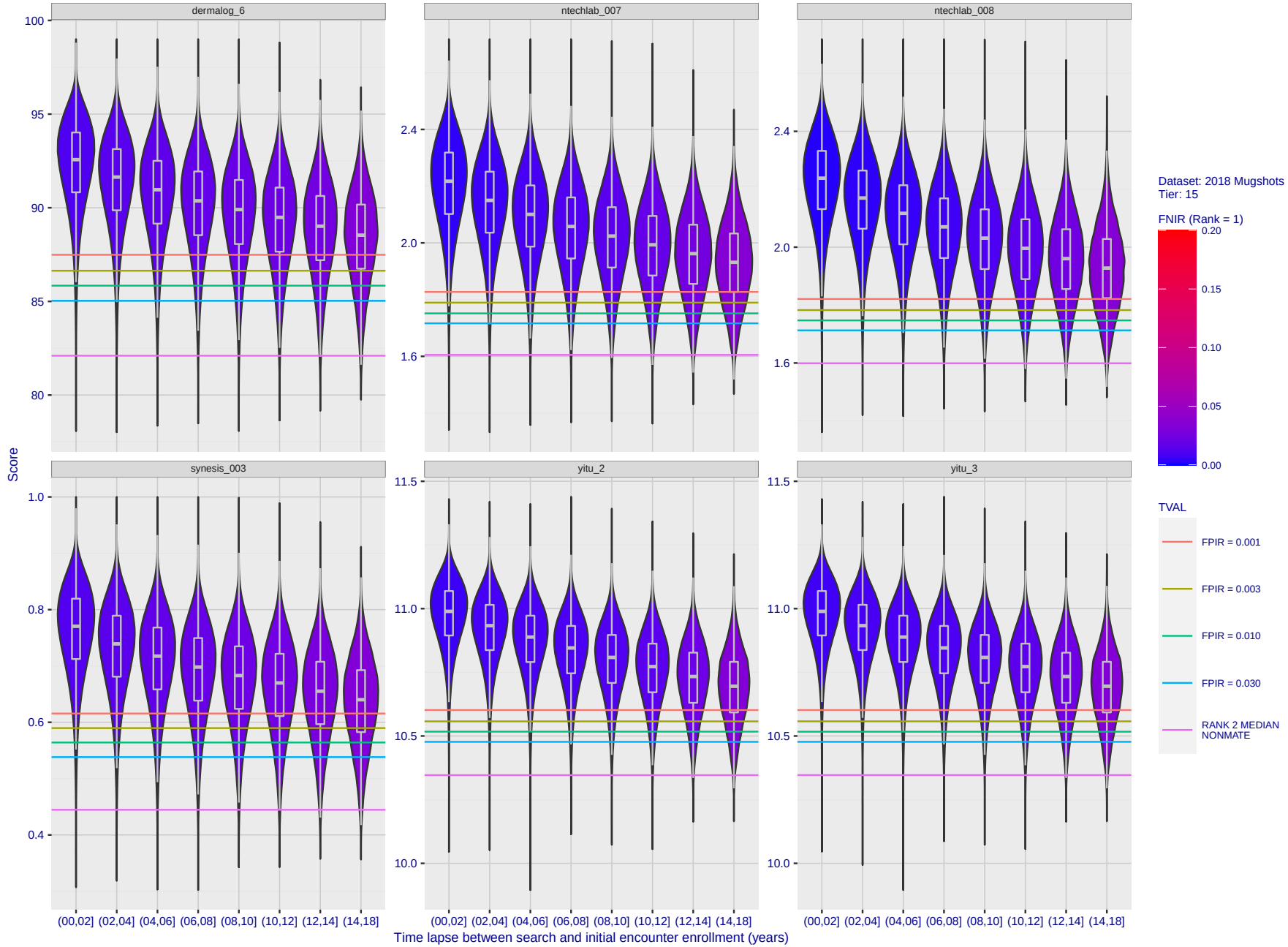

Figure 110: **[FRVT-2018 Mugshot Ageing Dataset] Native mate scores vs. time-elapsed**. *The oldest image of each individual is enrolled. Thereafter, all more recent images are searched. Mated score distributions are computed over all searches noted in row 17 of Table 1 binned by number of years between search and initial enrollment.*

This publication is available free of charge from: https://doi.org/10.6028/NIST.IR.8271

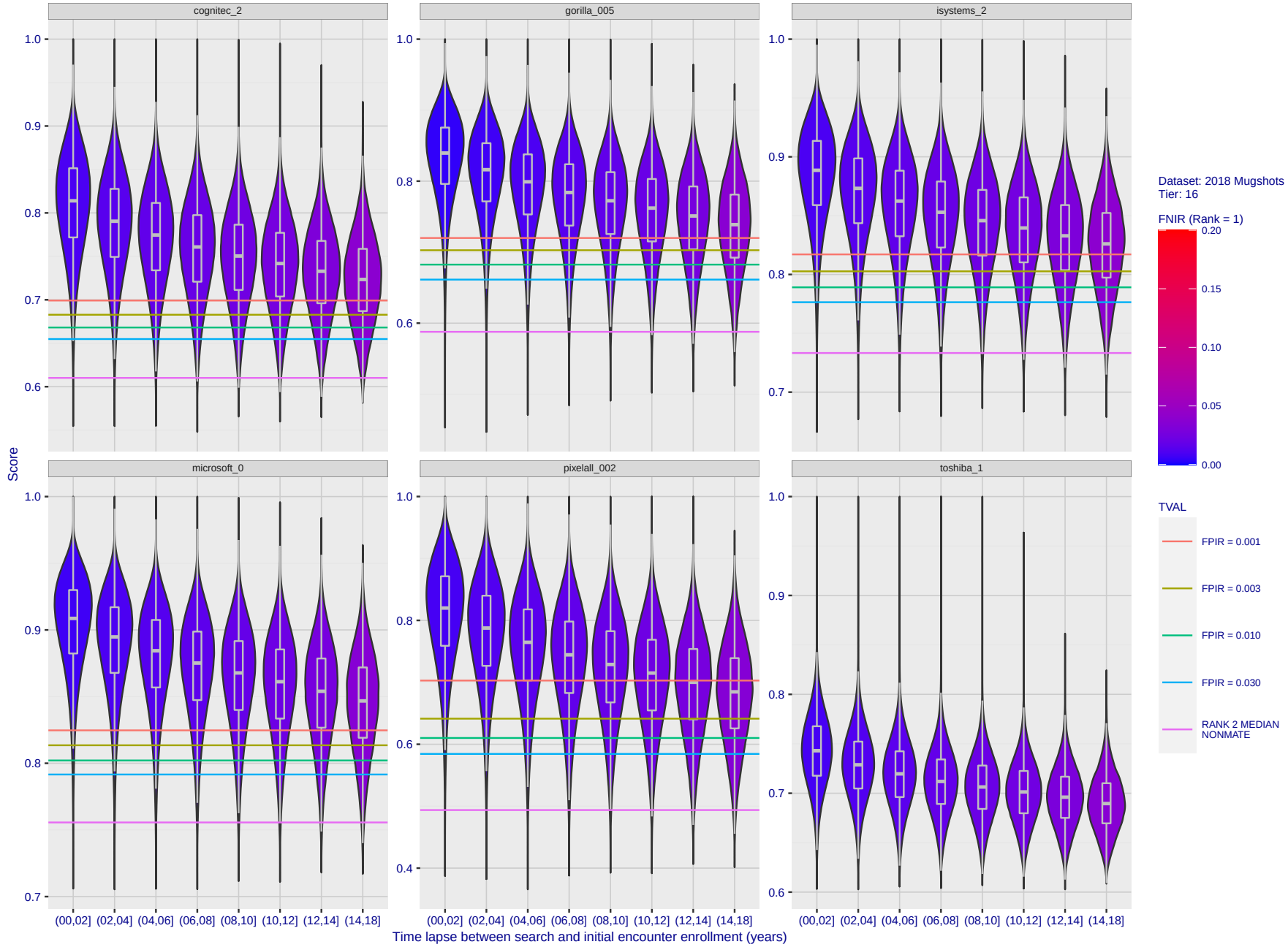

Figure 111: **[FRVT-2018 Mugshot Ageing Dataset] Native mate scores vs. time-elapsed**. *The oldest image of each individual is enrolled. Thereafter, all more recent images are searched. Mated score distributions are computed over all searches noted in row 17 of Table 1 binned by number of years between search and initial enrollment.*

This publication is available free of charge from: https://doi.org/10.6028/NIST.IR.8271

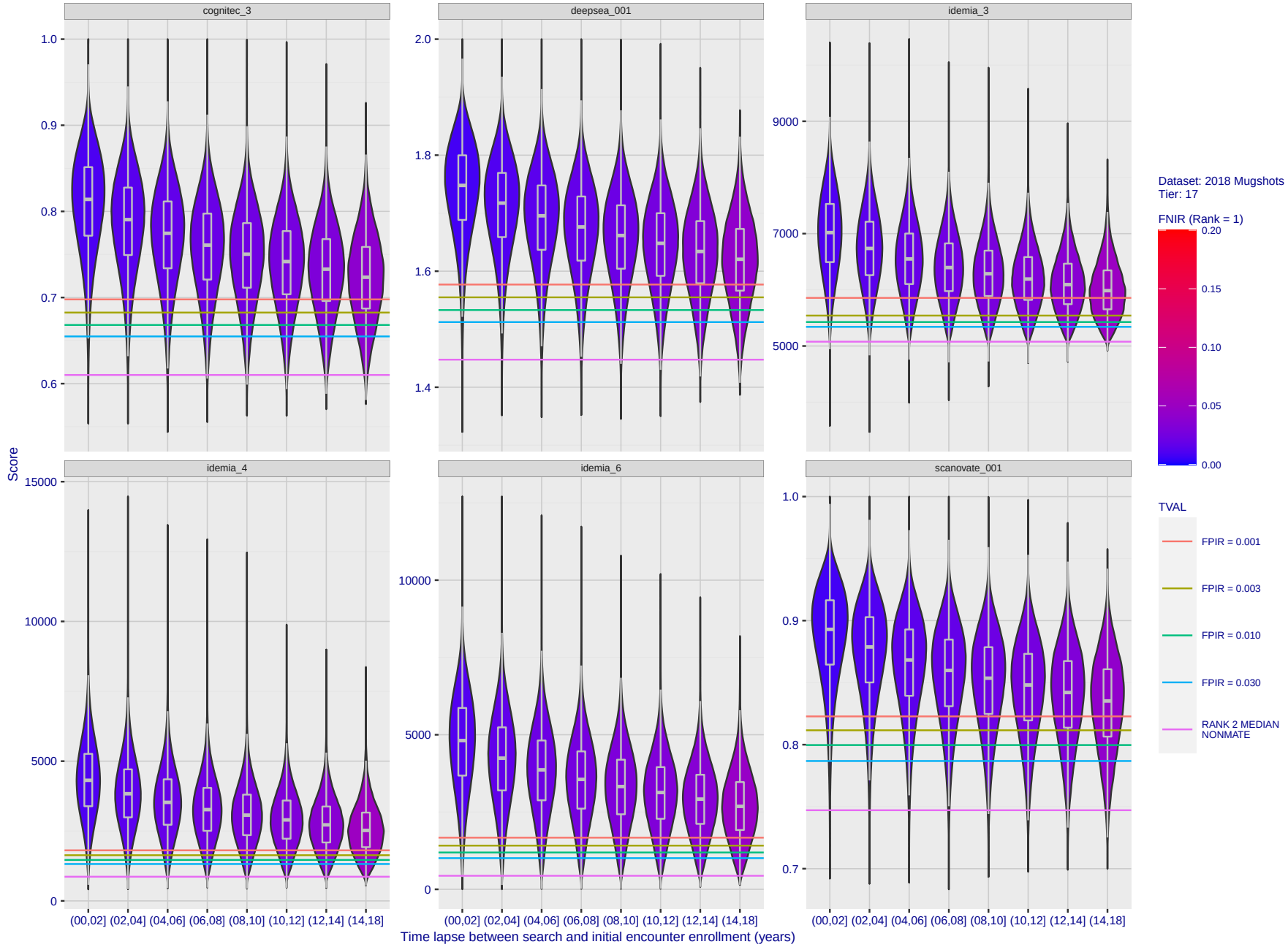

Figure 112: **[FRVT-2018 Mugshot Ageing Dataset] Native mate scores vs. time-elapsed**. *The oldest image of each individual is enrolled. Thereafter, all more recent images are searched. Mated score distributions are computed over all searches noted in row 17 of Table 1 binned by number of years between search and initial enrollment.*

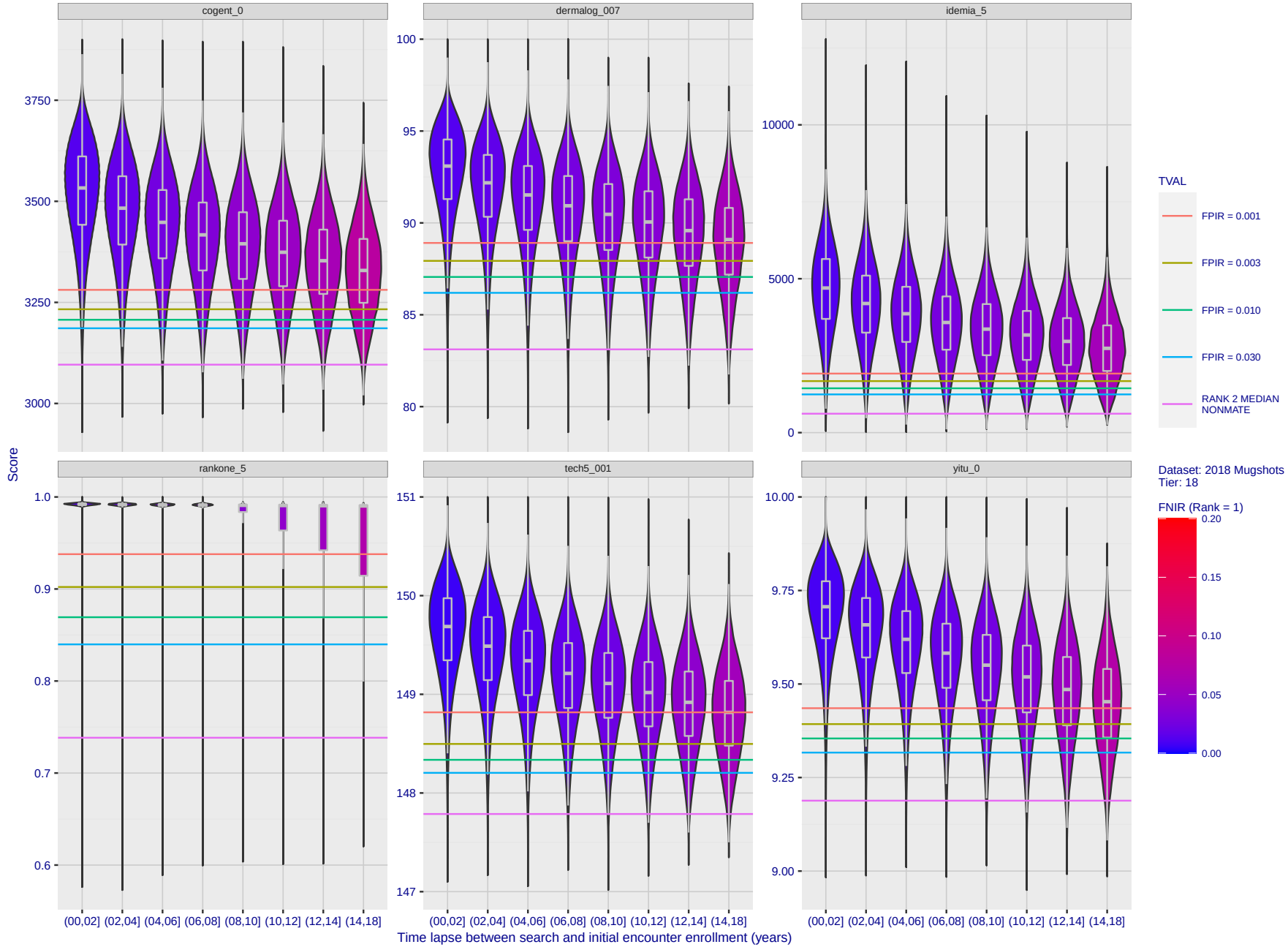

Figure 113: **[FRVT-2018 Mugshot Ageing Dataset] Native mate scores vs. time-elapsed**. *The oldest image of each individual is enrolled. Thereafter, all more recent images are searched. Mated score distributions are computed over all searches noted in row 17 of Table 1 binned by number of years between search and initial enrollment.*

This publication is available free of charge from: https://doi.org/10.6028/NIST.IR.8271

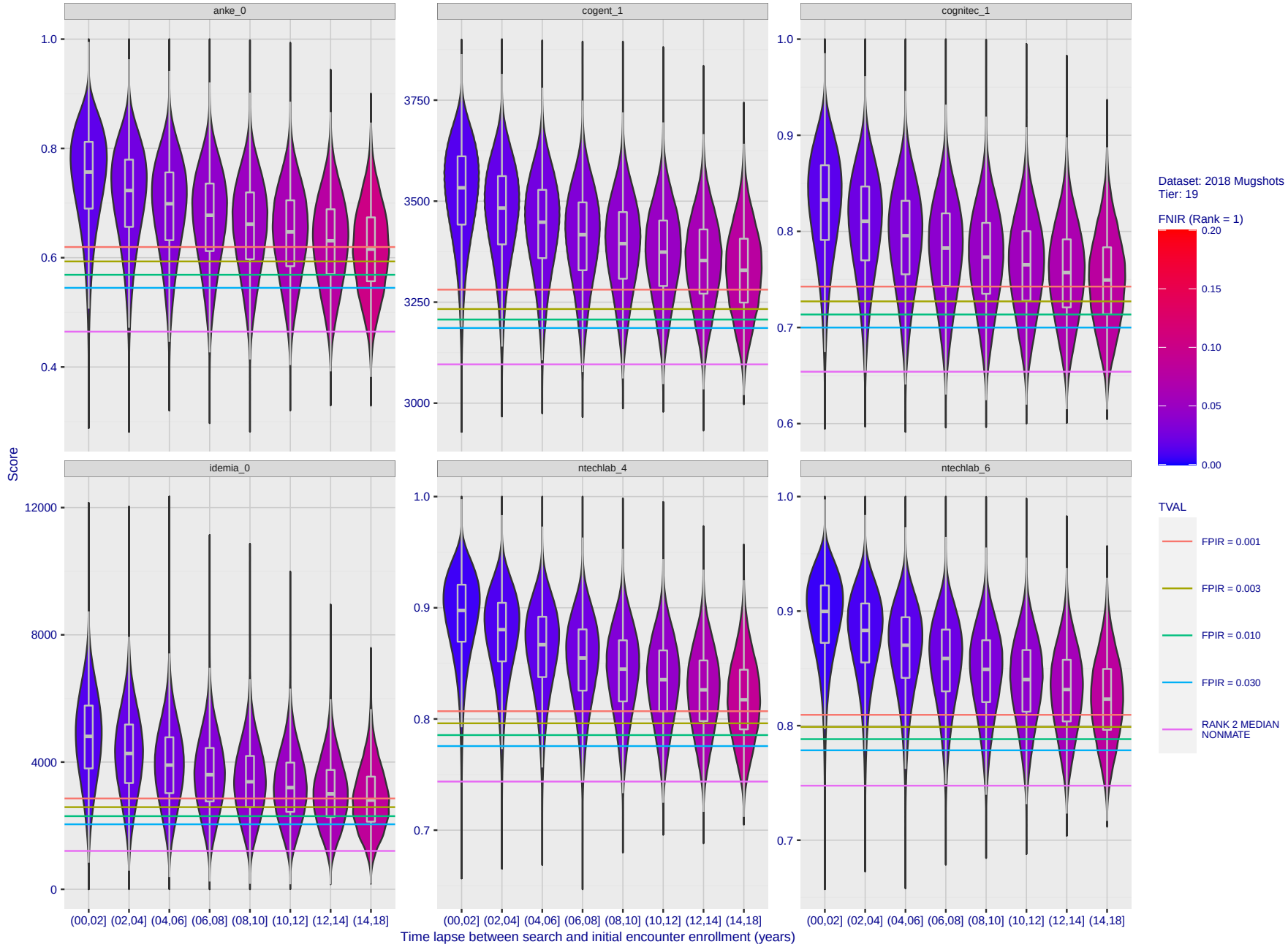

Figure 114: **[FRVT-2018 Mugshot Ageing Dataset] Native mate scores vs. time-elapsed**. *The oldest image of each individual is enrolled. Thereafter, all more recent images are searched. Mated score distributions are computed over all searches noted in row 17 of Table 1 binned by number of years between search and initial enrollment.*

This publication is available free of charge from: https://doi.org/10.6028/NIST.IR.8271

2022/06/13 18:09:57
FNIR(N, R, T) = False neg. identification rate
FPIR(N, T) = False pos. identification rate
N = Num. enrolled subjects
R = Num. candidates examined
T = Threshold
T = 0 → Investigation
T > 0 → Identification

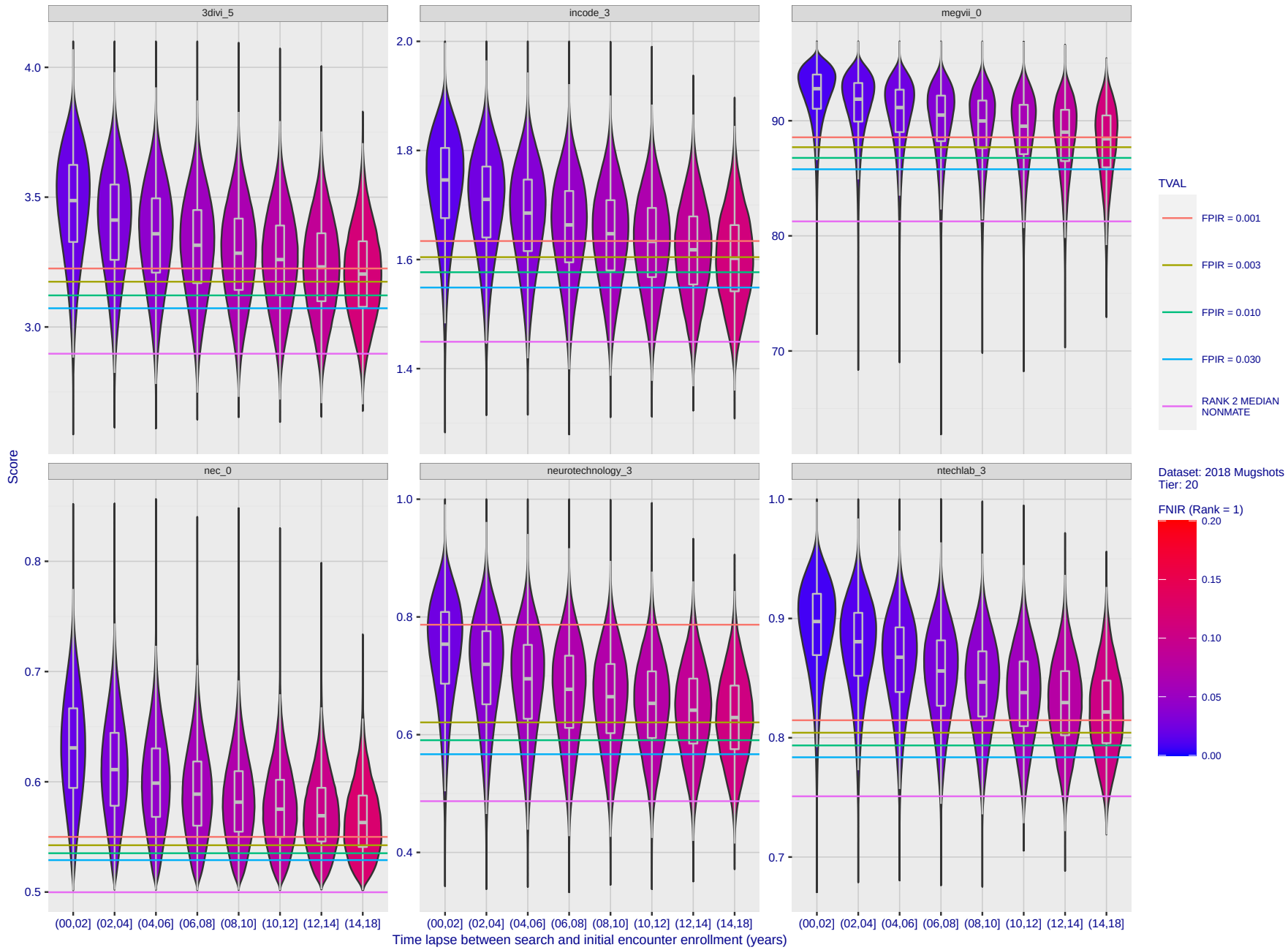

Figure 115: **[FRVT-2018 Mugshot Ageing Dataset] Native mate scores vs. time-elapsed**. *The oldest image of each individual is enrolled. Thereafter, all more recent images are searched. Mated score distributions are computed over all searches noted in row 17 of Table 1 binned by number of years between search and initial enrollment.*

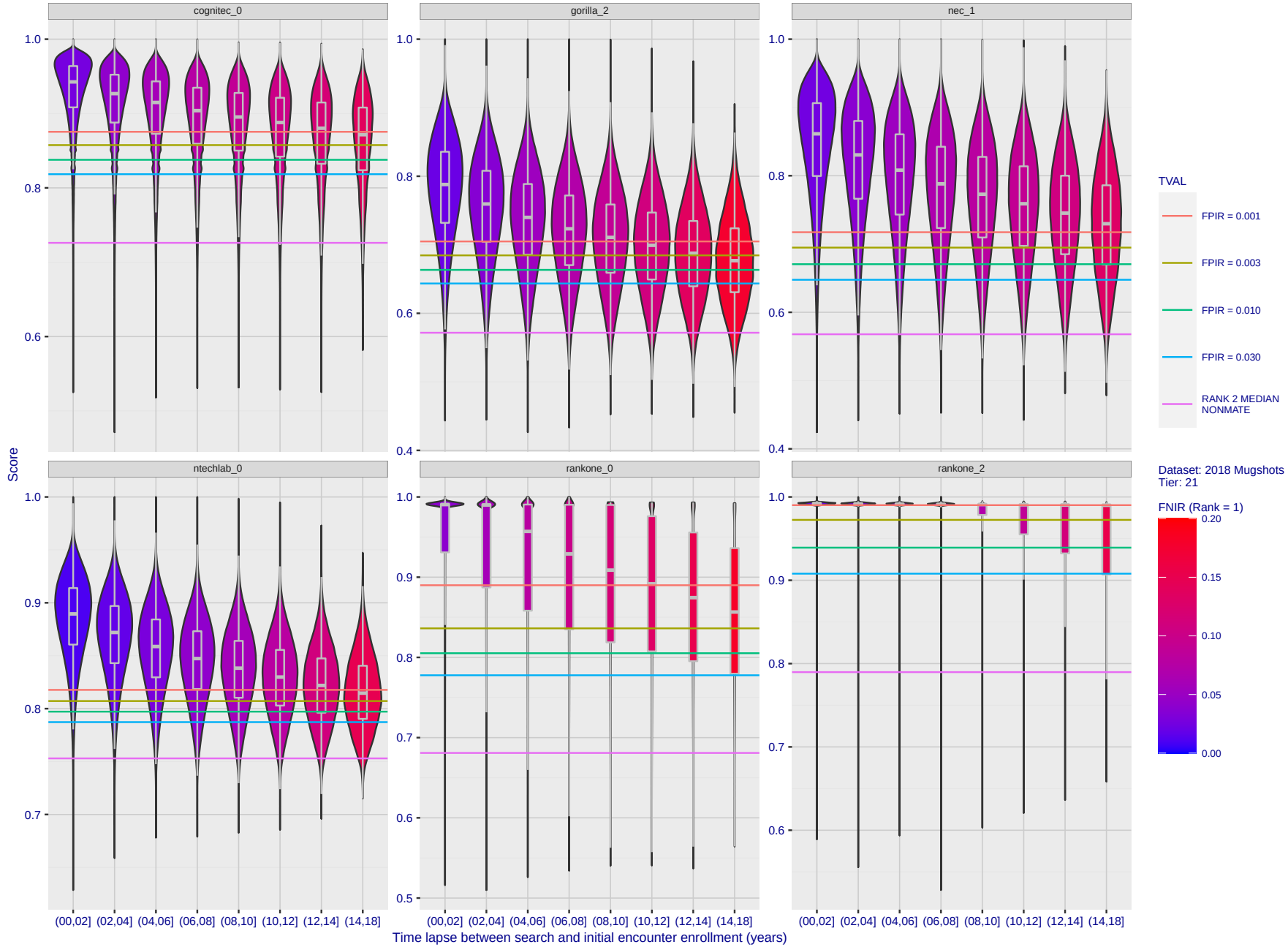

Figure 116: **[FRVT-2018 Mugshot Ageing Dataset] Native mate scores vs. time-elapsed**. *The oldest image of each individual is enrolled. Thereafter, all more recent images are searched. Mated score distributions are computed over all searches noted in row 17 of Table 1 binned by number of years between search and initial enrollment.*

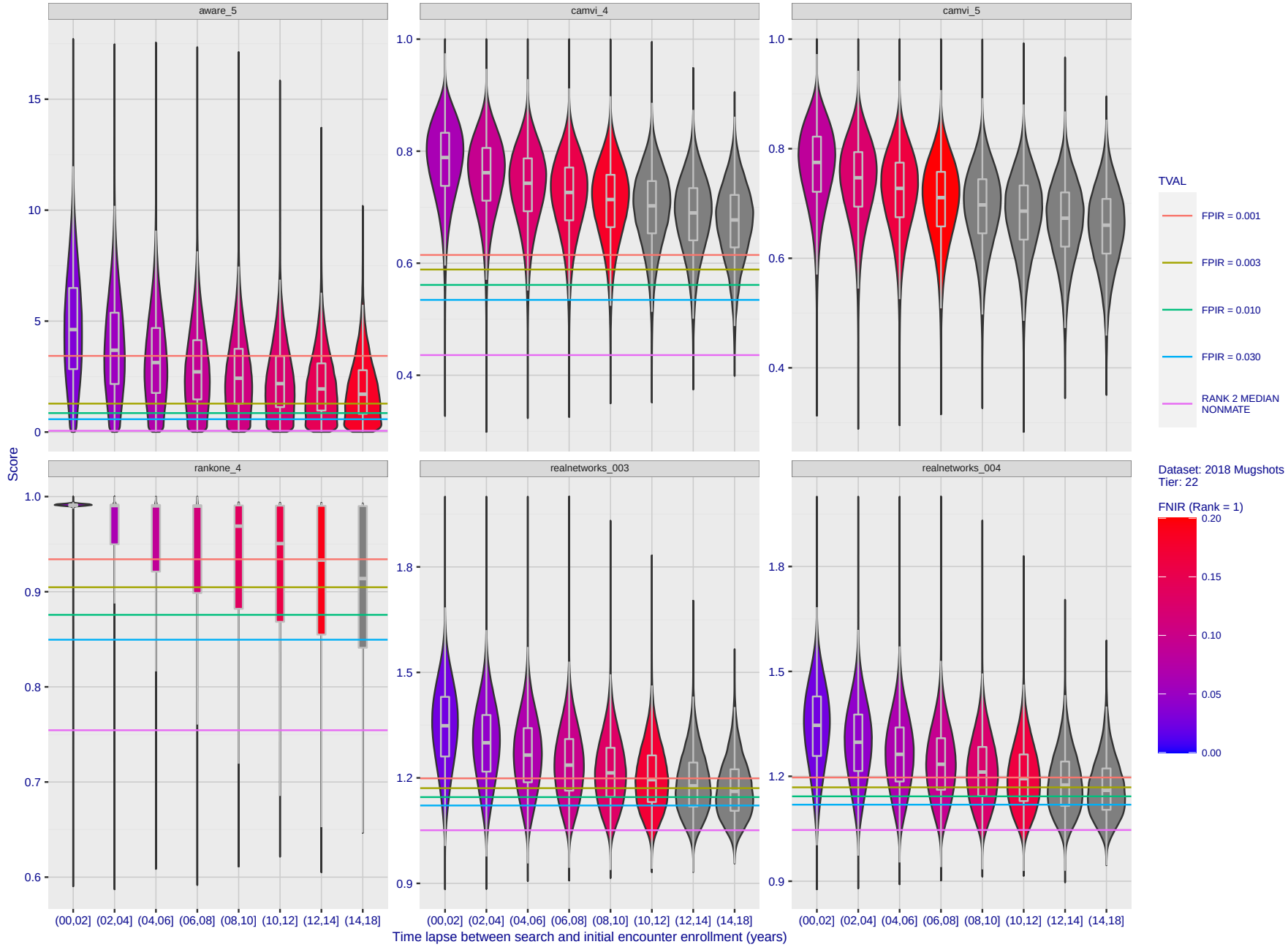

Figure 117: **[FRVT-2018 Mugshot Ageing Dataset] Native mate scores vs. time-elapsed**. *The oldest image of each individual is enrolled. Thereafter, all more recent images are searched. Mated score distributions are computed over all searches noted in row 17 of Table 1 binned by number of years between search and initial enrollment.*

This publication is available free of charge from: https://doi.org/10.6028/NIST.IR.8271

2022/06/13 18:09:57

FNIR(N, R, T) = False neg. identification rate
FPIR(N, T) = False pos. identification rate
N = Num. enrolled subjects
R = Num. candidates examined
T = Threshold
T = 0 → Investigation
T > 0 → Identification

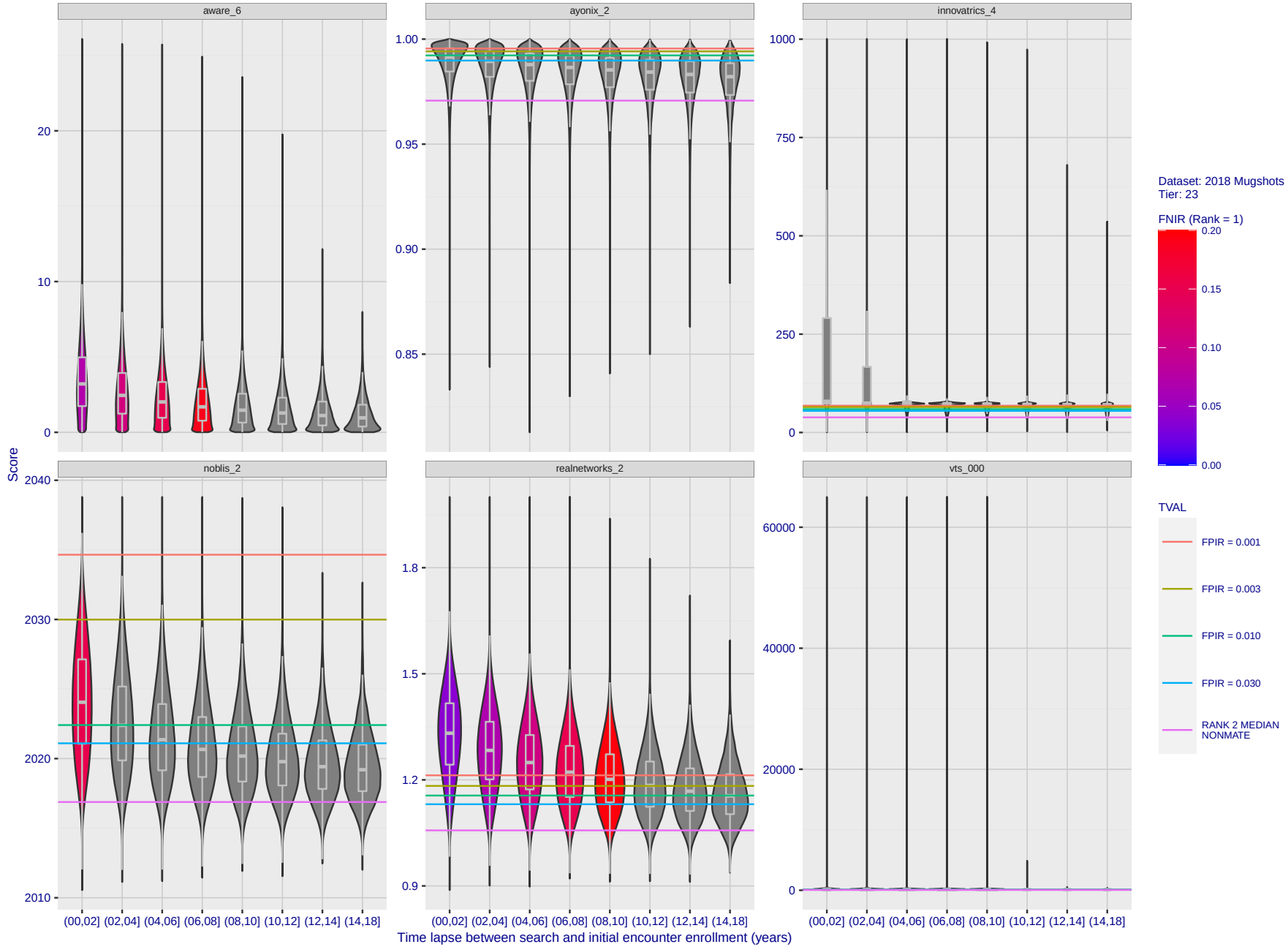

Figure 118: **[FRVT-2018 Mugshot Ageing Dataset] Native mate scores vs. time-elapsed**. *The oldest image of each individual is enrolled. Thereafter, all more recent images are searched. Mated score distributions are computed over all searches noted in row 17 of Table 1 binned by number of years between search and initial enrollment.*

This publication is available free of charge from: https://doi.org/10.6028/NIST.IR.8271

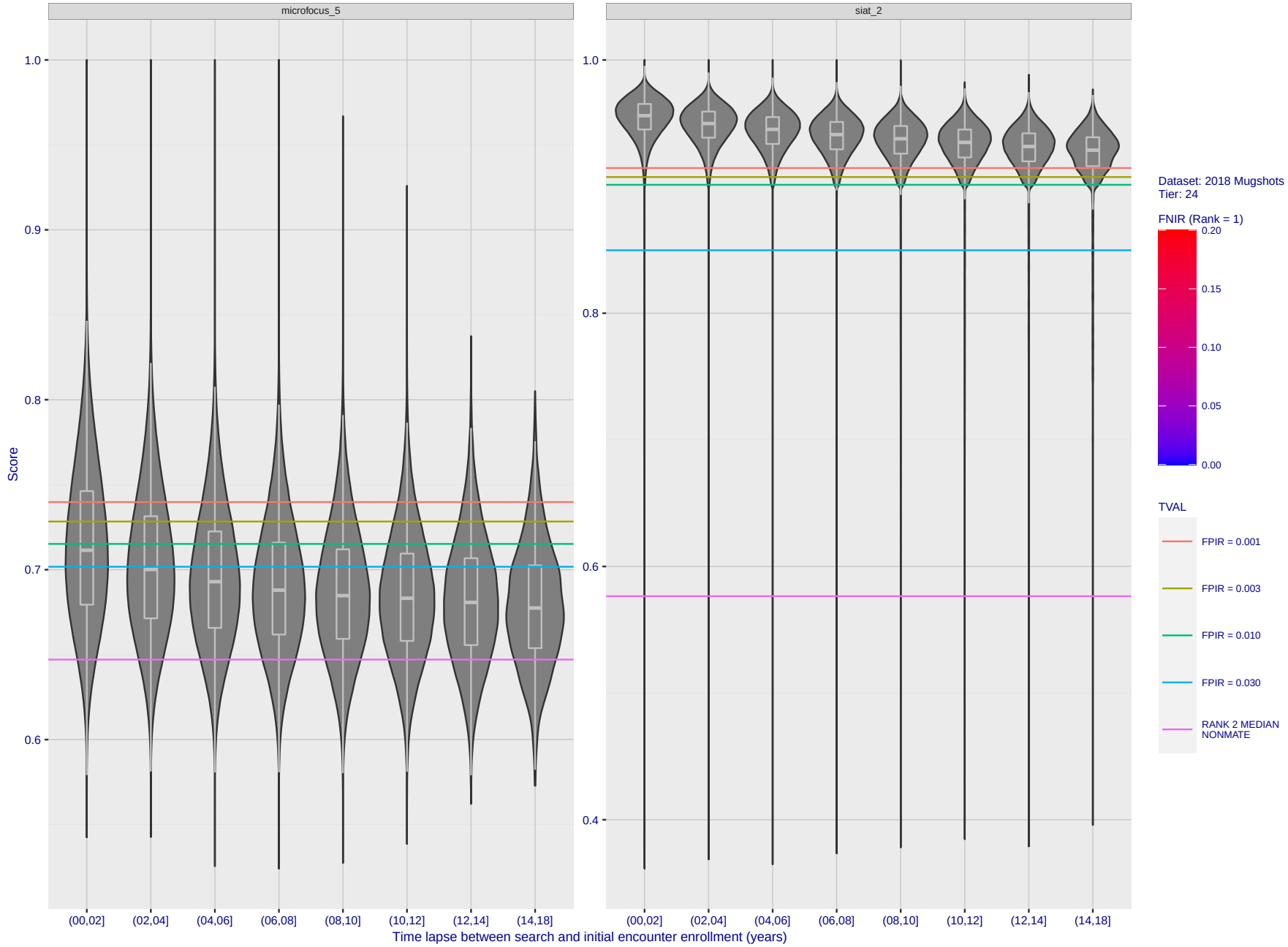

Figure 119: **[FRVT-2018 Mugshot Ageing Dataset] Native mate scores vs. time-elapsed**. *The oldest image of each individual is enrolled. Thereafter, all more recent images are searched. Mated score distributions are computed over all searches noted in row 17 of Table 1 binned by number of years between search and initial enrollment.*

Appendix C Effect of enrolling multiple images

This publication is available free of charge from: https://doi.org/10.6028/NIST.IR.8271

This publication is available free of charge from: https://doi.org/10.6028/NIST.IR.8271

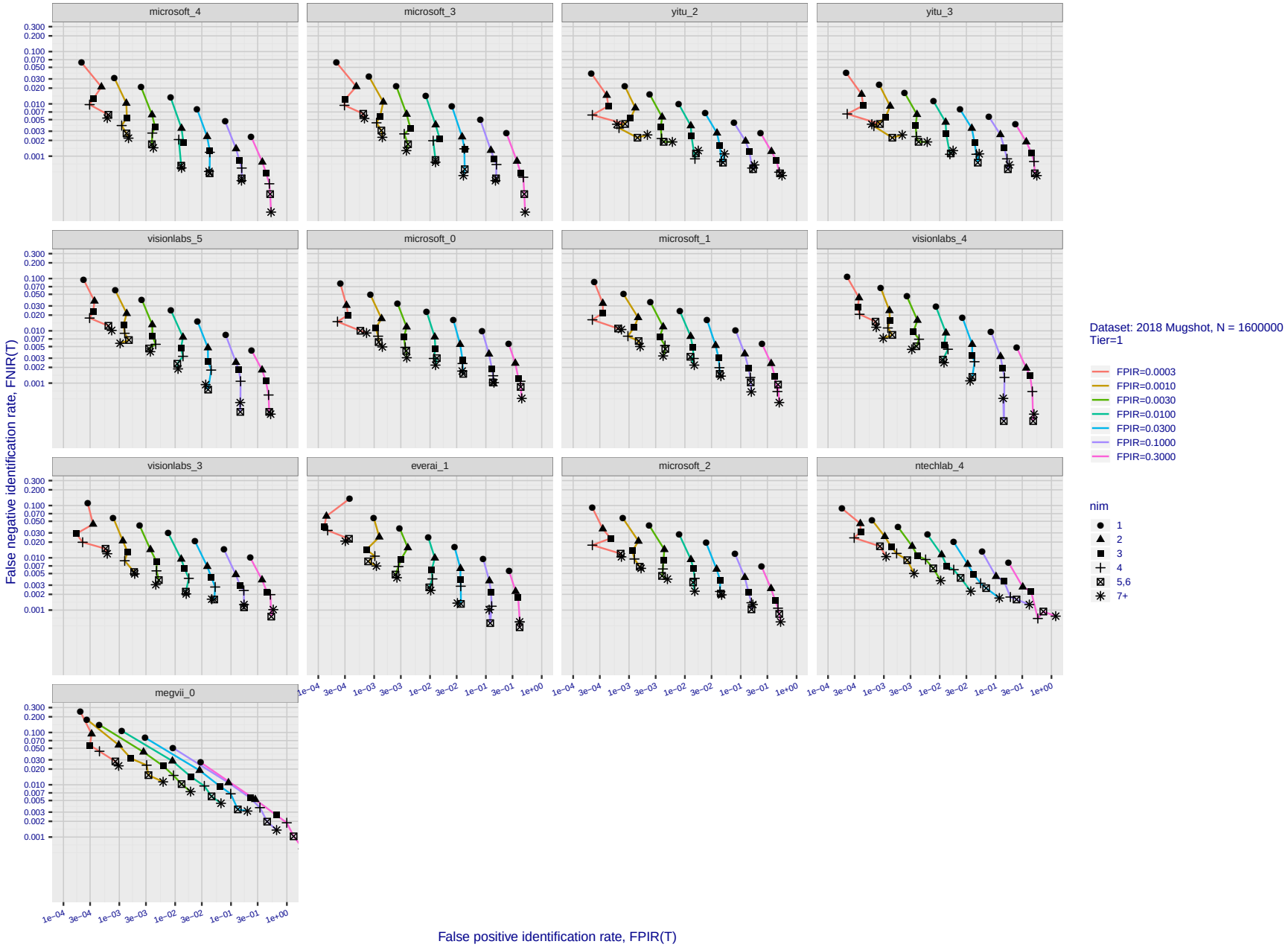

Figure 120: **[FRVT-2018 Mugshot Dataset] Effect of enrolling multiple images for each identity**. *The plot shows an identification miss rates vs. false positive rates, at seven operating thresholds. The enrolled population size is fixed. The images are enrolled with lifetime-consolidation - see section 2.3.*

This publication is available free of charge from: https://doi.org/10.6028/NIST.IR.8271

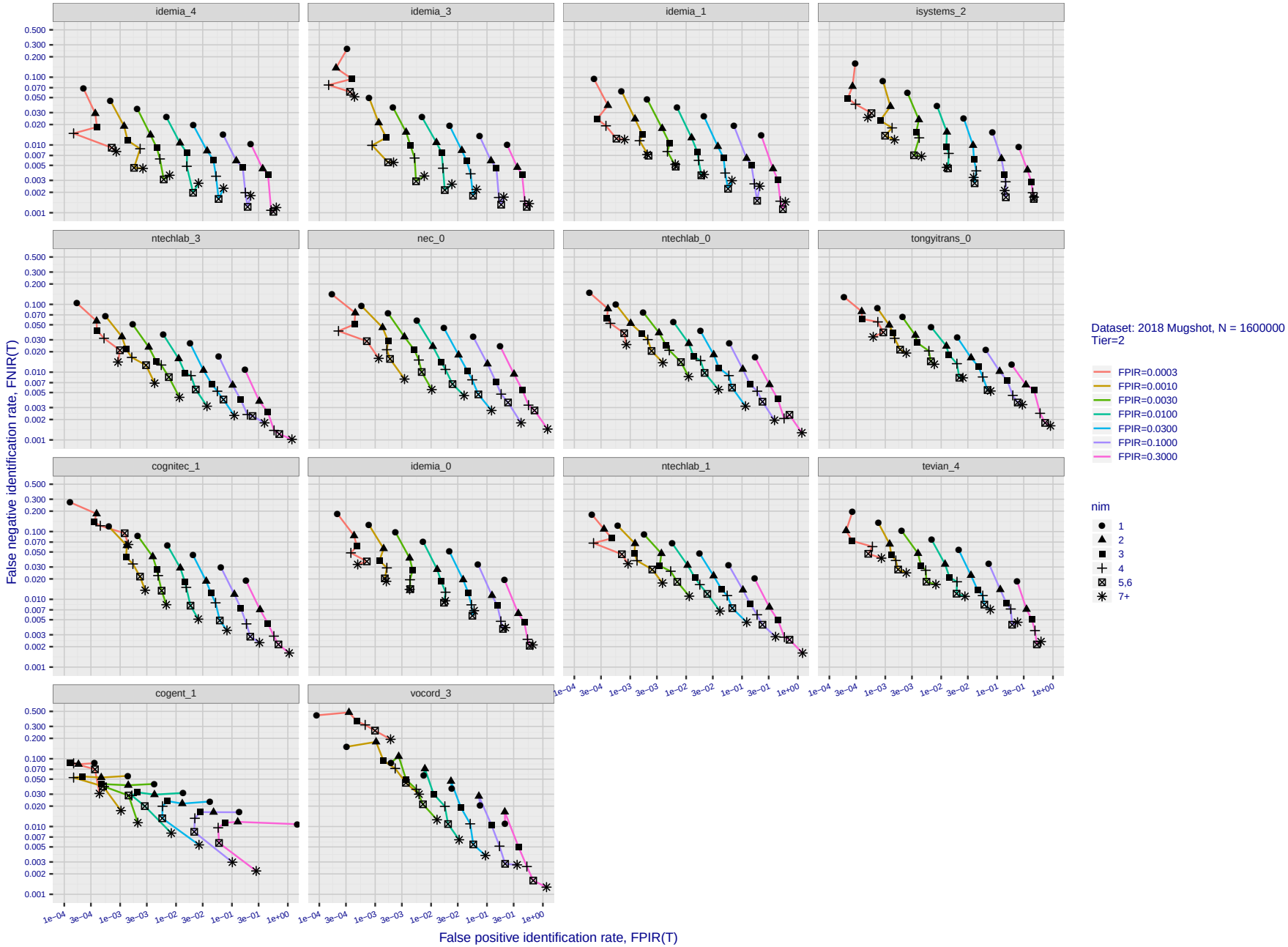

Figure 121: **[FRVT-2018 Mugshot Dataset] Effect of enrolling multiple images for each identity**. *The plot shows an identification miss rates vs. false positive rates, at seven operating thresholds. The enrolled population size is fixed. The images are enrolled with lifetime-consolidation - see section 2.3.*

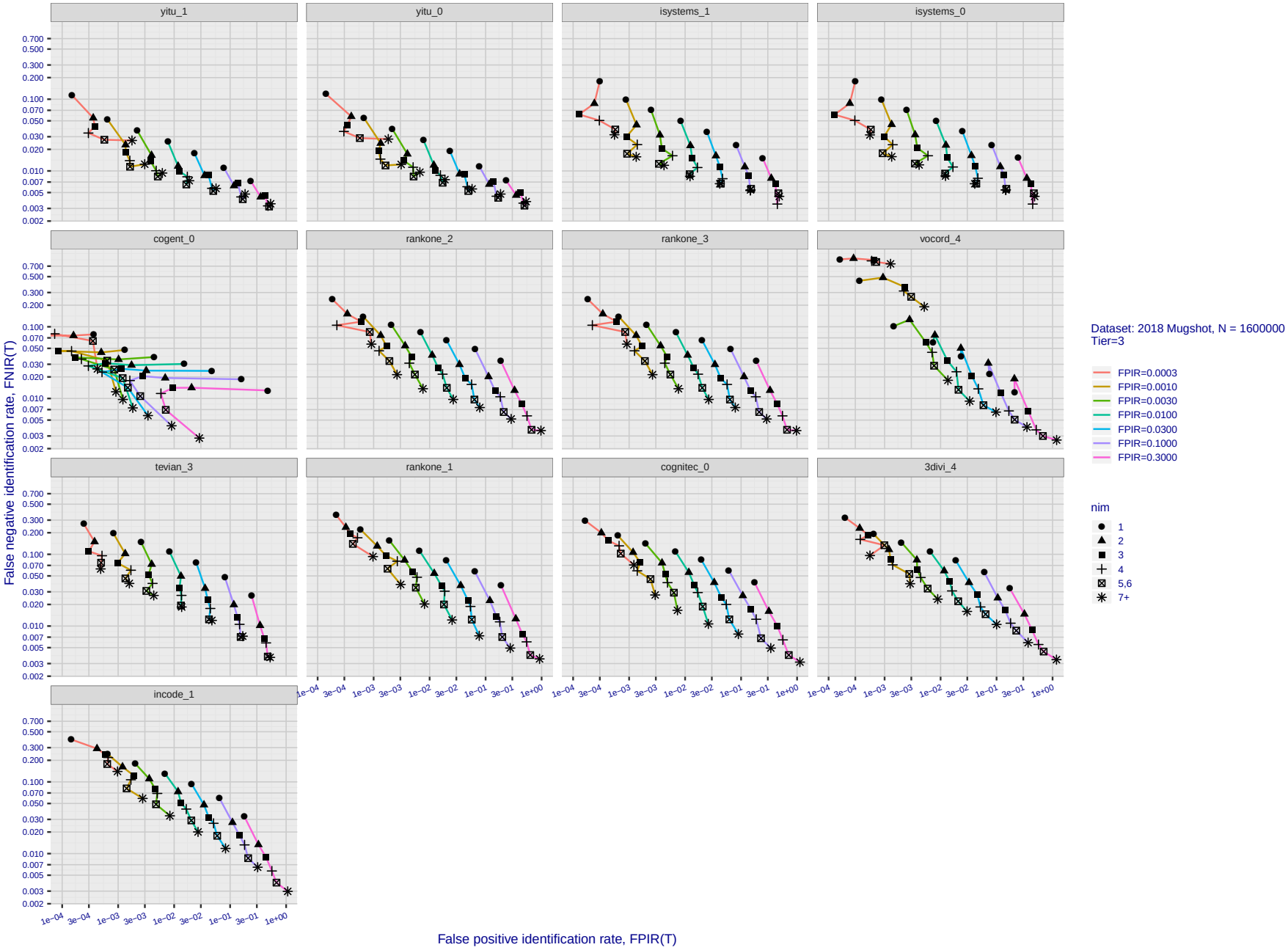

Figure 122: **[FRVT-2018 Mugshot Dataset] Effect of enrolling multiple images for each identity**. *The plot shows an identification miss rates vs. false positive rates, at seven operating thresholds. The enrolled population size is fixed. The images are enrolled with lifetime-consolidation - see section 2.3.*

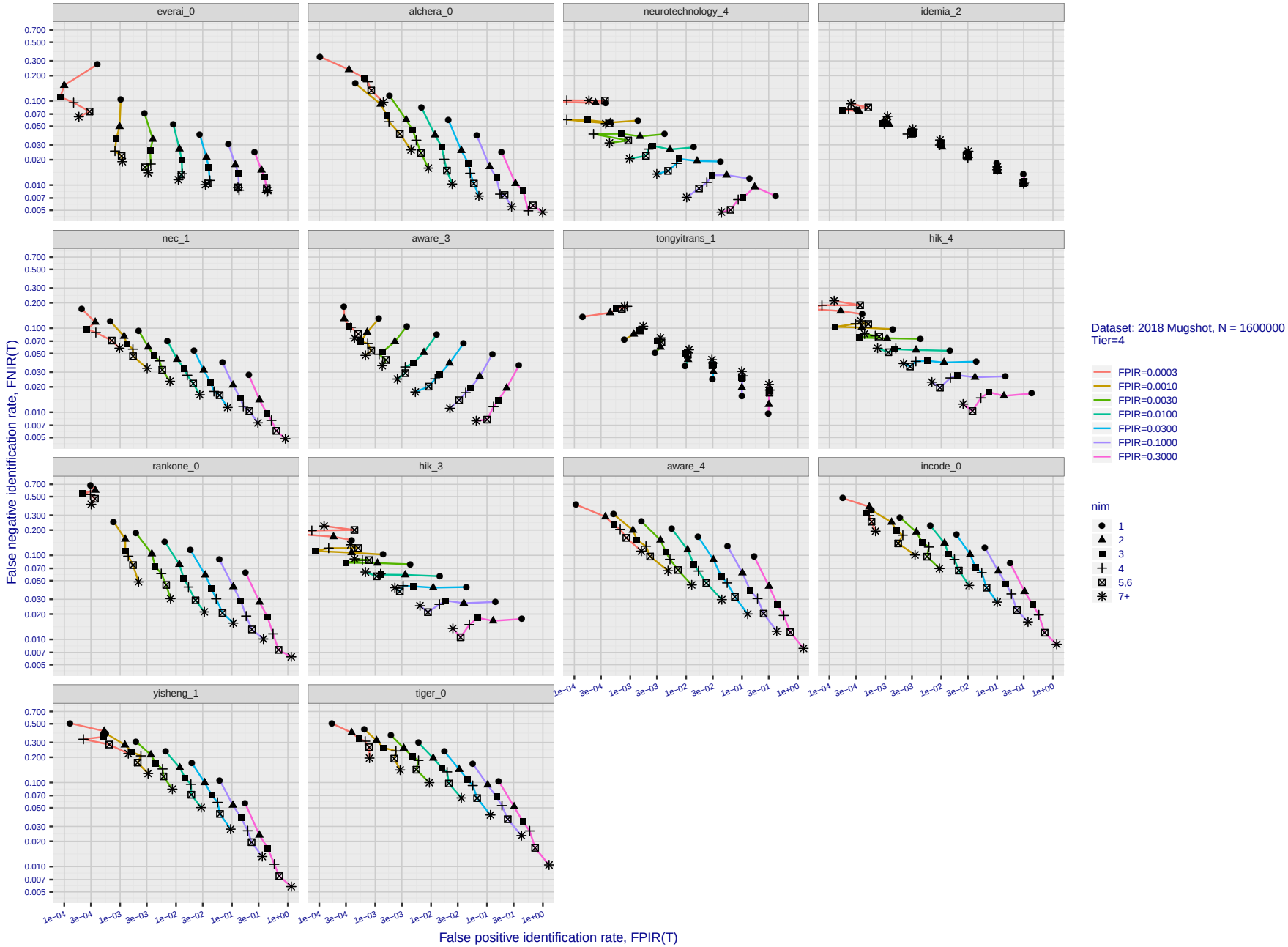

Figure 123: **[FRVT-2018 Mugshot Dataset] Effect of enrolling multiple images for each identity**. *The plot shows an identification miss rates vs. false positive rates, at seven operating thresholds. The enrolled population size is fixed. The images are enrolled with lifetime-consolidation - see section 2.3.*

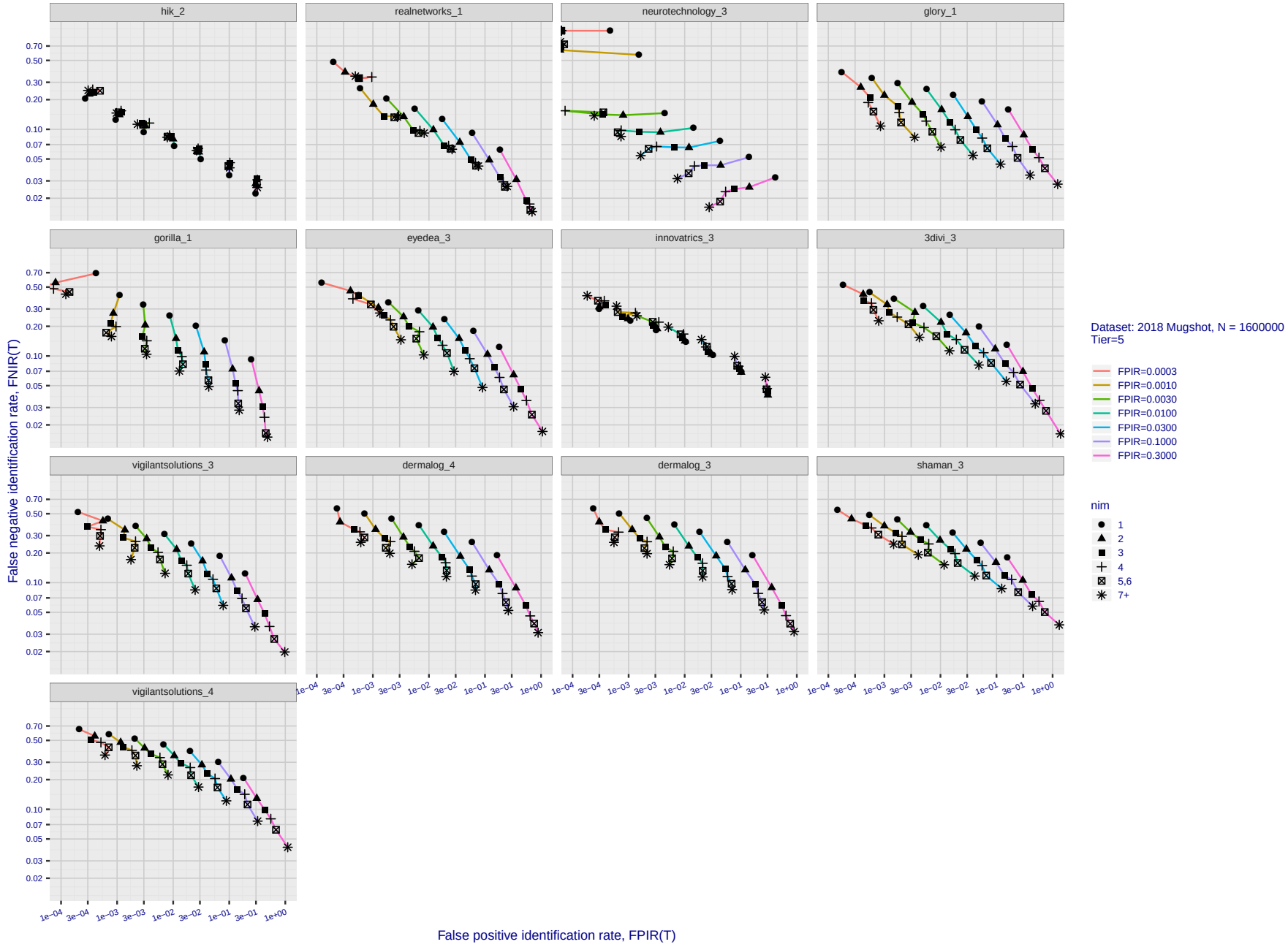

Figure 124: **[FRVT-2018 Mugshot Dataset] Effect of enrolling multiple images for each identity**. *The plot shows an identification miss rates vs. false positive rates, at seven operating thresholds. The enrolled population size is fixed. The images are enrolled with lifetime-consolidation - see section 2.3.*

FNIR(N, R, T) = False neg. identification rate
FPIR(N, T) = False pos. identification rate
N = Num. enrolled subjects
R = Num. candidates examined
T = Threshold
T = 0 → Investigation
T > 0 → Identification

This publication is available free of charge from: https://doi.org/10.6028/NIST.IR.8271

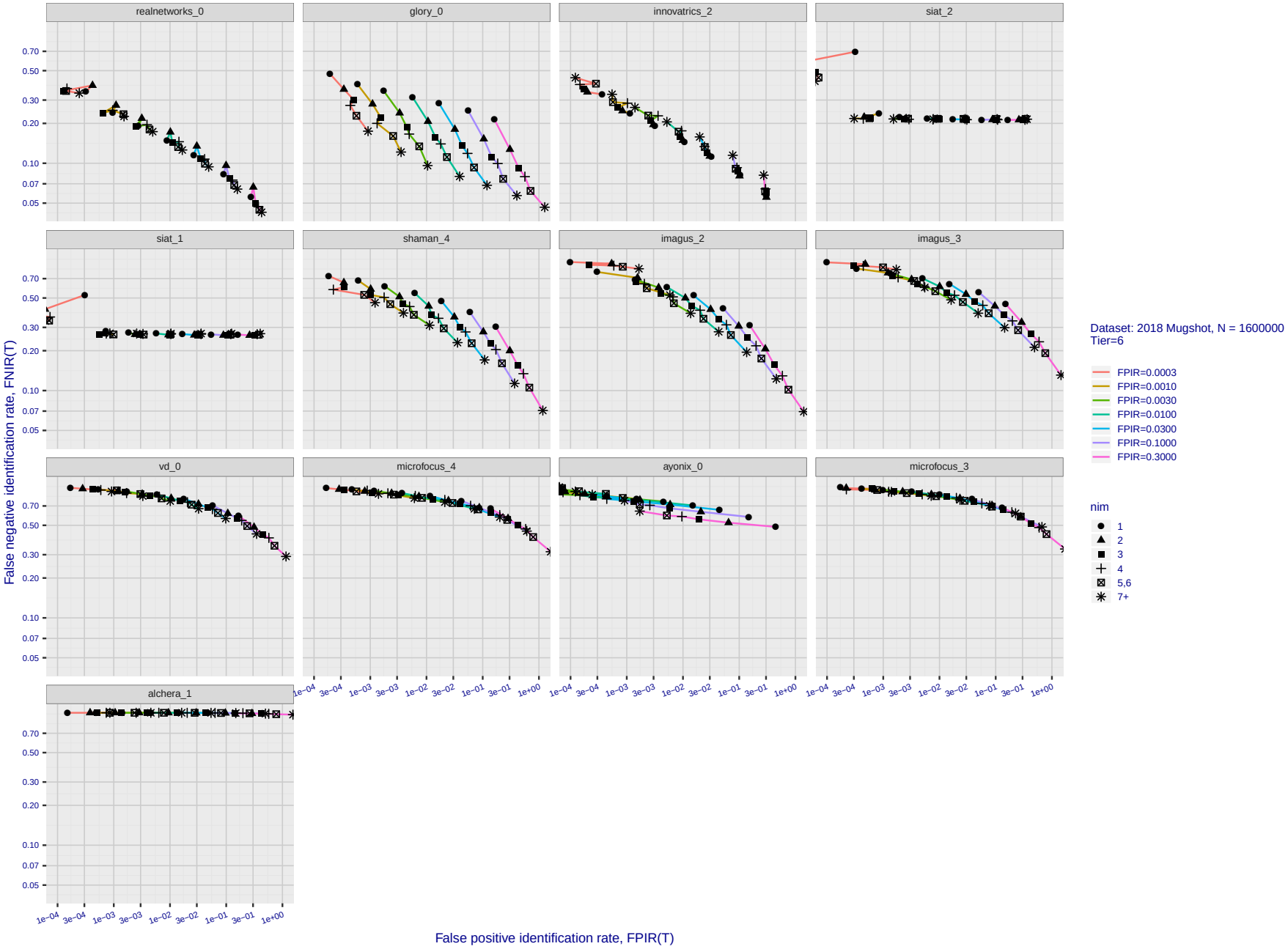

Figure 125: **[FRVT-2018 Mugshot Dataset] Effect of enrolling multiple images for each identity**. *The plot shows an identification miss rates vs. false positive rates, at seven operating thresholds. The enrolled population size is fixed. The images are enrolled with lifetime-consolidation - see section 2.3.*

Appendix D Accuracy with poor quality webcam images

This publication is available free of charge from: https://doi.org/10.6028/NIST.IR.8271

2022/06/13	FNIR(N, R, T) =	False neg. identification rate	N = Num. enrolled subjects	T = Threshold	$T = 0 \rightarrow$ Investigation
18:09:57	FPIR(N, T) =	False pos. identification rate	R = Num. candidates examined		$T > 0 \rightarrow$ Identification

This publication is available free of charge from: https://doi.org/10.6028/NIST.IR.8271

This publication is available free of charge from: https://doi.org/10.6028/NIST.IR.8271

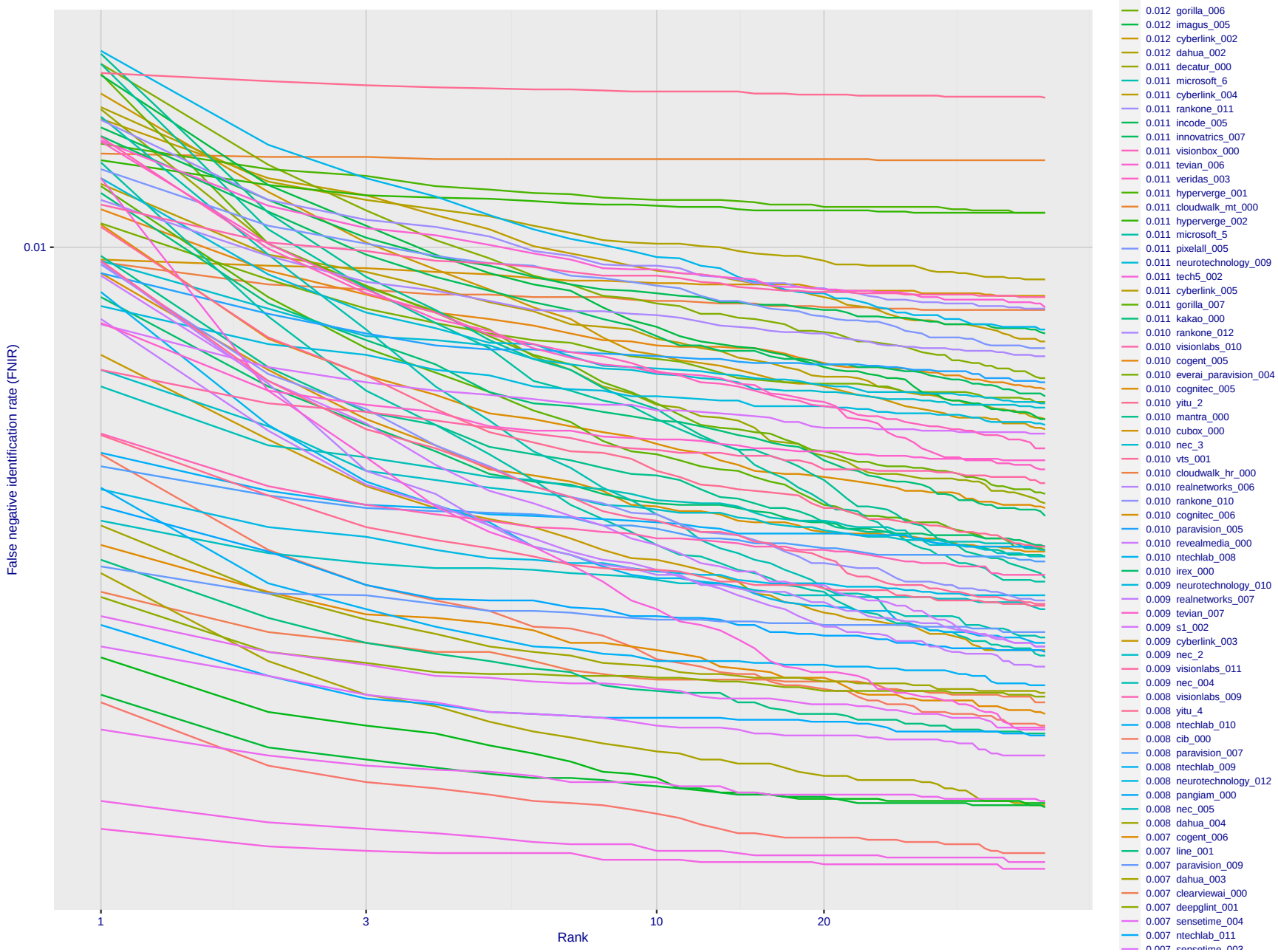

Figure 126: **[Webcam Dataset] Identification miss rates vs. rank**. *The results apply to cross-domain recognition in which webcams are searched against enrolled mugshots. The FNIR values are higher than those for mugshot-mugshot identification due to low image resolution, lighting and less constrained subject pose in webcam images - see Figure 6.*

This publication is available free of charge from: https://doi.org/10.6028/NIST.IR.8271

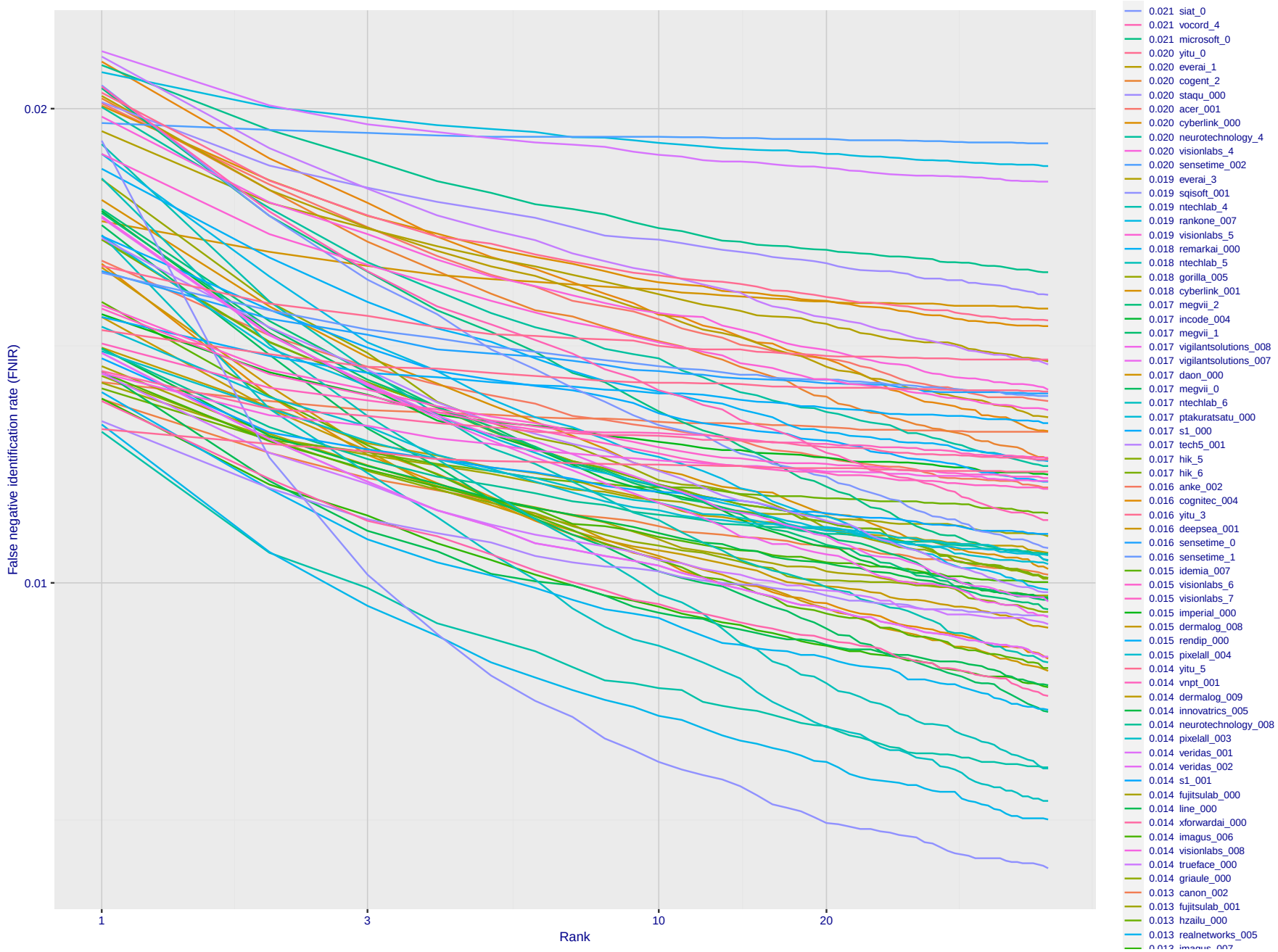

Figure 127: **[Webcam Dataset] Identification miss rates vs. rank**. *The results apply to cross-domain recognition in which webcams are searched against enrolled mugshots. The FNIR values are higher than those for mugshot-mugshot identification due to low image resolution, lighting and less constrained subject pose in webcam images - see Figure 6.*

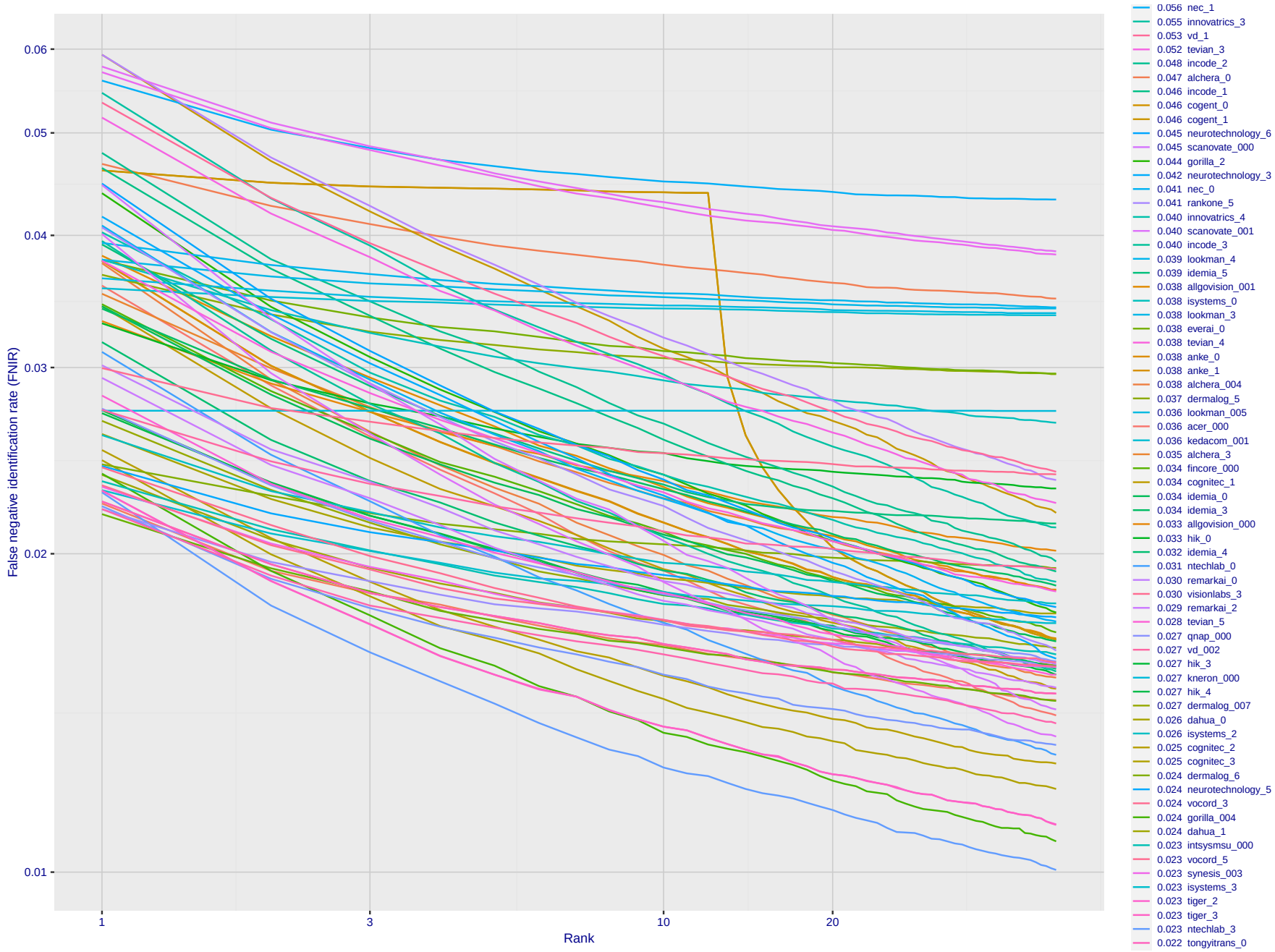

Figure 128: **[Webcam Dataset] Identification miss rates vs. rank**. *The results apply to cross-domain recognition in which webcams are searched against enrolled mugshots. The FNIR values are higher than those for mugshot-mugshot identification due to low image resolution, lighting and less constrained subject pose in webcam images - see Figure 6.*

This publication is available free of charge from: https://doi.org/10.6028/NIST.IR.8271

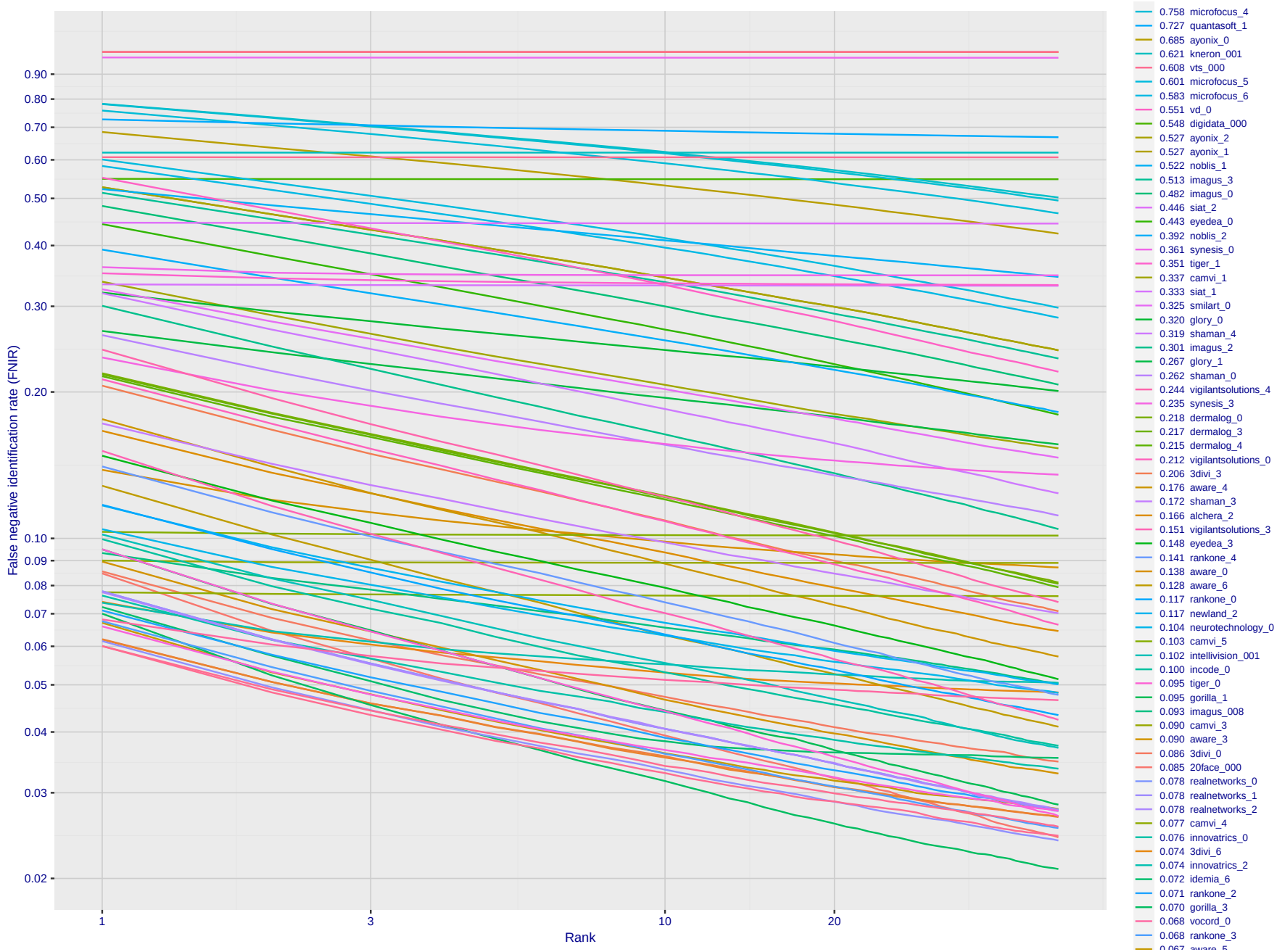

Figure 129: **[Webcam Dataset] Identification miss rates vs. rank**. *The results apply to cross-domain recognition in which webcams are searched against enrolled mugshots. The FNIR values are higher than those for mugshot-mugshot identification due to low image resolution, lighting and less constrained subject pose in webcam images - see Figure 6.*

2022/06/13	FNIR(N, R, T) =	False neg. identification rate	N = Num. enrolled subjects	T = Threshold	$T = 0 \rightarrow$ Investigation
18:09:57	FPIR(N, T) =	False pos. identification rate	R = Num. candidates examined		$T > 0 \rightarrow$ Identification

This publication is available free of charge from: https://doi.org/10.6028/NIST.IR.8271

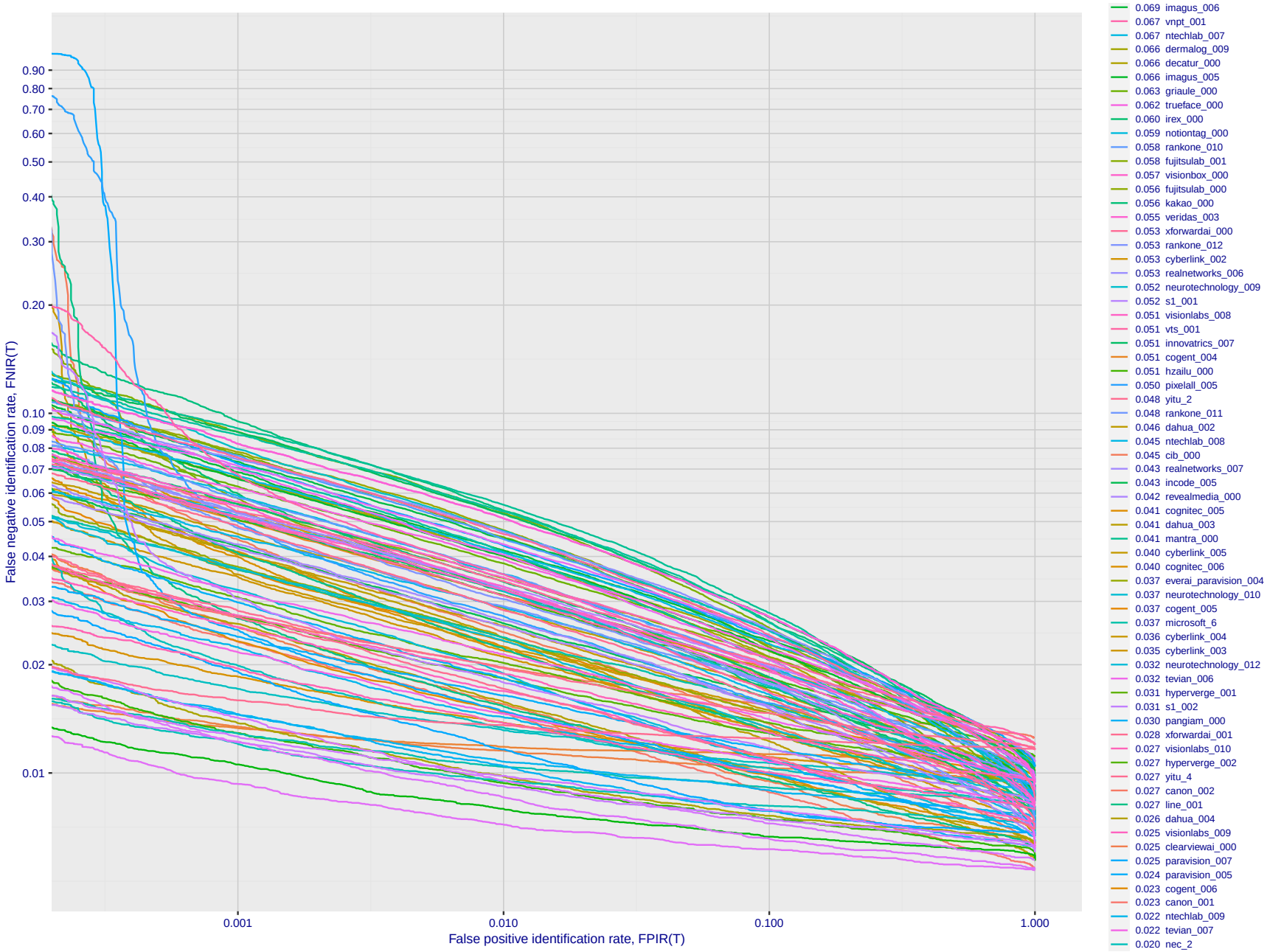

Figure 130: **[Webcam Dataset] Identification miss rates vs. false positive rates**. *The results apply to cross-domain recognition in which webcams are searched against enrolled mugshots. The FNIR values are higher than those for mugshot-mugshot identification due to low image resolution, lighting and less constrained subject pose in webcam images - see Figure 6.*

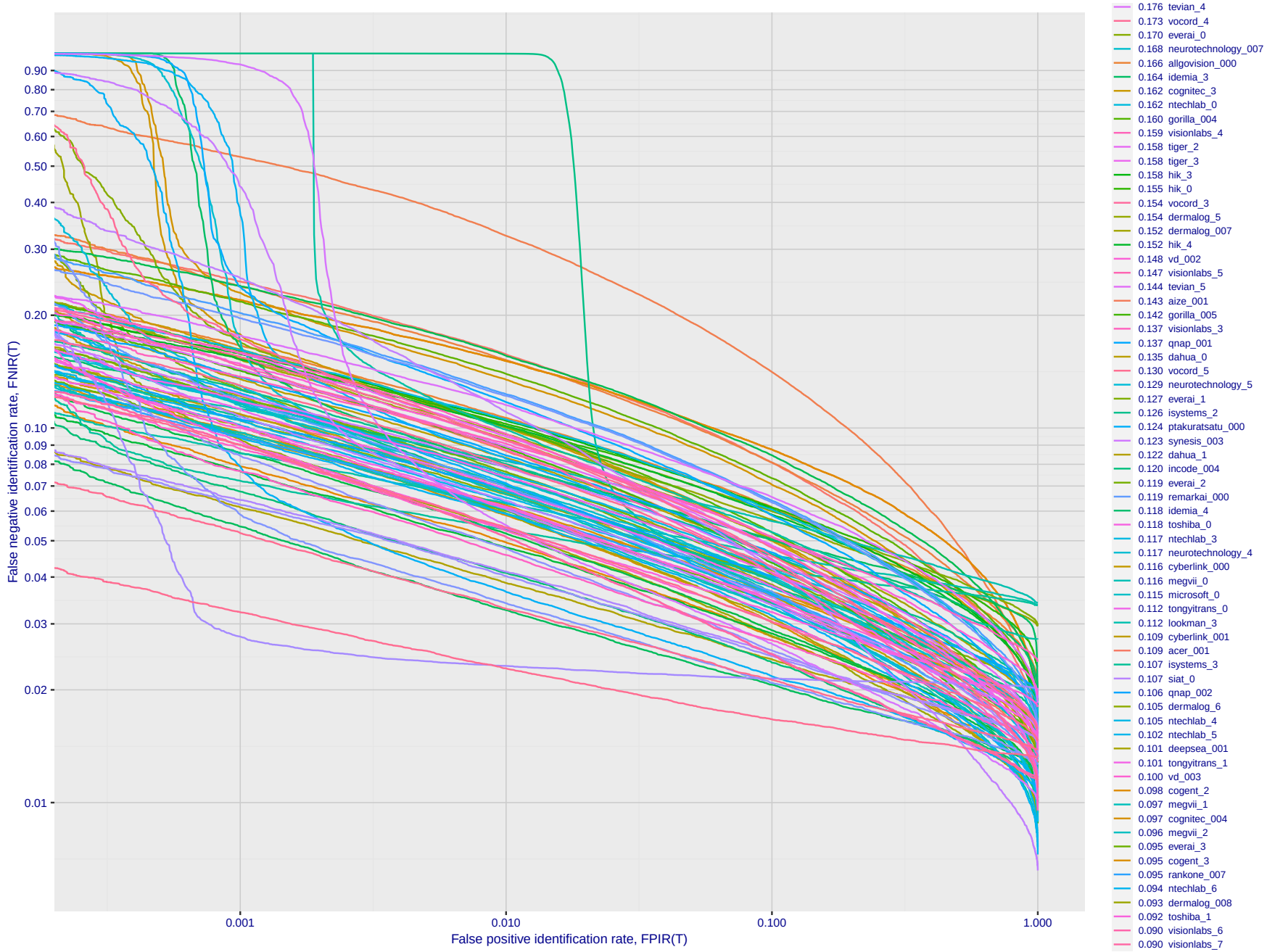

Figure 131: **[Webcam Dataset] Identification miss rates vs. false positive rates**. *The results apply to cross-domain recognition in which webcams are searched against enrolled mugshots. The FNIR values are higher than those for mugshot-mugshot identification due to low image resolution, lighting and less constrained subject pose in webcam images - see Figure 6.*

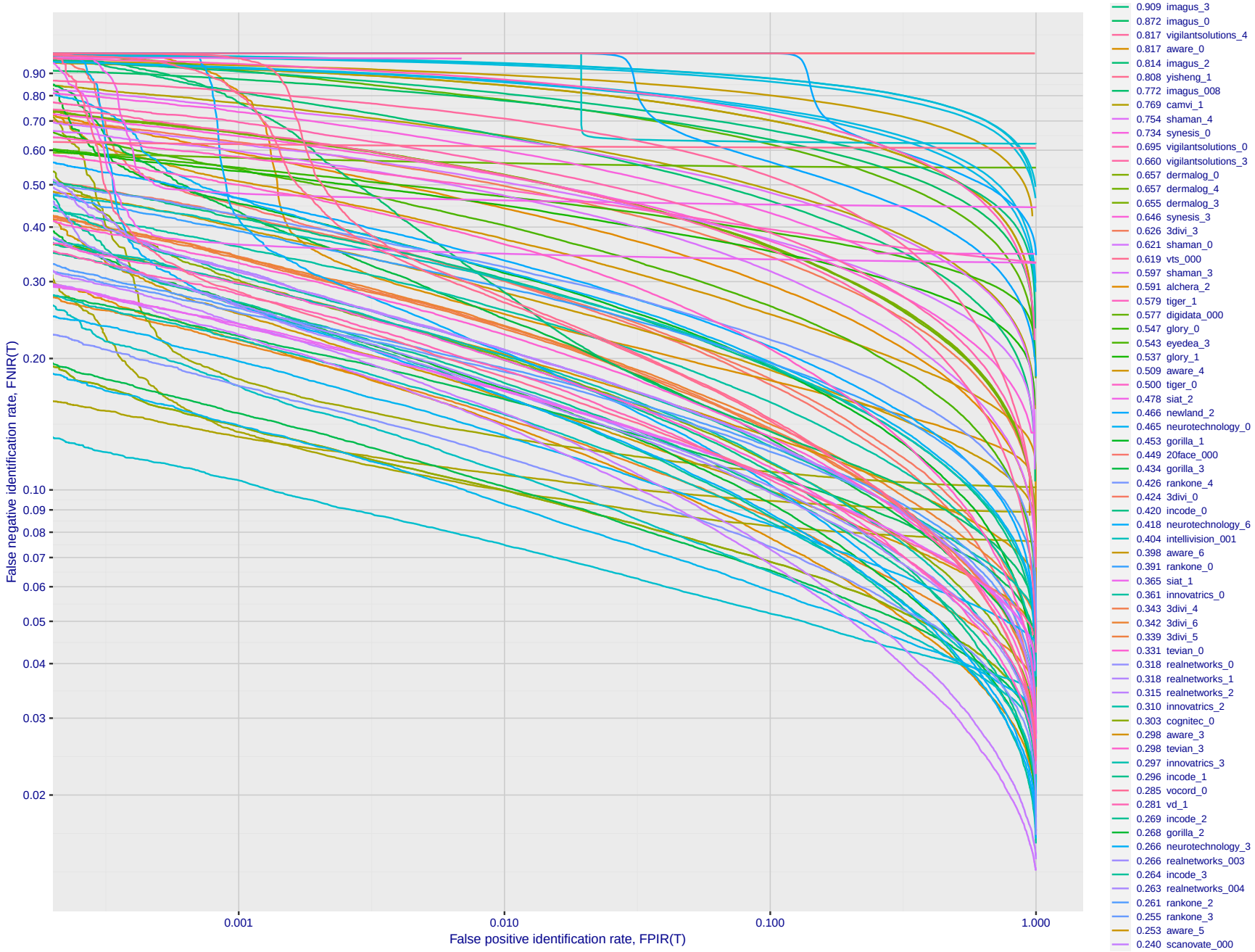

Figure 132: **[Webcam Dataset] Identification miss rates vs. false positive rates**. *The results apply to cross-domain recognition in which webcams are searched against enrolled mugshots. The FNIR values are higher than those for mugshot-mugshot identification due to low image resolution, lighting and less constrained subject pose in webcam images - see Figure 6.*

Appendix E Accuracy for profile-view to frontal recognition

Figures 133 - 135 gives accuracy results for searching 100 000 mated and 100 000 non-mated profile-view images against the same FRVT 2018 frontal enrollment dataset, N = 1 600 000, used in the main mugshot trials. This experiment corresponds to row-13 of Table 1. An example of profile-view image is given in Figure 7.

This publication is available free of charge from: https://doi.org/10.6028/NIST.IR.8271

This publication is available free of charge from: https://doi.org/10.6028/NIST.IR.8271

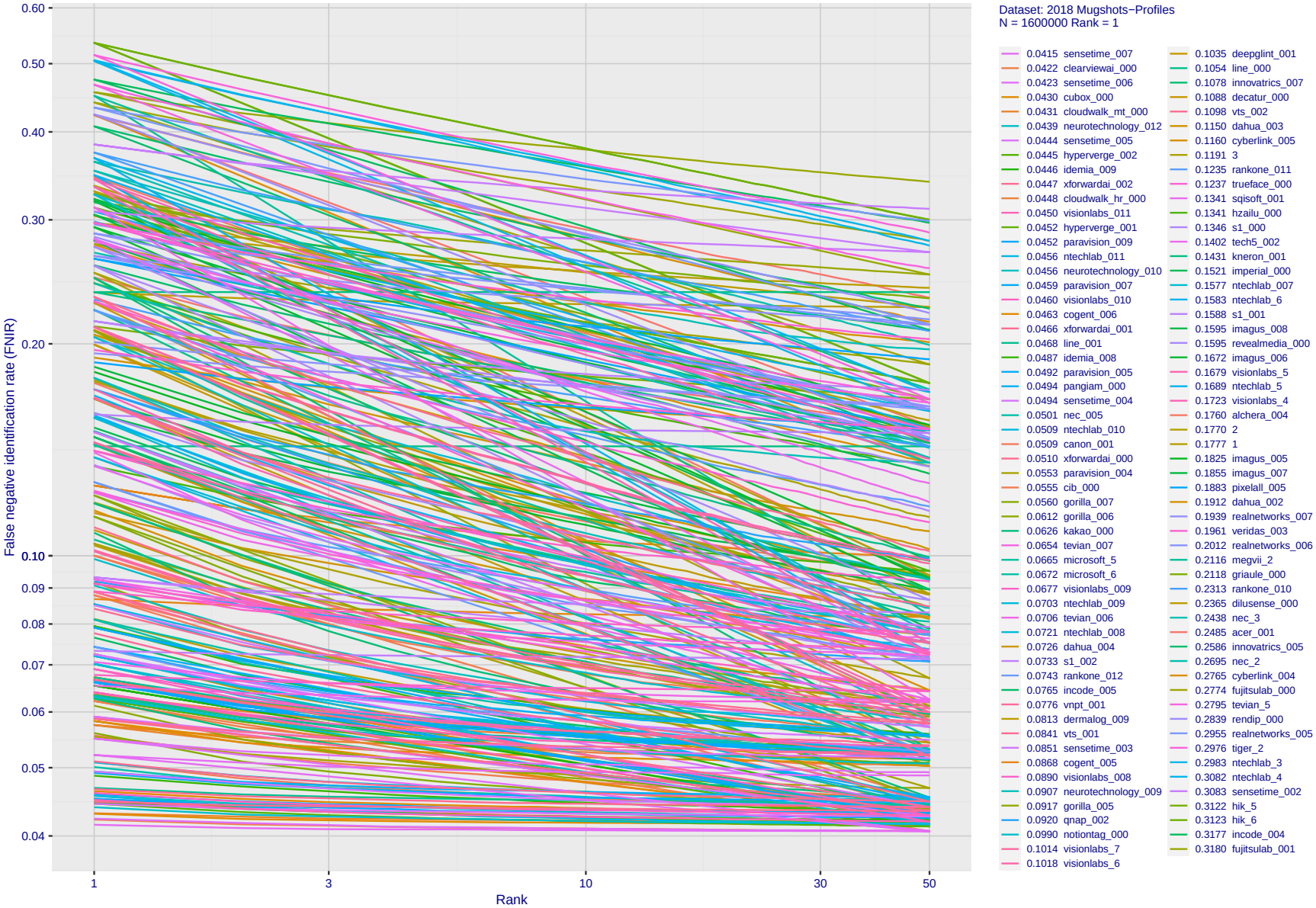

Figure 133: **[Mugshot and profile-view dataset] Rank-based accuracy**. *For some of the more accurate Phase 3 algorithms the figure plots error tradeoff characteristics for frontal and profile-view searches into an enrolled set of N = 1 600 000 frontal images. Note that some algorithms fail on profile-view images with FNIR → 1 - this evaluation did not ask developers to provide profile-view capability. Some algorithms, on the other hand, give FNIR approaching that for frontal-view searches using c. 2010 algorithms. The best result is that 91% of profile-view searches yield the correct mate at rank 1, and better than 94% in the top-50 candidates.*

This publication is available free of charge from: https://doi.org/10.6028/NIST.IR.8271

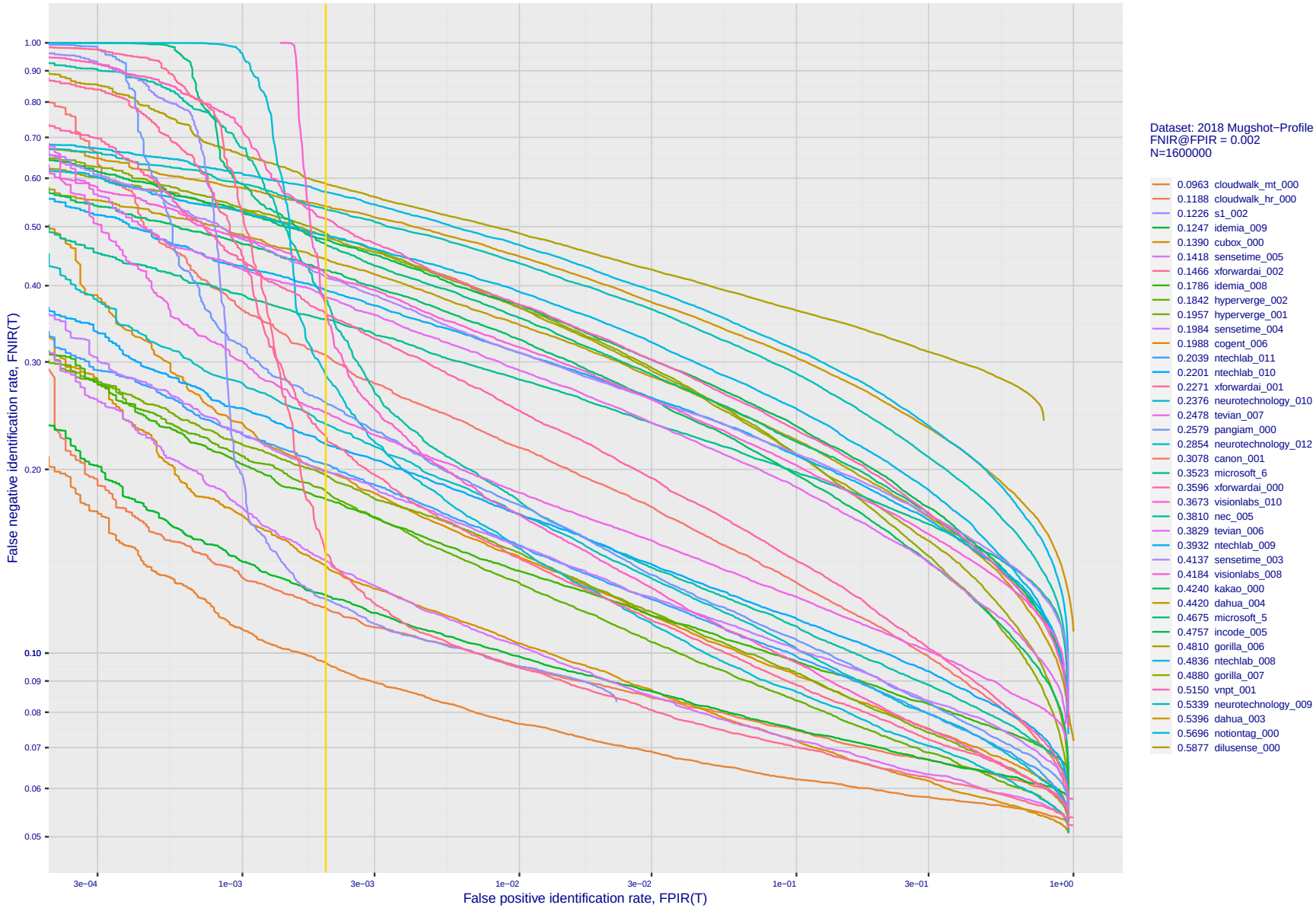

Figure 134: **[Mugshot and profile-view dataset] Threshold-based accuracy**. *For some of the more accurate Phase 3 algorithms the figure plots error tradeoff characteristics for frontal and profile-view searches into an enrolled set of N = 1 600 000 frontal images. Note that some algorithms fail on profile-view images with FNIR → 1 - this evaluation did not ask developers to provide profile-view capability. Some algorithms, on the other hand, give FNIR approaching that for frontal-view searches using c. 2010 algorithms.*

This publication is available free of charge from: https://doi.org/10.6028/NIST.IR.8271

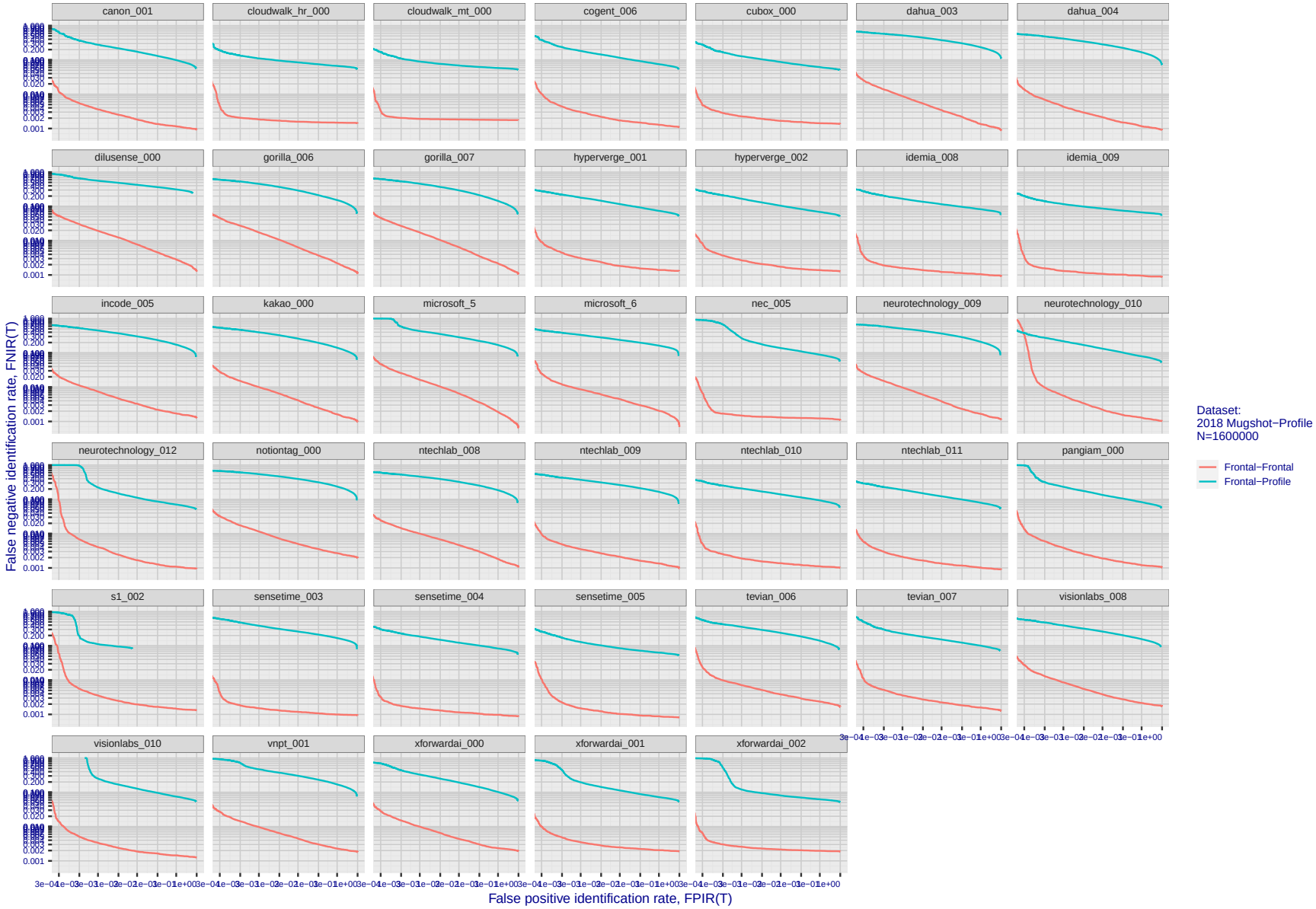

Figure 135: **[Mugshot and profile-view dataset] Speed-accuracy tradeoff**. *For some of the more accurate Phase 3 algorithms the figure plots error tradeoff characteristics for frontal and profile-view searches into an enrolled set of N = 1 600 000 frontal images. Some algorithms fail on profile-view images with FNIR → 1 - this evaluation did not ask developers to provide profile-view capability. Some algorithms, on the other hand, give FNIR approaching that for frontal-view searches using c. 2010 algorithms. Blue lines connect points of equal threshold from which it is evident that some algorithms would give markedly higher false positive outcomes if profile-view images were searched in a system configured for frontal searches. This would be a vulnerability in an access control system.*

Appendix F Search duration

As in and prior tests, this section documents search speeds spanning three orders of magnitude. In applications where search volumes are high enough, this will have implications for hardware requirements especially for large N or when search duration is appreciably larger than the time it takes to prepare a template from the search image(s). Further, given very large (and growing) operational databases, the scalability of algorithms is important. It has been reported previously [8] that search duration can scale sublinearly with enrolled population size N. Further there has been considerable recent research on indexing, exact [13] and approximate nearest neighbor search [1,13] and fast-search [14,16].

Figure 136 charts the search duration measurements presented earlier in Tables 2 - 4.

- ▷ Most algorithms scale linearly. For those in that category, there is a wide range in speed with search durations ranging from 82 milliseconds for a 12 million gallery (for NEC-3) to more than 40 seconds (for Yitu-3, Toshiba-2) and even higher for less accurate algorithms.
- ▷ Some developers (Camvi, Dermalog, EverAI, Innovatrics, and Visionlabs) provide algorithms whose template search durations grow approimately logarithmically i.e. $T(N)\tilde{a}\log N$ with the constant a varying between implementations. In the figure this model is fit using the point $T(1) = 0$, and $T(640\,000)$. This very sublinear behaviour affords extremely fast search times in very large galleries. One caveat for the sublinear algorithms is that their fast-search data structures can require considerable computation time - on the order of hours - for N in the millions, and this scales mildy super-linearly, i.e. $O(N^b), b > 1$. There are exceptions: the Camvi algorithms take minutes; and Innvovatrics' scale sublinearly.

This publication is available free of charge from: https://doi.org/10.6028/NIST.IR.8271

2022/06/13	FNIR(N, R, T) =	False neg. identification rate	N = Num. enrolled subjects	T = Threshold	$T = 0 \rightarrow$ Investigation
18:09:57	FPIR(N, T) =	False pos. identification rate	R = Num. candidates examined		$T > 0 \rightarrow$ Identification

This publication is available free of charge from: https://doi.org/10.6028/NIST.IR.8271

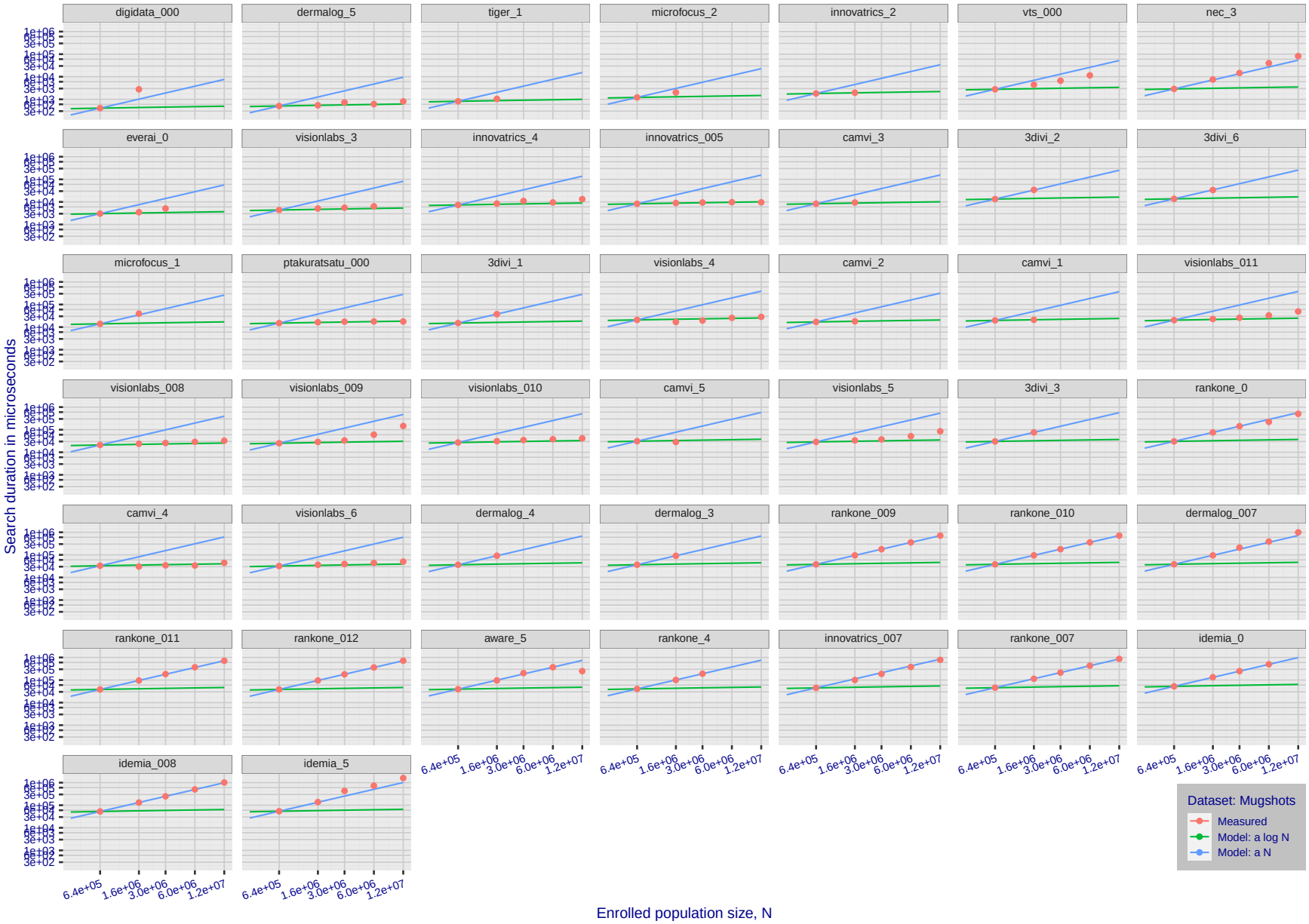

Figure 136: **[Mugshot Dataset] Search duration vs. enrolled population size**. *In red are the actual point durations measured on a single c. 2016 core. The blue shows linear growth from $N = 640\,000$. The green line shows logathmic growth from that point to $N = 1\,600\,000$. Note the sublinear growth from algorithms from Camvi, Dermalog, EverAI, Innovatrics, and Visionlabs. The tiger_1 algorithm is also sublinear, but inaccurate and inoperable at $N \geq 3000000$. This capability sometimes comes at the additional expense of converting a linear gallery data structure into whatever fast-search data structure is used. Note that search times are sometimes dominated by the template generation times shown in Table 24.*

This publication is available free of charge from: https://doi.org/10.6028/NIST.IR.8271

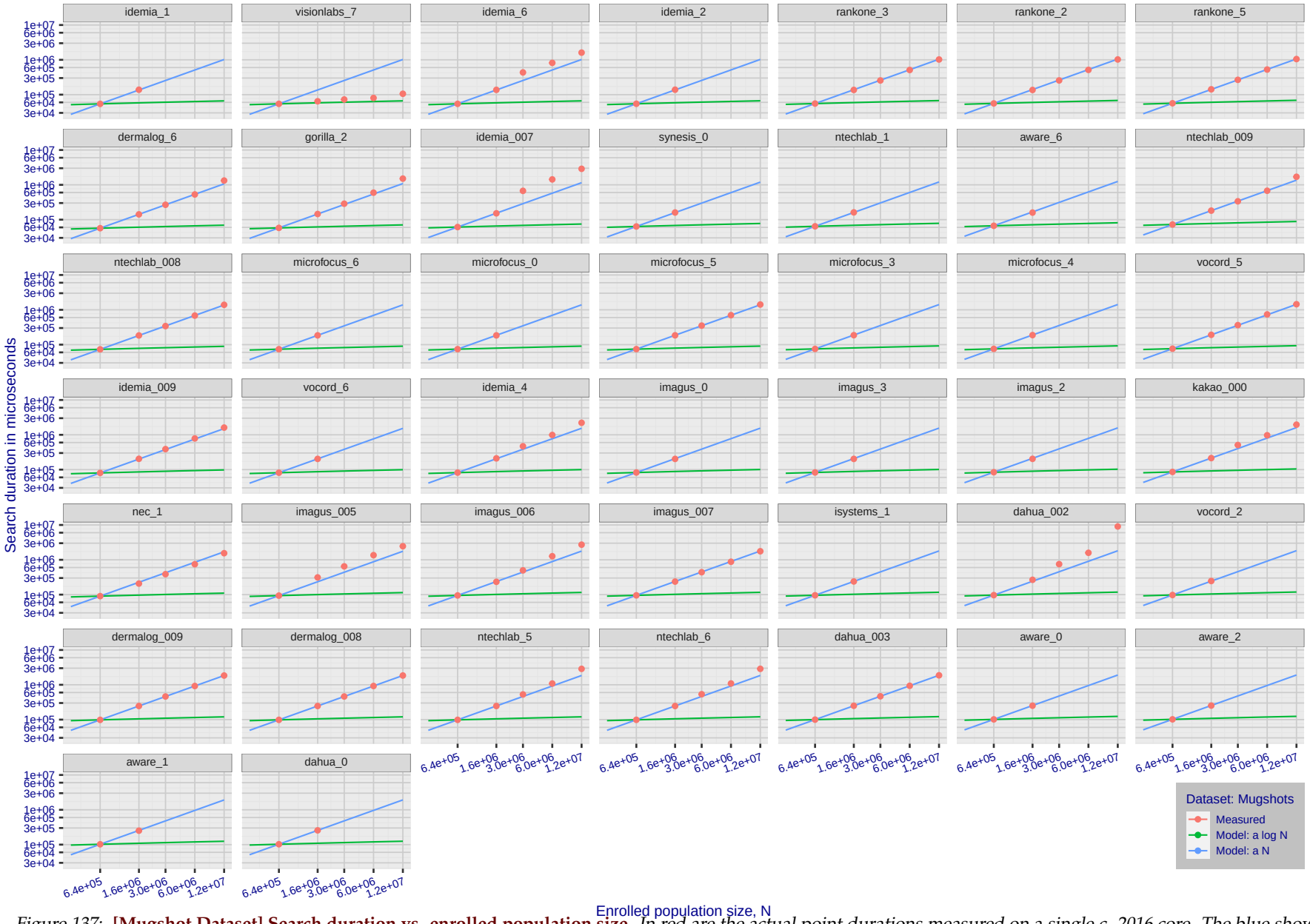

Figure 137: **[Mugshot Dataset] Search duration vs. enrolled population size**. *In red are the actual point durations measured on a single c. 2016 core. The blue shows linear growth from $N = 640\,000$. The green line shows logathmic growth from that point to $N = 1\,600\,000$. Note the sublinear growth from algorithms from Camvi, Dermalog, EverAI, Innovatrics, and Visionlabs. The tiger_1 algorithm is also sublinear, but inaccurate and inoperable at $N \geq 3000000$. This capability sometimes comes at the additional expense of converting a linear gallery data structure into whatever fast-search data structure is used. Note that search times are sometimes dominated by the template generation times shown in Table 24.*

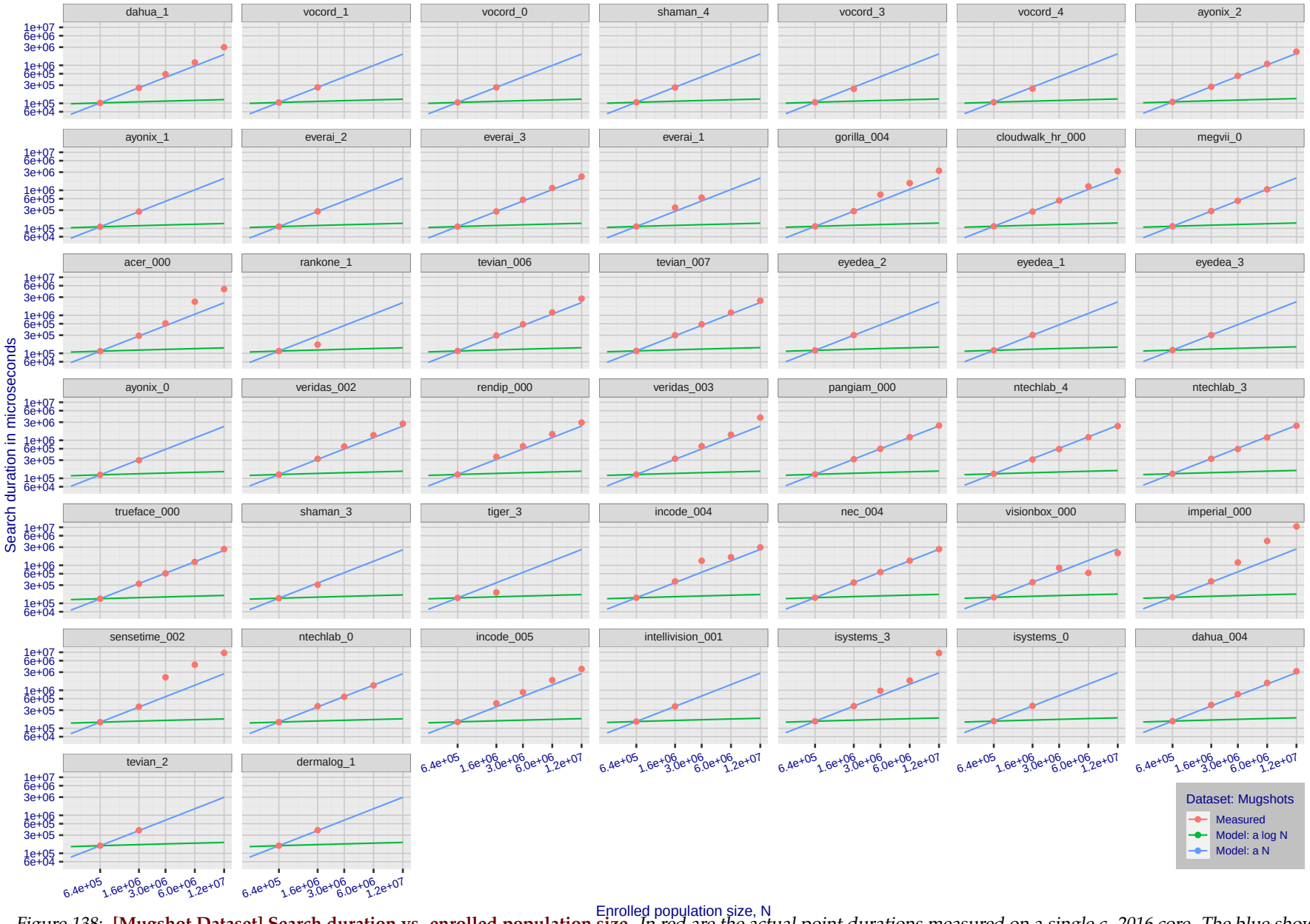

Figure 138: **[Mugshot Dataset] Search duration vs. enrolled population size**. *In red are the actual point durations measured on a single c. 2016 core. The blue shows linear growth from $N = 640\,000$. The green line shows logathmic growth from that point to $N = 1\,600\,000$. Note the sublinear growth from algorithms from Camvi, Dermalog, EverAI, Innovatrics, and Visionlabs. The tiger_1 algorithm is also sublinear, but inaccurate and inoperable at $N \geq 3000000$. This capability sometimes comes at the additional expense of converting a linear gallery data structure into whatever fast-search data structure is used. Note that search times are sometimes dominated by the template generation times shown in Table 24.*

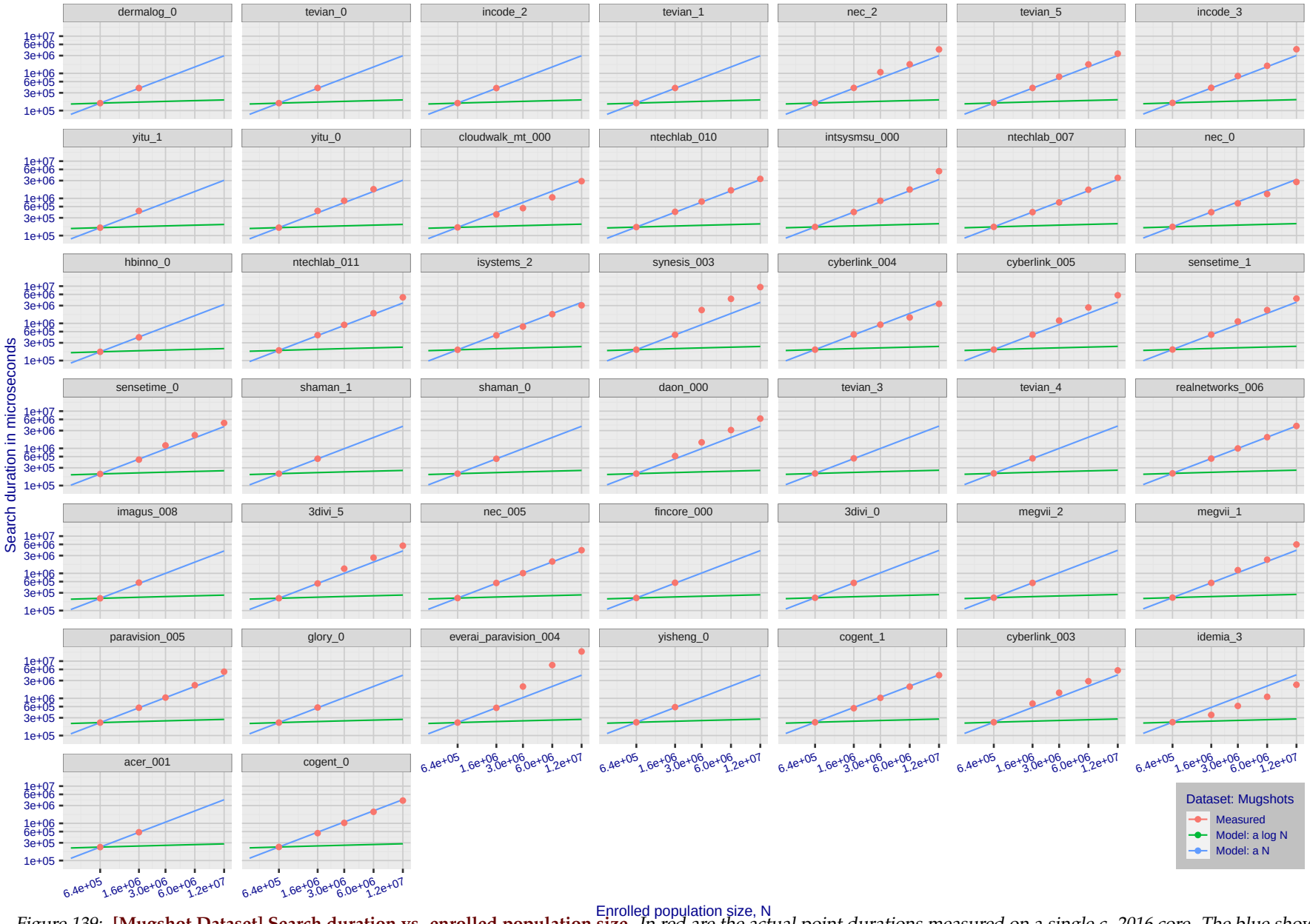

Figure 139: **[Mugshot Dataset] Search duration vs. enrolled population size**. *In red are the actual point durations measured on a single c. 2016 core. The blue shows linear growth from $N = 640\,000$. The green line shows logathmic growth from that point to $N = 1\,600\,000$. Note the sublinear growth from algorithms from Camvi, Dermalog, EverAI, Innovatrics, and Visionlabs. The tiger_1 algorithm is also sublinear, but inaccurate and inoperable at $N \geq 3000000$. This capability sometimes comes at the additional expense of converting a linear gallery data structure into whatever fast-search data structure is used. Note that search times are sometimes dominated by the template generation times shown in Table 24.*

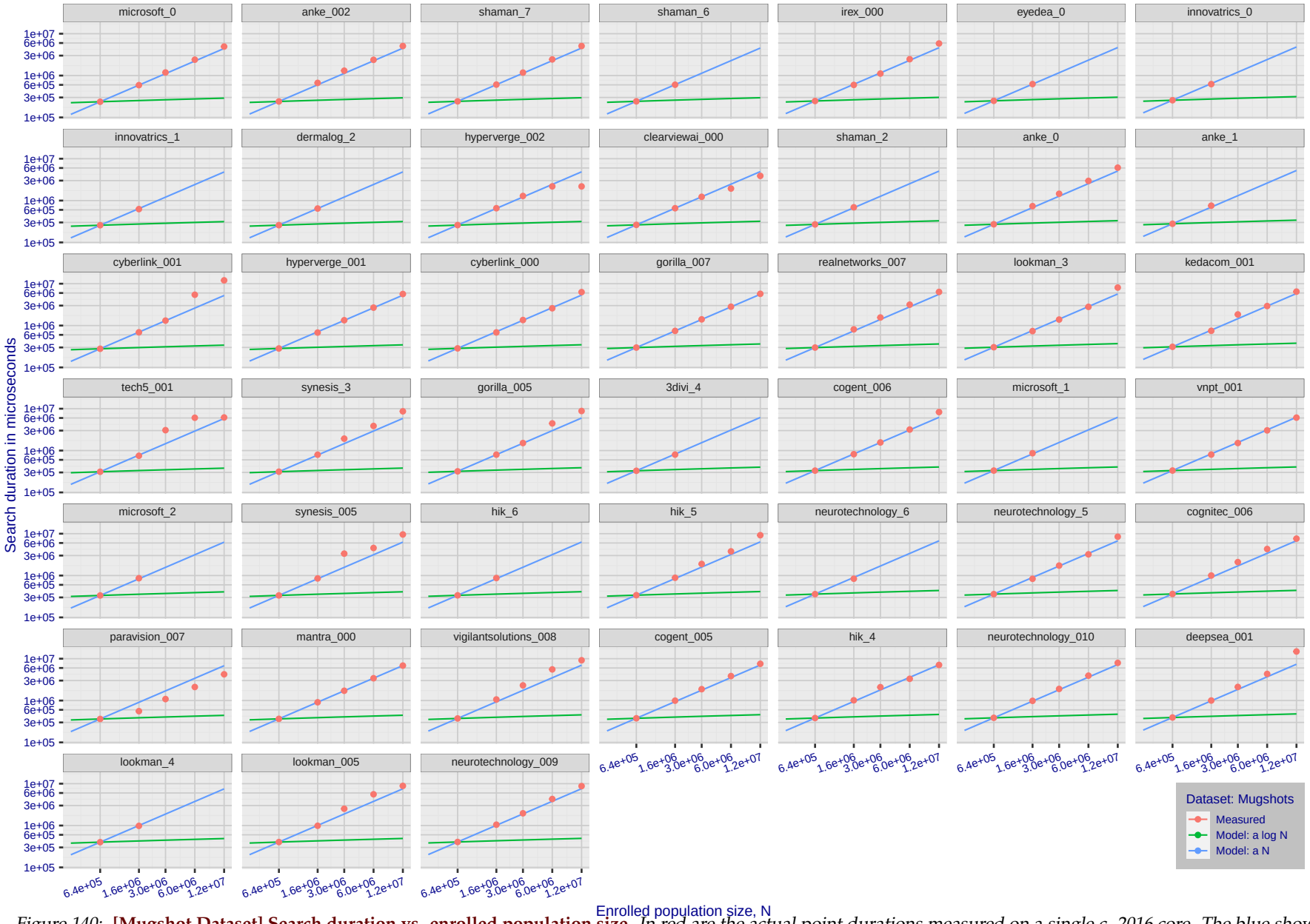

Figure 140: **[Mugshot Dataset] Search duration vs. enrolled population size**. *In red are the actual point durations measured on a single c. 2016 core. The blue shows linear growth from $N = 640\,000$. The green line shows logathmic growth from that point to $N = 1\,600\,000$. Note the sublinear growth from algorithms from Camvi, Dermalog, EverAI, Innovatrics, and Visionlabs. The tiger_1 algorithm is also sublinear, but inaccurate and inoperable at $N \geq 3000000$. This capability sometimes comes at the additional expense of converting a linear gallery data structure into whatever fast-search data structure is used. Note that search times are sometimes dominated by the template generation times shown in Table 24.*

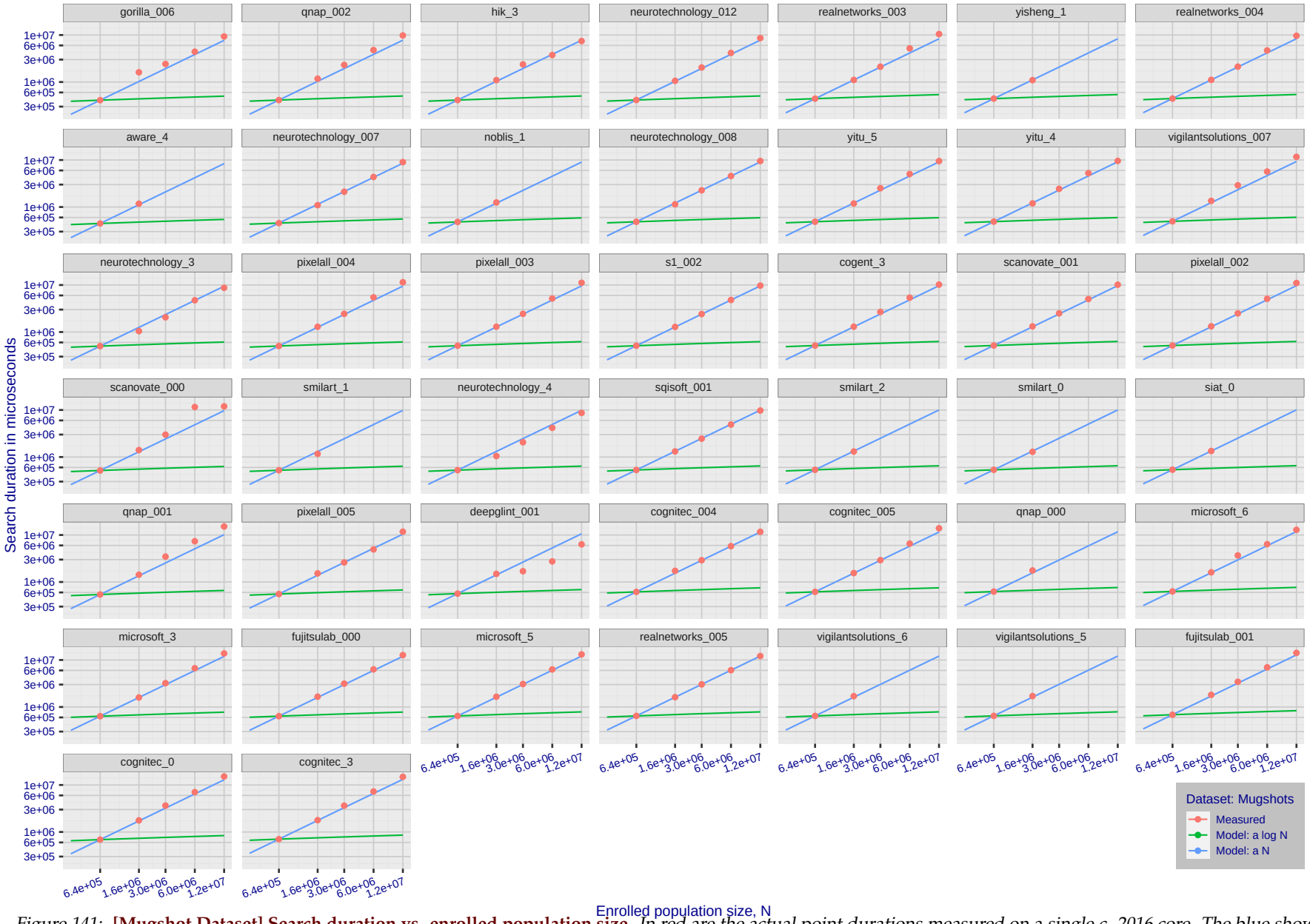

Figure 141: **[Mugshot Dataset] Search duration vs. enrolled population size**. *In red are the actual point durations measured on a single c. 2016 core. The blue shows linear growth from $N = 640\,000$. The green line shows logathmic growth from that point to $N = 1\,600\,000$. Note the sublinear growth from algorithms from Camvi, Dermalog, EverAI, Innovatrics, and Visionlabs. The tiger_1 algorithm is also sublinear, but inaccurate and inoperable at $N \geq 3000000$. This capability sometimes comes at the additional expense of converting a linear gallery data structure into whatever fast-search data structure is used. Note that search times are sometimes dominated by the template generation times shown in Table 24.*

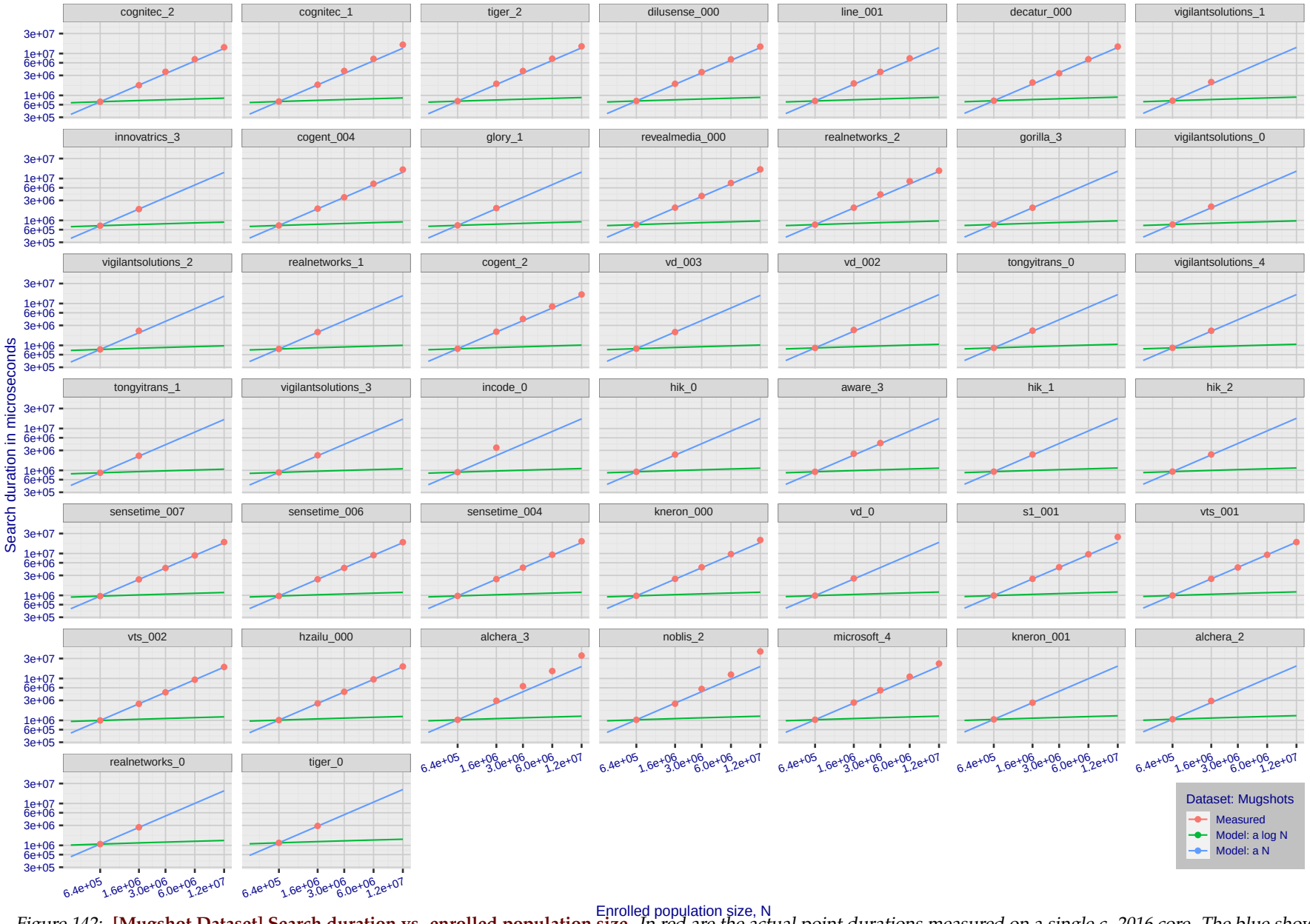

Figure 142: **[Mugshot Dataset] Search duration vs. enrolled population size**. *In red are the actual point durations measured on a single c. 2016 core. The blue shows linear growth from $N = 640\,000$. The green line shows logathmic growth from that point to $N = 1\,600\,000$. Note the sublinear growth from algorithms from Camvi, Dermalog, EverAI, Innovatrics, and Visionlabs. The tiger_1 algorithm is also sublinear, but inaccurate and inoperable at $N \geq 3000000$. This capability sometimes comes at the additional expense of converting a linear gallery data structure into whatever fast-search data structure is used. Note that search times are sometimes dominated by the template generation times shown in Table 24.*

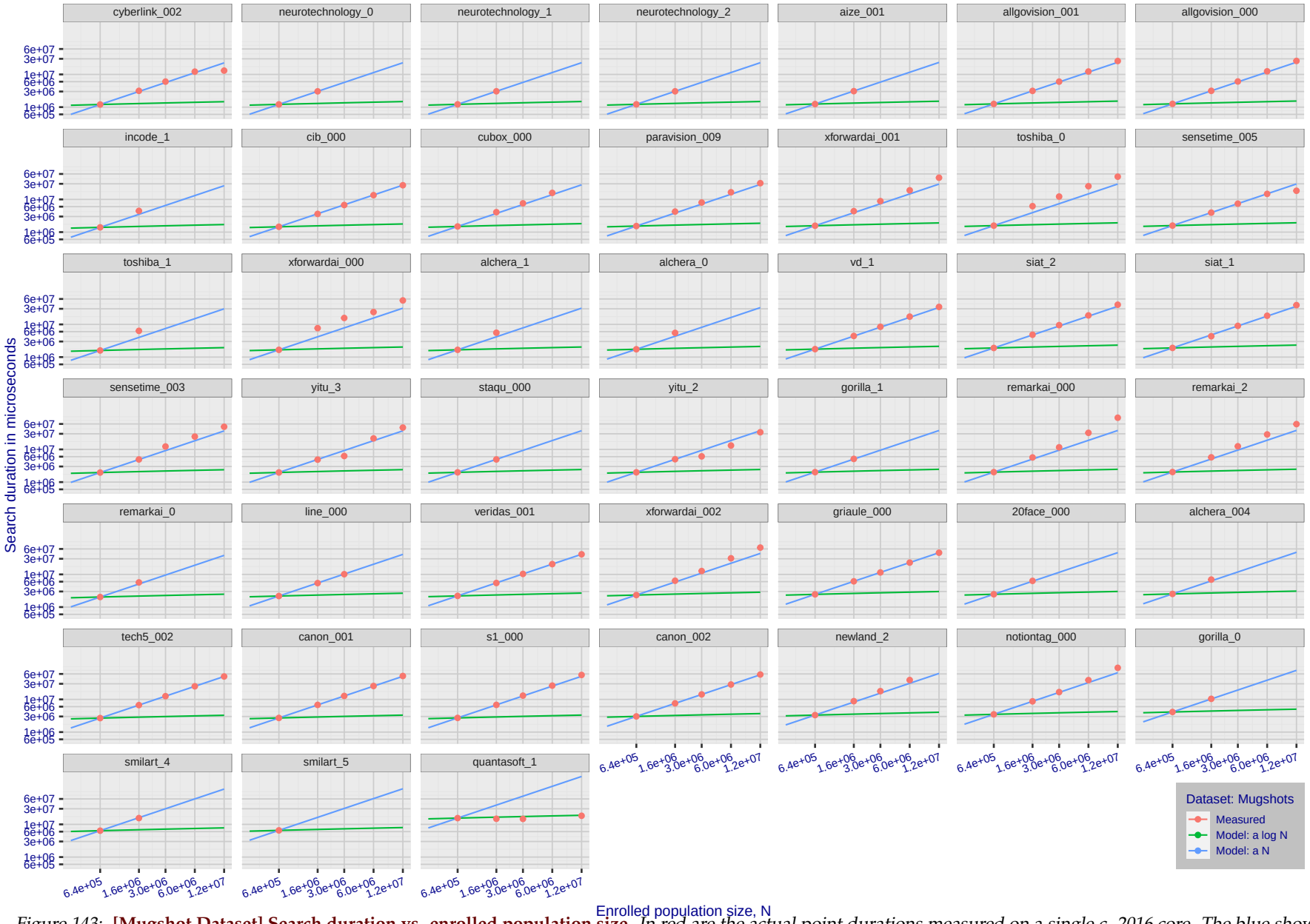

Figure 143: **[Mugshot Dataset] Search duration vs. enrolled population size**. *In red are the actual point durations measured on a single c. 2016 core. The blue shows linear growth from $N = 640\,000$. The green line shows logathmic growth from that point to $N = 1\,600\,000$. Note the sublinear growth from algorithms from Camvi, Dermalog, EverAI, Innovatrics, and Visionlabs. The tiger_1 algorithm is also sublinear, but inaccurate and inoperable at $N \geq 3000000$. This capability sometimes comes at the additional expense of converting a linear gallery data structure into whatever fast-search data structure is used. Note that search times are sometimes dominated by the template generation times shown in Table 24.*

Appendix G Gallery Insertion Timing

This publication is available free of charge from: https://doi.org/10.6028/NIST.IR.8271

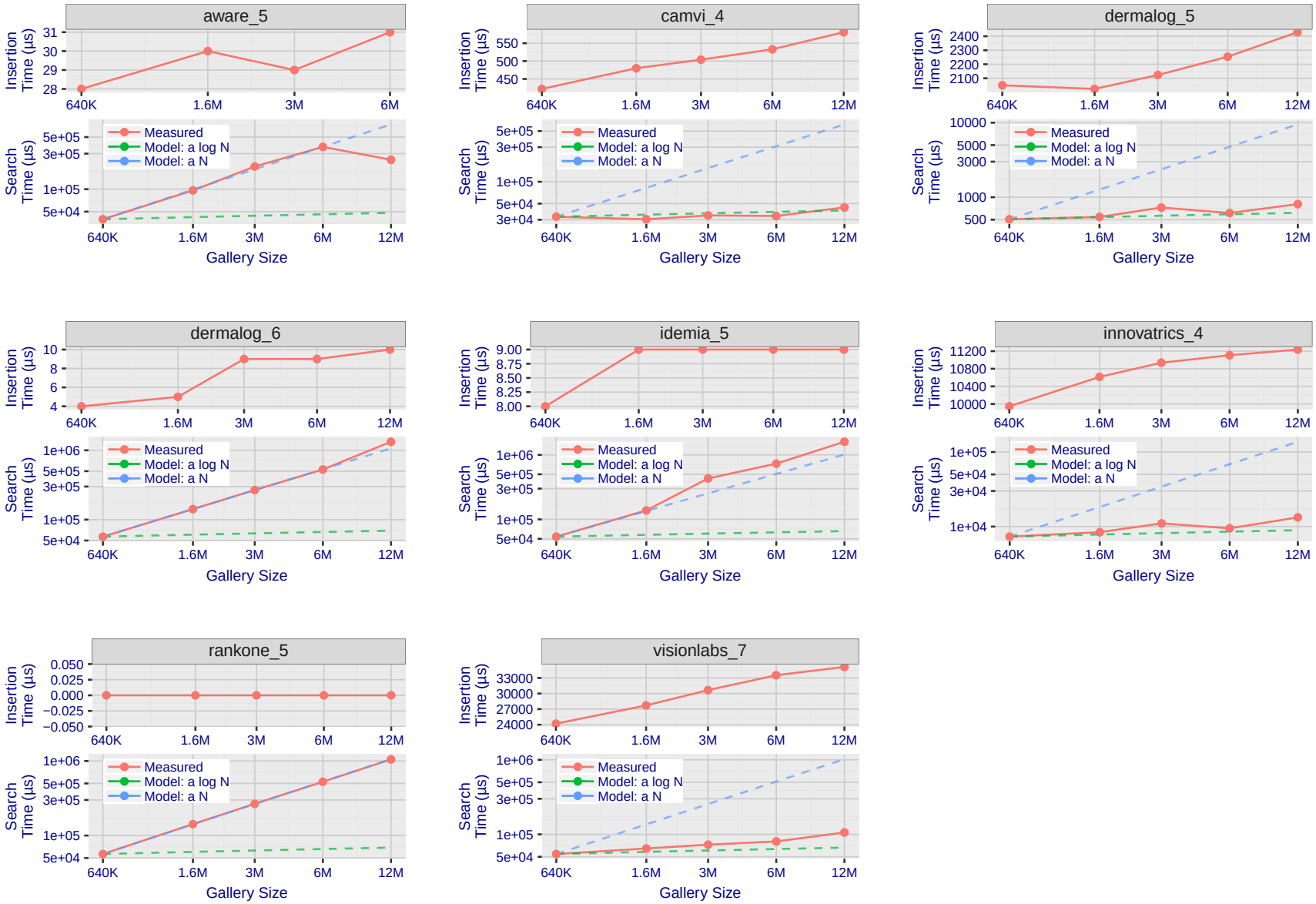

Figure 144: **[Mugshot Dataset] Gallery insertion duration vs. enrolled population size**. *This chart plots the time it takes to insert a single template into a finalized gallery, illustrated over increasing gallery sizes. For reference, search times on finalized galleries of corresponding sizes are plotted right underneath. Gallery insertion time plots were generated on algorithms that 1) successfully implemented gallery insertion with no errors and 2) that were run on galleries with N up to* 12 000 000. *Generally, only the more accurate algorithms were run on galleries with N up to* 12 000 000.

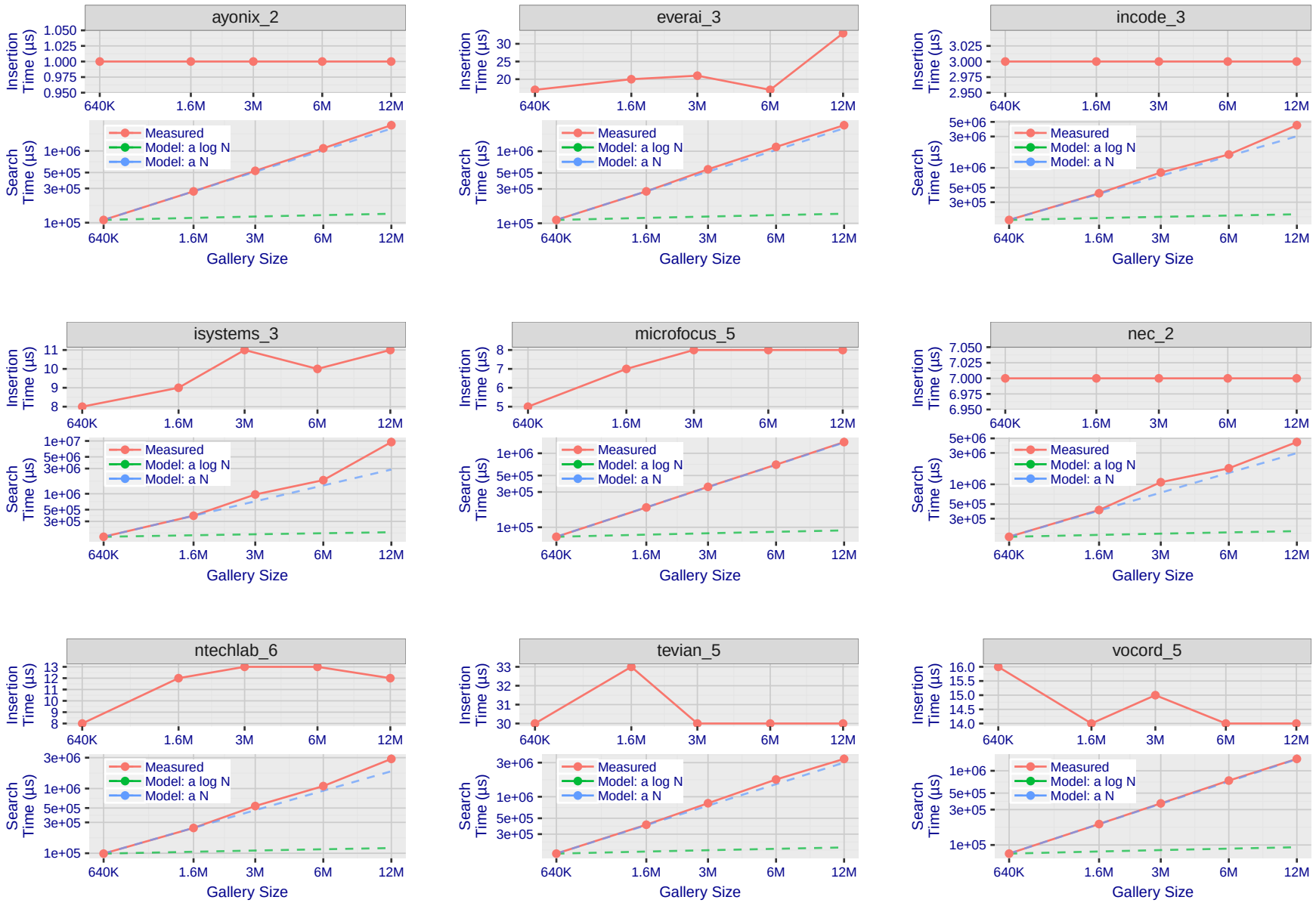

Figure 145: **[Mugshot Dataset] Gallery insertion duration vs. enrolled population size**. *This chart plots the time it takes to insert a single template into a finalized gallery, illustrated over increasing gallery sizes. For reference, search times on finalized galleries of corresponding sizes are plotted right underneath. Gallery insertion time plots were generated on algorithms that 1) successfully implemented gallery insertion with no errors and 2) that were run on galleries with N up to* 12 000 000. *Generally, only the more accurate algorithms were run on galleries with N up to* 12 000 000.

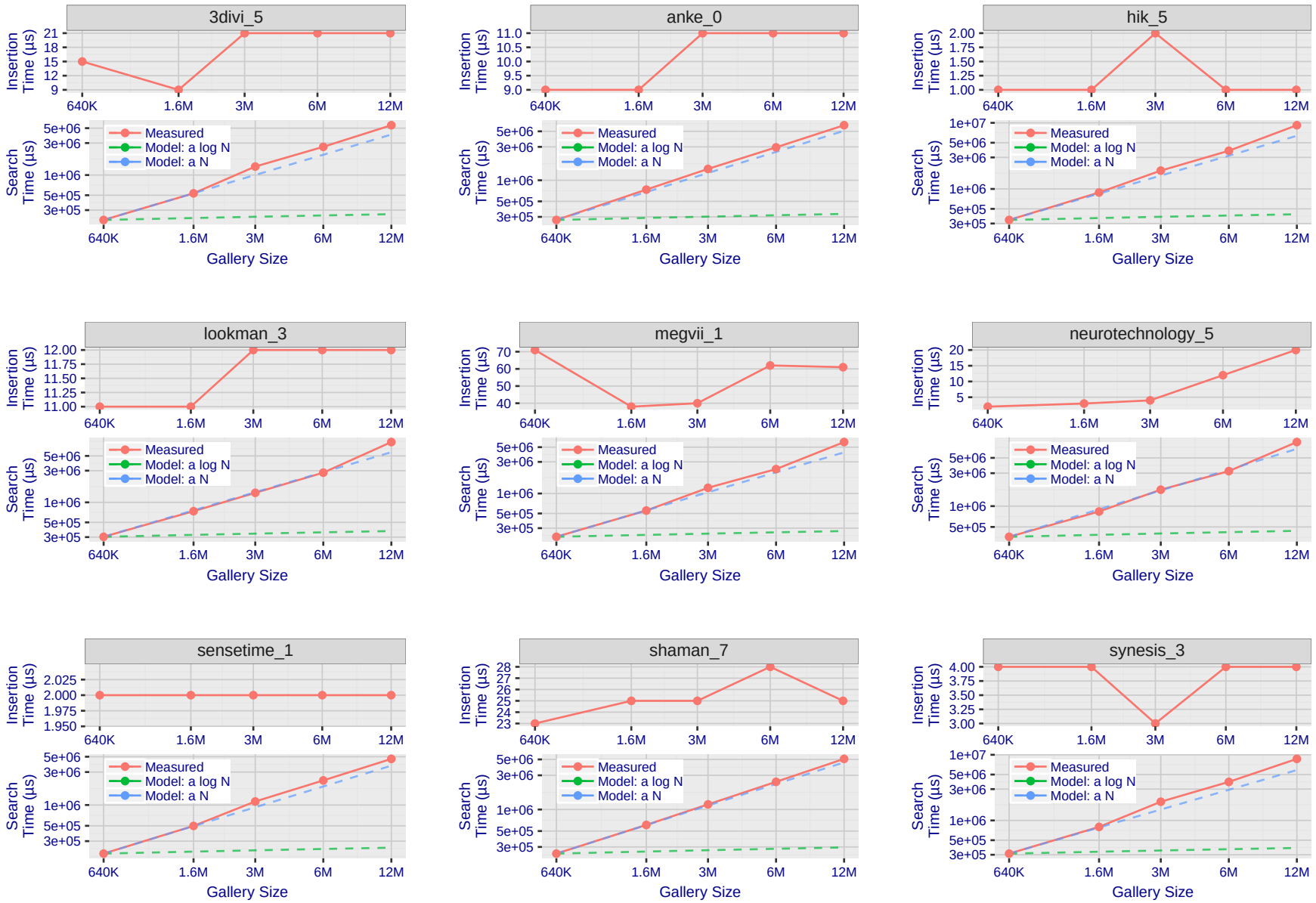

Figure 146: **[Mugshot Dataset] Gallery insertion duration vs. enrolled population size**. *This chart plots the time it takes to insert a single template into a finalized gallery, illustrated over increasing gallery sizes. For reference, search times on finalized galleries of corresponding sizes are plotted right underneath. Gallery insertion time plots were generated on algorithms that 1) successfully implemented gallery insertion with no errors and 2) that were run on galleries with N up to* 12 000 000. *Generally, only the more accurate algorithms were run on galleries with N up to* 12 000 000.

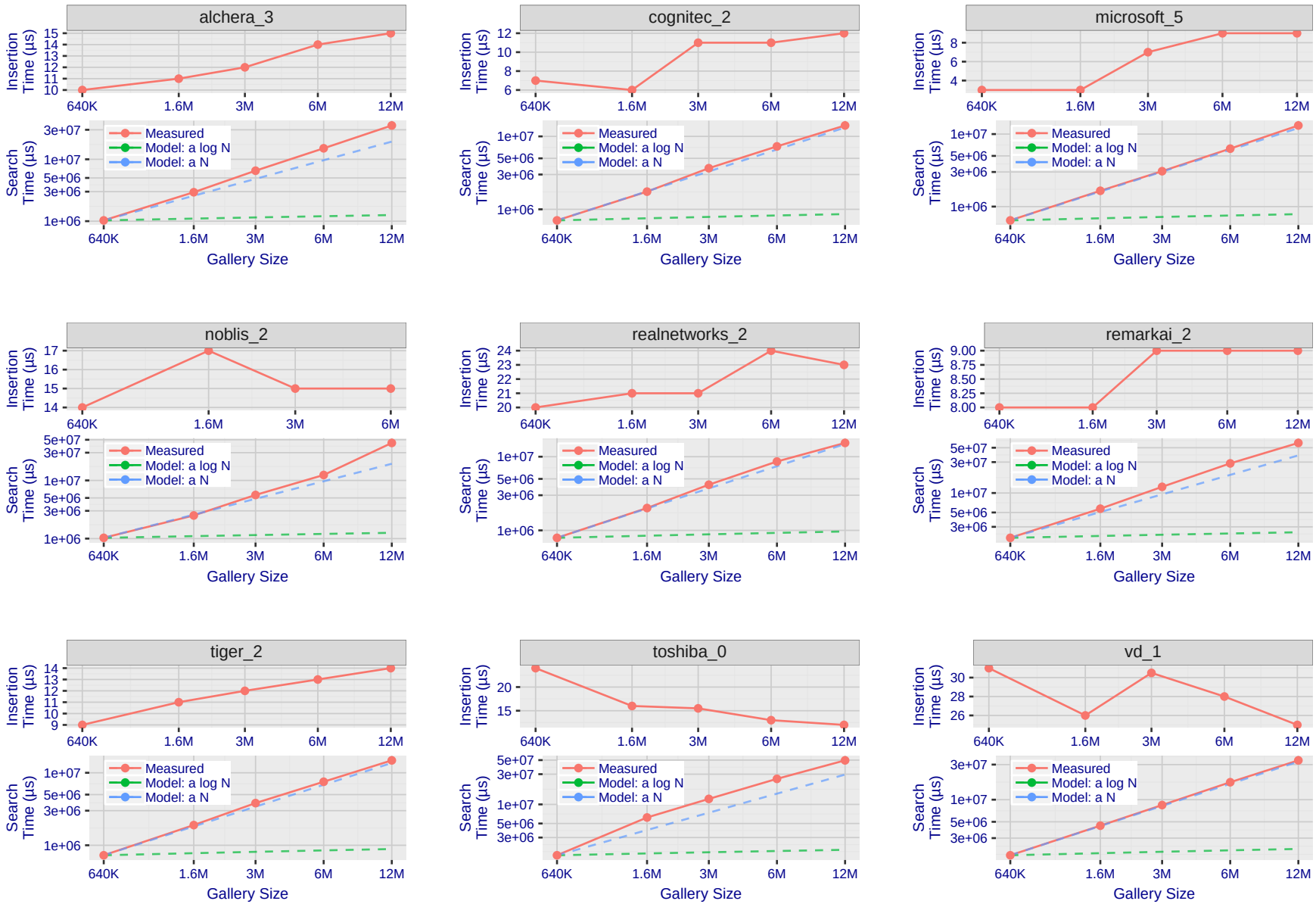

Figure 147: **[Mugshot Dataset] Gallery insertion duration vs. enrolled population size**. *This chart plots the time it takes to insert a single template into a finalized gallery, illustrated over increasing gallery sizes. For reference, search times on finalized galleries of corresponding sizes are plotted right underneath. Gallery insertion time plots were generated on algorithms that 1) successfully implemented gallery insertion with no errors and 2) that were run on galleries with N up to* 12 000 000. *Generally, only the more accurate algorithms were run on galleries with N up to* 12 000 000.

References

[1] Artem Babenko and Victor Lempitsky. Efficient indexing of billion-scale datasets of deep descriptors. In *The IEEE Conference on Computer Vision and Pattern Recognition (CVPR)*, June 2016.

[2] L. Best-Rowden and A. K. Jain. Longitudinal study of automatic face recognition. *IEEE Transactions on Pattern Analysis and Machine Intelligence*, 40(1):148–162, Jan 2018.

[3] Blumstein, Cohen, Roth, and Visher, editors. *Random parameter stochastic models of criminal careers*. National Academy of Sciences Press, 1986.

[4] Thomas P. Bonczar and Lauren E. Glaze. Probation and parole in the united statesm 2007, statistical tables. Technical report, Bureau of Justice Statistics, December 2008.

[5] White D., Kemp R. I., Jenkins R., Matheson M, and Burton A. M. Passport officers' errors in face matching. *PLoS ONE*, 9(8), 2014. e103510. doi:10.1371/journal. pone.0103510.

[6] P. Grother, G. W. Quinn, and P. J. Phillips. Evaluation of 2d still-image face recognition algorithms. NIST Interagency Report 7709, National Institute of Standards and Technology, 8 2010. http://face.nist.gov/mbe as MBE2010 FRVT2010.

[7] P. J. Grother, R. J. Micheals, and P. J. Phillips. Performance metrics for the frvt 2002 evaluation. In *Proceedings of Audio and Video Based Person Authentication Conference (AVBPA)*, June 2003.

[8] Patrick Grother and Mei Ngan. Interagency report 8009, performance of face identification algorithms. *Face Recognition Vendor Test (FRVT)*, May 2014.

[9] Patrick Grother, George Quinn, and Mei Ngan. Face in video evaluation (five) face recognition of non-cooperative subjects. Interagency Report 8173, National Institute of Standards and Technology, March 2017. https://doi.org/10.6028/NIST.IR.8173.

[10] Patrick Grother, George W. Quinn, and Mei Ngan. Face recognition vendor test - still face image and video concept, evaluation plan and api. Technical report, National Institute of Standards and Technology, 7 2013. http://biometrics.nist.gov/cs_links/face/frvt/frvt2012/NIST_FRVT2012_api_Aug15.pdf.

[11] K. He, X. Zhang, S. Ren, and J. Sun. Deep residual learning for image recognition. In *2016 IEEE Conference on Computer Vision and Pattern Recognition (CVPR)*, pages 770–778, June 2016.

[12] Gary B. Huang, Manu Ramesh, Tamara Berg, and Erik Learned-Miller. Labeled faces in the wild: A database for studying face recognition in unconstrained environments. Technical Report 07-49, University of Massachusetts, Amherst, October 2007.

[13] Masato Ishii, Hitoshi Imaoka, and Atsushi Sato. Fast k-nearest neighbor search for face identification using bounds of residual score. In *2017 12th IEEE International Conference on Automatic Face & Gesture Recognition (FG 2017)*, pages 194–199, Los Alamitos, CA, USA, May 2017. IEEE Computer Society.

[14] Jeff Johnson, Matthijs Douze, and Hervé Jégou. Billion-scale similarity search with gpus. *CoRR*, abs/1702.08734, 2017.

This publication is available free of charge from: https://doi.org/10.6028/NIST.IR.8271

[15] Ira Kemelmacher-Shlizerman, Steven M. Seitz, Daniel Miller, and Evan Brossard. The megaface benchmark: 1 million faces for recognition at scale. *CoRR*, abs/1512.00596, 2015.

[16] Yury A. Malkov and D. A. Yashunin. Efficient and robust approximate nearest neighbor search using hierarchical navigable small world graphs. *CoRR*, abs/1603.09320, 2016.

[17] Joyce A. Martin, Brady E. Hamilton, Michelle J.K. Osterman, Anne K. Driscoll, , and Patrick Drake. National vital statistics reports. Technical Report 8, Centers for Disease Control and Prevention, National Center for Health Statistics, National Vital Statistics System, Division of Vital Statistics, November 2018.

[18] O. M. Parkhi, A. Vedaldi, and A. Zisserman. Deep face recognition. In *British Machine Vision Conference*, 2015.

[19] P. Jonathon Phillips, Amy N. Yates, Ying Hu, Carina A. Hahn, Eilidh Noyes, Kelsey Jackson, Jacqueline G. Cavazos, Géraldine Jeckeln, Rajeev Ranjan, Swami Sankaranarayanan, Jun-Cheng Chen, Carlos D. Castillo, Rama Chellappa, David White, and Alice J. O'Toole. Face recognition accuracy of forensic examiners, superrecognizers, and face recognition algorithms. *Proceedings of the National Academy of Sciences*, 115(24):6171–6176, 2018.

[20] Florian Schroff, Dmitry Kalenichenko, and James Philbin. Facenet: A unified embedding for face recognition and clustering. *CoRR*, abs/1503.03832, 2015.

[21] Jeroen Smits and Christiaan Monden. Twinning across the developing world. *PLOS ONE*, 6(9):1–5, 09 2011.

[22] Yaniv Taigman, Ming Yang, Marc'Aurelio Ranzato, and Lior Wolf. Deepface: Closing the gap to human-level performance in face verification. In *Proceedings of the 2014 IEEE Conference on Computer Vision and Pattern Recognition*, CVPR '14, pages 1701–1708, Washington, DC, USA, 2014. IEEE Computer Society.

[23] A. Towler, R. I. Kemp, and D White. *Unfamiliar face matching systems in applied settings*. Nova Science, 2017.

[24] Working Group 3. Ed. M. Werner. *ISO/IEC 19794-5 Information Technology - Biometric Data Interchange Formats - Part 5: Face image data*. JTC1 :: SC37, 2 edition, 2011. http://webstore.ansi.org.

[25] David White, James D. Dunn, Alexandra C. Schmid, and Richard I. Kemp. Error rates in users of automatic face recognition software. *PLoS ONE*, 10:1–14, October 2015.

[26] Bradford Wing and R. Michael McCabe. Special publication 500-271: American national standard for information systems data format for the interchange of fingerprint, facial, and other biometric information part 1. Technical report, NIST, September 2015. ANSI/NIST ITL 1-2015.

[27] Andreas Wolf. Portrait quality - (reference facial images for mrtd). Technical report, ICAO, April 2018.

[28] D. Yadav, N. Kohli, P. Pandey, R. Singh, M. Vatsa, and A. Noore. Effect of illicit drug abuse on face recognition. In *2016 IEEE Winter Conference on Applications of Computer Vision (WACV)*, pages 1–7, Los Alamitos, CA, USA, mar 2016. IEEE Computer Society.

This publication is available free of charge from: https://doi.org/10.6028/NIST.IR.8271